DEPÓSITO LEGAL ppi 201502ZU4666
Esta publicación científica en formato digital
es continuidad de la revista impresa
ISSN 0041-8811
DEPÓSITO LEGAL pp 76-654

Revista de la Universidad del Zulia

Fundada en 1947
por el Dr. Jesús Enrique Lossada

Ciencias Exactas Naturales y de la Salud

Año 11 N° 30
Mayo - Agosto 2020
Tercera Época
Maracaibo-Venezuela

REVISTA DE LA UNIVERSIDAD DEL ZULIA

Tercera Época

Ciencias Exactas, Naturales y de la Salud

AÑO 11 N° 30 MAYO-AGOSTO 2020

Fundada en 1947 por el Dr. Jesús Enrique Lossada
Adscrita a la Cátedra Libre Historia de la Universidad del Zulia

PUBLICACIÓN AUSPICIADA POR LA
UNIVERSIDAD DEL ZULIA

Indizada, registrada y/o catalogada
electrónicamente en las siguientes bases de datos:

REVENCYT	WOS
LATINDEX	EZB- Elektronische Zeitschriftenbibliothek- Universität Regensburg
Actualidad Iberoamericana	Linkovaci Server SFX- Univerzita Karlova
CLASE	UBL -Universitas Bibliothek Leipzig
PERIÓDICA	ZDB- Zeitschriften Datenbank
Emerging Sources Citation Index (ESCI).	BSZ Bibliotheksservice Zentrum Baden-Wüuttemberg
BIBLAT-Bibliografía Latinoamericana	Issuu: http://Issuu.com/revistadelauniversidaddelzulia
FLACSO-Argentina	

REVISTA DE LA UNIVERSIDAD DEL ZULIA
©2020. Universidad del Zulia
DEPÓSITO LEGAL ppi 201502ZU4666
Esta publicación científica en formato digital es continuidad de la revista impresa
ISSN 0041-8811
DEPÓSITO LEGAL pp 76-654

Portada:
Concepto gráfico: Laura González
Diagramación final: Reyber Parra

REVISTA DE LA UNIVERSIDAD DEL ZULIA
Calle 67 (prolongación Cecilio Acosta) con Avenida 16 (Guajira)
Sede rectoral de la Universidad del Zulia. Edificio Fundadesarrollo
Maracaibo, estado Zulia, Venezuela.
Correo electrónico: revistadeluz@gmail.com

Revista de la Universidad del Zulia

Tercera Época

ISSN 0041-8811

El Dr. Jesús Enrique Lossada, luego de trabajar infatigablemente hasta lograr la reapertura de la Universidad del Zulia, el 01 de octubre de 1946, le aportó a esta institución su primera revista científica: la *Revista de la Universidad del Zulia*, fundada por este insigne zuliano, el 31 de mayo de 1947. En su Tercera Época la revista mantiene la orientación que le asignara su fundador: es un órgano científico de difusión de trabajos parciales o definitivos de investigadores y/o equipos de investigación nacionales y extranjeros. La revista posee un carácter multidiscliplinario, por ello su temática se divide en tres grandes ejes: a. ciencias sociales y arte; b. ciencias del agro, ingeniería y tecnología; c. ciencias exactas, naturales y de la salud. Su publicación es cuatrimestral. Cada número, de los tres del año, se corresponde con uno de los tres ejes temáticos. La *Revista de la Universidad del Zulia*, por su naturaleza histórica y patrimonial, está adscrita a la Cátedra libre Historia de la Universidad del Zulia.

Directores y Responsables Eméritos

Jesús Enrique Lossada
José Ortín Rodríguez
José A. Borjas Sánchez
Felipe Hernández
Antonio Borjas Romero
César David Rincón
Sergio Antillano

Directora

Imelda Rincón Finol (LUZ)

Editor-Coordinador

Reyber Antonio Parra Contreras (LUZ)

Comité Editorial

Imelda Rincón (LUZ)
Reyber Parra (LUZ)
Mario Ayala (Universidad Nacional de Tierra del Fuego UNTDF, Argentina)
José Lárez (UNERMB)
Diego Felipe Arbeláez (Revista Amazonia Investiga, Colombia)
Magda Julissa Rojas-Bahamón (I.E. Jorge Eliecer Gaitán, Colombia)

Comité Asesor

Nelson Márquez (LUZ)
Judith Aular (LUZ)
Rutilio Ortega (LUZ)
Tahís Ferrer (LUZ)
Alí López (ULA)
María Dolores Fuentes Bajo (Universidad de Cádiz, España)
Néstor Queipo (LUZ)
Ana Irene Méndez (LUZ)
Modesto Graterol (LUZ)
Tomás Fontaines (UTM Ecuador)
Enrique Pastor Seller (Universidad de Murcia, España)
Lourdes Molero (LUZ)
Marielis Villalobos (LUZ)
Teresita Álvarez (LUZ)
Jesús Medina (LUZ)

Autoridades

Judith Aular de Durán (E)
Rectora

Cleotilde Navarro
Vice Rector Académico (E)

Marlene Primera
Vice Rectora Administrativa (E)

Ixora Gómez (E)
Secretaria

Imelda Rincón Finol
Reyber Parra Contreras
Cátedra Libre
Historia de la Universidad del Zulia

REVISTA DE LA UNIVERSIDAD DEL ZULIA
CIENCIAS EXACTAS, NATURALES Y DE LA SALUD///
AÑO 11 N° 30, Mayo-Agosto 2020
ISSN 0041-8811

Contenido

Determinismo y noción tomista de la libertad en José Gregorio Hernández Cisneros

Reyber Parra Contreras *

Iniciamos nuestro número 30 de la *Revista de la Universidad del Zulia* (dedicado a las Ciencias Exactas, Naturales y de la Salud), con un análisis conciso acerca del pensamiento filosófico de José Gregorio Hernández[1], específicamente su noción tomista de la libertad y las críticas que, desde esta posición, formulase al determinismo psicológico. Pretendemos, de esta manera, abordar un aspecto concreto del conjunto de valores y virtudes que puede encontrarse en la vida de este venezolano, a quien reconocemos como ejemplo de vida cristiana, civilidad y auténtico patriotismo.

*Editor-Coordinador de la *Revista de la Universidad del Zulia*. ORCID- 000-0002-3231-9214, reyberparra@gmail.com

[1] Nace en Isnotú, estado Trujillo (Venezuela), el 26 de octubre de 1864, hijo de Benigno María Hernández y Josefa Antonia Cisneros Mansilla, de quienes recibió una sólida formación cristiana. En febrero de 1879, ingresa como interno al Colegio Villegas de Caracas. Culminados sus estudios de bachillerato filosófico, ingresa a la Escuela de Medicina de la Universidad de Caracas, donde obtiene el grado de doctor en Ciencias Médicas, el 29 de junio de 1888. Por disposición del presidente de la República, Dr. Juan Pablo Rojas Paúl, en julio de 1889 es becado para cursar estudios de microscopía, histología, bacteriología y fisiología experimental en París, con el compromiso de retornar al país a fin de impulsar el estudio de estas cátedras en el ámbito universitario. A su regreso, el presidente Dr. Raimundo Andueza Palacios, dictó un decreto de fecha 4 de noviembre de 1891, donde le confía la responsabilidad de fundar los estudios de histología, fisiología experimental y bacteriología en la Universidad de Caracas. Desde entonces y hasta 1908 transcurre su primera etapa como profesor universitario, la cual interrumpe para ingresar a la Cartuja de Farnetta, en Italia, donde intenta vivir una vocación contemplativa. En abril de 1909 retorna a Caracas y prosigue su servicio como médico y docente. Escribió varias obras de índole médica, literaria y filosófica, todas ellas signadas por su identidad católica (Obras completas, 1968). En vida fue considerado un hombre caritativo y servicial, comprometido con la atención de sus pacientes, especialmente los más pobres. Muere el 29 de junio de 1919, aniversario de su graduación de médico y día que marca el cese definitivo de la I Guerra Mundial, conflicto que le causó gran tristeza debido a la tragedia de quienes lo padecieron. Porras (2018: 2) sostiene que: "Su fama y popularidad no ha sido producto de una campaña publicitaria. Su personalidad y virtudes contrastan con la percepción negativa que los venezolanos tenemos de nosotros mismos. Sin embargo, es el prototipo de lo que cada coterráneo anhela ser aunque su conducta vaya por otras veredas". El 19 de junio de 2020, el papa Francisco firmó el decreto mediante el cual se autorizó la beatificación de J. G. Hernández.

El Dr. José Gregorio Hernández Cisneros es un personaje de gran valía en la historia de Venezuela, a tal punto que su vida y facetas científica, docente y cristiana (sobre todo esta última) se han mantenido presentes en la memoria colectiva de las generaciones de venezolanos de todo el siglo XX hasta la actualidad. De su legado se han escrito diversos trabajos que abordan estas facetas[2], siendo recurrentes los de índole hagiográfico, a tono con la permanente convicción de los venezolanos de la santidad del Dr. Hernández (De Gema, 1950; Maldonado, 1963; Díaz, 1980; Yáber, 1987, 2014; Castellanos, 1994; Carvallo, 1995; Suárez y Bethencourt, 2000; Duplá y Capriles, 2018). También se ha escrito sobre su desempeño como médico, científico y profesor universitario (Carvallo, 1951, 1953; Sanabria, 1977; Vélez, 1992, 1995; Briceño-Iragorry, 2005; Zambrano, 2014; Bandenier y López, 2019). No obstante, poco se ha avanzado en la comprensión de sus ideas filosóficas (Barnola, 1959; Varela, 2020).

En los escritos del Dr. Hernández (Obras completas, 1968), pueden identificarse varios trabajos con contenido filosófico. De estos, prestamos atención a dos, con el propósito de analizar su interpretación de la libertad y el determinismo.

En primer lugar, encontramos el libro: *Elementos de Filosofía*, del año 1912. La obra contiene una sinopsis de historia de la Filosofía, con énfasis en aspectos epistemológicos y ontológicos. En general, su contenido es descriptivo, a fin de ofrecer una síntesis de los postulados de diversas corrientes filosóficas; en ocasiones emergen los argumentos, con la intención de refutar ideas que son contrarias a la ortodoxia o pensamiento tradicional[3], como es el caso de la sección sobre la voluntad (tercera parte de la obra), donde se cuestiona el determinismo psicológico.

Un segundo escrito, también del año 1912, se titula *En un vagón*. Se trata de un cuento que da continuidad al proceso argumentativo esbozado en el trabajo anterior, esta vez con mayor profusión a pesar de la narrativa concisa que le caracteriza. El relato tiene el propósito de hacer

[2] No pretendemos presentar una relación de todos los trabajos que se han publicado acerca de la vida del Dr. Hernández. Tan sólo identificamos algunas obras relevantes, que dan cuenta de la importancia histórica de este venezolano.

[3] Nos referimos a la Filosofía que da fundamento a la civilización cristiana concebida por la Iglesia, y que tuvo su auge en la época medieval, para luego encontrar resistencia en corrientes del pensamiento de índole heterodoxa, como por ejemplo: el positivismo, el liberalismo, el modernismo y el marxismo.

ver algunos errores que el Dr. Hernández encuentra en la "novedad" expuesta por sistemas filosóficos (cientificismo y determinismo) que niegan la "buena doctrina" de la Iglesia.

La estrategia del autor para el logro de su cometido consiste en presentar la interacción de cuatro personajes alegóricos que se encuentran en el vagón de un tren, donde dos de ellos dan cause a un diálogo socrático que desemboca en el triunfo de la verdad proclamada por la Iglesia. Estos personajes y sus alegorías son los siguientes:

a) El joven Carlos, ávido de conocimientos, que por su inmadurez e ímpetu juvenil busca la verdad en "las novedades" del determinismo; representa a todos aquellos que pretenden conducir sus vidas al margen de las enseñanzas contenidas en el catecismo.

b) Felipe, el tío de Carlos, un adulto sosegado que conoce a cabalidad la ortodoxia; representa a quienes se rigen de forma cónsona con la autoridad de la Iglesia y, en consecuencia, dialoga con su sobrino a objeto de presentarle argumentos que lo disuadan de permanecer en el error.

c) La madre de Carlos (hermana del tío Felipe), una mujer que se ha esmerado en la educación cristiana de su hijo y ve con angustia la actitud rebelde de éste; ella representa la Iglesia, madre que "siembra" (Hernández, 1912 b) las verdades de la fe en sus hijos, y cuando estos se extravían no sólo se preocupa, sino que persiste para que den la "vuelta" de regreso a la verdad.

d) El cuarto personaje representa al Dr. Hernández: un espectador que observa con atención la interacción de los otros tres personajes, y de esta experiencia recoge una lección que se transmite al final de este cuento: "Yo me quedé con el corazón entristecido al pensar cuántos hay que permanecen definitivamente divorciados del Catecismo por carecer de una mano amiga y amante que les haga fácil la vuelta" (Hernández, 1912 b).

Al concebir esta obra, el Dr. Hernández parte del contenido de *Elementos de Filosofía*, de donde extrae una idea que quiso difundir mediante un cuento (género flexible, con mayor plasticidad para el autor y de más fácil comprensión para el lector), a fin de hacer saber que el ser humano es libre y capaz de ejercer su voluntad por encima de cualquier motivo[4], y por ende

[4] "El apetito inferior", según la explicación de Santo Tomás de Aquino (2001: 755), aunque forme parte de las cualidades corporales, está sometida al juicio racional del hombre.

sus actos no están determinados a priori porque en él prevalece la libertad de albedrío o libertad moral (Hernández, 1912 a).

De acuerdo con Hernández, el libre albedrío viene dado por la determinación de la voluntad o "el poder para elegir entre muchos actos posibles" (Hernández, 1912 a: 54), cualidad que sirve de fundamento a la personalidad. Cuando la persona guía su voluntad mediante principios racionales, desarrolla el carácter, donde convergen las convicciones y la voluntad firme (Hernández, 1912 a).

Este razonamiento se fundamenta en la doctrina tomista sobre la libertad (voluntad y libre albedrío), que a su vez se desprende del pensamiento aristotélico y las enseñanzas de los padres de la Iglesia. De acuerdo con Santo Tomás de Aquino (2001: 756) en el hombre hay libre albedrío o "juicio libre", lo que define como principio de un acto, "aquello en virtud de lo que el hombre juzga libremente". El "juzgar" nace de la condición racional del ser humano; su facultad cognoscitiva le permite discernir lo que debe evitar o buscar. Así, "es necesario que el hombre tenga libre albedrío, por lo mismo que es racional" (Santo Tomás de Aquino, 2001: 754).

El juicio libre o libre albedrío tiene dos atributos esenciales según Santo Tomás de Aquino (2001: 747-758): por un lado, su origen racional o atributo racional; por otro lado, la "facultad de elección", que remite a la voluntad, "pues somos dueños de nuestros propios actos en cuanto que podemos elegir esto o aquello". En este sentido, para el Doctor Angélico, "la naturaleza del libre albedrío debe ser analizada a partir de la elección", es decir, de la forma en que se conduzca o adhiera la voluntad, siendo realmente perfecta aquella que permite abrazar la bienaventuranza o fin último del hombre.

En concordancia con estos postulados de Santo Tomás de Aquino, el Dr. Hernández encuentra inadmisibles las coordenadas filosóficas trazadas por el determinismo, doctrina que pone en duda el poder de elección del hombre y afirma que las acciones de éste se encuentran condicionadas por factores ajenos a su voluntad. Spinoza (1632-1677) y Leibniz (1646-1716) desarrollaron tesis deterministas. El primero de ellos sostuvo que:

> "Los hombres se equivocan, en cuanto que piensan que son libres; y esta opinión solo consiste en que son conscientes de sus acciones e ignorantes de las causas por las que son determinados. Su idea de la libertad es, pues, esta: que no conocen causa alguna de sus acciones. Porque eso que dicen, de que las acciones humanas dependen de la voluntad, son palabras de las que no tienen idea alguna" (Spinoza, 2000: 73).

Leibniz, a su vez, creyó que "no hay acto voluntario sin motivo y la voluntad se determina siempre por el mejor (Determinismo psicológico)" (Hernández, 1912 a: 222). En este punto, el Dr. Hernández refiere que el método psicológico demuestra la existencia de la libertad al indagar en la conciencia, la cual atestigua que somos libres cuando resistimos nuestros apetitos y pasiones, y de esta manera optamos por aquello que juzgamos conveniente: "siempre la conciencia nos atestiguará la existencia de la libertad" (Hernández, 1912 b).

Por su parte, el determinismo intenta apoyarse en la estadística, de donde obtiene unos resultados que expresan regularidades o patrones de comportamientos, pero no explora "el estado psicológico de los individuos que ejecutaron dichos actos" (Hernández, 1912 a: 57) quedando, en consecuencia, al margen de la conciencia, "testigo perfecto de la existencia de la libertad humana" (Hernández, 1912 a: 59).

En su transitar por la modernidad, el determinismo transmutó a nihilismo. En efecto, al negar o condicionar la libertad del hombre, suprime en este la responsabilidad de sus actos y lo deja a merced de sus pasiones o apetito inferior. De esta manera, la moral -que el pensamiento tomista asocia al fin último – es irrelevante y carece de sentido.

En contraposición, la perfección moral está presente en el ideario del Dr. Hernández, convicción que se sustenta en la doctrina sobre la libertad de Santo Tomás de Aquino, donde la voluntad guiada por la razón, facultan al hombre para su perfección:

> "De suerte que la perfección del hombre consiste en el desarrollo total de sus facultades guiadas por la razón; y por esta razón el bien es aquello que contribuye a la perfección del ser del hombre, mientras que el mal es la carencia de la debida perfección.
> El hombre es un ser racional y libre; y es también un ser moral, es decir, capaz del bien y del mal" (Hernández, 1912 a: 143-144).

Al respecto, Santo Tomás de Aquino (2001: 755) refiere que la perfección moral y el acercamiento del hombre a la bienaventuranza o fin último, no depende totalmente de éste; el hombre necesita, aparte de la razón y la voluntad, ser "movido y ayudado por Dios (...) la elección nos pertenece, por supuesto que contando siempre con la ayuda divina". Esta combinación, de acuerdo con Hernández (1912 a) hace posible la vivencia de las virtudes o convicciones fuertes

(fortaleza, temperancia, castidad, caridad, justicia, bondad, piedad, esperanza y fe), capaces de moldear el carácter en cuanto atributo de la personalidad.

De esta manera, la noción de libertad, de la moral y la visión del hombre en su conjunto en el pensamiento de José Gregorio Hernández, se cimentan en la tradición escolástica, con énfasis en el tomismo: acá identifica la "buena doctrina" (Hernández, 1912 b), aquella que le da contenido a "mi filosofía, la mía, la que yo he vivido" y que conforma un mismo sistema con la "religión Santa que recibí de mis padres" (Hernández, 1912 a: 7).

Ciertamente, el Dr. Hernández abrazó la Filosofía Cristiana, entendida como "una especulación filosófica concebida en unión vital con la fe" (San Juan Pablo II, 1998). Además de él, otros intelectuales venezolanos de finales del siglo XIX -de condición seglar y universitaria-, asumieron esta orientación y la defendieron mediante publicaciones hemerográficas y bibliográficas donde confrontaban la "novedad" de las ideas heterodoxas (algunas modernistas, otras positivistas o evolucionistas). Cecilio Acosta, en la zona central (Parra, 2018); Manuel Dagnino y Francisco Ochoa en Maracaibo (Parra: 2014, 2017), fueron algunos de estos intelectuales.

Referencias

Barnola, Pedro Pablo (1959). Prólogo. En: Hernández, José Gregorio (1959). *Elementos de Filosofía* [Reimpresión]. Caracas: Bibliográfica Venezolana.

Bandenier de Suárez, Claudia; López Loyo, Enrique (2019). *José Gregorio Hernández: la epopeya de su laboratorio. Análisis descriptivo del primer laboratorio científico venezolano*. Caracas: UCV.

Briceño-Iragorry, Leopoldo (2005). José Gregorio Hernández, su faceta médica (1864-1919), *Gaceta Médica de Caracas*, 113 (4).

Carvallo Ganteaume, Marcel (1995). *José Gregorio Hernández: un hombre en busca de Dios*. Caracas: Trípode, p. 300.

Carvallo, Temístocles (1951). *Sinopsis sobre la obra científica del doctor José Gregorio Hernández fundador de la medicina experimental en Venezuela*. Caracas: Ediciones Millán, p.16.

Carvallo, Temístocles (1953). *José Gregorio Hernández: su obra científica y social en Venezuela*. 2a edición. Caracas: Imprenta Nacional, p. 147.

Castellanos, Rafael Ramón (1994). *El milagroso médico de los pobres en Isnotú*. 3a edición. Caracas: Italgráfica, p. 221.

De Gema, E. (1950). *El siervo de Dios doctor José Gregorio Hernández Cisneros: el hombre, el santo, el sabio: su vida*. Caracas: Imprenta Nacional.

Díaz Álvarez, Manuel (1980). *El médico de los pobres*. 2a edición. Caracas: Ediciones Paulinas, p. 155.

Duplá, Francisco J.; Capriles, Axel (2018). *Se llamaba José Gregorio Hernández*. Caracas: Fundación Amigos José Gregorio Hernández, p. 166.

Giacopini de Zambrano, María Isabel (2014). Dr. José Gregorio Hernández Cisneros. Ilustre Venezolano, Estudiante, Médico, Profesor e Investigador de la Universidad Central de Venezuela, *Revista Tribuna del Investigador*, 15 (1-2).

Hernández, José Gregorio (1912 a). *Elementos de Filosofía*. Caracas: Tipografía de la Empresa El Cojo, p. 236.

Hernández, José Gregorio (1912 b). En un vagón. *El Cojo Ilustrado*. Caracas, 1 de junio de 1912. En: Obras Completas del Dr. José Gregorio Hernández. Caracas: Universidad Central de Venezuela, p. 1277.

Maldonado, Francisco Armando (1963). *Cenizas inmortales*. Caracas: Ediciones Paulinas, p. 116.

Obras Completas del Dr. José Gregorio Hernández (1968), compilación y notas por el Dr. Fermín Vélez Boza. Caracas: Universidad Central de Venezuela, p. 1277.

Parra, Reyber (2014). Visión del socialismo en el pensamiento de Manuel Dagnino, *Revista de Filosofía*, 31 (78), 25-41. Maracaibo, Universidad del Zulia.

Parra, Reyber (2017). *Ideario del Dr. Francisco Ochoa. Primer Rector de la Universidad del Zulia.* Maracaibo: Academia de Historia del Estado Zulia-Cátedra Libre Historia de la Universidad del Zulia, p. 24. En: https://www.academiahistoriazulia.com/libros/

Parra, Reyber (2018). *Ideas socialistas y antisocialismo en el siglo XIX venezolano*. Cabimas (Venezuela): Universidad Nacional Experimental Rafael María Baralt/Universidad del Zulia, p.184. En: https://www.academiahistoriazulia.com/libros/

Porras, Baltazar (2018). Prólogo. En: Duplá, Francisco J.; Capriles, Axel (2018). *Se llamaba José Gregorio Hernández*. Caracas: Fundación Amigos José Gregorio Hernández, p. 166.

Sanabria, Antonio (1977). *José Gregorio Hernández de Isnotú (1864-1919): creador de la moderna medicina venezolana*. Caracas: Fundación Premio "José Gregorio Hernández", p. 163.

San Juan Pablo II (1998). *Fides et Ratio*. Carta Encíclica. Ciudad del Vaticano, 14 de septiembre de 1998. En: http://www.vatican.va/content/john-paul-ii/es/encyclicals/documents/hf_jp-ii_enc_14091998_fides-et-ratio.html

Santo Tomás de Aquino (2001). *Suma de Teología I*. Parte I. Cuarta Edición (reimpresión). Madrid: Biblioteca de Autores Cristianos. En: https://www.dominicos.org/media/uploads/recursos/libros/suma/1.pdf

Spinoza, Baruj (2000). *Ética demostrada según el orden geométrico*. Edición y Traducción de Atilano Domínguez. Madrid: Editorial Trotta, p.301.

Suárez, María M.; Bethencourt, Carmen (2000). *José Gregorio Hernández. Del lado de la luz*. Caracas: Fundación Bigott.

Varela, Nirso (2020). Filosofía del Dr. José Gregorio Hernández [Opinión]. Diario *Notica Al Día*, 13 de mayo de 2020. https://noticialdia.com/2020/05/filosofia-del-dr-jose-gregorio-hernandez-nirso-varela/

Vélez Boza F. (1995). La docencia médica del Dr. José G Hernández, *Revista de la Sociedad Venezolana de Historia de la Medicina*, 45 (69), 288-308.

Vélez Boza, F. (1992). José Gregorio Hernández: Profesor universitario, *Revista de la Sociedad Venezolana de Historia de la Medicina*, 41 (62), 17-42.

Yáber, M. (2014). *José Gregorio Hernández. Hombre de Dios, Siervo de los Enfermos*. Caracas: Ediciones Trípode.

Yáber, Miguel (1987). *José Gregorio Hernández*. Caracas: Trípode, 1987. Serie Modelos Venezolanos de Vida Cristiana, p. 157.

The Coherent and Thermal Photons Radiation in the Enzyme

Mehrad Gavahi *

ABSTRACT

This paper presents the theoretical states of radiation field in the mechanism of enzyme, for state of thermal and coherent radiation by concept of the quantum mechanics. For illustrating the energy and distribution of photon, we used simple concepts of the radiation field in the enzyme. We try to present the thermal radiation and coherent radiation happened in the biological microscopic system especially in the enzyme, and show that, these radiations could break the hydrogen bond pairs in the enzyme (substrate) at high temperature (above 323K) and show its effects on the relative activity of the enzyme.

KEYWORDS: Quantum Mechanics; Photon Radiation; Biophoton; Enzyme; Biological Physics.

La radiación de fotones coherentes y térmicos en la enzima

RESUMEN

Este artículo presenta los estados teóricos del campo de radiación en el mecanismo de la enzima, para el estado de radiación térmica y coherente por concepto de la mecánica cuántica. Para ilustrar la energía y la distribución del fotón, utilizamos conceptos simples del campo de radiación en la enzima. Tratamos de presentar la radiación térmica y la radiación coherente que se produjo en el sistema microscópico biológico, especialmente en la enzima, y mostramos que estas radiaciones podrían romper los pares de enlaces de hidrógeno en la enzima (sustrato) a alta temperatura (por encima de 323K) y mostrar sus efectos sobre la actividad relativa de la enzima.

PALABRAS CLAVE: Mecánica Cuántica; Radiación de fotones; Biofotón; Enzima; Física Biológica

*School of Science, Xi'an Jiaotong University, Xi'an 710049, China. ORCID iD: 0000-0001-5279-8008

Recibido: 02/04/2020 Aceptado: 15/06/2020

Introduction

Understanding the photon radiation happening in the biological system with respect to its effects on the biological systems is gaining an increased attention these days (Mayburov, 2009; Niggli, 2014; Mayburov, 2015).

There, biophoton describes photons in low frequency which are produced by a biological system. Biological physics and applying physical law in the biological system is more benefitial for both the academic knowledge and experimental framework. Living cells use a wide variety of cellular mechanisms for doing their activities. They do this at proper place at proper time.

The basic design idea of these nano-machines is based on the quantum physics, and in the quantum physics view, the enzyme is one kind of nano-machines. The enzyme plays an important role to explain how cells and proteins work inside a biological system. In a living system, there are various kinds of enzymes, however, the type of operation of all kinds of enzymes is usually the same (Cooper, 2000). In this paper, we would like to illustrate that the radiation state happens in the enzyme when the substrate binds to the active site.

Different types of enzymes have different classifications based on the kind of reactions they catalyze. We selected the enzyme worked on the temperature between 293K-353K i.e. before any reactions between the enzyme and the substrate, that enzyme's temperature is 293k. When the substrate binds to the enzyme (active site), the temperature is raised to 353k. In this case we probe the energy of each photon by two variables (the temperature and the frequency).

It is more benefitial to spend more time to know about DNA helix, because any living system is made up of DNA or RNA, and almost every cell in a human's body has DNA. DNA is made up of base pairs. The configuration of DNA is made of two long strands that called a double helix. The structure of the double helix is bonding many elements like C, O, N, H, etc. (Watson & Crick, 1993; Park & Lakes, 2007; Sheu et al., 2003). Those elements bond to each other and make the DNA double helix. The important bond in DNA double helix is hydrogen bond, the hydrogen bond is the heart of any biological structure. In this paper, we focus on the formation of hydrogen bonds in the alpha-helix and beta-sheet secondary structures. (Fig. 1)

In addition, hydrogen bonds are often playing the central role in the function of the catalytic active sites in the enzyme (Sneppen, & Zocch, 2005).

In Sec. 1, we show the description of the entire system (enzyme) and the type of operation. In Sec. 2, follows our design in the quantum thermal radiation for the temperature state. In Sec. 3, calculates the photon probability and the energy of photon in the coherent radiation. Finally, in sec 4, we numerically solve our model.

1. Enzyme and Operation (Model)

Enzymes are the organic particles living inside the cell. Enzymes accelerate the rate of all chemical reactions. They are vital for the life and serve the body, for example aiding in digestion and metabolism (Briegel & Popescu, 2013).

The enzyme and the substrate can bind to each other by two ways: the lock-and-key (Fig 2) and the induced-fit model, these two theories explain how enzymes work. This research focused on the lock-and-key model and in this model, the substrate and active site of the enzyme has the same configuration. When the substrate is binding to the active site, the chemical reactions start to effect the substrate and change it to product. Then the product leaves the active site of the enzyme and it goes on to catalyze the other reactions (Kaplan, 2010).

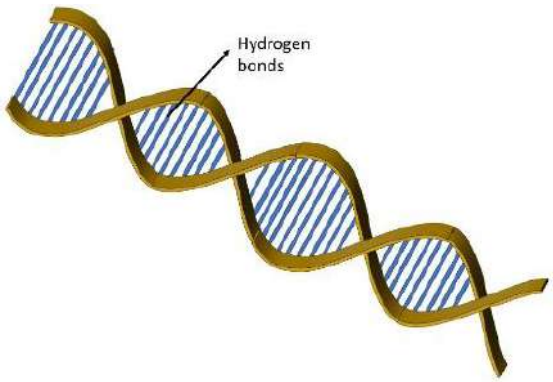

Figure 1: DNA helix is made up of the base pairs. These pairs have complex structures and are made up of particular elements like C, O, N, H, etc. Hydrogen is the most important element in these structures.

As mentioned, the human body is made up of many elements like sodium, potassium, calcium, magnesium, and hydrogen. These elements have electrical charges, called ions. All of our cells and sub-cells are made up of these elements. The electrical charge in our body has

studded in the bioelectric field (Elson & Haas, 2011). The enzyme is made up of some of these elements. It is convenient to suppose that the enzyme has electrical charge.

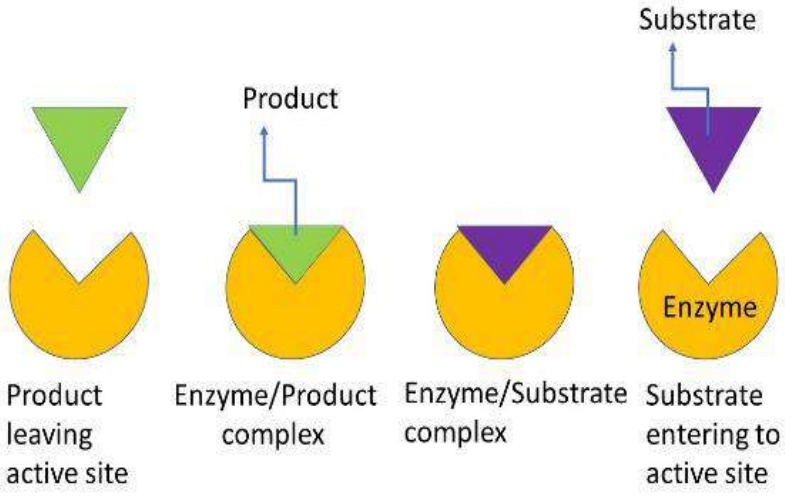

Figure 2: The enzyme has an active site in which the substrate could bind. A chemical reaction happens between the substrate and the enzyme when the substrate and the enzyme bind to each other, and due to the chemical reaction, the temperature rises. Then the chemical reaction causes the substrate convert to product and this product leaves the enzyme.

In the microscopic view, while the substrate and the enzyme are binding (enzyme/substrate complex), we supposed, the subsystem is made up of the alpha-helix and beta-sheet secondary structures and the hydrogen bond always oscillates with a high frequency, it is advantageous to ask how much free energy is related to the hydrogen bonds between these ranges 0.1-0.3 nm. The range of the order-of-magnitude for these ranges is 0.15-5.07 kJ/mol (Garrett & Grisham, 1997; Haynie, 2008; Van Der Spoel et al. 2006; Markovitch, & Agmon, 2007; Yakovchuk et al. 2006).

An important factor for the enzyme activity is *relatively activity*, which is the ratio between the activity of the enzyme and the activity of the temperature control, and it is expressed in percentage.

Before we introduce the thermal radiation and coherent radiation, let think about why we should focus on these two specific radiations. Biophotons are photons of light that are produced by a biological system. These photons lie down in the ultraviolet and low visible light ranges.

The emission of the biophotons is either non-thermal or thermal depending on the type of cells we select (Greffet et al., 2002; Bajpai, 1999), moreover, near the thermal source, we can also find the coherent radiation. Due to these reasons, we measure and find the energy of photons in both radiations. and the term of biophotons used here should not be confused with the Biophotonic Field, which studies the general interaction of light with the biological systems.

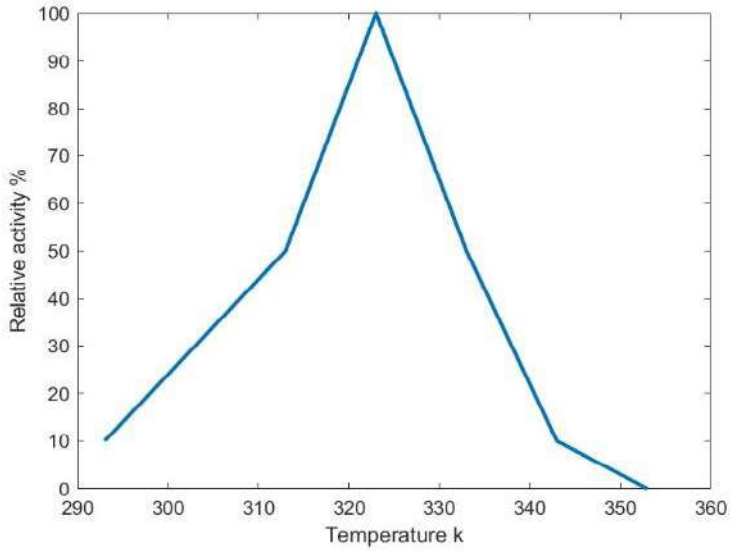

Figure 3: The effects of the temperature stress on the enzymatic relatively activity. The enzymatic activity starts below 20% at temperature 293k, when the substrate and the enzyme bind to each other; due to chemical reaction between the substrate and the enzyme, the temperature rises slightly. However, the enzymatic activity rises dramatically, the enzymatic activity at 323k is 100%. The enzymatic relatively activity rapidly decreases when the temperature rises above 323k. (De Freitas et al., 2014).

2. Thermal Radiation

This paper supposes that the interaction between the enzyme and the substrate stimulate photons with respect to changing temperature. The chemical reaction between the substrate and enzyme causes a rise in the temperature of the subsystem (enzyme/substrate complex), and it causes a change in the temperature of the nearest electron in the structure of the enzyme and then the substrate (electron) could emit the photon.

We suppose that, these photons are absorbed by the substrate with the fix frequency □ and given the state of polarization. The energy of photon is given by $E = \hbar$□, otherwise

the electron can diffuse n photons, the total energy of photons could be written by $E = n\hbar$ where $\hbar$ is plank's constant, and those photons are attracted by the substrate.

As mentioned, if the subsystem emits n of these photons, the energy essentially equals to $E = n\hbar$. The probability of photon is proportional to Boltzmann factor $E \sim e^{\frac{-\varepsilon}{kT}}$, where k is Boltzmann's constant and T is the temperature. We can write the probability of this system as follows:

$$P_n(E) = Ae^{-B\hbar n} \qquad (1)$$

where $B = \frac{1}{kT}$ and A is a normalizing factor. The radiation inside the substrate (cavity) can be regarded by the oscillator, and the energy inside the oscillator can be written by $E = \hbar\left(n + \frac{1}{2}\right)$. To determine what A is, we note that the sum of all probabilities must be equals to 1.

$$\sum_{n=0}^{\infty} P(E_n) = A\sum_{n=0}^{\infty} e^{-E_n/KT} = A\sum_{n=0}^{\infty} e^{-n\hbar\omega/KT} = 1. \qquad (2)$$

The above sum can be written in this form $\sum X = 1 + X^1 + X^2 + \cdots$, where $X = e^{-B\hbar}$ This series, called binomial expansion of $\frac{1}{1-x}$ (Beloussov, 2003). Hence $A = 1 - x = 1 - e^{-B\hbar}$, then

$$P_n(E) = Ae^{-B\hbar n} \qquad (3)$$

$$P_n(E) = (1 - e^{-B\hbar n})e^{-B\hbar n} \qquad (4)$$

The average number of photons with frequency and given polarization can be calculated in this form:

$$\langle n\rangle = \frac{1}{e^{B\hbar\square} - 1} \qquad (5)$$

For obtaining thermal energy of photon, we should multiply thermal average number of photons times with the energy per photon. This relation is known as the Planck distribution function:

$$\langle E_n\rangle = \hbar\square\langle n\rangle = \frac{\hbar\square}{e^{\hbar\square/KT} - 1} \qquad (6)$$

The factor $e^{B\hbar\square}$ can be very large or very small, depending on frequency and temperature. In this case, we have chosen $\hbar\square \gg KT$ and if we called $\langle n\rangle = \underline{n}$, photon distribution can be written by:

$$P_n = \frac{\underline{n}^n}{(\underline{n} + 1^{n+1})} \qquad (7)$$

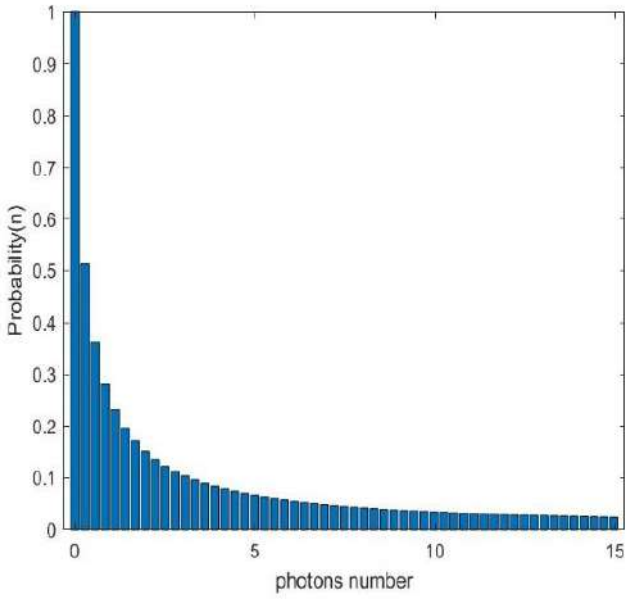

Figure 4: Photon distribution for thermal radiation of $P_n = \frac{\underline{n}^n}{(\underline{n}+1^{n+1})}$. It can be found that n = 0 has always the largest probability and the distribution falls off monotonically with increasing n.

The energy density is given by $u(\square, T)d\square dT = \frac{\hbar}{\pi^2 C^3}\frac{\square^3 d\square dT}{e^{B\hbar\square}-1}$. This energy density is very close to Stefan-Boltzmann law in the thermal radiation. However in the enzyme, the

temperature and the frequency are changed by the linear combination and it is the reason for the extra integral in the energy density.

The opposite side of the thermal radiation is the coherent radiation. In this subsystem, we modeled the oscillator coherent states.

3. Coherent Radiation

The main difference between the coherent and the thermal radiation is the wave phase. In fact, in thermal radiation the source emission wave is in the random phases *however* in the coherent source, waves are in the *same phases*. In the coherent thermal state, we should introduce displacement operator and density operator in phase-space.

The density matrix of the coherent thermal state is represented by:

$$\rho(\alpha,\beta) = \frac{D(\alpha)e^{-Bn\hbar}D^{+}(\alpha)}{\sum_{n=0}^{\infty} e^{-Bn\hbar}} \qquad (8)$$

where $D(\alpha)$ is the displacement operator generating the coherent state $D(\alpha)|0\rangle = |\alpha\rangle$ with the complex amplitude α

$$|\alpha\rangle = e^{-\frac{1}{2}|\alpha|^2 \sum_{r=0}^{\infty} \frac{\alpha^r}{\sqrt{r!}}|r\rangle} \qquad (9)$$

where $|r\rangle$ is photon number operator. Photon distribution (probability) of the coherent radiation can be calculated by

$$P_n = |\langle n|\alpha\rangle|^2 = e^{-\bar{n}}\frac{\bar{n}^n}{\bar{n}!} \qquad (10)$$

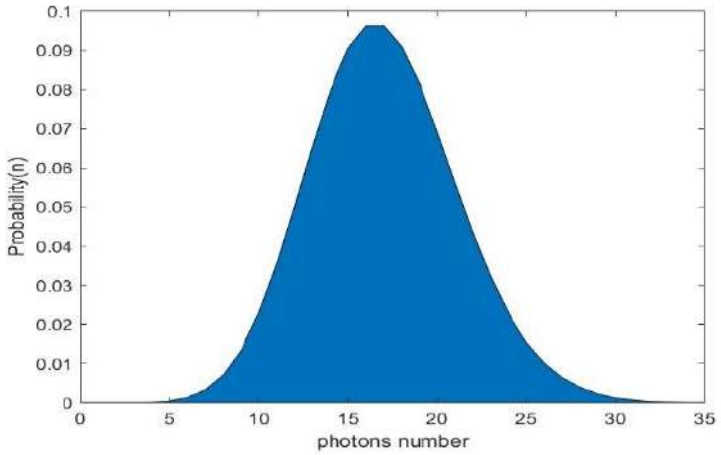

Figure 5: Photon distribution for the coherent radiation $P_n = e^{-\bar{n}}\frac{\bar{n}^n}{\bar{n}!}$ is Poissonian distribution.

4. Result and Discussion

We suppose that the enzyme emits photons with particular energy, and this energy depends on the specific frequency and temperature, i.e. if the enzyme seats on temperature T_1 then it emits the photon with the specific frequency $\square_1$ and in temperature T_2 emits $\square_2$. We will determine the energy of these photons for the thermal and coherent radiations. The energy to break the hydrogen bond of the alpha helices in isolated molecule is 4.79-5.57 KJ/mol, and the associated energy for this molecule in the water environment is 1.58-1.93 KJ/mol (Sheu et al., 2003).

We calculated, the maximum and the minimum content of the photon's energy respected to the thermal radiation that is 1.9 – 2.29 KJ/mol as shown in Fig. 6. As we mentioned in section I, many cells follow either the coherent or thermal radiation state. For thermal radiation of cell (enzyme), the energy of photon lies down between 1.9KJ/mol at temperature 294K and 2.3KJ/mol at temperature 360K.

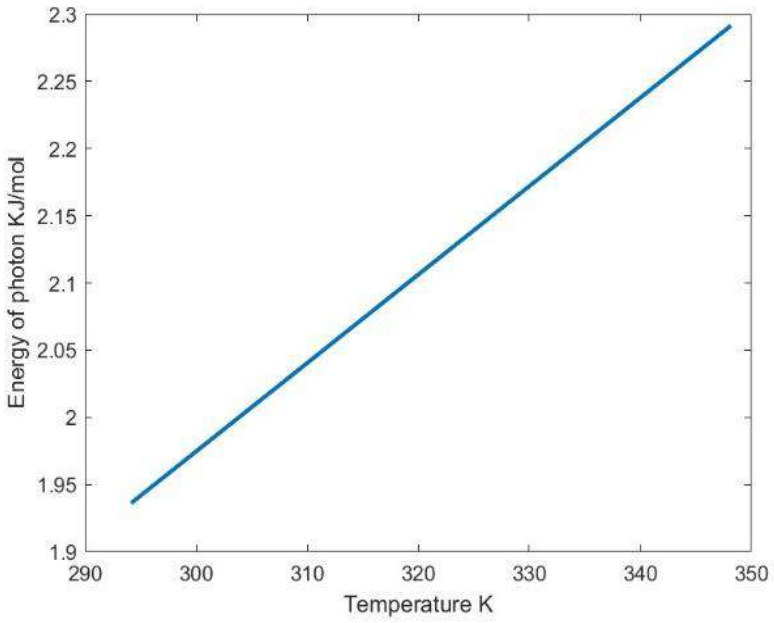

Figure 6: The minimum energy of photon is 1.9KJ/mol at temperature 294K, and the maximum energy of photon is 2.2915 KJ/mol at 358K without applying attenuation coefficient for the enzyme. The attenuation coefficient is a very small number depending on the enzyme classification. The energy of photon at 294K does not have enough power to break down the hydrogen bond, however when the temperature arises at 325K, the energy of photon is able to break the weakest hydrogen bond. At temperature 350K, the energy of photon can break all hydrogen bonds in the alpha helix in the water environment.

If we assume the alpha helix in the water environment follows the thermal equilibrium states, then at temperature 325K, the energy of photons can break down the hydrogen bond in the DNA alpha helices.

The energy of photons for the coherent radiation (squeeze state) Fig. 7 is between 3.87-4.73 KJ/mol. If we suppose that the hydrogen bond of the alpha helices in the isolated molecule follows the coherent radiation then the energy for breaking the hydrogen bond stands at 4.79-5.57 KJ/mol. However, we know that the distance between the hydrogen bond plays an important role for finding the energy bond. If we suppose that the hydrogen bond pair is 0.1nm, then the energy for the hydrogen bond in the isolated molecule is reduced to ~ 4.9KJ/mol for the stronger bond (Mitchell & Price, 1990).

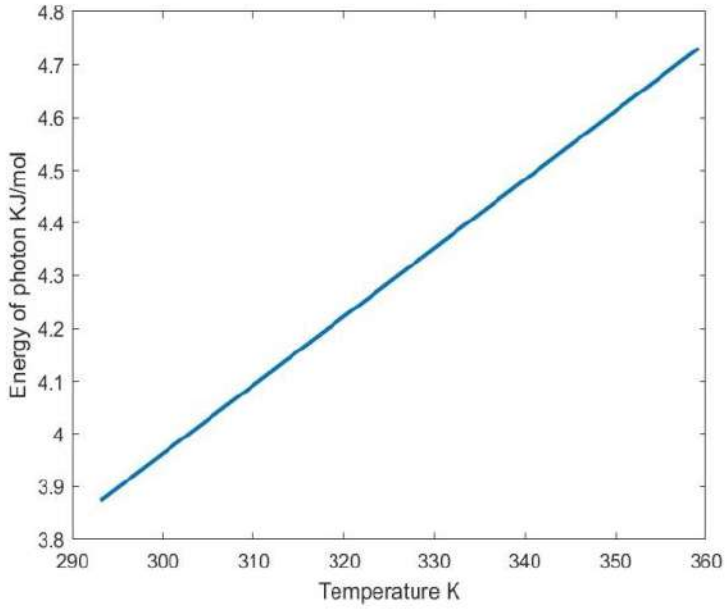

Figure 7: The minimum energy of the photon is 3.87 KJ/mol at temperature 294K, and the maximum energy of photon is 4.73 KJ/mol at temperature 358K.

It is found that the relative activity of the enzyme was shown in Fig. 3, when the temperature rises above 323k, the activity decreased dramatically. It may be because the enzyme starts to deform the shape and this deformation causes disconnection of the substrate and the enzyme. Regarding the radiation of the enzyme, it is reasonable to assume that the photons radiated by the enzyme can break down the pair of DNA helices, and these photons might play an important role to decrease the relative activity.

In the coherent modes, we could guess that after temperature 325K, the photons have enough energy for breaking down the weakest hydrogen bonds. When the temperature rises

above 325K, the energy of photons rises similarly, and thus these photons can break all the hydrogen bonds in the alpha helix. The photons radiated by the enzyme directly affects the relative activity of the enzyme.

Conclusion

In this paper, we supposed when the enzyme and substrate are binding to each other due to a chemical reaction, the temperature in the enzyme changes. Due to change of the temperature, the enzyme emits photons with respect to the thermal and coherent radiation. After calculating the energy of photons for both types of the radiations and comparing it with the DNA helix, we understood when the temperature sits at 293k, the energy of each photon could not break these bonds. However when the temperature rises above 293k, the energy of photon increases and it can break down the hydrogen bonds. By these results we noticed that the photons radiated by the enzyme plays a role for decreasing the relative activity in the enzyme.

The DNA helix is made up of the base pairs. These pairs have complex structures which are made up of the particular elements like C, O, N, H, etc. In this paper, we focus on hydrogen bond in the alpha-helix. The hydrogen energy bonding in the alpha-helix is between 1.58-1.93 KJ/mol for the water environment and 4.19-4.9 for the isolated mode. We assume when the enzyme's temperature rises above 325K, the photons emitted by the enzyme at this temperature can break the base pairs of DNA. In the other hand, as we observed in Fig 3, the relative activity starts to decrease when the temperature rises more than 293k. It is more benefital to mention that the enzyme begins to denature itself in high temperature. However, if the enzyme could not denature itself, these photons are able to break the connection between the enzyme and the product.

Conflict of Interests Statement

The authors declare that there is no conflict of interests.

References

Bajpai, R. P. (1999). Coherent nature of the radiation emitted in delayed luminescence of leaves. Journal of Theoretical Biology. http://doi.org/10.1006/jtbi.1999.0899

Beloussov, L.V. (2003). BioSystems 68, 199–212. Photon emission and quantum signalling in biological systems. DOI: 10.1016/S0303-2647(02)00096-5

Briegel, Hans J.; Popescu, Sandu (2013). Intra-molecular refrigeration in enzymes. Royal society, 469: 20110290.

Cooper, G. M. (2000). The Eukaryotic Cell Cycle (2nd ed). The Cell: A Molecular Approach. 2nd Edition. Sunderland (MA). http://doi.org/10.1017/S0003055408080179

De Freitas, A. C., Escaramboni, B., Carvalho, A. F. A., De Lima, V. M. G., & De Oliva-Neto, P. (2014). Production and application of amylases of Rhizopus oryzae and Rhizopus microsporus var. oligosporus from industrial waste in acquisition of glucose. Chemical Papers. http://doi.org/10.2478/s11696-013-0466-x

Elson M. Haas, M.D. (2011). Electrolyte Balance. ANATOMY AND PHYSIOLOGY, Chapter 26. Fluid, Electrolyte, and Acid-Base Balance.

Garrett, R. H., & Grisham, C. M. (1997). Biochemistry, Fifth Edition. Journal of Chemical Education,page16,figure1.13. http://doi.org/10.1021/ed074p189.2,

Greffet, J. J., Carminati, R., Joulain, K., Mulet, J. P., Mainguy, S., & Chen, Y. (2002). Coherent emission of light by thermal sources. Nature. http://doi.org/10.1038/416061a

Haynie, D. T. (2008). Biological thermodynamics: Second edition. Biological Thermodynamics: Second Edition. Chapter 2 The first law of thermodynamics Table 2.3 page 37. http://doi.org/10.1017/CBO9780511802690

Kaplan PCAT (2010). Edition, chapter 2.

Markovitch, O., & Agmon, N. (2007). Structure and energetics of the hydronium hydration shells. Journal of Physical Chemistry A. http://doi.org/10.1021/jp068960g.

Mayburov, S. (2009). Coherent and Noncoherent Photonic Communications in Biological Systems. ArXiv Preprint ArXiv:0909.2676.

Mayburov, S. N. (2015). Photon emission and quantum signaling in biological system. EPJ Web of Conferences ,95.03024 DOI: 10.1051

Mitchell, J. B. O. & Price, S. L. (1990). The nature of the N □ H...O□C hydrogen bond: An intermolecular perturbation theory study of the formamide/formaldehyde complex. https://doi.org/10.1002/jcc.540111014

Niggli H.J. (2014). Ultraweak Electromagnetic Wavelength Radiation as Biophotonic Signals to Regulate Life Processes. J Electr Electron Syst 3:126. DOI:10.4172/2332-0796.1000126

Park, J., & Lakes, R. S. (2007). Biomaterials: An introduction: Third edition. Biomaterials: An introduction: Third edition. http://doi.org/10.1007-978-0-387-37880-0

Sheu, S.-Y., Yang, D.-Y., Selzle, H. L., & Schlag, E. W. (2003). Energetics of hydrogen bonds in peptides. Proceedings of the National Academy of Sciences. http://doi.org/10.1073/pnas.2133366100

Sneppen, K., & Zocch, G. (2005). Physics in molecular biology. Physics in Molecular Biology. Chapter7, http://doi.org/10.1017/CBO9780511755699.

Van Der Spoel, D., Van Maaren, P. J., Larsson, P., & Tîmneanu, N. (2006). Thermodynamics of hydrogen bonding in hydrophilic and hydrophobic media. Journal of Physical Chemistry B. http://doi.org/10.1021/jp0572535

Watson, J. D., & Crick, F. H. C. (1993). Genetical implications of the structure of deoxyribonucleic acid. JAMA: The Journal of the American Medical Association. http://doi.org/10.1038/171964b0

Yakovchuk, P., Protozanova, E., & Frank-Kamenetskii, M. D. (2006). Base-stacking and base-pairing contributions into thermal stability of the DNA double helix. Nucleic Acids Research. http://doi.org/10.1093/nar/gkj454

Risk assessment in the Nanofluid stabilization process and optimization of process parameters by HAZOP methodology

Mehrzad Zandieh *

Mehrazad Zandieh **

ABSTRACT

In this article, a risk assessment of the Nanofluid stabilization process was made in order to optimize the process parameters using the HAZOP methodology. The results showed that the main parameters for the HAZOP risk assessment are as follows: the weight fraction of the surfactant, the temperature when the surfactant is used, the pressure and the speed of the fluid in the homogenizer, the PH solution, the time and the power of ultrasound, the temperature of the stabilization process, the volume fraction of nanoparticles, the size of the nanoparticles, the side surface to the volume of Nano particles, zeta potentials, Nanofluid concentrations. The results of the risk number calculations before control actions showed that after control actions, all risk numbers decreased 50% and more, so this decrease was significant. This decrease showed that all control actions were appropriate and effective.

KEYWORDS: Nanofluids; Risks evaluation; Process; Stabilization; HAZOP.

Evaluación del riesgo en el proceso de estabilización de Nanofluidos y optimización de parámetros del proceso por la metodología HAZOP

RESUMEN

En este artículo se hizo una evaluación del riesgo del proceso de estabilización de Nanofluidos a fin de optimizar los parámetros del proceso mediante la metodología HAZOP. Los resultados mostraron que los principales parámetros para la evaluación de riesgos HAZOP son los siguientes: la fracción en peso del surfactante, la temperatura cuando se usa el surfactante, la presión y la velocidad del fluido en el homogeneizador, la solución de PH, el tiempo y la potencia de ultrasonidos, la temperatura del proceso de estabilización, la fracción de volumen de nanopartículas, el tamaño de las nanopartículas, la superficie lateral al volumen de Nano partículas, potenciales zeta, concentraciones de Nanofluidos. Los resultados de los cálculos de números de riesgo antes de las acciones de control mostraron que después de las acciones de control, todos los números de riesgo disminuyeron 50% y más, por lo que esta disminución fue significativa. Esta disminución mostró que todas las acciones de control fueron apropiadas y efectivas.

PALABRAS CLAVE: Nanofluidos; Evaluación de riesgos; Proceso; Estabilización; HAZOP.

*Department of Chemical Engineering, Faculty of Engineering, Razi University, Kermanshah, Iran. Mehrzad.zandieh@yahoo.com, https://orcid.org/0000-0002-7566-5053

**Depatment of Biology, Faculty of science, Islamic Azad University, Qom, Iran. https://orcid.org/0000-0001-6866-7942

Recibido: 11/03/2020 Aceptado: 14/05/2020

Introduction

The suspension of solid particles in liquids is widely known to contribute to industrial liquid systems, such as heat transfer fluids, lubricant fluids, and magnetic fluids. Among these technologies, nanofluids as engineering materials consisting of nanometer-sized additives and base fluids have attracted interest because of their broad applications in heat transfer, cooling of microchips, drug delivery, and enhanced oil recovery. The method for the preparation of stable Nano fluids is a key concern for extending the application of Nano fluids (Mingwei Zhao et al., 2018). Due to the high demand for nanoparticle-based materials, two manufacturing approaches have developed over the years. The first is the top-down approach and involves reducing the size of bulk materials by physical or chemical processes. The final particle size, shape and surface structure are all dependent on the processing technique used. Furthermore, during the top-down approach surface imperfections are produced and ultimately influence the physicochemical properties of the manufactured nanoparticles. The second is the bottom-up approach and involves the assembly of individual atoms, molecules and smaller particles. Both approaches use a wide variety of physical and chemical manufacturing processes, which have evolved to produce nanoparticles with different sizes, shapes and compositions. Particle size, size distribution, shape and physicochemical properties are all influenced by process parameters. These parameters include initial reagent concentrations, temperature and reaction mixture pH. Moreover, during synthesis there are interactions taking place between precursor ions, reducing agents and the adsorption kinetics of the stabilizing agent. The competing parameters ultimately dictate the properties of the manufactured nanoparticles (Wisut Chamsa-ard, 2017).

Manoj Chopkar et al., (2006) studied Synthesis and characterization of nanofluid for advanced heat transfer applications. Nanofluid was prepared by dispersing about 0.2–2.0 vol.% nanocrystalline $Al_{70}Cu_{30}$ particles in ethylene glycol. The size/microstructure of the nanoparticles were characterized by X-ray diffraction and transmission electron microscopy, and the thermal conductivity of the nanofluid was measured using a modified thermal comparator. An improvement of up to two times in conductivity was recorded.

M. J. Kao et al., (2007) studied Copper-oxide brake nanofluid manufactured using arc-submerged nanoparticle synthesis system. This study revealed that a homemade machine can produce the CBN (copper-oxide brake nanofluid) which higher boiling point to reduce the occurrence of vapor-lock, higher viscosity and higher conductivity thus showing superior performance of copper brake nanofluid.

Tran X. Phuoc et al., (2007) studied Synthesis of Ag-deionized water nanofluids using multi-beam laser ablation in liquids. measurements of the thermal conductivity and viscosity of the produced samples showed that the thermal conductivity increased about 3–5% and the viscosity increased 3.7% above the base fluid viscosity even with the particle volume concentration as low as 0.01 %.

Ho Chang et al., (2008) studied Fabrication of Al_2O_3 nanofluid by a plasma arc nanoparticles synthesis system. The absorption properties of the Al_2O_3 nanofluid were analyzed using UV–Vis spectrophotometer. Moreover, the fuel calorific test showed that the combustion efficiency of 92 octane unleaded gas was greater when the weight concentration of the Al_2O_3 nanofluids was 3% .

S. Ananda Kumar et al., (2009) studied Synthesis and characterization of copper nanofluid by a novel one-step method. This study presented a novel one-step method for the preparation of stable, non-agglomerated copper nanofluids by reducing copper sulphate pentahydrate with sodium hypophosphite as reducing agent in ethylene glycol as base fluid by means of conventional heating. It was an in situ, one-step method which gave high yield of product with less time consumption. The characterization of the nanofluid was done by particle size analyzer, X-ray diffraction topography, UV–vis analysis and Fourier transform infrared spectroscopy (FT-IR) followed by the study of thermal conductivity of nanofluid by the transient hot wire method.

Xiaohao Wei et al., (2009) studied Synthesis and thermal conductivity of Cu_2O nanofluids. Suspensions of cuprous-oxide (Cu_2O) nanoparticles in water, and experimentally studied the effect of reactant molar concentration and nanofluid temperature on the thermal conductivity. Substantial conductivity enhancement up to 24% was achievable with the synthesized nanofluids. The nanoparticle shape was variable by adjusting some synthesis

parameters. The thermal conductivity showed both sensitivity and nonlinearity to the reactant molar concentration and the nanofluid temperature.

Xiaohao Wei et al., (2010) studied the chemical solution method to synthesize CuS/Cu_2S nanofluids and experimentally measured their thermal conductivity. The measured thermal conductivity showed that the presence of nanoparticles can either upgrade or downgrade fluid conductivity, a phenomenon predicted by the recent thermal-wave theory of nanofluids.

S. Suresh et al., (2011) studied Al_2O_3–Cu hybrid particles synthesized by hydrogen reduction technique from the powder mixture of Al_2O_3 and CuO in 90:10 weight proportions obtained from a chemical route synthesis. The experimental results showed that both thermal conductivity and viscosity of the prepared hybrid nanofluids increased with the nanoparticles volume concentration. The thermal conductivity and viscosity of nanofluids had been measured and it had been found that the viscosity increase was substantially higher than the increase in thermal conductivity.

Meher Wan et al., (2012) studied an effortless and fast novel route proposed to synthesize Polyaniline nanofibers and nanofluids of Polyaniline nanofibers in DI-water were obtained with conventional two step method. The effect of particle loading (0.08%, 0.16%, and 0.24% in volume) was also observed on the thermal conductivities of synthesized nanofluids. Thermal conduction performance in nanofluids was increased appreciably due to higher crystallinity and morphological uniformity of reinforced nanofibers.

M. Nabeel Rashin et al., (2013) studied Synthesis and viscosity of novel ecofriendly ZnO–coconut oil nanofluid. Novel nanofluid of zinc oxide in coconut oil has been synthesized in various concentrations through ultrasonically assisted two step method. The experimental viscosities of nanofluids were compared with the theoretical values obtained through Einstein, Batchelor and Wang models. A small deviation was observed which may arise due to the difference in the morphology, chemical composition and interactions. New empirical relations were proposed for predicting the viscosity of coconut oil based ZnO nanofluid at various temperatures and concentrations.

Yuvaraj Haldorai et al., (2014) studied a facile and residue free synthesis of copper oxide (CuO) nanospindles by the thermal decomposition of a 3D precursor complex, copper benzoate

dihydrazinate at 100 °C. The enhancement of the thermal conductivity of ethylene glycol (EG) in the presence of CuO nanospindles was examined. No surfactant was used as a dispersant. The volume fraction of CuO nanospindles suspended in EG was less than 5 vol%. The thermal conductivity of the CuO nanofluids increased with increasing particle loading.

M. Leena & S. Srinivasan (2015) studied Synthesis and ultrasonic investigations of titanium oxide nanofluids. Titanium oxide (TiO_2) nanoparticles (NPs) were synthesized by means of sol–gel method. Crystalline nature of synthesized TiO_2 NPs was confirmed by the X-ray powder diffractometry (XRD). It was observed that ultrasonic velocity was made visible on linearity with particle concentration and the results were discussed.

Gayatri Paul et al., (2016) studied Synthesis, characterization and studies on magneto-viscous properties of magnetite dispersed water based nanofluids. The observed increase in yield stress (calculated by fitting the Herschel and Bulkley model) with the applied magnetic field and concentration of dispersed nanoparticles confirmed the formation of large aggregates that restricted or prohibited the flow characteristics of the otherwise Newtonian magnetic nanofluid. The hysteresis observed during the application and withdrawal of magnetic field suggested that the chain or column like structures fail to relax within the allowed measurement time interval.

Sadegh Aberoumand et al., (2017) studied Experimental study on synthesis, stability, thermal conductivity and viscosity of Cu–engine oil nanofluid. The viscosity range for higher weight concentration nanofluid was observed from 235 cP to 35 cP in the applied temperature range. Finally, thermal conductivity and viscosity enhancements of 49% and 37% were observed for 1% weight fraction of utilized nanofluids.

Samarshi Chakraborty et al., (2018) synthesized Cu-Al Layered Double Hydroxide nanofluid at different molar ratios of Cu and Al by using co-precipitation technique and utilized this as a coolant in a pressure atomized spray to achieve high cooling rates in the temperature range of 900–600 °C for a 6 mm thick steel plate. With respect to concentration optimization, the maximum cooling rate of 168.6 °C/s was attained at a concentration of 160 ppm which was 26% higher than what was achieved by normal water spray. Results obtained from

the spray cooling experiments were further verified by the thermal conductivity analysis where highest enhancement of 15.17% was also observed at 160 ppm nanofluid concentration.

Aravinth Raj Arivalagan et al., (2019) studied Synthesis and characterization of Ag and Al doped ZnO dispersed nanofluids for heat transfer applications. It was observed that the addition of small amount of Al and Ag doped ZnO nanoparticles to the ethylene glycol-water mixture increased the thermal conductivity of the base fluid. The 50% EG-%50 Water mixture showed highest thermal conductivity enhancement of 37% compared to other base fluids when 1% Al and Ag doped ZnO nanoparticles were dispersed.

Shankar Amalraj et al., (2019) studied Synthesis and characterization of Al_2O_3 and CuO nanoparticles into nanofluids for solar panel applications. As a result, the cooling efficiency of both CuO and Al_2O_3 were found as 18.2%, which was higher than the conventional one. The obtained efficiency value also compared with the reported data. This showed that CuO and Al_2O_3 will be a promising candidate with a base fluid of water for solar panel applications.

The HAZOP method is the most comprehensive and effective safety evaluation to identify potential hazards of chemical installations. The HAZOP starts from the design intent of the unit. And it was applied to analyze the possible deviation of process state parameters in production operation and operation control as well as the possible causes and consequences of parameter deviation during the device running. Then not only is it definite that what the main dangers and hazards of a device or system are but also measures can be taken against the consequences of change. HAZOP is a technology developed by Imperial Chemical Industries. The HAZOP is a systematic and structural analysis method, which is on the risk and operability of chemical engineering process from an expert group of experienced professionals. The advantage of the method is that it can study the whole engineering process systematically and comprehensively, thus ensuring the safe operation of the production process (Ting-Ting Gao & San-Ming Wang, (2018).

In this applicable study, for the first time, it was investigated process risk assessment of stabilization processes of nanofluids for process parameters optimization by HAZOP methodology.

1. Methodology

HAZOP

Step 1 is knowing keywords in processes.

Table 1. Meaning of deviations in processes (L. Kotek, M. Tabas, 2012).

Keyword	Logical meaning	Example
NO	Total negation of the original function	No flow
MORE	Quantitative increase	Higher flow
LESS	Quantitative decrease	Lower flow
AS WELL AS	Qualitative increase (occurrence of another case)	Penetration of a water into the reactor
PART OF	Qualitative decrease	A compound is missing
REVERSION	Opposite function (activity)	Reverse flow of a medium
OTHER THAN	Total substitution	Presence of other substances
EARLY	Premature function (activity)	-
LATE	Delayed function (activity)	-
BEFORE	Relating to order or sequence	
AFTER	Relating to order or sequence	

Step 2 is identifying probability of occurrence in processes.

Table 2. Probability of the occurrence (L. Kotek, M. Tabas, 2012).

P	Probability of the occurrence	Meaning
1	< 0.0001	Very low
2	0.001 – 0.0001	Low
3	0.01 – 0.001	Middle
4	0.1 – 0.01	High
5	> 0.1	Very high

Step 3 is identifying numerical values of severities of consequences.

Table 3. Severity of consequence (L. Kotek, M. Tabas, 2012).

S	Loss	Harms
1	< 1000 EUR	No injury
2	1000 - 10 000 EUR	Minor injuries
3	10 000 - 100 000 EUR	Serious injuries
4	100 000 - 1 000 000 EUR	1 deadly injury
5	> 1 000 000 EUR	> 1 deadly injury

Step 4 is calculating and identifying risk levels.

Table 4. Risk number and its meaning (L. Kotek, M. Tabas, 2012).

Risk	R = P x S
1 - 3	Non-significant
3 – 7	Low significant
8 - 25	Significant

2. Results and discussions

Table 5. Risk assessment of processes of stabilization of Nano fluids by HAZOP method

Risk assessment by HAZOP / Stabilization of Nano fluids							
Number	KEY WORD	DEVIATION	CAUSES	EFFECTS	Risk1=S*P	Control Actions	Risk2=S*P
1	less	Low weight fraction of the surfactant added to the Nano fluid	Trial and error until the optimum amount of surfactant is reached	The coating required to generate electrostatic repulsion and van der Waals gravity compensation	=3*3=9	Control of surfactant concentration added to Nano fluid at optimum amount	=3*1=3

				is not created and as a result the required stability in nano fluid is not achieved and the thermal conductivity of nano fluid will be low.			
2	more	High weight fraction of the surfactant added to the Nano fluid	Trial and error until the optimum amount of surfactant is reached	The ratio of thermal conductivity coefficient of the Nano fluid to the base fluid decreases	=3*3=9	Control of surfactant concentration added to Nano fluid at optimum amount	=3*1=3
3	more	Increasing temperature (greater that 60°C) when using surfactant	High heating process	The bond between the nanoparticles and the surfactant may be damaged and the Nano fluid may lose its stability	=2*2=4	Set the temperature to below 60°C	=2*1=2
4	less	Very low amount of PH	Adding too much acid to the process	The result is that the absolute value of zeta potential is low, which makes the colloidal particles less stable and results in lower thermal conductivity	=2*3=6	Setting PH to optimum amount	=2*1=2
5	more	Very high amount of PH	Adding too much base to the process	The result is that the absolute value of zeta potential is low, which makes the colloidal particles less stable and results in lower thermal conductivity	=2*3=6	Setting PH to optimum amount	=2*1=3
6	more	Too increasing fluid pressure and velocity in homogenizer	Applying homogenizer with special design	The result is cavitation (bubble production) in	-	Positive risk (An opportunity to achieve	-

				the fluid and the high energy resulting from this phenomenon breaks down the clusters and ultimately increases the stability of the Nano fluid and increases its thermal conductivity.		desirable for process goals)	
7	more	increasing the ultra-sonication time and power	Setting ultrasonic device parameters to high amounts	having more dispersed and stable Nano fluids and leads to having higher thermal conductivity	-	Positive risk (An opportunity to achieve desirable for process goals)	-
8	more	increasing the ultra-sonication time and power	Setting ultrasonic device parameters to high amounts	In some special Nano fluids, leads Low stability of Nano fluids and to having lower thermal conductivity	=2*2=4	Use of optimum amount of sonication power and time	=2*1=2
9	more	Increasing stabilization process temperature normally	Heating of medium	Increasing thermal distributive coefficient and thermal conductivity	-	Positive risk-no demand of control action	-
10	less	Decreasing stabilization process temperature	Cooling of medium	Decreasing thermal distributive coefficient and thermal conductivity	=3*3=9	Increasing temperature to an optimum amount	=3*1=3
11	more	Increasing volume fraction of Nano particles normally	-	Increasing thermal conductivity	-	Positive risk-no demand of control action	-
12	less	Deceasing volume fraction of Nano particles	-	Decreasing thermal conductivity	=3*3=9	Setting volume fraction of Nano particles to an optimum value	=3*1=3
13	less	Deceasing Nano particles sizes	-	Increasing stabilization and thermal conductivity coefficient	-	Positive risk-no demand of control action	-

14	more	Increasing Nano particles sizes	-	Decreasing stabilization and thermal conductivity coefficient	=3*3=9	Being smaller of Nano particle sizes	=3*1=3
15	less	Decreasing of side surface to volume of Nano particles	-	Decreasing heat transfer rate	=3*3=9	Use of Nano particles with high ratio of side surface to volume	=3*1=3
16	more	Increasing side surface to volume of Nano particles	-	Increasing heat transfer rate	-	Positive risk-no demand of control action	-
17	more	zeta potentials between 40 and 60 mV	-	Stable Nano fluid	-	Positive risk-no demand of control action	-
18	more	zeta potentials greater than 60 mV	-	excellent stability of Nano fluid	-	Positive risk-no demand of control action	-
19	less	low zeta potentials	-	nanoparticle clustering and sedimentation	=3*3=9	Significant increase in zeta potential	=3*1=3
20	less	Application of fillers at low concentrations in Nano fluids	-	The nanoparticles will have many Brownian motions at high temperatures resulting in an increase in the effective conductivity.	-	Positive risk-no demand of control action	-
21	more	Application of fillers at high concentrations in Nano fluids	-	Nanoparticles tend to accumulate at high temperatures.	=3*3=9	Use of fillers at low concentrations	=3*1=3

It was identified 21 deviations in process parameters. Nine of these process parameters deviations caused to positive risks. These types of risks hadn't needed any preventive control actions. Because the consequences of these risk was high stability and high thermal conductivity of Nano fluids. But for 12 remain risks, these types of risks needed to control and corrective actions. Figure 1 shows the risk numbers before control actions. Figure 2 shows risk numbers after applying control actions. Also Figure 3 shows percent of risk number decrease (%).

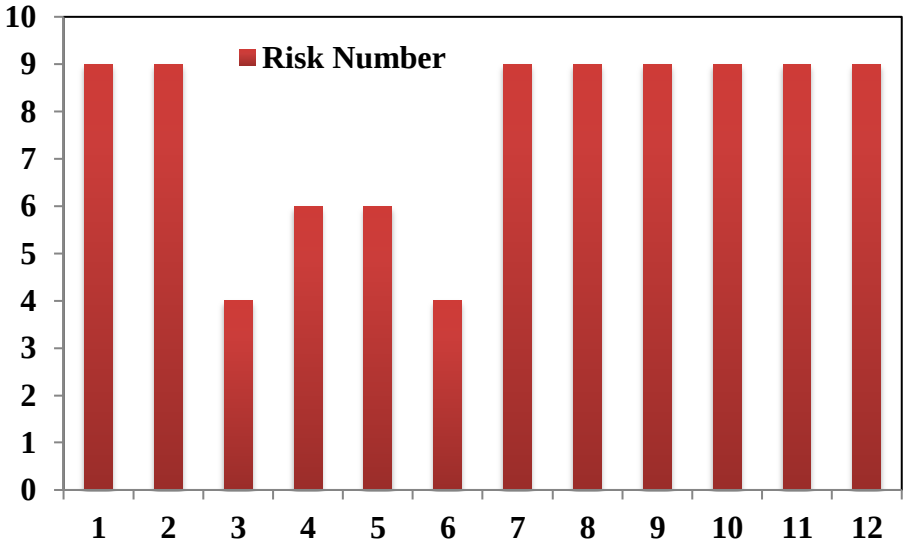

Figure 1: Risk numbers before control actions

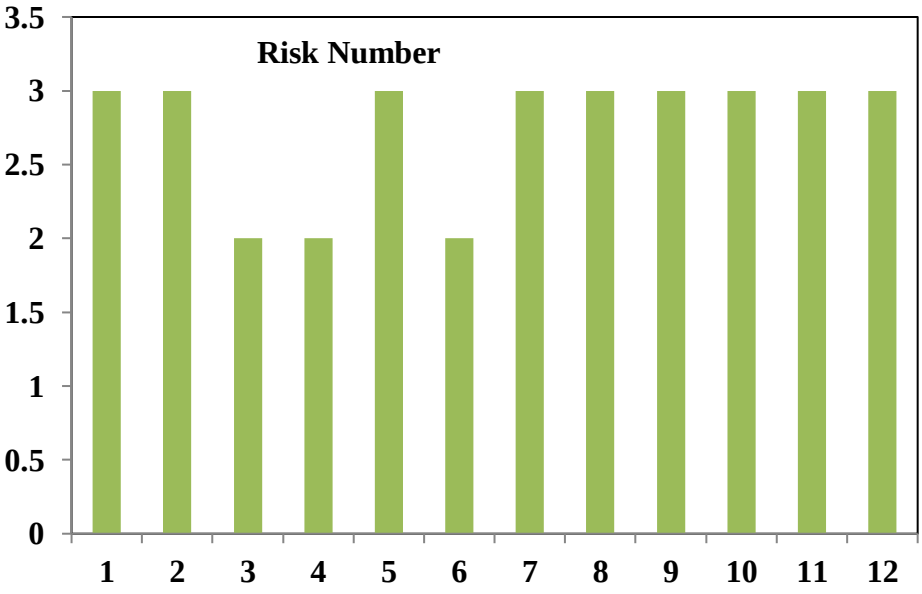

Figure 2: Risk numbers after control actions

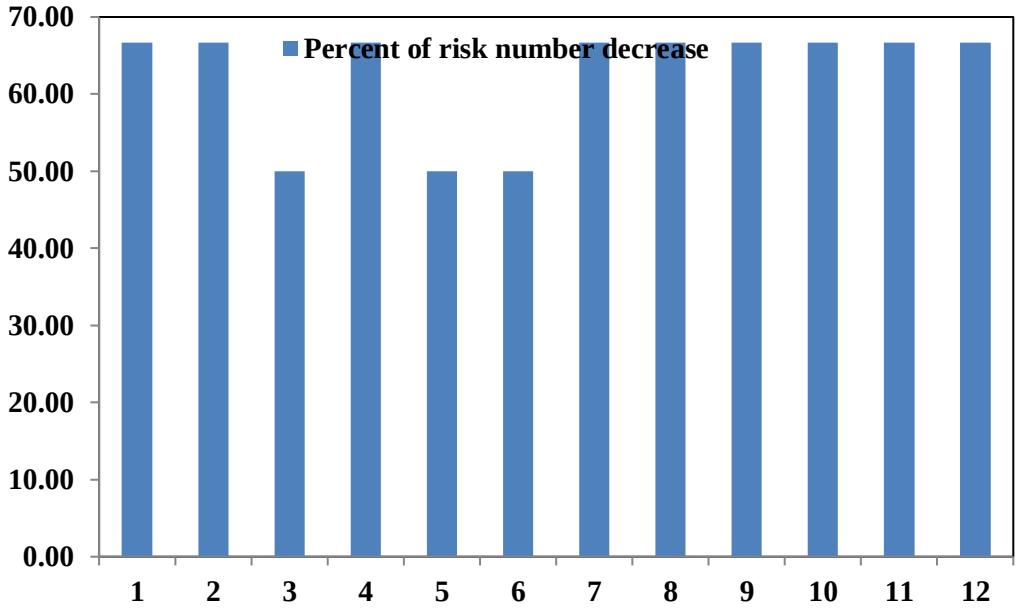

Figure 3: Percent of risk number decrease (%)

According to fig 1, eight number of risks was significant and four of them was low significant. After applying control actions, risk numbers decreased (fig 2). After decreasing risk numbers, level of them was non-significant (fig 2). Fig 3 shows the percent of decrease of risk numbers. This fig shows that decrease of risk numbers was completely significant. This means that suggested process control and preventive actions was effective for risk assessment of Nano fluids stabilization processes.

Conclusions

This investigation showed that chemical engineering scientific concepts are a powerful tool for risk assessment by HAZOP method. It was showed that a good process design can be effective and important as a basis in control actions in HAZOP method. This excellent process design is related to appropriate adjust of process parameters such as temperature, PH and also application of nanoparticles with desired observed features.

References

Aberoumand, Sadegh, Jafari Moghaddam, Amin, (2017). Experimental study on synthesis, stability, thermal conductivity and viscosity of Cu–engine oil nanofluid, *Journal of the Taiwan Institute of Chemical Engineers*, Volume 71, February 2017, Pages 315-322.

Amalraj, Shankar, Michael, Prawin Angel (2019). Synthesis and characterization of Al_2O_3 and CuO nanoparticles into nanofluids for solar panel applications, *Results in Physics*, Volume 15, December 2019, 102797.

Ananda Kumar, S., ShreeMeenakshi, K., Narashimhan, B. R. V., Srikanth, S., Arthanareeswaran, G., (2009). Synthesis and characterization of copper nanofluid by a novel one-step method, *Materials Chemistry and Physics*, Volume 113, Issue 1, 15 January 2009, Pages 57-62.

Ard, Wisut Chamsa, Brundavanam, Sridevi, Fung, Chun Che, Fawcett, Derek and Poinern, Gerrard (2017). Nanofluid Types, Their Synthesis, Properties and Incorporation in Direct Solar Thermal Collectors: A Review, *Nanomaterials 2017*, 7, 131; doi:10.3390/nano7060131.

Arivalagan, Aravinth Raj, Karthik, Vaduganathan, Ramji, R., Venkatakrishnan, P. G. (2019). Synthesis and characterization of Ag and Al doped ZnO dispersed nanofluids for heat transfer applications, material study, 2019.

Chakraborty, Samarshi, Sarkar, Ishita, Ashok, Avinash, Sengupta, Iman, Pal, Surjya K., Chakraborty, Sudipto, (2018). Synthesis of Cu-Al LDH nanofluid and its application in spray cooling heat transfer of a hot steel plate, *Powder Technology*, Volume 335, 15 July 2018, Pages 285-300.

Chang, Ho; Chang, Yu-Chun (2008). Fabrication of Al_2O_3 nanofluid by a plasma arc nanoparticles synthesis system, *Journal of Materials Processing Technology*, Volume 207, Issues 1–3, 16 October 2008, Pages 193-199.

Chopkar, Manoj, Das, Prasanta K., Manna, Indranil (2006). Synthesis and characterization of nanofluid for advanced heat transfer applications, *Scripta Materialia*, Volume 55, Issue 6, September 2006, Pages 549-552.

Gao, Ting-Ting, Wang, San-Ming (2018). Fuzzy integrated Evaluation Based on HAZOP, *Procedia Engineering*, 211 (2018) 176–182.

Haldorai, Yuvaraj, JinShim, Jae (2014). Facile synthesis of CuO nanospindles from a 3D coordination complex and its application to nanofluids, *Letters*, Volume, 1 February 2014, Pages 5-8.

Kao, M. J.; Lo, C. H.; Tsung, T. T.; Wu, Y. Y.; Jwo, C. S.; Lin, H. M. (2007). Copper-oxide brake nanofluid manufactured using arc-submerged nanoparticle synthesis system, *Journal of Alloys and Compounds*, Volumes 434–435, 31 May 2007, Pages 672-674.

Kotek, L.; Tabas, M. (2012). HAZOP study with qualitative risk analysis for prioritization of corrective and preventive actions, *Procedia Engineering* 42 (2012) 808 – 815.

Leena, M.; Srinivasan, S. (2015). Synthesis and ultrasonic investigations of titanium oxide nanofluids, *Journal of Molecular Liquids*, Volume 206, June 2015, Pages 103-109.

Nabeel Rashin, M.; Hemalatha, J. (2013). Synthesis and viscosity studies of novel ecofriendly ZnO–coconut oil nanofluid, *Experimental Thermal and Fluid Science*, Volume 51, November 2013, Pages 312-318.

Paul, Gayatri; Kumar Das, Prasanta; Manna, Indranil (2016). Synthesis, characterization and studies on magneto-viscous properties of magnetite dispersed water based nanofluids, *Journal of Magnetism and Magnetic Materials*, 48 (11), 29-39 http://dx.doi.org/10.1016/j.jmmm.2015.11.085

Phuoc, Than X.; Soong, Yee; Chyu, Minking K. (2007). Synthesis of Ag-deionized water nanofluids using multi-beam laser ablation in liquids, *Optics and Lasers in Engineering*, Volume 45, Issue 12, December 2007, Pages 1099-1106.

Suresh, S.; Venkitaraj, K. P.; Selvakumar, P.; Chandrasekar, M. (2011). Synthesis of Al_2O_3–Cu/water hybrid nanofluids using two step method and its thermo physical properties, *Colloids and Surfaces A: Physicochemical and Engineering Aspects*, Volume 388, Issues 1–3, 5 September 2011, Pages 41-48.

Wan, Meher; Yadav, R. R.; Yadav, K. L.; Yadaw, S. B. (2012). Synthesis and experimental investigation on thermal conductivity of nanofluids containing functionalized Polyaniline nanofibers, *Experimental Thermal and Fluid Science*, Volume 41, September 2012, Pages 158-164.

Wei, Xiaohao; Kong, Tiantian; Zhu, Haitao; Wang, Liqiu (2010). CuS/Cu_2S nanofluids: Synthesis and thermal conductivity, *International Journal of Heat and Mass Transfer*, Volume 53, Issues 9–10, April 2010, Pages 1841-1843.

Wei, Xiaohao; Zhu, Haitao; Kong, Tiantian; Wang, Liqiu (2009). Synthesis and thermal conductivity of Cu_2O nanofluids, *International Journal of Heat and Mass Transfer*, Volume 52, Issues 19–20, September 2009, Pages 4371-4374.

Zhao, Mingwei; Lv, Wenjiao; Li, Yuyang; Dai, Caili; Zhou, Hongda; Song, Xuguang and Wu, Yining (2018). A Study on Preparation and Stabilizing Mechanism of Hydrophobic Silica Nanofluids, *Materials 2018*, 11, 1385; doi:10.3390/ma11081385.

Soluciones numéricas para diferentes casos del modelo biológico no lineal de presa- depredador

Gilder Cieza Altamirano *
Manuel Jesús Sánchez-Chero **
Rafaél Artidoro Sandoval-Núñez ***
José Antonio Sánchez-Chero ****
María Verónica Seminario Morales*****

RESUMEN

La presente investigación se elaboró con el objetivo realizar una comparación de la solución numérica del modelo biológico no lineal de presa depredador, utilizando el método numérico Adams predicción-corrección junto con los métodos explícitos de Runge-Kutta. Los resultados numéricos para los métodos en mención comparan todos los casos de modelo de presa-depredador, encontrándose que los resultados se superponen entre si hasta un nivel de precisión de 7 a 8, cuando el intervalo se toma de [1,30] con el tamaño de paso de 1.

PALABRAS CLAVE: Modelo biológico; presa – depredador; no lineal; Runge – Kutta, método de Adams.

* Licenciado en Matemáticas. Universidad Nacional Autónoma de Chota. Perú. https://orcid.org/0000-0002-7936-1495

** Docente Investigador. Universidad Señor de Sipán S.A.C., Perú. https://orcid.org/0000-0003-1646-3037 E-mail: manuelsanchezchero@gmail.com

*** Licenciado en Estadística, Universidad Nacional Autónoma de Chota. Perú https://orcid.org/0000-0003-3930-2332

**** Docente posgrado. Universidad César Vallejo. Perú. https://orcid.org/0000-0002-3157-8935

***** Docente Auxiliar. Universidad Nacional de Frontera. Perú. https://orcid.org/0000-0002-6787-7371

Recibido: 8/04/2020 Aceptado: 4/06/2020

Numerical solutions for different cases of the non-linear biological model of prey-predator

ABSTRACT

The present investigation was carried out with the objective of making a comparison of the numerical solution of the non-linear biological model of predator prey, using the Adams prediction-correction numerical method together with the explicit Runge-Kutta methods. The numerical results for the mentioned methods compare all the predator-prey model cases, finding that the results overlap each other up to a precision level of 7 to 8, when the interval is taken from [1.30] with the step size of 1.

KEY WORDS: Biological model; prey - predator; nonlinear; Runge - Kutta, Adams method

Introducción

En los últimos años la comunidad investigadora está interesada en resolver los modelos biológicos. Los modelos biológicos se basan en las ecuaciones diferenciales lineales o no lineales. La mayoría de los modelos biológicos presentan el sistema de ecuaciones no lineales. El modelo presa- depredador es uno de ellos que muestra el sistema de ecuaciones no lineales. Este modelo tiene gran historia y ha sido presentado en el trabajo básico de Lotka y Volterra (Effati et al., 2015).

Este modelo se ha inventado para considerar el ejemplo de conejos y zorros: los zorros comen los conejos y los conejos comen el trébol. El número de conejos aumenta cuando el número de zorros disminuye y si el número de zorros aumenta, entonces comen conejos y, debido a esto, los conejos definitivamente disminuirán (Biazar, Montazeri, 2005).

El aumento o disminución de la población es el modelo de presa- depredador que representa el sistema de ecuaciones diferenciales no lineales dadas como (Solis, 2008):

$$\begin{cases} L'(x) = L(x)(a - bM(x)), \\ M'(x) = -M(x)(c - dL(x)), \\ L(0) = a_1, M \qquad (0) = a_2. \end{cases} \tag{1}$$

Donde *a*, *b*, *c y d* representan los valores de las constantes a_1 y a_2 son las condiciones iniciales y $L(x)$ y $M(x)$ son la cantidad de presas y depredadores en el tiempo *x*

Lotka y Volterra presentaron este modelo y (Holling, 1966) presentó tres porciones de las reacciones funcionales para la predicción de depredación para el modelo de presa – depredador.

En el campo biológico, la comunidad de investigación está interesada en resolver el sistema de ecuaciones diferenciales no lineales. Debido a la no linealidad, el sistema de ecuaciones de este modelo a menudo obtuvo las posiciones rígidas y poco realistas, lo que no es fácil de resolver. Existen pocos métodos disponibles en la literatura para resolver modelos de presa - depredador (Jing and Yang, 2006), (Elsadany, et al., 2012), (Danca et al., 1997), (Liu, and Xiao, 2007) y (Summers, et al., 2000), resolvió el modelo de presa- depredador utilizando sus propias técnicas y formas.

Algunos métodos bien conocidos que se han utilizado para resolver el modelo de presa – depredador son el método de Runge – Kutta – Fehlberg, transformación diferencial (Batiha, 2014), método de descomposición de Laplace Adomian (Paul, Mondal and Bhattacharya, 2016.), técnicas de elementos finitos (Garvie et al., 2015), método de análisis de homotopía (Yu and Yu, 2014), método de descomposición Sumudu (Bildik and Deniz, 2016), método de transformación diferencial fraccional (Ray, 2015), y método de dominio de confianza (Bashkirtseva and Ryashko, 2014) .

Todos los métodos anteriores tienen su propio impacto y significado. Sin embargo, el presente estudio está relacionado con la resolución del modelo de presa- depredador en el gran dominio del intervalo para los diferentes casos del modelo de presa- depredador utilizando las técnicas implícitas Adams y Runge-Kutta.

1. Métodos Numéricos

Para resolver el modelo biológico no lineal de presa- depredador, se ha utilizado el método numérico Adams predicción-corrección, junto con los métodos explícitos de Runge-Kutta.

1.1. Esquema de Adams numérico predicción - corrección

La formulación del método numérico predicción-corrección se aplica y se diseña en dos fases:

Fase 1: Los resultados aproximados de la predicción son competentes

Fase 2: Para calcular los medidores numéricos de corrección

$$\begin{cases} \frac{dL}{dx} = L(a - bM), & L(0) = a_1 \\ \frac{dM}{dx} = -M(c - dL), & M(0) = a_2 \end{cases}. \tag{2}$$

Para el método generalizado de Adams-Bashforth usando el método numérico predicción-corrección es:

$$\begin{cases} D_{n+1} = L_n + \frac{3}{2}Lh(x_n, L_n) - \frac{1}{2}Lh(x_{n-1}, L_{n-1}) \\ D_{n+1} = M_n + \frac{3}{2}Mh(x_n, M_n) - \frac{1}{2}Mh(x_{n-1}, M_{n-1}) \end{cases}. \tag{3}$$

La corrección de Adams-Moulton de dos pasos es:

$$\begin{cases} L_{n+1} = L_n + \frac{1}{2}[fh(x_{n+1}, D_{n+1}) + h(x_n, L_n)] \\ M_{n+1} = M_n + \frac{1}{2}[gh(x_{n+1}, D_{n+1}) + h(x_n, M_n)] \end{cases} \tag{4}$$

El método numérico predicción-corrección de 4 pasos es:

$$\begin{cases} D_{n+1} = L_n + \frac{f}{24}\left(55h(x_n, L_n) - 59f(x_{n-1}, L_{n-1}) + 37f(x_{n-2}, L_{n-2}) - 9f(x_{n-3}, L_{n-3})\right) \\ D_{n+1} = M_n + \frac{g}{24}\left(55h(x_n, M_n) - 59g(x_{n-1}, M_{n-1}) + 37g(x_{n-2}, M_{n-2}) - 9g(x_{n-3}, M_{n-3})\right). \end{cases} \tag{5}$$

El método de Adams-Bashforth Moulton se da como:

$$\begin{cases} L_{n+1} = L_n + \frac{f}{24}\left(9h(x_{n+1}, D_{n+1}) + 19f(x_n, L_n) - 5f(x_{n-1}, L_{n-1}) + f(x_{n-2}, L_{n-2})\right) \\ M_{n+1} = L_n + \frac{g}{24}\left(9h(x_{n+1}, D_{n+1}) + 19g(x_n, M_n) - 5g(x_{n-1}, M_{n-1}) + g(x_{n-2}, M_{n-2})\right) \end{cases} \quad (6)$$

1.2. Método explícito de Runge – Kutta

Para resolver el modelo presa – depredador biológico no lineal, se da el método explícito de Runge – Kutta y su forma General se presenta como:

$$\begin{cases} L_{n+1} = L_n + f\sum_{j=1}^{s} b_j k_j, k_{21} = h(x_n, L_n), \\ M_{n+1} = M_n + g\sum_{j=1}^{s} b_j k_j, k_{12} = h(x_n, M_n), \end{cases}$$

$$\begin{cases} k_{21} = h\left(x_n + c_2 f, L_n + f(a_{21}k_{11})\right) \\ k_{22} = h\left(x_n + c_2 g, M_n + g(a_{22}k_{21})\right) \end{cases}, \quad (7)$$

$$\begin{cases} k_{31} = h\left(x_n + c_3 f, L_n + f(a_{31}k_{11} + a_{32}k_{21})\right) \\ k_{32} = h\left(x_n + c_3 g, M_n + g(a_{31}k_{11} + a_{32}k_{21})\right) \end{cases} \ldots.$$

$$\begin{cases} k_{s1} = h\left(x_n + c_s f, L_n + f(a_{s1}k_{11} + a_{s2}k_{21} + \ldots + a_{ss-1}k_{s1-1})\right) \\ k_{s2} = h\left(x_n + c_s g, M_n + g(a_{s2}k_{21} + a_{s2}k_{22} + \ldots + a_{ss-1}k_{s2-1})\right) \end{cases}.$$

2. Simulaciones y Resultados

En esta sección se ha tomado una serie de casos utilizando diferentes valores constantes y las condiciones de contorno.

Caso I: Considerar $a = 0.1, b = 0.014, c = 0.012$ y $d = 0.08$, mientras $L(0) = 1$, $M(0) = 3$.

El sistema (1) se convierte en:

$$\begin{cases} L'(x) = L(x)(0.1 - 0.014M(x)), \\ M'(x) = -M(x)(0.012 - 0.08L(x)), \\ L(0) = 1, M \quad (0) = 3. \end{cases} \tag{14}$$

Caso II: Considerar $a = 0.5, b = 0.014, c = 0.012$ y $d = 0.08$, mientras $L(0) = 2$, $M(0) = 4$. El sistema (1) se convierte en:

$$\begin{cases} L'(x) = L(x)(0.5 - 0.014M(x)), \\ M'(x) = -M(x)(0.012 - 0.08L(x)), \\ L(0) = 2, M \quad (0) = 3. \end{cases} \tag{15}$$

Caso III: Considerar $a = 0.01, b = 0.014, c = 0.012$ y $d = 0.08$, mientras $L(0) = 3$, $M(0) = 5$. El sistema (1) se convierte en:

$$\begin{cases} L'(x) = L(x)(0.01 - 0.014M(x)), \\ M'(x) = -M(x)(0.012 - 0.08L(x)), \\ L(0) = 3, M \quad (0) = 5. \end{cases} \tag{16}$$

Caso IV: Considerar $a = 0.05, b = 0.014, c = 0.012$ y $d = 0.08$, mientras $L(0) = 4$, $M(0) = 6$.

El sistema (1) se convierte en:

$$\begin{cases} L'(x) = L(x)(0.05 - 0.014M(x)), \\ M'(x) = -M(x)(0.012 - 0.08L(x)), \\ L(0) = 4, M \quad (0) = 6. \end{cases} \tag{17}$$

Caso V: Considerar $a = 0.001, b = 0.014, c = 0.012$ y $d = 0.08$, mientras $L(0) = 5$, $M(0) = 7$.

El sistema (1) se convierte en:

$$\begin{cases} L'(x) = L(x)(2 - 0.014M(x)), \\ M'(x) = -M(x)(0.012 - 0.08L(x)), \\ L(0) = 5, M \quad (0) = 7. \end{cases} \tag{18}$$

Los resultados numéricos de todos los casos anteriores para L(x) y M(x) se dan en la tabla 1 al 5 para todos los casos de modelo de presa- depredador. Está claro que los resultados de los métodos Adams y Runge -Kutta se superponen entre si hasta un nivel de precisión de 7 a 8. El intervalo se toma como [1,30] con el tamaño de paso de 1 y las tablas se proporcionan como:

Tabla 1. Resultados de Adams y Runge – Kutta (RK), para el **caso I**

	$L(x)$		$M(x)$	
x	Adams	RK	Adams	RK
0	1.0000000	1.0000000	3.0000000	3.0000000
1	1.0581317	1.0581319	3.2185678	3.2185678
2	1.1159777	1.1159787	3.4691345	3.4691345
3	1.1725699	1.1725720	3.7563915	3.7563915
4	1.2267353	1.2267356	4.0855339	4.0855339
5	1.2770865	1.2770934	4.4621740	4.4621740
6	1.3220273	1.3220276	4.8922011	4.8922011
7	1.3597800	1.3597803	5.3815945	5.3815945
8	1.3884413	1.3884405	5.9356303	5.9356303
9	1.4060763	1.4060612	6.5590358	6.5590358
10	1.4108545	1.4108156	7.2545903	7.2545903
11	1.4012225	1.4012227	8.0219161	8.0219161
12	1.3761081	1.3760140	8.8589990	8.8589990
13	1.3351186	1.3350673	9.7567418	9.7567418
14	1.2787051	1.2786751	10.7037365	10.7037365
15	1.2082426	1.2081359	11.6835062	11.6835062
16	1.1259920	1.1259750	12.6744831	12.6744831
17	1.0349313	1.0349445	13.6542283	13.6542283
18	0.9384731	0.9385120	14.5994890	14.5994890

19	0.8401231	0.8401298	15.4896268	15.4896268
20	0.7431429	0.7432049	16.3048052	16.3048052
21	0.6502836	0.6503806	17.0329256	17.0329256
22	0.5636257	0.5636264	17.6670169	17.6670169
23	0.4845343	0.4846117	18.2023002	18.2023002
24	0.4137085	0.4137905	18.6420765	18.6420765
25	0.3512933	0.3512938	18.9914804	18.9914804
26	0.2970172	0.2970289	19.2568940	19.2568940
27	0.2503293	0.2503344	19.4474418	19.4474418
28	0.2105175	0.2105165	19.5721531	19.5721531
29	0.1768007	0.1767976	19.6399272	19.6399272
30	0.1483952	0.148395	19.6590185	19.6590185

Tabla 2. Resultados de Adams y Runge – Kutta (RK), para el **caso II**

	$L(x)$		$M(x)$	
x	**Adams**	**RK**	**Adams**	**RK**
0	2	2.0000000	4.0000000	4.0000000
1	3.101711	3.1017110	4.8324040	4.8324040
2	4.730434	4.7304335	6.5055707	6.5055707
3	6.962721	6.9627209	10.2229231	10.2229231
4	9.419416	9.4194161	19.4912043	19.4912043
5	10.2565	10.2564999	43.2289134	43.2289134
6	6.892167	6.8921671	87.1550423	87.1550423
7	2.521441	2.5214411	123.8051592	123.8051592
8	0.656411	0.6564110	136.8996036	136.8996036
9	0.155804	0.1558039	139.0959053	139.0959053
10	0.036782	0.0367825	138.3454748	138.3454748
11	0.008828	0.0088278	136.9092803	136.9092803
12	0.002165	0.0021645	135.3274036	135.3274036
13	0.000543	0.0005427	133.7256981	133.7256981
14	0.000139	0.0001392	132.1337083	132.1337083
15	0	0	130.5583790	130.5583790
16	0	0	129.0012501	129.0012501
17	0	0	127.4625420	127.4625420
18	0	0	125.9421474	125.9421474

19	0	0	124.4398775	124.4398775
20	0	0	122.9555241	122.9555241
21	0	0	121.4888757	121.4888757
22	0	0	120.0397216	120.0397216
23	0	0	118.6078534	118.6078534
24	0	0	117.1930649	117.1930649
25	0	0	115.7951524	115.7951524
26	0	0	114.4139146	114.4139146
27	0	0	113.0491527	113.0491527
28	0	0	111.7006699	111.7006699
29	0	0	110.3682722	110.3682722
30	0	0	109.0517680	109.0517680

Tabla 3: Resultados de Adams y Runge – Kutta (RK), para el **caso III**

	$L(x)$		$M(x)$	
x	**Adams**	**RK**	**Adams**	**RK**
0	3.0000000	3.0000000	5.0000000	5.0000000
1	2.8016233	2.8016233	6.2323044	6.2323044
2	2.5684641	2.5684641	7.6351788	7.6351788
3	2.3066467	2.3066467	9.1699569	9.1699569
4	2.0263048	2.0263048	10.7761278	10.7761278
5	1.7403375	1.7403375	12.3788660	12.3788660
6	1.4622571	1.4622571	13.9015337	13.9015337
7	1.2038410	1.2038410	15.2789995	15.2789995
8	0.9734164	0.9734164	16.4670913	16.4670913
9	0.7752420	0.7752420	17.4456316	17.4456316
10	0.6099094	0.6099094	18.2156418	18.2156418
11	0.4753429	0.4753429	18.7932270	18.7932270
12	0.3679266	0.3679266	19.2028774	19.2028774
13	0.2834431	0.2834431	19.4719757	19.4719757
14	0.2177178	0.2177178	19.6270922	19.6270922
15	0.1669797	0.1669797	19.6919583	19.6919583
16	0.1280154	0.1280154	19.6866577	19.6866577
17	0.0981893	0.0981893	19.6275852	19.6275852
18	0.0753970	0.0753970	19.5277901	19.5277901

19	0.0579894	0.0579894	19.3974731	19.3974731
20	0.0446898	0.0446898	19.2445163	19.2445163
21	0.0345183	0.0345183	19.0749581	19.0749581
22	0.0267277	0.0267277	18.8933957	18.8933957
23	0.0207493	0.0207493	18.7033196	18.7033196
24	0.0161519	0.0161519	18.5073705	18.5073705
25	0.0126079	0.0126079	18.3075464	18.3075464
26	0.0098694	0.0098694	18.1053550	18.1053550
27	0.0077476	0.0077476	17.9019359	17.9019359
28	0.0060993	0.0060993	17.6981475	17.6981475
29	0.0048155	0.0048155	17.4946380	17.4946380
30	0.0038127	0.0038127	17.2918954	17.2918954

Tabla 4. Resultados de Adams y Runge – Kutta (RK), para el **caso IV**

	$L(x)$		$M(x)$	
x	**Adams**	**RK**	**Adams**	**RK**
0	4.00000000	4.00000000	6.0000000	6.0000000
1	3.81198397	3.81198397	8.1087833	8.1087833
2	3.51400730	3.51400730	10.7481045	10.7481045
3	3.11122950	3.11122950	13.8512137	13.8512137
4	2.63171499	2.63171499	17.2267134	17.2267134
5	2.12280774	2.12280774	20.5869776	20.5869776
6	1.63668344	1.63668344	23.6350266	23.6350266
7	1.21339534	1.21339534	26.1597945	26.1597945
8	0.87200038	0.87200038	28.0804714	28.0804714
9	0.61253717	0.61253717	29.4277647	29.4277647
10	0.42371329	0.42371329	30.2945296	30.2945296
11	0.29035098	0.29035098	30.7906417	30.7906417
12	0.19798224	0.19798224	31.0163349	31.0163349
13	0.13476290	0.13476290	31.0519811	31.0519811
14	0.09177379	0.09177379	30.9574371	30.9574371
15	0.06262179	0.06262179	30.7753399	30.7753399
16	0.04285770	0.04285770	30.5352539	30.5352539
17	0.02943851	0.02943851	30.2573543	30.2573543
18	0.02030347	0.02030347	29.9552827	29.9552827

19	0.01406406	0.01406406	29.6382174	29.6382174
20	0.00978610	0.00978610	29.3123222	29.3123222
21	0.00684078	0.00684078	28.9817345	28.9817345
22	0.00480417	0.00480417	28.6492315	28.6492315
23	0.00338964	0.00338964	28.3166781	28.3166781
24	0.00240274	0.00240274	27.9853262	27.9853262
25	0.00171107	0.00171107	27.6560148	27.6560148
26	0.00122413	0.00122413	27.3293035	27.3293035
27	0.00087975	0.00087975	27.0055631	27.0055631
28	0.00063512	0.00063512	26.6850351	26.6850351
29	0.00046056	0.00046056	26.3678737	26.3678737
30	0.00033546	0.00033546	26.0541725	26.0541725

Tabla 5. Resultados de Adams y Runge – Kutta (RK), para el **caso V**

	$L(x)$		$M(x)$	
x	**Adams**	**RK**	**Adams**	**RK**
0	5	5	7.0000000	7.0000000
1	4.484123	4.484123	10.1176534	10.1176534
2	3.829592	3.829592	13.9521218	13.9521218
3	3.089425	3.089425	18.1868893	18.1868893
4	2.348923	2.348923	22.3300427	22.3300427
5	1.69112	1.69112	25.9136011	25.9136011
6	1.164451	1.164451	28.6756463	28.6756463
7	0.77603	0.77603	30.5935994	30.5935994
8	0.506095	0.506095	31.7972495	31.7972495
9	0.325827	0.325827	32.4647404	32.4647404
10	0.208397	0.208397	32.7591415	32.7591415
11	0.132988	0.132988	32.8060564	32.8060564
12	0.084912	0.084912	32.6937756	32.6937756
13	0.054342	0.054342	32.4812453	32.4812453
14	0.034898	0.034898	32.2066871	32.2066871
15	0.022504	0.022504	31.8944885	31.8944885
16	0.014578	0.014578	31.5600799	31.5600799
17	0.009488	0.009488	31.2131900	31.2131900
18	0.006206	0.006206	30.8599437	30.8599437

19	0.00408	0.00408	30.5041992	30.5041992
20	0.002695	0.002695	30.1483867	30.1483867
21	0.001789	0.001789	29.7940363	29.7940363
22	0.001194	0.001194	29.4421089	29.4421089
23	0.0008	0.0008	29.0932044	29.0932044
24	0.000539	0.000539	28.7476925	28.7476925
25	0.000365	0.000365	28.4057962	28.4057962
26	0.000248	0.000248	28.0676438	28.0676438
27	0.00017	0.00017	27.7333031	27.7333031
28	0.000117	0.000117	27.4028023	27.4028023
29	8.04E-05	8.04E-05	27.0761446	27.0761446
30	5.57E-05	5.57E-05	26.7533166	26.7533166

Conclusiones

La solución del modelo presa- depredador, que es un modelo biológico no lineal, se resuelve con éxito. Se han tomado cinco casos diferentes y se proporcionan sus resultados numéricos para resolver el modelo biológico histórico utilizando el método de Runge – Kutta y Adams. La superposición de los resultados numéricos hasta un mayor nivel de precisión se ha notado para resolver este famoso modelo biológico. Los resultados del modelo se tabulan para ambos parámetros.

Referencias

Ash, J. H. (1965). An Adams Runge-Kutta subroutine for systems of ordinary differential equations. Toronto. University of Toronto.

Batiha, B. (2014). The solution of the prey and predator problem by differential transformation method. International Journal of Basic and Applied Sciences, 4(1), pp.36-43.

Bashkirtseva, I. and Ryashko, L. (2014). Analysis of the noise-induced regimes in Ricker population model with Allee effect via confidence domains technique. BioMed research international, 2014.

Biazar, J. and Montazeri, R. (2005). A computational method for solution of the prey and predator problem. Applied Mathematics and Computation, 163(2), pp.841-847.

Bildik, N. and Deniz, S. (2016). The Use of Sumudu Decomposition Method for Solving Predator-Prey Systems. Mathematical Sciences Letters, 5(3), pp.285-289.

Danca, M., Codreanu, S., Bako, B. (1997). Detailed analysis of a nonlinear prey-predator model, J. Biol. Phys. 23 (1997) 11–20.

Effati, S., Mansoori, A. and Eshaghnezhad, M. (2015). An efficient projection neural network for solving bilinear programming problems. Neurocomputing, 168, pp.1188-1197

Elsadany, A. E. A., El-Metwally, H. A., Elabbasy, E. M. and Agiza, H. N. (2012). Chaos and bifurcation of a nonlinear discrete prey-predator system. Computational Ecology and Software, 2(3), p.169.

Garvie, M.R., Burkardt, J. and Morgan, J. (2015). Simple Finite Element Methods for Approximating Predator–Prey Dynamics in Two Dimensions Using Matlab. Bulletin of mathematical biology, 77(3), pp.548-578.

Holling, C. S. (1966). The functional response of invertebrate predators to prey density. Memoirs of the Entomological Society of Canada, 98(S48), pp.5-86.

Jing, Z. and Yang, J. (2006). Bifurcation and chaos in discrete-time predator–prey system. Chaos, Solitons & Fractals, 27(1), pp.259-277.

Liu, X. and Xiao, D. (2007). Complex dynamic behaviors of a discrete-time predator–prey system. Chaos, Solitons & Fractals, 32(1), pp.80-94.

Moulton, Forest R. (1926). New methods in exterior ballistics, University of Chicago Press.

Paul, S., Mondal, S.P. and Bhattacharya, P. (2016). Numerical solution of Lotka Volterra prey predator model by using Runge–Kutta–Fehlberg method and Laplace Adomian decomposition method. Alexandria Engineering Journal, 55(1), pp.613-617.

Ray, S.S. (2015). A New Coupled Fractional Reduced Differential Transform Method for the Numerical Solution of Fractional Predator-Prey System. CMES: Computer Modeling in Engineering & Sciences, 105(3), pp.231-249.

Solis, F. J. (2008). Self-limitation in a discrete predator–prey model. Mathematical and Computer Modelling, 48(1), pp.191-196

Summers, D., Cranford, J. G. and Healey, B.P. (2000). Chaos in periodically forced discrete-time ecosystem models. Chaos, Solitons & Fractals, 11(14), pp.2331-2342.

Yu, J. and Yu, J. (2014). Homotopy Analysis Method for a Prey-Predator System with Holling IV Functional Response. Applied Mechanics & Materials.

Modelos estadísticos para la interacción océano-atmósfera

Rafaél Artidoro Sandoval-Núñez *
Luis Cid-Serrano **
Eric J. Alfaro ***

RESUMEN

La presente investigación tiene como objetivo modelar la interacción del océano-atmósfera utilizando la relación entre la Oscilación del Sur y los eventos El Niño-La Niña como un sistema de entrada-salida. El modelamiento estadístico de este tipo de relaciones requiere del análisis de la función de correlación cruzada entre las series de entrada y salida. Los datos considerados corresponden a series de tiempo mensuales del Índice de la Temperatura Superficial del Mar de la Región del Niño 3.4 y del Índice de la Oscilación del Sur entre 1982 y 2015. Para representar la interacción del océano-atmósfera, se desarrollaron Modelos de Función de Transferencia y de retroalimentación. La eficiencia de estos modelos con datos hasta el 2015 fue comparada para pronosticar hasta septiembre del año 2019 por medio del error cuadrático medio de predicción, encontrando que el modelo de retroalimentación es más eficiente.

PALABRAS CLAVE: Modelos de Retroalimentación; Modelos de transferencia; ENSO; Oscilación del Sur; Temperatura Superficial del Mar.

* Profesor de la Universidad Nacional Autónoma de Chota – Perú, https://orcid.org/0000-0003-3930-2332. E-mail: rafaelsandonu@gmail.com

** Profesor de la Universidad del Bío-Bío – Chile.

*** Profesor de la Universidad de Costa Rica – Costa Rica, https://orcid.org/0000-0001-9278-5017.

Recibido: 30/04/2020 Aceptado: 25/06/2020

Statistical models for the ocean-atmosphere interaction

ABSTRACT

The present research aims to model the ocean-atmosphere interaction using the relationship between the Southern Oscillation and El Niño-La Niña events as an input-output system. Statistical modeling of this type of relationship requires analysis of the cross-correlation function between the input and output series. The data considered correspond to monthly time series of the Niño 3.4 Sea Surface Temperature Index and the Southern Oscillation Index between 1982 and 2015. To represent the interaction of the ocean-atmosphere, Function Models were developed Transfer and feedback. The efficiency of these models with data up to 2015 was compared to forecast until September 2019 by means of the mean squared error of prediction, finding that the feedback model is more efficient.

KEYWORDS: Feedback Models; Transfer Models; ENSO; Southern Oscillation; Sea Surface Temperature.

Introducción

Las interacciones a gran escala entre el océano y la atmósfera, particularmente en el Pacífico, junto con sus repercusiones en la variabilidad interanual del clima global, han sido objeto de numerosos estudios (Bjerknes, 1969; Enfield, 1989; Philander, 1990 y Trenberth, 1997). La manifestación más notable de estas interacciones es la aparición irregular del fenómeno de El Niño y La Niña cada pocos años. Después del trabajo de Bjerknes (1969), las variaciones atmosféricas, llamadas Oscilación del Sur (SO), y todo el proceso interactivo ha sido denominado como "El Niño-Oscilación del Sur" (ENSO). ENSO presenta las señales de variabilidad climática más prominentes y una de los más estudiados en términos de interacción océano-atmósfera (Wallace et al., 1998; Cid-Serrano et al., 1992; Enfield y Cid-Serrano, 1991; Trenberth, 1997 y Collins et al. 2010). Los eventos cálidos de ENSO, se caracterizan por un calentamiento oceánico de las aguas cercanas a la costa (a lo largo de la costa del Pacífico de América del Sur), así como un aumento en la temperatura superficial del mar (SST) en la zona ecuatorial del Pacífico central y oriental. La variabilidad atmósfera consiste en un aumento de la presión atmosférica en la zona de baja presión de Indonesia y el Norte de Australia, con una disminución simultánea de la presión en la región del Pacífico sudoriental de alta presión. Los cambios de presión causan una disminución en el Este - gradiente de presión hacia el Oeste que impulsa los intercambios que soplan normalmente

hacia el Oeste (Este), desde donde se produce un debilitamiento de los vientos del Este a lo largo del Ecuador.

Aunque los eventos cálidos de El Niño se describen típicamente en términos de un aumento anómalo de la temperatura de la superficie del océano, es bastante complejo. Se compone de grandes cambios en la estructura interna del océano, las precipitaciones, el nivel del mar, la presión atmosférica y otras variables climáticas. Para obtener información precisa sobre las fluctuaciones del sistema ENSO, es necesario considerar tanto el área amplia que afecta como las numerosas variables involucradas en el proceso. En los últimos años, se han obtenido muchos índices de diferentes variables meteorológicas en el Pacífico tropical y subtropical como la precipitación, presión atmosférica a nivel del mar (SOI), espesor atmosférico y otras variables. Los parámetros antes mencionados se han identificado como útiles para representar la SO (Chen, 1982; Quinn, 1983; Wallace et al., 1998; Cid-Serrano et al. 2015), entre los cuales el más utilizado es el SOI.

Mientras tanto, los eventos de La Niña o ENSO frío se estudian como el refuerzo de las condiciones normales del Pacífico ecuatorial oriental, con aguas más frías en esa región y una disminución de la presión atmosférica en la zona de Indonesia y el norte de Australia; también, se observa un aumento de la presión en la región del Pacífico sudoriental en estos eventos.

Los modelos estudiados muestran que las relaciones interactivas entre los cambios del océano y la atmósfera se pueden entender si se especifica un cambio en un medio y observamos los cambios físicos en el otro. Si se sabe que, la condición de límite inferior (SST) de un modelo numérico atmosférico recibe una anomalía positiva en la zona ecuatorial, ocasiona una perturbación en el campo de viento que es cualitativamente similar a lo que observamos durante El Niño (Rasmusson y Carpenter, 1982; Gill, 1980). De manera similar, podemos observar que un debilitamiento de la tensión del viento ecuatorial del Este traerá cambios oceánicos (Busalachi et al., 1983; Schopf y Harrison, 1983; Philander y Siegel 1985).

Aunque se acepta que los cambios en cada medio pueden provocar respuestas en el otro, ninguna de estas interacciones unilaterales es un verdadero indicador de causa y efecto, porque ambos medios fuerzan al otro simultáneamente. Si una anomalía se introduce por primera vez en la atmósfera (existe evidencia estadística de que esto ocurre), el océano puede responder e inducir cambios atmosféricos posteriores propios (Wright, 1985). Por ejemplo, las aguas más cálidas a lo largo del ecuador producirán un aumento en la temperatura de la

atmósfera, que a su vez se asocia con una mayor disminución de la presión atmosférica, también inducirá la advección de humedad de las áreas circundantes y la convección anómala. Estos eventos conducen a una perturbación mejorada en el campo de viento, que inicia una retroalimentación positiva en el océano con aumentos adicionales en la SST. Los cambios serán más significativos en la medida en que la SST persista. Del mismo modo, la temperatura del agua a lo largo de la banda ecuatorial persistirá en la medida en que se mantengan las anomalías climáticas en la zona. Por lo tanto, existe una potencial relación de las anomalías del océano y la atmósfera debido a la ocurrencia de retroalimentación positiva en los procesos de interacción aire-mar. La simulación efectiva de este comportamiento de la anomalía requiere que los modelos numéricos se acoplen de tal manera que reproduzcan los múltiples procesos de retroalimentación que ocurren.

Junto con el modelado numérico, se han adoptado enfoques estadísticos para simular las interacciones del sistema océano-atmósfera (Latif et al. 1994; 1998). Las herramientas más comunes son los estudios que examinan la respuesta oceánica (SST) a las condiciones preexistentes en ambos medios, utilizando métodos multivariados autorregresivos y medias móviles (ARMA) (Chu y Kast, 1985; Zwiers y von Storch, 1990); estos también se han utilizado, con cierto éxito, para la predicción a corto plazo (meses) (Barnett et al., 1988). Latif et al. (1994; 1998) mencionaron que los modelos estadísticos se basan, en general, en lineales avanzados (Xu y von Storch, 1990; Zwiers y von Storch 1990; Barnston y Ropelewski, 1992) y no lineales (Lima et al. 2009 y Ubilava y Helmers, 2012) técnicas estadísticas y se pueden clasificar en modelos que utilizan variaciones de baja frecuencia en la atmósfera (presión a nivel del mar o campo de viento), cantidades oceánicas (temperatura de la superficie del mar o una medida del contenido de calor del océano superior) (Lima et al., 2015; Suárez-Moreno y Rodríguez-Fonseca, 2015) o una combinación de valores oceánicos o atmosféricos como predictores (MacMartin y Tziperman, 2014). El uso de estos métodos, con grandes conjuntos de variables clave es prometedor, pero carece de un ingrediente esencial: la formulación explícita de la retroalimentación mutua en los algoritmos estadísticos (Cid-Serrano, 1986; Sandoval-Núñez, 2016). Este aspecto podría mejorar la habilidad de predicción de ENSO, que parece haber alcanzado una meseta a un nivel moderado (Chen y Cane, 2008). Además, Graham et al. (2015) mencionan que la naturaleza compleja de ENSO a menudo se simplifica mediante el uso de modelos conceptuales, cada uno de los cuales ofrece una perspectiva diferente sobre la retroalimentación océano-atmósfera que sustentan el ciclo ENSO.

Para modelar la relación océano-atmósfera, se puede hacer utilizando modelos de la función de transferencia (TFM) y de retroalimentación (FBM). Esto se hace posible porque los modelos de pronóstico actuales de ENSO, a pesar de sus grandes diferencias y complejidad, exhiben habilidades predictivas comparables (Chen y Cane, 2008).

Los modelos de series temporales binarias se activan por un proceso latente o un mecanismo de retroalimentación que modula la evolución del proceso observado. Este FBM hace posible el uso de una parametrización parsimoniosa de bajo rango para estructuras de datos complejas (Moysiadis y Fokianos, 2014). Cuando las variables de salida modulan las de entrada, hay un sistema de retroalimentación de circuito cerrado. Esta condición determina si las variables están relacionadas entre sí y se describen bajo las mismas condiciones (Chatfield, 2000).

Por lo expuesto anteriormente, el objetivo de esta investigación es modelar la interacción del océano-atmósfera aprovechando la relación entre la SST e IOS utilizando los modelos de función de transferencia (TFM) y retroalimentación (FBM), centrándose principalmente en la estimación y predicción de la SST como un indicador directo de la presencia de El Niño-La Niña. Pronosticando valores de SST hasta el año 2019, utilizando SOI como predictor, aprovechando la característica bidireccional de la relación, también se obtuvieron estimaciones del Índice de Oscilación del Sur (SOI) utilizando SST. Los resultados de las predicciones se compararon utilizando el error de predicción del cuadrado medio (PMSE). Según Wilby y Dawnson (2007), la principal fortaleza de los modelos TFM y FBM es la relativa facilidad computacional para su aplicación. La principal debilidad es que los modelos a menudo explican solo una fracción de la variabilidad climática observada y asumen la validez de los parámetros del modelo en condiciones climáticas futuras, pero las relaciones predictor-predicción a menudo no son estacionarias, especialmente cuando existe variabilidad climática de baja frecuencia.

1. Modelos estadísticos para el sistema océano-atmósfera

1.1. Modelos de funciones de transferencia

Esta representación se puede generalizar para incluir una variable explicativa $\{X_t\}$, con el modelo resultante conocido como Modelo de función de transferencia (TFM) (Box et al., 2015), que tiene la forma

$$Y_t = \nu(B)X_t + \xi(B)\varepsilon_t. \quad (1)$$

donde Y_t es la serie de salida, X_t es la entrada y ε_t es el término de componente aleatorio (ruido). $\nu(B)$ es un polinomio en B, llamado Función de transferencia. Sin embargo, esta expresión supone que los polinomios $\nu(B)$ y $\xi(B)$ en (1) tienen términos infinitos (Box et al., 2015), por lo que debemos encontrar una representación más parsimoniosa para ellos. Esto se logra al reemplazarlos por la relación de dos polinomios de orden finito en B como se muestra en (2),

$$Y_t = \frac{\omega_0 - \omega_1 B - \cdots - \omega_s B}{1 - \delta_1 B - \cdots - \delta_r B} X_t + \frac{\lambda_0 - \lambda_1 B - \cdots - \lambda_q B}{1 - \pi_1 B - \cdots - \pi_p B^p} \varepsilon_t \,, \quad (2)$$

donde s, r, q y p corresponden al orden del polinomio en el modelo. De manera equivalente, estos pueden escribirse como

$$Y_t = \frac{\omega_x(B)}{\delta_x(B)} X_t + \frac{\lambda(B)}{\pi(B)} \varepsilon_t. \quad (3)$$

La relación entre las series de entrada y salida, y el orden de los polinomios se definen inicialmente por la función de correlación cruzada (FCC), según lo definido por Box et al. (2015).

Aquí, ω, δ, λ y π son los parámetros a estimar y ε_t el término de ruido; s, r y p corresponden al orden de los polinomios, que representan el retraso entre las series; esto se determina principalmente utilizando el orden de los valores estadísticamente significativos de la FCC. Un sistema del tipo descrito por (2), se llama un sistema de circuito abierto, y ha sido utilizado por MacMartin y Tziperman (2014) para cuantificar la dinámica de ENSO en datos y modelos, por Alfaro y Cid (1999) y Alfaro y Soley (2001) para predecir el campo de precipitación en América Central y por Alfaro y Lizano (2001) para la predicción de SST en áreas afloradas de América Central, Pacífico Oriental Tropical.

1.2. Modelos de retroalimentación

Como se mencionó anteriormente, el orden del TFM está asociado con el número de rezagos significativos positivos del FCC (Box et al., 2015). Sin embargo, cuando la FCC tiene valores significativos en rezagos negativos, es razonable pensar que estamos en presencia de un sistema de retroalimentación (sistema de circuito cerrado) (Cid-Serrano, 1986; Hipel y Mc Leod, 1994) como lo representa (4) y (5).

$$Y_t = \sum_{i=1}^{k} \vartheta_i \, Y_{t-i} + \sum_{i=1}^{p} \gamma_i \, X_{t-i} + \eta_t \tag{4}$$

$$X_t = \sum_{i=1}^{q} \pi_i \, X_{t-i} + \sum_{i=1}^{r} \rho_i \, Y_{t-i} + \mu_t \quad , \tag{5}$$

η_t y μ_t, son los términos de error y $\vartheta_i, \gamma_i, \vartheta_{i_i}, \gamma_i$los parámetros a estimar. La ecuación (5) se conoce como ecuación de retroalimentación y ρ_i, $i = 1, 2, \ldots r$, se denominan parámetros de retroalimentación, y en ausencia de retroalimentación deben ser nulos, de modo que el sistema (4) y (5) se convierten en

$$Y_t = \sum_{i=1}^{k} \vartheta_i \, Y_{t-i} + \sum_{i=1}^{p} \gamma_i \, X_{t-i} + \eta_t \tag{6}$$

$$X_t = \sum_{i=1}^{q} \pi_i \, X_{t-i} + \mu_t \, . \tag{7}$$

1.3. Estimación de parámetros

Los parámetros de los modelos (2), y el sistema (4) y (5) o alternativamente (6) y (7), se estimaron por medio de mínimos cuadrados utilizando SAS y R Project (SAS, 2019 y R Core Team, 2019). La significancia estadística de los parámetros se determinó mediante pruebas T, con propiedades asintóticas respaldadas por la gran cantidad de observaciones ($n > 400$). Se determinó que todas las pruebas con valor $p \leq 0.05$ eran estadísticamente significativas. Utilizamos las estadísticas de prueba de Ljung y Box (1978) para la hipótesis de que los residuos son ruido blanco y el criterio para encontrar el mejor modelo fue el error cuadrático medio de predicción (MSEP).

1.4. Datos

En principio, se utilizaron series de tiempo mensuales del año 1950-2015, pero los modelos de transferencia y retroalimentación presentaron un error cuadrático medio alto y falta de estabilidad estructural que afectó las predicciones. En consecuencia, los resultados pueden ser muy sensibles, por lo que, pueden suponer diferentes conclusiones (Sánchez, 2008). Entonces, el uso de series temporales desde 1982 tiene la intención de mejorar la precisión de los modelos. Aunque el modelo original solo buscaba evaluar las relaciones entre

SOI y SST, la naturaleza interactiva del fenómeno requiere la representación de los procesos por medio de sus índices y su inclusión en un modelo estadístico de circuito cerrado. Para este análisis, se consideró dos series temporales de datos mensuales para el período 1982 – 2015 como son la SST y SOI. La a SST (medida en el Pacífico tropical ecuatorial), en la región Niño 3.4 (5 ° N - 5 ° S, 120 ° W -170 ° W, N34) (para una descripción ver Trenberth, 1997; Trenberth y Stepaniak, 2001) y el Índice de Oscilación del Sur (SOI), donde este último corresponde a la diferencia estandarizada en la presión del nivel del mar entre Tahití y Darwin, Australia. Ambos se descargaron del sitio web del Centro de Predicción Climática de NOAA (http://www.cpc.ncep.noaa.gov/data/indices/).

La selección de un SOI apropiado para ser usado en el contexto de este análisis se basó en la experiencia de Chen (1982) y Rasmusson y Carpenter (1982). Descubrieron que los cambios atmosféricos en Tahití provocan cambios en Darwin en aproximadamente un mes. El retraso entre Rapa Nui y la Isla de Pascua también fue de aproximadamente un mes. Se descubrió que tanto Rapa Nui como Easter lideraron Tahití por varios meses. En general, esto significa que los cambios en la presión atmosférica de la superficie cerca del centro del Pacífico Sur (Rapa Nui e Isla de Pascua) conducen a los que se encuentran en latitudes más bajas en el Pacífico Sur Central (Tahití), y también provocan cambios del signo opuesto en la vecindad del bajo australiano-indonesio.

La serie original de la SST no es estacionaria, contiene un fuerte componente anual (12 meses). Para corregir este problema, se restó el promedio mensual correspondiente a cada observación para que la serie resultante muestre componentes no periódicos. Obteniendo la serie de anomalía de la SST (denominada Y_t en los modelos de la sección 2.5) muestra los eventos ENSO del período.

La serie SOI (se define como X_t en los modelos de la sección 2.5) exhibe un fuerte componente de ruido y también muestra los eventos ENSO del período. La serie original tiene valores atípicos, que fueron reemplazados utilizando el método propuesto por Chen y Liu (1993). Este procedimiento no elimina los valores atípicos, pero los reemplaza usando un algoritmo que preserva la estructura autocorrelativa de la serie.

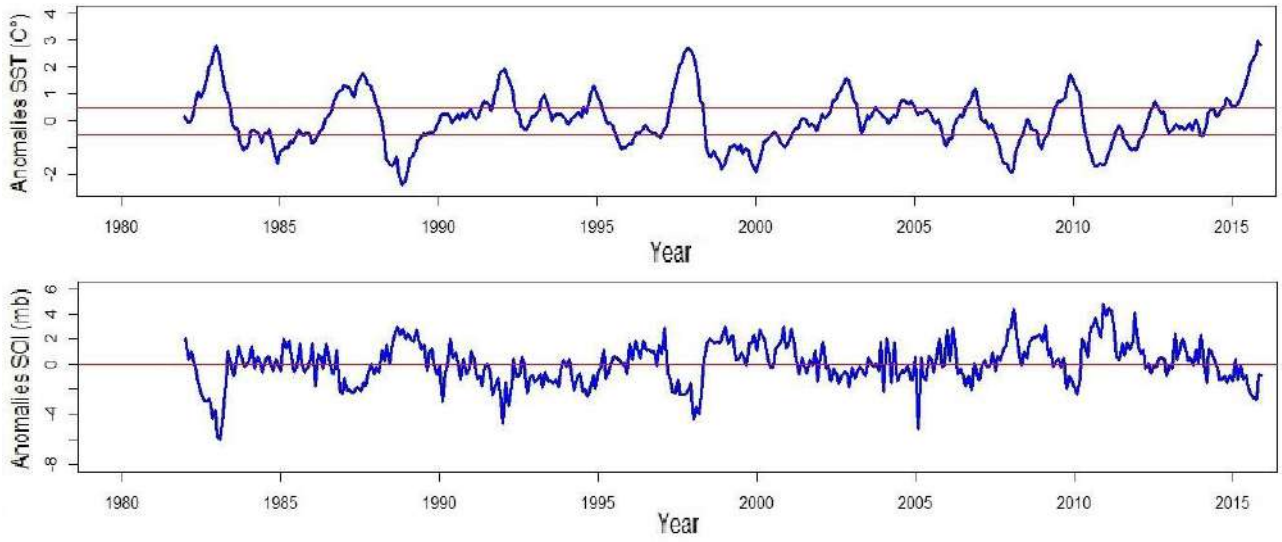

Figura 1. Series de anomalía de la SST (arriba) y SOI (abajo). Las líneas rojas en el panel superior indican los indicadores de +/- 0.5 °C de los eventos de El Niño o La Niña cuando persisten durante 5-6 meses o más.

1.5. Resultados de los modelos para representar la interacción del océano-atmósfera

1.5.1. Modelos de función de transferencia

La función de transferencia describe la relación de entrada-salida dependiente de la frecuencia entre cualquier par de variables causalmente relacionadas y puede estimarse a partir de la serie temporal (MacMartin y Tziperman, 2014). Inicialmente, ajustamos el TFM (2, utilizando SOI como serie de entrada y la SST como salida. Aquí, la identificación de la relación (rezagada) entre la entrada y la salida se basa en el FCC entre ellos después del preblanqueamiento de la serie, para lo cual se necesita encontrar un modelo ARMA para la serie de entrada (Box et al., 2015). Se descubrió que el mejor modelo ARMA(p, q) para el SOI de entrada era un modelo autorregresivo de orden 3, AR (3). Los resultados para el TFM correspondiente se muestran en la ecuación (8) a continuación, que muestra valores rezagados significativos de N34 de hasta dos meses.

$$Y_t = \frac{-0.0218 \; - \; 0.06526\, B}{1 \; - \; 1.16815\, B + 0.45492 B^2} X_t + \frac{1}{1 - 1.27895\mathrm{B} + 0.37875 B^2}\, \varepsilon_t. \qquad (8)$$

Se utilizó una metodología similar para ajustar un TFM con SOI como salida y N34 como entrada. El modelo ajustado (9) muestra valores rezagados significativos de hasta dos meses.

$$X_t = \frac{-0.8519 \; - \; 0.70438B}{1 \; + \; 0.57732\mathrm{B} \; - \; 0.35292\, B^2} Y_t + \frac{1 \; - \; 0.78912\, B + 0.13652\, B^2}{1 \; - \; 0.98268\,\mathrm{B}} \varepsilon_t \,. \qquad (9)$$

1.5.2. Modelos de retroalimentación

El primer enfoque fue considerar un sistema bivariado para SOI y para la anomalía de la SST. Aquí la identificación del sistema de circuito cerrado se basa en el FCC entre ellos, al observar valores significativos de la FCC para retrasos negativos (Cid-Serrano, 1986). Primero ajustamos el sistema (4) y (5) usando SOI como entrada y SST como serie de salida, aunque esta clasificación podría ser engañosa, dada la estructura de retroalimentación del sistema. Los parámetros se estimaron utilizando la estimación de Mínimos Cuadrados Generalizados. Los resultados del proceso de estimación se muestran en las ecuaciones (10) y (11) a continuación. El AIC muestra el mejor modelo que incluye variables rezagadas hasta el orden 4. Tenga en cuenta que hay dos parámetros de retroalimentación significativos, correspondientes a ρ_1 y ρ_5 en la ecuación (11) (valor $p \; < 0.05$). Por lo tanto, concluimos que hay parámetros de retroalimentación estadísticamente significativos en el sistema con un retraso de hasta cinco meses, como se muestra a continuación.

$$Y_t = 1.2751Y_{t-1} - 0.3593Y_{t-2} - 0.0564Y_{t-3} - 0.0689X_{t-1} + 0.0262X_{t-3} \qquad (10)$$

$$X_t = -0.9474Y_{t-1} + 0.1937Y_{t-5} + 0.3474X_{t-1} \,. \qquad (11)$$

1.5.3. Pronóstico y comparación de los modelos

Una vez que se ha encontrado un modelo, una forma útil de evaluar la calidad de los resultados es examinar cómo funciona al pronosticar los valores de las variables de respuesta. Las figuras 2 y 3 muestran los valores observados y pronosticados de las series de la anomalía de la SST y SOI, respectivamente hasta el año 2019, utilizando las parametrizaciones que se muestran en (10) y (11). Para fines comparativos, también estimamos MSEP para ambas series usando TFM en (8) y (9), para SST y SOI, respectivamente.

La Tabla 1, muestra los resultados de los procesos de pronóstico de PMSE calculados para el año 2019, para cada modelo y respuesta. La tabla muestra que el modelo de retroalimentación funciona mejor al predecir los valores de SST y SOI para el año 2019, lo que

refuerza la idea de que un FBM es un mejor modelo para representar las relaciones océano-atmósfera en el área.

Tabla 1. Valores del error cuadrático medio de predicción para los dos modelos y variables.

	Salida	TFM	FBM
MSEP	SST	0.4476	0.4143
	SOI	1.4736	0.6860

Las Figuras 2 y 3 a continuación muestran los resultados del pronóstico de la anomalía SST y SOI para el año 2019, utilizando tanto TFM como FBM.

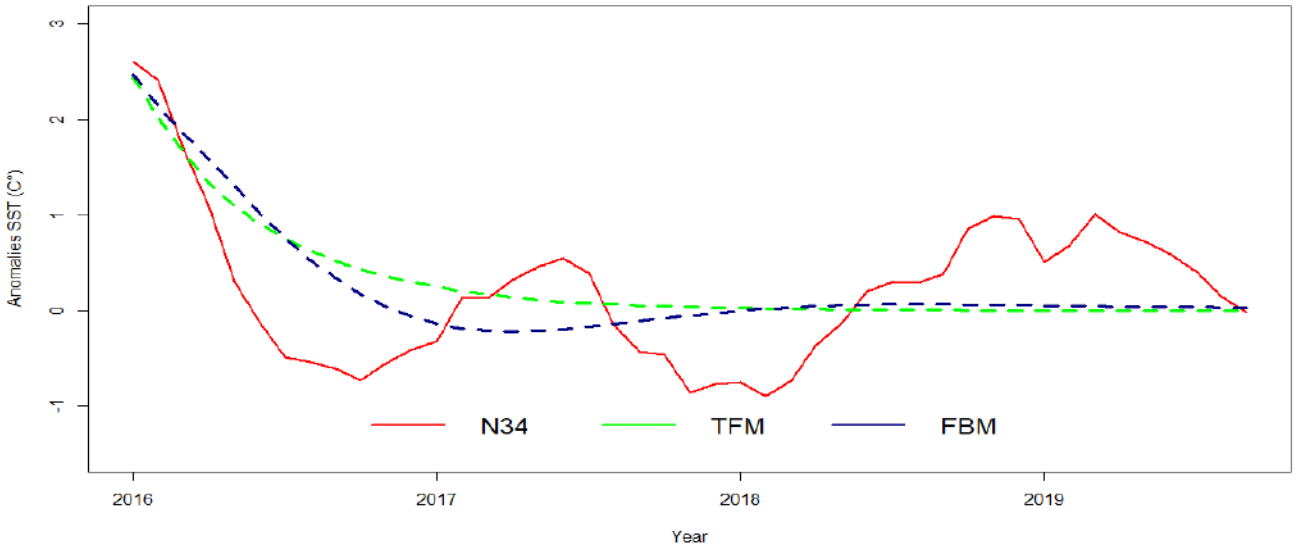

Figura 2. Comparación de los valores mensuales pronosticados de las anomalías de SST para el año 2019, utilizando los modelos de las ecuaciones 8 y 10.

La Figura 2, muestra una mejor proximidad de los valores observados a los valores pronosticados cuando se usa el FBM, mientras que la Figura 3 muestra una mejor proximidad de los valores observados de SOI a los valores pronosticados cuando se usa el FBM. Tenga en cuenta que los valores SOI observados presentan una variabilidad mucho mayor que la

anomalía de la SST, variabilidad que se refleja en valores más altos del PMSE para SOI que para la SST.

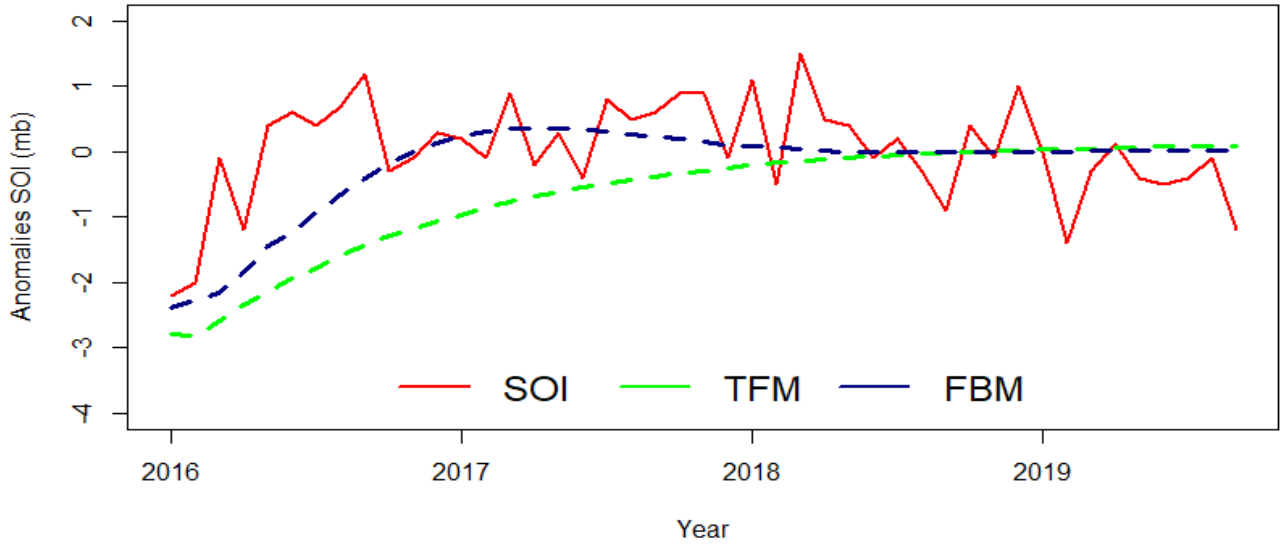

Figura 3. Comparación de los valores mensuales pronosticados de SOI para el año 2019, utilizando los modelos de las ecuaciones 9 y 11.

2. Discusión y conclusiones

En este estudio, se ha implementado un método estadístico que permite modelar la presencia de retroalimentación en los sistemas climáticos, con una aplicación específica a la interacción océano-atmósfera a través del estudio de ENSO. Según Ubilava y Helmers (2012), estos resultados son importantes para los agentes económicos y los encargados de formular políticas en todo el mundo, ya que ofrecen mejores pronósticos de ENSO e inferencias económicas y sociales más precisas.

Un enfoque natural para representar dicha interacción es el uso de TFM. Sin embargo, el análisis del FCC entre SOI y N34, que es un paso previo para el ajuste del modelo de función de transferencia, indica que hay valores significativos en la FCC para los retrasos no positivos; Esto, junto con la naturaleza física conocida del fenómeno ENSO, es una clara indicación de la presencia de retroalimentación en el sistema. Tanto SOI como SST son parte de un sistema global que involucra una serie de otros procesos, como la cobertura de nubes, el viento y la radiación, que también ha sido documentado por Wright (1985) y Cid-Serrano (1986) y están relacionados por una retroalimentación mecanismo. Dado que Tahití lidera a Darwin por solo un mes, parece más conveniente usar un SOI basado en estas dos series para reducir el desfase temporal entre las dos regiones, como lo sugiere Chen (1982). Por lo tanto, adoptamos el SOI

como el que mejor representa las características de la Oscilación del Sur. Chu y Katz (1985) encontraron que las anomalías mensuales pueden describirse utilizando un modelo de promedio móvil autorregresivo (ARIMA) con parámetros (1,7,1) (ver Box et al., 2015), mientras que las series trimestrales siguen un ARMA(1,1) modelo.

Chen (1982) examinó la capacidad de varios índices SLP para representar adecuadamente el SO analizando series obtenidas de estaciones ubicadas en la Isla de Pascua, localmente conocida como Rapa Nui- o Tahití, en el Pacífico oriental, y Darwin, Australia en el Pacífico occidental (ubicado en el centro de la región de baja presión de Indonesia). Los índices utilizados se calculan, en la mayoría de los casos, como la diferencia en la presión atmosférica estandarizada entre las estaciones ubicadas en cada una de esas dos antípodas climáticas del Pacífico Tropical (Rasmusson y Carpenter, 1982). Trenberth (1984) discutió la utilidad de usar un índice simple restando las medidas de Tahití estandarizado menos Darwin estandarizado dividida entre la desviación estándar mensual de la diferencia de ambos índices. Este índice, es definido como SOI y es el más utilizado para definir el SO.

Aunque claramente estamos tratando con un sistema de retroalimentación, para fines comparativos ejecutamos TFM para las diferentes combinaciones de la serie, SOI y SST. La Tabla 1 mostró que la SST se predijo mejor que SOI para todos los casos, mostrando una estructura de atmósfera más caótica en comparación con la inercia oceánica.

Las ecuaciones (10) y (11) mostraron que las retroalimentaciones de SOI en SST y viceversa, con retrasos de hasta cuatro meses. Sin embargo, encontramos que el mejor modelo (con respecto al PMSE) para predecir N34 es el FBM (10), que usa el SOI como serie de entrada, en lugar del TFM (8), retroalimentando a SST con un retraso de entre uno y tres meses (10). Por lo tanto, los valores altos (bajos) de SOI están asociados con valores bajos (altos) de SST. Aunque todos los modelos fueron estadísticamente significativos (valor p <0.05), vale la pena mencionar que la serie SOI es extremadamente ruidosa, afecta la naturaleza del proceso de ajuste (al aumentar la varianza de los estimadores) y mejora el PMSE de los modelos en el que se incluye SOI.

Como en MacMartin y Tziperman (2014), pudimos comparar cuantitativamente diferentes procesos individuales entre las observaciones. Nótese que las ecuaciones (10) y (11) describen, de manera implícita, las relaciones de un sistema de retroalimentación que contiene los elementos clave presentados en la mayoría de los modelos dinámicos utilizados en la predicción canónica de ENSO (Fernández y Pacheco 2000; Chen y Cane 2008); como el

modelo de oscilador unificado (Graham et al., 2015) o el modelo de oscilador retrasado (MacMartin y Tziperman, 2014). Comenzando con un frío (anomalías SOI positivas) o una condición ENSO normal, los vientos alisios ecuatoriales pueden generar una ola Kelvin ascendente hacia el este en el Pacífico occidental. Dado que la termoclina en el Pacífico oriental es poco profunda, la SST podría disminuir (anomalías negativas en el SST). Esta ola Kelvin se refleja contra la costa este continental de América del Sur y regresa al oeste como una ola de hundimiento de Rossby, casi sin efecto en el campo SST. Cuando esta ola de Rossby llega a la costa occidental continental, se refleja como una forma Kelvin de hundimiento hacia el este, lo que aumenta la profundidad de la termoclina en el Pacífico central y oriental. Esto podría estar asociado con un evento ENSO cálido (anomalías positivas de SST) y disminuye la fuerza de los vientos alisios ecuatoriales orientales, al tiempo que aumenta la convección profunda en el Pacífico ecuatorial oriental (anomalías negativas de SOI). Tenga en cuenta que el punto de partida de la descripción sintetizada anterior en un sistema de retroalimentación es arbitrario, pero Suárez-Moreno y Rodríguez-Fonseca (2015) mencionaron que un comportamiento no estacionario de las teleconexiones en los océanos tropicales, como la Barrera de previsibilidad de primavera (Lai et al., 2018), podría ser un tema importante a considerar en la predicción futura de ENSO.

Además, los estudios dinámicos han demostrado que los sistemas ENSO de retroalimentación, como el que se encuentra en las ecuaciones (10) y (11), implican que cuando el valor de SOI es alto (anomalías positivas de SOI), podemos esperar la región de baja presión. para ser más intenso más profundo y el subtropical alto para ser más fuerte. Estas condiciones están asociadas con fuertes intercambios en el sureste y vientos del este ecuatoriales, que mejoran el afloramiento ecuatorial y causan que el isotérmico baje y la SST disminuya en el este (anomalías negativas de SST). Junto con esto, hay un patrón característico de lluvia para la región, con precipitaciones sobre Indonesia y condiciones secas que se extienden desde la costa sudamericana hacia el oeste a lo largo del ecuador, al menos hasta la fecha. Estas características comprenden la llamada condición de La Niña hacia el este y la región de Australia-Indonesia en el oeste (Rosenzweig y Hillel, 2008).

Cuando el SOI cae desde picos que no son de ENSO hacia valores bajos de ENSO, la baja presión ecuatorial "se llena" (aumenta la presión) y migra hacia el Este a lo largo del Ecuador mientras el sistema subtropical de alta presión se debilita. Los vientos alisios del Este se relajan y se produce una situación de El Niño. La afluencia ecuatorial disminuye y la SST del

Pacífico central aumenta. Las precipitaciones aumentan en el Pacífico ecuatorial central, a lo largo de la costa de Ecuador y el Norte de Perú y las tierras altas andinas Centro-Norte de Indonesia, Australia y Surinam experimentan condiciones severas de sequía (Marshall y Plumb, 2007). Sin embargo, el efecto más característico es el gran aumento anómalo de la SST desde Ecuador hasta el Norte de Chile. La presión atmosférica a nivel del mar es un aspecto clave en la alternancia de El Niño-La Niña. Este patrón a gran escala contrasta la presión atmosférica en ambos lados del Pacífico tropical de América del Sur.

Rasmusson y Carpenter (1982), Quinn (1983) y Chen (1982) mostraron que los cambios en la fase del SOI llevan estadísticamente cambios en la SST a lo largo de la costa del Perú por varios meses. Esto, sumado a la conexión estadística ya descrita, sugiere que el SOI puede ser muy útil para predecir las variaciones de la SST del Pacífico oriental si se encuentra un modelo estadístico adecuado, como los de las ecuaciones (8), (9), (10) y (11) Esto es consistente con los argumentos a menudo citados de que la atmósfera generalmente fuerza al océano (por ejemplo, Davis, 1976), pero Zerefos y Bais (1997) reconocieron el sistema océano-atmósfera como un sistema acoplado. El océano es impulsado por la radiación solar a través de la interfaz aire-agua, incorporando los cambios que ocurren en la interfaz océano-atmósfera. También explican la existencia de un acoplamiento cercano entre la atmósfera y el océano a través de la radiación solar. Magaña et al (1999) siguen este enfoque de retroalimentación para explicar, por ejemplo, los sucesos de la sequía de mediados de verano en el Pacífico tropical oriental. Según Ubilava y Helmers (2012), los avances y resultados presentados aquí sobre la predicción de ENSO son de interés para los investigadores y los encargados de formular políticas en los campos de la dinámica climática, la producción agrícola y la gestión ambiental, como los que participan en los Foros Regionales de Perspectiva Climática (García-Solera y Ramírez, 2012).

Referencias

Alfaro, E. y Cid L. (1999). Ajuste de un modelo VARMA para los campos de anomalías de precipitación en Centroamérica y los índices de los océanos Pacífico y Atlántico Tropical. *Atmósfera*, 12(4), 205-222.

Alfaro, E. y Lizano O. (2001). Algunas relaciones entre las zonas de surgencia del Pacífico Centroamericano y los Océanos Pacífico y Atlántico Tropical. *Revista de Biología Tropical*, 49(Supl. 2), 185-193.

Alfaro, E. y Soley F. (2001). Ajuste de un modelo VAR como predictor de los campos de anomalías de precipitación en Centroamérica. *Revista de Matemática: Teoría y Aplicaciones*, 8(1), 99-116.

Barnett, T. P., Graham, N., Cane, M., Zebiak, S., Dolan, S., Obrien, J. y Legler, D. (1988). On the prediction of El Niño 1986-1987. *Science*, 241. 192-196. https://doi.org/10.1126/science.241.4862.192

Barnston, A. G. y Ropelewski, C. F. (1992). Prediction of ENSO episodes using canonical correlation analysis. *Journal of Climate*, 5(11), 1316-1345. https://doi.org/10.1175/1520-0442(1992)005<1316:POEEUC>2.0.CO;2

Bjerknes, V. (1969). Atmospheric teleconnections from Equatorial Pacific. *Monthly Weather Review*, 97, 163-172.

Box, G., Jenkins, E. P., Reinsel, C.G. y Ljung, G. M. (2015). *Time Series Analysis: Forecasting and Control*. Fifth Edition. John Wiley & Sons, Inc.

Busalachi, A. J., Takeuchi, K. y O´Brien, J. J. (1983). Interannual variability of the equatorial Pacific- Revisited. *Journal of Geophysical Research*, 88, 7551-7562. https://doi.org/10.1029/JC088iC12p07551

Chatfield, C. (2000). *Time-series forecasting*. Chapman and Hall/CRC.

Chen, W. Y. (1982). Assessment of the Southern Oscillation sea level pressure indices. *Monthly Weather Review*, 110, 800-807. https://doi.org/10.1175/1520-0493(1982)110<0800:AOSOSL>2.0.CO;2

Chen, D. y Cane, M. A. (2008). El Niño prediction and predictability. *Journal of Computational Physics*, 227(7), 3625-3640. https://doi.org/10.1016/j.jcp.2007.05.014

Chen, C. y Liu, L. M. (1993). Joint Estimation of Model Parameters and Outlier Effects in Time Series. *Journal of the American Statistical Association*, 88, 284-297.

Chu, P.S. y Katz, R.W. (1985). Modeling and forecasting the Southern Oscillation: A time domain approach. *Monthly Weather Review*, 113,1875-1888.

Cid-Serrano, L. (1986). *Estimation of the parameters in a closed-loop system: A geophysical problem*. Ph.D. Thesis Oregon State University.

Cid-Serrano, L., Enfield D. y González, U. (1992). Distributional properties of the recurrence intervals of El Niño/Southern Oscillation Events. *Gayana Oceanologica*, 1, 17-25

Cid-Serrano, L., Ramirez, S. y Alfaro, E. (2015). Analysis of the Latin American west coast rainfall predictability using an ENSO Index. *Atmósfera*, *28(3)*, *191-203. DOI: https://doi.org/10.20937/ATM.2015.28.03.04*

Collins, M., An, S., Cai, S., Ganachaud, A., Guilyardi, E., Jin, F., Jochum, M., Lengaigne, M., Power, S., Timmermann, A., Vecchi, G. y Wittenberg, A. (2010). The impact of global warming on the tropical Pacific Ocean and El Niño. *Nature Geoscience*, 3 (6), 391-397.

Davis, R. E. (1976). Predictability of the sea surface temperature and sea level pressure over the North Pacific Ocean. *Journal of Physical Oceanography*, 6(3), 249-267. https://doi.org/10.1175/1520-0485(1976)006<0249:POSSTA>2.0.CO;2

Enfield, D. B. (1989). El Niño past and present. *Reviews of Geophysics*, 27, 159-187. DOI: https://doi.org/10.1029/RG027i001p00159

Enfield, D. y Cid-Serrano, L. (1991). Low-frequency changes in El Niño/Southern Oscillation. *Journal of Climate*, 4(12), 1137-1146. DOI: https://doi.org/10.1175/1520-0442(1991)004<1137:LFCIEN>2.0.CO;2

Fernández, I. y Pacheco, J. M. (2000). Bases para la predicción del ENSO. In: *El Niño: climatología, efectos y predicción* (R. García Herrera and E. Hernández Martín, Eds.). MAPFRE, Madrid, pp. 93-131.

García-Solera, I. y Ramírez, P. (2012). Central America's seasonal climate outlook forum. *Climate Services Partnership*, 8 pp. Available at: http://www.climate-services.org/wp-content/uploads/2015/09/CRRH_Case_Study.pdf

Gill, A. (1980). Some simple solutions to the heat-induced tropical circulation. *Quarterly Journal of the Metorological Society*, 106, 447-462. https://doi.org/10.1002/qj.49710644905

Graham, F. S., Brown J. N., Wittenberg A. T. y Holbrook N. J. (2015). Reassessing conceptual models of ENSO. *Journal of Climate*, 28(23), 9121–9142. https://doi.org/10.1175/JCLI-D-14-00812.1

Hipel, W. H. y McLeod, A. L. (1994). *Time Series Modelling of Water Resources and Environmental Systems, Volume 45, 1st Edition*. Elsevier Science.

Lai, A. W., Herzog, M. y Graf H. (2018). ENSO Forecasts near the Spring Predictability Barrier and Possible Reasons for the Recently Reduced Predictability. *Journal of Climate*, 31(2), 815-838. https://doi.org/10.1175/JCLI-D-17-0180.1

Latif, M., Anderson, D., Barnett, T., Cane, M., Kleeman, R., Leetmaa, A., O'Brien, J., Rosati, A. y Schneider, E. (1998). A review of the predictability and prediction of ENSO. *Journal of Geophysical Research*, 103(C7), 14375-14393. https://doi.org/10.1029/97JC03413

Latif, M., Barnett, T.P., Cane, M.A., Fliigel M., Graham N.E., von Storch H., Xu J. S. y Zebiak S.E. (1994). A review of ENSO prediction studies. *Climate Dynamics*, 9, 167-179. https://doi.org/10.1007/BF00208250

Lima, C. H. R., Lall, U., Jeraba, T. y Barnston, A. G. (2009). Statistical Prediction of ENSO from Subsurface Sea Temperature Using a Nonlinear Dimensionality Reduction, *Journal of Climate*, 22(17), 4501–4519. DOI: https://doi.org/10.1175/2009JCLI2524.1

Lima, C.H.R., Lall, U., Jebara, T. y Barnston A.G. (2015). *Machine Learning Methods for ENSO Analysis and Prediction. In: Machine Learning and Data Mining Approaches to Climate Science*. Springer, Cham, pp. 13-21. https://doi.org/10.1007/978-3-319-17220-0_2

Ljung, G. M. y Box, G. E. P. (1978). On a measure of lack of fit in time series models. *Biometrika*, 65(2), 297-303. https://doi.org/10.1093/biomet/65.2.297

MacMartin, D. G. y Tziperman, E. (2014). Using transfer functions to quantify El Niño Southern Oscillation dynamics in data and models. *Proceedings of the Royal Society A: Mathematical, Physical & Engineering Science*, 470, 20140272. http://dx.doi.org/10.1098/rspa.2014.0272

Magaña, V., Amador, J. A. y Medina, S. (1999). The Midsummer Drought over Mexico and Central America. *Journal of Climate*, 12(6), 1577–1588. https://doi.org/10.1175/1520-0442(1999)012%3C1577:TMDOMA%3E2.0.CO;2

Marshall, J. y Plumb, A. (2007). *Atmosphere, ocean, and climate dynamics: an introductory text.* Massachusetts, Academic Press.

Moysiadis, T. y Fokianos, K. (2014). On binary and categorical time series models with feedback. *Journal of Multivariate Analysis*, 131, 209-228. https://doi.org/10.1016/j.jmva.2014.07.004

Philander, S. G. H. y Siegel, A. D. (1985). Simulation of El Niño 1982-83, *Hydrodynamic of the Equatorial Ocean.* Elsevier Science.

Philander, S. G. H. (1990). El Niño, La Niña and the Southern Oscillation. Academic Press, San Diego, CA.

Quinn, W. (1983). Long term variations in the Southern Oscillation, El Niño and Chilean subtropical rainfall. *Fishery Bulletin*, 81, 363-374.

Rasmusson, E. M. y Carpenter, T. H. (1982). Variations in the tropical sea surface wind fields associated with the Southern Oscillation/El Niño. *Monthly Weather Review*, 110, 354-384.

R Core Team. (2019). R: A language and environment for statistical computing. *R Foundation for Statistical Computing* (Version 3.6.2), Vienna, Austria. URL:(http://www.R-project.org/).

Rosenzweig, C. y Hillel, D. (2008). *Climate variability and the global harvest: impacts of El Niño and other oscillations on agroecosystems*. Oxford University Press, Inc.

Sandoval-Núñez, R. A. (2016). *Estudio de las Variaciones Oceanográficas-Atmosféricas Asociadas con las Tendencias Climáticas a partir del Año 1951*. Tesis, Magíster en Matemática, Mención en Estadística, Universidad del Bío-Bío, Concepción, Chile.

SAS. (2019). SAS® University Edition. USA: SAS Institute Inc, 2016. URL:(https://www.sas.com/en_us/home.html).

Sánchez, P. A. (2008). Cambios estructurales en series de tiempo: una revisión del estado del arte. Revista Ingenierías Universidad de Medellín, 7(12), 115-140.

Shopft P. S., and Harrison D.E., 1983. Influence of initial states on wave induced currents and warmings. Journal of Physical Oceanography, 13, 936-948.

Suárez-Moreno, R. y Rodríguez-Fonseca, B. (2015). S^{4}CAST v2.0: sea surface temperature based statistical seasonal forecast model. *Geosci. Model Dev.*, 8, 3639–3658. doi:10.5194/gmd-8-3639-2015

Trenberth, K. E. (1984). Signal versus noise in the Southern Oscillation. *Monthly Weather Review*, 112, 326-332.

Trenberth, K. E. (1997). The definition of El Niño. *Bulletin of the American Meteorological Society*, 78(12), 2771–2778.

Trenberth, K. E. y Stepaniak, D. (2001). Indices of El Niño evolution. *Journal of Climate*, 14, 1697-1701.

Ubilava, D. y Helmers, C. G. (2012). Forecasting ENSO with a smooth transition autoregressive model, *Environmental Modelling & Software*, 40, 81-190. http://dx.doi.org/10.1016/j.envsoft.2012.09.008

Wallace, J., Mitchell, T., Rasmusson, E., Kousky, V., Sarachik, E. y von Storch H. (1998). On the structure and evolution of ENSO-related climate variability in the Tropical Pacific: Lessons from TOGA. *Journal of Geophysical Research*, 103, 14,241–14,260.

Wilby, R.L. y Dawnson, C.W. (2007). *SDSM 4.2 – A decision support tool for the assessment of regional climate change impacts*. Tech. Note, UK. (Visited: July 30, 2018. Available at: https://sdsm.org.uk/).

Wright, P. B. (1985). The Southern Oscillation: An Ocean-Atmosphere Feedback System?. *Bulletin of the American Meteorological Society*, 66, 4, 398-412.

Xu, J. y von Storch, H. (1990). Predicting the state of the Southern Oscillation using POP analysis. *Journal of Climate*, 3, 1316-1329.

Zerefos, C. S. y Bais, A. F. (1997). *Solar Ultraviolet Radiation Modelling, Measurements and Effects*. New York: Springer-Verlag Berlin Heidelberg.

Zwiers, F. y von Storch, H. (1990). Regime dependent autoregressive time series modelling of the Southern Oscillation. *Journal of Climate*, 3, 1347-1363.

La Matemática recreativa en la mejora de la capacidad de resolución de problemas: caso I.E. Miguel Cortés – Castilla – Piura

María Verónica Seminario Morales *
Manuel Jesús Sánchez Chero **
Marcos Timaná Alvarez ***
José Antonio Sánchez Chero ****
Gilder Cieza Altamirano *****

RESUMEN

La presente investigación basada en la capacidad de resolución de problemas, tuvo como objetivo "Determinar el efecto de la matemática recreativa en la mejora de la capacidad de resolución de problemas en alumnos del primero de secundaria de la IE Miguel Cortés– Castilla"; basado en el método de Polya. Su importancia radica en que servirá como soporte didáctico para el trabajo del docente. Esta investigación experimental, cuasi experimental, trabajó con dos grupos no equivalentes. La muestra fue de 50 alumnos y se les aplicó un pre test y post test, cuya hipótesis se validó con la t de Student. Los resultados mostraron que antes del cuasi experimento las t calculadas eran menores que las t de tablas, además en el post test el grupo experimental en las tres capacidades de estudio sobre un total de 60 puntos, obtuvieron una diferencia de incrementos a su favor de 8.52 puntos. Por lo que se afirma que el grupo experimental ha tenido efectos positivos después de haberles aplicado el programa, en comparación con el grupo control. Con estos resultados se estima haber contribuido con los docentes en mención y con la ciencia matemática en el mejoramiento de la capacidad de resolución de problemas.

PALABRAS CLAVE: Matemática recreativa, pre test, post test, cuasi experimental, programa.

* Docente Auxiliar. Universidad Nacional de Frontera. Perú. https://orcid.org/0000-0002-6787-7371
** Docente Investigador. Universidad Señor de Sipán S.A.C., Perú. https://orcid.org/0000-0003-1646-3037. E-mail: manuelsanchezchero@gmail.com
*** Docente Auxiliar. Universidad Nacional de Frontera. Perú. https://orcid.org/0000-0002-4222-7372
**** Docente Auxiliar. Universidad Nacional de Frontera. Perú. https://orcid.org/0000-0002-3157-8935
***** Licenciado en Matemáticas. Universidad Nacional Autónoma de Chota. Perú. https://orcid.org/0000-0002-7936-1495

Recibido: 22/04/2020 Aceptado: 25/06/2020

Recreational Mathematics in improving problem solving capacity: case I.E. Miguel Cortés - Castilla - Piura

ABSTRACT

This research based in the capacity of solving problems, the objective was to "determine the effect of the of recreational mathematics on improving the ability of the seventh grade students at Miguel Cortés School to solve problems"; this program was based on the method of Polya and took place in Castilla. Its importance is to serve as a didactic support for the work of teachers. This experimental research, quasi-experimental, worked with two non-equivalent groups. The sample consisted of 50 students and answered a pre-test and post-test, the hypothesis was validated with the Student t. The results showed that before the t test calculated quasi-experiment were lower than t table, besides in the post-test the experimental group in all three study capacities on a total of 60 points, a difference of increments obtained for the experimental group of 8.52 points. By what affirms the experimental group had positive effects after the application of the program, compared with the control group. With these results is estimated to have contributed with teachers in mention and with the mathematical science on improving the capacity of solving problems.

KEYWORDS: Recreational mathematics, pre-test, post-test, quasi-experimental, program.

Introducción

La capacidad de resolución de problemas cobra gran importancia en la tarea educativa de los docentes especialmente de matemática. Esta se convierte en un conjunto de conocimientos que, al ser utilizados mediante habilidades de pensamiento matemático en distintas situaciones, generan destrezas que permiten organizar información y procesarla para encontrar la solución de situaciones problemáticas (Ministerio de Educación del Perú, 2001).

Las investigaciones que tienen una estrecha relación con el presente trabajo son las siguientes:

Alzamora (2002), "Técnicas Lúdicas grupales para despertar el interés por la matemática en tercer grado de primaria del Colegio San Ignacio de Loyola del distrito de Castilla", quien concluyó que: La aplicación de técnicas lúdicas grupales, permiten que los alumnos de diferentes

niveles y capacidades establezcan entre ellos procesos de ayuda, comentarios, permitiendo avanzar a todos ellos en el cálculo oral y escrito. Además, las técnicas lúdicas proporcionan en los alumnos un valor motivacional, actitudinal y de predisposición al estudio de la matemática, promoviendo el proceso de socialización estableciendo relaciones de aceptación, de cumplimiento de reglas; también fomenta valores educativos como saber escuchar, conversar, convencer, comunicar, establecer estrategias, reconocer sus propias capacidades y las de sus compañeros.

Así mismo la investigación de Jara et al. (2010) de la Universidad Nacional de Educación Enrique Guzmán y Valle de Lima- Perú, "Modelos de Interacción como estrategia metodológica en la resolución de problemas para el aprendizaje de la matemática en los alumnos del 6to. grado de educación primaria, en las Instituciones Educativas Estatales, UGEL Nº 1, San Juan de Miraflores". Concluyeron que los modelos de resolución de problemas: normativo, iniciativo, aproximativo, Pólya, y Guzmán ayudan a los estudiantes en el aprendizaje del área de Matemática, conjuntamente con la aplicación de estrategias para la resolución de problemas matemáticos ayuda a mejorar en forma significativa el rendimiento conceptual de los alumnos en el área de Matemática.

En esta investigación el problema fue: ¿Es posible mejorar la capacidad de resolución de problemas en los alumnos del primero de secundaria de la Institución Educativa Miguel Cortés, mediante la aplicación de la matemática recreativa? Y su objetivo general: determinar el efecto del programa experimental de matemática recreativa en el mejoramiento de la capacidad de resolución de problemas en alumnos del primero de secundaria de la IE Miguel Cortés– Castilla, basado en el método de Polya (1957). Así mismo sus objetivos específicos fueron: Determinar y comparar el nivel de logro de la capacidad de resolución de problemas en el área de matemática en los alumnos del grupo experimental y del grupo control antes de cuasi experimento; evaluar y comparar el nivel de logro de la capacidad de resolución de problemas de los alumnos del grupo experimental y grupo control después del cuasi experimento. Se trabajó con 50 alumnos (25 grupo experimental y 25 grupo control). Su importancia radica en que servirá como soporte didáctico para el trabajo del docente.

1. Metodología

Para la presente investigación se aplicó el diseño Cuasi-experimental, se trabajó con dos grupos no equivalentes; grupo experimental y grupo control.

Los instrumentos empleados fueron: prueba escrita: Pre test- Post test, guía de análisis de documentos, escala de Likert, y lista de cotejo; los cuales se aplicaron durante las sesiones de aprendizaje al grupo experimental; para el grupo control sólo se aplicó la prueba escrita antes y después de la aplicación del programa. Estos instrumentos fueron validados por especialistas en el tema. Y un profesional de estadística para que opine sobre la confiabilidad de dichos instrumentos, se dió confiabilidad de 0.878 (confiabilidad alta- Alfa de Cronbach) a la Escala de Likert más no a los demás instrumentos.

La información recogida fue sistematizada en tablas con su descripción correspondiente. Se hizo uso de las medidas estadísticas: media aritmética, varianza, desviación estándar; en la interpretación de los resultados se procedió a tener en cuenta los promedios y luego se aplicó la prueba t de Student para muestras relacionadas con el objeto de comparar los resultados obtenidos en la aplicación de la prueba exploratoria, tanto al inicio como al final del cuasi-experimento.

2. Resultados

Objetivo 1: Determinar y comparar el nivel de logro de la capacidad de resolución de problemas en el área de matemática en los alumnos del grupo experimental y del grupo control antes de cuasi experimento.

De acuerdo a la tabla 1, se aprecia que los alumnos del grupo experimental, en la capacidad 1: "Aplica los conceptos de divisor, múltiplo, criterios de la divisibilidad, MCD y MCM" alcanzaron según la escala vigesimal una media aritmética de 9.52 puntos, mientras que los del grupo control 12.56 puntos. Respecto a la capacidad 2: "Aplica la adición y sustracción de números enteros", los alumnos del grupo experimental, obtuvieron según la escala vigesimal una media aritmética de 10.2 puntos, en cambio los del grupo control 11.16 puntos. En relación con la capacidad 3: "Analiza situaciones que involucran números racionales", los alumnos del grupo experimental consiguieron de acuerdo a la escala vigesimal una media aritmética de 6.64 puntos, en tanto que los del grupo control 7.76 puntos. En los resultados generales de la prueba escrita aplicada, los alumnos del grupo experimental, lograron sobre un puntaje total de 60 puntos, una

media aritmética de 26.36 puntos, pero los del grupo control 31.48 puntos. La tabla evidenció que los resultados de la t calculada de las tres capacidades mencionadas anteriormente y el resultado total de la prueba, al compararlo con la t de tabla, todos estos valores son menores; deducciones que son coherentes con la teoría científica de la t-Student.

Tabla 1. RESULTADOS DE LA T- STUDENT DEL PRE TEST

CAPACIDADES	GRUPO EXPERIMENTAL			GRUPO CONTROL			t CALCULADA COMPUTO	t TABLA	GRADOS DE LIBERTAD	NIVEL DE SIGNIFICANCIA	NIVEL DE CONFIANZA
	n=25			n=25							
	$\overline{X}$	S^2	S	$\overline{X}$	S^2	S					
CAPACIDAD 1	9.52	4.0896	2.02	12.56	2.73	1.65	-5.82	-1.67	48	0.05	0.95
CAPACIDAD 2	10.2	2.88	1.70	11.16	3.49	1.87	-1.90				
CAPACIDAD 3	6.64	2.79	1.67	7.76	1.54	1.24	-2.69				
TOTAL	26.36	12.23	3.50	31.48	8.41	2.90	-5.63				

Fuente: Resultados Pre test

Objetivo 2: Evaluar y comparar el nivel de logro de la capacidad de resolución de problemas de los alumnos del grupo experimental y grupo control después del cuasi experimento.

En la tabla 2 se puede observar, que los alumnos del grupo experimental, en la capacidad 1: "Aplica los conceptos de divisor, múltiplo, criterios de la divisibilidad, MCD y MCM" obtuvieron según la escala vigesimal una media aritmética de 14.04 puntos, en tanto que los del grupo control 14.88 puntos. En la capacidad 2: "Aplica la adición y sustracción de números enteros" los alumnos del grupo experimental lograron según la escala vigesimal una media aritmética de 14.64 puntos, mientras que los del grupo control 12.4 puntos. También se puede apreciar que los alumnos del grupo experimental, con respecto a la capacidad 3: "Analiza situaciones que involucran números racionales", alcanzaron según la escala vigesimal una media aritmética de 12.2 puntos, pero los del grupo control 10.2 puntos. De igual forma los alumnos del grupo experimental, con respecto a los resultados generales de la prueba escrita aplicada obtuvieron sobre un puntaje total de 60 puntos, una media aritmética de 40.88 puntos, mientras

que los del grupo control 37.48 puntos. En los resultados de la t calculada de las tres capacidades mencionadas anteriormente y el resultado total de la prueba y al compararlo con la t de tabla, los valores de la capacidad 2, 3 y el total son mayores, resultados que son coherentes con la teoría científica de la t-Student; sin embargo: el resultado de la capacidad 1 ha sido menor.

Tabla 2. RESULTADOS DE LA T - STUDENT DEL POST TEST

CAPACIDADES	GRUPO EXPERIMENTAL n=25			GRUPO CONTROL n=25			t CALCULADA COMPUTO	t TABLA	GRADOS DE LIBERTAD	NIVEL DE SIGNIFICANCIA	NIVEL DE CONFIANZA
	$\overline{X}$	S^2	S	$\overline{X}$	S^2	S					
CAPACIDAD 1	14.04	3.00	1.73	14.88	1.39	1.18	-2.01	1.67	48	0.05	0.95
CAPACIDAD 2	14.64	2.39	1.55	12.4	1.68	1.30	5.55				
CAPACIDAD 3	12.2	2.96	1.72	10.2	1.20	1.10	4.90				
TOTAL	40.88	10.11	3.18	37.48	5.45	2.33	4.31				

Fuente: Resultados Post test

Objetivo 3. Determinar el efecto del programa experimental de matemática recreativa en la mejora de la capacidad de resolución de problemas en alumnos del primero de secundaria de la IE Miguel Cortés– Castilla.

Con respecto a la capacidad 1 el puntaje de ganancia de los estudiantes del grupo experimental, entre el pre test y el post test, fue de 4.52 puntos según la escala vigesimal, mientras que en los estudiantes del grupo control fue de 2.32 puntos; lo que demuestra una diferencia de incrementos a favor del grupo experimental de 2,20 puntos. En relación con la capacidad 2, el puntaje de ganancia de los estudiantes del grupo experimental, entre el pre test y el post test, fue de 4.44 puntos según la escala vigesimal, pero en los estudiantes del grupo control fue de 1.24 puntos; destacando una diferencia de incrementos a favor del grupo experimental de 3.20 puntos. Con respecto a la capacidad 3, el puntaje de ganancia de los estudiantes del grupo experimental, entre el pre test y el post test, fue de 5.56 puntos según la escala vigesimal, en tanto en los estudiantes del grupo control fue de 2.44 puntos; registrándose una diferencia de incrementos a favor del grupo experimental de 3.12 puntos. Se evidencia, respecto al total de 60 puntos, que el puntaje de ganancia de los estudiantes del grupo

experimental, entre el pre test y el post test, fue de 14.52 puntos, mientras que en los estudiantes del grupo control fue de 6.00 puntos; lo que muestra una diferencia de incrementos a favor del grupo experimental de 8.52 puntos. Así mismo se encontró que antes del cuasi experimento (Pre test) el grupo experimental tenía menor nivel de logro en la Capacidad de resolución de problemas, y en sus tres capacidades especificas del área de matemática que el grupo control, además las t calculadas eran menores que las t de tablas, mientras que después del cuasi experimento (Post Test) el grupo experimental tiene mayor nivel de logro en la Capacidad de resolución de problemas, y en las capacidades 2 y 3 y en el total del área de matemática que el grupo control, rechazando las respectivas hipótesis nulas, razón por la cual se afirma que las hipótesis de investigación quedan aceptadas (Hernández et al., 2010).

Tabla 3. **EFECTOS DEL PROGRAMA EXPERIMENTAL DE MATEMÁTICA RECREATIVA EN LA MEJORA DE LA CAPACIDAD DE RESOLUCIÓN DE PROBLEMAS EN ALUMNOS DEL PRIMERO DE SECUNDARIA DE LA IE MIGUEL CORTÉS– CASTILLA.**

CAPACIDADES	Grupo Experimental(n=25)							Grupo Control(n=25)							Diferencia de $\Delta\bar{y}$
	Pre Prueba			Post Prueba			Ptje Ganancia	Pre Prueba			Post Prueba			Ptje Ganancia	
	$\bar{y}$	S^2	S	$\bar{y}$	S^2	S	$\Delta\bar{y}$	$\bar{y}$	S^2	S	$\bar{y}$	S^2	S	$\Delta\bar{y}$	
C-1	9,52	4,09	2,02	14,04	3,00	1,73	4,52	12,56	2,73	1,65	14,88	1,39	1,18	2,32	2,20
C-2	10,2	2,88	1,70	14,64	2,39	1,55	4,44	11,16	3,49	1,87	12,4	1,68	1,30	1,24	3,20
C-3	6,64	2,79	1,67	12,2	2,96	1,72	5,56	7,76	1,54	1,24	10,2	1,20	1,10	2,44	3,12
Total	26,36	12,23	3,50	40,88	10,11	3,18	14,52	31,48	8,41	2,90	37,48	5,45	2,33	6,00	8,52

3. Discusión

Los resultados antes de la aplicación del programa no son coherentes con lo que manifiesta el Ministerio de Educación del Perú (2006: 19), el cual sugiere que durante la resolución de problemas a los estudiantes se les permita que observen, analicen, reflexionen, comprueben y expliquen las estrategias utilizadas, las hipótesis formuladas; a través de medios y materiales concretos, representaciones gráficas, cálculos y expresiones analíticas que les permita comprender y resolver problemas. Los estudiantes desarrollan habilidades como:

Identificar y comprender situaciones matemáticas del contexto. Analizan con sentido crítico, comprenden información oral, gráfica y textual de situaciones reales o simuladas para ser resueltas. Dada una situación problemática ya sea en forma oral, gráfica o simbólica reconocen información importante, las partes, la condición, que se sabe, que no se sabe, cuáles fueron las soluciones posibles, etc. Usan materiales concretos, representaciones gráficas, cálculos aritméticos, en suma, utilizan recursos conforme a las condiciones del problema para su resolución. También estos resultados se corroboran según la investigación realizada por Del Valle y Margarita (2008), titulada "La resolución de problemas como estrategia de enseñanza y aprendizaje" quienes concluyeron que de acuerdo a los participantes de la muestra la enseñanza y aprendizaje de la Resolución de Problemas, están estrechamente vinculados a procesos repetitivos y a acciones que validan este proceso resolutivo. Sin embargo, el juicio crítico carece de sentido si el estudiante no cambia estas formas, estas acciones repetitivas con el fin de obtener mejores calificaciones sacrificando su aprendizaje.

Corresponde al docente dar las herramientas y los elementos que permitan que el estudiante desarrolle sus estrategias de aprendizaje y elementos metacognitivos que contribuyan en su aprendizaje. El profesor debe presentar las actividades y orientar su discurso de tal forma que el estudiante pueda reconocer de otras maneras los fenómenos, de reflexionar y de explicar sobre ellos. Para ello es necesario que se produzca un cambio en la forma de conceptualizar y entender que es enseñar. Esta investigación dio mucho aporte para el desarrollo del programa experimental.

Los resultados después de la aplicación del programa son coherentes como lo que manifiesta Paulo Abrantes citado por Giménez et al (2007: 117): Para aprender matemáticas hay que "hacer matemáticas" y cuando hacemos matemáticas hemos de desarrollar las capacidades de resolver problemas y razonar. Al mismo tiempo que estimulamos el valor de las matemáticas y damos confianza a los alumnos y alumnas.

De la misma manera lo expresa Giménez et al. (2007: 118), promover el aprendizaje cooperativo y el trabajo en grupo. Resolver una problemática en grupo implica descubrir, razonar, intercomunicar, compartir, explicar, aprender, enseñar descubriendo las matemáticas como una actividad que permite la interacción y comunicación. Y también Alzamora, en su trabajo de investigación denominado Técnicas Lúdicas grupales para despertar el interés por la

matemática en tercer grado de primaria del Colegio San Ignacio de Loyola del distrito de Castilla, concluyó que: La aplicación de técnicas lúdicas grupales, permiten que los alumnos de diferentes niveles y capacidades establezcan entre ellos procesos de ayuda, comentarios, permitiendo avanzar a todos ellos en el cálculo oral y escrito. Las técnicas lúdicas proporcionan en los alumnos un valor motivacional, actitudinal y de predisposición al estudio de la matemática, promoviendo el proceso de socialización estableciendo relaciones de aceptación, de cumplimiento de reglas; también fomenta valores educativos como saber escuchar, conversar, convencer, comunicar, establecer estrategias, reconocer sus propias capacidades y las de sus compañeros. En el proceso de enseñanza aprendizaje de la matemática es efectiva la metodología lúdica pues fomenta la socialización, promueve destrezas, habilidades, fomenta la creatividad y sobre todo despierta el interés por el estudio.

En los resultados también observamos que antes del cuasi experimento las t calculadas eran menores que las t de tablas, mientras que después del cuasi experimento (Post Test) el grupo experimental tuvo mayor nivel de logro en la capacidad de resolución de problemas, y en las capacidades 2 y 3 y en el total del área de matemática que el grupo control, rechazando la respectivas hipótesis nulas, razón por la cual se afirma que las hipótesis de investigación quedan aceptadas (Hernández et al, 2010).

La información anterior corrobora con lo que especifica el Ministerio de Educación del Perú (2009: 186):

> "Ser competente matemáticamente supone tener habilidad para usar los conocimientos con flexibilidad y aplicar con propiedad lo aprendido en diferentes contextos. Es necesario que los estudiantes desarrollen capacidades, conocimientos y actitudes matemáticas, pues cada vez más se hace necesario el uso del pensamiento matemático y del razonamiento lógico en el transcurso de sus vidas: matemática como ciencia, como parte de la herencia cultural y uno de los mayores logros culturales e intelectuales de la humanidad; matemática para el trabajo, porque es fundamental para enfrentar gran parte de la problemática vinculada a cualquier trabajo; matemática para la ciencia y la tecnología, porque la evolución científica y tecnológica requiere de mayores conocimientos matemáticos y en mayor profundidad."

Los hallazgos, tanto de los resultados como del sustento teórico son avalados por el trabajo de investigación de Jara et al. (2010) de la Universidad Nacional de Educación Enrique Guzmán y Valle de Lima- Perú, quienes en su trabajo titulado "Modelos de Interacción como estrategia

metodológica en la resolución de problemas para el aprendizaje de la matemática en los alumnos del 6to. grado de educación primaria, en las Instituciones Educativas Estatales, UGEL Nº 1, San Juan de Miraflores"; concluyeron que los modelos de resolución de problemas: normativo, iniciativo, aproximativo (Pólya, 1957) ayudan a los estudiantes en el aprendizaje del área de Matemática, conjuntamente con la aplicación de estrategias para la resolución de problemas matemáticos ayuda a mejorar en forma significativa el rendimiento conceptual de los alumnos en el área de Matemática.

Conclusiones

Analizando los resultados de todo el proceso de Investigación incluyendo la aplicación del programa de Matemática Recreativa para mejorar la capacidad de resolución de problemas en los alumnos, se afirma lo siguiente:

- Los alumnos del grupo experimental, antes del cuasi experimento, en la capacidad 1, capacidad 2 y capacidad 3, obtuvieron una media aritmética menor que los del grupo control y lo mismo se obtuvo en los resultados generales.
- Los alumnos del grupo experimental, después del cuasi experimento, en la capacidad 2, capacidad 3 y en el total lograron mejores resultados que los alumnos del grupo control con excepción de la capacidad 1.
- Los alumnos del grupo experimental han tenido efectos positivos después de haberles aplicado el programa porque en las tres capacidades sobre un total de 60 puntos, se mostró una diferencia de incrementos a favor del grupo experimental de 8.52 puntos. Además, antes del cuasi experimento las t calculadas eran menores que las t de tablas, mientras que después del cuasi experimento (Post Test) el grupo experimental tuvo mayor nivel de logro en la capacidad de resolución de problemas, y en las capacidades 2 y 3 y en el total del área de matemática que el grupo control, rechazando las respectivas hipótesis nulas, razón por la cual se afirma que las hipótesis de investigación quedan aceptadas (Hernández et al., 2010).

Referencias

Alzamora, T. Z. (2002). *Técnicas lúdicas grupales para despertar el interés por la matemática en tercer grado*

de primaria (Tesis de Maestría). Universidad Nacional de Piura. Piura

Del Valle Coronel, M. y Margarita Curotto, M. (2008). La resolución de problemas como estrategia de enseñanza aprendizaje. *Revista Electrónica de Enseñanza de las Ciencias*. Volumen 7, Número 2. http://www.saum.uvigo.es/reec/volumenes/volumen7/ART11_Vol7_N2.pdf

Giménez, J., Santos, L. y Da Ponte, P. (2007). *La actividad matemática en el aula. Homenaje a Paulo Abrantes.* Segunda edición. Barcelona: GRAO de IRIF, S. L.

Hernández, R., Fernández, C., Baptista, L. (2010). *Metodología de la investigación, Vol (5)*. México: McGraw-Hill

Jara, M., y otros (2010). Modelos de Interacción como Estrategia Metodológica en la Resolución de Problemas para el Aprendizaje de la Matemática en los alumnos del 6to. Grado de Educación Primaria, en las Instituciones Educativas Estatales, UGEL Nº 1, San Juan de Miraflores. Lima, Perú: Universidad Nacional de Educación Enrique Guzmán y Valle. Dirección del Instituto de Investigación. Recuperado de http://goo.gl/WxNbn

Ministerio de Educación del Perú (2009). *Diseño Curricular Nacional de Educación Básica Regular.* Lima: Fimart S.A.C Editores e Impresores.

Ministerio de Educación del Perú (2006). *Orientaciones para el Trabajo Pedagógico de Matemática* Lima: Fimart S.A.C Impresores

Ministerio de Educación del Perú (2001). *Capacitación Docente en Formación Continua*. Curso para Consultores. Huampaní. Lima. Perú. Recuperado de http://goo.gl/UU7jc

Pólya, G. (1957). How to Solve It.A new aspect of Mathematical Method.2nd. Edition. New Jersey: Princeton University Press. Disponible en http://www.hep.manchester.ac.uk/u/hywel/downloads/polya.pdf

Simplificación del cálculo del volumen de activación y el valor zP para los modelos lineales de inactivación microbiana, enzimática o retención nutricional

William Rolando Miranda Zamora *
Manuel Jesús Sánchez Chero **
José Antonio Sánchez Chero ***
Karina Gutiérrez Valverde ****

RESUMEN

Los cálculos de procesos de alta presión hidrostática implican cinéticas de reacción de primer orden las cuales han sido comúnmente descritas por el método del tiempo de muerte de presión en el campo de la ingeniería de los alimentos. El objetivo de esta investigación fue revisar un análisis de varios ejemplos recogidos de la literatura científica de la metodología de simplificación. Los datos para obtener las constantes de volumen de activación (Va) y las constantes de resistencia a la presión (zP) han sido recuperados de la literatura y clasificados en microorganismos, enzimas y nutrientes. La mayoría de los datos están disponibles en la forma de ecuaciones por lo que ha sido necesario escoger literatura que cuenta con los datos para poder volver a calcular con el nuevo planteamiento la constante de volumen de activación (Va) y la constante de resistencia a la presión (zP). Los resultados de las ecuaciones con el nuevo procedimiento predicen tan igual que las de la literatura, pero éstas permiten el fácil manejo de los datos cinéticos con solamente un ajuste, como se muestran hasta ocho (8) maneras de poder determinar las constantes de Va y valor zP, que son resumidas en tablas.

PALABRAS CLAVE: Volumen de activación; valor zP; alta presión hidrostática; reacción de primer orden.

* Docente Asociado. Universidad Nacional de Frontera. Perú. https://orcid.org/0000-0002-0829-2568.
** Docente Investigador. Universidad Señor de Sipán S.A.C., Perú. https://orcid.org/0000-0003-1646-3037. E-mail: manuelsanchezchero@gmail.com
*** Docente. Universidad César Vallejo. Perú. https://orcid.org/0000-0002-3157-8935
**** Docente. Universidad Nacional de Frontera. Perú. https://orcid.org/0000-0001-8079-8371

Recibido: 30/04/2020 Aceptado: 25/06/2020

Simplification of the calculation of the activation volume and the zP value for the linear models of microbial, enzymatic, or nutritional retention

ABSTRACT

Calculations of high hydrostatic pressure processes involve first order reaction kinetics which have been commonly described by the pressure death time method in the field of food engineering. The aim of this research was to review an analysis of several examples collected from the scientific literature of the simplification methodology. The data to obtain the activation volume constants (Va) and the pressure resistance constants (zP) have been recovered from the literature and classified into microorganisms, enzymes and nutrients. Most of the data are available in the form of equations so it has been necessary to choose literature that has the data in order to recalculate the activation volume constant (Va) and the pressure resistance constant (zP) with the new approach. The results of the equations with the new procedure predict as well as those of the literature, but they allow the easy handling of the kinetic data with only one adjustment, as shown up to eight (8) ways to be able to determine the constants of Va and zP value, which are summarized in tables.

KEYWORDS: Activation volume; zP value; high hydrostatic pressure; first order reaction.

Introducción

El proceso de pascalización (como un homenaje a Blaise Pascal) (Jay et al., 2005), bridgmanización, (como un homenaje a Percy Williams Bridgman Nobel de física en 1946 por su trabajo de la física de las altas presiones) (Leake, 2018), alta presión (HP por sus siglas en inglés) (Evrendilek, 2018; Parekh et al., 2017), ultra alta presión (UHP por sus siglas en inglés) (Lin et al., 2017), alta presión (Calzada, 2015; Barboza-Cánovas y Bermudez-Aguirre, 2010) o alta presión hidrostática (HHP por sus siglas en inglés) (Ruiz, 2017, Andrés, 2016, Toledo et al., 2015) es un método para conservar los alimentos. El procesamiento con alta presión hidrostática ha sido considerado una tecnología innovadora en el procesamiento de alimentos debido a su procesamiento mínimo de las características técnicas de los productos alimentarios (Jia et al., 2019). El proceso de alta presión hidrostática, como un proceso no térmico, puede usarse para inactivar microorganismos mientras se minimizan las reacciones químicas (color, sabor y nutrición), conservando así la frescura de los alimentos (Huang et al. 2014). La alta presión hidrostática permite procesar

alimentos seguros de alta calidad. La determinación de los parámetros de la velocidad de inactivación microbiana, enzimática o retención tales como los valores DP y zP se da para caracterizar la reducción microbiana o la retención de nutrientes bajo presión hidrostática. La alta presión hidrostática para alimentos se aplica desde 100 MPa a más (Yamamoto, 2017) a temperatura ambiente o calor moderado (Jia et al., 2019).

Este artículo presenta una metodología para manejar datos de prueba utilizando curvas de tipo semilogarítmico para determinar a partir de la pendiente de una sola curva tanto él Va como el valor zP. Las curvas de tipo semilogarítmico son útiles para verificar la unicidad de la solución.

El efecto de la presión en las reacciones alimentarias se explica a través de la teoría del estado de transición (Eyring, 1935), el cual considera al volumen de activación (Eyring y Magee, 1942; Stearn y Eyring, 1941), en el estado de transición de la reacción. En el estado de transición de la reacción (Hernalsteens y Pereira, 2019), la dependencia de la temperatura de una constante de velocidad k sobre la presión P se puede expresar como:

$$\left(\frac{\partial \ln k}{\partial P}\right)_T = -\frac{V_a}{RT} \qquad (1)$$

Siendo: P = presión (MPa), k = constante de velocidad de reacción (min-1), R = constante de los gases (8,3144 m3 MPa (mol K)-1 en el sistema internacional de unidades), T = temperatura absoluta (K en el sistema internacional de unidades), Va = volumen de activación (m3/mol).

Los efectos de presión correspondientes en los valores de Ea son los mostrados en la Tabla 1.

Tabla 1. Efectos de la presión sobre la Ea.

Va	Ea
‹ 0 (negativo)	Disminuye
= 0	sin cambio
› 0 (positivo)	Aumenta

Los efectos de presión correspondientes en la velocidad de reacción se muestran en la Tabla 2.

Tabla 2. Efectos de la presión sobre la velocidad de reacción.

Va	Velocidad de reacción
‹ 0 (negativo)	Aumenta
= 0	sin cambio
› 0 (positivo)	Disminuye

Cuanto mayor es la magnitud del Va (positiva o negativa), mayor es la sensibilidad de una reacción química a la presión, mientras que las reacciones con Va = 0 son independientes de la presión (Valdez-Fragoso et al., 2011; Mussa y Ramaswamy, 1997).

Para el caso de un nutriente, un volumen de activación negativo (Va ‹ 0) indica que la degradación del nutriente aumenta con un aumento de la presión (Tola y Ramaswamy, 2015).

El principio de Henri-Louis Le Châtelier (Le Châtelier, 1884, Le Châtelier, 1888) o denominado el principio de Le Châtelier-Braun (De Heer, 1957; Ehrenfest, 1911; Braun, 1887; Braun, 1888) en honor a Karl Ferdinand Braun (Süsskind, 1980) establece que "un sistema químico en condiciones de equilibrio experimentaría un cambio de reacción, acompañado de una disminución en el volumen cuando aumenta la presión y viceversa" (Jaeger et al., 2012; Yordanov y Angelova, 2010; Butz y Tauscher, 1998). Según este principio, cuando se altera el equilibrio de un sistema, el sistema responde para minimizar la perturbación acelerando las reacciones asociadas con la reducción de volumen y suprimiendo las reacciones que conducen a un aumento en el volumen (Anandharamakrishnan & Ishwarya, 2019).

La dependencia de la presión del valor DP se expresa mediante el valor zP a temperatura constante, por ejemplo, cuando un incremento de 200 MPa en la presión del proceso cambia el valor D de 20 a 2 min, el valor zP es 200 MPa (Farkas y Hoover, 2000) y de manera viceversa la dependencia de la temperatura del valor DT se expresa mediante el valor zT a presión constante (Miranda-Zamora y Heldman, 2018) (Tabla 3).

Existen muchas formas de encontrar el volumen de activación, Va y el valor zP a partir de los datos de las constantes de velocidad de reacción, si fueran los años en los que Hite (1899) usó la alta presión hidrostática para procesar leche se usaría el papel semilogarítmico, que tiene un eje en una escala logarítmica y el otro en una escala lineal, para encontrar la pendiente entre las constantes de activación, k y la presión a una

temperatura constante, T, tal como se aprecia en la Figura 1. Es común su uso en la literatura científica.

Tabla 3. Constantes de tiempo de reducción decimal y de resistencia a la temperatura y presión.

Valor	a temperatura constante	a presión constante
DT		Tiempo de reducción decimal. Se calcula a partir de curvas de sobrevivientes o retenciones de concentración trazadas.
DP	Tiempo de reducción decimal. Se calcula a partir de curvas de sobrevivientes o retenciones de concentración trazadas.	
zP	Resistencia a la presión. La presión requerida para reducir el valor DP en un 90%.	
zT		Resistencia térmica. La temperatura requerida para reducir el valor DT en un 90% o en un factor de 10 .

Fuente: Adaptado de Tola y Ramaswamy (2015), Patazca et al. (2006), Mussa y Ramaswamy (1997).

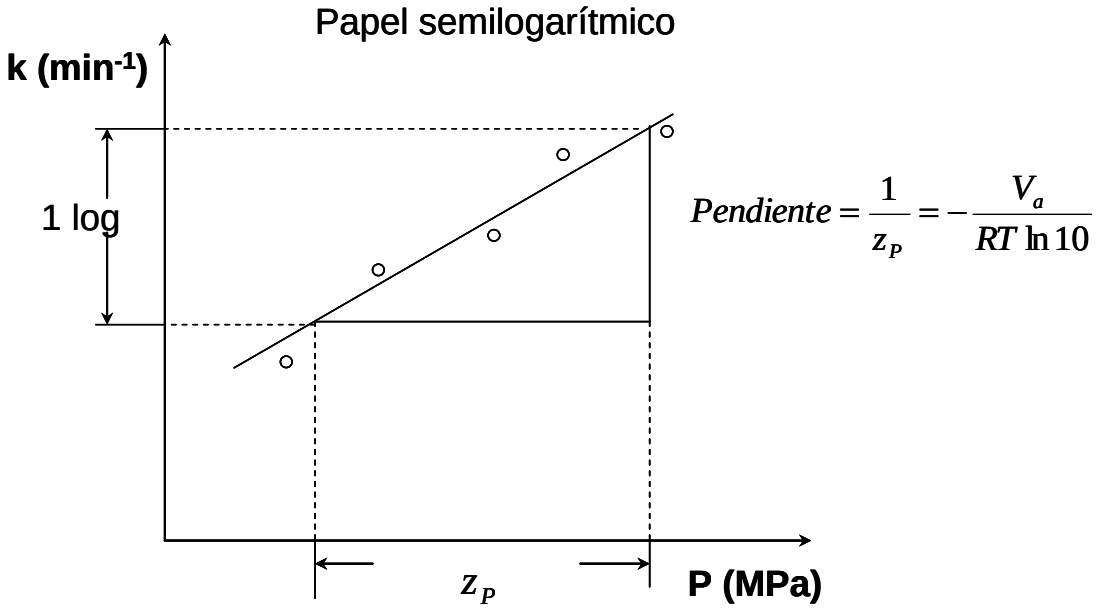

Figura 1. Determinación gráfica del valor zP y del volumen de activación. Gráfica entre la constante de activación, k y la presión.

La pendiente del ajuste lineal nos permite encontrar el volumen de activación, Va y el valor zP.

La segunda forma de encontrar el volumen de activación y el valor zP usando el papel semilogarítmico es graficando el 1/k versus la presión, a una temperatura constante, T, tal como se aprecia en la Figura 2.

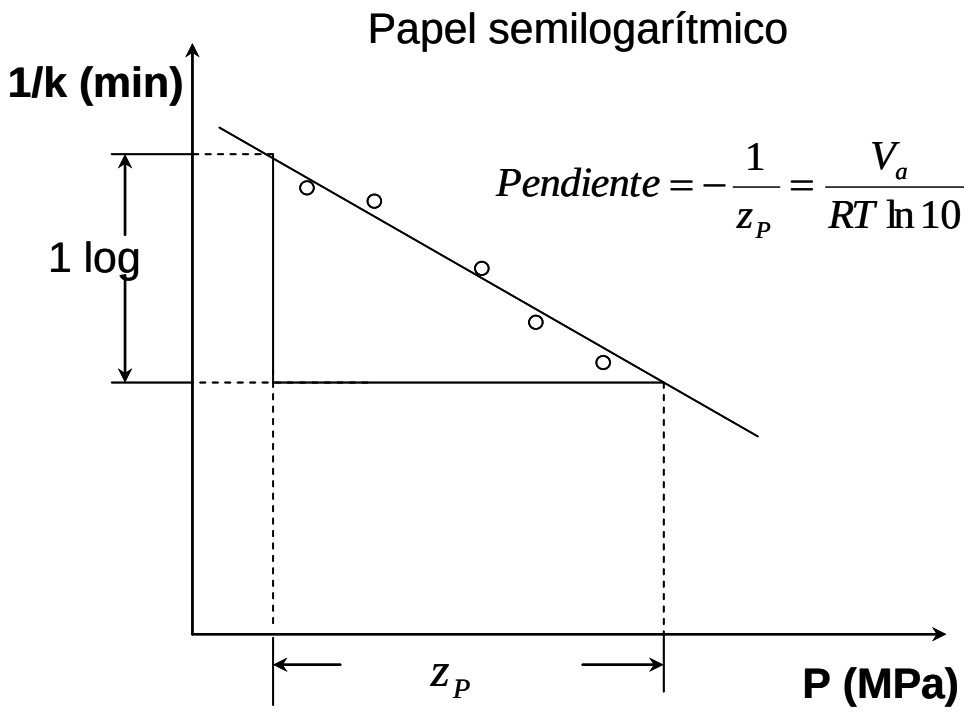

Figura 2. Determinación gráfica del valor zP y del volumen de activación. Gráfica entre el inverso de la constante de activación, 1/k y la presión. Se plantea su uso.

Una tercera forma de encontrar el volumen de activación y el valor zP usando el papel semilogarítmico es graficando el valor DP versus la presión, a una temperatura constante, T, tal como se aprecia en la Figura 3. Es común su uso en la literatura científica.

Una cuarta forma de encontrar el volumen de activación y el valor zP usando el papel semilogarítmico es graficando el valor 1/DP versus la presión, a una temperatura constante, T, tal como se aprecia en la Figura 4.

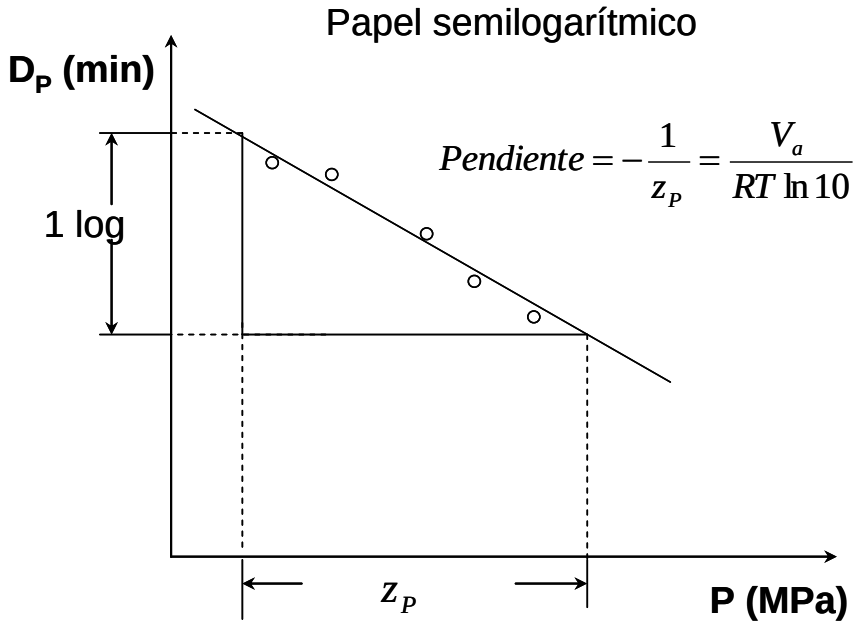

Figura 3. Determinación gráfica del valor zP y del volumen de activación. Gráfica entre el valor DP y la presión.

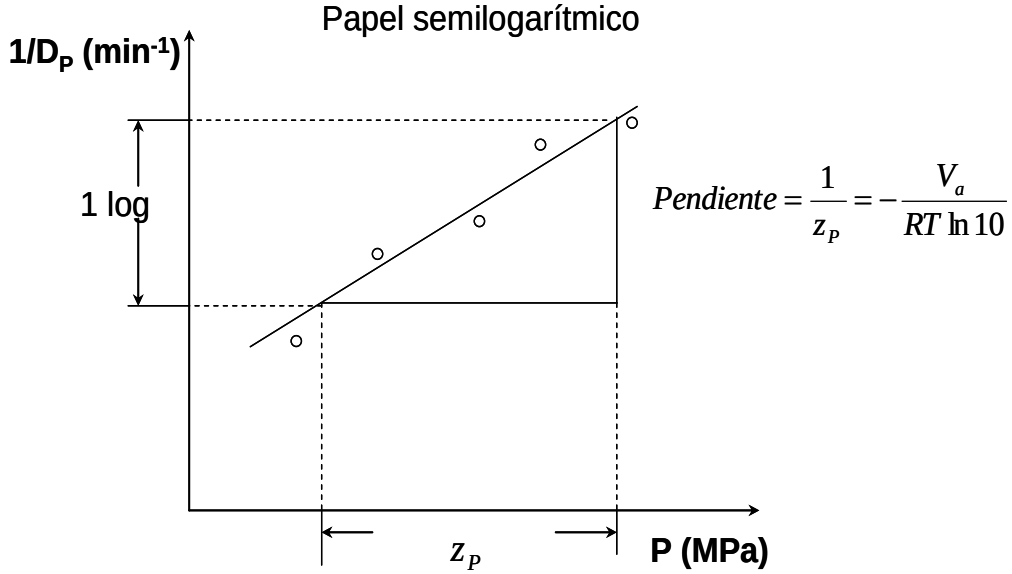

Figura 4. Determinación gráfica del valor zP y del volumen de activación. Gráfica entre el valor 1/DP y la presión. Se plantea su uso.

El papel gráfico semilogarítmico (Theodore y Behan, 2018; Roe et al., 2018; Turgeon, 2015; Yang, 2015; Onur y Palabiyik, 2015) facilita el trazado los procesos exponenciales ya que se asumen líneas rectas.

Al no encontrarnos en los años que vivió Hite (1866-1921) (Leake, 2018) tenemos que utilizar las herramientas computacionales como las hojas de cálculo: VisiCalc (Parsons, 2017), SuperCalc (Gassner, 1985), Lotus 1-2-3 (Sachs, 2007) y en la actualidad Excel de Microsoft (Poli, 2019; Guerrero, 2019; Alexander y Kusleika, 2019; Tiziano, 2019; Alexander y Kusleika, 2018; Quirk, 2013). El Excel es una herramienta utilizada en ingeniería de alimentos (Toledo et al., 2018; Singh y Heldman, 2013) para resolver diferentes tipos de análisis, como por ejemplo el ajuste por mínimos cuadrados para el análisis de regresión (Kato et al., 2019; Sreehari y Ghantasala, 2019; Paolella, 2019; Kavuncuoglu et al., 2018; Li et al., 2015; Ramsundar y Zadeh, 2018).

Para resolver tal como están los datos sin hacer ninguna aplicación de logaritmos podemos usar el análisis de regresión exponencial (Prataviera et al., 2019; Henriquez y Oxenham, 2018; Braide y Diema, 2018).

1. Metodología

La metodología de simplificación se ha logrado tras el análisis de varios ejemplos recogidos de la literatura científica (Kaushik et al., 2014; Salvi et al., 2017; Tola y Ramaswamy, 2015; Kaushik et al., 2014; Fachin et al., 2004; Fachin et al. 2003; Nienaber y Shellhammer, 2001; Van den Broeck et al., 2000).

La simplificación permite los cálculos y el manejo de datos de una manera ágil y sencilla usando una hoja de cálculo de Excel para poder determinar el valor zP y el volumen de activación.

2. Resultados y Discusión

El análisis de regresión exponencial pertenece a la regresión no lineal, el Excel trae incorporada esta herramienta (Bisht y Soni, 2019) que se puede usar para ajustar los datos de constantes de velocidad de reacción, k versus presión y poder luego encontrar zp y él Va. El Excel tiene muchas funciones y herramientas incorporadas que podemos usar (McFedries, 2019; Bluttman, 2019) para encontrar las constantes de resistencia a la presión y el volumen de activación.

Se muestran en el presente trabajo hasta ocho (8) maneras de poder determinar las constantes de Va y valor zP, que son resumidas en la Tabla 4.

Tabla 4. Formas para determinar el valor ZP y él Va.

Graficar	zP	Va
log k versus P	1/Pendiente	-Pendiente x R x T x ln10
log 1/k versus P	-1/Pendiente	Pendiente x R x T x ln10
ln k versus P	ln10/Pendiente	-Pendiente x R x T
ln 1/k versus P	-ln10/Pendiente	Pendiente x R x T
log DP versus P	-1/Pendiente	Pendiente x R x T x ln10
log 1/DP versus P	1/Pendiente	-Pendiente x R x T x ln10
ln DP versus P	-ln10/Pendiente	Pendiente x R x T
ln 1/DP versus P	ln10/Pendiente	-Pendiente x R x T

Si se tuviera una hoja de cálculo de Excel los datos de la presión y la velocidad de reacción ordenados de la manera que se observa en la Figura 5.

	A	B	C
1	**Presión, P (MPa)**	**Velocidad de reacción, k (min^{-1})**	
2	.	.	
3	.	.	
4	.	.	
5	Pendiente	=PENDIENTE(LOG(B2:B4);A2:A4)	
6			

Figura 5. Datos de presión y velocidad de reacción en una hoja de Excel.

En la Tabla 5 se resumen las formas más sencillas de encontrar la pendiente en una hoja de cálculo de Excel para luego proceder a encontrar el valor zP y él Va de acuerdo a las Figuras 5 y 6.

Tabla 5. Resumen de las maneras de encontrar la pendiente de acuerdo a las Figuras 5 y 6.

Graficar	Pendiente
log k versus P	=PENDIENTE(LOG(B2:B4);A2:A4)
log 1/k versus P	=PENDIENTE(LOG(1/(B2:B4));A2:A4)
ln k versus P	=PENDIENTE(LN(B2:B4);A2:A4)
ln 1/k versus P	=PENDIENTE(LN(1/(B2:B4));A2:A4)
log DP versus P	=PENDIENTE(LOG(D2:D4);C2:C4)
log 1/DP versus P	=PENDIENTE(LOG(1/(D2:D4));C2:C4)
ln DP versus P	=PENDIENTE(LN(D2:D4);C2:C4)
ln 1/DP versus P	=PENDIENTE(LN(1/(D2:D4));C2:C4)

	C	D	E
1	**Presión, P (MPa)**	**Valor D_P (min^{-1})**	
2	.	.	
3	.	.	
4	.	.	
5	Pendiente	=PENDIENTE(LOG(D2:D4);C2:C4)	
6			

Figura 6. Datos de presión y valor DP en una hoja de Excel.

A partir de la revisión de la literatura científica, por ejemplo, Kaushik et al. (2014), trabajan con la inactivación de un grupo de microorganismos (mesófilos aerobios, levaduras y mohos, coliformes, bacterias ácido lácticas y psicrotrofos) en pulpa de mango calculando la pendiente de las curvas log DP versus la presión y ln k versus la presión haciendo uso de dos ecuaciones, cuando se puede simplificar, y a partir de una de las dos curvas se puede obtener tanto él Va como el valor zP, tal como se plantea en la Tabla 4.

Conclusiones

Se ha presentado un análisis de la constante de volumen de activación y la constante de resistencia a la presión (zP) para el manejo de datos cinéticos.

Un procedimiento, con cuatro nuevas ecuaciones son presentadas y permiten predecir (constante de volumen de activación y la constante de resistencia a la presión) en un solo paso.

Referencias

Alexander, M., Kusleika, R. (2018). Excel 2019 bible. Wiley.

Alexander, M., Kusleika, R. (2019). Excel 2019 power programming with VBA. John Wiley & Sons.

Anandharamakrishnan, C.; Ishwarya, S.P. (2019). Essentials and applications of food engineering. CRC Press.

Andrés, V. (2016). Efecto del tratamiento de altas presiones hidrostáticas y del almacenamiento sobre la seguridad y la calidad nutricional, sensorial y funcional de

smoothies como alternativa a las bebidas mixtas comerciales. Tesis doctoral. Universidad Complutense de Madrid. Facultad de Farmacia. Departamento de Nutrición y Bromatología II. Bromatología. Madrid-España.

Barboza-Cánovas, G.V.; Bermudez-Aguirre, D. (2010). Procesamiento no térmico de alimentos. Scientae Agropecuaria, 1: 81-93.

Bisht, A.S., Soni, U. (2019). Application of linear regression modeling on continuous and categorical data using R programming scripts. International Journal of Applied Engineering Research, 14 (4): 965-976.

Bluttman, K. (2019). Excel® formulas & functions for dummies®. 5th Edition. John Wiley & Sons.

Braide, S.L., Diema, E.J. (2018). Analysis of Least Square and Exponential Regression Techniques for Energy Demand Requirement (2013-2032). American Journal of Electrical and Electronic Engineering, 6(2), 38-59.

Braun, F. (1887). Untersuchungen über die Löslichkeit fester Körper und die den Vorgang der Lösung begleitenden Volum- und Energieänderungen. Zeitschrift Für Physikalische Chemie, 1U(1).

Braun, F. (1888). Ueber einen allgemeinen qualitativen Satz für Zustandsänderungen nebst einigen sich anschliessenden Bemerkungen, insbesondere über nicht eindeutige Systeme. Annalen Der Physik Und Chemie, 269(2), 337–353.

Butz, P., Tauscher, B. (1998). Food chemistry under high hydrostatic pressure. High Pressure Food Science, Bioscience and Chemistry, 133–144.

Calzada, J. (2015). Prevención de la sobremaduración y de la formación de aminas biógenas en quesos mediante tratamientos de altas presiones. Tesis Doctoral. Facultad de Veterinaria. Departamento de Nutrición, Bromatología y Tecnología de los Alimentos. Universidad Complutense de Madrid. Madrid-España.

De Heer, J. (1957). The principle of Le Châtelier and Braun. Journal of Chemical Education, 34(8), 375.

Ehrenfest, P. (1911). Das Prinzip von Le Chatelier-Braun und die reziprozitätssätze der thermodynamic. Zeitschrift für physikalische Chemie, 227-244.

Evrendilek, G.A. (2018). Effects of high pressure processing on bioavaliability of food components. Journal of Nutrition & Food Sciences, 8 (2): 676.

Eyring, H. (1935). The Activated Complex in Chemical Reactions. The Journal of Chemical Physics, 3(2), 107–115.

Eyring, H.; Magee, J.L. (1942). Application of the theory of absolute reaction rates to bacterial luminescence. Journal of Cellular and Comparative Physiology, 20(2), 169–177.

Fachin, D., Smout, C., Verlent, I., Ly Nguyen, B., Van Loey, A.M., Hendrickx, M.E. (2004). Inactivation Kinetics of Purified Tomato Polygalacturonase by Thermal and High-Pressure Processing. Journal of Agricultural and Food Chemistry, 52(9), 2697–2703.

Fachin, D., Van Loey, A.M., Nguyen, B.L., Verlent, I., Indrawati, Hendrickx, M.E. (2003). Inactivation kinetics of polygalacturonase in tomato juice. Innovative Food Science & Emerging Technologies, 4(2), 135–142.

Farkas, D.F.; Hoover, D.G. (2000). High pressure processing. Journal of Food Science, 65, 47–64.

Gassner, F. (1985). Bankkunden-beratung mit SuperCalc auf Osborne – und allen CP/M-betriebssystemen. Springer Fachmedien Wiesbaden.

Guerrero, H. (2019). Excel data analysis: modeling and simulation. Springer.

Henriquez, A.C., Oxenham, M.F. (2018). New distance-based exponential regression method and equations for estimating the chronology of linear enamel hypoplasia (LEH) defects on the anterior dentition. American Journal of Physical Anthropology.

Hernalsteens, S.; Pereira, C.G. (2019). Thermodynamics of Reactions in Food Systems. Thermodynamics of Phase Equilibria in Food Engineering, 593–631.

Hite, B.H. (1899). The effect of pressure in the preservation of milk. West Virginia University. Agricultural Experiment Station, 58, 15-35.

Huang, H.-W.; Lung, H.-M.; Yang, B.B.; Wang, C.-Y. (2014). Responses of microorganisms to high hydrostatic pressure processing. Food Control 40: 250–259.

Jaeger, H.; Reineke, K.; Schoessler, K.; Knorr, D. (2012). Effects of emerging processing technologies on food material properties. Food Materials Science and Engineering, 222–262.

Jay, J.M.; Loessner, M.J.; Golden, D.A. (2005). Modern Food Microbiology. 7 ed. Springer.

Jia, J.; Liu, D.; Ma, H. (2019). Advances in food processing technology. Springer Singapore.

Kato, T., Kobayashi, A., Oishi, W., Kadoya, S., Okabe, S., Ohta, N., Amarasiri, M., Sano, D. (2019). Sign-constrained linear regression for prediction of microbe concentration based on water quality datasets. Journal of Water and Health, 17(3), 404–415.

Kaushik, N., Kaur, B.P., Rao, P.S., Mishra, H.N. (2014). Effect of high pressure processing on color, biochemical and microbiological characteristics of mango pulp (Mangifera indica cv. Amrapali). Innovative Food Science & Emerging Technologies, 22, 40–50.

Kavuncuoglu, H., Kavuncuoglu, E., Karatas, S.M., Benli, B., Sagdic, O., Yalcin, H. (2018). Prediction of the antimicrobial activity of walnut (Juglans regia L.) kernel aqueous extracts

using artificial neural network and multiple linear regression. Journal of Microbiological Methods, 148, 78–86.

Le Châtelier, H.L. (1884). A general statement of the laws of chemical equilibrium. Comptes Rendus 99: 786–789.

Le Châtelier, H.L. (1888). Recherches expérimentales et théoriques sur les équilibres chimiques. Dunod, Paris.

Leake, L.L. (2018). HPP: A 'cool' innovation in food packaging. Food Quality & Safety, 25(4). Wiley.

Li, Z., Cao, X., Ding, X., Chen, H. (2015). Prediction Model of Multiple Linear Regression Analysis in Grain Production. 5th International Conference on Information Engineering for Mechanics and Materials (ICIMM) 1290-1293.

Lin, Y.H.; Li, C.H.; Lin, C.H.; Yan, Y.Z.; Chuang, Y.Y.; Chen, G.W. (2017). Application and development status of an ultra-high pressure processing technique in aquatic food. Haidayu 47, 17-32.

McFedries, P. (2019). Microsoft Excel 2019 formulas and functions. Pearson education.

Miranda-Zamora, W.R.; Heldman, D.R. (2018). Diseño de procesos térmicos y alta presión de alimentos. AMV ediciones.

Mussa, D.M.; Ramaswamy, H.S. (1997). Ultra high pressure pasteurization of milk: kinetics of microbial destruction and changes in physico-chemical characteristics. LWT - Food Science and Technology, 30(6), 551–557.

Nienaber, U., Shellhammer, T.H. (2001). High-Pressure Processing of Orange Juice: Kinetics of Pectinmethylesterase Inactivation. Journal of Food Science, 66(2), 328–331.

Onur, M., Palabiyik, Y. (2015). Nonlinear parameter estimation based on history matching of temperature measurements for single-phase liquid-water geothermal reservoirs. Proceedings World Geothermal Congress 2015, Melbourne, Australia, 19-25.

Paolella, M.S. (2019). Linear models and time-series analysis: regression, ANOVA, ARMA and GARCH. John Wiley & Sons.

Parekh, S.L., Aparnathi, K.D., Sreeja, V. (2017). High Pressure Processing: A potential technology for processing and preservation of dairy foods. International Journal of Current Microbiology and Applied Sciences, 6(12): 3526-3535.

Parsons, J.J. (2017). New perspectives on computer concepts 2018: comprehensive. Edition 20. Cengage Learning.

Patazca, E., Koutchma, T., Ramaswamy, H.S. (2006). Inactivation kinetics of Geobacillus stearothermophilus spores in water using high-pressure processing at elevated temperatures. Journal of Food Science, 71(3), M110–M116.

Poli, P. (2019). Excel 2019: formule e analisi dei dati. Hoepli.

Prataviera, F., Vasconcelos, J.C.S., Cordeiro, G.M., Hashimoto, E.M., Ortega, E.M.M. (2019). The exponentiated power exponential regression model with different regression structures: application in nursing data. Journal of Applied Statistics, 1–30.

Quirk, T.J. (2013). Excel 2013 for engineering statistics: a guide to solving practical problems. Springer International Publishing.

Ramsundar, B., Zadeh, R.B. (2018). Tensorflow for deep learning: from linear regression to reinforcement learning. O'Reilly Media.

Roe, J., deForest, R., Jamshidi, S. (2018). Mathematics for sustainability. Springer.

Ruiz, P. (2017). Conservación de alimentos por altas presiones hidrostáticas. Trabajo de fin de grado. Universidad Complutense. Madrid-España.

Sachs, J. (2007). Recollections: developing Lotus 1-2-3. IEEE Annals of the History of Computing, 29(3), 41–48.

Salvi, D., Arserim, E., Karwe, M. (2017). Innovative Processing Technologies for Mango Products. Handbook of Mango Fruit, 169–193.

Singh, R.P., Heldman, D.R. (2013). Introduction to food engineering. Fifth edition. Academic Press.

Sreehari, E., Ghantasala, P.G.S. (2019). Climate changes prediction using simple linear regression. Journal of Computational and Theoretical Nanoscience, 16(2), 655–658.

Stearn, A.E., Eyring, H. (1941). Pressure and Rate Processes. Chemical Reviews, 29(3), 509–523.

Süsskind, C. (1980). Ferdinand Braun: Forgotten Forefather. Advances in Electronics and Electron Physics, 241–260.

Theodore, L., Behan, K. (2018). Introduction to optimization for environmental and chemical engineers. CRC Press.

Tiziano, B. (2019). How to model and validate expected credit losses for IFRS9 and CECL: a practical guide with examples worked in Excel, R, and SAS. Elsevier Science & Technology.

Tola, B.; Ramaswamy, H. (2015). Temperature and high pressure stability of lycopene and vitamin C of watermelon Juice. African Journal of Food Science. 9. 351-358.

Toledo, J.; Grande, M.J.; Lucas, R.; Gálvez, A.; Pérez Pulido, R. (2015). Inactivación de patógenos en vegetales mediante el uso de altas presiones hidrostáticas. Biosaia: Revista de los másteres de Biotecnología Sanitaria y Biotecnología Ambiental, Industrial y Alimentaria, 1(4).

Toledo, R.T., Singh, R.K, Kong, F. (2018). Fundamentals of food process engineering. Fourth edition. Springer.

Turgeon, M.L. (2015). Linne & Ringsrud's clinical laboratory science: concepts, procedures, and clinical applications. Seventh edition. Elsevier, Mosby.

Valdez-Fragoso, A.; Mújica-Paz, H.; Welti-Chanes, J.; Torres, J.A. (2011). Reaction kinetics at high pressure and temperature: effects on milk flavor volatiles and on chemical compounds with nutritional and safety importance in several foods. Food and Bioprocess Technology, 4(6), 986–995.

Van den Broeck, I., Ludikhuyze, L.R., Van Loey, A.M., Hendrickx, M.E. (2000). Inactivation of orange pectinesterase by combined high-pressure and -temperature treatments: a kinetic study. Journal of agricultural and food chemistry, 48(5), 1960–1970.

Yamamoto, K. (2017). Food processing by high hydrostatic pressure. Bioscience, Biotechnology, and Biochemistry, 81(4), 672–679.

Yang, W. (2015). Effect of chlorine dioxide gas treatment on bacterial inactivation inoculated on spinach leaves and on pigment content. Master of Science, Ohio State University, Food, Agricultural and Biological Engineering.

Yordanov, D.G.; Angelova, G.V. (2010). High pressure processing for foods preserving. Biotechnology & Biotechnological Equipment, 24(3), 1940–1945.

Variations of graphene nanotube membrane support layer in outlet flux of PAFO system

Leila Javarani*
Mohammad Malakootian**
Amir Hessam Hassani***
Amir Hossein Javid ****

ABSTRACT

The PAFO system is a solution in the desalination of seawater using a hydraulic pressure of 5 bar, which competes with the FO system (direct osmosis). The project includes four stages of pilot construction, entrainment detection, graphene nanotube membrane synthesis and, finally, efficiency determination and outflow modeling of the PAFO system. High Flux is the most important parameter of the system test for practical application. According to the results, the highest flow of current (120 l / m2.hr) was calculated at the osmotic pressure of 55, indicating a 50% increase in the flow of water with KOH fertilizer as entrainment solution and membrane of low thickness backing layer. Outflow values were calculated using theoretical modeling (MATLAB software). The results show the consistency of the outflow with the flow of the proposed chi model.

KEY WORDS: Forward Osmosis; Flow; Drag solution; Support layer.

* Department of Natural Resources and Environment, Science and Research Branch, Islamic Azad University, Tehran, Iran.

**Environmental health engineering research center, Kerman University of medical science. Kerman, Iran. ORCID: 0000-0002-4051-6242

***Department of Natural Resources and Environment, Science and Research Branch, Islamic Azad University, Tehran, Iran. ORCID:0000-0003-2569-5446 (corresponding author)

****Department of Natural Resources and Environment, Science and Research Branch, Islamic Azad University, Tehran, Iran.

Recibido: 23/04/2020 Aceptado: 25/06/2020

Variaciones de la capa de soporte de membrana de nanotubos de grafeno en el flujo de salida del sistema PAFO

RESUMEN

El sistema PAFO es la solución en la desalinización de agua de mar utilizando una presión hidráulica de 5 bar, que compite con el sistema FO (ósmosis directa). El proyecto incluye cuatro etapas de construcción piloto, detección de solución de arrastre, síntesis de membrana de nanotubos de grafeno y, finalmente, determinación de eficiencia y modelado de flujo de salida del sistema PAFO. High Flux es el parámetro más importante de la prueba del sistema para una aplicación práctica. Según los resultados, se calculó el flujo más alto de corriente (120 l / m2.hr) en la presión osmótica de 55, lo que indica un aumento del 50% en el flujo de agua con fertilizante KOH como solución de arrastre y membrana de capa de soporte de bajo espesor. Los valores de flujo de salida se calcularon mediante el modelado teórico (software MATLAB). Los resultados muestran la consistencia del flujo de salida con el flujo del modelo de chi propuesto.

PALABRAS CLAVE: Osmosis adelante; flujo; solución de arrastre; capa de soporte.

Introduction

Osmosis is the transfer process of water through a semi-permeable membrane. In this process, water molecules are allowed and the solute molecules are returned. The osmotic force in the process is obtained from the drag solution and the final driving force is obtained from the difference between the osmotic pressure $\Delta\pi$and the hydraulic pressure Δp. The fundamental challenges of the forward osmosis process is an access to drag solution with high osmotic pressure and proper membrane.

Maryam Amini et al. 2012, used the forward osmosis system using NaCl solution as feed and drag solution. The results show an increase in water permeability and salt return. The water flux of $95(^{L}/_{m^2})$ was estimated (Maryam Amini et al. 2012).

Andrea Achilli et al. (2010), the process of forward osmosis analysis in this study involves the screening of 14 draw solutions and the study of water flow and salt diffusion. The best draw solutions were $CaCl_2$, $Ca(No_3)$, NaCl (Andrea Achilli et al. 2010).

Shrubphuntsho et al. (2011), in this research, the Fo system and agricultural fertilizers were used to desalinate seawater and agricultural uses. 9 fertilizers were selected as a drag solution from the relevant list, and their efficiency was evaluated by determining the pure water flux and return drag solution. According to the results, fertilizers with the highest solubility in water produce high osmotic pressure than seawater. The most appropriate drag solutions were introduced as KCl–$NaNo_3$ and KNO_3. Each kilogram of fertilizer separates about 11-29 liters of water from the sea (Shrubphuntsho et al. 2011).

Changquan Qiu et al. (2011), the forward osmotic membrane was successfully done using layer-by-layer (lbl) deposition, the results of bonded and non-bonded membranes were investigated using shape, water permeation structure, salt return, and solute flux. The water flux was estimated to be $100(^{L}/_{m^2.hr})$, which indicates high capability of lbl membranes for high flux (Changquan Qiu et al. 2011, 81).

Yan Kim et al. 2012, according to research on AFO process efficiency, showed that water flux is increased with the use of hydraulic pressure and solute return is reduced. Driving force control in AFO is easier than Fo, which leads to flexibility in system design and operation (Gaetanjlandin et al., 2013).

Sang Min et al. (2013), numerically predicted Foefficiency by the equilibrium copper equation for the feed and drag solution ratio associated with the water flux model. According to the results, a high concentration drag solution improves water flux. Water flux in opposite or reverse flow conditionis 10% higher than direct flow. A series of feed solution flow and parallel drag solution are effective in increasing water flux (Sang Min et al. 2013).

Gaetenjlandin et al. (2013), investigated the effect of hydraulic pressure on Fo. A 6 bar pressure on feed solution had doubled the water permeability. Moreover, salt diffusion was significantly reduced. This study investigates the limitations of the flow method to determine water permeability and membrane properties (Gaetenjlandin et al.2013).

Coworker et al. 2015, designed PVDF nanofibers for water desalination. Membranes prepared for drinking water.

Zhuqing et al. (2018), designed super-hydrophobic PVDF, containing nanofiber and fluoropropane and CNT (nanotubes), which were designed by electro method. The hydrophobic

and mechanical properties were investigated by the concentration of CNTs. In another study, produced a thin film nanocomposite (TFN) containingsilica nanoparticles pores through interfacial polymerization. Huetal et al. made Go layer-by-layer (LbL) nano sheet son poly sulfane coated with polyamine and nano GO membrane benzene tricarbonyl trichloride binder and the outlet flux is estimated (Tiging et al. 2016).

David Chaen et al. 2015, investigated the simulation and modeling of nano graphene and outlet flux (Chaen et al. 2015).

The present study investigates and evaluates the efficiency of the PAFO systemin seawater salt desalination in various operating situations. In many studies, by building new membranes in forward osmosis systems, the water flux is raised successfully, but none of these plans were commercial. Consequently, changes in inlet pressure on feed solution, inlet water flow, concentration, flow direction, and membrane contact surfacelead to changes in osmotic pressure, concentration polarization, and osmotic pressure between the two solutions. Thus, providing information and collecting data for better design and operation in the future and making strong incentives for development of FO processes in a commercial scale are the main goals of this project, so the results are reported in real conditions using seawater (Persian Gulf) with very high EC.

1. Research method

Experimental studies were conducted in the HSE laboratory of the National Iranian Oil Company of the Pars Special Economic Energy Zoneduring 2016-2018. Determining FO efficiency is the result of the combination of tests. Drag and membrane were selected to determine pilot efficacy with 11 fertilizer solutions at a concentration of 50 mg/L as drag solution and sea water with EC=48000as feed solution. Graphene nanotube membranes were made by reducing the thickness of the support layer. Finally, the effects of nanomembranes made along with auxiliary pressure on the efficiency of the system were investigated.

1.1. Devices and equipment used

Tensiometer	model K20
Viscometer	ulv
EC-meter	conductivity module
Experimental laboratory precision of 0.1	CS Series
Maximum flow diaphragm pump of 100 and maximum pressure of 7 bar l/min	

Table 2-1: List of devices used

Material	Chemical formula
Graphene nanotube suspension	$CNT\text{-}NH_2$
Cyclohexane extra pure ›99%	C_6H_{12}
Potash	KoH
Calcium nitrate	$Ca(No_3)_2$
Complete fertilizer	$N_{20}\times K_{20}\times P_{20}$
Complete fertilizer	$K_{40}\times P_{53}$
Urea phosphate	CH_4N_2O
Calcium chelate	OligoCalcium EDTA/Ca
High +Urea phosphate potash	CH_4N_2O + KoH
Calcium + High potash nitrate	KoH + $Ca(No_3)_2$
Calcium + High potash chelate	KoH + Oligo Calcium
Complete fertilizer Potash + 20x20x20	KoH + $N_{20}K_{20}P_{20}$
Complete fertilizer Potash + 34x52	KoH + $K_{40}P_{53}$

Table 2-2: Chemicals consumed

1.2. Pilot construction

In order to achieve the correct results of the laboratory pilot, PAFO was designed and constructed. Figure 1.2 shows a diagram of the PAFO system in the laboratory.

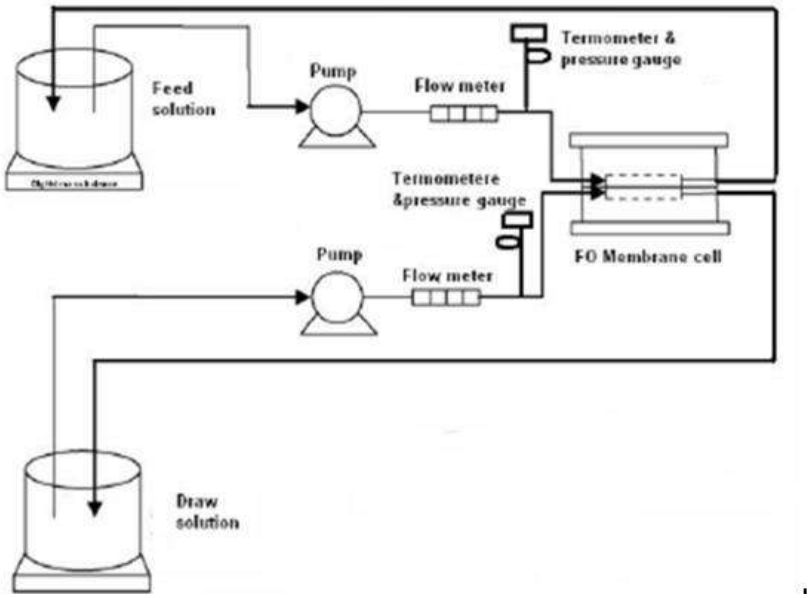

Figure 1.2: Diagram of forward osmosis system

- **Pilot specifications:**
- Plexiglas cell (3.75 m^2)
- Graphene nanotube membranes (15*25cm)
- Diaphragm pump for draw and feed solution flow (maximum flow of 100 l/min and maximum pressure of 7 bar)
- 200 liter tanks

Each piece of cell has an inlet tube and an outlet tube entering the flow through the piece to the diffusion channels, which are opposite to each other. Generally, the active layer that is brighter is towards the feed solution and back of membrane is towards the drag solution. Plexiglas membrane cell with the transverse flow consist of a series of symmetrical channels on

each side. The dimensions of cell, length, width and depth, are 25cm, 15cm and 0.3cm, respectively, in the form of a hollow rectangle. Graphene nanotube membranes is made of thin support layer and has an effective surface of 139cm^2 mounted in a 139cm^3cell. Two diaphragm pumps are used for constant speed flow. The water velocity and drag solution are considered the same. The solution is rotating. The solution is passed from the feed solution to the drag solution until the osmotic pressure becomes equal on both sides.

1.3. Selecting drag solution

A list of fertilizers (synthetic or mineral) was investigated for selection. Selection criteria are solvability, generality of use, osmotic pressure, and diffusion coefficient. Chemical details are presented in Table 1-3. According to the table, most fertilizer shave osmotic pressure higher than seawater. In the initial screen,9 fertilizers were selected.

1.4. Inlet feed

Inlet feed in all phases was water of Persian Gulf with EC=48000.

1.5. Membrane synthesis

Membrane synthesis method with graphene nanotubes

1.6. Measuring method of parameters

1.6.1. Osmotic pressure

Due to the absence of osmotic pressure analyzer in Iranian laboratories, theoretical prediction method was used. Osmotic pressure is a function of dissolved solids concentration, the value of which is PSI=1.1–0.6 per TDS=100ppm.

1.6.2. Diffusion coefficient

To measure the diffusion coefficient, first, the surface tension must be calculated. Surface tension was measured at temperature of 20 °C using plate or ring method according to National Iranian Standard 2976. The diffusion coefficient was determined by formulaic calculations.

S= diffusion coefficient

Yc= Surface tension of cyclohexane (mN/m)

Yf=Surface tension of fertilizer solution (mN/m)

Y= Interfacial tension of foam solution and cyclohexane (mN/m)

(1-2) S=Yc-Yf-Y

(National Iranian Standard 3778)

1.6.3. Viscosity

The viscosity of the solutions in torque was measured between 10 and 100 by Brookfield apparatus.

1.6.4. Water flux

Water flux was consistently recorded by the laboratory scale from the difference of the initial and final weights as the amount of water flux over time.

1.6.5. Water permeability coefficient (A)

A is the membrane water permeability coefficient. Increased permeability increases the flux water during operation of Fo and PAFo systems.

$$A = J_w / (\Delta\pi + \Delta P) \quad (2.2)$$

J_w=Water flux ($L/m^2.hr$)

$\Delta\pi$= Osmotic pressure difference

ΔP= Hydraulic pressure difference

A solution with zero osmotic pressure (distilled water) was used for in vitro measurement. The system was designed in a way to fix the hydraulic pressure and current. Data were collected every 5 minutes and 3 averages were determined.

1.6.6. Permeability coefficient of solute (B)

B is the permeability coefficient of the solute (drag material). Diffusion indicates the inverted solute. In the PAFo process, the value of parameter B must be limited.

(2.3) $J_s = B\Delta C$

ΔC= Concentration differences over the membrane

J_s= Drag solution or drag solute flux $^{gr}/_{m^2.hr}$

B= Permeability of the solute

(2.4) $$B = \exp\frac{J_w}{K} \times J_w\frac{1-R}{R}$$

If overlooking the concentration polarization in above flow, the feed solution B is equal to zero

(2.5) $$B = J_w\frac{1-R}{R}$$

C_P and C_F= Solute concentration in the feed and permeation solution

1.6.7. Water flux modeling

1.6.7.1. Osmosis

Osmosis is the spontaneous transfer of molecules from a dilute solution to a concentrated solution. The semi-permeable membrane allows the passage of solvent molecules, but it doesn't allow the passage of solute. Osmotic pressure is a function of the number of solute molecules(n), solvent volume (V), temperature (T), and ideal gas constant (R).

$\pi_{=\frac{n}{v}.iRT}$(2.6)

(Sang Min et al. 2013, 27).

1.6.7.2. Water flux equations

Equation for FO systems with zero hydraulic pressure adjustment is zero. Lee et al. developed the water flux equation based on resistance method against fouling and internal and external concentration polarization for the FO system.

In the FO system, the feed water is in contact with active membrane layer and drag solution is in contact with the support layer. The equation is as follows:

(2.7) $J_w=A(\pi+B/A)e^{-(J_w/k_m)-}(\pi+B/A).e^{(J_w/k_{ECP})}$

(Sang Min et al. 2013, 27)

A, B= Water and salt permeability coefficient

K_m, K_{ECP}= External concentration polarization (ECP) and internal concentration polarization (ICP)

K_m= Mass transfer coefficient

K_m= D/S=D.E/&.T (2.8)

(Sang Min et al. 2013, 27)

D= Drag material diffusion coefficient

S= Structure parameter

E= Membrane porosity

&=Layer thickness

T= Membrane curvature

1.6.7.4. General equation for FO water flux system

General equation for water flux in forward osmosis is obtained by Lee et al. and the modified equation by Mica Cheaon.

(2.9) $J_w = A\left[(\pi_D \exp(-J_w K_a) - \pi_F \exp(^{J_w}/_{k_b})\right]$ Type equation here.

(Sang Min et al. 2013, 27)

J_w= Water flux

A= Pure membrane water permeability

π_D=Osmotic pressure of drag solution

π_F= Osmotic pressure of feed solution

k_a= Soluble specific resistance coefficient (solute resistance to diffusion to the pores)

k_b= Mass transfer coefficient

-$k_a$calculation (soluble specific resistance coefficient)

(2.10) $$k_a = \frac{t\tau}{D\epsilon} s = \frac{t\tau}{\varepsilon}$$

(Sang Min et al. 2013, 27)

t= Membrane layer thickness

τ= Membrane curvature

ε= Pores

D= Drag strength diffusion coefficient

s= Membrane structure parameter

As a result, with respect to substitution of a membrane structural parameter in the equation, ka is obtained:

(2.11) $$k_a = \frac{s}{D}$$

(Sang Min et al. 2013, 27)

Dis drag solution diffusion coefficient measured by Tensiometer and s is the membrane structure parameter, and in the FO system, s can be estimated for the system. Parameters is constant for each membrane in different states.

Structure parameter s calculations

(2.12) $$s = \left(\frac{D}{J_w}\right) \times Ln\left(\left(B + A \times \pi_D\right) \Big/ \left(\beta + J_w + A \times \pi_F\right)\right)$$

(Yan Kim et al. 2012)

D= Drag strength diffusion coefficient

π_D=Osmotic pressure of drag solution

π_F= Osmotic pressure of feed solution

A= Water permeability coefficient

β= Salt permeability coefficient

Membrane structure parameter (s)indicates the resistance of the membrane support layer in diffusion of solute. According to the research, it was found that with a decrease in parameter s, the water flux is increased.

-$k_b$calculation (mass transfer coefficient)

(2.13) $$k_b = \frac{shD}{d_h}$$

(Sang Min et al. 2013, 27)

Sh= Sherwood number

D= Drag strength diffusion coefficient

d_h=Hydraulic diameter

Sherwood number, known as mass transfer Nuselet number, is a non-dimensional number in the mass transfer science that indicates the mass transfer rate from convection to mass permeability.

$$\frac{Mass\ transfer\ coefficient}{Diffusion\ transfer\ coefficient}$$

- Sherwood number calculation

(2.14) $$sh = 1.85\left[Re \times Sc \times \frac{d_h}{L}\right]^{0.33} \quad \rightarrow \quad Re \leq 2100$$

(Inger Lise et al., 2013: 5)

(2.15) $$sh = 1.85[Re^{0.75} \times Sc^{0.33}] \quad \rightarrow \quad Re \geq 2100$$

(Inger Lise et al., 2013: 5)

(2.16) $$Re = \frac{d_h V \rho}{u}$$

(Inger Lace et al., 2013: 5)

Sc= Schmidt number

Re= Reynolds number

$\frac{\rho}{u}$= Kinematic viscosity

D_h= Hydraulic diameter

(2.17) $$d_h = \frac{4\times \text{Soaked area}}{Soaked\ area}$$ Type equation here.

(Inger Lace et al. 2013, 5)

-Schmidt number calculation (**Wilhelm Schmidt)**

A non-dimensional number that indicates theratio of the momentum diffusion (viscosity) to the mass diffusion (diffusion coefficient).

(2.18) $$\frac{u}{D} = \frac{Dynamic\ viscosity}{Diffisuion\ coefficient} = \frac{\left(Pa.s\ \ or\ \ \text{N}.\frac{s}{m^2}\right)}{(m^2/s)}$$

(Inger Lise et al., 2013)

1.6.7.5. Water flux model in PAFO system

Achilli et al (2010) presented a new equation for PAFO (FO and RO hybrid system)

(19-2) $$J_w = A\left(\Delta p + \left(\pi_D \exp\left(-\frac{J_w}{k_d}\right) - \pi_F \exp(\frac{J_w}{k_F})\right)\right)$$

(Inger Lise et al., 2013)

(20-2) $$J_w = A(\pi - \pi) + \Delta p$$ Type equation here.

(Inger Lise et al., 2013)

A= Membrane water permeability coefficient

Δp= System hydraulic pressure

π_D= Osmotic pressure of draw solution

π_F= Feed osmotic pressure

$k_F$and$k_d$areequal to k or 1/k in equation, respectively.

2. Results

2.1. Primary evaluation of flux system

After pilot startup, the outlet flux from the pilot is reduced after a 2-hour period, because the drag solution became thinner and the feed solution became thicker over time. The water transfer from the feed water to the drag solution occurs by the osmotic process reach the osmotic equilibrium (zero osmotic gradient).

Flux changes over time are in accordance to curve 3.1.

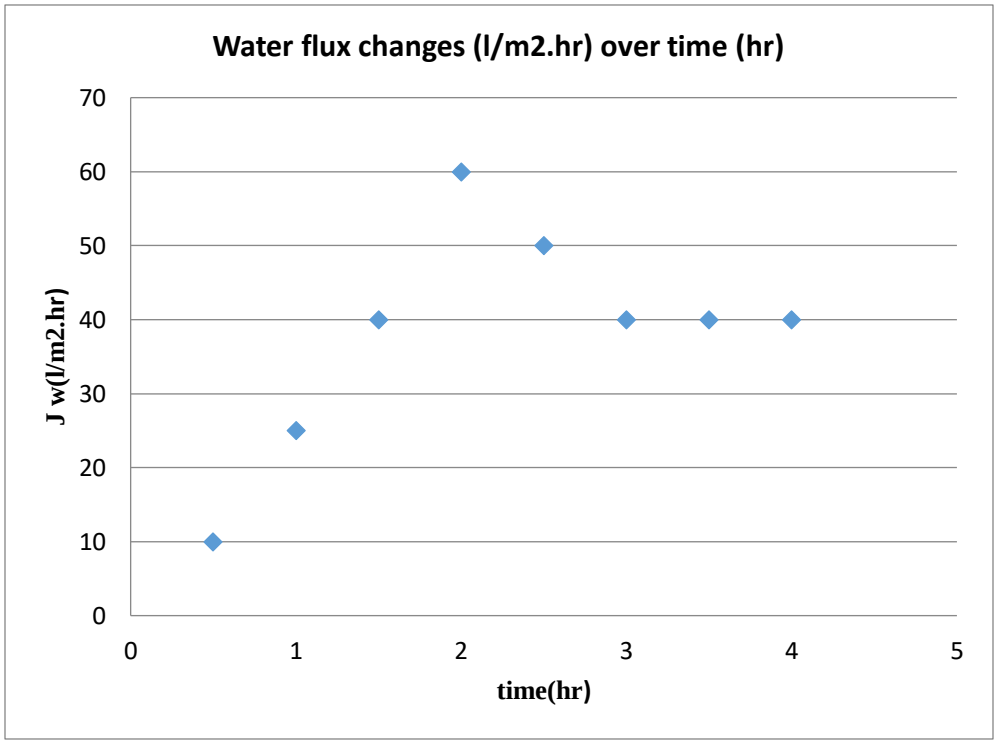

Figure 3.1: Water flux changes over time in FO system

2.2. Results of the effect of osmotic pressure on flux (J_w)

Details of chemical fertilizers used are presented in Table 3.1, and the drag soltion in this project was prepared by dissolving fertilizer compounds in distilled water at a concentration of 50 mg/L.

Table 3.1: Chemical physical properties of fertilizers

No	Fertilizer	Chemical formula	Concentration $(^{mg}/_{l})$	EC n $(^{s}/_{cm})$	π Osmotic pressure (bar)	Diffusion coefficient (D)
1	Potash	KoH	50 mg/l	92000	55	1.1
2	Calcium nitrate	$Ca(No_3)_2$	50 mg/l	116000	70	1/31
3	Complete fertilizer	$N_{20}\times K_{20}\times P_{20}$	50 mg/l	65000	35	1/04
4	Complete fertilizer	$K_{40}\times P_{53}$	50 mg/l	65000	39	1/04
5	Urea phosphate	CH_4N_2O	50	15000	9	1.91
6	Calcium chelate	OligoCalcium EDTA/Ca	50 mg/l	23000	14	1.06
7	Urea phosphate +High potash	CH_4N_2O + KoH	25+25 mg/l	57000	34	1.91
8	High potash + Calcium nitrate	KoH + $Ca(No_3)_2$	25+25 mg/l	114000	68	1.06
9	High potash + Calcium chelate	KoH + Oligo Calcium	25+25 mg/l	79000	47	1.04
10	Complete fertilizer 20x20x20 +Potash	KoH + $N_{20}K_{20}P_{20}$	25+25 mg/l	111000	67	1
11	Complete fertilizer 34x52 + Potash	KoH + $K_{40}P_{53}$	25+25 mg/l	90000	54	1.38

Ca(NO3)2 has the highest osmotic pressure at a concentration of 50 mg/L equal to 70 bar and the urea phosphate at osmotic pressure of 9 bar has the minimum osmotic pressure. According to the table, most selected fertilizers have higher osmotic pressure than seawater. According to the results presented in the table, the calcium nitrate has the highest diffusion coefficient of 1.31 and the complete fertilizers have the lowest diffusion coefficient of 1.04. This indicates a correlation between the diffusion coefficient and high osmotic pressure. Draw solutions with high diffusion coefficient and high osmotic pressure have higher water flux.

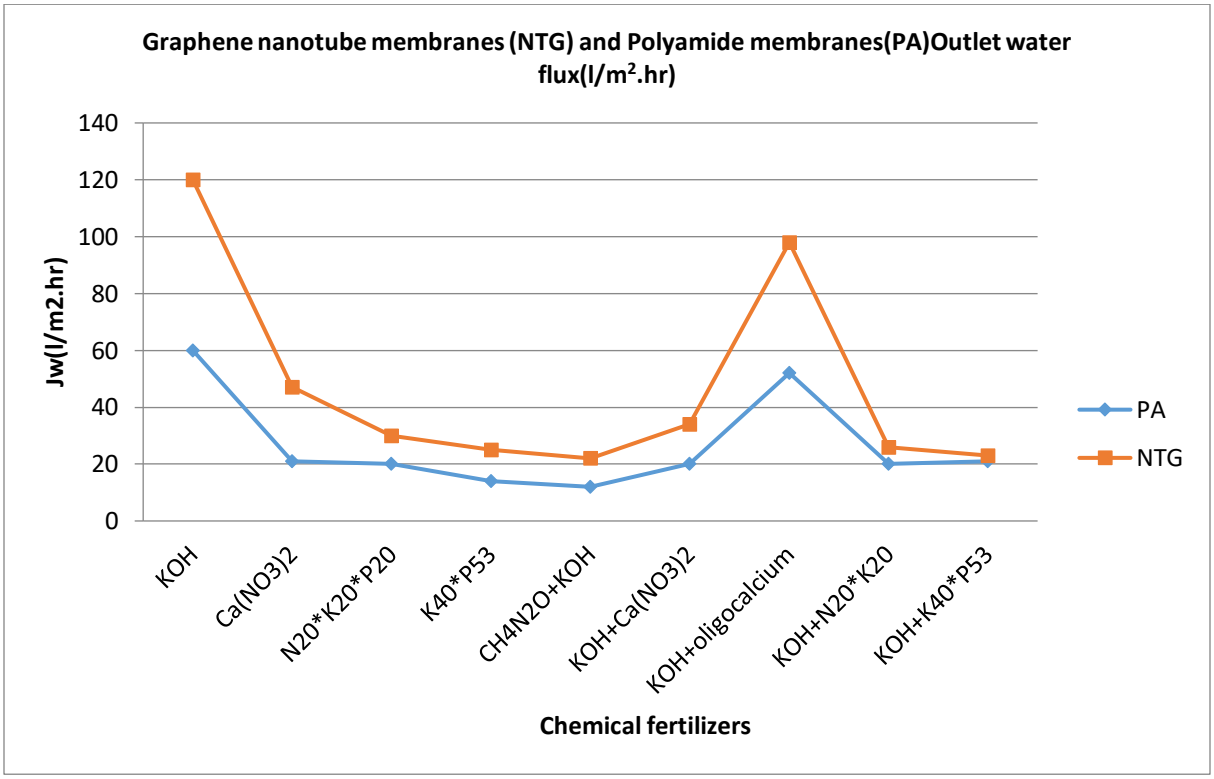

Figure 3.2: Outlet water flux values J_w(l/m^2.hr) with drag solutions of PAFO system

Outlet water flux for draw solutions are presented in Figure 3.2. The lowest and highest fluxes of 120 (l/m^2.hr) and 22(l/m^2.hr) are at osmotic pressure of 55 bar and 34 bar, respectively. In this project, the same concentration is considered. It can be said that pure water flux is a function of the concentration and osmotic pressure of the draw solution. There is a linear correlation coefficient between water flux and predicted osmotic pressure. Some fertilizers have low correlation coefficient. Among the selected fertilizers, the fertilizer with higher molecular

weight has the greatest impact on internal polarization and flux reduction. The abnormal relationship of osmotic pressure of drag solution and water flux in the forward osmosis process indicates internal polarization in the water flux flow. The internal polarization reduces flux and pressure across membranes.

In Table 3.2. Outlet flux of the system with graphene nanotube membranes and reverse osmosis membranes are presented.

Table 3.2: Outlet flux of the system with NTG and PA membranes

No	Fertilizer	RO membrane flux $J_w \left(L/m^2.hr\right)$	Graphene nanotube membrane flux $J_w \left(L/m^2.hr\right)$
1	Potash	60	120
2	Calcium nitrate	21	47
3	Complete fertilizer $N_{20} \times K_{20} \times P_{20}$	20	30
4	Urea phosphate + high potash	12	22
5	High potash + calcium nitrate	20	34
6	Potash + calcium chelate	52	98
7	Complete fertilizer + potash $N_{20} \times K_{20} \times P_{20}$	20	26
8	Complete fertilizer + potash $N_{40} \times P_{53}$	21	23
9	Complete fertilizer $N_{40} \times P_{53}$	14	25

According to the table, the highest outlet flux with PA and graphene nanotube membranes is 60 (l/m2.hr)and 120(l/m^2.hr)respectively.

PAFO against FO systems is a new solution with an aim of putting pressure on the feed solution to increase water permeability through membranes. Once a 5 bar pressure is applied on a feed solution, the permeability and flux is multiplied compared to the FO system. The results of research from 2010 to 2017 on the outlet flux from osmotic systems with different membranes are presented in Table 3.3, indicating the high importance in choice of membrane in these systems.

Highest water flux with nanographene membranes is estimated up to 50-300 (l/m^2.hr).

Table 3.3: Research results of FO system

System	Type of membranes	Drag solution	Flux	Reference
FO	LbL(PAH/PSS)	MgCL2	100	Changquan Qiuetal (2011)
MBR		MgSO4	6.3	Kiwa Water Research (2009)
Fo	CTA	Fertilizer	5-10	Andereaachili-Tzahi (2010)
AFO	CTA	Sea water	8	Gaetenjlandin-Arne (2013)
FO	CTA	Sea water	2-6	Shrubphuntsho-Hokyonshon (2011)
FO	TFN	Sea water	95	Maryamamini-Mohsenjahanshahi (2012)
RO	GO nano	-	80-276	Glenn L-Martin Hall (2013)
FO	-	Graphen hydrogel	2	Yaozengling Giu-Kunwang (2012)
RO	GO nano	-	50-300	Shahin Homaegohar (2017)

2.3. Calculation results of water permeability (A)

Water permeability values are presented in Table 3.4. The maximum water permeability is 8.6 (l/m^2.hr) and minimum water permeability is 0.9 (l/m^2.hr). According to the results, the maximum graphene nanotube membrane permeability coefficient is approximately increased by 50% compared to the maximum RO membrane permeability coefficient.

Table 3.4: PA membrane and thin graphene nanotube membrane permeability A values

No	Fertilizer	$\Pi_F - \Pi_D$ (bar)	P_H (bar)	Membrane permeability coefficient Ro(A)	Graphene nanotube membrane permeability coefficient(A)
1	Potash	103	5	4.3	8.6
2	Calcium nitrate	25	5	0.7	1.56
3	Complete fertilizer $N_{20} \times K_{20} \times P_{20}$	10	5	1.33	2
4	Urea phosphate + high potash	11	5	0.75	1.43
5	High potash + calcium nitrate	20	5	0.71	1.36
6	Potash + calcium chelate	2	5	7.41	13
7	Complete fertilizer + potash $N_{20} \times K_{20} \times P_{20}$	22	5	1.42	2.30
8	Potash + complete fertilizer $N_{40} \times P_{53}$	9	5	0.77	0.9
9	Complete fertilizer $N_{40} \times P_{53}$	106	5	1.27	2.9

Water permeability is improved in new membrane. Increased hydrophilicity of membranes and the existence of nanotubes as water passage channel are the main causes of this increase. The results of water permeability variations with osmotic pressure and hydraulic pressure are similar to the changes in Gaetenjlandin-Arne et al. (2013) in the evaluation project of the effects of hydraulic pressure on forward osmosis system.

2.4. Results of B/A values

Permeability values of the solute are presented in Table 3-5. The maximum and minimum permeability values (B) equal to 120 ($l/m^2.hr$) are calculated with potash fertilizer and potash fertilizer.

According to the results, the minimum graphene nanotube membrane permeability coefficient of solute (B)is approximately decreased by 50% compared to the minimum RO membrane permeability coefficient.

This indicates proper efficiency of graphene nanofiber membranes with low-thickness support layer.

Table 3.5: Comparing permeability values of solute (B) and B/A ratio and return percentage (PA membranes and thin graphene nanotube membranes)

Fertilizer	R% (PA)	R% (NTG)	B (PA)	B (NTG)	B/A (PA)	B/A (NTG)
KoH	30	50	121	120	28	13
$Ca(No_3)_2$	47	65	23	24	33	16
$N_{20} \times K_{20} \times P_{20}$	18	30	91	69	35	34
$K_{40} \times P_{53}$	20	30	56	58	44	21
CH_3N_2O + KoH	17	21	37	82	52	57
KoH + $Ca(No_3)_2$	50	63	20	20	28	14

KoH + Oligo Calcium	38	50	84	98	11	7
KoH + $N_{20}K_{20}P_{20}$	46	58	23	19	16	8
KoH + $K_{40}P_{53}$	37	51	35	22	46	24

According to research, water permeability and flux of graphene nanotubes depends on the chemistry and geometric shape of the nanotubes, hydrated radius, and the properties of the transition ions. The critical diameter for salt return is between 0.6 and 0.8 nm. It is also found in the hydrogenated graphene membranes, salt return is higher than hydroxyl graphene membranes.

B/A represents the return flux of solute. Evaluation of B/A efficiency of drag solutions is essential, because it reduces the quality of production of concentrated solution. B/A of drag solution variable depends on the type of drag solution and the capacity of ions in the solution. Among the non-composted fertilizers, KOH has the lowest B/A. This fertilizer contains univalent elements, while in case of bivalent elements, B/A of higher values are created. Thus, it can be concluded that fertilizers with univalent ions are a priority for the PAFO system. It should be noted that the ratio of B/A in graphene nanotube membranes is lower than other membranes, including cellulose acetate.

In contrast to expectations, increased hydraulic pressure followed by decreased B/A. This ratio is reduced with graphene nanofibers membranes. A decrease is caused by different factors and it can be estimated that with increased hydraulic pressure and increased permeability, the concentration polarization in the membranes is increased, but after a short period of time, a high osmotic pressure on the other side of the membrane reduces the polarization. These two phenomena on both sides of the membrane prevent an increase in B/A.

In Figure 3.3, a comparison of B/A ratio with PA membrane and graphene nanotube are presented.

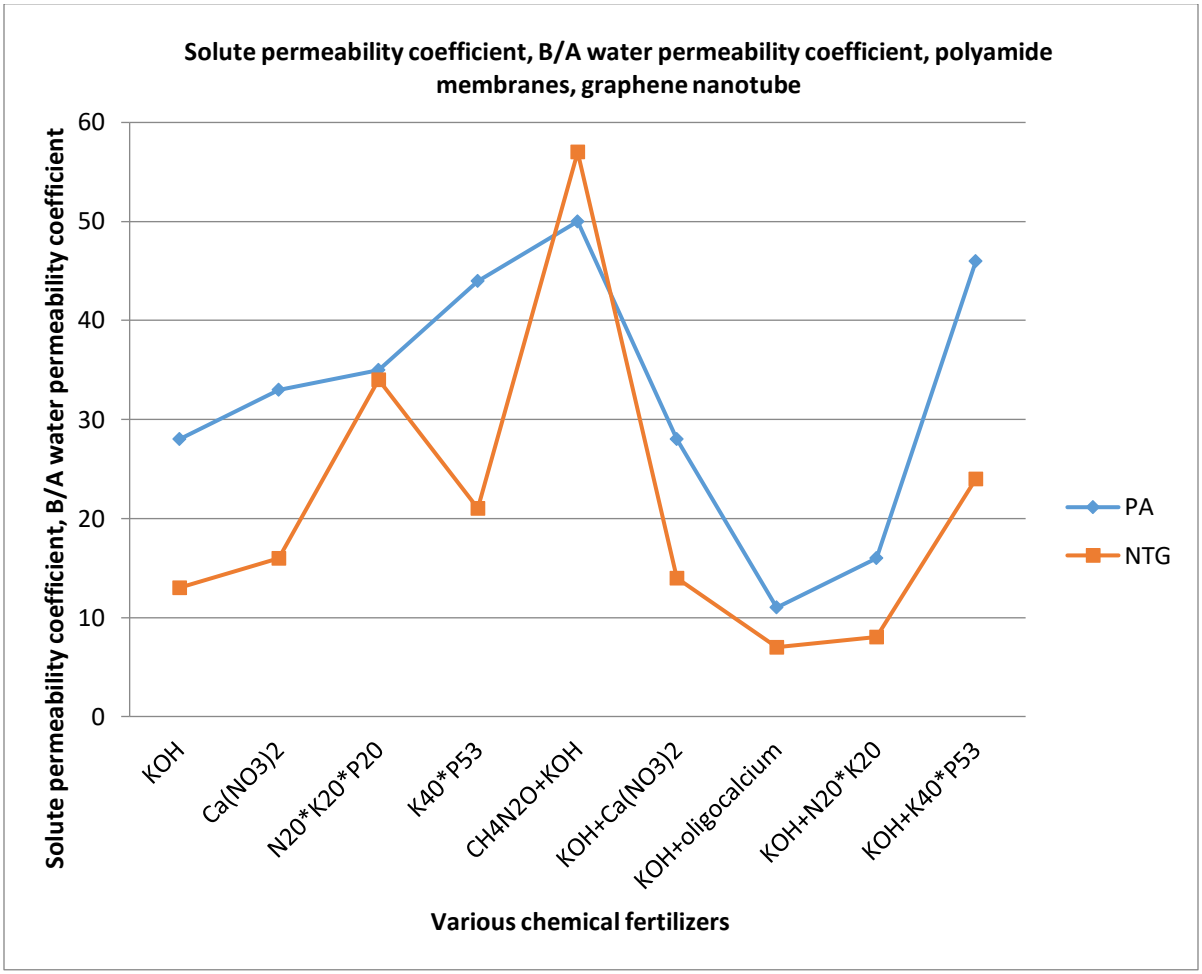

Curve 3.3: Comparing B/A ratio of PA membrane and thin graphene nanotube membrane

The results of changes in water permeability with osmotic pressure and hydraulic pressure are similar to the changes in Gaetenjlandin et al. (2013) in the evaluation project of the effects of hydraulic pressure on forward osmosis system. We need to know that PA membranes have no proper efficiency to be used in forward osmosis systems. A few studies and examinations have been done in this field. In PA membranes, the internal polarization of solute is high and internal polarization reduces the osmotic pressure difference and causes a severe limitation in the water flux. Although forward osmosis commercial membranes are developed by hydration technology and water permeability (A) is almost equal to 1 ($l/m^2.hr$), but the water flux is still low and equal to 9 ($l/m^2.hr$).

In recent studies and developments, the thin film composite (TFC) membranes are made. The permeability of these membranes is over 1($l/m^2.hr$), which approximately had doubled

water flux, but due to the high costs, these membranes are limited, while graphene membranes are not expensive and are affordable.

According to Andrea Achilli et al. (2010), in the field of forward osmosis (FO) using membranes cellulose triacetate, water flux is reported to be equal to 5-10 (l/m2.hr), 8 (l/m2.hr), 6 (l/m2.hr), which also indicates low water flux with cellulose membranes in comparison with the present project (Achilli, 2010).

Changquan et al. (2011), in this study, the forward osmotic membrane synthesis with layer-by-layer membrane and electrolytes was conducted. Water flux is 100 (l/m2.hr) and permeability is 6 (l/m2.hr), indicating the capability of lbl membranes for high flux.

In comparison with results of this project, where seawater and fertilizer were used as feed solution and drag solution, the water flux is 120(l/m^2.hr) and maximum permeability is 8.6 l/m2.hr, which indicates a few percent increase in the water flux with the graphene nanotube membranes in this research.

According to the results, water flux, water permeability, and salt return are improved in the low-thickness support layer nanographene membranes. Such membranes have a great potential for being used in the forward osmosis process, which is due to the increased and improved structural properties. The internal nanotubes and inner pores of nanotube are the solvent crossing paths, which cross the water without pressure.

According to the research conducted at the Babol Noshirvani University, entitled "Nanocomposite Membrane Preparation for Forward Osmosis by Surface Polymerization 2012", salt water was used as drag and feed solution. The produced water flux was estimated to be 95 (l/m^2.hr). In this research the drag and feed solutions do not show the real conditions, because brine osmotic pressure is very different from the seawater osmotic pressure, while in the present project, the seawater with EC of 48000and chemical fertilizer solution have been used as a solution, indicating the real conditions in water treatment. Furthermore, the thickness of membrane support layer has been modified to change and improve the membrane properties, indicating improved water flux of 120(l/m^2.hr) in comparison with project of the Babol Noshirvani University.

2.5. Modeling the outlet flux of the PAFO system

Theoretical modeling of PAFO was performed, and the results of the laboratory measurements were compared with the predicted model. The outlet results are presented in Figure 3.4. The theoretical flux was calculated by Chi equation for PAFO system using MATLAB software.

Table 3.6: Theoretical flux values of the PAFO system

Pilot flux (l/m2.hr)	Modeling predicted flux (l/m2.hr)
120	103
47	35
25	20
30	23
23	20
34	25
98	81
33	24
26	19

According to the diagram below, in all cases, PAFO efficiency is higher than the results of the predicted model.

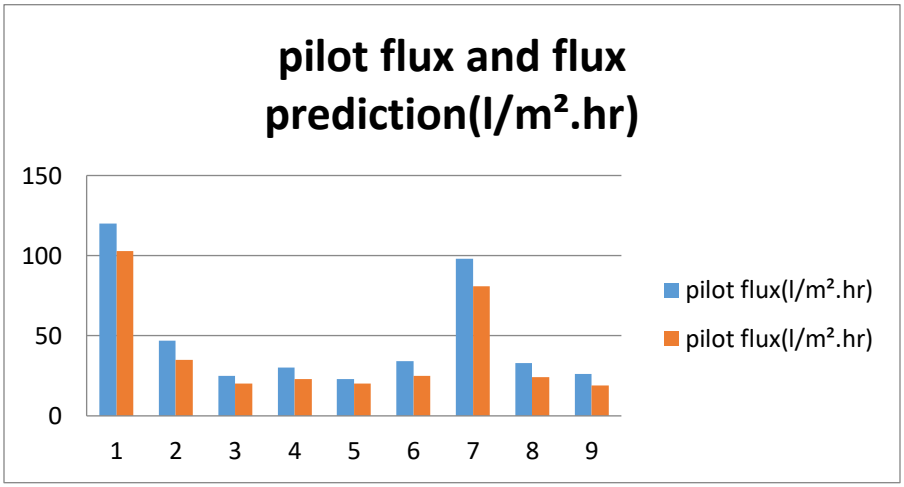

Figure 3.4. Comparing testing and modeling pilot flux

According to the results presented in Table 3-6, the measurements are partly consisted with predictions on developed water flux modeling the process.

The important cases in modeling osmotic systems are membrane orientation and membrane deformation and varied membrane structure parameter. The flux increase rate in the PAFO process is clearly different based on membranes in the research. PAFO modeling with TFC membranes was not confirmed in comparison with laboratory observations due to the membrane malfunction. Thus, it is suggested to define and analyze the membrane structure for proper modeling of these systems.

Conclusion

This study is a main framework for assessment of PAFO system and effective factors on the water flux of this this system. The system efficiency was examined by fertilizer as a drag solution and graphene nanotube membrane with thickness ssupport layer. High flux is the most important parameter to cofirm FO technology for practical application. According to this study, KOH fertilizer of 55 barosmotic pressure and diffusion coefficient of 1.31 has the highest water flux of 120 ($^{L}/_{m^2.hr}$)According to the results, the maximum graphene nanotube membrane permeability coefficient is approximately increased by 50% compared to the maximum PA membrane permeability coefficient. According to the results, the minimum graphene nanotube membrane permeability coefficient of solute (B)is approximately decreased by 50% compared to the minimum PA membrane permeability coefficient, which indicates proper efficiency of graphene nanofiber membranes. The PAFO system overcomes the FO system and makes up the limitations of this system, such low flux. The increased hydraulic pressure and decreased thickness of support layer in the graphene nanotube membranes synthesis significantly affects the outlet flux of the PAFO system. In fact, the PAFO system is the application of the FO+RO hybrid system, which is specially designed for high recovery.

References

Achilli, Andrea; Amy E. Childress (2010). Selection of organ: c – based draw solutions for forward osmosis applications, *Journal of Membrane Science* 364 (2010) 233-249

Changquan Qui, Saren Qi, Chuyang Y. Tang (2011). Synthesis of high flux forward osmosis membranes by chemically crosslink layer-by-layer polyelectrolytes Journal of Membrane Science 381(2011) 74-80

Gaetanjlandin, Arne Rd. Verliefde, Chuyang Y. Tang, Amy E. Childress (2013). Validation of assisted forward osmosis (Afo) process. impact of hydraulic pressure, Journal of membrane Science 447(2013) 1-11

Inger Lise Alswik and May Britt (2013). Pressure retarded osmosis and forward osmosis membrance. *Journal Polymer* (2013),5,303-327.

Maryam Amini, Mohsen Jahanshahi, Ahmad Rahimpour Synthesisof (2013). Novel thin film nanocomposite (TFN) forward osmosis membran using functionalized multi-walled Carbon NanoTubes. Nanotechnology Research institute, School of Chemical (2013).

Sang-Min Shim and Woo-Seungkim (2013). Anumerical study on the performance prediction of forward osmosis process- *Journal of Mechanical Science and Technology* 27 (4) (2013) 1179-1189

Sherubphuntsho, Hongkwan Shon, Seungkwan Hong, Sang Youplee (2011). A novel low energy fertilizer driven forward osmosis desalination for direct fertigation: evaluating the performance of fertilizer draw solutions, *Journal of Membrane Science* 375(2011) 172-181

Zhuqing Wang, Aiguo Wa, Licio Colombi Ciacchi and Gang Wei (2018). Recent advance in nanoporous membrance for water purification, *Journal of Nano Material* (2018), 65-80

Method for analyzing the stability of information transfer between unmanned aerial vehicles in the formation

G. S. Vasilyev *
O. R. Kuzichkin **
I. A. Kurilov ***
D. I. Surzhik ****

ABSTRACT

The use of a formation consisting of adaptive autonomous mobile agents allows solving a wide range of tasks that are often beyond the capabilities of individual agents. A multi-agent formation is a complex high-order dynamic system, so analyzing the stability of such a system is a complex task. At present, the problem of estimating the stability of a formation formed by substantially nonlinear high-order agents with variable dynamic parameters is not sufficiently considered. This task is particularly important for a formation that is affected by complex unstable environmental conditions, in particular for the formation of unmanned aerial vehicles (UAVs). A method for analyzing the stability of formations of nonlinear agents with different types and orders of transfer function has been developed for studying information exchange in UAV networks. The new approach is based on the use of the Popov frequency criterion and the piecewise linear approximation of the hodograph. A computational experiment was performed to analyze the stability of a formation with transfer functions of various types and orders from the 1st to the 10th. The conducted studies revealed a significant difference in the calculated boundary coefficients of formation stability in the linear and nonlinear modes, which confirms the need to analyze the nonlinear stability under the influence of strong destabilizing influences on the formation.

KEYWORDS: multi-agent formation; mobile agent formation; unmanned aerial vehicle; UAV; data transmission; stability; Nyquist criterion; Popov criterion.

* Belgorod State University, Belgorod, 308015, Russia (E-mail: Belova-t@ores.su, https://orcid.org/0000-0003-1681-5223).

** Belgorod State University, Belgorod, 308015, Russia (E-mail: eav@ores.su, https://orcid.org/0000-0003-0817-223X).

*** Vladimir State University, Vladimir, 600000, Russia (E-mail: global@ores.su, https://orcid.org/0000-0003-1901-7411).

**** Vladimir State University, Vladimir, 600000, Russia (E-mail: russia@prescopus.com, https://orcid.org/0000-0002-0101-3503).

Recibido: 03/04/2020 Aceptado: 01/06/2020

Método para analizar la estabilidad de la transferencia de información entre vehículos aéreos no tripulados en la formación

RESUMEN

El uso de una formación que consiste en agentes móviles autónomos adaptativos, permite resolver una amplia gama de tareas que a menudo están más allá de las capacidades de los agentes individuales. Una formación de múltiples agentes es un sistema dinámico complejo de alto orden, por lo que analizar la estabilidad de dicho sistema es una tarea compleja. En la actualidad, el problema de estimar la estabilidad de una formación integrada por agentes de alto orden sustancialmente no lineales con parámetros dinámicos variables, no se considera suficientemente. Esta tarea es particularmente importante para una formación que se ve afectada por condiciones ambientales complejas e inestables, en particular para la formación de vehículos aéreos no tripulados (UAV). Se ha desarrollado un método para analizar la estabilidad de las formaciones de agentes no lineales con diferentes tipos y órdenes de función de transferencia para estudiar el intercambio de información en redes UAV. El nuevo enfoque se basa en el uso del criterio de frecuencia de Popov y la aproximación lineal por partes del hodógrafo. Se realizó un experimento computacional para analizar la estabilidad de una formación con funciones de transferencia de varios tipos y órdenes del 1 al 10. Los estudios realizados revelaron una diferencia significativa en los coeficientes límite calculados de la estabilidad de la formación en los modos lineal y no lineal, lo que confirma la necesidad de analizar la estabilidad no lineal bajo la influencia de fuertes influencias desestabilizadoras en la formación.

PALABRAS CLAVE: formación de múltiples agentes; formación de agentes móviles; vehículos aéreos no tripulados; UAV; transmisión de datos; estabilidad; criterio de Nyquist; criterio de Popov.

Introduction

Using a formation consisting of adaptive autonomous mobile agents allows to solve a wide range of tasks that are often beyond the capabilities of individual agents. In particular, such tasks include positioning mobile robots in production, automating traffic, monitoring the environment with unmanned aerial vehicles (UAVs), and others. Cooperation of individual agents in the formation is based on the interaction protocols of network systems (Amelina, 2011; Wu, 2007).

A multi-agent formation is a complex dynamic system of high order, so analyzing the stability of such a system is a complex task. Existing approaches to assessing the stability of

mobile agent formations are based on a number of simplifying assumptions. Thus, in (Fax & Murray, 2004) the assumption is made about the linearity and identity of the dynamics models of the agents in a formation. The stability analysis of the formation in this paper is based on checking the stability condition of an individual agent using the Nyquist frequency criterion, taking into account the spectrum of the Laplace matrix describing the graph of information transfer between agents. Synchronization in networks of passive agents (including nonlinear ones) has been studied in a number of papers, for example (Proskurnikov, 2014). Most of the known results assume that the graph of agent formation is constant, or that there is a positive delay (dwell-time) between changes. In (Proskurnikov, 2014), the problem of consensus of nonlinear agents of the 2nd order (double integrators) is investigated, in addition, non-stationary communication functions are considered. A number of papers consider the problems of adaptive synchronization of interconnected dynamic subsystems (Chopra & Spong, 2006; Arcak, 2007) and adaptive management of agents with significantly different dynamic properties. The influence of the bandwidth of the information exchange channel between agents on the stability of the agent system and its dynamic properties as a whole is studied (Andrievsky et al., 2010; Amelin, et al., 2019). At the same time, the problem of estimating the stability of a formation formed by essentially nonlinear high-order agents with variable dynamic parameters is not sufficiently considered. This problem is particularly relevant for a formation that is affected by complex unstable environmental conditions, in particular, for a UAV formation.

The aim of this work is to develop a method for analyzing the stability of high-order non-linear agent formations with variable dynamic parameters for information exchange in UAV networks.

1. Method for analyzing the absolute stability of the UAV formation as high-order nonlinear agents

Consider the UAV formation as a network of interconnected dynamic subsystems represented in the Lurie form (a dynamic linear unit (LU) with a static non-linear unit (NLU) in feedback). According to (Fax & Murray, 2004), $K(s)$ stabilizes the dynamics of agent formation with many inputs and many outputs of $P(s)$ if

$$\rho(W(j\omega)) < M^{-1} \forall \omega \in (-\infty; \infty),$$

where $W(s) = P(s)K(s)(I + P(s)K(s))^{-1}$, I is the unit matrix. This condition allows us to check the stability of the formation of linear agents according to the Nyquist criterion. When exposed to destabilizing perturbations on formation agents operate in a significantly nonlinear regime, so the condition of Nyquist stability criterion can be broken, and it is necessary to study the stability of nonlinear system by Popov criterion. According to the Popov criterion (Krasovsky, 1987; Popov, 1970), for absolute stability of the equilibrium of a nonlinear system with a stable LU, the existence of a real g for which the condition is satisfied is sufficient

$$\forall \omega \geq 0 : \mathrm{Re}\left[(1 + j\omega g)W(j\omega)\right] > -1/k, \quad (1)$$

where k is the angle of absolute stability, $W(j\omega) = \dfrac{A_1(\omega) + jA_2(\omega)}{B_1(\omega) + jB_2(\omega)}$ is the complex transfer function of the LU, and I is order of the LU. The highest and lowest k values, at which the condition (1) is met, determine, respectively, the lower and upper bounds of the area of stable operation of the agent in a formation.

Let's divide the complex transfer function of a LU into real and imaginary parts:

$$W(j\omega) = W_R(\omega) + jW_I(\omega), \quad (2)$$

where $W_R(\omega) = \dfrac{A_1(\omega)B_1(\omega) + A_2(\omega)B_2(\omega)}{B_1^2(\omega) + B_2^2(\omega)}$ is real frequency characteristic of the LU, $\mathrm{W_I}(\omega) = \dfrac{A_2(\omega)B_1(\omega) - A_1(\omega)B_2(\omega)}{B_1^2(\omega) + B_2^2(\omega)}$ is imaginary frequency characteristic of the LU, polynomials $A_{1,2}(\omega) = \sum_{i=0}^{I} A_{1,2_i}(\omega)$ and $B_{1,2}(\omega) = \sum_{i=0}^{I} B_{1,2_i}(\omega)$ are defined according to the expressions:

$$A_{1_i}(\omega) = \mathrm{Re}\left[A_i(j\omega)\right] = \alpha_{4i}\omega^{4i} - \beta_{4i+2}\omega^{4i+2},$$

$$B_{1_i}(\omega) = \mathrm{Re}\left[B_i(j\omega)\right] = \beta_{4i}\omega^{4i} - \beta_{4i+2}\omega^{4i+2},$$

$$A_{2_i}(\omega) = \mathrm{Im}\left[A_i(j\omega)\right] = \alpha_{4i+1}\omega^{4i+1} - \alpha_{4i+3}\omega^{4i+3},$$

$$B_{2_i}(\omega) = \mathrm{Im}\left[B_i(j\omega)\right] = \beta_{4i+1}\omega^{4i+1} - \beta_{4i+3}\omega^{4i+3},$$

where α_i, β_i are coefficients of the polynomials in the numerator and denominator of the LU transfer function. Dividing the LU transmission coefficient into real and imaginary parts allows a simple geometric interpretation of the Popov criterion.

We introduce a modified complex transfer function

$$W^*(j\omega) = W_R(\omega) + jW_I^*(\omega), \quad (3)$$

where $W_I^*(\omega) = \omega W_I(\omega)$.

By converting (1) considering (3), we obtain a sufficient condition of absolute stability in the form $W_R(\omega) - gW_I^*(\omega) > -1/k$. For the boundary values of the coefficient k, the condition takes the form of equation (the Popov line equation)

$$W_R(\omega) - gW_I^*(\omega) = -1/k. \quad (4)$$

The line defined by equation (4) passes through the point -1/k on the real axis with a slope of 1/g.

To conduct an analytical study of the absolute stability of the formation, it is necessary to obtain an expression of the Popov line for a specific type of LU $W(j\omega)$. It is not possible to solve the problem in a generalized form for an arbitrary type and order of LU. This difficulty arises from the non-linear nature of the left part of equation (4) and the presence of two unknowns g and k. Approximation of the frequency characteristics of the LU based on continuous piecewise linear functions (CPLF) (Kurilov & Romanov, 2002) allows us to linearize (4), eliminate the unknown g, and conduct an analytical study of the absolute stability of the formation in general.

Let's set the following approximation parameters: variable range from ω_0 to ω_N, N is maximum number of approximation nodes, n and m are current numbers of approximation nodes. Frequency characteristics change most quickly in the region of small values and slowly in the region of large values. Thus, in order to reduce the error, the nodes are arranged in an exponential manner. Expressions of lines that approximate the left part (4) in the current nodes will take the form

$$W_{I\,m,n}^*(W_R) = g_{m,n}(W_R - b_{m,n}), \quad (5)$$

where $g_{m,n} = (W_{I\,m}^* - W_{I\,n}^*)/(W_{R\,m} - W_{R\,n})$ are angular coefficients, $W_{I\,m,n}^* = W_I^*(\omega_{m,n})$, $W_{R\,m,n} = W_R(\omega_{m,n})$, abscissas of the approximating straight lines are defined as

$$b_{m,n} = W_{R\,m} - W_{I\,m,n}^* / g_{m,n}. \quad (6)$$

As a result, we get N^2 coefficients $b_{m,n}$. Among the obtained abscissa values, it is necessary to exclude those that are located outside the interval $\omega_n \div \omega_m$ and are "false". To do

this, include the CPLF $Q_{m,n}(\vartheta)=K_\sigma\sum_{\lambda=0}^{1}\sum_{\gamma=0}^{1}(-1)^{\lambda+\gamma}\left|\vartheta+\vartheta_n-\vartheta_m(1-\gamma)-\frac{\lambda}{2K_\sigma}\right|$, where K_σ is the steepness of the side components of the inclusion function. Function $Q_{m,n}(\vartheta)$ takes value 1 if its argument belongs to the $[\omega_n;\omega_m]$ section, and 0 otherwise.

The corresponding inclusion function for" false" abscissa values is zero, and for true values $Q_{m,n}(b_{m,n})=1$. To exclude "false" values of $b_{m,n}$, it is enough to multiply (6) by $Q_{m,n}(b_{m,n})$

$$b^*_{m,n}=b_{m,n}Q_{m,n}(b_{m,n}). \quad (7)$$

The boundary values of k for each true abscissa are obtained by substituting (7) in the right part (4)

$$\mathrm{k}_{m,n}=-1/b^*_{m,n}. \quad (8)$$

Let's denote N_2^{low} and N_2^{up} - the lower and upper bounds of the range of N^2 values in which the formation of agents remains stable. That is, the area of stability is a segment $N_2^{low}\le N_2\le N_2^{up}$.

To find the boundaries of the area of absolute stability, it is necessary to select one negative and one positive nearest to zero from all values (8).

The lower bound of N_2 is defined as the maximum of all negative values $k_{m,n}$

$$\tilde{N}_2^{low}=\max\left\{k_{m,n}\left[1-\tilde{q}(k_{m,n})\right]\right\}, \quad (9)$$

where $\tilde{q}(\vartheta)=\frac{1}{2\Delta}\left[|\vartheta+\Delta|-|\vartheta|+\Delta\right]$ is the inclusion CPLF, which takes value 1 for $\vartheta\ge0$ and 0 for $\vartheta<0$. The multiplier $1-\tilde{q}(\mathrm{k}_{m,n})$ in (9) excludes positive roots.

The upper bound of N_2 corresponds to the minimum of all positive values $k_{m,n}$

$$\tilde{N}_2^{up}=\min\left\{N_{2\mathrm{k}}\tilde{q}(k_{m,n})\right\}. \quad (10)$$

As an example, we calculate the area of absolute stability of the agent formation, when the LU is described by the transfer function of the low-pass filter (LPF) of the 5th order $W(p)=1/(1+Tp)^5$, where T is the LU time constant.

The real and imaginary frequency characteristics of LU are obtained by expression (2) based on polynomials $A_{1,2}(\omega)$ and $B_{1,2}(\omega)$. Take the time constant of LU equal to T=1 s and make an approximation of the frequency characteristics in the range of variables

$\omega_0 = 0.01\ \text{s}^{-1}$, $\omega_N = 7\,\text{s}^{-1}$, N=30. From all N^2=900 abscissas (6), we determine the true ones (7). According to (9) and (10), $\tilde{N}_2^{low} = -1.006$ and $\tilde{N}_2^{up} = 2.9$.

Figure 2 shows the usual W and modified W^* hodographs of the frequency characteristic of the LU under consideration, approximated by the CPLF. Abscissa of approximating lines corresponding to the boundaries of the absolute stability region, $\tilde{b}_{low} = -1/\tilde{N}_2^{low} = 0.994$, $\tilde{b}_{\text{up}} = -1/\tilde{N}_2^{up} = -0{,}345$. The Popov lines for $\tilde{N}_2^{low,up}$, indicated in Fig. 2 as $W^*_{I\ low,up}$, are obtained by (5).

The stability of a formation formed by linear agents, in accordance with (Yakovlev, 2003; Voronov, 1986), is determined by the condition that the Nyquist hodograph intersects the abscissa axis ($W_I(\omega) = 0$), the boundary values are equal to $N_2^{low} = -1$, $N_2^{up} = 2.885$, that is, the stability region of the formation of linear agents of the 5th order represents a segment $-1 \le N_2 \le 2.885$

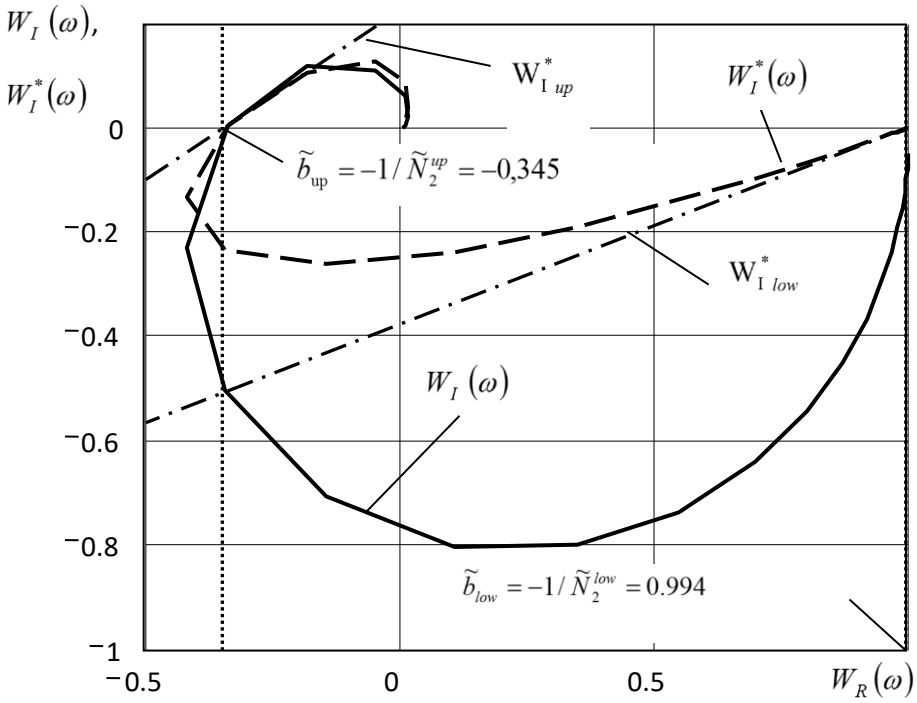

Fig. 1. Regular (W) and modified (W^*) hodographs of the 5th order agent formation

From the comparison of hodographs in Fig. 2 it is seen that the regions of stability of the formation of linear agents and absolute stability of the formation of nonlinear agents coincide. A small error of $\tilde{N}_2^{low,up}$ (less than 1%) is caused by an error in the approximation of frequency characteristics. Similarly, the stability of formations of other orders is analyzed.

In the case of the 5th-order LPF considered above, the stability regions of the forms in the linear and nonlinear modes of the agents' functioning coincide. It is also possible that they differ for some types of LU. As an example, we can also calculate the area of absolute stability of the formation, the transfer function of which is described by a complex filter of the 4th order. The filter consists of sequentially connected integrating, inertial-integrating, and oscillating links. Transfer function of the LU formation

$$W(p)=\frac{1}{p(1+Tp)\left(\beta+2\xi Tp+T^2p^2\right)}, \tag{11}$$

where T is time constant of LU. We assume T=ξ=1, β=10.

After calculating the LU coefficients α_i, β_i, we get the real and imaginary frequency response of the LU by substituting these coefficients in (2).

The approximation of the frequency characteristics is performed in the same range of variables $\omega_0=0.01\ \mathrm{s}^{-1}$, $\omega_N=7\,\mathrm{s}^{-1}$ as for LPF5. The number of approximation nodes is increased to N=50 to improve accuracy. Of all the N^2=2500 abscesses (6), we determine the true ones by (7). By (9) we get $\tilde{N}_2^{low}=-1/0\to-\infty$. The upper absolutely stable value of N_2 is obtained by (10): $\tilde{N}_2^{up}=1/0.045=22.2$. The area of absolute stability represents a segment $0\le N_2\le 22.2$.

From a comparison of the regular $W_I(\omega)$ and modified $W_I^*(\omega)$ hodographs in Fig. 3 it can be seen that the stability regions of the formation differ in the linear and nonlinear modes of agents' functioning. Thus, the stability "in small" is determined by the abscissa of the point at which $W_I(\omega)=0$: $b_{\text{up}}=-0.034$, $N_2^{up}=1/0.034=29.4$. The stability region in "small" is a segment $0\le N_2\le 29.4$. The general method for analyzing the stability of the form in the linear mode (for small perturbations) is based on the application of the Nyquist frequency criterion and the piecewise linear approximation of the hodograph.

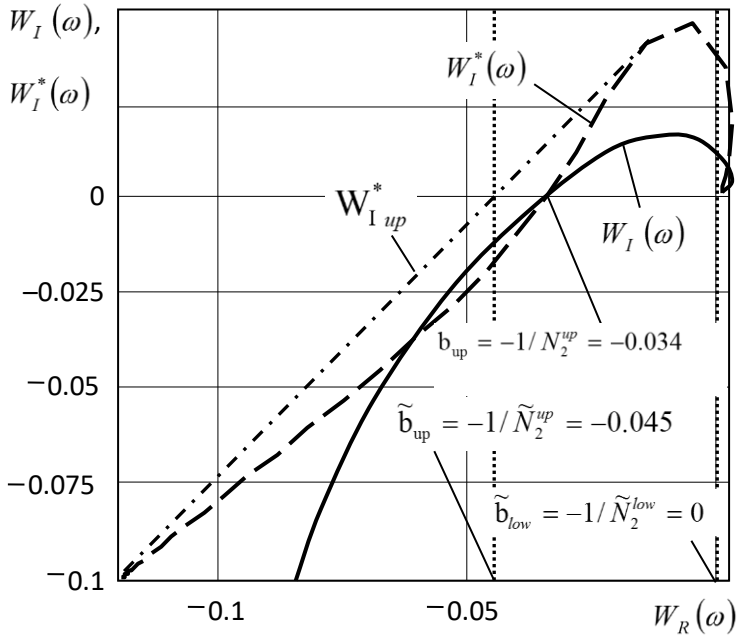

Fig. 3. Regular and modified hodographs of the formation described by a complex oscillation-integrating LU of the 4th order

The upper limit value of N_2 in the nonlinear mode is significantly less than in the linear mode (1.32 times). This imposes restrictions on the choice of acceptable dynamic parameters of formation agents for large impacting perturbations.

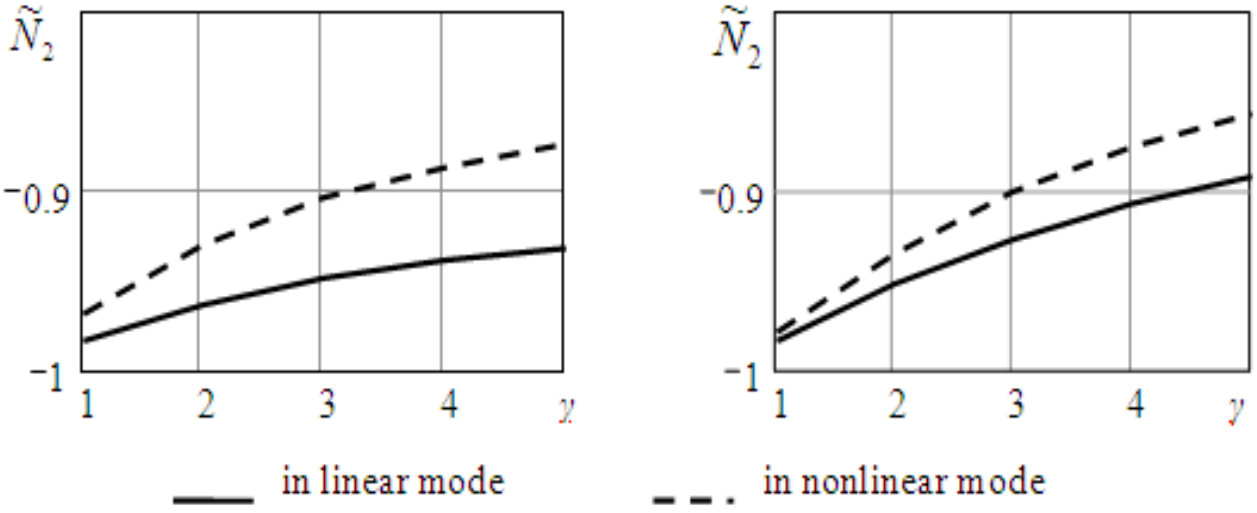

a) $\tilde{N}_2^{low}$ for NF of the 4th order

b) $\tilde{N}_2^{low}$ for NF of the 6th order

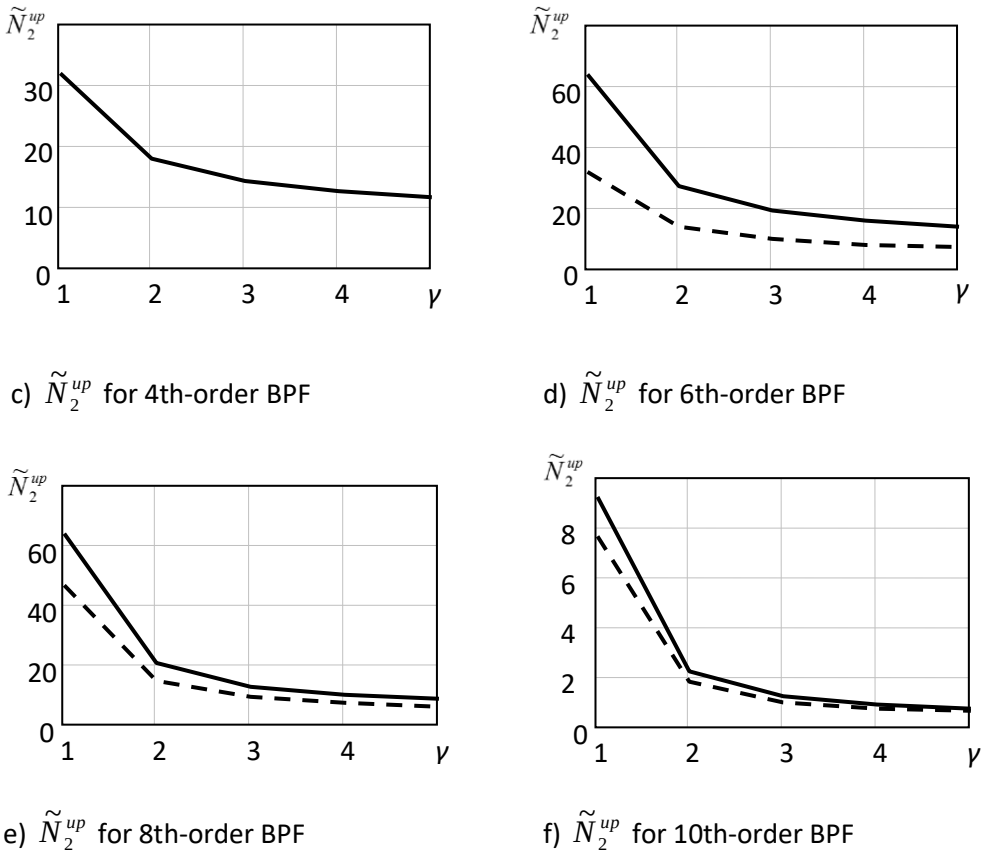

Fig. 4. Dependences of the boundary stable coefficients N_2 on γ in the linear and non-linear mode for different filter types and orders

Fig. 4 also shows graphs of stable coefficients N_2 of the formations with LU described by bandpass (BPF) and notch (NF) filters of different orders (4, 6, 8, 10). Filter transfer functions have the form:

$$M_2^{LPF}(p) = 1/(1+Tp)^I,\ M_2^{HPF}(p) = (Tp)^I/(1+Tp)^I,$$

$$M_2^{BPF}(p) = \mathrm{H}_{\mathrm{LPF}}(p)\mathrm{H}_{\mathrm{HPF}}(p) = (\gamma Tp)^{0.5I}/\left[(1+Tp)(1+\gamma Tp)\right]^{0.5I},$$

$$M_2^{NF}(p) = 1 - M_2^{BPF}(p).$$

Here, T is the time constant of the link in the LPF and HPF, γ is the ratio of the time constants of the LPF and HPF links in the BPF and NF. When the agents switch to the nonlinear mode of operation, the stability region of the formation significantly narrows from the top (by a factor of 2 for the 6th-order PF at γ=1 (Fig. 4d): $N_2^{up} = 64$ in linear mode, $\widetilde{N}_2^{up} = 32$ in nonlinear mode). The results of the calculation of the lower limit of absolute stability for BPF coincide with the results of the calculation for the linear mode. Based on

absolutely stable values N_2 of a formation with LU at form of low-pass filter (LPF) and high-pass filter (HPF) coincide with the values for stability "in the small" for any filter order to 10-th inclusive.

Expressions are obtained that define the range of the loop amplification coefficient of the feedback circuit corresponding to the stable operation of the formation "as a whole" (for large amounts of influences). The use of CPLF allows us to study the absolute stability of formations of essentially nonlinear agents with different types and orders of the transfer function of the LU.

Conclusions

The relevance of the study of the absolute stability of formations of high-order non-linear agents for the analysis of information exchange in UAV networks with an arbitrary amount of impacting perturbations (stability "as a whole") is noted. A method for analyzing the absolute stability of formations of nonlinear agents with different types and orders of the transfer function of LU is developed. The new approach is based on the use of the Popov frequency criterion and a piecewise linear approximation of the hodo-graph. The choice of a specific transfer function of the LU is carried out by simply substituting its coeffi-cients in the resulting expressions (1)-(10). A computational experiment was conducted to analyze the stability of a formation with LU of various types and orders from the 1st to the 10th. The conducted re-search revealed a significant difference in the calculated boundary stability coefficients of the formation in the linear and nonlinear mode, which confirms the need to analyze the nonlinear stability under the influence of strong destabilizing influences on the formation.

Acknowledgments

The work was supported by RFBR grant 19-29-06030-MK "Research and development of wireless ad-hoc network technology between UAVs and smart city dispatch centers based on adaptation of transmission mode parameters at different levels of network interaction". The theory was prepared in the framework of the state task FZWG -2020-0017 "Development of theoretical foundations for building information and analytical support for telecommunication systems for geo-ecological monitoring of natural resources in agriculture".

References

Amelin, K. S., Andrievsky, B. R., Tomashevich, S. I., Fradkov, A. L. (2019). Data transfer with adap-tive encoding between quadrocopters in formation", UBS, 62 (2016), 188-213; Autom. Remote Con-trol, 80(1),150-163

Amelina N. O. (2011). Multiagent technologies, adaptation, self-organization, consensus creation. Stochast. optimization in computer science, 7(1), 149-185.

Andrievsky, B. R., Matveev, A. S., & Fradkov, A. L. (2010). Management and evaluation under in-formation constraints: towards a unified theory of control, computation, and communication. Auto-matics and telemachanics, 4, 34-99.

Arcak, M. (2007). Passivity as a design tool for group coordination. IEEE Trans. Autom. Control, 52(8), 1380–1390.

Chopra, N., & Spong, M.W. (2006). Passivity-based control of multi-agent systems. Kawa-mura S., Svinin M. (eds.). Advances in robot control. Berlin: Springer-Verlag, 107–134.

Fax, J., & Murray, R. (2004). Information Flow and Cooperative Control of Vehicle Formations. IEEE Trans. Automat. Con-tr, 8, 1465–1476

Krasovsky, A. A. (1987). Handbook on theory of automatic control / A. G. Aleksandrov, V. M. Arte-myev, V. V. Afanas'ev [et al.]; under the editorship of A. A. Krasovsky. - Moscow: Nauka,. – 712 p.

Kurilov, I. A., & Romanov, D. N. (2002). Piecewise-linear continuous approximation of characteris-tics. Data, information and processing: Collection of scientific articles. under the editorship of S. S. Sadykov, D. E. Andrianov. - MOSCOW: Hotline-Telecom, 175 – 180.

Popov, V. M. (1970). Hyperstability of automatic systems / V. M. Popov. - Moscow: Nauka, - 456 p.

Proskurnikov, A.V. (2014). Frequency criteria for consensus in multi-agent systems with nonlinear sector connections. Automatics and telemachanics, 11, 110-126

Voronov, A. A. (1986). Automatic control theory: a textbook for universities in the specialty "Auto-mation and telemechanics" / A. A. Voronov, D. P. Kim, V. M. Lokhin [and others]; ed. by A. A. Voro-nov. - -Vol. 2. - Moscow: Higher school, - 504 p.

Wu, Z., GUAN, Z., WU, X., & LI, T. (2007). Consensus Based Formation Control and Trajectory Tracing of Multi-Agent Robot Systems. J. Intelligent and Robotic Systems, 48(3), 397–410.

Yakovlev, V. B. (2003). Theory of automatic control: a textbook for universities / S. E. Dushin, N. S. Zotov, D. H. Imaev [and others]; edited by V. B. Yakovlev. - Moscow: Higher school,. – 567 p.

Development of methods to model UAVS nonlinear automatic control systems

G. S. Vasilyev *
O. R. Kuzichkin **
I. A. Kurilov ***
D. I. Surzhik ****

ABSTRACT

When modeling Automatic Control Systems (ACS) of an unmanned aerial vehicle (UAV), it is often necessary to take into account the nonlinearity of an aircraft's reaction when the controls drift, as well as the strong influence of various destabilizing factors that make the system go out of linear mode. When known analytical and numerical methods are used to analyze dynamic systems, it is problematic to obtain general solutions that are valid for the variable parameters of the system under study and, at the same time, provide the required error value. A method has been developed to model dynamic processes in automatic non-linear UAV control systems based on linear approximation by parts and crosslinking of partial solutions with consideration of the initial conditions. An example of using the technique to model the transition characteristics of an ACS UAV with a single non-linear link is considered. Based on the analysis of errors in the calculation of the transition process, the effectiveness of the proposed approach is shown.

KEY WORDS: Unmanned aerial vehicle; UAV; non-linear automatic control system; linear approximation by parts; transitional process.

* Belgorod State University, Belgorod, 308015, Russia (E-mail: Belova-t@ores.su, https://orcid.org/0000-0003-1681-5223).

** Belgorod State University, Belgorod, 308015, Russia (E-mail: eav@ores.su, https://orcid.org/0000-0003-0817-223X).

*** Vladimir State University, Vladimir, 600000, Russia (E-mail: global@ores.su, https://orcid.org/0000-0003-1901-7411)

**** Vladimir State University, Vladimir, 600000, Russia (E-mail: russia@prescopus.com, https://orcid.org/0000-0002-0101-3503)

Recibido: 10/03/2020 Aceptado: 20/05/2020

Desarrollo de métodos para modelar sıstemas de control automátıco no lıneal de UAVS

RESUMEN

Al modelar sistemas de control automático (ACS) de un vehículo aéreo no tripulado (UAV), a menudo es necesario tener en cuenta la no linealidad de la reacción de una aeronave cuando los controles se desvían, así como la fuerte influencia de varios factores desestabilizadores que hacen que el sistema salga del modo lineal. Cuando se utilizan métodos analíticos y numéricos conocidos para analizar sistemas dinámicos, es problemático obtener soluciones generales que sean válidas para los parámetros variables del sistema en estudio y, al mismo tiempo, proporcionen el valor de error requerido. Se ha desarrollado un método para modelar procesos dinámicos en sistemas de control automático de UAV no lineales basado en aproximación lineal por partes y reticulación de soluciones parciales con consideración de las condiciones iniciales. Se considera un ejemplo de uso de la técnica para modelar las características de transición de un UAV ACS con un solo enlace no lineal. Con base en el análisis de errores en el cálculo del proceso de transición, se muestra la efectividad del enfoque propuesto.

PALABRAS CLAVE: Vehículo aéreo no tripulado; UAV; sistema de control automático no lineal; aproximación lineal por partes; proceso transitorio.

Introduction

To ensure flight safety and successfully solve a wide range of tasks based on unmanned aerial vehicles (UAVs), an effective UAV control system (ACS) is required at the physical level of the UAV communication network (Advanced Control of Aircraft, 2011; Austin, 2011). The development of such systems is impossible without an adequate mathematical model describing the operation of ACS in a wide range of parameters. A large number of studies consider the linear dynamics of UAVs (Lebedev and Chernobrovkin, 1973; Moiseev, 2013) and the linearity of their control systems (Zheng, et al., 2014; Kuriki and Namerikawa, 2014). The task of modeling and analyzing UAV ACS is significantly complicated when the non-linearity of the aircraft's response is manifested in case if the controls are deviated (Xiang et al., 2017; Raffo et al., 2010). In addition, the nonlinearity of processes in control systems is caused by the strong influence of various destabilizing factors that cause the system to exit the linear mode. In most cases, there are no convenient analytical expressions for describing nonlinear systems. Therefore, we have to use numerical methods for solving differential

equations that describe the dynamics of UAVs (Marino et al., 2016). This approach does not allow us to obtain general solutions for the variable parameters of the system under study. At the same time, the use of linearization of ACS characteristics based on the Taylor series is convenient for analytical research, but is often unacceptable because of the unacceptably high approximation error in a wide range of changes in impacts and response.

A promising approach is piecewise linear approximation of the system characteristics (Balashkov, 2010; Bogachev and Chapliga, 1976). The approach makes it possible to obtain analytical solutions for dynamic processes in control systems that are valid for individual linear sections of the characteristics of nonlinear parts of the system. Crosslinking of partial solutions is performed taking into account the initial conditions for each current section of the transition process up to the established mode.

The purpose of this work is to develop a method for modeling dynamic processes in nonlinear automatic control systems of UAVs based on piecewise linear approximation.

1. The dynamics of the UAV the longitudinal flight mode

The mathematical model of UAV movement in the longitudinal flight mode is described by a system of nonlinear differential equations (Gutsevich, 2018):

$$
\begin{aligned}
&m\frac{dV}{dt} = P\cos\alpha - X_a - mg\sin\theta,\\
&mV\frac{d\theta}{dt} = P\sin\alpha - Y_a - mg\cos\theta,\\
&\vartheta = \theta + \alpha,\\
&I_z\frac{d\vartheta}{dt} = M_z.
\end{aligned}
$$

In this system, m is the mass of the UAV, V – vector of linear velocity, P is the power of the engine thrust, α angle of attack, X_a is drag, Y_a is lifting force, g is the gravitational acceleration, ϑ – pitch, θ is the slope of the trajectory of the mass center of the aircraft, I_z is the moment of inertia of the UAV along the z-axis, M_z is the moment of the aerodynamic forces.

Similar nonlinear differential equations describe other UAV flight modes (start, landing, coordinated u-turn, spiral descent, etc.), while UAV dynamics in these modes

generally also have nonlinear properties. In general, the nonlinearity of UAV dynamics should be taken into account when modeling and developing UAV ACS.

2. Representation of the UAV ACS scheme based on the model of amplitude-phase signal conversion

The functional diagram of the aircraft height stabilization circuit is shown in Fig. 1 (Gordin, 2000).

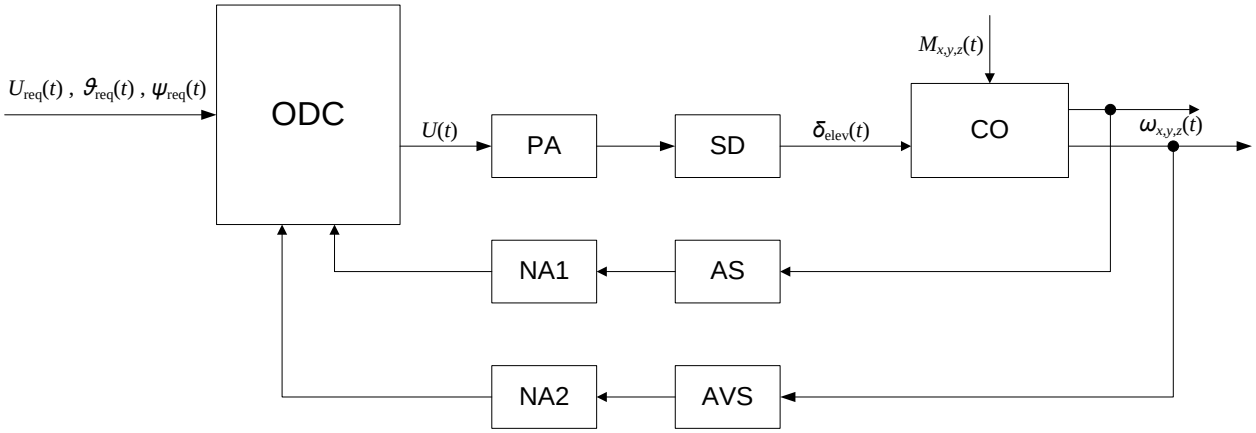

Figure 1. Functional diagram of the UAV control system

In Fig. 1 the following designations are accepted: ODC - onboard digital computer, PA – pre-amplifier, SD – servo drive, CO – control object; AS – angle sensor; AVS – angular velocity sensor; NA1, NA2 – normalizing amplifiers; $U_{req}(t)$, $\vartheta_{req}(t)$, $\psi_{req}(t)$ – the required values of roll, pitch, and yaw angles; $\delta_{elev}(t)$ – deviation angle of the elevator; $M_{x,y,z}(t)$ – disturbing effects; $U(t)$ –obtained pitch angle value; $\omega_{x,y,z}(t)$ – angular roll, pitch, and yaw speeds.

To analyze the two-channel scheme (Figure 1), we present each control channel based on the amplitude-phase signal conversion (APC) model (Vasilyev et al., 2011, 2013). The model of the converter with deviation control (Fig. 2) includes a similar APC* a control device (CD), a control path (CP), and a weight distributor (WD). The control device (CD) controls the amplitude and (or) phase of the input signal. The CP consists of a detector for deviation of the signal amplitude and (or) phase (D), as well as a filter (F). The values of the WD transmission coefficients determine the proportions of signal transmission from its

inputs to its outputs. The diagram shows: U_1, u_1 и U_2, u_2 – input (main, additional) and output signals, u – control signal.

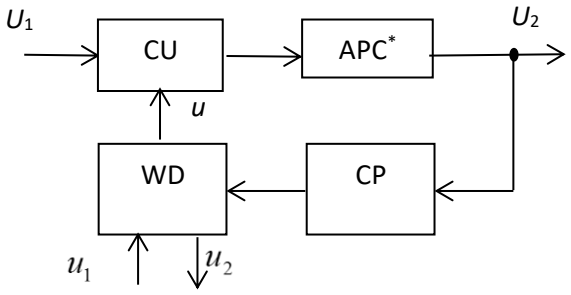

Fig. 2. Model of an amplitude-phase signal converter with deviation control

Transfer functions of APC model blocks (Fig. 2), equivalent to representing the control scheme (Fig. 1), have the form:

$K_{APC*} = K_{PA} \cdot K_{SD}$, $K_{CP}^{(1)} = K_{NA1} \cdot K_{AS}$, $K_{CP}^{(2)} = K_{NA2} \cdot K_{AVS}$, $K_{CU} = K_{WD} = 1$.

3. UAV ACS modeling technique based on the APC model and piecewise linear approximation

To obtain analytical expressions of the dynamic characteristics (transients) of a non-linear UAV ACS, we approximate the nonlinear characteristic of the D based on piecewise linear functions (Kurilov et al. 2010, 2012). After approximation, the characteristic looks like the sum of M linear sections, where M is the maximum number of the approximation node. The equation of the approximating line segment for the node m: $f_{Dm}=K_m y+B_m$, where y is a parameter (amplitude or phase) of the output signal of the converter, K_m and B_m are approximation coefficients. Let's denote the transfer coefficient of K_{APC*} as K^* and assume $u_1=u_2=0$. The equation of the converter at the section m $[Y_m; Y_{m+1}]$

$$y_m = x_m - K^* \left[K_y n_p M(p) \left(K_m y_m + B_m \right) \right],$$

where x is a parameter (amplitude or phase) of the input signal, $M(p)$ is a transmission coefficient of the CP filter, $p = d/dt$ is operator, t is time, K_{CU} and K_{WD} are transmission coefficients of corresponding blocks.

We denote $N_m = K_y n_p K_m$ - the control coefficient and $B_m^* = K_y n_p B_m$. The Laplace image of the output parameter on the *m* section will take the form

$$y_m = x_{\text{m}} - K^*[M(p)(\text{N}_{\text{m}} y_m + B_m^*)]. \quad (1)$$

This is a linear differential equation of the APC at the interval [*m*, *m*+1], presented in operator form. The general nonlinear equation of the converter can be represented by the sum of equations (1) for all parts of the approximation. Let's present the filter transfer function as

$$M(p) = A(p)/B(p) = \sum_{i=0}^{I} \alpha_i p^i \Big/ \sum_{i=0}^{I} \beta_i p^i , \quad (2)$$

where α_i, β_i are coefficients of the filter.

Substitute (2) in equation (1), which after the conversion will take the form

$$y_m \sum_{i=0}^{I} \beta_i p^i = x_{\text{m}} \sum_{i=0}^{I} \beta_i p^i - K^* \left[\sum_{i=0}^{I} \alpha_i p^i \left(\text{N}_{\text{m}} y_m + B_m^* \right) \right].$$

Let's replace the Laplace operator *p* with a differential d/dt in the resulting expression

$$\sum_{i=0}^{I} \beta_i \frac{d^i y_m}{dt^i} = \sum_{i=0}^{I} \beta_i \frac{d^i x_{\text{m}}}{dt^i} - K^* \left[\sum_{i=0}^{I} \alpha_i \frac{d^i \left(\text{N}_{\text{m}} y_m + B_m^* \right)}{dt^i} \right]. \quad (3)$$

Let's make an operator equation for (3) taking into account the initial conditions:

$$y_m(t) \leftarrow Y_m(p), \quad y'_m(t) \leftarrow pY_m(p) - y_m(0), \quad y''_m(t) \leftarrow p^2 Y_m(p) - pY_m(0) - y'_m(0),$$

$$y^{i'}{}_m(t) \leftarrow p^i Y_m(p) - p^{i-1} y_m(0) - p^{i-2} y'_m(0) - \ldots$$

$$- y_m{}^{i-1}(0) = p^i Y_m(p) - \sum_{k=1}^{i} y_m{}^{(k-1)}(0) p^{i-k}.$$

We assume that all derivatives except the first one are null: $y^{(i)}{}_m(0) = 0, i > 1$. Similarly, we present an image of the impact and its derivatives. Then

$$x^{(i)}{}_m(t) \leftarrow p^i X_m(p) - p^{i-1} x_m(0) - p^{i-2} y'_m(0). \quad (4)$$

Given (4), the expression (3) will take the form

$$\sum_{i=0}^{I} \beta_i \left[p^i Y_m(p) - p^{i-1} y_m(0) - p^{i-2} y'_m(0) \right] =$$

$$= \sum_{i=0}^{I} \beta_i \left[p^i X_m(p) - p^{i-1} x_m(0) - p^{i-2} x'_m(0) \right] -$$

$$- K^* N_m \sum_{i=0}^{I} \alpha_{\text{i}} \left[p^i Y_m(p) - p^{i-1} y_m(0) - p^{i-2} y'_m(0) \right] -$$

$$- \frac{K^* B_{\text{m}}^*}{p} \sum_{i=0}^{I} \alpha_{\text{i}} p^i .$$

From the resulting equation, we express $Y_m(p)$:

$$Y_m(p) = \frac{pB(p)X(p) - K^* B_m^* A(p) + pC_m(p)}{p\left[B(p) + K^* N_m A(p)\right]}, \quad (5)$$

$C_m(p) = C^{(y)}(p) - C^{(x)}(p) - C^{(G)}(p)$ - polynomial of initial conditions.

$C^{(y)}(p) = \left[\tilde{B}_1(p) + K^* N_m A_1(p)\right] y_m(0) + \left[\tilde{B}_2(p) + K^* N_m A_2(p)\right] y_m'(0)$ - polynomial of initial response conditions,

$C^{(x)}(p) = \tilde{B}_1(p)x(0) + \tilde{B}_2(p)x'(0)$ - polynomial of initial impact conditions,

$C^{(G)}(p) = \begin{cases} K^* B_m^* A_1(p), m \neq m_н \\ 0, m = m_{ini}, \end{cases}$ $\tilde{B}_k(p) = \sum_{i=k}^{I} \beta_i p^{i-k}$, $A_k(p) = \sum_{i=k}^{I} \alpha_i p^{i-k}$.

Initial conditions for different *m* take the following values:

1) $m = m_н$, then $x_{m_н}(0) = y_{m_н}(0) = 0$, $x'_{m_н}(0) = y'_{m_н}(0) = 0$.

For APC with filters of the second and higher orders ($I \geq 2$) $y'_{m_н}(0) = 0$, it corresponds to zero initial values of the stresses on the reactive elements of the filter (Lebedev and Chernobrovkin, 1973).

2) For each subsequent section ($m \neq m_{ini}$), the APC response values at the border of the sections are the same:

$y_m(0) = Y_{m+\bar{q}_m}$, $y'_m(0) = y'_{m-1+2\bar{q}_m}(t_{m-1+2\bar{q}_m})$, where t_m is the end time of a particular solution, $\bar{q}_m = q\left[y_m(t-\Delta) - y_m(t)\right]$ - the direction of the transition process ($\bar{q}_m$=1 when decreasing and $\bar{q}_m$=0 when increasing), $\Delta \to 0$, $q(y)$ - the CPLF of inclusion, equal to 1 at $y \geq 0$ and 0 at y<0, $y'_m(t) = \frac{y_m(t+\Delta) - y_m(t)}{\Delta}$. To calculate t_m, we must determine the abscissa of the intersection points $y_m(t)$ with Y_m line.

The initial value of the impact and its derivative on the m-th section are determined by the time shift: $\tilde{t}_m$: $x_m(0) = x(\tilde{t}_m)$, $x'_m(0) = x'(\tilde{t}_m)$. For each current section, the shift will consist of the sum of the transition durations for each of the previous sections. Let's denote k=0...K-1 is the number of a particular transient solution, K is the total number of particular solutions (k=0 corresponds to m_k=m_0=m_{ini}, k=K-1 corresponds to m_{K-1}=m_{end}. Thus, the time shift of a particular transient solution is defined as

$$\tilde{t}_{mk} = \sum_{\tilde{k}=0}^{k-1} t_{\tilde{k}}, \quad (6)$$

$\tilde{t}_{m_н} = 0$.

4. UAV ACS modeling based on the APC model and piecewise linear approximation

Based on the developed method, the simulation of the transition characteristics of the UAV ACS was performed. Accepted K_y=1, n_p=2, K^*=1. The characteristic of the filter F, which describes the inertia of the feedback circuit of the control loop of the system, is given by the expression $M(p) = (1+ p)^{-1}$. The characteristic of the detector D, describing the non-linearity of the ACS, is approximated by two and three straight lines (Fig. 3a and 3b). The calculated transient characteristic of the UAV ACS when approximating the D with two and three linear sections is shown in Fig. 4. A solid line highlights the component formed by the initial section of the characteristic D and described by the expression $y_1(t) = e^{-2t}$. The dotted line marks the next section of the transition characteristic described by the expression $y_0(t - t_1) = 0{,}125 + 0{,}375e^{-4t}$, where t_1 = 0.34 s is the time shift of the second partial solution. The result of calculating the transition process for three parts of the D approximation is shown by a dashed line (time shifts of the second and third partial solutions (t_2 = 0.087; t_1 = 0.43). The figure shows that the error in the representation of D by three sections is significantly less, especially at the end setting stage.

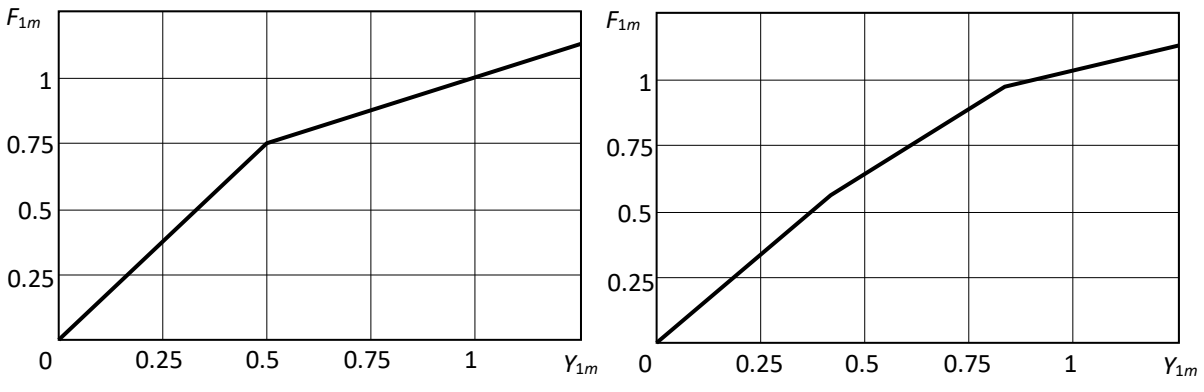

Fig. 3. Approximation of the characteristics of a nonlinear UAV ACS link: a) two linear sections: b) three linear sections

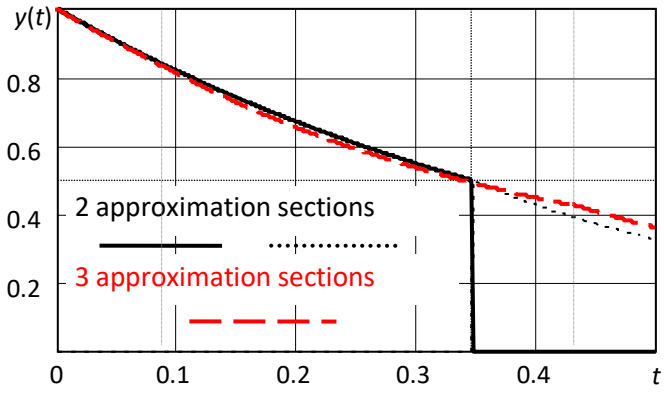

Fig. 4. Transient characteristics of a UAV ACS when approximating a nonlinear link with two or three linear sections

Conclusions

The task of modeling and analyzing UAV ACS is significantly complicated by factors such as the nonlinearity of the aircraft's response when the controls are deviated, as well as the strong influence of various destabilizing factors that cause the system to exit the linear mode. Known numerical and analytical methods do not allow us to obtain general solutions for the variable parameters of the system under study and at the same time provide the required error value.

A method for modeling dynamic processes in nonlinear UAV automatic control systems based on piecewise linear approximation is developed. The approach makes it possible to obtain analytical solutions for dynamic processes in control systems that are valid for individual linear sections of the characteristics of nonlinear parts of the system. Crosslinking of partial solutions is performed taking into account the initial conditions for each current section of the transition process up to the established mode. In the framework of the proposed approach, a representation of the ACS scheme that performs the function of UAV height stabilization is performed on the basis of a model of amplitude-phase signal conversion with deviation control. Analytical expressions describing dynamic processes in UAV ACS with a single nonlinear link are obtained based on the signal conversion model and piecewise linear approximation.

Based on the developed method, the UAV ACS with a nonlinear link represented by two and three linear sections is simulated. It is found that the error in calculating the

transition process when presenting the link characteristic by three approximation sections is significantly less, especially at the end setting stage. Thus, the effectiveness of the proposed approach is shown. When analyzing the dynamic modes of a specific UAV control system, approximated by the signal conversion model with deviation control, its characteristics can be obtained by substituting the corresponding numerical coefficients of the device into general expressions of the dynamic characteristics of the converter.

Acknowledgments

The work was supported by RFBR grant 19-29-06030-MK "Research and development of wireless ad-hoc network technology between UAVs and smart city dispatch centers based on adaptation of transmission mode parameters at different levels of network interaction"

References

Advanced Control of Aircraft, Spacecraft and Rockets Ashish Tewar, 2011 John Wiley & Sons, Ltd. ISBN 978-0-470-74563-2, 454 p.

Austin, R. (2011). Unmanned aircraft systems: UAVS design, development and deployment (Vol. 54). John Wiley & Sons.

Balashkov, M. V. (2010). Development of methods for the analysis of piecewise linear systems and minimization of phase instability of transistor amplifiers: PhD thetis. - Moscow, Russia, - 148 p.

Bogachev, V. M., & Chapliga, V. M. (1976). On the calculation of periodic modes in systems with piecewise linear characteristics under harmonic influence. Radio engineering and electronics, 21(4), 906.

Gordin, A. G. (2000). Unmanned aerial vehicles as control objects. Ucheb.stipend. - Kharkiv: State aerospace university "Kharkiv. aviation institute", - 140 p.

Gutsevich, D. E. (2018). Modeling the behavior of an airplane-type aircraft with automatic control in various flight modes. Mathematical modeling, computer and field experiment in natural Sciences, 1.

Kuriki, Y., & Namerikawa, T. (2014). Formation control of UAVs with a fourth-order flight dynamics. SICE Journal of Control, Measurement, and System Integration, 7(2), 74-81.

Kurilov, I. A., Vasilyev, G. S., & Harchuk, S. M. (2010). Dynamic characteristics analysis of signal converters based on continuous piecewise linear functions. Nauchno-tekhnichesky vestnik Povolzhya, (1), 100-104.

Kurilov, I. A., Vasilyev, G. S., Kharchuk, S. M., & Surzhik, D. I. (2012). Vasilyev G. S. Investigation of the stability of a signal converter based on continuous piecewise linear functions. Radio Engineering and telecommunication systems, 1, 4-7.

Lebedev A. A., Chernobrovkin L. S. (1973). Flight Dynamics of unmanned aerial vehicles. – Study book for universities. - Moscow: Mashinostroenie,. – 616 p.

Marino, M., Gardi, M. A., Sabatini, R., Watkins, M. D., & Watkins, M. R. (2016). DEVELOPMENT OF A VALIDATED DYNAMICS MODEL FOR THE STOPROTOR UAV REPORT 2: Rotary Wing Configuration Experimental and Numerical Methods.

Moiseev, V. S. (2013). Applied theory of control of unmanned aerial vehicles: monograph. Kazan: GBU «Republican Center for Monitoring the Quality of Education»(Series «Modern Applied Mathematics and Informatics»).–768 p.

Raffo, G. V., Ortega, M. G., & Rubio, F. R. (2010). An integral predictive/nonlinear H∞ control structure for a quadrotor helicopter. Automatica, 46(1), 29-39.

Vasilyev, G. S., Kurilov, I. A., Kharchuk, S. M., & Surzhik, D. I. (2013, September). Analysis of dynamic characteristics of the nonlinear amplitude-phase converter at complex input influence. In 2013 International Siberian Conference on Control and Communications (SIBCON) (pp. 1-4). IEEE.

Vasilyev, G., Kurilov, I., & Kharhuk, S. (2011, September). Research of static characteristics of converters of signals with a nonlinear control device. In 2011 International Siberian Conference on Control and Communications (SIBCON) (pp. 93-96). IEEE.

Xiang, X., Liu, C., Su, H., & Zhang, Q. (2017). On decentralized adaptive full-order sliding mode control of multiple UAVs. ISA transactions, 71, 196-205.

Zheng, E. H., Xiong, J. J., & Luo, J. L. (2014). Second order sliding mode control for a quadrotor UAV. ISA transactions, 53(4), 1350-1356.

Soil-Forming and Evolution Related to the Geological Formations, A Case Study of the Southern Part of Urmia Plain

Hengameh Javadi *
Mohammad Hassan Masihabadi **
Reza Sokouti ***
Ebrahim Pazira****

ABSTRACT

The objective of this article was to study the effect of geographical features and geological formations on some physicochemical properties of soils in order to better identify the soil and optimize land management for sustainable agriculture in the southern part of the plain. Urmia, with an area of 35000 (ha) in the province of Western Azarbaijan, Iran. In this investigation, satellite images, aerial photographs, topographic and geological maps were used to identify and distinguish different land forms, soil series classified based on geomorphological and geophysical methods. 30 soil profiles were drilled and the FAO standard dimensions were described. Samples were taken from five soil profiles in each genetic horizon and transferred to the laboratory. The soil moisture and temperature regime was determined as Xeric and Mesic. The soils of the studied area were classified as Fluventic Inceptisols and grid subgroups. The most dominant formations in the Barandoz and Ghasemlou river basins were limestone and lime, which is one of the determining factors in rock formation in different soils in the study area. On the other hand, physiography and topography have also played an important role, so that the upper terraces have more developed soils and some sloping regions have younger and less developed soils. With the decrease in height and proximity to Lake Urmia, the effect of the groundwater level and its salinity on the profiles is evident. Meanwhile, the river bank has young and uncovered soils due to the sediments of the current era.

KEY WORDS: Soil evolution, Urmia plain, geological formation, physiography.

*Ph.D. student of Soil Science, Department of Soil Science, Islamic Azad University, Science and Research Branch of Tehran, Tehran, Iran. CP: 5715784501, Tel :(+98) 9145505489, necklace.h@gmail.com, https://orcid.org/0000-0001-8177-9041

**Professor of Soil Science Department of Islamic Azad University, Science and Research Branch of Tehran, Tehran, Iran. CP: 1394934311 Tel :(+98) 9121307990. Corresponding author Email address: H.masih@yahoo.com, https://orcid.org/0000-0003-3650-9426

***Associate Professor, Department of Soil Conservation and Watershed Research, Agriculture and Natural Resources Research Center of West Azarbaijan, Agricultural Research, AREEO, Urmia, Iran. CP: 5717115759, Tel :(+98) 9144480614, rezasokouti@gmail.com, https://orcid.org/0000-0001-8662-9886

****Professor of Soil Science Department of Islamic Azad University, Science and Research Branch of Tehran, Tehran, Iran. CP: 1346815473, Tel :(+98) 9121860376, ebrahimpazira@gmail.com, https://orcid.org/0000-0003-0258-1710

Recibido: 29/04/2020 Aceptado: 16/06/2020

Formación de suelos y evolución relacionada con las formaciones geológicas, un estudio de caso en la parte Sur de la Llanura de Urmia

RESUMEN

El objetivo de este artículo fue estudiar el efecto de los accidentes geográficos y las formaciones geológicas en algunas propiedades fisicoquímicas de los suelos con el fin de identificar mejor el suelo y optimizar la gestión de la tierra para la agricultura sostenible de la parte sur de la llanura de Urmia, con un área de 35000 (ha) en la provincia de Azarbaijan Occidental, Irán. En esta investigación, se utilizaron imágenes satelitales, fotografías aéreas, mapas topográficos y geológicos para identificar y distinguir diferentes formas de tierra, series de suelo clasificadas en base a métodos geomorfológicos y geofísicos. Se perforaron 30 perfiles de suelo y se describieron las dimensiones estándar de la FAO. Se tomaron muestras de cinco perfiles de suelo en cada horizonte genético y se transfirieron al laboratorio. El régimen de humedad y temperatura de los suelos se determinó como Xeric y Mesic. Los suelos del área estudiada se clasificaron como Inceptisoles y subgrupos de rejilla de Fluventic. Las formaciones más dominantes en la cuenca del río Barandoz y Ghasemlou fueron la piedra caliza y la cal, que es uno de los factores determinantes en la formación de rocas en diferentes suelos en el área de estudio. Por otro lado, la fisiografía y la topografía también han desempeñado un papel importante, de modo que las terrazas superiores tienen suelos más desarrollados y algunas regiones inclinadas tienen suelos jóvenes y menos desarrollados. Con la disminución de la altura y la proximidad al lago Urmia, el efecto del nivel del agua subterránea y su salinidad en los perfiles es evidente. Mientras tanto, el margen de los ríos tiene suelos jóvenes y sin recubrimiento debido a los sedimentos de la época actual.

PALABRAS CLAVE: Evolución del suelo, llanura de Urmia, formación geológica, fisiografía.

Introduction

Although the study of the geological factors helps a deeper understanding of how soil formation and transformation. Few studies have been done about the role of geological formations and landforms on soil characteristics. Different characteristics of parent materials do not change at the same rate (Rabenhorst & Wilding, 1986). Over time and soil development, changes in the soil are less controlled by parent materials and are more likely to be determined by climates and topographies (Caspari et al., 2006). Under these conditions, the morphology of neighboring soils formed on different materials tends to be similar. However, the color, stratification, and reaction of materials are influenced by high-speed soil-forming processes (Buol et al., 2011). On the contrary, some of the characteristics of soil parent materials are very stable and they affect their effects on a long time on the soil.

Clay and sand materials can be made heavy and light texture soils respectively (Costantini & Damiani, 2004). Other materials which have large amounts of weather-sensitive minerals produce loamy soils. Also, the type of parent matter controls the severity of soil processes due to its effect on the texture and specific surface of the soil (Wilding et al., 1983). Generally, soil development in sandy material is faster due to better penetration of the weather, and the thickness of the soil in these materials is deeper (Schaetzl & Anderson, 2005).

Sarvak Formation is a typical example of Kermanshah limestone, which is transformed into two tectonic units of Sanandaj-Sirjan and Zagros Folded. Their constituent materials include fine-grained, intermediate-to-thick, and radial-shaped limestones, whose topography is characterized by rock outcrop and debris, shallow soil, thinness vegetation, and low erosion. In contrast, clastic and shale formations which form at the bottom of the hills, are susceptible to degradation mainly due to Marl. Formations of Amiran, Keshkan, and Ilam are parts of Gurpi, Gachsaran and Aghajari forms of this category. These formations include marl, chert, and shale with layers of limestone and conglomerate. Such formations play the greatest role in soil erosion and its various consequences including sediment production. Differences in the morphological, physical and chemical characteristics of soils reflect the difference in the chemical composition of materials (Irmak et al., 2007). The least amount of lime is found in soils from igneous formations and its maximum in soils from calcareous and dolomite formations. Marls in dry areas are considered to be material with high sensitivity to erosion and the origin of sediment production (Sheklabadi, 2000).

As a result, the degree of development of the horizons and the depth of the soil in this organization is low. Soils formed on calcareous rocks of the Cretaceous have a calcareous and petrochemical horizon more than the calcareous horizons, while in the wetter regions; the clay accumulation horizon has been formed (Rabenhorst & Wilding, 1986). Leaching, clay accumulation, carbonates, and salts were the main soil-forming process in the Azarak Basin in northeastern Jordan (Khresat & Qudah, 2006). In the Azarak region, the process of clay accumulation at a wetter time of the past has led to an increase in clay in the lower horizons and as a result of the formation of an Argillic horizon, and the state of the soil horizons are the result of the clay formation, alteration, and

destruction. On the other hand (Egli et al., 2008) showed that weathering of soils is strongly related to the climate. Moazallahi and Farpoor (2009) in their studies in Kerman, the region concluded that the soil properties and many of the pedogenic properties of the soil such as the formation and deposition of calcium carbonate depend on the weather (Moazallahi & Farpoor, 2009). In arid and semi-arid regions, the types of complications of limestone and gypsum are observed. Calcium carbonate accumulation is a common characteristic and a very important soil-forming process in arid and semi-arid soils (Gunal & Ransom, 2006). Calcium carbonate is produced as a result of complex processes of dissolution, transfer; sedimentation, and re-accumulation of carbonates that are either present in soil material or from external sources that are added to the soil (Blank & Fosberg, 1990).

Owliaie et al. (2006) concluded that the physical and chemical properties of Iran's soils in a dry and semi-arid climate are completely dependent on the calcareous rock, which has been influenced by chemical and physical evacuation over time, and the existence of lime-rich soils brings. Based on geological maps in Urmia, a large part of the soils of the Urmia plain and its surrounding areas are located on quaternary sediments, and most of the agricultural, livestock and natural resources activities are concentrated in this formation (Soltani Sisi, 2005). These quaternary sediments have been expanded on two sides of Lake Urmia and cover a relatively large surface and are more uncoated to semi-hard sand and clay-sand, often forming agricultural lands and fields (Farzamnia et al., 2013). The watershed basins, the rivers leading to the Urmia plain, consist of Cretaceous and Third Age formations, especially Eocene and Miocene, which are sensitive to erosion because of their marl content. In these basins carbonate formations are characterized by different weathering processes with surface erosion, low sediment yield, mountainous geomorphology and steep slope (Ahmadi & Feiznia, 1999).

Review of the research results has shown that to preserve the land and increase the possibility of exploitation of the soil, it is necessary to provide Physico-chemical, morphological data related to the soil and to classify them so that they can be properly planned for their management in different conditions of the land. However, soil-specific studies have been conducted for analyzing the relationship between soil formation and management with geological and topographical factors are low. Therefore, this study aimed

to study the effect of landform and geological formations on some physicochemical properties of soils to better identify soils to optimize land management and promote sustainable agriculture.

1. Materials and Methods

1.1. Study Area

The study area includes the southern part of Urmia plain with an area of 17000 (ha) in the West Azarbaijan Province, Iran, is located between the coordinates of 500786 and 528396 E to 4132305 and 4159466 N. (Figure 1). The height of the Urmia plain is 1,350 meters above sea level in length and the shape of the land in the study area are alluvial plain, piedmont, and the lowlands. Geologically, the catchment area is more covered by the Oligomiocene Formations, which is Permian limestone. The climate of Urmia station with an average temperature of 8.9 ° C in summer is roughly hot, and cold in winter. The rainy season begins in late October and the beginning of November and continues until May. The average long-term rainfall in Urmia (1965-2017) is 339 mm and is a total of 120 days of the frosty period.

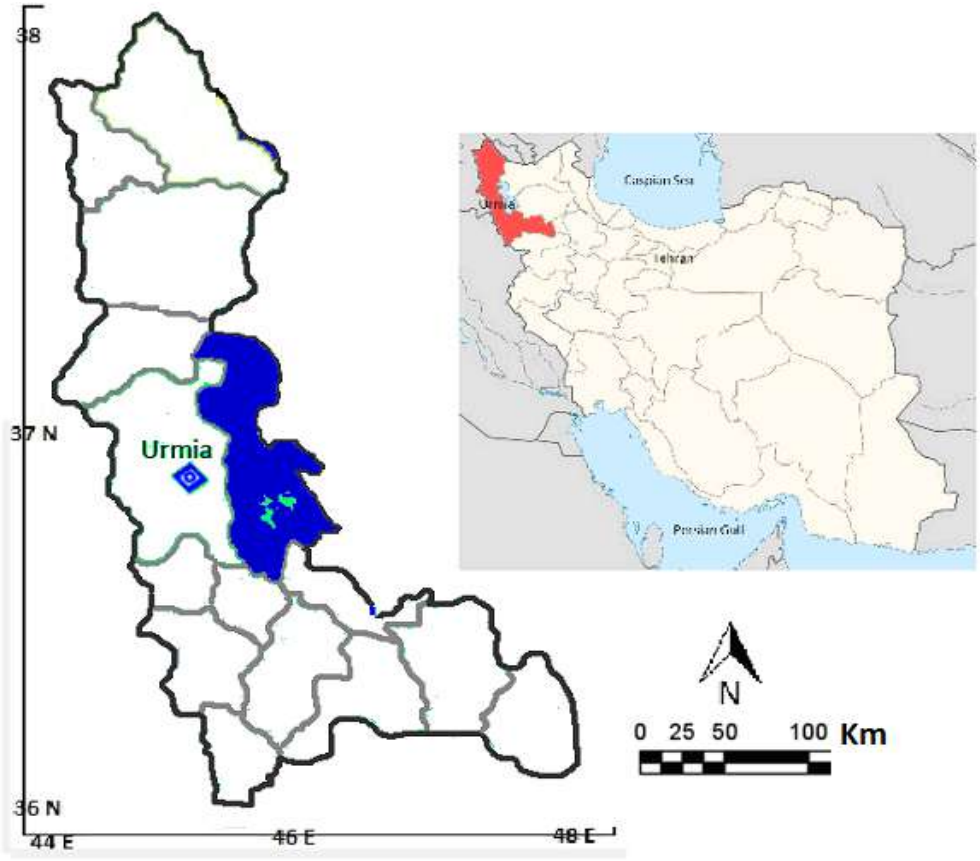

Figure 1. Location of the study area in the West Azerbaijan province

1.2. Research Method

In this research, satellite imagery, aerial photos, topographic maps, and geological maps were used to identify and distinguish different forms of land. The separation of soil series was carried out based on geomorphologic and geophysical processes. The coordinates of the study were determined from topographic maps, satellite imagery, and aerial photos and transmitted to the Global Positioning System. 30 soil profiles were drilled and described by the guidelines for soil mapping. Five soil profiles were selected and after sampling every genetic horizon, transferred to the laboratory.

The soil samples were then air-dried and passed through a 2 mm sieve. Experiments including determination of soil texture by hydrometer (Gee & Bauder, 1986), determination of bulk density by paraffin (Blake & Hartge, 1986), measurement of calcium carbonate equivalent Chloridic acid neutralization and titration with profit, Gypsum measurements by means of acetone method (Nelson, 1982), soil reaction, electrical conductivity of saturated flower extracts by conductivity method, organic matter using modified Valky and Black, capacity Cation exchange was carried out using sodium acetate (Rhoades, 1983). The classification of soils in the American classification system up to the family level was carried out based on the 2014 key (Smith, 2014).

2. Results

The basin of the Barandoz Chay River, with an area of 1203 km2, consists of two major branches, Barandoz and Qasemlou, and originates from the Dalamper, Banhool and Helaleh mountains at the borderlands of Iran and Turkey. The mainstream extends 75 kilometers westward to the east after passing the Urmia Plain Discharged to the Urmia Lake. The maximum height in this basin is 3500 meters above sea level (masl) and the minimum height at the outlet is 1250 (masl). The two rivers flow from the southwest to Urmia. Based on the average rainfall and temperature of the Urmia station, the soil moisture and temperature regime were determined as Xeric and Mesic respectively using NEWHALL software (Fig. 2).

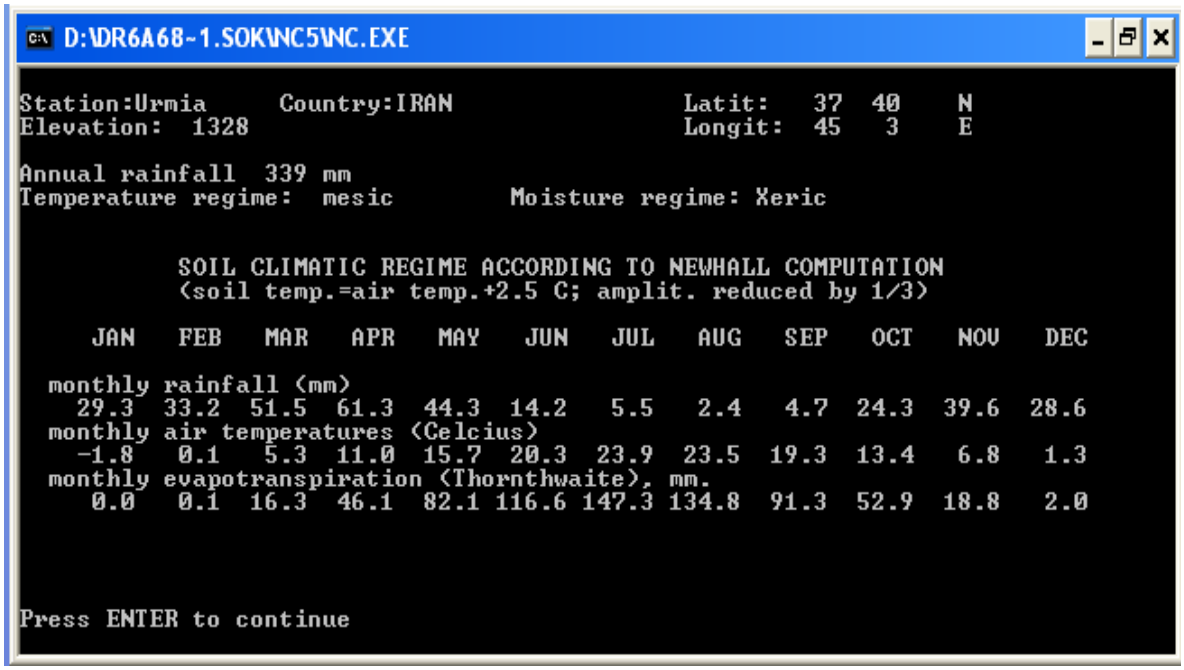

Figure 2. Soil moisture and temperature regime of the study area

2.1. Soils

Along the path of the Barandoz river from the catchment to the Urmia plain toward the Urmia Lake, the characteristics of the soils are as follows.

Soil 1: Soil is very deep, dark brown (10YR 4/4) with moderate texture and clay structure on a dark-browned layer (10YR 4/4) with a heavy texture and a relatively cuboid Strong structure.

The soil classified as Fine loamy, mixed-mesic - Typic Calcixerepts.

Soil 2: Very deep, dark brown (10YR 4/4) with moderate texture and clayey structure and the material is dark to dark brown (10YR 4/4) with medium texture and cuboid structure. The corner is fairly strong

The soil classification is Fine Loamy Mixed, Mesic-Fluventic Haploxeropts.

Soil 3: Soil is very deep, brown (10YR4/3) with moderate texture and clay structure on a brownish layer with a relatively strong cubic structure. The above layers are placed on a dark gray (10YR 4/2) with very heavy texture, and in the lower layer there is a grayish-gray to very dark gray (10 YR 3/4) with a very heavy texture It has a very solid cubic structure.

The classification of this soil is Fine Mixed, Mesic-Fluventic Haploxerepts.

Soil 4: Moderately deep, dark brown (10 YR 4/4), moderate texture and clay structure is located on a dark brown (10 YR 4/4) with moderate texture and weak cortical cubic structure. These layers are also on a layer with more than 75% gravel and sandy texture.

This soil classified as Loamy over sandy skeletal, mixed, mesic-Fluventic Haploxerepts.

Soil 5: Soil is very deep, dark gray (10YR 4/2) with a very heavy texture and clay structure on a very dark gray layer (10YR 3/2) with very heavy texture and building The column is fairly strong. The above classes are located on a very dark gray (10YR 3/2), medium-sized, and poorly-formed cortical structure, which is generally on a dark brown layer (10 YR 2/2) and light texture and cuboid structure with weak corners.

The classification of this soil is Fine Mixed, Mesic-Typic Haplaquepts.

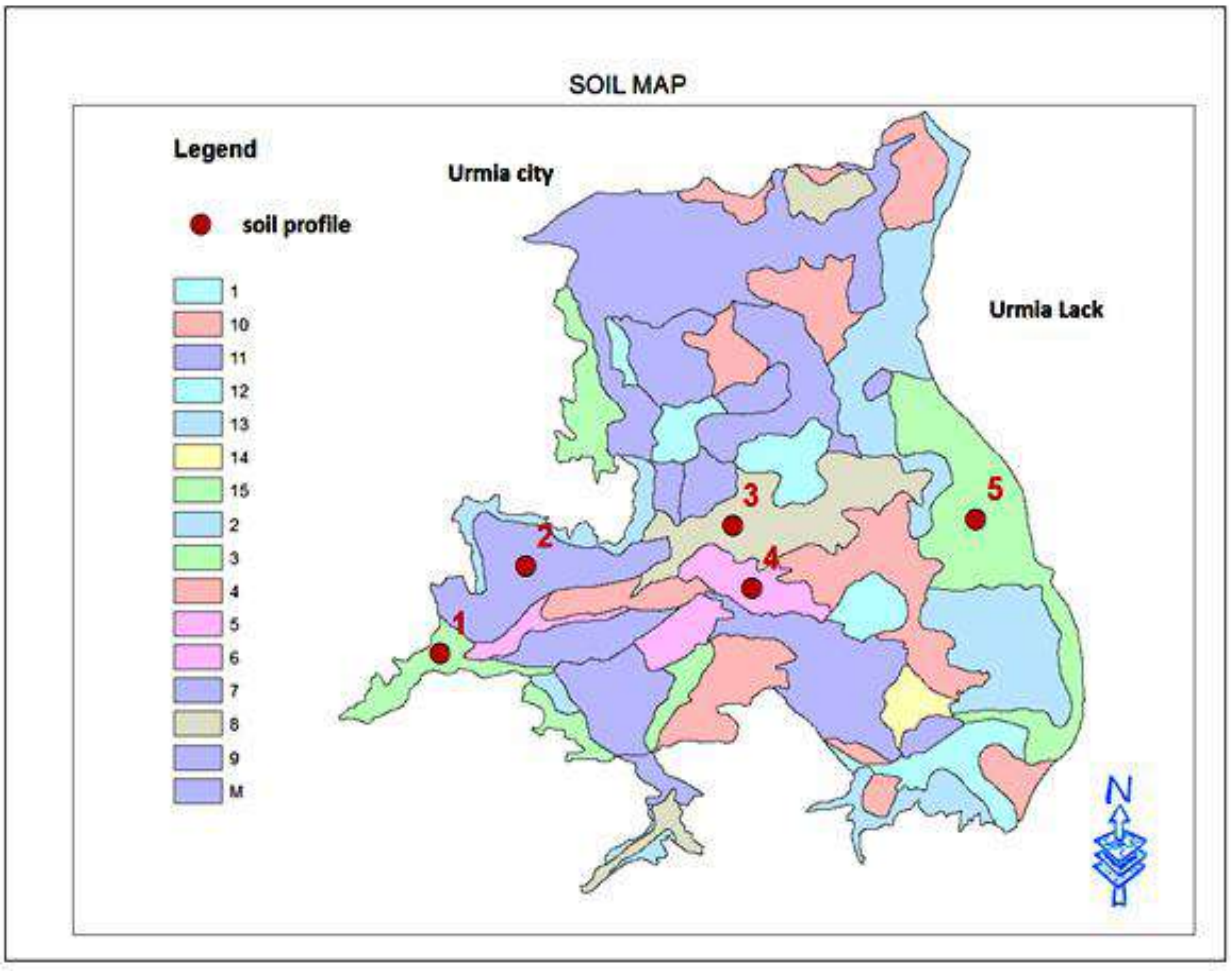

Figure 3. Soil series in the study area

Some of the physicochemical, morphological characteristics of selected soils are presented in Table 1.

Table 1. Some characteristics of the soil sample in the study area

profile	Depth (cm)	layer	texture	Ec ds/m	pH	OC(%)	TNV(%)	SAR
1	0 - 20	AP	L	0.59	7.9	0.83	11.0	
	55	Bw1	CL	0.62	7.8	0.51	23.5	
	135	Bk1	CL	0.35	7.9	0.18	11.0	
2	0 - 20	Ap	L	0.46	7.9	1.19	5.5	
	50	Bw1	L	0.34	7.9	0.59	4.0	
	80	Bw2	L	0.32	8.0	0.59	4.5	
	130	Bw3	L	0.40	8.0	0.61	4.5	
3	0-30	AP	SiL	2.11	7.6	1.17	13.3	
	60	Bw1	Cl	1.14	7.9	1.17	16.3	
	100	Bg1	SiC	1.01	8.0	0.84	19.8	
	145	Bg2	SiC	0.97	8.2	0.43	15.8	
4	0-30	AP	L	0.83	7.6	0.88	19.0	
	55	Bw1	L	0.61	7.9	0.50	19.5	
	130	Cz	S	0.69	7.9	0.40	14.3	
5	0-30	A	SiC	28.04	8.0	1.52	27.0	70
	80	Bg1	C	24.7	8.3	0.44	22.5	87
	130	Bg2	SiL	10.97	8.4	0.02	29.3	61
	150	Bg3	SL	9.47	7.9	0.17	19.0	59

2.2. Geological formations

Formations in the region include the southern part of Urmia Plain and the highlands of the Barandoz chay River catchment have a variety of sedimentary rocks including dolomitic limestone and Permian limestone such as the Ruteh and Mila formations along with the new Quaternary sediments in the Urmia plain (Fig. 4).

The igneous rocks, such as granite without age, are also exposed in parts of the region that are highly tectonized and crushed. The function of these granite influences on most limestone rocks has also led to adjacent alterations. The Colored Mélange of Ophiolite complexes is also found in the region, which is, in fact, a collection of rocks and ultrasonic layers. The Colored Mélange is seen in the main branches of the Barandoz River catchment and the mountainous highlands of Buz-sina.

Ruteh Formation consists of Permian deposits composed of fine-layered, fine-grained lime and dolomitic lime, which is found in the eastern and western parts of the Barandoz catchment, which branches originate from the mountain peaks of Helaneh.

The Mila Formation is one of the geological formations that include dolomite, limestone, shale, and marl, and is dispersed in the upstream areas and western branches of Barandoz, parallel to the Iranian border with Turkey.

Young alluvial deposits, consisting of a series of coarse deposits (rock blocks, coarse and fine rubble, sand and clay). The vast part of the Urmia Lake is composed of soft lake sediments that are swampy and muddy.

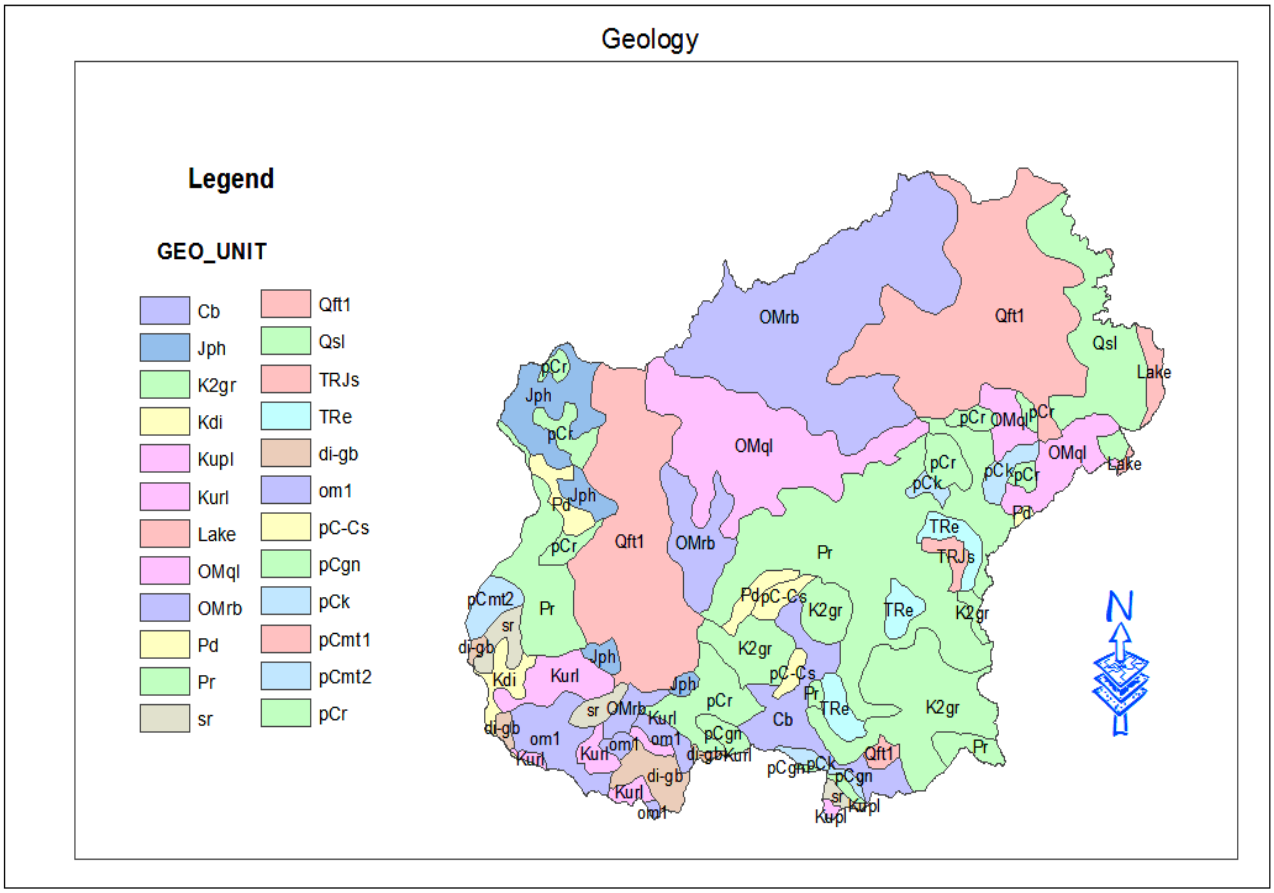

Guide

Cb - Baroot Formation (Shale Lime, Dolomite)
PeK - Kalhor Formation (Murad and Kalhor series)
Fm = pd - Drood Formation
TRe - Elika Formation
J ph - Hamadan fillites
Om1 - ophiolite colored mixes
OMrb - sandstone, gypsiferous marls
Pe.CS - Soltanieh Formation
Pc cr-Rizu Series
pr - Rute limestone
TR js - Shemshak Formation
K2gr – granite
OMQ1- limestone

Figure 4: Geological Formations of the Barandoz chay River catchment and Urmia Plain

Conclusion

Based on the meteorological data of the region, the soil moisture and temporal regime are determined as the Xeric and Mesic respectively. Geological surveys also showed that rock formations located at the Barandoz and Qasemlou catchments are limestone (Soltani Sisi, 2005). Although the amount of gypsum is also high in some formations, lime is one of the factors determining the rock in the formation of different soils in the region. On the other hand, physiography and topography have also played a significant role, so that the upper terraces have more developed soil and regions with a sloping land and less aging less evolved soils. With decreasing height and proximity to Lake Urmia, the effect of groundwater level and its salinity on the profiles is evident. In the meantime, the soils of the river margin and the channels have young and uncoated soils due to the sediments of the present age.

In this research, the selected five soil profiles were studied and classified in different situations and almost homogenous sequence. Selected soils clearly show how soil changes in terms of soil-forming factors including climate, parent materials, time and slope, and biological factors.

Soil 1 is located on the oldest sediments and upper terrace of the area. Given sufficient time and climate, opportunities for the formation of calcic horizons and the accumulation of lime in the middle layers were provided. Constantine and Damieni (2004) have also come up with this trend in their studies (Costantini & Damiani, 2004).

Soil 2, located in relatively old plains, has a lower evolutional soil and only the Cambic horizon is formed in the middle layers, and the effects of coherence and continuous sedimentation on these soils are still evident. These results are consistent with the findings of Mirkhani et al. (2005) and Farzamnia et al. (2013).

Soil 3 is located along with the soil 2 and has almost the same common characteristics. In these soils, the soil's low development time is poor and the effects of the sedimentation of the continuous periods are evident. Laurence et al. (2011) also found similar results in their research (Quénard, Samouëlian, Laroche, & Cornu, 2011). Soil 4 is located at the margin of the Barandoz River and has not a long time passed since their sedimentation, so the soils are well observed with coarse and fine sediments. Finally, the

soil 5 located at the end of the Urmia sedimentary plain and the alluvial fan of the Barandoz River, has a very fine texture. Regarding its proximity to Lake Urmia and the high groundwater level is highly saline and Sodic. In this soil, salinity and sodium content are predominant on other soil properties and are known as saline and sodic soil. Vahidi et al. (2012) also reported similar results.

In general, what is evident in field studies and experimental results, has played an important role in the soil formation is parent materials. The lime in all soils, both geogenic and pedogenic, is of maternal origin. Lime has been the main contributor to most of the watershed formations. Formations such as Baroot, Soltanieh, Kalmard, Dorood, Elika, etc. all have a lot of lime and dolomite. Gypsum is also found in some basin rocks that are likely to be transported to the underlying layers and are not dominated by profiles, especially in higher elevations.

References

Ahmadi, H., & Feiznia, S. (1999). Quaternary formations, theoretical and applied principles in natural resources., niversity of Tehran: Publication.

Blake, G. R., & Hartge, K. (1986). Bulk density. Methods of soil analysis: Part 1 Physical and mineralogical methods, 5, 363-375.

Blank, R. R., & Fosberg, M. A. (1990). Micromorphology and classification of secondary calcium carbonate accumulations that surround or occur on the undersides of coarse fragments in Idaho (USA) Developments in soil science (Vol. 19, pp. 341-346): Elsevier.

Buol, S. W., Southard, R. J., Graham, R. C., & McDaniel, P. A. (2011). Soil genesis and classification: John Wiley & Sons.

Caspari, T., Bäumler, R., Norbu, C., Tshering, K., & Baillie, I. (2006). Geochemical investigation of soils developed in different lithologies in Bhutan, Eastern Himalayas. Geoderma, 136(1-2), 436-458.

Costantini, E. A., & Damiani, D. (2004). Clay minerals and the development of Quaternary soils in central Italy. Revista Mexicana de Ciencias Geológicas, 21(1), 144-159.

Egli, M., Merkli, C., Sartori, G., Mirabella, A., & Plötze, M. (2008). Weathering, mineralogical evolution and soil organic matter along a Holocene soil toposequence developed on carbonate-rich materials. Geomorphology, 97(3-4), 675-696.

Farzamnia, P., Manafi, S., & Momtaz, H. (2013). The study of physico-chemical properties of soils formed on Quaternary sediments in some lands of Urmia Plain. Paper presented at the Proceeding of the national Congress of soil and Sustainable agriculture, Malayer University.

Gee, G. W., & Bauder, J. W. (1986). Particle-size analysis. Methods of soil analysis: Part 1 Physical and mineralogical methods, 5, 383-411.

Gunal, H., & Ransom, M. (2006). Genesis and micromorphology of loess-derived soils from central Kansas. Catena, 65(3), 222-236.

Irmak, S., Surucu, A., & Aydogdu, I. (2007). Effects of different parent material on the mineral characteristics of soils in the arid region of Turkey. Pakistan Journal of Biological Sciences, 10(4), 528-536.

Khresat, S., & Qudah, E. (2006). Formation and properties of aridic soils of Azraq Basin in northeastern Jordan. Journal of arid environments, 64(1), 116-136.

Krivova, N. R. (2020). Improvement of oil production in low permeability deposits with a system of horizontal wells, *Revista de la Universidad del Zulia*, 11 (29), 205-216.

Mirkhani, R., Shaaban, P., & Saadat, S. (2005). Using Particle Size Distribution and Organic Carbon Percentage to Predict the Cation Exchange Capacity of Soils of Lorestan Province.

Moazallahi, M., & Farpoor, M. H. (2009). Soil micromorphology and genesis along a climotoposequence in Kerman Province, Central Iran. Australian Journal of Basic and Applied Sciences, 3(4), 4078-4084.

Nelson, R. (1982). Carbonate and gypsum En: Methods of soil analysis: part 2; chemical and microbiological. 172-181.

Owliaie, H., Abtahi, A., & Heck, R. (2006). Pedogenesis and clay mineralogical investigation of soils formed on gypsiferous and calcareous materials, on a transect, southwestern Iran. Geoderma, 134(1-2), 62-81.

Quénard, L., Samouëlian, A., Laroche, B., & Cornu, S. (2011). Lessivage as a major process of soil formation: A revisitation of existing data. Geoderma, 167, 135-147.

Rabenhorst, M., & Wilding, L. (1986). Pedogenesis on the Edwards Plateau, Texas: II. Formation and Occurrence of Diagnostic Subsurface Horizons in a Climosequence 1. Soil Science Society of America Journal, 50(3), 687-692.

Rhoades, J. (1983). Cation exchange capacity. Methods of Soil Analysis: Part 2 Chemical and Microbiological Properties, 9, 149-157.

Schaetzl, R., & Anderson, S. (2005). Soils: Genesis and Geomorphology. Cambridge University Press, Cambridge, UK (817 pp.).

Sheklabadi, M. (2000). Relative erosivity of soils affected by some geological formations and its relation to some physical and chemical properties of Golabad watersheds. Master's Degree of Soil Science, Isfahan University of Technology.

Smith, D. (2014). Soil survey staff: keys to soil taxonomy. Washington: Natural Resources Conservation Service.

Soltani Sisi, G. (2005). Geological map of Iran, 1: 100000 series, sheet No, 5065. Geological survey and mineral Exploration of Iran.

Vahidi, M., Jafarzadeh, A., & Oustan Sh, S. F. (2012). Effect of land use on physical, chemical and mineralogical properties of soils in Southern Ahar. Water Soil Sci, 22(1), 33-48.

Wilding, L. P., Smeck, N. E., & Hall, G. (1983). Pedogenesis and soil taxonomy: the soil orders: Elsevier.

Wastewater treatment by coagulatıon wıth countercurrent sludge return

E.V. Alekseev *

ABSTRACT

Industrial wastewater contains pollutants that do not oxidize under the biological wastewater treatment conditions of populated areas. The treatment of wastewater containing persistent organic substances can be effective in its extraction. Using only water treatment separation methods does not provide sufficient efficiency. Significantly better results are obtained by combining the persistent organic pollutant coagulation method with subsequent separation processes. The disadvantage of coagulation is the need to use large doses of reagents and a large number of wastewater treatment processes. The objective of the research was to determine the possibility of reducing the doses of mineral coagulants and related reagents while maintaining sufficient efficiency in the treatment of contaminant water by countercurrent transfer of the solid phase of the sludge to the previous separation stages. . For the experimental investigation, a facility was used, which included a three-section block of sedimentation chambers, equipment for the manufacture and dosage of reagents, devices for pumping sludge and water sampling. The research was carried out in aqueous solutions of contaminants: persistent synthetic dyes used in the textile industry. The concentration of the dye solutions was assumed to be constant, equal to 150 mg / l. Three series of experiments were carried out with different conditions to dose the coagulant and return the hydroxyl mud. The results of the experiments were analyzed using the Langmuir adsorption equation and the graphical constructions of the equilibrium and the lines of work of the contaminant extraction process. Compared to the traditional single-stage coagulation scheme, which includes a single addition of reagents without reusing the sludge, the use of solid-phase countercurrent transfer coagulation schemes was found, based on the research results. of sludge conductors gives a significant reduction in the number of reagents consumed and, consequently, a decrease in the amount of sludge removed.

KEYWORDS: wastewater; persistent organic pollutants; synthetic dyes; coagulation; sludge; countercurrent return.

* Moscow State University of Civil Engineering (National Research University).

Recibido: 03/03/2020 Aceptado: 08/05/2020

Tratamiento de aguas residuales por coagulación con devolución de lodos a contracorriente

RESUMEN

Las aguas residuales industriales contienen contaminantes que no se oxidan bajo las condiciones de tratamiento biológico de aguas residuales de áreas pobladas. El tratamiento de aguas residuales que contienen sustancias orgánicas persistentes puede ser eficaz en su extracción. El uso de solo métodos de separación de tratamiento de agua no proporciona suficiente eficiencia. Se obtienen resultados significativamente mejores al combinar el método de coagulación de contaminantes orgánicos persistentes con procesos de separación posteriores. La desventaja de la coagulación es la necesidad de utilizar grandes dosis de reactivos y una gran cantidad de procesos de tratamiento de aguas residuales. El objetivo de la investigación fue determinar la posibilidad de reducir las dosis de coagulantes minerales y reactivos relacionados al tiempo que se mantiene la eficiencia suficiente del tratamiento del agua de los contaminantes por transferencia a contracorriente de la fase sólida del lodo a las etapas previas de separación. Para la investigación experimental, se utilizó una instalación, que incluía un bloque de tres secciones de cámaras de sedimentación, equipos para la fabricación y dosificación de reactivos, dispositivos para bombear lodos y muestreo de agua. La investigación se llevó a cabo en soluciones acuosas de contaminantes: colorantes sintéticos persistentes utilizados en la industria textil. Se supuso que la concentración de las soluciones colorantes era constante, igual a 150 mg / l. Se realizaron tres series de experimentos con diferentes condiciones para dosificar el coagulante y devolver el lodo de hidroxilo. Los resultados de los experimentos se analizaron utilizando la ecuación de adsorción de Langmuir y las construcciones gráficas del equilibrio y las líneas de trabajo del proceso de extracción de contaminantes. Según los resultados de la investigación, se encontró que, en comparación con el esquema tradicional de coagulación de una sola etapa, que incluye una sola adición de reactivos sin reutilizar el lodo, el uso de esquemas de coagulación con transferencia a contracorriente de la fase sólida de los conductores de lodo da una reducción significativa en el número de reactivos consumidos y, en consecuencia, una disminución en la cantidad de lodo eliminado.

PALABRAS CLAVE: aguas residuales; contaminantes orgánicos persistentes; colorantes sintéticos; coagulación; lodos; retorno a contracorriente.

Introduction

Water sphere pollution with persistent organic substances is a big problem for many countries and territories. At the same time, many organic substances are purposefully created

resistant to natural factors. For example, synthetic dyes, finishing preparations and other chemicals used in the production of fabrics (Kant, 2012; Majcen Le Marechal et al, 2012).

Solutions to the problem are to reduce the discharge of these substances with wastewater and to use effective methods for extracting these substances from water. Among the processes of water treatment from persistent organic substances, separation processes are the most environmentally friendly. These processes provide real water treatment as a result of the extraction of pollutants (Zaharia & Suteu 2012; Sojkaledakowicz et al, 1998).

However, it is not possible to purify water from dissolved, colloidal and microdispersed pollutants present in the wastewater of textile and many other enterprises using separation methods.

Different methods of water treatment are used to extract these groups of pollutants (Chandrakant et al, 2016). The method of coagulation with mineral salts of metals has a wide range of applications in the treatment of municipal and industrial wastewater, including for water treatment from persistent organic pollutants (Gonzalez et al, 2007; Verma & Kumar 2016). The main drawback of the method of water treatment by coagulation is the need to use large doses of reagents to extract pollutants. This is typical for wastewater treatment processes from persistent organic substances. High doses of coagulants and the consequent need for reagent correction of the pH value lead to an increase in the mineralization of treated water and an increase in sludge. In the practice of water treatment, the problem of high doses of reagents is partially solved by a combination of coagulation with methods of destruction of organic pollutants and separation processes (Sarasa et al, 1998; Alekseev 2018). The combined application of coagulation methods and separation processes increases significantly the efficiency of wastewater treatment plants. The combination of coagulation processes with separation processes has a multi-factor effect on the entire system of pollutants. This explains the versatility of combined water treatment processes (Anjaneyulu,et al, 2005; Ahmadi & Kord Mostafapour 2017).

In wastewater coagulation processes, pollutants are extracted by reacting with slightly soluble metal hydroxides of the coagulant. According to the works of many researchers, the theory of adsorption interactions can be applied to describe the process of water treatment with mineral coagulants (Al-Qodah, 2000; Abdel-Fatah et al, 2015).

The Langmuir isotherm equation, which reflects the sorption process in a wide range of their concentrations, was assumed as the main equation for describing the process of extraction of pollutants (Lin & Wang 2009; Ayari et al, 2008):

$$a_x = A_\infty K_i X_i/(1+ K_i X_i), \qquad (1)$$

where a_x – specific adsorption of the extracted substance, mg/mg;

A_∞ - the maximum adsorption (according to Langmuir), mg/mg;

K_i – the constant of adsorption equilibrium;

X_i – equilibrium concentration, mg/l.

The transfer of the mass of pollutants from water to the surface of the solid phase of metal hydroxides formed during coagulation can be represented by the material balance equation:

$$-Q dC = G da_x, \qquad (2)$$

where Q – volume flow rate of wastewater, m^3/s;

C – mass concentration of pollutants, kg/m^3;

G – mass flow rate of the coagulant dosing, kg/s;

a_x – specific adsorption of pollutants at equilibrium concentration, kg/kg.

For a single addition of a coagulant, which is common in the practice of coagulation, the dose value at known coefficients of the sorption isotherm equation can be found by integrating the material balance equation within the limits of the target water treatment problem (C_{en}; C_{ex}):

$$G\int_0^{a_{ex}} da_{(x)} = Q\int_{Cen}^{Cex} dC,$$

from which

$$Ga_{ex} = -Q\,(C_{ex} - C_{en}), \qquad (3)$$

where C_{en} and C_{ex} –concentration of pollutants in the water entering and exiting the treatment, respectively;

a_{ex} – specific adsorption of pollutants corresponding to the exiting concentration C_{ex}.

At ensuring the dynamic stability of the process, when the flows Q_w and G are constant in value, equation (3) takes the form:

$$G/Q = (C_{en} - C_{ex}) / a_{ex} \qquad (4)$$

Expression (4) represents the equation of the working line of the pollutant extraction process, and the ratio G/Q is the specific flow rate of the coagulant, that is, its dose. It follows that in order to achieve the required concentration of pollutants in treated water C_{ex} by limiting indicator, the required dose of coagulant, D_c, can be determined by the expression:

$$D_c = (C_{en} - C_{ex}) / a_{ex}\,, \qquad (5)$$

where D_c – dose of coagulant.

According to expression (5), the required dose of coagulant is determined for the minimum value of specific adsorption corresponding to the minimum concentration of pollutants in the water after its treatment. This necessitates the use of large doses of coagulants and related reagents.

Theoretically, reducing the required dose of reagents can be achieved by increasing the specific adsorption and reducing the difference between the initial and final concentrations of pollutants. This is possible by ensuring multiple contacts of wastewater with the sorption surface of the formed hydroxyl sludge with a constant increase in the equilibrium concentration.

One way to achieve this result may be to transfer repeatedly and add the resulting sludge to the treated water in the direction opposite to the movement of the water.

Countercurrent transfer of the formed sludge can be repeated. In this case, it is necessary to assign intervals of change in the concentration of pollutants ($\Delta C = C_n - C_{n-1}$), and the integration of equation (2) to perform within the specified intervals of concentrations of pollutants:

$$-Q\int_{C_{n-1}}^{C_n} dC = G\int_{a_{n-1}}^{a_n} da_{(x)} \qquad (6)$$

If the flows Q_w and G are constant in a given range of concentrations of removed pollutants (ΔC), we come to the following expression:

$$-G/Q = (C_{n-1} - C_n) / (a_{n-1} - a_n), \qquad (7)$$

where a_{n-1} and a_n – values of specific adsorption of pollutants at equilibrium concentrations C_n and C_{n-1}, respectively;

n – number of separation stages; $(n-1)$ – number of sludge transfers.

Formula (7) is an equation of the section of the working line of the coagulation process at a given range of concentrations of pollutants ΔC, and the ratio G/Q is the average dose of the coagulant at this interval.

It follows that within each separation stage, the dose of coagulant required at each separation stage can be determined by the equation:

$$D_c = -(C_{n-1} - C_n) / (a_{n-1} - a_n), \qquad (8)$$

here $C_n = C_{ex}$ and $a_n = a_{ex}$

However, the final analytical solution of equation (8) presents difficulties due to the interdependence of C_n and a_n at specific separation stages.

The aim of the research was to determine the possibility of reducing the doses of mineral coagulants and related reagents while maintaining sufficient efficiency of water treatment from pollutants by countercurrent transfer of the solid phase of the sludge to the previous stages of separation.

The objectives of the experimental research included the following:

Carrying out the process of extraction of pollutants with a single introduction of a coagulant and confirmation of the possibility of using the Langmuir isotherm to describe the quantitative relationship between the dose of the reagent and the amount of extracted pollutants;

Determining the coefficients of the Langmuir equation;

Carrying out the process of extraction of pollutants using the principle of countercurrent transfer of sludge containing aluminum hydroxide;

Analysis of the results of coagulation according to the scheme of countercurrent transfer of the solid phase of the resulting sludge containing aluminum hydroxide.

1. Materials and methods

Studies were conducted on aqueous solutions containing persistent organic pollutants. Persistent synthetic dyes used in the textile industry were selected as such substances (pollutants). The concentration of dye solutions was assumed to be constant,

equal to 150 mg/l, which corresponded to the average value of their content in the wastewater of textile dyeing plants.

Determination of the dye concentration was carried out by colorimetric method using a photometer UNICO 2800. Aluminum sulfate was used as a mineral coagulant.

Experimental studies were performed on a model of a flow facility. The scheme of the experimental facility is shown in Fig. 1.

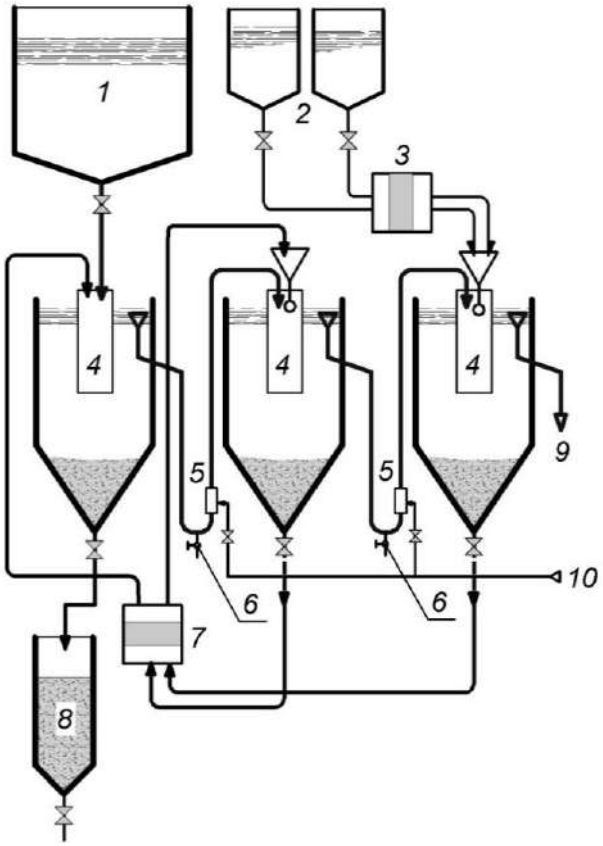

Fig.1. Experimental facility model: 1 – feed tank; 2 – tanks for the preparation of reagent solutions; 3, 7 –peristaltic pumps; 4 – chambers for settling; 5 – airlifts; 6 – samplers; 8 – a container for collecting sludge; 9 – treated water; 10 – air supply.

The main stage of separation of aluminum hydroxide sediment and adsorbed dyes formed in the process of coagulation was adopted by the model of sedimentation tank with a vertical movement of the water flow. The choice of a model of this type of equipment is determined by the simplicity of design, clarity of the process of formation and separation of the precipitate hydroxyl, a relatively small sludge moisture content and possibility of use under field conditions.

The facility included three identical chambers for settling, connected in series by means of airlift devices. The design of the airlift devices made it possible to take water samples, and maintain a predetermined position of the water level in the next settling chamber.

The test water came from a feed tank. Maintaining a given dose of coagulant during the experiment was achieved by proportional supply of solutions of coagulant and alkali. Multi-channel peristaltic pumps were used as proportional feeders. The concentration of the alkali solution was pre-selected according to the concentration of the working solution of the coagulant under the condition of maintaining the required pH value in their mixture. At the facility, it was possible to study the treatment of water with different schemes of transfer of the solid phase of the resulting sediment.

The methodological basis of the experiments included three series of experiments.

In the first series of experiments, the coagulation of the test water was carried out in contact (without a flow) mode with constant fixed doses of reagents (coagulant and neutralizer, if necessary, pH control), introduced into the first settling chamber. The coagulant doses were varied from 20 to 250 mg/l calculated from anhydrous salt. After that, the water was not stirred for 30 minutes. The subsequent chambers of settling (the second and third) were not used in this series of experiments. The sludge was being dumped.

The second and third series of experiments were carried out in flow mode on water. Water was supplied to the beginning of the facility, passing successively all the settling chambers. Reagents were continuously added to the third settling chamber. Doses of coagulant in specific experiments varied in the range of 50 ... 250 mg/l on anhydrous salt in increments of 50 mg/l.

In the second series of experiments, coagulation was carried out according to a two-stage scheme. The sludge that falls in the third settling chamber is pumped to the second settling chamber along with the incoming water. The sludge from the second settling chamber was discharged. Water samples were taken at the end of the facility and from the airlift device of the second settling section to determine the residual concentration of pollutants (dyes).

The third series of experiments was conducted on a three-stage scheme. The difference was that the sludge from the second chamber was pumped to the distribution device of the

first settling chamber, which received water from the feed tank. The sludge from the first chamber was discharged.

Water samples were taken at the end of the installation and from the airlift devices of the first and second settling sections.

2. Results and Discussion

The results of the first series of experiments on a single-stage scheme with a single use of a coagulant are shown in table 1 and in Fig. 2.

Table1: Indicators of water treatment from dyes on a single-stage scheme with a single coagulation without the use of sludge

Dc, mg/l	Cex , mg/l	Cen – Cex, mg/l	a1 , mg/mg
0	150	0	0
20	130	20	0,99
35	118	32	0,97
50	101	49	0,98
100	69	81	0,81
150	45	105	0,70
200	29	121	0,61
250	22	128	0,51

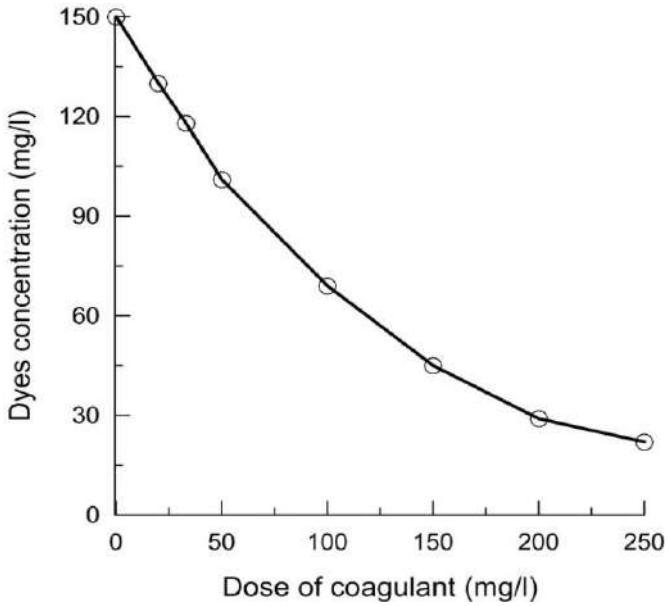

Fig. 2. Effect of the coagulant dose on reducing the dye content

The obtained values of residual dye concentrations with a single introduction of the coagulant are approximated by the Langmuir equation.

As a result of processing the experimental data, the values of the constants of the Langmuir isotherm equation were determined: a□=1.234 and Ki=0.0323. Accordingly, the Langmuir isotherm equation (f. 1) for this process will have the form:

$$ax = 0{,}04Xi /(1+ 0{,}0323Xi), \quad (9)$$

A graphical interpretation of the Langmuir isotherm is shown in Fig. 3.

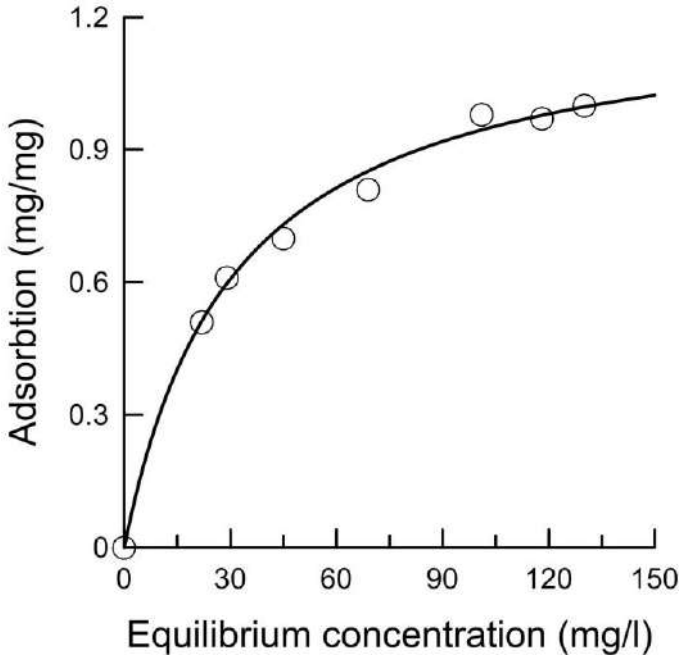

Fig.3. The effect of the equilibrium concentration on the specific adsorption of dyes (according to Langmuir)

The view of the isotherm line confirms the adsorption mechanism of dye extraction. The solution to the water treatment objective is to extract pollutants as much as possible. Therefore, their equilibrium concentration will be minimal. The isotherm shows that the minimum value of the equilibrium concentration will also correspond to the minimum value of the specific adsorption.

According to the results of the experiments given in table 1 and the values of the Langmuir isotherm constants the equilibrium line equation for this coagulation process was obtained:

$$Xi = 1{,}548\square 104\ ax / (617\text{-}500\ ax), \qquad (10)$$

where Xi – equilibrium concentration of dyes in water, mg/l;

ax – specific adsorption of dyes, mg/mg, at equilibrium concentration.

The equilibrium line (curve 1) establishes the relationship between the content of the extracted substance (sorptive) in water and on the solid surface of the sediment (sorbate).

For single-stage coagulation of a dye solution with a fixed dose of 150 mg/l coagulant (see table 1) the equilibrium and working lines of the process are constructed, which are shown in Fig. 4.

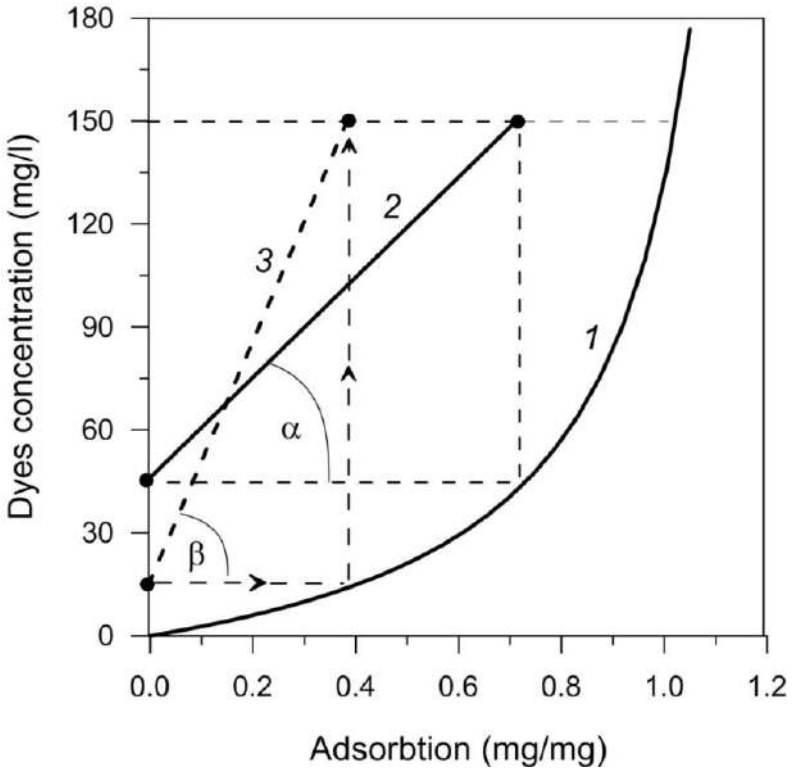

Fig.4. Lines of single-stage process of coagulation of dyes: 1 - the equilibrium line of the process; 2 - working line of single coagulation process with dose Dc = 150 mg/l; 3 - working line of single coagulation process with dose Dc = 330 mg/l.

The working line of the coagulation process (curve 2) establishes the relationship between the initial content of pollutants and their concentration in treated water at a given dose of coagulant. In accordance with equation (8), the slope of the working line at an angle (□) sets the value of the required dose of coagulant. Accordingly, the dose of the coagulant is equal to the tangent of the angle of inclination of the working line.

In the general case of water treatment by coagulation, the specific adsorption of pollutants (C/Dc) theoretically cannot be below the equilibrium line for the corresponding equilibrium concentration. However, the approximation of the working line to the equilibrium one characterizes the greater completeness of the use of the coagulant.

In the first series of experiments the initial value of the working line of a single-stage coagulation (curve 2) is arranged on the concentrations of the dyes at the end of the process Cex = 45 mg/l, which corresponds to the value of specific adsorption by the formula (9), equal to 0.72 mg/mg. This leads to low utilization of the sorption capacity of hydroxyl sludge coagulant. In practice, this means that if you need to implement a deeper water treatment, you will need significantly higher doses of reagents. For example, the process of water treatment of a similar composition, up to the value Cex = 15 mg / l, is illustrated by a working line (curve 3), located at an angle which corresponds to an increase in the required dose of coagulant to 330 mg/l.

The results of the second and third series of experiments with the return of sludge, conducted under flowing conditions, are shown in tables 2 and 3.

Table 2. Indicators of water treatment from dyes in a two-stage scheme with a single countercurrent transfer of sludge

The dose of coagulant, Dc, mg/l	Settling chambers					
	The 1st chamber		The 2nd chamber		The 3rd chamber	
	Cex(1) , mg/l	a(1) , mg/mg	Cex(2), mg/l	a(2) , mg/mg	Cex(3) , mg/l	a(3) , mg/mg
50	150	-	150	-	102,0	0,97
100	150	-	127	0,99	51,0	0,77
150	150	-	81	0,89	16,6	0,43
200	150	-	44	0.72	5,6	0,19
250	150	-	28	0,59	2,8	0,10

Table 2 shows the results of coagulation of a mixture of dyes with an initial concentration of 150 mg/l. Doses of aluminum sulfate were changed in the range from 50 to 250 mg/l. Coagulation was carried out according to a two-stage scheme with a single

countercurrent transfer of the sludge to the second chamber. In the first chamber, the water was not treated.

The results of coagulation of water with a dose of 50 mg/l for all schemes of introduction of reagents are almost identical. Reducing the concentration of pollutants to the dose of coagulant C/Dc 1, which means approaching the theoretically possible value of adsorption. This means that the dose of coagulant in this case is insufficient for effective removal of dyes. Increasing the dose of coagulant to 250 mg/l leads to a significant (more than 18 times) decrease in the content of dyes in purified water. At the same time, the potential stock of the sorption capacity of the hydroxides remains high. This explains the significant effect of reducing the dye content after the second settling chamber.

Carrying out the coagulation process using a three-stage scheme with two-fold transfer of the solid phase of the sediment using a countercurrent scheme has demonstrated the possibility of reducing significantly the consumption of reagents at comparable doses and achieving significant efficiency of water treatment (table 3). For example, coagulation with a dose of Dc = 150 mg/l with a single transfer of the sludge reduces the dye content to 16.6 mg/l. Coagulation with a double transfer of the sludge under similar conditions reduces the dye content to 6.5 mg/l.

The analysis of the results shown in table 3 shows that the sorption capacity of the aluminum hydroxide precipitate is used almost completely during two-fold countercurrent transfer of the solid phase of the sediment. Comparison of the results of coagulation in the range of doses Dc (150...200) mg/l with coagulation on a single-stage scheme (see table 1) fully confirms the advantages of the technology of countercurrent transfer of hydroxyl precipitation of coagulation both in terms of efficiency of water treatment and in terms of reagent consumption.

The use of a coagulant dose of more than 200 mg/l provides a deep extraction of pollutants from the water. However, the sorption capacity of the sediment is not completely exhausted. In this case, it can be assumed that adding another solid phase transfer stage to the coagulation process scheme will increase the efficiency of water treatment at the same doses of coagulant. With equal efficiency of water treatment, it is possible to reduce the dose of reagents. This can be explained by a more complete use of the precipitation sorption capacity.

Table 3: Indicators of water treatment from dyes according to a three-stage scheme with double countercurrent sludge transfer

The dose of coagulant, Dc, mg/l	Sedimentation tank sections					
	The 1st chamber		The 2nd chamber		The 3rd chamber	
	Cex(1) , mg/l	a(1) , mg/mg	Cex(2), mg/l	a(2) , mg/mg	Cex(3) , mg/l	a(3) , mg/mg
50	150	-	147	0,99	100	0,94
100	146	0,99	123	0,98	48	0,75
150	109	0,96	38,6	0,68	6,5	0,21
200	47	0,75	7,2	0,23	0,82	0,032
250	29	0,59	3,2	0,12	0,29	0,011

Figure 5 shows the curves of the equilibrium and working lines of the coagulation process using two-stage and three-stage coagulation schemes.

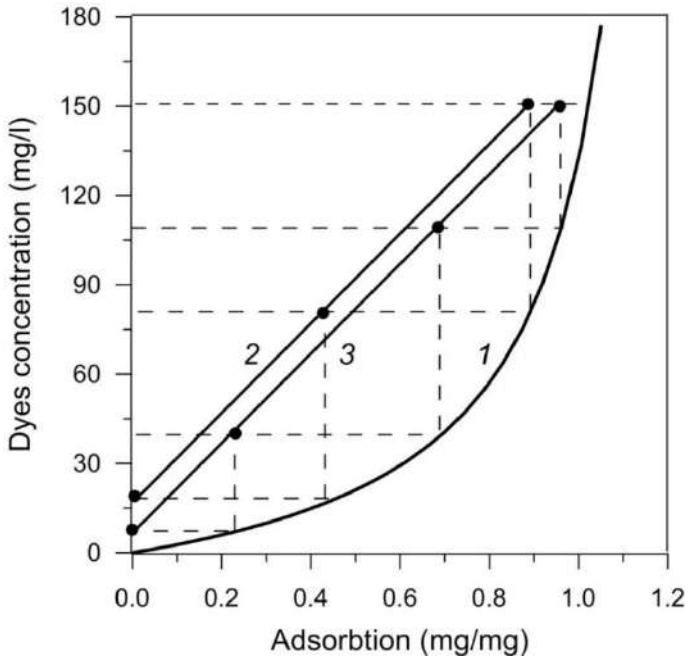

Fig.5. Lines of process of water treatment from dyes on two-stage and three-stage schemes of coagulation: 1 - equilibrium line of the coagulation process; 2 - working line of the coagulation process with a dose of Dc=150 mg/l with a single countercurrent transfer of sludge; 3 - working line of the coagulation process with a dose of Dc =150 mg/l with double countercurrent transfer of sludge.

Coagulation using a two-stage scheme with a single countercurrent transfer of sludge (working line 2, Fig.5) significantly exceeds the depth of water treatment according to a single-stage scheme (working line 1, Fig. 4). According to the single-stage scheme, this result could only be obtained at a dose of coagulant Dc=330 mg/l (Fig.4).

Parallel displacement of the working line of the three-stage coagulation process with a two-time transfer of the sludge towards the equilibrium line (Fig. 5, line 3) corresponds to a greater depth of water treatment and greater completeness of the sorption capacity of the hydroxyl precipitate at the same dose of coagulant.

Conclusion

The results of studying different schemes of the coagulation process show that with a lack of reagents, the specific adsorption of pollutants approaches the theoretical limit. In this case, the complication of the scheme of the coagulation process cannot increase its effectiveness. At the same time, with an excessive dose of coagulant, the greatest efficiency of water treatment is achieved with a finite number of separation stages with the return of the solid phase of the sludge. Further complication of the scheme of the coagulation process does not lead to an increase in the efficiency of water treatment.

The conducted research confirmed the possibility of a significant increase in the efficiency of coagulation processes and other methods of water treatment, the regularities of which are described by the Langmuir isotherm equation. This can be achieved by applying several steps of coagulation with a countercurrent transfer of the sludge. Compared to coagulation by traditional single-stage scheme, including a single addition of reagents without recycling sludge, the use of schemes of coagulation with a countercurrent transfer of the solid phase of the sediment leads to a significant reduction in the consumption of reagents and, accordingly, decreases the quantity of diverted sludges

References

Abdel-Fatah M. A., Sherif H.O., Agour F., Hawash S. I. (2015). Textile waste water treatment by chemical coagulation technology. - Global Journal of Advance Engineering Technology and Sciences. No.2(12). Pp.20-28.

Ahmadi S., Kord Mostafapour, F. (2017).Treatment of Textile wastewater using a combined Coagulation and DAF processes, Iran, 2016.- Arch Hyg Sci.Vol.6, No.3. pp.229-234.

Alekseev E.V. (2018). Abatement of environmental pollution by effluents of textile industry. - Pollution Research, Vol. 37 (1). Pp. 278-284.

Al-Qodah Z. (2000). Adsorption of dyes using shale oil ash. - Water Research, No.34 pp. 4295-4303.

Anjaneyulu,Y., Sreedhara Chary N., Suman Raj D.S. (2005). Decolourization of industrial effluents – available methods and emerging technologies – a review. - Reviews in Environmental Science and Bio/Technology, Vol.4, pp. 245-273.

Ayari F., Srasra E., Trabelsi-Aydi M. (2008), Low-cost adsorbents for a dye uptake from contaminated water modeling of adsorption isotherms: the Langmuir, Freundlich and Elovich models. - Surface Engineering and Applied Electrochemistry, No.6, pp. 76–86.

Chandrakant R. Holkar, Ananda J. Jadhav, Dipak V. Pinjari, Naresh M. Mahamuni, Aniruddha B. Pandit (2016). A critical review on textile wastewater treatments: Possible approaches. - Journal of Environmental Management. Vol. 182. pp.351-366.

Gonzalez T., Dominguez J., Beltran-Heredia J., Garcia H., Snachez-Lavado F. (2007). Aluminum sulfate as coagulant for highly polluted cork processing wastewater: evaluation of settleability parameters and design of a clarifier–thickener unit. - Journal of Hazardous Materials. Vol.148. pp 6–14.

Kant R. (2012). Textile dyeing industry an environmental hazard. - Natural Science. Vol.4 No.1, pp. 22-26.

Lin J.X., Wang L. (2009). Adsorption of dyes using magnesium hydroxide-modified diatomite. - Desalination and Water Treatment. No.8, pp.1–9.

Majcen Le Marechal A., Krianec B., Vajnhandl S., Volmajer J. (2012). Textile Finishing Industry as an Important Source of Organic Pollutants. Organic pollutants ten years after the Stockholm Convention – Environmental and Analytical Update.- InTech, pp. 26–54.

Sarasa J., Roche M.P., Ormad M.P., Gimeno E., Puig A., Ovelleiro J.L. (1998). Treatment of wastewater resulting from dye manufacturing with ozone and chemical coagulation. - Water Research Vol.32, No.9, pp. 2721-2727.

Sojkaledakowicz J., Koprowski T., Machnowski W., Knudsen H. (1998). Membrane filtration of textile dyehouse wastewater for technological water reuse. - Desalination. Vol. 119, (1-3). Pp. 1-10.

Verma M., Kumar R.N. (2016). Can coagulation-flocculation be an effective pre-treatment option for landfill leachate and municipal wastewater co-treatment? - Perspectives in Science . Vol. 8, September, pp. 492-494.

Zaharia C., Suteu D. (2012). Textile organic dyes–characteristics, polluting effects and separation/elimination procedures from industrial effluents—a critical overview. - Organic pollutants ten years after the Stockholm Convention – Environmental and Analytical Update.- InTech, pp. 55–86.

Hierarchical model of information signals formation at the physical layer in FANET

G. S. Vasilyev *
O. R. Kuzichkin **
I. A. Kurilov ***
D. I. Surzhik ****

ABSTRACT

Creation of reliable and efficient flying ad-hoc networks (FANET) requires detailed development of the model of the physical layer of data transmission, determined by the conditions of operation of the networks. The problems of well-known software simulators of communication networks are the simplified nature of the physical layer, as well as the inability to obtain specific analytical solutions in the process of simulation. The hierarchical model of formation of information signals which allows to represent various types of communication channels and the channel-forming equipment, for providing their analytical description and the further analysis is developed. The model allows to describe communication channels between UAVs and (or) ground control centers taking into account the effects of attenuation, intersymbol interference, multipath propagation of signals; schemes of terminal and intermediate network equipment with linear and nonlinear signal conversion; circuits with forward regulation, backward regulation and combined regulation; circuits with multi-channel signal generation and processing, as well as cross-links between channels. Analytical expressions of the transfer function of the generalized hierarchical model for an arbitrary number of disclosed levels of hierarchy are obtained. An example of the presentation and study of the UAV transmitter circuit on the basis of a hierarchical model of signal formation is considered.

KEYWORDS: unmanned aerial vehicles; FANET; physical layer; basic network; communication channel; hierarchical model.

* Belgorod State University, Belgorod, 308015, Russia (E-mail: Belova-t@ores.su, https://orcid.org/0000-0003-1681-5223).

** Belgorod State University, Belgorod, 308015, Russia (E-mail: eav@ores.su, https://orcid.org/0000-0003-0817-223X).

*** Vladimir State University, Vladimir, 600000, Russia (E-mail: global@ores.su, https://orcid.org/0000-0003-1901-7411).

**** Vladimir State University, Vladimir, 600000, Russia (E-mail: russia@prescopus.com, https://orcid.org/0000-0002-0101-3503).

Recibido: 17/03/2020 Aceptado: 22/05/2020

Modelo jerárquico de formación de señales de ınformación en la capa física en FANET

RESUMEN

La creación de redes de vuelo ad-hoc confiables y eficientes (FANET) requiere un desarrollo detallado del modelo de la capa física de transmisión de datos, determinada por las condiciones de operación de las redes. Los problemas de los simuladores de software conocidos de las redes de comunicación son la naturaleza simplificada de la capa física, así como la incapacidad de obtener soluciones analíticas específicas en el proceso de simulación. Se desarrolla el modelo jerárquico de formación de señales de información que permite representar varios tipos de canales de comunicación y el equipo de formación de canales, para proporcionar su descripción analítica y el análisis posterior. El modelo permite describir canales de comunicación entre UAV y (o) centros de control en tierra teniendo en cuenta los efectos de atenuación, interferencia entre símbolos, propagación de señales por trayectos múltiples; esquemas de equipos de red terminales e intermedios con conversión de señal lineal y no lineal; circuitos con regulación hacia adelante, regulación hacia atrás y regulación combinada; circuitos con generación y procesamiento de señales multicanal, así como enlaces cruzados entre canales. Se obtienen expresiones analíticas de la función de transferencia del modelo jerárquico generalizado para un número arbitrario de niveles de jerarquía revelados. Se considera un ejemplo de la presentación y estudio del circuito transmisor UAV sobre la base de un modelo jerárquico de formación de señal.

PALABRAS CLAVE: vehículos aéreos no tripulados; FANET; capa física; red básica; canal de comunicación; modelo jerárquico.

Introduction

Flying ad-hoc networks (FANET), which are a kind of mobile ad-hoc networks (MANET), are used to solve a wide class of tasks based on unmanned aerial vehicles (UAVs): the organization of protection (Sun et al., 2011), signal relay between two networks (De Freitas et al., 2010; Jiang, 2010), monitoring of the natural environment (Cho et al, 2011; Xiang &Tian, 2011) and technical objects (Maza et al., 2011; Semsch et al., 2009), etc. The effectiveness of FANET largely depends on the organization of the physical layer. Creating a robust FANET data architecture requires a detailed model representation of the physical layer. At this layer, radio wave propagation models (Ahmed et al., 2011; Abualhaol & Matalgah, 2011) and antenna structures (Ramanathan, 2001; Noubir, 2004) are considered. The variation of a large number of heterogeneous factors (environmental conditions, radio

signal reflection characteristics, natural and intentional interference, etc.) makes it difficult to create reliable models of network interaction in FANET at the physical layer. The modeling problem is further complicated by the extremely high mobility of nodes (Wang et al., 2010; Kuiper & Nadjm, 2006).

Currently, there are a number of specialized software simulators of computer networks, for example, OPNET, NS-2, NS-3, Omnet++, allowing to model the protocols of ad-hoc networks of different layers of the OSI model (from the lower physical to the upper application) (Abuarqoub et al., 2016). However, the problem with such software tools is the simplified nature of the physical layer. When using such simulators, it is difficult or impossible to reliably take into account factors such as the simultaneous influence of a large number of destabilizing perturbations in the simulation process. It is also problematic to carry out modeling considering the transfer functions of communication equipment, causing distortion of information signals due to various inertials and nonlinearities of the component blocks.

These problems determine the relevance of the analysis of communication networks and use of general-purpose software packages, such as MatLAB / Simulink (Gilat,2004). Due to the large number of built-in functions of digital and analog signal processing, this environment allows to explore a wide class of effects of the physical layer of wireless networks (the impact of noise with different spectra and distribution laws, the propagation of radio signals in the atmosphere and transmission paths). In (Qutaiba, 2012; Qutaiba et al., 2011), a simulation of a wireless sensor network using MatLAB/Simulink was performed, as a result of the simulation, the nature of signals at different noise levels was revealed. The disadvantage of this approach is the lack of general analytical solutions for varying the parameters of the channel or signal processing paths.

The aim of the work is to develop and apply a hierarchical model of information signals formation for numerical and analytical modeling of UAV networks at the physical layer.

1. Hierarchical model of information signals formation at physical layer

The hierarchical model of information signals formation should allow representation of various kinds of communication channels and the channel-forming equipment, for ensuring their analytical description and the further analysis. The generalized model should

provide a representation of communication channels between UAVs and (or) ground control centers, taking into account the effects of attenuation, intersymbol interference, multipath propagation of signals. In addition, the model should allow the study of terminal and intermediate network equipment circuits with linear and nonlinear signal conversion; circuits with forward regulation (FR), backward regulation (BR) and combined regulation; circuits with multi-channel signal generation and processing, as well as with cross-links between channels.

To simplify the analysis, the construction of a hierarchical model should be carried out on the basis of a minimum number of similar blocks with possibility of their arbitrary increase. At the same time, the integrity of the general forward, backward and channel links must be maintained. The generalized model contains an arbitrary number of parallel, dependent channels - "lines" that form a "frame". It can be disclosed (unfolded) in a raster way on "lines" (disclosure on levels) and on "frame", with any lengths of "lines" and their quantity.

Each "line" of the scheme is a generalized transformer of signals (TS) of a certain level of disclosure (Fig. 1). The structure of the TS includes: similar to it TS, control unit (CU), control path (CP) and weighted summator (WS).

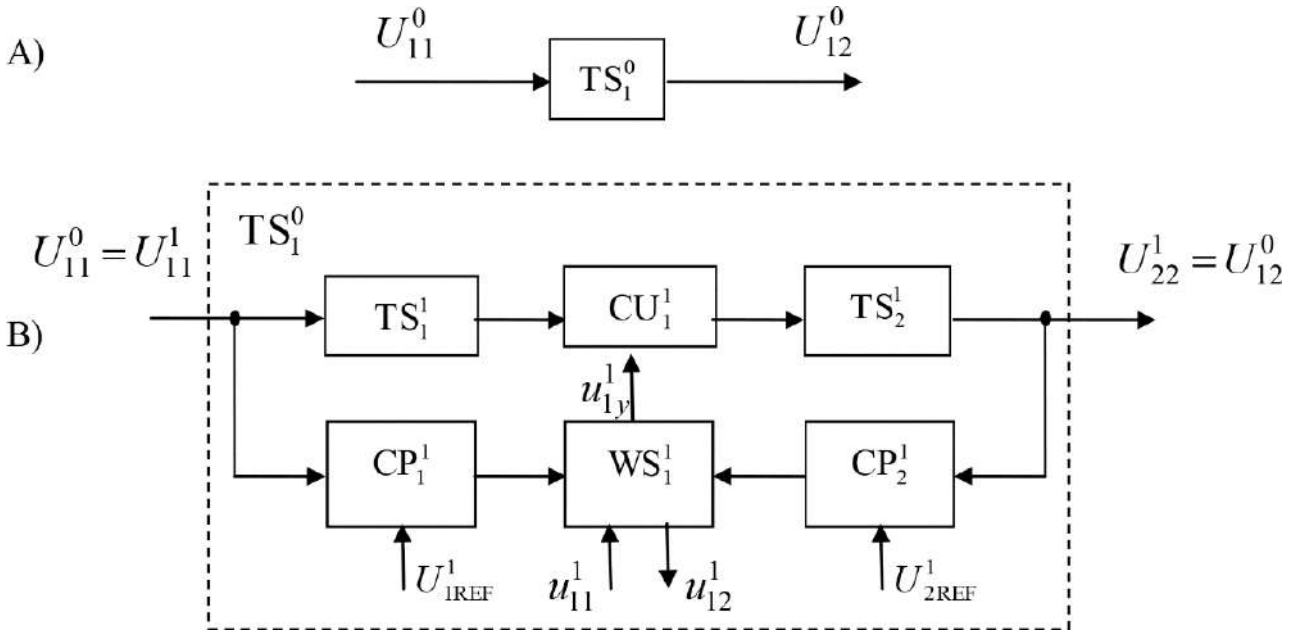

Figure 1. Structure of the generalized transformer of signals

The generalized signal generator contains two control circuits – FR and BR. Each CP generates a control signal and includes a series-connected detector (D) and a filter (F). As D,

the model may contain amplitude, frequency or phase detectors, depending on the type of modulation used at the physical layer. The CU model describes the control of the amplitude, phase and (or) frequency of the signal. WS (Fig. 2) commutes signals. The WS coefficients determine the summation sign and the ratio of the signal transmission from the WS inputs to the WS outputs.

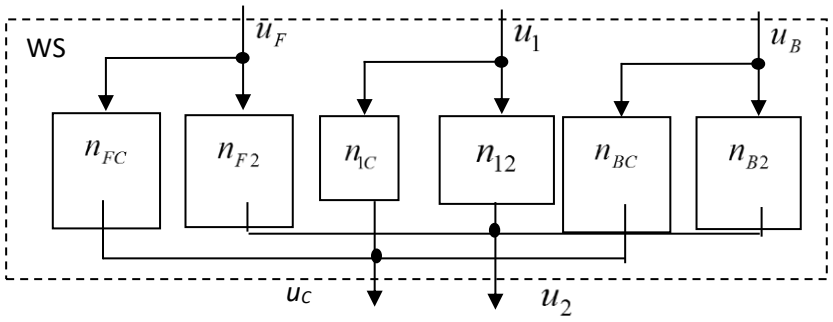

Figure 2. Model of the weight summation

The following designations of blocks are accepted on schemes: $TS^{x_1}_{x_2}$, where x1 is a level number, x2 is a block number. The *U* symbols denote the external main input and output signals, and the *u* symbols denote the auxiliary signals.

The upper and lower indices of the signals are denoted as $U^{y_1}_{y_2\ y_3}$, where y_1 is the level number, y_2 is the block number to which the signal belongs, y_3 is a signal identifier. The identifier y_3 can take the following alphabetical and numerical designations: 1 – input unit, 2 – output, *REF* – signal of the reference oscillator, *F* – forward regulation path, *B* – backward regulation path, *u* – CU control signal.

Figure 3 shows several hierarchical levels of disclosure of the TS model. Zero level (Fig. 1A) corresponds to a folded transformer. Level 1 (Fig. 1B) is the basic TS. Its further disclosure allows to arbitrarily increase the number of signal transformations in the "line" (channel). Each disclosure of the next level is carried out by the disclosure of the TS scheme (Fig. 1B) contained in the previous level.

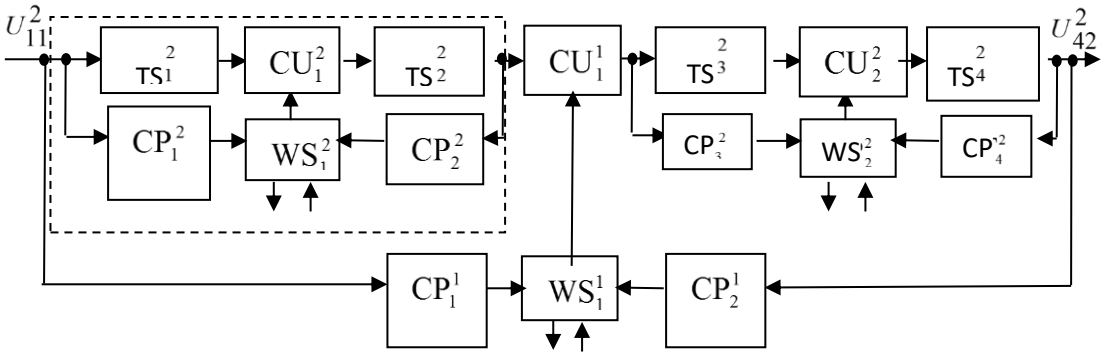

Figure 3. Unfolding of the transformer model

Let us denote the transfer functions of the blocks: TS→ Π, CU → K, WD→ n, CP→ W. Let the upper and lower indices of the functions fully correspond to the upper and lower indices of their blocks. According to Fig. 1, Fig. 3 the TS transfer functions of different levels are obtained by multiplying the transfer functions of the constituent blocks and have the form

level 0 $Q^0 = \Pi_1^0$ – folded TS,

level 1 $Q^1 = \Pi_1^1 K_1^1 \Pi_2^1$,

level 2 $Q^2 = \Pi_1^2 K_1^2 \Pi_2^2 K_1^1 \Pi_3^2 K_2^2 \Pi_4^2$,

level 3 $Q^3 = \Pi_1^3 K_1^3 \Pi_2^3 K_1^2 \Pi_3^3 K_2^3 \Pi_4^3 K_1^1 \Pi_5^3 K_3^3 \Pi_5^3 K_3^3 \Pi_6^3 K_2^2 \Pi_7^3 K_4^3 \Pi_8^3$.

The general expression of the transfer function for an arbitrary number of disclosed levels $A \geq 1$

$$Q^A = \prod_{\alpha=1}^{A} \prod_{\beta=1}^{B} \prod_{\gamma=1}^{G} \Pi_\beta^\alpha K_\gamma^\alpha ,$$

where α is a current number of disclosed layer, A is the maximum number of layers disclosed in TS, β, γ are coefficients (number of transfer functions) of the TS and CU, respectively, $B = 2^\alpha$, $G = 2^{\alpha-1}$ are maximum values of β, γ.

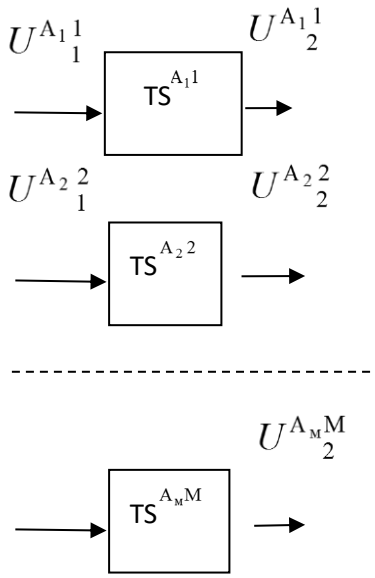

Figure 4. Parallel unfolding of the transformer model

A generalized model of signal formation containing M "strings" ("lines") is presented in Fig. 4. The upper right indices of blocks, signals and transfer functions correspond to the "line" number.

The totality of input and output signals denote through the matrices $\boldsymbol{U}^{A_M M}_{1,2}$, and through the matrix $\boldsymbol{Q}^{A_M M}$ - a set of transfer functions. Then the generalized model is described by a system of equations

$$\boldsymbol{U}^{A_M M}_{2} = \boldsymbol{Q}^{A_M M} \boldsymbol{U}^{A_M M}_{1}.$$

The principle of constructing a model based on raster signals formation allows us to reduce model-specific channel in the FANET or scheme specific device of channel-formation equipment to a transfer characteristics in the corresponding "frame" element of generalized hierarchical model.

2. Investigation of UAV transmitter circuit on the basis of hierarchical model of signal formation

Consider the UAV transmitter circuit with amplitude (phase) modulation and automatic gain control (AGC) (Fig. 5A), and its representation on the basis of a hierarchical model of signal formation (Fig.5B).

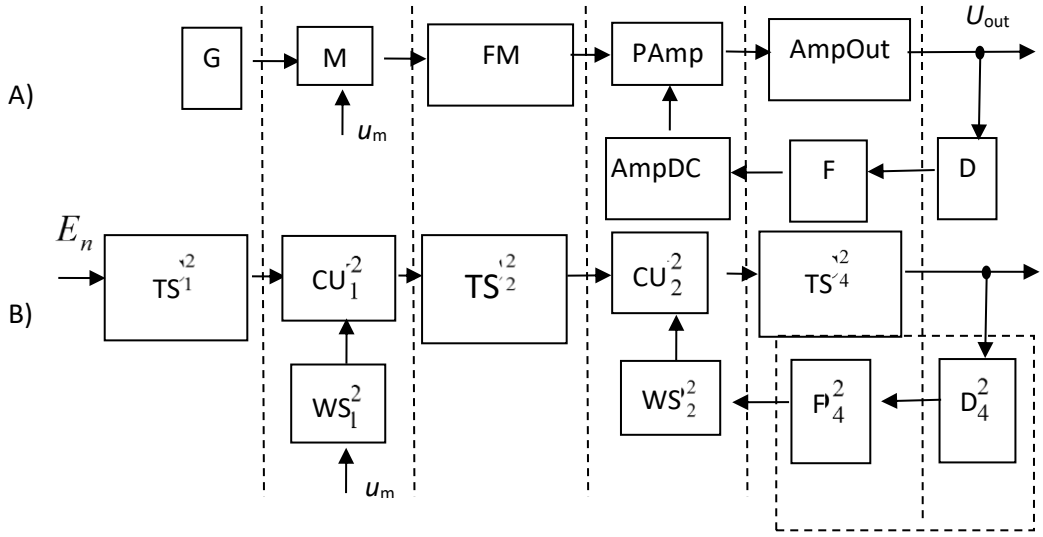

Figure 5. Block diagram of the UAV transmitter

Here the following designations are accepted:

G – transmitter generator, M – modulator, FM – frequency multiplier, PAmp – adjustable power amplifier, AmpOut – output power amplifier, D, F and AmpDC – detector, filter and DC amplifier of the AGC system, accordingly;

u_m – modulating signal, E_P – power supply voltage.

Let us also denote $U_G = U_m \cos \omega t$ – the output signal of the generator, U_m – amplitude, ω – carrier frequency, t – time;

K_M, K_{FM}, K_{PAmp}, K_{AmpOut}, D_A, M_A, n_A – transmission coefficients of modulator, frequency multiplier, adjustable and output power amplifiers, detector, filter and DC amplifier of AGC, respectively.

Then the transfer functions of the blocks of the generalized model:

$\Pi_1^2 = (U_m / En)\cos \omega t$, $K_1^2 = K_M$, $\Pi_2^2 = K_{FM}$, $K_2^2 = K_{PAmp}$, $\Pi_4^2 = K_{AmpOut}$, $K_1^1 = \Pi_3^2 = n_1^2 = 1$, $W_1^1 = W_2^1 = W_1^2 = W_2^2 = W_3^2 = 0$, $D_4^2 = D_A$, $M_4^2 = M_A$, $n_{2BC}^2 = n_A$.

Their substitution in the final transfer functions of the generalized scheme allows to immediately obtain expressions for dynamic, amplitude-frequency modulation and other characteristics of a particular transmitter. The submission required one "row" and two levels of TS disclosure. If necessary, the output of the model Fig. 5 can be added in series connected

units, describing the transfer function of the communication channel and the transfer function of the input paths of the UAV receiver or control center. This approach can be used for analysis of a wide class of network equipment circuits with multi-channel signal generation and processing, as well as cross-links between channels.

Thus, the developed generalized hierarchical model and analysis methodology based on it can simplify the process and reduce the time spent on the study of specific channels or network equipment in UAV networks at the physical layer.

Conclusions

The effectiveness of FANET networks is highly dependent on the physical layer. A reliable description of the physical layer of the FANET requires the creation of an adequate model describing the radio signal propagation in the atmospheric communication channel, the formation and conversion of signals in the paths of the transmitter and receiver of the UAV or ground control center, signal conversion in the antenna system. Varying a large number of heterogeneous factors makes it difficult to create reliable models of network interaction in FANET at the physical layer. Serious disadvantages of many specialized and universal software simulators of communication networks are the simplified nature of the physical layer, as well as inability to obtain the necessary analytical solutions in the process of simulation.

The developed hierarchical model of information signals formation allows to consider various kinds of communication channels and channel-forming equipment, provide their analytical description and further analysis. Attenuation and intersymbol interference in the communication channel are taken into account in the model by the introduction of inertial frequency-dependent links, multipath propagation of signals - summation of signals on individual beams considering their time shifts. Due to the presence of frequency-dependent filtering units and nonlinear detection units, the model allows to study the schemes of terminal and intermediate network equipment with linear and nonlinear signal conversion. Due to the presence of forward and backward control circuits, the hierarchical model allows to describe a wide class of network equipment circuits with multi-channel signal generation and processing, as well as cross-links between channels.

Acknowledgments

The work was supported by RFBR grant 19-29-06030-MK "Research and development of wireless ad-hoc network technology between UAVs and control centers of "smart city" on the basis of adaptation of transmission mode parameters at different levels of network interaction". The theory was prepared in the framework of the state task FZWG - 2020-0017 "Development of theoretical foundations for building information and analytical support for telecommunication systems for geo-ecological monitoring of natural resources in agriculture".

References

Abualhaol, I. Y.; Matalgah, M. M. (2011). Performance analysis of cooperative multi-carrier relay-based UAV networks over generalized fading channels, International Journal of Communication Systems 24 (8) (2011) 1049–1064.

Abuarqoub, A.; Hammoudeh, M.; Alfayez, F.; Aldabbas, O. (2016). A Survey on Wireless Sensor Networks Simulation Tools and Testbeds. In book: Sensors, Transducers, Signal Conditioning and Wireless Sensors Networks Advances in Sensors: Reviews, Vol. 3 Chapter: 14 Publisher: IFSA. 2016.

Ahmed, N.; Kanhere, S.; Jha, S. (2011). Link characterization for aerial wireless sensor networks, in: GLOBECOM Wi-UAV Workshop, 2011, pp. 1274–1279.

Cho, A.; Kim, J.; Lee, S.; Kee, C. (2011). Wind estimation and airspeed calibration using a UAV with a single-antenna GPS receiver and pitot tube, IEEE Transactions on Aerospace and Electronic Systems 47 (2011) 109–117.

De Freitas, E. P.; Heimfarth, T.; Netto, I. F.; Lino, C. O.; Pereira, C. E.; Ferreira, A. M.; Wagner, F. R.; Larsson, T. (2010). UAV relay network to support WSN connectivity, ICUMT, IEEE, 2010, pp. 309–314.

Gilat, A. (2004). MATLAB: An Introduction with Applications 2nd Edition. John Wiley & Sons. ISBN 978-0-471-69420-5.

Jiang, F.; Swindlehurst, A. L. (2010). Dynamic UAV relay positioning for the ground-to-air uplink, in: IEEE Globecom Workshops, 2010.

Kuiper, E.; Nadjm-Tehrani, S. (2006). Mobility models for UAV group reconnaissance applications, in: Proceedings of International Conference on Wireless and Mobile Communications, IEEE Computer Society, 2006, p. 33

Maza, I.; Caballero, F.; Capitán, J.; Martínez de Dios, J. R.; Ollero, A. (2011). Experimental results in multi-UAV coordination for disaster management and civil security applications, Journal of Intelligent and Robotics Systems 61 (1–4) (2011) 563–585.

Noubir, G. (2004). On connectivity in ad hoc networks under jamming using directional antennas and mobility, in: Wired/Wireless Internet Communications, Lecture Notes in Computer Science, vol. 2957, Springer, Berlin/Heidelberg, 2004, pp. 521–532.

Qutaiba, A. (2012). Simulation Framework of Wireless Sensor Network (WSN) Using MATLAB/SIMULINK Software. In book: MATLAB - A Fundamental Tool for Scientific Computing and Engineering Applications, 2012, Volume 2. 10.5772/46467.

Qutaiba, A.; Abdulmaowjod, A.; Hussein, M. (2011). Simulation & performance study of wireless sensor network (WSN) using MATLAB, Conference: Energy, Power and Control (EPC-IQ), 2010, pp. 307 - 314.

Ramanathan, R. (2001). On the performance of ad hoc networks with beamforming antennas, in: Proceedings of the 2nd ACM International Symposium on Mobile Ad Hoc Networking &Computing, MobiHoc '01, ACM, New York, NY, USA, 2001, pp. 95–105.

Semsch, E.; Jakob, M.; Pavlícek, D.; Pechoucek, M. (2009). Autonomous UAV Surveillance in Complex Urban Environments, in: Web Intelligence, 2009, pp. 82–85.

Sun, Z.; Wang, P.; Vuran, M. C.; Al-Rodhaan, M.; Al-Dhelaan, A.; Akyildiz, I. F. (2011). BorderSense: border patrol through advanced wireless sensor networks, Ad Hoc Networks 9 (3) (2011) 468–477.

Wang, W.; Guan, X.; Wang, B.; Wang, Y. (2010). A novel mobility model based on semi-random circular movement in mobile ad hoc networks, Information Science 180 (3) (2010) 399–413.

Xiang, H.; Tian, L. (2011). Development of a low-cost agricultural remote sensing system based on an autonomous unmanned aerial vehicle, Biosystems Engineering 108 (2) (2011) 174–190.

Development of a methodology to model the dynamic properties of UAVS and high-order control systems

G. S. Vasilyev *
O. R. Kuzichkin **
I. A. Kurilov ***
D. I. Surzhik ****

ABSTRACT

When modeling the dynamic properties of an unmanned aerial vehicle (UAV) and an automatic control system (ACS), it is often necessary to take into account factors such as the lack of rigidity of the aircraft structure, the influence of control and destabilizing factors, which leads to an increase in the order of the model under study. The known numerical and analytical methods do not allow us to obtain general solutions for the variable parameters of the high-order system under study, and at the same time provide the required amount of error and computational costs. A method is developed to model the dynamic properties of UAVs and high-order control systems based on the spectral method, the linear approximation by parts of the input control actions and the spectrum of the system's output signal. An example of using the technique to model the dynamic properties of different orders ACS UAVs (from 1 to 10) with different types of inertia is considered. Based on the analysis of errors in the calculation of the transition process, the effectiveness of the method for analyzing high-order systems is shown based on the required computational costs.

KEY WORDS: unmanned aerial vehicle; UAV; automatic control system; linear approximation by parts; spectral method; transition process.

* Belgorod State University, Belgorod, 308015, Russia (E-mail: Belova-t@ores.su, https://orcid.org/0000-0003-1681-5223).
** Belgorod State University, Belgorod, 308015, Russia (E-mail: eav@ores.su, https://orcid.org/0000-0003-0817-223X).
*** Vladimir State University, Vladimir, 600000, Russia (E-mail: global@ores.su, https://orcid.org/0000-0003-1901-7411).
**** Vladimir State University, Vladimir, 600000, Russia (E-mail: russia@prescopus.com, https://orcid.org/0000-0002-0101-3503).

Recibido: 06/04/2020 Aceptado: 02/06/2020

Desarrollo de una metodología para modelar las propıedades dınámıcas de los UAVS y los sıstemas de control de alto orden

RESUMEN

Al modelar las propiedades dinámicas de un vehículo aéreo no tripulado (UAV) y un sistema de control automático (ACS), a menudo es necesario tener en cuenta factores como la falta de rigidez de la estructura de la aeronave, la influencia de las señales de control y los factores desestabilizadores, lo que conduce a un aumento en el orden del modelo en estudio. Los métodos numéricos y analíticos conocidos no nos permiten obtener soluciones generales para los parámetros variables del sistema de alto orden en estudio, y al mismo tiempo proporcionan la cantidad requerida de error y costos computacionales. Se desarrolla un método para modelar las propiedades dinámicas de los UAV y los sistemas de control de alto orden basado en el método espectral, la aproximación lineal por partes de las acciones de control de entrada y el espectro de la señal de salida del sistema. Se considera un ejemplo del uso de la técnica para modelar las propiedades dinámicas de UAV ACS de diferentes órdenes (del 1 al 10) con diferentes tipos de inercia. Con base en el análisis de errores en el cálculo del proceso de transición, se muestra la efectividad del método para analizar sistemas de alto orden por el criterio de los costos computacionales requeridos.

PALABRAS CLAVE: vehículo aéreo no tripulado; UAV; sistema de control automático; aproximación lineal por partes; método espectral; proceso de transición.

Introduction

The design of automatic control systems (ACS) for unmanned aerial vehicles (UAVs) is based on models of the dynamic properties of aircraft in various flight modes. A large number of studies consider the linear dynamics of UAVs (Lebedev & Chernobrovkin, 1973; Moiseev, 2013), and the linearity of their control systems (Byard & McLain, 2015; Kuriki & Namerikawa, 2013). An aircraft of rigid construction with fixed rudders has, like any absolutely solid body, 6 degrees of freedom, and its movement in space is described by a system of 12 differential equations (Lebedev & Chernobrovkin, 1973). The non-rigidity of the aircraft structure or the presence of control actions causes the appearance of additional degrees of freedom, which causes an increase in the order of the UAV models and the control system. At the same time, convenient analytical models describing the dynamics of UAVs and control systems are obtained on the basis of a number of simplifying assumptions for the studied systems of the 4th order maximum (Kuriki & Namerikawa, 2013). Analytical

expression for such models can be obtained on the basis of the operator method of Laplace transformations (Dech, 1971). In the simplest cases, the solutions are determined directly from the table of originals and images according to Laplace (Dwight, 1977; Makarov & Mensky, 1978) in more complex cases-using the decomposition theorem of the fractional rational function (Ditkin & Prudnikov, 1961; Shostak, 1972). When the order of the system under study increases, the resulting expressions according to the decomposition theorem become dramatically more complex, especially if the characteristic polynomial of the system has multiple roots. At the same time, lowering the order of the UAV or control system dynamics model may be unacceptable because of the unacceptably high approximation error.

The use of numerical methods for solving differential equations, explicit (Runge-Kutta, Adams) (Lambert, 1991; Godunov & Ryaben'kii, 1962) or implicit for rigid systems (the Bulirsch–Stoer algorithm based on the extrapolation of Richardson, Krank-Nicholson, and others) (Hairer, & Wanner, 1996; Crank, & Nicolson, 1947), allows us to study the dynamics of high-order systems, but does not allow us to obtain analytical solutions that are valid for the modifiable parameters of the model. In addition, when using such methods, as a rule, the computational cost increases significantly with increasing model order.

The aim of this work is to develop a technique for numerical and analytical modeling of UAV dynamics and a high-order control system that is less demanding on computational resources when increasing the model order in comparison with known methods.

1. Generalized model of dynamic properties of UAVs and control systems

Studies have shown that the dynamic properties of UAVs in various flight modes (start, landing, coordinated turn, spiral descent, etc.) and flight control systems (stabilization and guidance systems) are described by a fractional rational transfer function

$$H_{xy}(\mathrm{j}\omega)=\frac{\zeta_{xy}+N_{1xy}M_1(\mathrm{j}\omega)}{1+N_{2xy}M_2(\mathrm{j}\omega)}=\frac{\sum_{i=0}^{I}\alpha_i(\mathrm{j}\omega)^i}{\sum_{i=0}^{I}\beta_i(\mathrm{j}\omega)^i}, \quad (1)$$

where $j\omega$ is the complex frequency, x – the input control, the response (output parameter) of the system, ζ_{xy} is coefficient, taking values 0 or 1, depending on the specific transfer function, $N_{1,2x,y}$ are coefficients of the forward and backward control circuits (FCS and BCS) for x and y

parameters, I is the order of the system, α_i, β_i are coefficients of the numerator and denominator of the transfer function. A generalized model of the dynamic properties of UAVs and ACS is shown in Fig. 1.

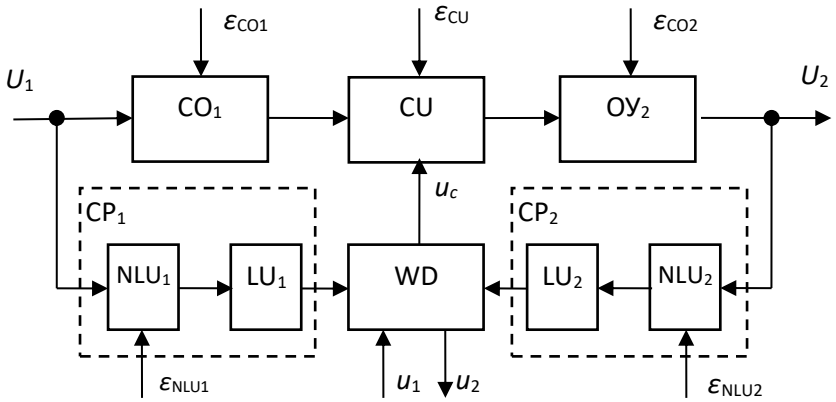

Fig. 1. Generalized model of dynamic properties of UAVs and control system

In the model (Fig. 1) the control object (CO) can be located both at the input of the control unit (CU) – CO_1, and at the output of the CU (CO_2). In addition, the model includes control paths (CP1, 2) and a weight distributor (WD). The CU controls the amplitude and (or) phase of the input action. Each control path in the model is represented by a sequential connection of a nonlinear unit (NLU) and a linear unit (LU). Paths CP_1 and CP_2 implement the principle of forward and backward regulation, respectively. The following designations are accepted in the model: $U_{1,2}$ – main input and output signals of the model, $u_{1,2}$ – auxiliary input and output signals, u_c – control signal, ε - destabilizing factors. For example, the required values of the UAV's angular parameters (roll, pitch, yaw) can be used as input effects, and the achieved values of the corresponding angular velocities can be used as output parameters of the ACS. Nonlinear, inertial and amplifying properties of ACS blocks (angle sensors, servos, etc.) are taken into account at the transfer functions of the corresponding blocks of the generalized model.

2. Methodology for modeling dynamic properties of UAVs and high-order control systems

The use of the spectral method allows us to perform a piecewise linear approximation of the input control actions and the spectrum of the output signal of the system under study,

and then obtain the desired expressions of dynamic characteristics by performing the inverse Fourier transform from the output spectrum (Vasilyev et al., 2013; Kurilov et al., 2014). Using a simple approximation with linear segments allows you to get analytical solutions in the same type of record for describing different models of ACS and the control object - UAV. In this case, the computational cost is determined by the number of approximation nodes that must be increased with increasing order of the system under study. However, it should be noted that in terms of computing costs, the proposed approach is less sensitive to the growth of the model order than numerical methods for integrating differential equations.

The conversion of signals in a linear system is described by the expression (Chen, 1998):

$$S_{out}(j\omega) = S_{in}(j\omega) \cdot H_{xy}(j\omega), \tag{2}$$

where $S_{in}(j\omega)$, $S_{out}(j\omega)$ - the spectra of the input control action and the output signal (response) of the system, $H_{xy}(j\omega)$ is the complex transfer function (1).

It is difficult or impossible to obtain an analytical expression of its spectrum $S_{in}(j\omega)$ if the input control action has a complex form. Approximation of the effect based on the switching continuous piecewise function (CPF) (Vasilyev et al., 2013; Kurilov et al., 2014; Vasilyev et al., 2011):

$$q_i(t) = \frac{A_i}{2\Delta_i}\left(\left|t - t_i\right| - \left|t - t_i + \Delta_i\right| + \Delta_i\right), \tag{3}$$

allows us to obtain a compact generalized expression of the spectrum using the direct Fourier transform:

$$S_{in}(j\omega) = \sum_{i=0}^{N-1} \frac{A_i}{\Delta_i \omega^2}\left[e^{-j\omega(t_i+\Delta_i)} - e^{-j\omega t_i}\right], \tag{4}$$

Here it is indicated: i – the number of the current approximation node, t_i – the time in the current node, Δ_i – approximation step, $A_i = x(t_i + \Delta_i) - x(t_i)$ - the difference between the values of the impact parameter at the time $t_i + \Delta_i$ and t_i..

In general, the spectral density of the output parameter of the system can be represented as a real and imaginary part. In (Polivanov, 1972) it is shown that to find the original $y(t) \leftarrow S_{out}(j\omega)$, it is sufficient to use only the real $S_R(\omega)$ or imaginary part $S_I(\omega)$:

$$y_R(t) = \frac{2}{\pi}\int_{0+}^{\infty} S_R(\omega)\cos(\omega t)d\omega + \frac{1}{\pi}\int_{0-}^{0+} S_R\cos(\omega t)d\omega; \quad (5)$$

$$y_I(t) = \frac{2}{\pi}\int_{0+}^{\infty} S_I\sin(\omega t)d\omega + \frac{1}{\pi}\int_{0-}^{0+} S_I\sin(\omega t)d\omega. \quad (6)$$

These expressions are suitable in some cases for analytical research of dynamic modes. Analytical calculation of transients of real systems using expressions (5) and (6) is not always possible due to the complexity of the resulting expressions of the output signal spectrum. We have to resort to numerical methods, for example, the Philo method for numerical integration of rapidly oscillating functions (Chrysos, 1995; Krylov, 1968). The application of the operator method is also difficult, since the table original for the image of the transition process of a high-order system is usually absent (Dwight, 1977; Makarov & Mensky, 1978). The calculation of the time function by the method of deductions (Hazewinkel, 2001) is generally associated with finding high-order derivatives of several fractional-rational functions. This transformation has to be performed separately for each individual system, which makes research difficult.

Solving integrals in (5) and (6) can be very difficult for a complex transfer function of the system or a complex form of influence. It is convenient to use approximation using switching CPFs (3). We approximate the real $S_R(\omega)$ and imaginary spectrum $S_I(\omega)$ of the output signal by switching CPFs and transform expressions (5) and (6). We first find the dynamic characteristic of the system $y_{R,I}^{(i)}(t)$ in the simplest case, when the spectral density of the output signal has the form of a single switching function.

Based on the approximation of the real output spectrum

$$y_R^{(i)}(t) = -\frac{2}{\pi t}\frac{a_{0i}}{2\Delta_i}\int_{\omega_i-\Delta_i}^{\omega_i+\Delta_i}\sin\omega t d\omega = \frac{2}{\pi t}\frac{a_{0i}}{2\Delta_i}\left[\cos(\omega_i+\Delta_i)t - \cos(\omega_i-\Delta_i)t\right] = 2\frac{a_{0i}\omega_i}{\pi}\frac{\sin\omega_i^* t}{\omega_i^* t}\frac{\sin\Delta_i^* t}{\Delta_i^* t}, \quad (7)$$

where $a_{0i} = S_R(\omega_i) - S_R(\omega_{i+1})$ is coefficient of the CPF approximating $S_R(\omega)$ at the current segment $[\omega_i;\omega_{i+1}]$, $\Delta_i^* = \Delta_i/2$, $\omega_i^* = \omega_i + \Delta_i/2$ is the central frequency of the inclined side of the *i*-th switching CPF.

Based on an approximation of the imaginary output spectrum

$$y_I^{(i)}(t)=\frac{2}{\pi t}S_I(\delta_\omega)+\frac{2}{\pi t}\frac{b_{0i}}{2\Delta_i}\int_{\omega_i-\Delta_i}^{\omega_i+\Delta_i}\cos\omega t d\omega=\frac{2}{\pi t}S_{вых2}(\delta_\omega)+$$

$$+\frac{b_{0i}}{\pi t^2\Delta_i}\left[\sin(\omega_i+\Delta_i)t-\sin(\omega_i-\Delta_i)t\right]= \quad (8)$$

$$=\frac{2}{\pi t}S_I(\delta_\omega)+2\frac{b_{0i}\omega_i}{\pi}\frac{\cos\omega_i^* t}{\omega_i^* t}\frac{\sin\Delta_i^* t}{\Delta_i^* t},$$

where $b_{0i}=S_I(\omega_i)-S_I(\omega_{i+1})$ is the coefficient of the CPF approximating $S_I(\omega)$ in the i-th segment. We apply an approximation based on switching CPF at N nodes for the real and imaginary spectrum of the output parameter of the system:

$$S_R(\omega)=\sum_{i=0}^{N-1}a_i(\omega),\quad S_I(\omega)=\sum_{i=0}^{N-1}b_i(\omega). \quad (9)$$

Dynamic characteristic based on the real output spectrum has the form

$$y_R(t)=\frac{2}{\pi}\sum_{i=0}^{N-1}a_{0i}\omega_i\frac{\sin\omega_i^* t}{\omega_i^* t}\frac{\sin\Delta_i^* t}{\Delta_i^* t}. \quad (10)$$

Dynamic characteristic based on the imaginary output spectrum is obtained by summing (8) over N approximation nodes:

$$y_I(t)=\frac{2}{\pi t}S_I(\delta_\omega)+\frac{2}{\pi}\sum_{i=0}^{N-1}b_{0i}\omega_i\frac{\cos\omega_i^* t}{\omega_i^* t}\frac{\sin\Delta_i^* t}{\Delta_i^* t},\quad \delta_\omega\to 0. \quad (11)$$

The use of expressions (10) and (11) is incorrect if the output spectrum contains a 2nd-order gap at a certain frequency: $S_R(j\omega_k)\to\infty$. To avoid such situations, we present the complex transfer function of the converter in the form $H(j\omega)=H(j\omega_k)+\left[H(j\omega)-H(j\omega_k)\right]$ and denote $H^*(j\omega)=H(j\omega)-H(j\omega_k)$. Then

$$S_{out}(j\omega)=S_{out0}(j\omega)+S_{out}^*(j\omega)=S_{in}(j\omega)\cdot H(j\omega_k)+S_{in}(j\omega)\cdot H^*(j\omega),$$

and for the time dependence of the signal, we get

$$y_R(t)=x(t)\cdot H(j\omega_k)+\frac{2}{\pi}\sum_{i=0}^{N-1}a_{0i}^*\omega_i\frac{\sin\omega_i^* t}{\omega_i^* t}\frac{\sin\Delta_i^* t}{\Delta_i^* t} \quad (12)$$

$$y_I(t)=x(t)\cdot H(j\omega_k)+\frac{2}{\pi}\sum_{i=0}^{N-1}b_{0i}^*\omega_i\frac{\cos\omega_i^*}{\omega_i^*}\frac{\sin\Delta_i^* t}{\Delta_i^* t}, \quad (13)$$

where $a_{0i}^*=S_R^*(\omega_i)-S_R^*(\omega_{i+1})$, $b_{0i}^*=S_I^*(\omega_i)-S_I^*(\omega_{i+1})$ - coefficient of the i-th switching CPF.

3. Modeling the dynamic properties of UAV ACS

The transient characteristics of ACS with combined control and unit control coefficients for forward (FCS) and backward control (BCS) (N_1=N_2=1) calculated using expressions (12) and (13) are shown in Fig. 2-4. A single step function (Heaviside function) was adopted as the input control action U1. The characteristics of a system with three types of filters of different order in the FCS and BCS circuits are shown: with low-pass filters (LPF, Fig. 2), high-pass filters (HPF, Fig. 3) and bandpass filters (BPF, Fig. 4). In each case, two identical filters were used in the FCS and in the BCS. In the examples considered, the LPF and HPF have the 1st, 2nd, 3rd, and 5th order; the BPF is the 2th, 4th, 6th, and 10th order. High-order filters are formed by a series of 1st-order filters of the corresponding type. The ratio of the time constants of the LPF and HPF links in the BPF in Fig. 4 is assumed to be γ=1.

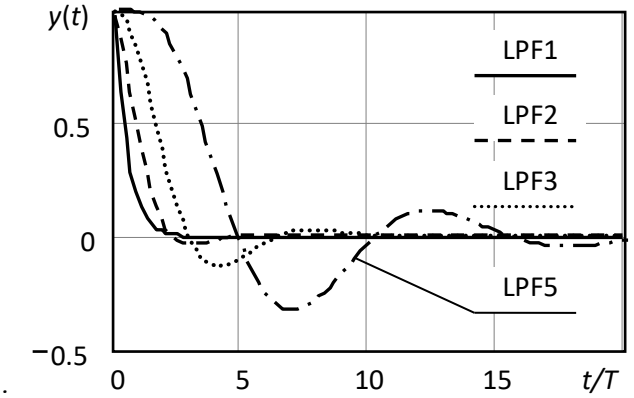

Fig. 2. Transient characteristics of the UAV ACS with low-pass filters of different orders

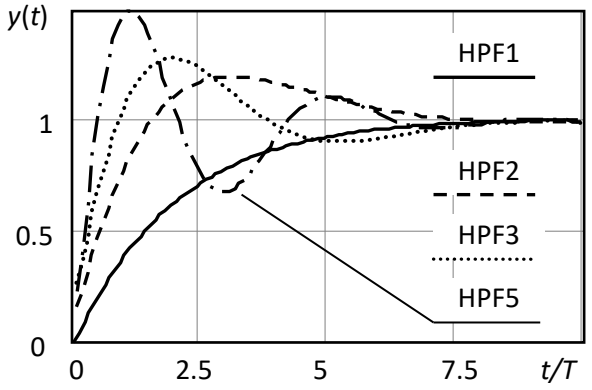

Fig. 3. Transient characteristics of the UAV ACS with high-pass filters of different orders

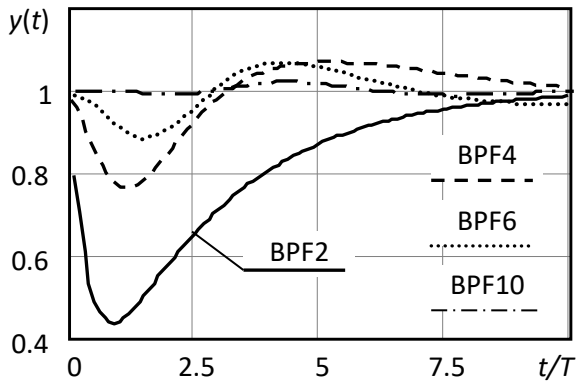

Fig. 4. Transient characteristics of the UAV ACS with bandpass filters of different orders

The study has shown that for transients of different types (aperiodic, oscillatory), for different order of the system and type of inertia, the mean square error of the calculation was from $5 \cdot 10^{-4}$ to $9 \cdot 10^{-4}$ at N=100 approximation nodes.

Conclusions

The task of modeling and analyzing the dynamic properties of the UAV and control system is significantly complicated by factors such as the non-rigidity of the aircraft structure, the influence of control signals and destabilizing factors, which leads to an increase in the order of the model under study. Known numerical and analytical methods do not allow us to obtain general solutions for the variable parameters of the high-order system under study, and at the same time provide the required error value. In addition, when using numerical methods for integrating differential equations, as a rule, computational costs increase significantly with increasing model order.

A generalized model of the dynamic properties of UAVs and high-order ACS is proposed, which allows for the simulation of dynamics to take into account the influence of control signals, destabilizing factors, and characteristics of sensors and actuators in the transfer functions of the corresponding blocks of the generalized model. A method for modeling the dynamic properties of UAVs and high-order control systems has been developed. The use of the spectral method, as well as piecewise linear approximation of the input control actions and the spectrum of the output signal of the system, allowed us to obtain similar analytical expressions for systems of different orders. Based on the developed method, the dynamic properties of UAV ACS of different orders (from the 1st to the 10th)

with different types of inertia were simulated. The study has shown that for transients of different types (aperiodic, oscillatory), for different order of the system and type of inertia, the mean square error of the calculation was from 5·10−4 to 9·10−4 at N=100 approximation nodes. Thus, with an increase in the order of the system under study, the number of approximation nodes (and, consequently, computational costs) does not need to be increased, and acceptable accuracy is provided for a fixed N. Thus, the efficiency of the method for analyzing high-order systems based on the criterion of required computational costs is shown.

Acknowledgments

The work was supported by RFBR grant 19-29-06030-MK "Research and development of wireless ad-hoc network technology between UAVs and smart city dispatch centers based on adaptation of transmission mode parameters at different levels of network interaction"

References

Byard, R. W., & McLain, T. W. (2015). Small unmanned aerial vehicles: theory and practice. Moscow: TECHNOSPHERA.

Chen, C. T. (1998). Linear system theory and design. Oxford University Press, Inc.

Chrysos, M. (1995). An extension of the Filon method for the accurate numerical integration of rapidly varying functions. Journal of Physics B: Atomic, Molecular and Optical Physics, 28(11), L373.

Crank, J., & Nicolson, P. (1947). A practical method for numerical evaluation of solutions of partial differential equations of the heat conduction type. Proc. Camb. Phil. Soc, 43(1), 50–67. doi:10.1017/S0305004100023197..

Dech, G. (1971). Guide to the Practical Application of the Laplace Transform. Moscow: Nauka, 1971. – 288 p.

Ditkin, V. A., & Prudnikov, A. P. (1961). Integral transformations and operational calculus. - Moscow: Fizmatgiz,. – 524 p.

Dwight, G. B. (1977). Tables of integrals and other mathematical formulas. - Moscow: Nauka. 244 p.

Godunov, S. K., Ryaben'kii, V. S. (1962). Introduction to the theory of difference schemes. - Moscow: Fizmatgiz.

Hairer, E., & Wanner, G. (1996). Solving ordinary differential equations II: Stiff and different-algebraic problems, second edition, Springer Verlag, Berlin, ISBN 3-540-60452-9.

Hazewinkel, M., ed. (2001) [1994], "Residue of an analytic function", Encyclopedia of Mathematics, Springer Science+Business Media B.V. / Kluwer Academic Publishers, ISBN 978-1-55608-010-4.

Krylov, V. I. (1968). Reference book on the numerical reversal of the Laplace transform. - Minsk,. – 296 p.

Kuriki, Y., & Namerikawa, T. (2013). Formation control of UAVs with a fourth-order flight dynamics. 52nd IEEE Conference on Decision and Control, Firenze, 6706-6711

Kurilov, I. A., Romashov, V. V., Zhiganova, E. A., Romanov, D. N., Vasilyev, G. S., Kharchuk, S. M., & Surzhik, D. I. (2014). Methods of analysis of radio devices based on the functional approximation. Electronic and telecommunications systems, (1), 13.

Lambert, J. D. (1991). Numerical methods for ordinary differential systems: the initial value problem. John Wiley & Sons, Inc.

Lebedev A. A., & Chernobrovkin L. S. (1973). Flight dynamics of unmanned aerial vehicles. – Study book for universities. - Moscow: Mashinostroenie, – 616 p.

Makarov, I.M., & Mensky, B.M. (1978). Tables of inverse Laplace transformations and inverse z-transformations. Fractional-rational images. Moscow: Higher school, – 247 p.

Moiseev, V. S. (2013). Applied theory of control of unmanned aerial vehicles: monograph. Kazan: GBU «Republican Center for Monitoring the Quality of Education»(Series «Modern Applied Mathematics and Informatics»).–768 p.

Polivanov, K. M. (1972). Theoretical foundations of electrical engineering, 1. - Moscow: Energia,. - 240 p.

Shostak R. Ya. (1972). Operational calculus. Training manual for higher education institutions. Ed. 2nd. - M.: Higher school, – 280 p.

Vasilyev, G. S., Kurilov, I. A., Kharchuk, S. M., & Surzhik, D. I. (2013, September). Analysis of dynamic characteristics of the nonlinear amplitude-phase converter at complex input influence. In 2013 International Siberian Conference on Control and Communications (SIBCON) (pp. 1-4). IEEE.

Vasilyev, G., Kurilov, I., & Kharhuk, S. (2011, September). Research of static characteristics of converters of signals with a nonlinear control device. In 2011 International Siberian Conference on Control and Communications (SIBCON) (pp. 93-96). IEEE.

A method for designing the logical structure of a distributed telecommunication environment

G. S. Vasilyev *
V. T. Eremenko **
O. R. Kuzichkin ***
A. V. Eremenko ****
D. I. Surzhik *****
S. V. Eremenko ******

ABSTRACT
The article presents a methodology for the development of information exchange tools based on the apparatus of hierarchical Petri nets, characterized by the possibility of simultaneous events and allows solving the problem of correctness analysis and verification of protocols. Protocol objects and access points are represented on the basis of the Petri nets apparatus: the simplest object of the reception/transmission protocol, the queue object, a single object and a trivial object. It describes the construction of complex structures of objects and operations on them, the management of timeouts based on the timer object, the specification of protocol objects, the specification of protocols and levels of logical structure. The proposed method is relevant for the analysis of complex communication systems of large size, which are mobile ad-hoc networks with a large number of nodes, characterized by topology instability due to unstable communication channel characteristics and high nodes mobility, and especially flying ad-hoc networks of aircraft (FANET) and flying sensor networks (FSN).

KEYWORDS: distributed system; transport protocol; Petri net; flying ad-hoc network; FANET; flying sensor network; FSN.

* Belgorod State University, Belgorod, 308015, Russia (E-mail: Belova-t@ores.su, https://orcid.org/0000-0003-1681-5223).

** Orel State University, Orel, 302026, Russia (E-mail: ssv@ores.su, https://orcid.org/0000-0002-5650-9151).

*** Belgorod State University, Belgorod, 308015, Russia (E-mail: eav@ores.su, https://orcid.org/0000-0003-0817-223X)

**** Orel State University, Orel, 302026, Russia (E-mail: info@ores.su, https://orcid.org/0000-0003-3119-9123).

***** Vladimir State University, Vladimir, 600000, Russia (E-mail: russia@prescopus.com, https://orcid.org/0000-0002-0101-3503).

****** Orel State University, Orel, 302026, Russia (E-mail: editor@ores.su, https://orcid.org/0000-0001-8766-3816).

Recibido: 23/03/2020 Aceptado: 27/05/2020

Método para diseñar la estructura lógica de un entorno de telecomunicaciones distribuida

RESUMEN

El artículo presenta una metodología para el desarrollo de herramientas de intercambio de información basada en el aparato de redes jerárquicas de Petri, que se caracteriza por la posibilidad de eventos simultáneos y permite resolver el problema del análisis de corrección y verificación de protocolos. Los objetos de protocolo y los puntos de acceso se representan sobre la base del aparato de redes de Petri: el objeto más simple del protocolo de recepción / transmisión, el objeto de cola, un único objeto y un objeto trivial. Describe la construcción de estructuras complejas de objetos y operaciones en ellos, la gestión de tiempos de espera basados en el objeto temporizador, la especificación de objetos de protocolo, la especificación de protocolos y niveles de estructura lógica. El método propuesto es relevante para el análisis de sistemas de comunicación complejos de gran tamaño, que son redes móviles ad-hoc con una gran cantidad de nodos, caracterizados por la inestabilidad de la topología debido a las características inestables del canal de comunicación y la alta movilidad de los nodos, y especialmente a Redes hoc de aeronaves (FANET) y redes de sensores de vuelo (FSN).

PALABRAS CLAVE: sistema distribuido; protocolo de transporte; red Petri; red ad-hoc voladora; FANET; red de sensores voladores; FSN.

Introduction

The most important characteristics of the telecommunication environment are largely determined by the properties of the protocols used – the rules of interaction between various objects, including remote ones. Here a special role is played by the properties of logical correctness, i.e. the absence of logical errors such as deadlocks, unproductive cycles, overflows.

This problem was dealt with by a number of scientists who made a significant contribution to the development of general theory and specific applications to the specific field of communication protocols. Works of R. Milner, K. Petri, C. Hoare are known (Hoare, 1989). A number of significant achievements in solving fundamental and applied problems in this area are associated with the names of Russian researchers: N. A. Anisimov (1989, 1990); O. L. Bandman, V. I. Varshavsky, Yu. G. Karpov (Karpov,

1987); V. E. Kotov (1984); V. G. Lazarev (Eremenko, 2018); E. I. Pilya, S. A. Yuditsky (Eremenko, 2019). The results obtained by them in the description and analysis of protocols of distributed environments are applicable to systems of small size. In a more complex environment based on the construction and analysis of a set of achievable states, the practical need involves further development of protocols. Examples of such a complex environment are mobile ad-hoc networks with a large number of nodes, characterized by topology instability due to unstable communication channel characteristics and high node mobility (Konstantinov et al., 2018, 2019). First of all, these are flying ad-hoc networks of aircraft (FANET) (Bekmezci et al., 2013; Karan, 2015) and flying sensor networks (FSN) (Purohit and Zhang, 2009; Ahmed and Kanhere, 2011).

The main purpose of developing the logical structure of a distributed telecommunications environment at system level is the design of an open system, i.e. the logical structure of the communication module. In this case, network objects are used as elementary units – logical modules that have certain external characteristics (protocol object, auxiliary objects of system management, timer objects). The process of designing at the system level is based on the composition of objects to obtain the necessary configuration. Objects can interact with each other in various ways.

The element that characterizes the direction of interaction of the object is called an access point through which you can access the medium of information transmission. There are two types of access points – *P*-points (positions) and *t*-points (transitions) (Anisimov, 1990; Kotov, 1984; Eremenko, 2018).

For a formal description of the protocol level, it is necessary to build an N-level protocol model consisting of two copies of the *n*-object and (*N* – 1)-service, i.e. to build a logical implementation of the *N*-service. Next, it is necessary to compare it with the reference *N*-service and, in the case of equivalence of these objects, we can talk about the correctness of the *N*-level protocol. The problem statement requires the introduction of the concept of equivalence of objects and methods of its verification.

To implement the task requires the creation of a formal apparatus and requirements for the design methodology of the transport level.

1. Representation of protocol objects and access points

An object is a logical module that performs certain functions. The execution of functions is accompanied by interaction with other objects, for which there are access points in the object. An interaction of two objects is realized by connecting their respective access points. The interaction itself is an exchange of primitive commands, in which parameters and data can be transferred between objects.

This characteristic of the object allows us to formally define it as a Petri net with many *t*-access points, each of which formalizes the concept of an access point to the object.

A Petri net object is a set

$$E = \langle \sum, \Gamma \rangle,$$

where $\sum = (P, T, F, M_0)$ is a labeled network called *an object structure*; $\Gamma = \{\alpha_1,...,\alpha_n\}$ – a set of *t*-access points to the network $\sum$, where each point $\alpha_i = \langle tid_i, Alph_i, \sigma_i \rangle$ specifies an access point to the object. Each point α_i has its own name tid_i, by which one point will differ from another (Anisimov, 1989).

The Petri net tid_i defines the internal structure of an object and therefore its behavior. You can interact with an object and observe its behavior only through access points. Obviously, the triggering of some transition *t* can be "seen" from all access points, but under different names. If at some point the transition is marked with a τ-symbol, then at this point it is "not visible", it is impossible to interact through it at this point. If the transition is "not visible" from all access points, it is considered to be completely internal. The entire set of access point names of the object $E = \langle \sum, \Gamma \rangle$ is denoted as $Id(E) = \{tid_a \mid \alpha \in \Gamma\}$ (Kotov, 1984).

Network objects are depicted as a Petri net, where transitions can be labeled with multiple names. For each name, a colon-delimited access point is specified. These names are separated from each other by semicolons. For example, if the transition *t* at the point α in the object $E[\alpha, \beta]$ marked with name *a*, and at the point β with name *b*, then this corresponds to the expression "α: *a*; β: *b*". If at some access point the transition is "not visible", i.e. marked with a τ-symbol, then this entry is omitted.

The simplest object of the protocol of reception/transfer is shown on Fig. 1. An object that implements the simplest acknowledgement receive/transmit protocol has two access points, *U* and *L*, to connect to the user and the transmission line, respectively.

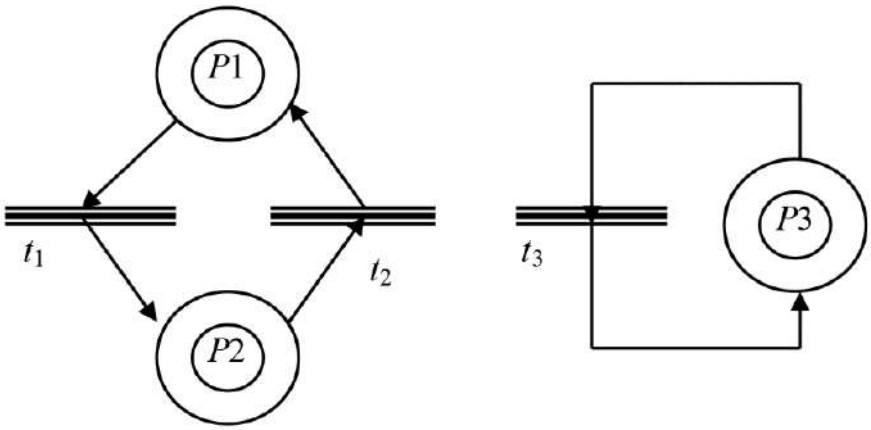

Fig. 1. Example of an object of the simplest protocol of reception / transfer $E_1[U, L]$

Transitions *t* have the following trigger conditions:

t_1 at point *U* – receiving a data request from the user (*DatReq*);

t_1 at point *U* – sending data block (*sDT*);

t_2 at point *L* – receiving acknowledgement on data block (*rACK*);

t_3 at point *L* – receiving a data block and sending confirmation to it (*rDT* + *sACK*);

t_3 at point *L* – indication of incoming data (*DatInd*).

Thus, triggering the t_1 transition means receiving a data request from the user and simultaneously sending it to the line. Receiving confirmation of this data corresponds to the operation of the transition t_2. Note that in this case the user is not informed in any way, because at point *U* this transition is "not visible". Data reception consists in triggering the transition t_3, which corresponds to receiving data from the line (*rDT*) with immediate return of acknowledgement (*sACK*) and transfer to the user of the received block (*DatInd*). Marking the transition t_3 is a good illustration of the specification of simultaneous logical events. Simultaneity can be implemented both

within the same access point (*rDT* and *sACK*) and at different points (*rDT*, *sACK* and *DatInd*).

The queue object. The E_2 object shown as an example in Fig. 2 describes a queue of capacity three. The object has two access points *in* and *out*, through which you can respectively put and retrieve items from the queue. Transition t_1 (*in*: *x*) is "visible" only from point *in* and corresponds to the statement operation, and transition t_4 (*out*: *x*) is "visible" from point *out* and corresponds to the extraction operation. The transitions t_2 and t_3 corresponding to the internal promotion of messages are completely internal and invisible from the outside.

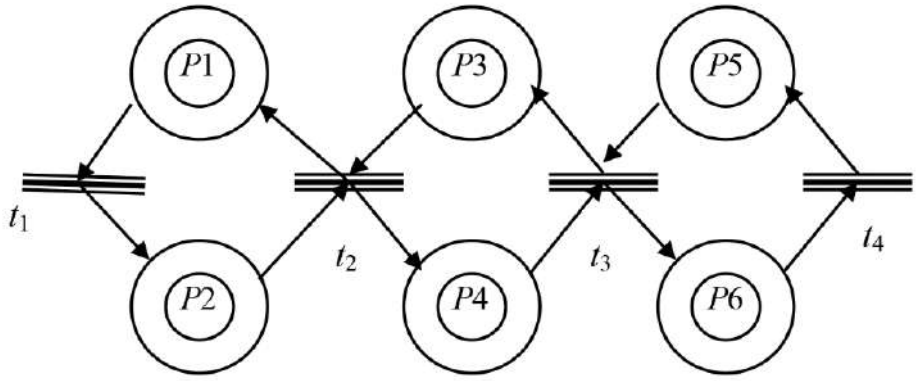

Fig. 2. An example of the queue object $E_2[in, out]$

A single object. Let $A = \{\alpha_1,...,\alpha_n\}$ be some set of names. If we construct an object with two points α and β so that its network is equal to

$(\varnothing, A, F, 0)$, where $F = \{\langle 0, a, 0\rangle \mid a \in A\}$, and the access points are equal to $\langle \alpha, A, \sigma_\alpha\rangle$ and $\langle \alpha, A, \sigma_\alpha\rangle$ with $\sigma_\beta(a) = \sigma_\beta(a) = a$ for all $a \in A$, then this object will only consist of transitions, and for each name $a \in A$ one transition starts, visible from α and β under the name *a*. Since transitions do not have preconditions, then at any time any shift (a multiset of transitions) can work, which is visible equally from the points α and β. Such an object is denoted as $1_A[\alpha, \beta]$ and is called a *repeater object*.

A trivial object. An object may have no access points at all, i.e. $\Gamma = \varnothing$. In this case, the object does not manifest itself in the external world. From the point of view of an external observer, i.e. from the point of view of compositionality, it does not seem to

exist, because it is impossible to interact with it. It is intuitively clear that such an object $E_1 = \langle \sum_1, \varnothing \rangle$ is equivalent to any other object $E_2 = \langle \sum_2, \varnothing \rangle$. Such an object is denoted as 0.

If some object $E = \langle \sum, \Gamma \rangle$ has two different access points $\alpha, \beta \in \Gamma$ and $\alpha \neq \beta$ have the same identifiers $tid_\alpha = tid_\beta$, then such an object does not allow to uniquely identify access points by identifiers. Therefore, a special normalization procedure called α-normalization is necessary (Karpov, 1987).

2. Construction of complex structures of objects and operations on them

For manipulation with objects, building more complex structures from them, appropriate operations are necessary.

Separate unification of objects. We will call an object

$$E = E_1 \oplus E_2 = \langle \Sigma_1 \oplus \Sigma_2, \ \widetilde{\Gamma}_1 \cup \widetilde{\Gamma}_2 \rangle$$

as a separate union of the two objects $E_1 = \langle \sum_1, \Gamma_1 \rangle$ and $E_2 = \langle \sum_2, \Gamma_2 \rangle$.

Separate unification simply allows two objects to be represented as a single object. In this case, the result object may not be α-normalized.

The operation of abstraction of the object. Let $E = \langle \sum, \Gamma \rangle$ be some object and $H \subseteq \Gamma$ be some subset of access points. Then the abstraction of the object E with respect to H is called the new object $E' = \tau_H(E) = \langle \sum, \Gamma \setminus H \rangle$.

The abstraction operation removes a subset of access points from the object definition without changing its structure (network $\sum$) and therefore without changing the behavior of the object in the remaining access points.

The operation of composition of objects. Let $E_1 = \langle \sum_1, \Gamma_1 \rangle$ and $E_2 = E = \langle \sum_2, \Gamma_2 \rangle$ be two objects in normal form, $\alpha \in \Gamma_1$ and $\beta \in \Gamma_2$ are their access points. Then, composition E_1 and E_2 in relation to α and β is called a new object $E' = (E_1 {}_\alpha||_\beta E_2) = norm(E)$, where an object $E = \langle \sum, \Gamma \rangle$ is constructed as follows:

1. $\sum = \langle (N_1 {}_\alpha|_\beta N_2), M_{01} \cup M_{02} \rangle$;
2. $\Gamma = \{ \tilde{\gamma} \mid \gamma \in \Gamma_1 \cup \Gamma_2 \setminus \{\alpha, \beta\}\}$;

The structure (network) of the resulting object is formed by a parallel composition of the source networks through the access points α and β. In this case, the original transitions intended for synchronization (T_{out}) are converted into synchronization transitions (T_{sync}) by a linear combination. The set of access points of this object is formed as a union of transformed access points of the original objects without points α and β as having played a role. Obviously, the transformation is necessary, because the structure of the network changes with the composition. After that, the resulting object is normalized, i.e. consistently be subject to the procedures α– и λ-normalization. This is really necessary because, at first, E_1 и E_2 can have access points with the same identifiers. Secondly, as a result of the operation, transitions that are λ-redundant can be formed.

Renaming of access points. Let $E = \langle \Sigma, \Gamma \rangle$ be an object and $\alpha = \langle tid, Alph, \sigma \rangle \in \Gamma$ its access point. Then renaming the access point α from the name *tid* to the name *tid'* gives a new object

$E[tid'/tid] \stackrel{def}{=} norm(E')$, where $E' = \langle \Sigma, \Gamma \setminus \{\alpha\} \cup \{\alpha'\} \rangle$, $\alpha' = \langle tid', Alph, \alpha \rangle$. Renaming multiple points at once will be denoted as $E[tid'_1 / tid_1, tid'_2 / tid_2, ..., tid'_k / tid_k]$.

To solve a number of problems related to the correctness of protocols, it is necessary to have an equivalence relation between objects, which allows comparing them from the external, behavioral side. The isomorphism relation is not suitable for this, because it is too discriminatory. The most convenient for these purposes is to use bisimulation equivalence of Petri nets.

Equivalence of objects in the access points. Let the objects $E_1 = \langle \Sigma_1, \Gamma_1 \rangle$ and $E_2 = \langle \Sigma_2, \Gamma_2 \rangle$ with access points $\alpha \in \Gamma_1$ and $\beta \in \Gamma_2$ be given in normal form. These objects will be called interleavingly equivalent at points α and β, written as $E_1 \ {}_{\alpha}\approx^{i}_{\beta} \ E_2$ if

1. $tid_\alpha = tid_\beta$;

2. $\Sigma_1 \ {}_{\alpha}\approx^{i}_{\beta} \ \Sigma_2$

These objects will be called stepwise equivalent, written as $E_1 \ {}_{\alpha}\approx^{s}_{\beta} \ E_2$, if in condition 2 the superscript *i* is replaced by *s*.

In other words, objects are equivalent at access points if, firstly, these points have the same identifier, and, secondly, labeled networks of objects are bisimulatively equivalent at these points. Like bisimulation, the object equivalence relation has two variants – interleaving and stepwise.

In addition to the equivalence at certain points, we will be interested in the equivalence of objects as a whole – simultaneously at all access points.

Equivalence of objects. The objects of $E_1 = \langle \Sigma_1, \Gamma_1 \rangle$ and $E_2 = \langle \Sigma_2, \Gamma_2 \rangle$ in normal form are called interleavingly equivalent, denoted as $E_1 \approx^i E_2$, if there exists a relation of bisimulation *R* such that $\forall \alpha \in \Gamma_1 \exists \beta \in \Gamma_2 : E_{1\,\alpha} \approx^i_\beta E_2$ with respect to bisimulation *R* and vice versa.

The step equivalence of objects denoted as $E_1 \approx^i E_2$ is defined similarly, only the superscript *i* in the condition is replaced by *s*.

Thus, full object equivalence is defined as equivalence at all access points *at the same time*. This simultaneity is provided by the uniform bisimulation relation *R* for all equivalences. Obviously, equivalent objects have the same number of access points, and for each point of one object there is a point of another object with the same identifier.

Objects equivalence, based on bisimulation, allows identification of objects that have different internal structure, but the same external behavior. However, in order to make active use of this equivalence, such as replacing one object in a model with an equivalent one without disrupting the behavior of the whole system, it is necessary that this equivalence relation be *congruent* with respect to operations on objects. If you take the operation of objects composition, the congruence property says that if $E_1 \approx E_2$, then $E_\alpha||_\beta E_1 \approx E_\alpha||_\beta E_2$.

3. Specification of enterprise telecommunication environment

With the help of the Petri net object concept, the concept of service and its architectural components is formalized. A service specification can be defined using a network object whose access points are interpreted as service access points. The alphabet of each access point is a set of service primitives (PS), where the names of the

transitions correspond to the names of the service primitives, and the set of terms – the parameters of the primitive. In particular, the connection endpoints specification is implemented using a special parameter, the connection endpoint identifier, assigned to each service primitive.

Thus, the specification of the service in this case is nothing but a Petri net, in which the transitions are mapped to the PS, and their triggering is treated as the execution of these primitives. It is easy to see that the rules of functioning of Petri nets completely satisfy the rules of execution of PS – their operation is an indivisible instantaneous operation. In general, the behavior of such a system specifies the behavioral part of the service, from which, in particular, you can derive information about possible valid sequences of execution of service primitives, including the values of their parameters. An object in this interpretation is called *a service object*.

Data transfer in violation of the order. One of the simplest services is the transfer of data block from one point to another, in which the order of messages is not preserved. In this case, two service access points are defined to send (*s*) and receive (*r*) blocks of data. Sending is done by executing *DatReq*(*x*) at point *s*, and receiving is done by executing *DatInd*(*x*) at point *r*. Parameter x contains the transmitted data. If there are labels in position P_1, the transition t_2 can work by deriving one of the arbitrary labels from position P_1, whose parameter *x* is "visible" from point *r*. It is obvious that the order of the data blocks is not respected here. In addition, this service does not limit the number of data blocks in it.

Data block transfer service. This service is provided by the transport protocol (parametric version). It is initially point-to-point, i.e. assumes only two users sending and receiving users, denoted by access points *s* and *r*.

Fig. 1 shows a service object that specifies a data block transfer service. The service object has two access points *s* and *r*. At point *s* the primitive *DatReq*(*x*) may be executed corresponding to the transmission request data block *x*. At the point *r* the primitive *DatInd*(*x*) is executed, the corresponding to indication for the user about the receipt of data block *x*. From the network view, we can draw the following conclusions concerning this service. First, the execution of query primitives and data indication at

points *s* and *r* alternate. Secondly, the block of data transmitted from point *s* is delivered to point *r* without changes, which is provided by the parameter *x*. Indeed, after the transition t_1 is triggered, the variable *x* takes one of the valid values, which is assigned to the label at position P_2. Next, the same value appears when the transition t_2 is triggered, which corresponds to the execution of the *DatInd*(*x*) primitive.

The final capacity queue. The data block transfer service and the T-service specify a buffer of the capacity queue type equal to one. It is not difficult to specify a transmission service with an arbitrary finite capacity. Fig. 2 shows an object describing a service that transfers three blocks of data at the same time (queue capacity three).

Here the transitions t_2 and t_3 are completely internal and correspond to the "advance" of the data block *x* inside the queue.

The queue with loss and duplication (Fig. 3). The previous examples described a fairly high quality service, i.e. a service that provides error-free data transmission. However, in practice, for a number of reasons, a lower quality service with errors is often used. One such type of error, associated with a violation of the order of transmission of blocks, was considered earlier. Other typical errors of such services are loss and duplication of data blocks. All such properties can be expressed in terms of the Petri net apparatus.

Triggering of the internal transition t_4 corresponds to loss of the data unit in the queue, and triggering of the internal transitions t_2 and t_5 corresponds to duplication of block *x*, number *z*, resulting in an additional unit *x* with the number one more than the [$y = z + 1$]. A service with only one kind of error is easily obtained by removing the corresponding transition along with the surrounding arcs (t_4 or t_5).

4. The timer object

Most protocols use a time service called a *timer* in their operation. Different protocols impose approximately the same requirements on the timer. Therefore, it is advisable to allocate the timer in an independent object and use it in composition with protocol objects both individually and in the separation mode (Fig. 4).

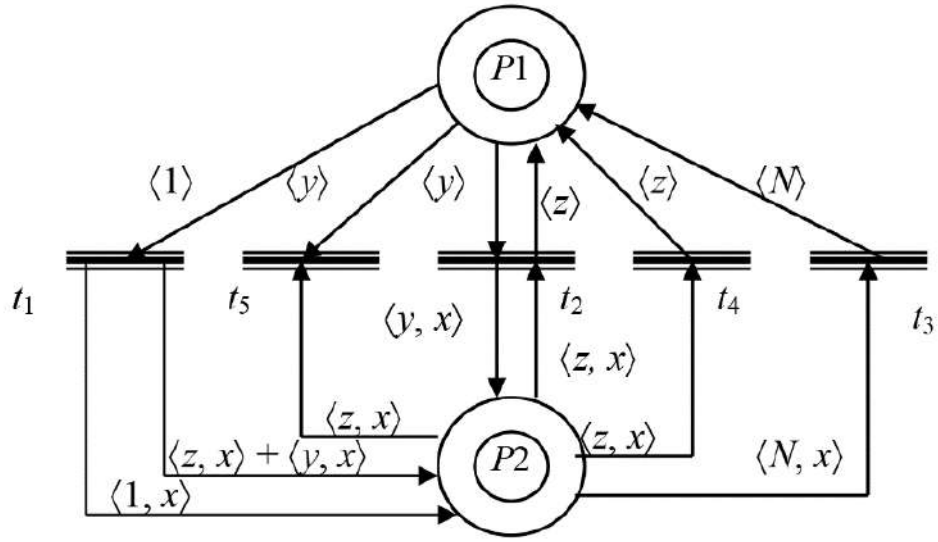

Fig. 3. Service object with loss and duplication *FIFO N-LD* [*s*, *r*]

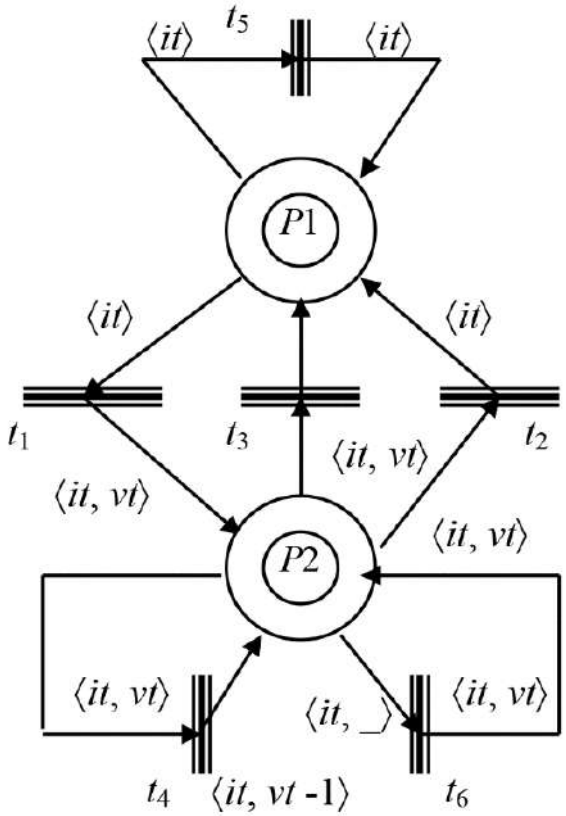

Fig. 4. The timer object

Based on the analysis of the existing ways of using the timer protocols, we can make the following conclusions about its functions. The timer should provide management of timeouts: start of a timeout with a certain value of an interval; its

shutdown before the moment of the expiration and alarm to the user about its expiration. Moreover, it is often necessary to restart the timeout, i.e. to set the enabled timeout to a new value of the time interval (Eremenko, 2015).

The timer object has one access point *u* for communication with users. A timer can manage multiple timeouts at the same time, in this case *n* instances. For each timeout, a label with a unique identifier it_i is allocated. Initially, all timeouts are disabled (all labels (it_i) are in position P_1). The timeouts are controlled by four commands that define the conditions for triggering transitions:

t_1 – start of timeout *ON* (*it*, *vt*);

t_2, t_5 – timeout *OFF* (*it*);

t_3 – end of time (expiration) timeout *EXP*(*it*), [*vt* = 0];

t_4 – timeout execution [*vt* › 0];

t_6 – restart timeout *RS*(*it*, *vt*)

The *vt* parameter in *ON* and *RS* commands specifies the timeout interval.

If the user needs to run a timeout of the value *vt*, he issues the command *ON* (*it*, *vt*), where the parameter *it* can be free (i.e. not defined in advance). After executing this command (t_1 transition triggered), one of the free it_i identifiers is moved from position P_1 to position P_2, and its value is returned to the user for further work with this timeout. Further, the triggering of the internal transition t_4, gradually decreases the value of *vt* and when it becomes zero, the command *EXP*(*it*) is executed that indicates expiration of the timeout with identifier it_i. The user may, before the expiration of the specified interval, to turn off the timeout command *OFF*(*it*) that translates the tag it_i from position P_2 to P_1. It may happen that this command will be issued by the user after the *EXP* command. In this case, the t_5 transition will be triggered which does not change the state of the timer objects. The user may need to restart the pending timeout by setting its interval to a new value. To do this, it can use the *RS*(*it*, *vt*) command, which does not change the timeout state, but only changes its value.

5. Specification of protocol objects

A protocol object is a logical module that interacts with various objects, among which there are necessarily protocol objects of the upper and lower neighboring levels and, possibly, some auxiliary objects. A protocol object implements a protocol of corresponding level.

Using the apparatus of objects of Petri nets, it is possible to represent schematically the protocol object in the most general form. The protocol object of *N*-level is represented as a network object $PE_N[S_N, S_{N-1}, P_N, T_m, C]$ having five access points. Here S_N and S_{N-1} are access points to protocol objects of the upper and lower neighboring levels, respectively. The alphabet of these access points are the service primitives of the *N* - and (*N*–1)-levels, respectively. The P_N access point describes the interaction of a protocol object over a "clean" protocol with a remote protocol object of this level. The alphabet of this access point is a set of protocol commands and the behavior of the object from this access point is "seen" as the execution of protocol rules for the exchange of protocol commands. Between points P_N and S_{N-1} there is a certain communication since protocol commands from P_N are actually forwarded through an access point S_{N-1} in the form of data of service primitives. For this reason, the P_N point is redundant, because protocol interaction can be restored from the behavior of the object at the S_{N-1} point.

In addition, the protocol object includes two auxiliary access points *Tm* and *C*, designed to interact with the timer object (in cases where it is convenient to have a common time service for all objects) and the control object. It is possible that the protocol object may have other auxiliary access points.

A protocol object specification in its most general form is called *a complete protocol object specification*. To solve specific problems of protocol engineering, simplified specifications, which are called *problem-oriented* specifications, are enough. For example, for protocol implementation purposes, a complete specification is required except for the P_N point, which can be obtained by the abstraction operation: $\tau_{\{PN\}}(PE_N)$. To analyze protocols for the presence/absence of deadlocks, as will be seen later, a specification with one P_N point is sufficient: P_N: $\tau_{\{SN, SN-1, Tm, C\}}(PE_N)$.

Transport protocol (T-protocol, Fig. 1). The T-protocol is asymmetric, i.e. it has two types of protocol objects – receiving *TPEr*[*r*, *b*] and transmitting *TPEs* [*s*, *a*] objects.

The transmitting TPES object[*s*, *a*] has two access points: point *s* for the user and point *a* for the service being used. At point *s*, the object receives a block of data *x* from the user (PS *UDatReq*(*x*)) and immediately passes it to the protocol command *DT* (*x*). This protocol command is actually transmitted through the service used by the *LDatReq*(*DT*(*x*)) primitive, after which the object goes into the state of waiting for the protocol command acknowledgement ACK, which comes in the *LDatInd*(ACK) primitive and then the object goes to the initial state. In this version of the T-protocol, two logical actions of receiving a block of data from the user and its transmission in the service primitive are performed simultaneously as a result of performing a single transition. Indeed, as common sense dictates, there is no need to perform these operations separately. This possibility of specifying several logical actions simultaneously in one physical action is one of the most important advantages of the introduced apparatus, which increases its expressive capabilities.

The receiving object *TPEr*[*r*, *b*] has two access points *r* and *b*, designed respectively for the user and the service used. Its behavior consists in repeated triggering of one transition that, however, includes performance of several logical actions – reception of the protocol command *DT*(*x*) with data *x* in PS *LDatInd* from the lower level; transfer to the user of the received block *x* in PS *UDatInd*(*x*); return of the protocol command of confirmation ACK in PS *LDatReq*. This object also has significant differences from the original version.

In addition to simultaneous interaction at different access points, there is simultaneous execution of several primitives at one point. Namely, at point *b*, the transition is labeled with the *MultiSet LDatInd*(*DT* (*x*)) + *LDatReq* (ACK), which specifies the simultaneous execution of these primitives. This mechanism is also very useful and powerful, because it avoids unnecessary intermediate states and, in the end, leads to a greater degree of compactness.

From this description it is possible to allocate "pure" protocol, having projected behavior of object on a set of protocol commands *DT* and ACK. The sending *TPEs* object

sends PS *DT*(*x*) (data) and waits for confirmation. The receiving *TPEr* object, having received *DT*(*x*), returns a confirmation ACK. After that, *TPEs*, having received ACK, goes to the initial state.

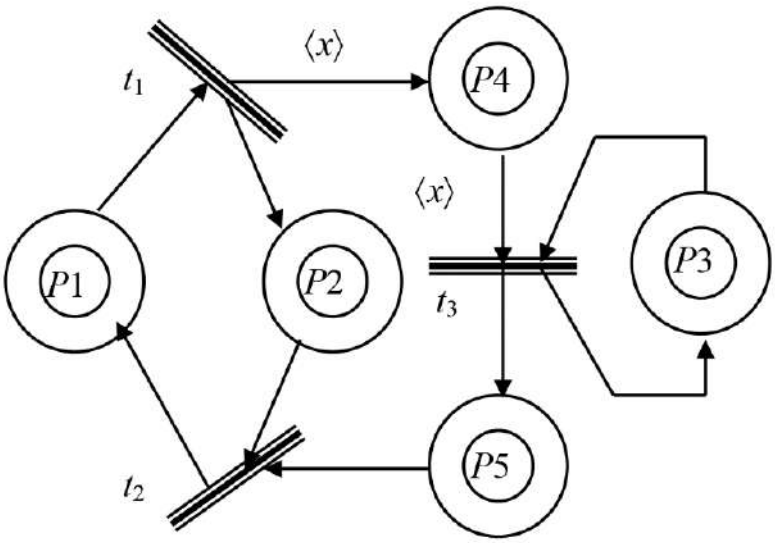

Fig. 5. Specification of means of information exchange
(three-level T-protocol)

6. Specification of protocols and logical structure levels

As a rule, work on the formal specification of protocols and levels of the logical structure of the telecommunication environment is performed at different levels of compositionality. At the system level, the final architectural actions are performed when objects specified at other levels of compositionality are combined into the final configuration.

Thus, depending on the protocol model, the protocol specification is completed by the composition of protocol objects and the object of the underlying service or data medium (Fig. 5). The last three-level model of the protocol is a specification of the entire level of the logical structure, which includes the specification of protocol objects, objects of the underlying and provided service.

As an example, here is the specification of the T-protocol. To do this, we take two protocol objects *TPEs* [*s*, *a*] and *TPEr*[*r*, *b*] (Fig. 1), the simplest duplex service *SE*1 and combine them as follows: *TL*[*s*, *r*] = (*TPEs* || *SE*1 || *TPEr*).

Conclusions

The presented technique allows to create a formal basis for the development of the logical structure of the distributed telecommunication environment at the system level. Its implementation allows:

- formally define a concept of object as a certain logical module with access points specifying directions of interaction with object;

- define rules for composing objects through access points, allowing to build complex configurations for determining the final means of information exchange, and for subsequent analysis of protocol implementations;

- provide the ability to determine the equivalence relationship between objects and the availability of key means of its verification;

- introduce a new concept of a network object, defined as a Petri net with several marks – access points to the object. The most important advantage of the objects is the possibility of specification of simultaneous events, which significantly increases the expressive and analytical capabilities of the device and compactness of the resulting descriptions. Graphical representation of network objects in architectural and network forms is introduced;

- introduce operations on objects that allow to design complex configurations of objects, the central of which is the operation of the composition of objects. The standard properties of operations that allow efficient manipulation of objects are shown;

- introduce the concept of objects equivalence based on the bisimulation equivalence of Petri nets. It is shown that this equivalence is a congruence with respect to all operations on objects.

- to interpret key concepts of the logical structure of the telecommunication environment, such as protocol, service, data transmission medium in terms of network

objects. In terms of the apparatus, the main tasks of development of the system level of logical structure, including the task of specification, are strictly formulated and solved.

Acknowledgments

The work was supported by RFBR grant 19-29-06030-MK "Research and development of wireless ad-hoc network technology between UAVs and control centers of "smart city" on the basis of adaptation of transmission mode parameters at different levels of network interaction".The theory was prepared in the framework of the state task FZWG -2020-0017 "Development of theoretical foundations for building information and analytical support for telecommunication systems for geo-ecological monitoring of natural resources in agriculture".

References

Ahmed, S., Kanhere, S. (2011). Jha, Link characterization for aerial wireless sensor networks, in: GLOBECOM Wi-UAV Workshop, 2011, pp. 1274–1279.

Anisimov, N. A. (1989). Recursive definition of the hierarchy of protocols based on Petri nets. Fourteenth all-Union school-seminar on computer networks. (Minsk, 1989). – Moscow; Minsk: VINITI, 1989, CH. 2, pp. 101-106.

Anisimov, N. A. (1990). Hierarchical composition of protocols. Automation and computer engineering, 1990, No. 1, pp. 3-10.

Bekmezci, L., Sahingoz, O.K., Temel, S. (2013). Flying Ad-Hoc Networks (FANETs): A Survey, Ad Hoc Networks, 2013, Vol. 11, № 3, pp. 1254–1270;

Eremenko, V. T. (2018). Mathematical models and methods for solving problems of optimization of reliability of systems with complex structure / D. S. Mishin, V. T. Eremenko, M. Yu. Rytov / / Bulletin of the Bryansk state technical University. 2018-No. 4 (65). - Pp. 88-95

Eremenko, V. T. (2019). Mathematical models of information exchange algorithms of ad-hoc networks of geographically distributed construction objects. / V. A. Eremenko, V. T. Eremenko, V. M. Haramohan. Information systems and technology. 2019. - No. 2 (112). - Pp. 41-47

Eremenko, V.T. (2015). Method of forming test kits for security protocols in data processing systems. V. T. Eremenko, V. M. Haramohan. Information systems and technology. - 2015. - No. 2 (88). Pp. 131-137.

Hoare, H. (1989). Communicating sequential processes. – Moscow: Mir, 1989. - 264 pp.

Karan Palan, Priyanka Sharma. (2015). FANET Communication protocols: A Survey, Volume 7, Number 1, Sept 2015 - March 2016, pp. 219-223. DOI: 10.090592/IJCSC.2016.034.

Karpov, Yu. G. (1987). On the property of protocol coherence. Automatics and computer engineering, 1987, No. 4, pp. 38-40.

Konstantinov, I.S., Vasilyev, G.S., Kuzichkin, O.R., Surzhik, D.I., Lazarev, S.A. (2018). Numerical and Analytical Modeling of Wireless UV Communication Channels for the Organization of Wireless Ad-Hoc Network. IJCSNS - International Journal of Computer Science and Network Security - 2018. - Vol. 18, No. 8, pp. 98-104. Open access: http://paper.ijcsns.org/07_book/201808/20180815.pdf.

Konstantinov, I.S., Vasyliev, G.S., Kuzichkin, O.R., Surzhik, D.I., Kurilov, I.A., Lazarev, S.A. (2019). Development Of UV Communication Channels Characteristics Modeling Algorithm In A Mobile Ad-Hoc Network / Journal of Advanced Research in Dynamical and Control Systems (JARDCS) / ISSN: 1943-023X / Volume 11 | 08-Special Issue, 2019. Pages: 1920-1928. http://www.jardcs.org/abstract.php?id=2543

Kotov, V. E. (1984). Petri Nets. – Moscow: Nauka, 1984. - 160 pp.

Polshchykov, K.; Lazarev, S.; Kiseleva, E. (2019). Decision-making supporting algorithm for choosing the duration of the audio communication session in a mobile ad-hoc network, *Revista de la Universidad del Zulia*, 10 (27), 101-107.

Purohit, A., Zhang, P. (2009). Sensor Fly: a controlled-mobile aerial sensor network, in: Proceedings of the 7th ACM Conference on Embedded Networked Sensor Systems, SenSys '09, ACM, New York, NY, USA, 2009, pp. 327–328.

Los aportes de la Neurociencia a la enseñanza de las Ciencias Naturales: reflexiones desde la experiencia de los estudiantes de educación secundaria

Daniel Rubén Tacca Huamán*
Francisco Chire Bedoya**

RESUMEN

La investigación en neurociencia cognitiva aporta conocimiento sobre el funcionamiento cerebral que podría ser útil para la enseñanza de las ciencias naturales. Por ello, el objetivo principal de la investigación fue conocer, desde la experiencia de los estudiantes de educación secundaria, la contribución de los principios de la neurociencia a la enseñanza de las ciencias naturales. El enfoque fue cualitativo, con diseño fenomenológico y con 24 sujetos participantes que estudiaban el último año de educación secundaria. Se utilizó la técnica conocida como grupo focal y se elaboró una guía con 20 ítems. Los resultados indican que los sujetos informantes perciben un cambio positivo en la enseñanza de las ciencias naturales, especialmente en la motivación, presentación de contenidos, evaluación, actividades de indagación, experiencias prácticas, relación docente-estudiante y perspectiva de estudio en áreas científicas.

PALABRAS CLAVE: neurociencia; enseñanza; ciencias naturales; estudiantes; secundaria.

*Universidad Tecnológica del Perú, https://orcid.org/0000-0002-0694-5262, C17500@utp.edu.pe
**Asociación Educativa Estándares, Perú, https://orcid.org/0000-0002-3109-341X, francischire@gmail.com

Recibido: 30/01/2020 Aceptado: 20/03/2020

The contributions of Neuroscience to natural sciences teaching: reflection from the experience of high school students

ABSTRACT

The research in Cognitive neuroscience provides knowledge about brain functioning that could be useful for teaching the natural sciences. Therefore, the main objective of the research was to know, from the experience of high school students, the contribution of the principles of Neuroscience to the teaching of natural sciences. The approach of this study was qualitative, with a phenomenological design and with 24 participating subjects studying the last year of high school. The technique called focus group was used and a question guide with 20 items was prepared. The results indicate that the informant subjects perceive a positive change in the teaching of the natural sciences, especially in motivation, presentation of content, evaluation, research activities, practical experiences, student-teacher relationship and study perspective in scientific areas.

KEY WORDS: Neuroscience; teaching; natural sciences; students; high school.

Introducción

Cuando se estudia el proceso de aprendizaje en los adolescentes, es imposible dejar de lado los aportes de la psicología sobre el desarrollo cognoscitivo, el estadio de las operaciones formales de Piaget y las propuestas del aprendizaje sociocultural de Vygotsky. Durante la adolescencia, la maduración cognoscitiva permite, paulatinamente, que los jóvenes alcancen un razonamiento abstracto, elaboren juicios morales y realicen planes sobre su futuro (Papalia et al., 2010). Lo anterior significa que, los adolescentes desarrollan el pensamiento abstracto, adquieren la capacidad de emplear símbolos para representar conceptos, pueden comprender metáforas, analizar posibilidades y plantear hipótesis. La educación, como proceso de humanización, socialización y culturización, debe promover el desarrollo y fortalecimiento de estas habilidades "naturales", pues son de vital importancia para la vida del adolescente y para el futuro adulto.

En la mayoría de países, el programa curricular del nivel secundario está organizado por materias. Esta segmentación permitió, en un inicio, profundizar y especializar el conocimiento sobre una determinada disciplina; sin embargo, como explican Sanmartí y Márquez (2017), esta educación tradicional no permite el desarrollo habilidades científicas. La enseñanza de las Ciencias Naturales en la secundaria no debe ser entendida como un proceso aislado de otras materias ni de la realidad; si bien se necesita cierto grado de

especialización, tanto a nivel escolar como universitario, es imposible que los estudiantes desarrollen habilidades "aprendiendo" un contenido enlatado y aislado. Según López (2015), uno de los principales problemas de la enseñanza de las ciencias es el uso de estrategias tradicionales que no contribuyen a la comprensión de temas relacionados con el desarrollo científico y tecnológico.

El principal objetivo de la enseñanza de las Ciencias Naturales es que el estudiante conozca y comprenda la complejidad del mundo en el que vive, para que luego pueda transformarlo (Tacca, 2011). Memorizar contenidos, fórmulas, ecuaciones, etc. descontextualiza el aprendizaje, no resulta viable en una educación globalizada y lleva al analfabetismo científico (Matthews, 2017). Como explica Romero-Ariza (2017), la alfabetización científica es un constructo que hace referencia a lo que las personas deben conocer y a las acciones que podrían realizar en un contexto donde aspectos de la ciencia y tecnología están implicados. En este sentido, continua el autor, para la evaluación de la alfabetización científica a través de la prueba PISA (Programm for International Student Assessment) del año 2015 se consideró cuatro aspectos muy importantes: el contexto, el conocimiento, las competencias, y las actitudes. Según lo anterior, estas cuatro dimensiones no podrían ser evaluadas por separado, se deberían integrar y amalgamar en el desempeño de los estudiantes.

En la propuesta de Arteaga et al. (2016), se puede distinguir seis finalidades de la enseñanza de las ciencias, entre ellos: (1) promover la elección de estudios relacionados al ámbito científico, (2) facilitar la toma de decisiones democráticas respecto a temas científicos y tecnológicos, (3) desarrollar habilidades para el mundo laboral, (4) culturizar a los estudiantes, (5) desarrollar la capacidad de aprender fuera de clase y (6) fomentar los valores para aportar al contexto más cercano. No se trata únicamente de desarrollar contenidos y preservar el rol transmisor del profesor, se trata de enseñar a aprender para que el estudiante pueda construir su conocimiento.

Reimers y Chung (2016) plantea que las habilidades requeridas para el contexto actual son: pensamiento crítico, innovación, creatividad, pensamiento científico, autoconocimiento, autocontrol y trabajo en equipo. Con la enseñanza de las Ciencias Naturales se pueden desarrollar muchas habilidades en los estudiantes (Rivero et al., 2017); sin embargo, todavía es posible observar que algunos profesores, y no solo a nivel escolar, siguen con el dictado y exposición de contenidos, convirtiendo a las ciencias naturales en algo aburrido y tedioso

(Tacca, 2011). Para Arteaga et al. (2016), es necesario propiciar el aprender a aprender, desarrollar la observación, clasificación, modelación, la formulación de hipótesis, solución de problemas, motivar el trabajo académico, entre otros; lo anterior representa los principales retos al momento de enseñar ciencias.

Según Aguilera et al. (2018), enseñar ciencias haciendo ciencia es un reto que involucra corregir ciertas actitudes negativas, concepciones equivocadas y sobre todo mejorar la experiencia de aprendizaje a partir de sensaciones y emociones positivas. Si un profesor desea enseñar ciencias y generar actitudes positivas hacia ella, la mejor forma es a través de la indagación (Rojas-Bahamón et al., 2018) y considerando los aspectos afectivos y motivacionales (Bevins y Price, 2016). Existen diversos estudios que exponen resultados positivos de la indagación como estrategia para promover el pensamiento, la argumentación y la comprensión de las ideas científicas (Romero-Ariza, 2017). Por ejemplo, Flórez-Nisperuza y De la Ossa Albis (2018) reportaron que las actividades de indagación mediadas por el profesor tuvieron mayor efecto en el aprendizaje que aquellas actividades de trabajo netamente autónomo; lo anterior significaría que, si bien el estudiante es el centro del aprendizaje, el acompañamiento que ofrece el docente es relevante para el cumplimiento de los objetivos educativos.

Rivero et al. (2017) sugieren que cualquier mejora educativa necesita que los profesores conozcan los principios teóricos y prácticos de las nuevas propuestas, esto representa un reto que incluye la formación inicial del profesorado. Delord et al. (2017) explican que un profesor puede innovar y cambiar su forma de enseñanza si es que comparte sus experiencias, fortalece la reflexión colectiva y la ayuda mutua con los colegas. Delord y Porlán (2018) comentan que la evaluación de los aprendizajes es el tópico más resistente a la innovación; además, aclaran que para innovar en las clases es necesario el apoyo del área académica de la institución. Monroy y Peón (2019) sugieren integrar diversos enfoques pedagógicos en un modelo híbrido para responder adecuadamente a las actuales exigencias educativas; además, como los modelos pedagógicos son provisionales y no son infalibles, recomiendan que estos lineamientos generales incorporen a su propuesta los avances logrados en el campo científico y tecnológico. De esta manera, el docente puede contar con mayores recursos didácticos, tecnológicos y, sobre todo, basados en la investigación científica.

En los últimos años la neurociencia cognitiva ha contribuido en la comprensión de cómo se desarrollan las funciones superiores (Tacca, 2018). Hoy se sabe que el desarrollo del

cerebro es un proceso heterocrónico (Tacca, 2016); las hormonas intervienen en el proceso organizativo y en el funcionamiento del cerebro (Crone, 2019); el proceso de poda y mielinización integran conexiones que permiten la aparición de juicios y discernimientos basados en el análisis completo de una determina situación, el cerebro busca la gratificación, la sociabilidad y las reacciones emocionales (Siegel, 2016); la memoria es una colección de conexiones neuronales que se recupera al momento de la acción y, en cuanto a la atención, se percibe solo aquello en lo que estamos interesados (Manes y Niro, 2014); el cerebro, con ayuda de los sentidos, está en la capacidad de construir circuitos neuronales con la información que percibimos producto de nuestras experiencias (Hüther, 2013); un ambiente estimulante, que brinda todas las posibilidades para desarrollar el potencial, maximiza la capacidad de generar ideas y estimula la creatividad (Bachrach, 2016); los estímulos liberan neurotransmisores y estos activan o desactivan ciertas redes neuronales, además, dichas redes se fortalecen con la repetición, las emociones, la novedad y la focalización de la atención (Bachrach, 2015). La bioquímica cerebral es la responsable de la construcción del conocimiento, por ello, González (2017) aconseja que los profesores deben considerar las características del funcionamiento cerebral en el desarrollo de las clases. Una enseñanza novedosa e interesante contribuye a cambiar la estructura y la actividad electroquímica del cerebro (Paniagua, 2013).

Como el aprendizaje de la ciencia está ligado a diversas capacidades y habilidades que, al parecer, se pueden desarrollar con la indagación; y, por otra parte, la neurociencia cognitiva ha descubierto cómo funciona el cerebro y que el aprendizaje lo modifica (Tacca et al., 2019), el presente trabajo de investigación tuvo como objetivo principal conocer, desde la experiencia de los estudiantes de educación secundaria, la contribución de los principios de la neurociencia a la enseñanza de las Ciencias Naturales.

1. Diseño de la investigación

En la presente investigación se buscó recoger las experiencias de los estudiantes de educación secundaria sobre el proceso de enseñanza de las ciencias naturales por parte de sus profesores a partir de la incorporación de los principios y aportes de la neurociencia cognitiva. La información que se recolectó fue producto de la experiencia compartida y se basó en la subjetividad de las percepciones de cada estudiante; por lo que, según Hernández-Sampieri

y Mendoza (2018), el trabajo se desarrolló bajo el enfoque cualitativo con diseño fenomenológico.

1.1. Participantes

Fueron 24 sujetos informantes que cursaban el quinto año de educación secundaria en una institución educativa pública. Todos los estudiantes pertenecían al mismo año de escolaridad, tenían el mismo horario de estudio, compartían los mismos compañeros y los docentes desarrollaban el mismo programa curricular en la misma cantidad de horas por materia. Todos los participantes presentaron el consentimiento informado de sus padres o apoderados legales para participar en forma voluntaria durante la investigación. Representaron el 33% del total de los estudiantes del grado, siendo la edad promedio de 16.4 años, 13 fueron varones y 11 mujeres.

1.2. Instrumento de recolección de datos

Se realizó una revisión sistemática de la literatura especializada sobre la enseñanza de las Ciencias Naturales y los resultados de las investigaciones en neurociencia cognitiva; además, se realizó una serie de visitas a la institución donde se pudo observar cómo se desarrollan las clases del área de Ciencias y Tecnología del quinto de secundaria. Con toda esta información, y luego de un proceso de reflexión, se identificaron las siguientes categorías a investigar: (1) secuencia metodológica, (2) experiencias prácticas, (3) relación docente-estudiante, (4) sistema de evaluación y (5) perspectiva de estudios en áreas científicas. En este proceso, se elaboró una batería de preguntas abiertas que en su redacción incluían aspectos relacionados con los aportes de la neurociencia cognitiva, de esta forma, los participantes podrían evaluar desde su perspectiva la posible contribución o no de dichos descubrimientos. Todos los ítems fueron organizados en una guía de preguntas. El instrumento denominado Guía de preguntas estuvo constituido por 20 ítems.

1.3. Procedimiento

Del total de estudiantes, 27 entregaron el consentimiento informado, pero solo 24 decidieron participar efectivamente. Se decidió usar la técnica denominada grupo de enfoque o *focus group*, ya que, como explican Hernández-Sampieri y Mendoza (2018), esta técnica

permite comprender las experiencias de los sujetos informantes a través de su interacción. Se realizaron 4 grupos focales, cada uno con 6 integrantes distribuidos al azar. En cada sesión, los investigadores realizaron una breve presentación personal; luego de empatizar con los estudiantes, se informó sobre los objetivos del trabajo y se distribuyeron formando un círculo en el cual todos se podían observar y compartir información. Cada sesión duró, aproximadamente, 45 minutos y se desarrollaron todas las preguntas que se habían propuesto en la guía. Para un adecuado análisis de las respuestas, se obtuvo un registro en audio de todas las sesiones.

2. Resultados

Las respuestas de los participantes fueron analizadas según las categorías indicadas anteriormente, de acuerdo a esto se obtuvieron los siguientes resultados:

2.1. Categoría 1: secuencia metodológica

En esta categoría, los participantes comentaron que en los últimos dos años percibieron que los docentes de ciencias cambiaron la forma de iniciar las clases. Todos recordaban que, en los primeros años de secundaria, las clases empezaban con un saludo y rápidamente se colocaba el título del tema que el profesor iba a dictar. Sin embargo, todos transmitieron gran satisfacción porque sienten que los profesores se esfuerzan en presentar alguna imagen o video que llama su atención y que se relaciona con el tema a tratar; también revelan que gracias a que el profesor les hace recordar lo trabajado la clase anterior, ellos pueden evocar con mucha mayor facilidad los principales conceptos y actividades desarrolladas.

En cuanto al desarrollo de la clase, los estudiantes manifestaron que en años anteriores las lecciones las recibían en carpetas que prácticamente no se movían, se dedicaban a escuchar, tomaban nota cuando el profesor dictaba y las actividades las realizaban por la calificación que iban a obtener y no por desarrollar la actividad misma. Durante este año, los estudiantes percibieron que las actividades grupales en el aula han aumentado: a todos les parece que es mejor aprender en grupo que de forma individual, pues les permite identificar las fortalezas y debilidades de los integrantes que hay que mejorar. Según los participantes, aprenden más cuando el profesor plantea una situación problemática relacionada con su

contexto más cercano, con vivencias propias de la comunidad o de la ciudad donde viven. Además, perciben que los profesores están más preocupados por su aprendizaje, debido a que plantean las preguntas: ¿Cómo va el trabajo? ¿Entendieron la explicación? ¿Puedes apoyar a tu compañero? Expresan que hay más libertad para expresarse, pueden proponer ideas que el profesor no ha previsto y si estas son aceptadas por sus compañeros, el profesor la incorpora como parte de la clase.

En el cierre y evaluación del trabajo en el aula, los estudiantes explican que los profesores ya no usan el color rojo para calificar los cuadernos o pruebas, ahora utilizan azul, verde u otro color. A tres estudiantes no les interesa el cambio de color, dos no se dieron cuenta, pero el resto ha interpretado este cambio como positivo, ya que perciben que el color rojo se asocia con el peligro o les trae recuerdos negativos de pruebas desaprobadas en el pasado. Así mismo, consideran positivo que los profesores realicen un balance de los aprendizajes ya que de esta forma pueden darse cuenta de sus aciertos y errores en la resolución de las actividades. Consideran que ahora comprenden mejor lo que pasa a su alrededor, perciben que en los últimos meses han aprendido a relacionar lo desarrollado en el colegio con el mundo que los rodea.

2.2. Categoría 2: experiencias prácticas

Durante las experiencias prácticas, los estudiantes han identificado otro cambio en la dinámica de las clases de Ciencias Naturales. A diferencia de años anteriores, hoy son conscientes que es muy importante formular hipótesis en el trabajo de las ciencias, consideran que esta respuesta tentativa a la pregunta de investigación es muy importante porque de alguna forma guía su trabajo y al final deben argumentar si fue correcta o no. El valor atribuido a los debates y a la argumentación es positivo. Consideran que este tipo de dinámicas les permite contrastar activamente sus teorías, argumentos e ideas. Una de sus actividades preferidas es la de socializar sus puntos de vista porque están convencidos que la participación grupal enriquece su aprendizaje.

La manipulación de los equipos y materiales en el laboratorio sigue siendo parte fundamental en la enseñanza de las Ciencias Naturales. Algunos estudiantes comentan que sus padres solo escucharon como es un tubo de ensayo o un matraz, nunca pudieron experimentar porque el laboratorio no existía o porque no estaba implementado. Se sienten afortunados porque el colegio donde estudian les brinda la oportunidad, en la medida de lo

posible, de trabajar con material de vidrio, de plástico y reactivos; ellos lo llaman: "hacer ciencia de verdad". Han aprendido que para observar un fenómeno es necesario usar los cinco sentidos, son conscientes que la información entra por todos los sentidos y no solo por la vista. Muestran una reacción positiva cuando recuerdan la sesión de clase donde el profesor les plantea una experiencia que ellos no pueden resolver a priori. La consideran retadora y prueban varias veces la hipótesis (repiten el experimento) hasta obtener un resultado coherente con los principios que plantean al inicio. No se sientes frustrados si sus hipótesis están equivocadas, se sienten satisfechos de que el trabajo realizado cumpla con los pasos del método científico y la construcción argumentativa sea lógica y coherente.

Comentan que en algunas ocasiones han salido del colegio a recolectar muestras biológicas, siempre con los permisos respectivos y apoyo del docente. Perciben que de esta forma la enseñanza de las ciencias naturales, por parte del docente, se hace vivencial y significativa. Dentro de las recomendaciones, las que obtuvieron apoyo de la mayoría de participantes fueron: (1) incrementar las clases prácticas porque consideran que así aprenden más y (2) implementar no solo su laboratorio, sino los laboratorios de ciencia de todos los colegios.

2.3. Categoría 3: relación docente-estudiante

Consideran que los profesores han adoptado una actitud empática al estar más cercanos dentro y fuera del aula. Ellos manifiestan que mientras desarrollan las actividades, los profesores se acercan a apoyarlos o preguntan si todo está claro. Según comentan los informantes, en años anteriores se les recriminaban por el uso errado de algún implemento del laboratorio y los profesores resaltaban los errores en las pruebas escritas y orales; sin embargo, ahora se han percatado de un cambio de actitud, ya que los profesores los alientan a seguir aprendiendo, a formular nuevas hipótesis, a experimentar y a probar nuevos procedimientos. Este cambio se considera positivo porque han encontrado un apoyo emocional, son conscientes que como estudiantes adolescentes se pueden equivocar, a pesar de ello, valoran la actitud proactiva y empática de los docentes para promover el aprendizaje de las ciencias naturales. De todos los participantes, cuatro tienen al menos un hermano que está cursando estudios universitarios y manifiestan, según testimonio del familiar directo, que la enseñanza de las ciencias en la universidad no es igual que en el colegio. Saben que el

nivel académico es diferente, pero según expresan, no esperan ver un profesor aburrido, que solo escribe en la pizarra y que deja fórmulas para memorizar.

2.4. Categoría 4: sistema de evaluación

Uno de los comentarios más resaltantes y recurrentes en esta categoría fue: "el examen parcial y final ya no son tan importantes". Los estudiantes explicaron que con la nueva "forma" de evaluación de los profesores, estos exámenes no influyen mucho en la calificación final. Según comentan, en años anteriores solo se evaluaba de esa forma y era un sistema donde se "jugaban la vida" en un curso, ya que si se desaprobaba ambos exámenes se desaprobaba la asignatura. Sin embargo, hoy reconocen que los profesores han asignado un valor importante al trabajo en aula, a las presentaciones que realizan, a la participación, a los trabajos que entregan, a las actividades de campo, a los experimentos realizados y al trabajo colaborativo. Para ellos, esta "forma de evaluación" es mejor ya que se considera el trabajo continuo en cada clase y así recuerdan más rápido los términos especializados y las teorías pues los utilizan constantemente. Según comentan, en el sistema anterior, estudiaban uno o dos días antes de los exámenes, les costaba trabajo recordar la información y no podían explicar ciertos procedimientos; pero ahora, los recuerdan por la frecuencia de uso del conocimiento científico.

Otro cambio importante que comentan es que antes se evaluaba con preguntas de opción múltiple o de falso y verdadero, pero ahora han visto un incremento de las preguntas abiertas. En este sentido, comentan que al inicio tuvieron problemas para responder dichas preguntas, pues no estaban acostumbrados a argumentar sus ideas y a justificar sus concusiones. Sin embargo, hoy son conscientes que la argumentación de ideas es una habilidad que necesitan desarrollar.

2.5. Categoría 05: Perspectiva de estudios en áreas científicas

En esta parte del estudio, más de la mitad de los participantes manifestaron que no les interesaba estudiar una carrera ligada a las ciencias naturales, a pesar que en las pruebas psicológicas de orientación vocacional los resultados mencionaban que poseían algunas aptitudes para dichas carreras. Por otra parte, ocho participantes declararon que si les interesaría estudiar Ingeniería, Química, Biología, Medicina, Enfermería u otra carrera

relacionada con las ciencias. Cuando fueron consultados del porqué de su decisión, los ocho manifestaron que en los últimos meses han comprendido que las ciencias naturales son importantes para la vida del hombre, ayuda a comprender el mundo y con la investigación científica se puede producir conocimiento valioso para el progreso de la sociedad. Según explicaron, los factores en orden de importancia para tomar dicha decisión fueron: (1) los resultados del test vocacional donde se identificaron las aptitudes hacia la ciencia, (2) la metodología de análisis crítico en la enseñanza de las ciencias y (3) el posible beneficio que traerán a su comunidad.

Según comentan, por conversaciones con estudiantes universitarios cercanos a ellos, son conscientes que en los niveles superiores de estudio la "forma" como se enseña las ciencias naturales no es "tan divertida" ni "tan activa". Los estudiantes de secundaria actualmente se concentran en obtener buenas calificaciones para poder postular a la universidad y, una vez dentro, afirman que se adaptaran al sistema "antiguo" de enseñanza.

3. Discusión y conclusiones

Como se puede apreciar, los principios de la neurociencia cognitiva han contribuido a la enseñanza de las ciencias naturales según la experiencia de los estudiantes de educación secundaria. Si bien las preguntas no incluían tecnicismos propios de la neurociencia ni de la psicología, los participantes pudieron brindar información valiosa y evidenciaron el cambio producido en las clases de Ciencias Naturales.

Según la información recolectada, los cambios realizados al inicio de clases han tenido buen recibimiento por parte de los estudiantes. La presentación de imágenes y otros recursos coincide con los planteamientos de Bachrach (2016), quien comenta que el aprendizaje se beneficia cuando se enseña con imágenes y texto y cuando se presentan ambos recursos al mismo tiempo. En este sentido, Small y Vorgan (2009) explican que un grado adecuado de estimulación del cerebro puede convertirse en algo sano y placentero; de esta forma, es posible que los estímulos que se presentan al inicio de las clases hacen que los contenidos teóricos de las ciencias sean percibidos como algo accesible y no generan expectativas negativas en los estudiantes. Esto parece coincidir con la propuesta de Waipan y Lerker (2017) sobre la captura de la atención como primer paso para el aprendizaje, luego, según los autores, es necesario mantener cierto grado de expectativa y ofrecer oportunidades de logro para mantener la motivación.

En cuanto a la importancia de recordar lo trabajado en la clase anterior, Blakemore y Frith (2016) explican que la formación de imágenes visuales puede crear cambios en el estado emocional, incluso en el sistema hormonal e inmunitario. Esto significaría que, al recordar los saberes previos, los estudiantes pueden evocar imágenes mentales y también recordar las sensaciones y emociones asociadas a dicho recuerdo. Un inicio emocional y disruptivo es vital, como sugiere Bachrach (2016), el cerebro recuerda primero el componente emocional, luego vienen los detalles, el aspecto, etc. Según Siegel (2016), ciertos estímulos gratificantes y novedosos ayudan a la liberación de dopamina, neurotransmisor asociado a la sensación de bienestar. Esto significaría, que un inicio emocionalmente positivo podría contribuir al aprendizaje. Lo anterior resulta ser importante no solo para la enseñanza de las ciencias naturales, sino para todas las áreas curriculares de los diferentes niveles educativos.

Según Oliverio (2018) el objetivo de utilizar los conocimientos sobre el cerebro es aprovechar su capacidad y estimular diversas áreas para crear conexiones neuronales que almacenan conocimiento. Massa et al. (2015) explican que cuando se habla de crear conocimiento, se hace referencia a un proceso complejo en el que se establecen relaciones permitiendo la articulación de conceptos para formar preposiciones y teorías. Como se ha visto, la clase magistral no puede ser vista como única fórmula válida para que el estudiante se apropie del conocimiento científico. Si bien la explicación es importante, según los resultados del presente trabajo, el diálogo, los debates y el interrogatorio didáctico constituyen estrategias válidas y funcionales para abandonar el pensamiento dogmático. El pensamiento en equipo permite plantear diversas soluciones a un problema y promueve el aprendizaje dialéctico.

En opinión de los estudiantes, la aplicación del método científico y del aprendizaje por indagación ha mejorado la dinámica educativa en la enseñanza de las ciencias naturales. Waipan y Merker (2017), explican que la acción de memorizar no garantiza el aprendizaje; sin embargo, cuando el sujeto experimenta y se emociona construye redes de información más significativas. Según Perez y Meneses (2018), en la actualidad existen diferentes propuestas para la planificación, ejecución y evaluación de las actividades indagatorias; sin embargo, la problemática, las hipótesis, el contraste de las hipótesis, la interpretación de resultados, la elaboración de conclusiones y la comunicación de los mismos, son elementos indispensables en cualquier escenario. Lo que se ha evidenciado, es que los estudiantes consideran que este tipo de metodología les ha permitido aprender en forma dinámica, significativa y sobre todo

vivencial. Lo anterior permite afirmar, siguiendo el planteamiento de Fraiha et al. (2018), que con la indagación es posible potenciar el desarrollo de habilidades relacionadas con la resolución de problemas.

Según Bachrach (2015), el cerebro es dinámico y va cambiando su organización y funcionamiento en respuesta a las actividades que el sujeto realiza o a las experiencias que vive. De esta forma, asegura el autor, es posible que para desarrollar ciertas habilidades es necesario introducir un cambio en la rutina, este nuevo hábito debe ser practicado, repetido y probado varias veces hasta que las conexiones sinápticas se fortalezcan y constituyan una estructura cerebral nueva. Esto indicaría que mientras más se ejerciten ciertas habilidades y actitudes, los estudiantes pueden desarrollar destrezas específicas relacionadas con el quehacer científico. Por ello, era necesario cambiar la forma como se enseñaba las ciencias naturales; se ha pasado del "dictado" tradicional a una enseñanza que promueve constantemente la construcción de argumentos, la elaboración de hipótesis, la realización de experimentos, etc. Si se analiza en perspectiva, esta forma de enseñar ciencias estaría fortaleciendo el desarrollo de la actitud científica en los estudiantes.

Por otra parte, todo indicaría que la implementación de actividades retadoras en la enseñanza de las Ciencias Naturales contribuye a un mejor aprendizaje. Las actividades de baja demanda cognitiva pueden presentar resultados positivos; sin embargo, la comprensión de información, la conexión de conceptos y su potencial aplicación necesitan un contexto de exigencia que no se puede olvidar (Salcedo, 2019). Las actividades retadoras que se implementaron tienen un componente emocional; como explica Hüther (2013), las emociones nacen cuando se perciben estímulos que no corresponden a nuestras expectativas, que rompen la armonía actual de los procesos cerebrales. Según Waipan y Lerker (2017), el cerebro está acostumbrado a la seguridad que le ofrecen los patrones de resolución de problemas; sin embargo, cuando aparece un estímulo que no encaja con lo que el cerebro sabe y puede hacer, casi automáticamente empieza a buscar la forma de solucionarlo, incorpora una nueva rutina y guarda de manera profunda y significativa la información. De esta forma, un estímulo sorpresa, disruptivo o conflictivo, cognitivamente hablando, se convierte en pieza fundamental en la enseñanza de las ciencias naturales.

Parece que la preocupación de los profesores durante el desarrollo de las clases es bien recibida por los estudiantes. Si bien durante la adolescencia se produce un avance importante en el desarrollo emocional y mental de la persona (Manes y Niro, 2014), la comprensión y

gestión de las emociones termina constituyendo el pilar de las relaciones interpersonales en todas las etapas de la vida (Oliverio, 2018). Es el sistema límbico, según Bachrach (2015), el responsable de las emociones; este sistema neurológico es el que "decide" si la información se guarda como un recuerdo agradable o no y también modula la motivación. El ser humano es un ser social, la empatía no solo involucra el aspecto afectivo de la persona, sino también ciertos procesos reflexivos (Manes y Niro, 2014). Waipan y Merker (2017) explican que el clima en el aula supone una interacción socio-afectiva y una convivencia saludable, por lo que, la convivencia entre pares, el acercamiento del profesor, el lenguaje asertivo, inclusivo y motivador que emplea en las clases parecen contribuir a un adecuado ambiente de aprendizaje.

En cuanto a la evaluación, se ha observado que los estudiantes valoran el cambio de discurso del profesor en cuanto a resaltar los avances y no los errores. Siegel (2016) recomienda centrarse en los aspectos positivos del proceso de aprendizaje, sin castigos e impulsando la reflexión sobre las posibles mejoras. Según Waipan y Merker (2017), los adolescentes buscan sentirse valorados, tener cierta independencia para tomar decisiones y mostrar a los demás que pueden solucionar problemas. De esta forma, el proceso de evaluación deja de ser un proceso de calificación, y pasa a convertirse en un momento para reflexionar lo aprendido e impulsar las posibilidades de mejora.

Una revelación interesante se produjo cuando un grupo de estudiantes comentaron sus sensaciones sobre el color que emplea el profesor para corregir los avances y las pruebas. Como explica Canté (2017), los colores que se usan en una presentación o durante la clase pueden convertirse en desencadenes psicológicos que evocan emociones, sentimientos y logran cambiar la percepción del sujeto y mejora el aprendizaje. Si bien la evidencia encontrada sugiere que algunos de los estudiantes han asignado un valor al color de las revisiones, es probable que se necesite mayor investigación sobre el aspecto valorativo que realizan las personas para corroborar los principios de la psicología del color.

La enseñanza tradicional no se caracterizaba por dar espacio a la creatividad de los estudiantes. El contexto y los factores socioculturales influyen en la estimulación o inhibición de la capacidad creativa (Manes y Niro, 2014); es por lo anterior que, si no se presta atención a las ideas o propuestas innovadoras de los estudiantes, el entorno educativo habrá perdido todo sentido de existencia. Si no se promueve la innovación, los estudiantes están en peligro de repetir el círculo vicioso del aprendizaje memorista por el cual pasaron, probablemente,

sus padres. La enseñanza de las Ciencias Naturales en este nivel tiene la oportunidad de sembrar la semilla de la innovación, de promover ideas creativas y de incentivar el uso del pensamiento divergente.

El presente estudio, por su naturaleza cualitativa, ha recogido la percepción de los estudiantes respecto a las actividades didácticas que planifica y pone en ejecución el profesor en las clases de ciencias naturales. Se ha podido conocer que la aplicación del conocimiento del cerebro y de aspectos fundamentales de la neurociencia cognitiva ha contribuido a mejorar la enseñanza y el aprendizaje en sus tres componentes: conceptual, procedimental y actitudinal. Como explican Waipan y Merker (2017), si la percepción que construyen los estudiantes sobre las ciencias naturales no es gratificante y positiva, es posible que se pierda un gran capital humano que, de ser encaminado, puede convertirse en un talento del futuro.

Si bien esta investigación se ha desarrollado a nivel escolar, es válido plantear las siguientes interrogantes ¿Se obtendrán las mismas percepciones en otros colegios respecto a los aportes de la neurociencia a la enseñanza de las ciencias naturales? ¿Es posible replicar las experiencias descritas por los participantes en otras áreas curriculares? ¿En qué medida las percepciones de los estudiantes son objetivas? ¿Se puede implementar los principios de la neurociencia a la docencia universitaria? ¿Los docentes estamos dispuestos a innovar? La investigación en neurociencia cognitiva ha contribuido al conocimiento del cerebro cuando el sujeto aprende, pero según Blakemore y Frith (2016), hoy se sabe poco de lo que sucede en el cerebro cuando uno enseña. Sin embargo, es necesario estar atentos a los futuros aportes de la neurociencia y psicología ya que, por el volumen de información que se produce a través de la investigación científica, es probable que lo que se entiende como cierto ahora no se desfase en unos cuantos años.

Referencias

Aguilera, D., Martín-Páez, T., Valdivia-Rodríguez, V., Ruiz-Delgado, A., Williams-Pinto, L., Vílchez-González, J., & Perales-Palacios, F. (2018). La enseñanza de las ciencias basada en indagación. Una revisión sistemática de la producción española. *Revista de Educación*, (381), 259-284. Recuperado de https://digibug.ugr.es/bitstream/handle/10481/54384/19144.pdf?sequence=1&isAllowed=y

Arteaga, E., Armada, L., & Del Sol, J. (2016). La enseñanza de las ciencias en el nuevo milenio. Retos y sugerencias. *Universidad y Sociedad*, 8(1), 169-176. Recuperado de https://rus.ucf.edu.cu/index.php/rus/article/view/321

Bachrach, E. (2015). *En Cambio. Aprende a modificar tu cerebro para cambiar tu vida y sentirte mejor*. Buenos Aires: Sudamericana.

Bachrach, E. (2016). *Il cervello geniale. Migliora la tua vita con le scoperte delle neuroscienze*. Milano: TEA

Blakemore, S., & Frith, U. (2016). *Cómo aprende el cerebro. Las calves para la educación*. Barcelona: Editorial Ariel.

Bevins, S., & Price, G. (2016) Reconceptualising inquiry in science education. *International Journal of Science Education*, *38*(1), 17-29. doi:10.1080/09500693.2015.1124300

Canté, J. (2017). Psicología del color aplicada a los cursos virtuales para mejorar el nivel de aprendizaje en los estudiantes. *Grafica*, *5*(9), 51-56. Recuperado de https://www.raco.cat/index.php/Grafica/article/view/v5-n9-cante

Crone, E. (2019). *El cerebro adolescente: Cambios en el aprendizaje, en la toma de decisiones y en las relaciones sociales*. Madrid: Narcea Ediciones.

Delord, G. & Porlán, R. (2018). Del discurso tradicional al modelo innovador en enseñanza de las ciencias: obstáculos para el cambio. *Didáctica de las ciencias experimentales y sociales*, *35*, 77-90. doi:10.7203/DCES.35.12193

Delord, G., Porlán, R. & Harres, J. (2017). La importancia de los proyectos y redes innovadoras para el avance de la Enseñanza de las Ciencias: El caso de un profesor de la Red IRES. *Revista Eureka sobre Enseñanza y Divulgación de las Ciencias*, *14*(3), 653-665. Recuperado de http://hdl.handle.net/10498/19514

Flórez-Nisperuza, E., & De la Ossa Albis, A. (2018). La indagación científica y la transmisión-recepción: una contrastación de modelos de enseñanza para el aprendizaje del concepto densidad. *Revista Científica*, *31*(1), 55-67. doi:10.14483/23448350.12452

Fraiha, S., Paschoal, W., Perez, S., Tabosa, C., & Silva, C. (2018). Atividades indagativas e o desenvolvimento de habilidades e competências: um relato de experiencia no curso de Física da Universidade Federal do Pará. *Rev. Brasileira de Ensino de Física*, *40*(4).

González, S. (2017). La Neurociencia en la enseñanza universitaria. *Sinopsis educativa. Revista venezolana de investigación*, *17*(1-2), 46-52.

Hernández-Sampieri, R., & Mendoza, C. (2018). *Metodología de la investigación. Las rutas cuantitativa, cualitativa y mixta*. México: Mc Graw Hill Education

Hüther, G. (2013). *Il cevello umano:istruzioni per l'uso. Come percezioni, emozioni e conoscenza possono trasformare le nostre capacità intelletive*. Roma: Castelvecchi.

López, Z. (2015). La enseñanza de las ciencias naturales desde el enfoque de la *apropiación* social de la ciencia, la tecnología y la innovación ASCTI, en educación básica-media. *Revista científica*,*2*(22), 75-84. doi:10.14483/10.14483/udistrital.jour.RC.2015.22.a6

Manes, F., & Niro, M. (2014). *Usar el cerebro. Conocer nuestra mente para vivir mejor*. Buenos Aires: Planeta.

Massa, M., Foresi, M., & Sanjurjo, L. (2015). *La enseñanza de las Ciencias Naturales en la escuela media.* Santa Fe: Homo Sapiens Ediciones.

Matthews, M. (2017). *La enseñanza de la ciencia. Un enfoque desde la historia y la filosofía de la ciencia.* México: FCE.

Monroy, M., & Peón, I. (2019). Modelo pedagógico de integración sinérgica para la enseñanza de las ciencias experimentales. *RIDE. Revista Iberoamericana para la Investigación y el Desarrollo Educativo, 10*(19). doi:10.23913/ride.v10i19.573

Oliverio, A. (2018) *Il cervello che impara. Neuropedagogia dall'infanzia allá vecchiaia*. Bergamo: Giunti.

Paniagua, M. (2013). Neurodidáctica: una nueva forma de hacer educación. *Fides et Ratio - Revista de difusión cultural y científica de la Universidad La Salle en Bolivia*, 6(6), 72-77. Recuperado de http://www.scielo.org.bo/pdf/rfer/v6n6/v6n6_a09.pdf

Papalia, D., Olds, S., & Feldman, R. (2010). *Desarrollo Humano*. México: Mc Graw Hill.

Perez, S., & Meneses, J. (2018). La competencia científica en las actividades de aprendizaje incluidas en los libros de texto de Ciencias de la Naturaleza. *Revista Eureka sobre Enseñanza y Divulgación de las Ciencias, 17*(2). doi:10.25267/Rev_Eureka_ensen_divulg_cienc.2020.v17.i2.2101

Reimers, F. y Chung, C. (2016). *Enseñanza y aprendizaje en el siglo XXI: metas, políticas educativas y currículo en seis países*. México: FCE.

Rivero, A., Martín del Pozo, R., Solís, E., Azcárate, P., & Porlán, R. (2017). Cambio del conocimiento sobre la enseñanza de las ciencias de futuros maestros. *Enseñanza de las Ciencias*, *35*(1), 29-52. doi:10.5565/rev/ensciencias.2068

Rojas-Bahamón, M.; Arbeláez-Campillo, D. F.; Prieto, J. D. (2018). The investigation as an environmental education strategy, *Revista de la Universidad del Zulia*, 9 (25), 89-97.

Romero-Ariza, M. (2017). El aprendizaje por indagación: ¿existen suficientes evidencias sobres sus beneficios en la enseñanza de las ciencias? *Revista Eureka sobre Enseñanza y Divulgación de las Ciencias, 14*(2), 286-299. Recuperado de https://www.redalyc.org/articulo.oa?id=920/92050579001

Sanmartí, N. & Márquez, C. (2017). Aprendizaje de las ciencias basado en proyectos: del contexto a la acción. *Ápice. Revista de Educación Científica, 1*(1), 3-16. doi:10.17979/arec.2017.1.1.2020

Salcedo, A. (2019). Las ideas fundamentales de la estadística en textos escolares de matemáticas. En J. M. Contreras, M. M. Gea, M. M. López-Martín y E. Molina-Portillo (Eds.),

Actas del Tercer Congreso Internacional Virtual de Educación Estadística. Recuperado de www.ugr.es/local/fqm126/civeest.html

Siegel, D. (2016). *Tormenta cerebral. El poder y propósito del cerebro adolescente.* Barcelona: Alba Editorial.

Small, G., & Vorgan, G. (2009) *El cerebro digital. Cómo las nuevas tecnologías están cambiando nuestra mente*. Barcelona: Urano.

Tacca, D. (2011). La enseñanza de las ciencias naturales en la educación básica. *Investigación educativa*, *14*(26), 139-152. Recuperado de https://revistasinvestigacion.unmsm.edu.pe/index.php/educa/article/view/4293/3429

Tacca, D. (2016). ¿Cómo aprende el que aprende? La importancia de las emociones en el aprendizaje. *Revista Peruana de Psicología y Trabajo Social*, 5(1), 53-65.

Tacca, D. (2018). *Compendio Pedagógico*. Lima: Estándares Ediciones.

Tacca, D., Tacca, A., & Alva, M. (2019). Estrategias neurodidácticas, satisfacción y rendimiento académico en estudiantes universitarios. *Cuadernos de Investigación Educativa*, *10*(2), 15-32. doi:10.18861/cied.2019.10.2.2905

Waipan, L., & Lerker, A. (2017). *El cerebro adolescente va al aula: Neuroeducación adolescencia y escuela secundaria*. Buenos Aires: Bonum.

The value of the prooxidant-antioxidant system in ensuring the immunity of plants

Mariia Bobrova *
Olena Holodaieva **
Hanna Arkushyna ***
Olena Larycheva ****
Olha Tsviakh *****

ABSTRACT

Aim of the research: to identify changes in the state of the prooxidant-antioxidant system in the organs of different plant varieties, depending on their level of resistance to disease. The **subject** of the research is the role of individual components of the prooxidant-antioxidant system in ensuring plant resistance to disease. **Methodology**. Quantitative determination of PAS status was performed on onion tissue samples taken from the following varieties: "Globus" (high-resistant variety), "Rainbow" (medium-resistant variety) and "Donetsk Golden" (low-resistant variety). For biochemical analysis, tissues from the top of the leaf, the middle of the leaf, the scales of the onion-turnip, stem, flower, roots, and seeds were used. The concentration of superoxide anion radical, TBA-active products, superoxide dismutase activity, catalase, GSH-peroxidase, the concentration of ascorbic acid, glutathione, cytochrome oxidase activity were determined. The **results** of the research show that in the tissues of photosynthetic vegetative organs of onions, there is an increase in both parts of the prooxidant-antioxidant system; in tissues that are not capable of photoproduction, there is an advantage of the antioxidant link in accordance with the increased resistance of the variety to disease. Initiation of germination processes enhances the activity of both parts of the prooxidant-antioxidant system and is highest in flower cells. Onion seed tissues, which are at rest, have the advantage of a prooxidant link and an increase in the concentration of low molecular weight antioxidants. **Practical consequences**. As a result of the correlation analysis of the studied indicators, the presence of a close relationship between the concentration of TBA-active products and the activity of cytochrome oxidase and superoxide dismutase, ascorbate with glutathione was established.

KEYWORDS: ascorbic acid, catalase, superoxide anion radical, superoxide dismutase, cytochrome oxidase.

* PhD in Biology, Senior Lecturer of the Department of Biology and Methods of Teaching of the Volodymyr Vynnychenko Central Ukrainian State Pedagogical University, Ukraine. ORCID ID: 0000-0001-7703-651X.

** PhD in Chemistry, Associate Professor of the Department of General and Biological chemistry #2 Donetsk national medical university, Ukraine. ORCID ID: 0000-0002-4922-7033

*** PhD in Biology, Associate Professor of the Department of Biology and Methods of Teaching of the Volodymyr Vynnychenko Central Ukrainian State Pedagogical University, Ukraine. ORCID ID: 0000-0002-5261-7315

****PhD in Biology, Associate Professor of the Department of Pharmacy, Pharmacology, Medical, Bioorganic and Biological Chemistry of the Petro Mohyla Black Sea National University, Ukraine. ORCID ID: 0000-0001-7399-3339

*****PhD in Biology, Associate Professor of the Department of Chemistry of the V.O. Sukhomlynskyi Mykolaiv National University, Ukraine. ORCID ID: 0000-0002-1119-2170

Recibido: 22/04/2020 Aceptado: 17/06/2020

El valor del sistema prooxidante-antioxidante para garantizar la inmunidad de las plantas

RESUMEN

Objetivo de la investigación: identificar cambios en el estado del sistema prooxidante-antioxidante en los órganos de diferentes variedades de plantas, dependiendo de su nivel de resistencia a las enfermedades. El tema de la investigación es el papel de los componentes individuales del sistema prooxidante-antioxidante para garantizar la resistencia de las plantas a las enfermedades. **Metodología**. La determinación cuantitativa del estado de PAS se realizó en muestras de tejido de cebolla tomadas de las siguientes variedades: "Globus" (variedad de alta resistencia), "Rainbow" (variedad de resistencia media) y "Donetsk Golden" (variedad de baja resistencia). Para el análisis bioquímico, se utilizaron tejidos de la parte superior de la hoja, la mitad de la hoja, las escamas del nabo, el tallo, la flor, las raíces y las semillas. Se determinó la concentración de radicales anión superóxido, productos activos TBA, actividad superóxido dismutasa, catalasa, GSH-peroxidasa, la concentración de ácido ascórbico, glutatión, actividad citocromo oxidasa. **Los resultados** de la investigación muestran que en los tejidos de los órganos vegetativos fotosintéticos de las cebollas, hay un aumento en ambas partes del sistema prooxidante-antioxidante. En los tejidos que no son capaces de fotoproducción, existe una ventaja del enlace antioxidante de acuerdo con el aumento de la resistencia de la variedad a la enfermedad. El inicio de los procesos de germinación mejora la actividad de ambas partes del sistema prooxidante-antioxidante y es más alto en las células de las flores. Los tejidos de semillas de cebolla, que están en reposo, tienen la ventaja de un enlace prooxidante y un aumento en la concentración de antioxidantes de bajo peso molecular. **Consecuencias prácticas**: Como resultado del análisis de correlación de los indicadores estudiados, se estableció la presencia de una estrecha relación entre la concentración de productos activos TBA y la actividad de citocromo oxidasa y superóxido dismutasa, se estableció ascorbato con glutatión.

PALABRAS CLAVE: ácido ascórbico, catalasa, radical anión superóxido, superóxido dismutasa, citocromo oxidasa.

Introduction

Changes in the values of the state of the prooxidant-antioxidant system (PAS) accompanies all physiological and pathological processes, so it is the object of study of clinical medicine and gerontology (Kasote et al., 2015; Marrocco et al., 2017; Pacheco et al., 2018; Ye, 2013). The prospect of using and modifying certain components of antioxidant protection (AOP) to increase the body's immune defenses opens new areas of research in the

field of immunology, breeding, biotechnology, and genetic engineering and draws scientists' attention to the problem of PAS (Kohen & Nyska, 2002; Kostyuk, 2004). A feature of PAS of plants is the enhancement of prooxidant activity due to photosynthesis and generation of reactive oxygen species (ROS) by plastids, peroxisomes, apoplast, cytosol (Merzlyak, 1999; Polesskaja, 2007). The connection between the immunity of plants and their adaptation to the conditions of existence in terms of changes in the values of PAS indicators; the role of individual components of PAS in ensuring plant resistance to diseases, biochemical and molecular mechanisms of this resistance; features of the distribution of components of PAS in various organs of an organism of plants has not been studied. Recently, in an unfavorable environmental situation, increased attention to the quantitative content of antioxidants, ROS, and products of free radical peroxidation (FRPO) of biopolymers that enter our body with foods of plant origin. It is important to study the dynamics of their change with increasing duration of storage of edible vegetative parts of plants (Baiano et al., 2015; Xu et al., 2017; Song et al., 2010).

Aim of the research: to identify changes in the state of the prooxidant-antioxidant system in the organs of different plant varieties, depending on their level of resistance to disease. To achieve this aim, the following **tasks** were identified:

1. To identify the state of the components of PAS in photosynthetic and non-photosynthetic vegetative organs of onions.
2. To identify the state of the components of the PAS of the generative organs of onions.
3. To establish the relationship between the indicators of the state of PAS among themselves and with the level of resistance of plant varieties to disease.

1. Literature review

The formation of ROS in the process of life of plant and animal organisms was first established by M. Shenbein. In the formation of ideas about the participation of ROS and free radicals in biochemical processes of great importance were: the theory of Bach-Engler peroxidation, the theory of chain free radical oxidation, developed by M.M. Semenov, as well as a study by American scientist I. Fridovich, who proved the formation of oxygen radicals in enzymatic reactions and discovered the ability to inactivate some ROS with enzymes (Merzlyak, 1999). According to the works of O.P. Dmitrieva and Zh.M. Kravchuk, ROS in

plant cells are by-products of normal metabolism due to leaks in electron transport chains (ETC) in chloroplasts, mitochondria, as well as in those compartments where there are enzymes of redox reactions. In a normally functioning cell, there is a certain balance between activation and deactivation of Oxygen, so the number of its active forms remains at a safe level, but damage to plant tissues under stress, usually leads to activation of Oxygen, while disturbing the balance between ROS formation and destruction (Dmytriyev & Kravchuk, 2005). The generation of ROS by the plant cell occurs in response to environmental stressors of abiotic origin (Apel & Hirt, 2004; Foyer & Noctor, 2005; Gill & Tuteja, 2010; Pacheco et al., 2018; Kohen & Nyska, 2002). In the works of I.V. Maksimov, I.A. Tarchevsky, A.A.Averyanov noted an increase in total AFO production by plants during the invasion of pathogens (bacteria, fungi, mycoplasmas) and described the mechanisms of hypersensitivity reactions (Maksimov, 2006; Aver'yanov, 1991; Tarchevskiy, 2002). O.P. Dmitriev and Zh.M. Kravchuk in his work "Oxygen Active Forms and Plant Immunity" note the importance of ROS in the formation of acquired systemic resistance of plants to pathogens as signal intermediates for the activation of genes of enzymes involved in the synthesis of AO and phytoalexins (Dmytriyev & Kravchuk, 2005). At the present stage, the British School of Biochemistry, headed by Dr. Nicholas Smirnoff, is developing the problem of ROS and AOS of plant organisms, one of the most powerful complex works of which is "Antioxidants and reactive oxygen species in plants" (Smirnoff, 2005). In general, the question of the importance of ROS and AO in the plant cell is not unambiguous and exhaustive and requires careful study and systematization.

According to the works of O.G.Polesskaja is most important for plant cells singlet oxygen, superoxidation ion radical, hydrogen peroxide, and hydroxyl radical (Polesskaja, 2007). The system of antioxidant protection (AOP) of plants includes prevention of formation of ROS, their inactivation, break of a chain of reactions of FRPO, inactivation of products of FRPO, repair of damages (Halliwell, 2006). According to the literature, the most important enzymatic AOs present in all plant cells and organs are SOD, catalase, a number of peroxidases, ascorbate-glutathione cycle enzymes and cytochrome oxidase (Pacheco et al., 2018; Kostyuk, 2004; Shao, 2008; Smirnoff, 2005; Xu et al., 2017). Many authors (Pacheco et al., 2018; Kostyuk, 2004; Shao, 2008; Smirnoff, 2005; Xu et al., 2017) agree that the most important non-enzymatic low molecular weight antioxidants of the plant organism are AA,

α-tocopherol, reduced GSH, carotenoids, flavonoids, and isoprene. Estimation of the FRPO level of biopolymers of membranes is carried out on the value of an indicator of the activity of cytochrome oxidase.

The study of the role of ROS in anti-infective protection of animals, oxidative explosion processes, mechanisms of aging and apoptosis has opened up prospects for the search for analogs in the plant world. This area is the subject of research A.A. Averyanov, according to whose work in a normally functioning plant cell there is a balance between activation and deactivation of oxygen, so the number of its active forms remains at a safe level (Aver'yanov, 1991). However, structural and functional disorders of plant tissues, as a rule, lead to the activation of oxygen. The normal balance between the formation and disposal of ROS can be disturbed in a variety of pathological conditions of plants (Dmytriyev & Kravchuk, 2005). Since the activation of oxygen is one of the first responses of the plant cell, ROS may play an important role in inhibiting the development of pathogens. Thus, when carrying out a hypersensitivity reaction, phenols are released from vacuoles and their enzymatic oxidation. And since this process is accompanied by the generation of activated oxygen in toxic concentrations, it is possible that it is the cause of death of both infected host cells and invading pathogens (D'yakov et al., 2002). In I.A.Tarchevsky's laboratory, it is established that pathogenic microorganisms induce in a plant cell a cascade of protective reactions long before stability or susceptibility is shown in full. This is achieved by the functioning of signaling systems, the main of which are in the plant body: calcium, lipoxygenase, NADPH-oxidase (superoxide synthase), NO-synthase, adenylate cyclase, phosphoinositol, and MAP-kinase (Tarchevskiy, 2002). ROSs play a key role in the functioning of the first four of them. This information, and the ever-increasing number of publications on the involvement of ROS in other important physiological processes (metabolism and synthesis of phytohormones, regulation of photosynthetic reactions and mitochondrial oxidation, apoptosis, aging), require a more detailed, qualitatively new approach to studying the biological role of ROS and AO plant life (Foyer & Noctor, 2005; Pacheco et al., 2018).

2. Research methodology

Quantitative determination of PAS status was performed on onion tissue samples taken from the following varieties: "Globus" (high-resistant variety - 9th class of disease resistance), "Rainbow" (medium-resistant variety - 7th class of disease resistance) and "Donetsk Golden" (low-resistant variety - 5th class of resistance to diseases). For biochemical analysis, tissues from the top of the leaf, the middle of the leaf, the scales of the onion-turnip, stem, flower, roots, and seeds were used. The tops of the onion leaf were cut at a distance of up to 0.5 cm from the point of growth, the middle of the leaf was selected geometrically, the analysis of onion-turnip scales was carried out on its cross-section, onion roots were cut at a distance of 0.1 cm from the tillering node. The studied parts of the plants were in the growth stage. The stem was selected at the stage of the flowering of the plant. Tissues of cross-section of the middle of the stem were used for analysis. Onion flowers were selected at the stage of flowering, flowers without peduncles were used for analysis. Onion seeds were analyzed at dormant sites. In parallel, the seeds were examined during the initiation of germination, which was carried out by the previous 12-hour soaking in clean stagnant water. Each experimental group included 10 samples, so the experiment analyzed 2880 samples.

Evaluation of the level and sources of ROS *generation* was performed by spectrophotometric NBT test. For analysis, 0.1 g of tissue was homogenized with glass sand in 0.9 cm^3 of phosphate buffer (pH = 7.4, composition per 1 dm^3 of a solution – 5.37 g of $KH_2PO_4 \cdot 12\ H_2O$, 8.5 g of NaCl, 1.5 g NaOH). 0.05 cm^3 of homogenate was taken in 3 tubes: 0.05 cm^3 of buffer solution was added to I (to determine the total main unstimulated activity); in AI was added 0.05 cm^3 of NaF solution (w = 0.01%, stimulation of Ca^{2+} messenger system); in III – 0.05 cm^3 of yeast solution (w = 1%, stimulation of oxidative explosion), in IV – 0.05 cm^3 of NADH solution (w = 3%, stimulation of mitochondrial generation), in V – 0.05 cm^3 of NADPH solution (w = 3%, stimulation of microsomal generation). The samples were shaken for 2 min, added to each of 0.05 cm^3 NBT, stirred, incubated in a thermostat at 24^0C. After 30 minutes (for test tubes I– III) and after 10 minutes. (for IV–V tubes), 2 cm^3 of solvent (dimethyl sulfoxide-chloroform in a volume ratio of 2:1) was added, shaken for 1 minute, and centrifuged for 5 minutes at 1500 rpm. From the obtained centrifugal, a colored supernatant was taken and photometered against the appropriate control at 540 nm on a microphotoelectrocolorimeter in a 1 cm^3 cuvette 0.5 cm thick.

To prepare the reagent control, the following solutions were poured into three tubes: 0.05 cm^3 of a buffer, 0.05 cm^3 of water, and 0.05 cm^3 of NBT. Added: in I – 0.05 cm^3 of water; in II – 0.05 cm^3 of NaF solution (w = 0.01%); in II – 0.05 cm^3 of yeast solution (w = 1%), in IV– 0.05 cm^3 of NADH solution (w = 3%), in V – 0.05 cm^3 of NADPH solution (w = 3%) were incubated min, for test tubes I–III, 10 min. for test tubes IV–V) in a thermostat at 24^{0}C and eluted color. To build a standard calibration graph in test tubes typed 0.01, 0.02, 0.05, 0.07, 0.1, 0.2 cm^3 NBT (w = 0.2%), 0.1 cm^3 KOH (C (KOH) = 1 mol /dm^3) and 0.1 cm^3 of AK solution (18 mg /10 cm^3), stirred and incubated for 10 min at 24 ^{0}C. The color of 2 cm^3 of the solvent was eluted, the extinction (E) of each sample was determined and a calibration graph was plotted. According to the schedule, superoxide production was found in nmol per sample (n nmol ●O_2^-) and translated into nmol per g of tissue per second of incubation.

Assessment of the level of FRPO was carried out by the concentration of TBA-active products (TBA_{ap}). Analysis of the level of TBA_{ap} was carried out in the following sequence: 0.5 g of tissue was homogenized in 4.5 cm^3 of buffer solution (pH = 7.4, preparation: 1.9 g of tris-(oxy)-methylaminomethane was placed in a volumetric flask per 1 l with 0,5 l of distilled water, added 50 cm^3 of a solution of HCl (C (HCl) = 0.1 mol/dm^3), 1.4 g of ascorbic acid, 32 mg of $FeSO_4{\cdot}7H_2O$ in the specified order, after dissolving the previous component, added water below the mark; the finished solution was left for a day to adjust the pH, as evidenced by the change in its color from blue-violet to yellow). To determine the basic level of TBA_{ap} (TBA_{ap0}) to 2 cm^3 of the selected homogenate was immediately added a solution of trichloroacetic acid (w = 30%) and centrifuged for 30 minutes at 3000 rpm. To 2 cm^3 of centrifugate was added 3 cm^3 of thiobarbituric acid solution (w = 0.338%, extempore preparation, incubation in a water bath at 80^0 C until the reagent dissolved, and another 50 min in a boiling water bath) followed by photometry of the formed trimethine complex at 540 nm against the control, which did not contain homogenate (control composition for reagents: 1.2 cm^3 of buffer solution, 0.7 cm^3 of trichloroacetic acid, 0.1 cm^3 of water and 3 cm^3 of TBA reagent). To initiate an increase in the level of TBA_{ap} ($TBA_{ap1,5}$), the sample was pre-incubated for 90 minutes (1.5 hours, therefore $MDA_{1,5}$) in prooxidant iron-ascorbate buffer, shaking every 20 minutes. Further analysis was performed similarly to the determination of TBA_{ap0}. The calculations were carried out according to the formula:

$$C = E \cdot 240.4$$

where C is the concentration of TBA_{ap} in μmol/kg;

E – extinction;

240.4 – coefficient taking into account molar extinction and dilution.

The magnitude of the increase in the level of TBA_{ap}, which is inversely proportional to the antioxidant supply of tissue, was calculated according to the formula:

$$\Delta\ TBA_{ap} = |\ TBA_{ap1,5} - TBA_{ap0}\ |\ /\ TBA_{ap0} \cdot 100\%$$

where $\Delta\ TBA_{ap}$ – increase in the level of TBA_{ap}, expressed as a percentage;

TBA_{ap0}, $TBA_{ap1,5}$ – basic and stimulated levels of TBA_{ap} in μmol/kg, respectively.

The level of antioxidant protection was assessed by the activity of enzymatic and the concentration of non-enzymatic antioxidants. To determine the activity of SOD 0.5 g of tissue was homogenized in 0.5 cm^3 of water after 10 minutes added 2 cm^3 of pigment precipitant (ethanol chloroform in a volume ratio of 5: 3), stirred with a glass rod and kept at -4^0 C day. Then stirred and centrifuged at 3000 rpm 15 min. Control (average for several determinations before, in the middle and at the end of a series of experimental samples): in a cuvette with an optical path length of 1 cm scored successively 4.4 cm^3 of carbonate buffer solution (C = 0.2 mol/dm^3; pH = 10.2, for the preparation of which in 1 dm^3 of distilled water was dissolved 4.5 g of anhydrous sodium bicarbonate and 9.5 g of decahydrate sodium carbonate), 0.1 cm^3 of distilled water (to establish the optical zero) and added 0.5 cm^3 of adrenaline solution (C = 0.01 mol/dm^3) in citric acid (C = 0.01 mol /dm^3). Turn on the stopwatch, stir with a glass rod, and note the extinction every minute until it stops increasing. Instead of water, 0.1 cm^3 of the centrifuge was introduced into the experimental sample, followed by similar procedures. Temperature range 23-27^{0}C.

The calculation of SOD activity was carried out according to the formula:

$$T = (E_1 - E_2) \cdot 100 / E_1$$

T is the percentage of inhibition of oxidation of ●O_2^- adrenaline to adrenochrome (%);

E_1 – average extinction control for 1 min (E/t);

E_2 – average extinction of the experiment for 1 min;

100 – the maximum percentage (%) of inhibition.

SOD activity was expressed in conventional units (OD):

$$OD = T / (100 - t)$$

where 1 OD corresponds to the inhibition of the reaction rate by 50%.

To determine the activity of catalase: 0.1 g of tissue was homogenized in 20 cm^3 of distilled water. 7 cm^3 of distilled water was taken from the flasks, then 1 cm^3 of homogenate was added to the experimental sample, and 1 cm^3 of boiled homogenate was added to the control sample, in which the enzyme was thermally destroyed. To both samples was added 2 cm^3 of hydrogen peroxide (w = 1%), stirred and left at room temperature for 30 minutes, shaking every 10 minutes. Then 3 cm^3 of sulfuric acid solution (w = 10%) was added to both samples and titrated with potassium permanganate solution ($C(1/5KMnO_4) = 0.1$ mol/dm^3) to a pale pink color that does not disappear within 30 seconds. The calculation of catalase activity was carried out by the formula:

$$A = (V_{control} - V_{experimental}) \cdot 1.7$$

A – catalase number;

$V_{control}$ – volume of solution $KMnO_4$ ($C(1/5\ KMnO_4) = 0{,}1$ mol /dm^3), spent on titration of the control sample, cm^3;

$V_{experimental}$ – volume of solution $KMnO_4$ ($C(1/5\ KMnO_4) = 0{,}1$ mol /dm^3), spent on titration of the experimental sample, cm^3;

1.7 – amount of H_2O_2 (mg), which corresponds to 1 cm^3 of $KMnO_4$ solution ($C(KMnO_4) = 0.002$ mol/dm^3).

Used the international unit of activity (μmol of substrate per unit time per unit mass of protein), which was calculated by the formula:

$$A = (V_{control} - V_{experimental}) \cdot 1.7/t \cdot M\ (H_2O_2)$$

t – incubation time of the sample (30 s);

M (H_2O_2) - molar mass of H_2O_2 (34 g/mol).

To determine the activity of GSH-peroxidase, 0.1 cm^3 of tissue was homogenized in 1.9 cm^3 of water. In the experimental and control tubes were collected 0.1 cm^3 of sodium azide solution ($C(Na_3N) = 0.01$ mol/dm^3), 0.25 cm^3 of a solution of reduced glutathione ($C(GSH) = 0.004$ mol/dm^3; on phosphate buffer, pH = 7.05), 0.05 cm^3 of homogenate and 1.8 cm^3 of water. Incubate for 5 minutes at 37 ^0C. 0.25 cm^3 of H_2O_2 solution was added to the experimental sample (0.04 cm^3 of H_2O_2 (w = 33%) was dissolved in 100 cm^3 of water), and the same amount of water was added to the control sample. Incubate for 10 minutes at 37^0 C, add 0.75 cm^3 of trichloroacetic acid (w = 30%), stirred, centrifuged at 3500 rpm for 15 minutes. The reduced

glutathione was determined in the supernatant photometrically at a wavelength of 412 nm (cuvette per 1 cm). The calculation was carried out according to the formula:

$$A = (C_{control} - C_{experimental}) \cdot K$$

A – activity of glutathione peroxidase (OD, μmol/cm^3·min or μmol/g·min);

$C_{control}$ and $C_{experimental}$ – concentrations of reduced glutathione before and after incubation (in control and experimental samples);

K is the coefficient that takes into account the dilution and incubation time.

Determination of GSH concentration was performed in the following order: 0.1 g of tissue was homogenized with 2.4 cm^3 of trichloroacetic acid solution. After 10 minutes samples were centrifuged for 15 min at 3000 rpm, 0.2 cm^3 of the centrifuge was taken, 0.05 cm^3 of NaOH solution (w = 20%) and 5 cm^3 of Tris-buffer were added, for preparation at 1 dm^3 used 6.06 g of Tris-oxymethylaminomethane, 14.85 g of EDTA for binding of divalent cations and 275 ml of HCl, C (HCl) = 0.1 mol/dm^3). The pH of the sample was checked and, if necessary, the pH was adjusted to 8.0-8.1 with weak solutions of HCl or NaOH (because at pH ‹8 the reaction is almost non-existent, and at pH›8.1 DTNBK hydrolyzes to thionitrophenyl anion, which overestimates the analysis results). Then added 0.1 cm^3 of Elman's reagent (99 mg of DTNBK in 25 cm^3 of ethanol). Stirred and kept for 20 minutes in the dark. Photometered at 412 nm in a cuvette at 1 cm against control for reagents that did not contain homogenate. The calculation of the analysis results was performed according to the standard calibration schedule.

Determination of the concentration of AA was carried out by direct titrimetry. To do this, in a porcelain mortar 1 g of the test material was thoroughly ground with quartz sand. To the obtained homogenate was added 9 cm^3 of HCl solution (w = 2%), defended for 10 minutes, and filtered. For quantification, 3 cm^3 of the filtrate was taken (test sample), added to the flasks, and titrated with a solution of 2.6-dichlorophenolindophenol (C (1/2 2.6 – DFIF) = 0.001 mol / dm^3) until a pink color appeared which persisted for 30 s. To control the reagents, 3 cm^3 of the filtrate was boiled with 3 drops of 3% H_2O_2, followed by titration. The calculation of the content of AA was carried out according to the formula:

$$C = Q \cdot (A_{exp} - A_{contr}) \cdot V_0 / (V_1 \cdot a)$$

C – AA content, mmol/kg;

Q is the amount of ascorbic acid, which corresponds to 1 cm^3 of a solution of 2.6-dichlorophenolindophenol (C (1/2 2.6-DFIF) = 0.001 mol/dm^3) (0.088 mg);

V_0 – total amount of extract, cm3;

V_1 – volume of extract taken for titration, cm3;

a – the amount of test substance, g;

A_{contr}, A_{exp} - volume of solution of 2,6-dichlorophenolindophenol spent on titration of control and experimental sample, cm^3 (C (1/2 2.6 DFIF) = 0.001 mol/dm^3).

Evaluation of the effects of PAS changes was performed by changes in cytochrome oxidase activity.

Procedure: 0.5 g of tissue on ice was thoroughly homogenized with 4.5 cm^3 of phosphate buffer solution (pH 7.6). 1 cm^3 of homogenate was collected in the test tube, and 1 cm^3 of diluted buffer solution in the control tube. Extempore quickly prepared the reaction mixture by merging 0.25 cm^3 of α-naphthol (w = 0.1%; 50 mg of α-naphthol was dissolved in 50 cm^3 of ethanol (w = 22%)), 0.35 cm^3 of a solution of N,N-dimethyl- para-phenylenediamine hydrochloride (w = 0.1%; 5 mg of reagent was dissolved in 5 cm^3 of distilled water), 0.25 cm^3 of dilute buffer solution, 0.15 cm^3 of cytochrome c solution (w = 0,02%). Preincubated the mixture for 2 minutes at 37^0C.

Added to the control and test sample 1 cm^3 of the reaction mixture, stirred, incubated under the same conditions for 5 minutes. 10 cm^3 of an ethereal alcohol mixture (diethyl ether and ethanol in a volume ratio of 9:1) were added, shaken, and placed in the cold (4^0C, 30 min), shaking periodically.

Adjust the volume of the essential alcohol extract to 10 cm^3 and photometer at 540 nm against the control. The calculations were carried out according to the formula:

$$A = E_{exp} \cdot 10 / E_{st} \cdot 5 = 2\ E_{exp} / E_{st}\ ,$$

A – cytochrome oxidase activity in indophenolic units per gram of tissue per minute;

E_{exp} – extinction of the test sample;

E_{st} – extinction of the standard, calculated from the calibration graph at a dose of 100 mg / cm3 of α-naphthol (1 cm^3 in the mixture; it is possible to equate to a conventional unit proportional to the amount of indophenol);

10 – breeding; 5 – incubation time.

Standard solutions for plotting the calibration graph (α-naphthol – 100 μg / cm^3, n-phenylenediamine – 150 mg / cm^3 and potassium dichromate – 210 mg / cm^3) were taken in

the first series of 0.1 cm^3, in the second – 0.2 cm^3 and so on to portions of 1.2 cm^3; incubated for 5 min, extracted with 10 cm^3 of the ether-alcohol mixture and photometered.

The results obtained by us have undergone mathematical and statistical processing.

3. Results and discussion

Analysis of the distribution of PAS components in different organs of onion. As a result of quantitative analysis of the prooxidant activity of onion tissues by spectrophotometric NBT test revealed an increase in the basic production of superoxide in photosynthetic (leaf, stem) and generative (flower, seed) cuttings. A possible explanation for the obtained distribution is that the most reliable ROS generator of a plant cell is chloroplasts. Photosynthetic products $\bullet O_2^-$ is carried out by ETC thylakoids of photosystem I, where electrons are intercepted from 4Fe-4S clusters and from reduced ferredoxin. In photosystem II $\bullet O_2^-$ is formed at Q_A and Q_B sites. In addition, the source of $\bullet O_2^-$ is O_2^1, which is formed by chlorophyll (Polesskaja, 2007). The fact of the predominance of the basic level of generation of $\bullet O_2^-$ by the tissues of the top of the onion leaf of all three experimental varieties in comparison with the tissues of the middle of the leaf (Fig. 1) is noteworthy.

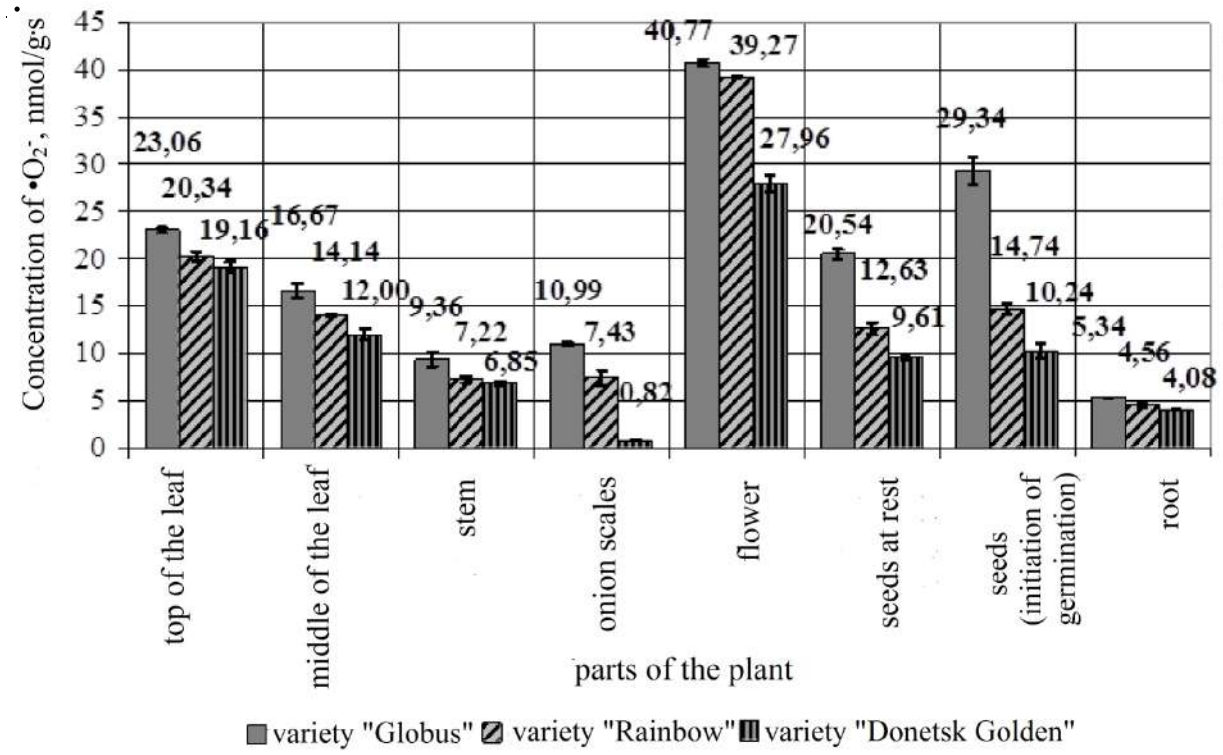

Fig. 1. Comparison of the concentration of superoxide in the tissues of onions (basic level of generation)

A possible explanation for this phenomenon is that the leaves of onions grow at the base, so the ROS of the cells of the top of the coot accompanies the aging process. Thus, ROS are involved in the synthesis of enzymes that destroy chlorophyll and cell membranes, activate lipoxygenase, which induces lipid peroxidation of thylakoid membranes. There is also evidence that high levels of ROS are important for blocking cell division. Thus, the tissues of the apex of the onion leaf are equipped with a group of cells at rest, with a minimum frequency of division. The content of AA in these cells is also low because all the ascorbate is oxidized by ascorbate oxidase, the activity of which, on the contrary, is quite high. Low levels of AA, GSH-peroxidase, and cytochrome oxidase activity in this area lead to an increase in the level of ROS, which causes a low frequency of cell division. The role of ROS cells of the apex of the leaf in the chain of the signaling cascade of the growth reaction through the activation of Ca^{2+} channels and, as a consequence, the determination of the direction of growth of the organ is possible. The opposite is the explanation of the reduced generation of superoxide by the cells of the middle and base of the leaf, providing growth of the organ. It is known that active cell division processes occur in the tissues of the meristem of the base of the onion leaf, while the cells of the middle leaf, in addition to photosynthesis, provide organ growth by stretching, which is carried out by ROS involved in processes aimed at weakening the links between cell wall polymers. Thus, OH● cuts the polymers of cell walls, promoting their stretching during growth. The formation of OH● in the apoplast is strictly controlled by enzyme systems, in particular, peroxidases, which are able in the presence of added NADH to induce reactions leading to the formation of ROS, with: oxidation of phenolic compounds by peroxide forms NAD-radical that spontaneously reduces O_2 to $●O_2^-$, which in turn quickly turns into H_2O_2 either with the participation of SOD or due to the oxidation of another NADH (Polesskaja, 2007).

It should be noted that due to the small pool of NADH and NADPH in the apoplast, the concentration of OH formed is insignificant (up to 1 mM), which significantly reduces its contribution to growth processes by stretching. Closing cells of the stomata of the leaves contain chloroplasts, so they are characterized by the enhanced generation of ROS. ROSs are involved in conducting the signal that occurs when ABA acts on the closing cells of the stomata. Thus, under the action of ABA closure of the stomata is preceded by the accumulation in the closing cells of H_2O_2 formed in the apoplast. It is known that in the

closing cells of the stomata the expression of genes encoding the synthesis of NADPH oxidase is higher compared to other leaf cells, and is able to increase under the action of ABA. Formed with the participation of NADPH-oxidase $\bullet O_2^-$ under the action of SOD turns into H_2O_2, which is included in a number of signal reactions, the end result of which is the closure of the stomata. Thus, according to a number of scientists (Kolupaev, 2007; Maksimov, 2006; Polesskaja, 2007), H_2O_2 induces an increase in the cytosolic concentration of Ca^{2+} and hence the activation of potential-dependent Ca^{2+} channels in the plasmalemma of closing cells. ROS regeneration occurs in the apoplast with the participation of NADPH oxidase and SOD. The relationship between the level of ROS and the state of Ca^{2+} channels is carried out through signaling pathways: Ca^{2+} channels can be regulated through phosphorylation, and ROS triggers individual signaling reactions that lead to the activation of the corresponding protein kinases or protein phosphatases. In addition to H_2O_2, $\bullet O_2^-$ and $OH\bullet$ are also included in the signaling processes as ROS.

The study found that the onion stem also has a slightly enhanced generation of $\bullet O_2^-$, but the lowest of all photosynthetic organs. A possible explanation for this is the ability of stem cells to photoproduct, the presence of the respiratory system, but its main transient function.

It is established that the highest generation of both basic and stimulated levels of superoxide is carried out by flower cells of all experimental varieties of onions (Fig. 2, Fig. 3).

This distribution may be explained by the participation of ROS in the reception of specific areas of the pollen grain membrane by the pistil receptacle during pollination, pathogen recognition with the subsequent triggering of signaling processes to include protective reactions, especially activated at the time of pollination and fertilization.

An increase in the level of ROS is also observed during pollen germination. It is a known fact that the addition of AO, in particular, ascorbic acid inhibits the process of pollen germination. Onion pistil also performs photosynthesis, equipped with stomata, contains polyploid cells, participates in the protective reaction of hypersensitivity, hormonal regulation of growth processes in the cells of the germ. According to one version of the formation of parcarp gynoecium, onion occurs by apoptotic destruction of the inner shells of carpels with the formation of a cavity. This process is initiated by mitochondrial and microsomal generation $\bullet O_2^-$.

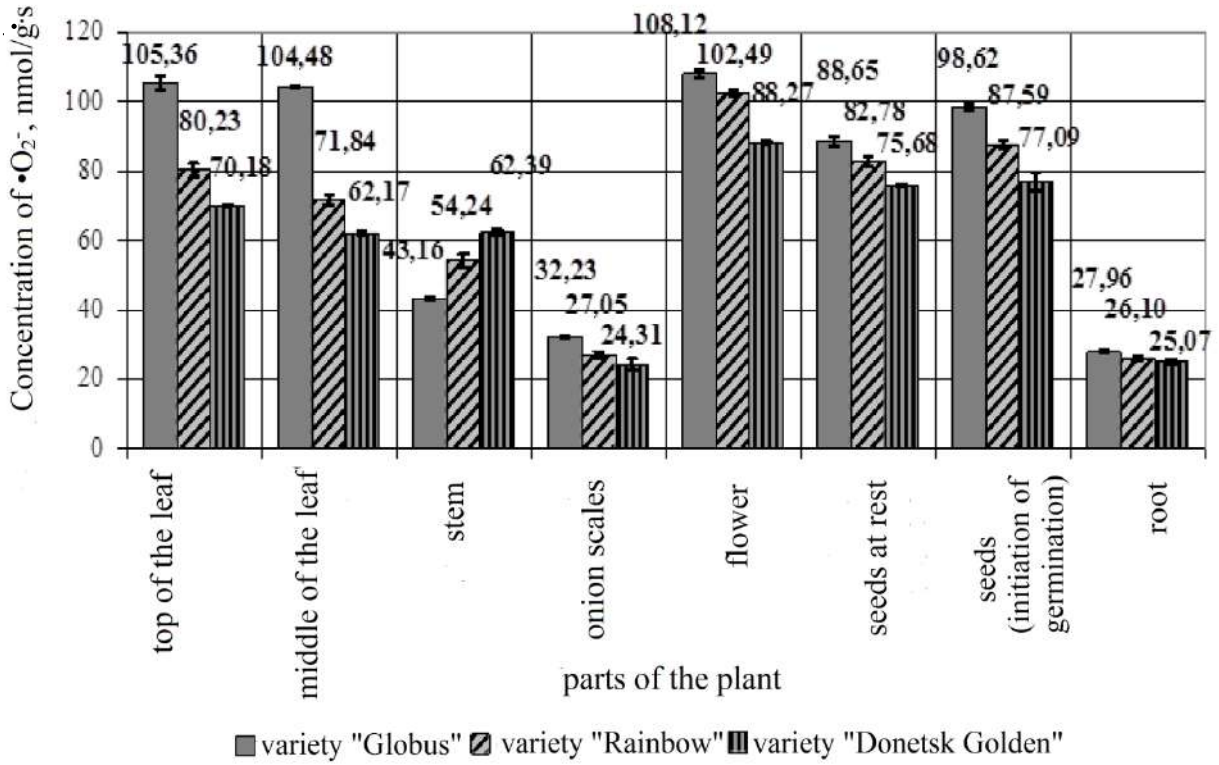

Fig. 2. Comparison of superoxide concentration in onion tissues (NADP·H stimulation).

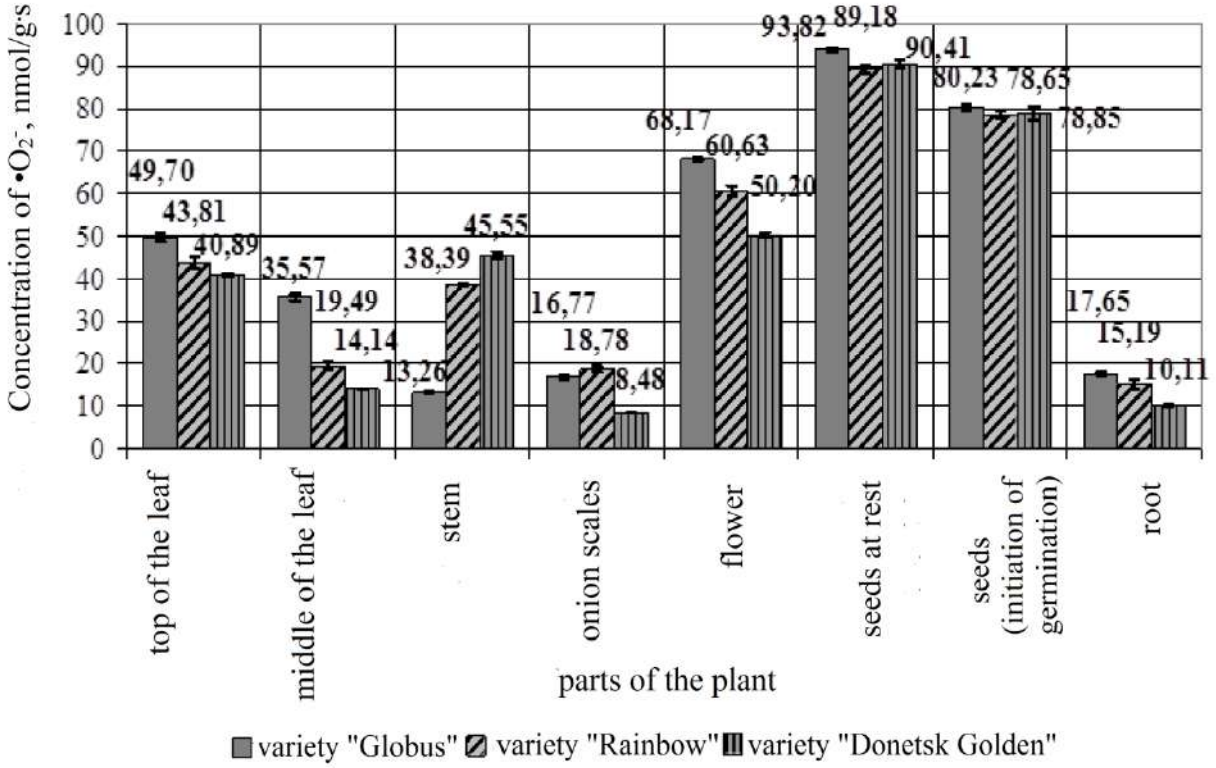

Fig. 3. Comparison of the concentration of superoxide in onion tissues (stimulation of NAD·H).

It was found that onion scales have a slightly reduced level of generation $\bullet O_2^-$, which may be due to their inability to photosynthesis and perform the main storage function. However, the tissues of the scales are capable of the formation of the protective flavonoid pigment quercetin, which is a highly toxic chemical barrier to parasite damage and accumulates in the dead cells of the outer covering scales.

It was experimentally found that the root of the onion has one of the lowest basic levels of superoxide generation, but is characterized by a significant increase in all types of stimulation. A possible explanation for this phenomenon is the increase in the level of ROS during the growth of root hairs, reception when interacting with the soil microflora, participation in the gravitropic reaction, and polar growth. Thus, upon receipt of gravistimulus, the pressure of amyloplasts on the membrane activates Ca^{2+} channels, indirectly leads to the redistribution of auxin transporters in cell membranes, followed by its concentration on the underside of the root. With the orientation of the plant horizontally, there is a rapid increase in the level of ROS in the apical part of the root, which includes the root cover, meristem, and part of the stretching zone (Tsebrzhinskiy, 1992).

ROSs also control the growth of root hairs, which is associated with the activation of Ca^{2+} channels when Ca^{2+} enters the apical part of the cell and its active pumping from the opposite side with the participation of Ca^{2+}-ATPase. Thus, with increasing cytosolic concentration of Ca^{2+}, there is an increase in the level of ROS in the apex as a result of the activation of NADPH oxidase. ROS in the apex of the rhizoderm cells activates Ca^{2+}channels, resulting in a growing cell, a gradient of Ca^{2+} ions, which provides polar growth of root hairs. Root meristems are also equipped with a group of dormant cells with a minimum division rate maintained by a high concentration of ROS, resulting in a decrease in the level of AOS of root cells, including catalase, SOD, AA, GSH, and GSH peroxidase.

The analysis revealed the enhanced generation of superoxide in onion seeds of all studied varieties, which may be explained by the fact that the seeds belong to the generative organ formed directly from the pistil of the flower. It should be noted that the seed cells are at rest, so the level of $\bullet O_2^-$ in them is lower compared to the flower.

Attention is drawn to the experimentally established fact of the growth of $\bullet O_2^-$ generation at the initiation of seed germination, which confirms the participation of ROS in the start of germination processes. It should be noted that the detected increase in the level

of $\bullet O_2^-$ is observed both when stimulated with NAD●H and under the action of NADP●H, NaF, and yeast in all experimental varieties of onions. The results of the analysis show that the largest increase in $\bullet O_2^-$ is observed when stimulated with a solution of NAD●H and NADP●H, which means that the largest contribution to increasing the concentration of $\bullet O_2^-$ when starting seed germination processes are mitochondria and microsomes, and for onion seed tissues "Globus" is dominated by microsomal generation, and for "Donetsk Golden" – mitochondrial. When comparing the increase in the level of $\bullet O_2^-$ under the action of NaF and yeast, it was found that stimulation by yeast enhances the generation of $\bullet O_2^-$ to a greater extent than the Ca^{2+}-messenger system.

Analyzing the results of the study of the level of AOP in the tissues of different organs of onions revealed the similarity of a number of decreases in the activity of SOD to a number of decreases in the level of generation $\bullet O_2^-$ (Fig. 4). A possible explanation for the established distribution is that the first powerful line of protection against the harmful effects of $\bullet O_2^-$ is SOD, which utilizes $\bullet O_2^-$ by decomposing it into H_2O_2 and triplet O_2. It was also found that the activity of SOD in the tissues of the onion flower variety "Globus" and "Rainbow" ranks third after the top and middle of the leaf (II for the tissues of the onion "Donetsk Golden"), while in a number of decreasing generation $\bullet O_2^-$ flower index is in the first place.

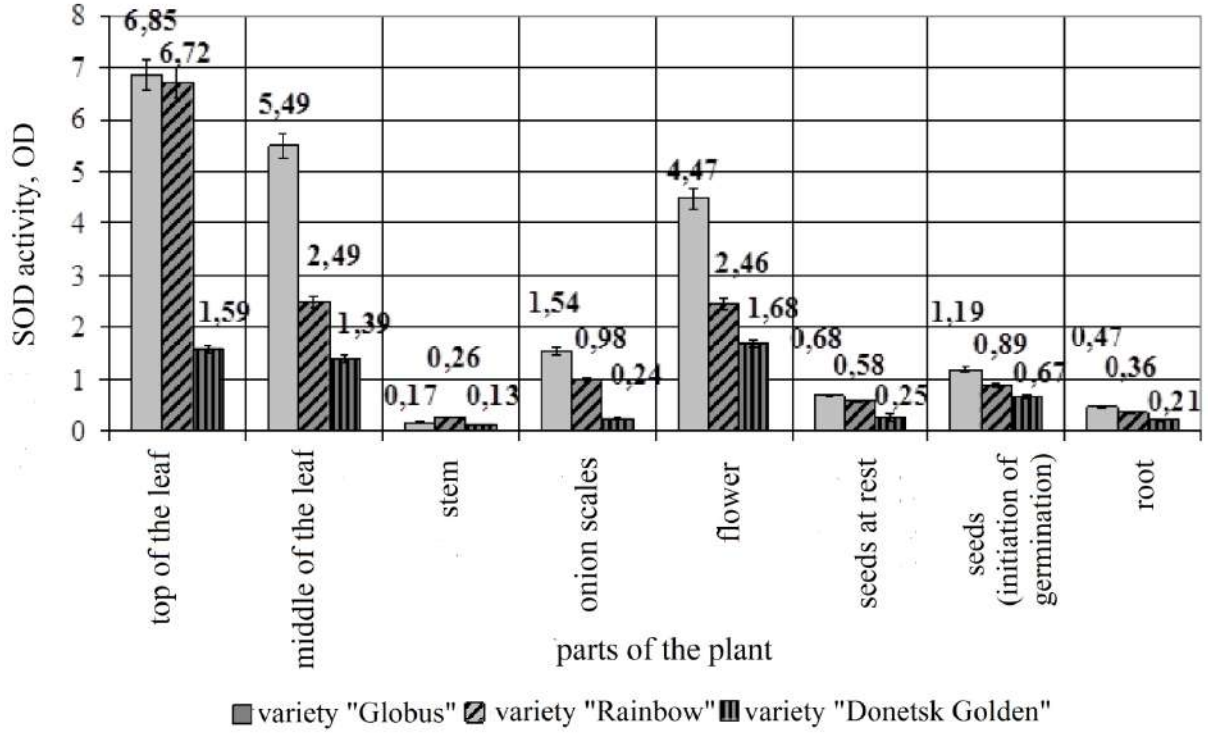

Fig. 4. Comparison of SOD activity in onion tissues

A similar discrepancy is observed in relation to seed tissues when activating germination, which takes the second place after the flower in terms of concentration $\bullet O_2^-$ and V place in a number of SOD, as well as the opposite correspondence of the arrow and root. A possible explanation for this phenomenon is the presence of another competing method of recycling $\bullet O_2^-$, which is carried out through the operation of the Hallivel-Asada cycle. The general pattern of both ways of utilization $\bullet O_2^-$ is the formation of H_2O_2 as the final product. It is also known that the utilization of H_2O_2 is possible with the participation of catalase, AA, GSH, and GSH peroxidase. Thus, as a result of the research, it was found that the top activity of SOD has the top of the onion leaf of the variety "Globus", "Veselka" and "Donetska Zolotista" which naturally has the highest activity of catalase (Fig. 5). Quite a high level of H_2O_2, formed as a result of utilization $\bullet O_2^-$ in the cells of the flower and the middle of the leaf neutralizes AA, the concentration of which is highest in the cells of these tissues.

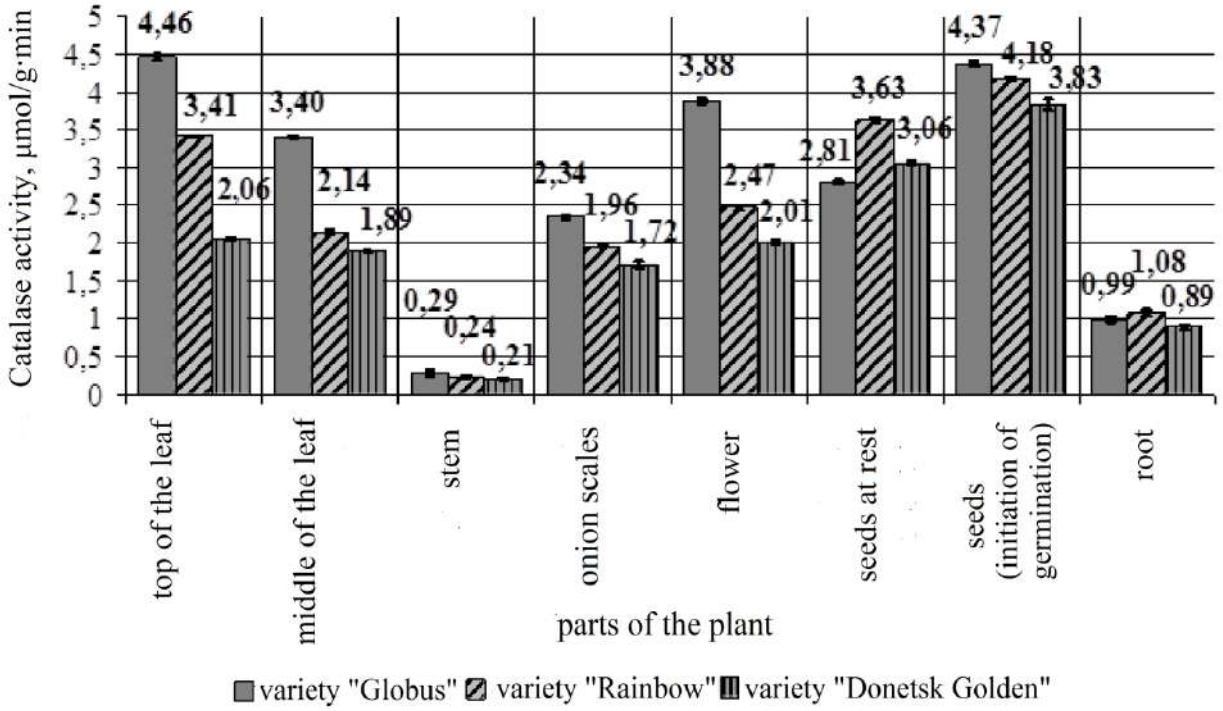

Fig. 5. Comparison of catalase activity in onion tissues

The significant similarity was also found in the series of organotropic decreases in catalase and GSH-peroxidase activity. According to the literature, a characteristic feature of plant catalase is its low specificity to the substrate and the increasing role of peroxidases in the utilization of H_2O_2. The compensatory role of GSH-peroxidase is probably explained by

the fact that the onion globe has the lowest catalase activity but the highest GSH-peroxidase activity, and the leaf apex tissues – on the contrary – are characterized by the highest catalase activity and one of the lowest GSH activity. It was found that changes in the activities of catalase and GSH-peroxidase of other organs show almost complete compliance.

As a result of the analysis of low molecular weight AO, it was found that the highest value of the concentration of AA is inherent in flower cells and all photosynthetic organs of onions of the three experimental varieties (Fig. 6). A possible explanation for this phenomenon is, experimentally confirmed by us, the highest level of generation $\bullet O_2$. In addition, AA is a major non-enzymatic antioxidant, a precursor to many plant metabolism compounds and a cofactor of enzymes. Thus, AA affects the synthesis of gibberellins, growth, stretching, cell morphogenesis. AA is a potential donor of hydrogen atoms and electrons used to reduce free radicals and H_2O_2, tocopherol, oxidized forms of many AOS enzymes such as ascorbate peroxidase, polyphenol oxidase, cytochrome oxidase, peroxidase. The analysis revealed the highest content of AA in those vegetative organs that are capable of photosynthesis (leaf, arrow), which naturally confirms the literature, which states that the concentration of AA in chloroplasts may exceed the concentration of chlorophyll, promoting its biosynthesis and recovery.

The lowest concentration of AA in seed cells, which is at rest, and the roots of all three experimental varieties of onions. A possible explanation for this distribution is that the synthesis of AA begins with UDF-glucose and is significantly enhanced with the appearance of the first photosynthetic leaves. An increase in the concentration of AA during the initiation of the germination process was recorded, which is probably associated with increased generation of ROS and the need for AOS by direct utilization of ROS and restoration of oxidized forms of antioxidants. A small percentage increase in the concentration of AA in the seeds during germination, compared with other AO, due to heterotrophic nutrition of the embryo using carbohydrate reserves before the first photosynthetic leaves and the inability to synthesize large amounts of AA from UDF-glucose. The participation of AA in the maintenance of the ascorbate-glutathione cycle is also known.

The highest concentration of GSH was found in the cells of the generative organs of onions of all experimental varieties, which may be explained by the participation of GSH in almost all stages of metabolism and its importance as a key AO of plant cells.

A characteristic feature of the transition of seeds to germination is a decrease in the level of GSH, which is inherent in the tissues of all experimental varieties of onions. This may be due to the use of GSH to restore oxidized forms of AO, which are actively used during germination to protect against elevated levels of AO in cells. For the same reason, the established concentration of GSH decreases during the transition from the tissues of the apex of the leaf to the photosynthetically active middle leaf of the onion varieties "Globus", "Rainbow" and "Donetsk Golden".

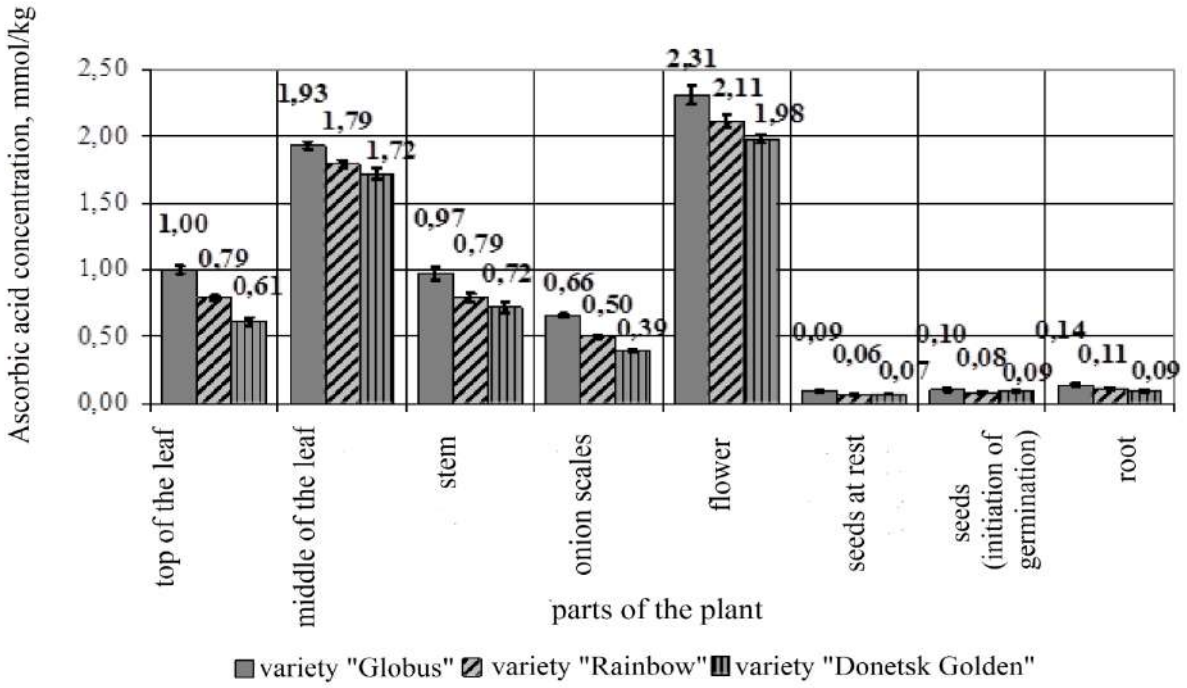

Fig. 6. Comparison of the concentration of ascorbic acid in the tissues of onions.

The lowest level of GSH is recorded in the roots of Globus and Veselka onions, which may be due to the constant use of GSH as a key participant in the detoxification of plant-absorbed xenobiotics and excretory metabolic products. The difference between the concentration of GSH levels in the tissues of the roots and arrows of the onion variety "Donetsk Golden" is insignificant, although the numerical value of the indicator is minimal, which does not contradict the general pattern and may be a variety-specific feature.

Experimentally established the highest level of generation $\bullet O_2^-$ in the cells of the onion flower of all three experimental varieties naturally causes the highest concentration of TBA_{ap}, both background and stimulated level. Similarly, a fairly high concentration of TBA_{ap}

in the seeds, which was initiated by germination and a significant increase in the level of TBA_{ap0} and $TBA_{ap1.5}$ during the transition of seeds from dormancy to germination (Fig. 7).

The sequence of changes in the indicator TBA_{ap0} and $TBA_{ap1,5}$ photosynthetic organs of onions "Globus" can be displayed as the following series: stem › middle of the leaf › top of the leaf, which may be due to the experimentally established most powerful enhancement of the activity cells of the middle of the leaf, which shifts the PAS towards the formation of prooxidants and the functional purpose of the stem with the proven minimum level of AOS (catalase, SOD, GSH) in comparison with other photosynthetic organs. It should be noted that for the fabrics of onion varieties "Rainbow" and "Donetsk Golden" the top of the leaf has a higher level of TBA_{ap0} compared to the middle of the leaf, and the tissues of the middle of the leaf were characterized by increased concentration of $TBA_{ap1.5}$ compared to the top.

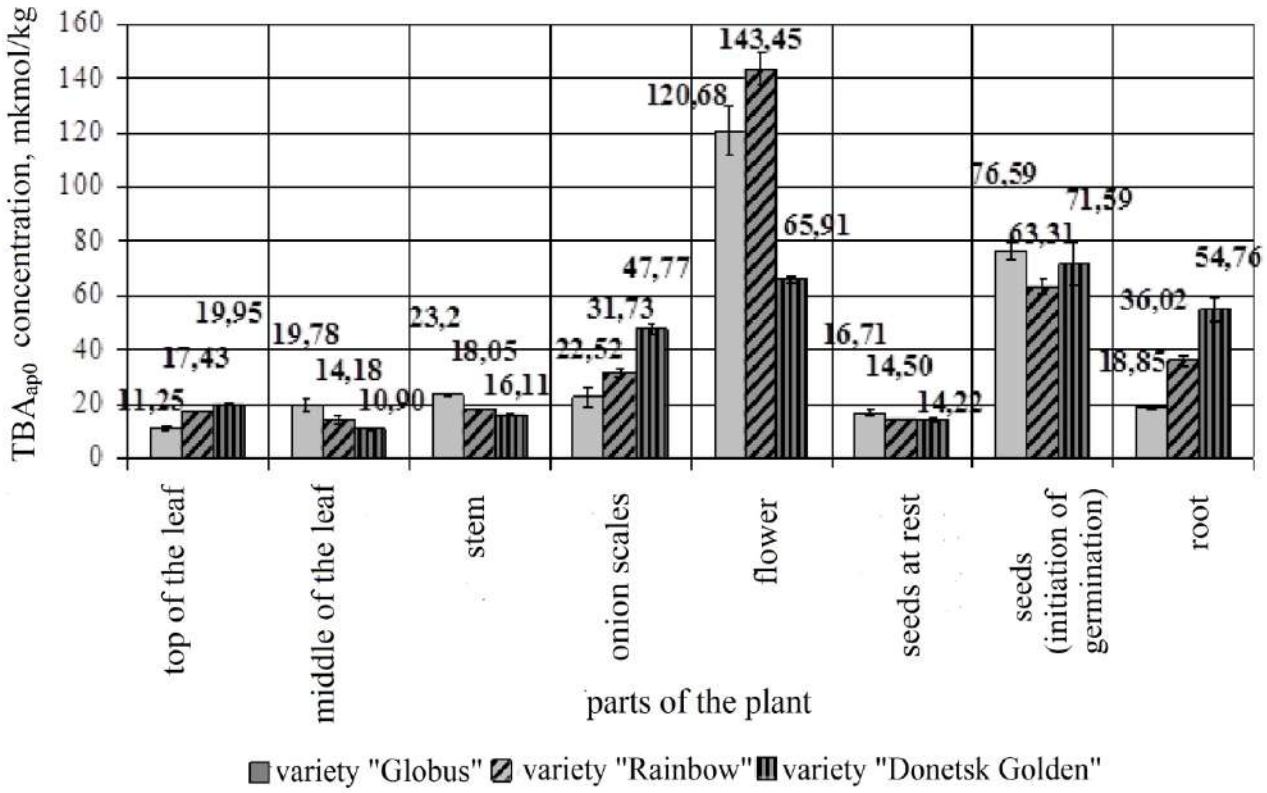

Fig. 7. Comparison of the TBA_{ap0} concentration of in the tissues of different onions

Since the highest level of $\bullet O_2^-$ generation is experimentally established in the tissues of the top of the onion leaf of all three experimental varieties, this discrepancy can be explained by the imperfection of the ROS utilization system, which is manifested in a decrease in the level of activity of the AOS system. Similarly, the increase in the concentration of TBA_{ap} in the tissues of the roots and scales of onion-turnip medium- and low-disease-

resistant variety can be explained. The decrease in the concentration of TBA_{ap} in the tissues of onion scales of the "Globus" variety can be attributed to the lack of a photosynthetically conditioned source of ROS generation. The lowest level of TBA_{ap0} among vegetative organs has onion root, which may be explained not only by the lowest level of generation $\bullet O_2^-$ but also by increased activity of GSH-peroxidase, SOD, and one of the highest levels of cytochrome oxidase compared to onion scales.

The marker of FRPO intensity is the activity of cytochrome oxidase, which transfers electrons from cytochromes to oxygen according to the scheme: $4H + 4e^- + O_2 \rightarrow 4H_2O$. Free radical peroxide degradation of membrane lipids reduces the activity of the enzyme, so the natural explanation for the low activity of cytochrome oxidase in the tissues of the apex of leaves, seeds, and flowers of onions of all experimental varieties is the highest level of generation of O_2 cells by these organs (Fig. 8).

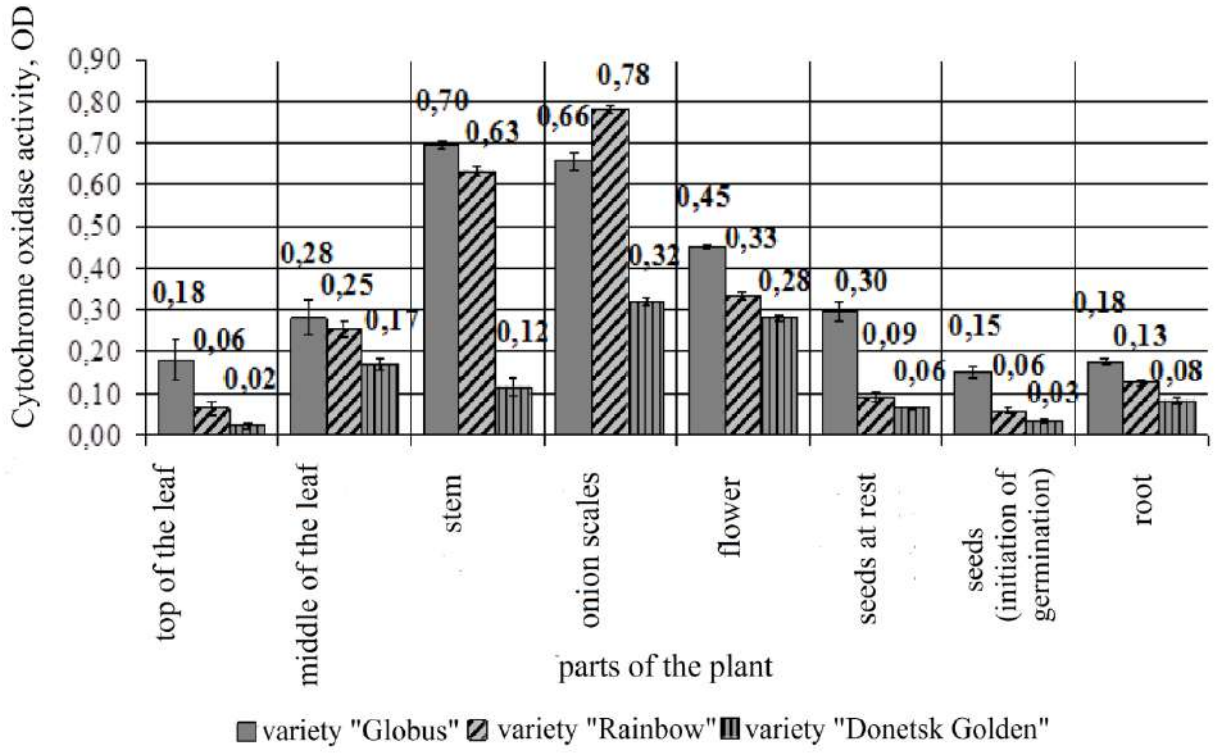

Fig. 8. Comparison of cytochrome oxidase activity in onion tissues.

The diagram shows that the highest level of enzyme activity among photosynthetic organs has a stem, among other vegetative organs – the root and scales of onions. As shown in Fig. 1 and 2, the tissues of these organs are characterized by a relatively low prooxidant activity, which is a possible explanation for this distribution of cytochrome oxidase activity.

As a result of statistical processing of experimentally obtained data, a characteristic feature of the state of PAS tissues of onion varieties "Globe" was a close relationship between concentrations of $\bullet O_2^-$ with GSH (r = + 0.65) and with catalase activity (r > + 0.77) in seed tissues, connection with AA (r > + 0.63) and SOD (r = + 0.75) in onion-turnip tissues, as well as with GSH-peroxidase in leaf apex tissues (r = + 0.93) and the middle of the leaf (r = + 0.67) onion. Variety "Rainbow" is characterized by a close dependence of the concentration of $\bullet O_2^-$ with AA (r > + 0.65) and catalase (r < -0.63) in the tissues of the apex of the leaf; catalase correlates with GSH-peroxidase (r = + 0.86) in the tissues of the middle of the leaf; in flower tissues, TBA_{ap} and SOD are closely related (r = + 0.67), $\bullet O_2^-$ and GSH-peroxidase (r = 0.86); in root tissues – $\bullet O_2^-$ directly correlates with AA, catalase, SOD and GSH (r > + 0.63), and in seed tissues – SOD with GSH and TBA_{ap} (r > + 0.63). For the tissues of the onion flower of the «Donetsk Golden» variety, a direct proportional relationship between the concentration of TBA_{ap} and the activity of catalase and cytochrome oxidase (r > + 0.63) was revealed; in seeds, the associated feedback is GSH-peroxidase and TBA_{ap} (r < -0.63); at the roots – directly associated catalase with TBA_{ap} (r = + 0.71); revealed an inverse relationship of TBA_{ap} with GSH and GSH-peroxidase (r < - 0.63) in the tissues of the scales and leaves of onions, as well as a direct connection with catalase (r > + 0.63) in the tissues of the stem, which is likely, are variety-specific traits.

Therefore, the results of correlation analysis indicate a possible connection of the synthesis of these components of PAS, their interdependent participation in the chains of biochemical reactions, including reactions to ensure the resistance of the variety to disease.

Comparative characteristics of quantitative indicators of the state of PAS of onions depending on the level of resistance of the variety to diseases. The results of the biochemical analysis and inter-varietal comparison of the values of indicators indicate that the tissues of the apex of the onion leaf variety "Globus" have the highest background level of generation $\bullet O_2^-$ compared to the variety "Rainbow" and "Donetsk Golden", but the level of TBA_{ap0} and $TBA_{ap1,5}$ is minimal and increases in the transition from stable to low-resistant variety. A possible explanation for this phenomenon is the experimentally confirmed significant predominance of catalase, SOD, and AA concentrations in onions of the highly disease-resistant Globus onion and the decrease in the value of these indicators in the transition to the low-resistance Donetsk Golden variety. The result of the established predominance is the lowest level of destructive

peroxide damage to tissue membranes of highly disease-resistant varieties, as evidenced by the almost predominance of cytochrome oxidase activity in the tissues of the leaf tips of the onion variety "Globus" in 2.81 ($p < 0.05$) and 8.18 ($p < 0.05$) times compared to "Rainbow" and "Donetsk Golden", respectively. Therefore, the obtained results confirm the connection between ROS and AO in ensuring the resistance of onion varieties to diseases.

Cross-varietal comparison of the values of the PAS of the tissues of the middle leaf of the onion also revealed the predominance of the background level of superoxide generation in the onion of the high-resistance variety. However, in the transition from the apex to the middle of the leaf there is a significant weakening of mitochondrial and enhancement of microsomal generation $\bullet O_2^-$, while in the tissues of medium- and low-resistant varieties there is a slight strengthening of both links of generation $\bullet O_2^-$, which may be varietal-specific.

It was found that mid-leaf tissues of all experimental onion varieties are characterized by a decrease in SOD and catalase activity, but a compensatory increase in GSH-peroxidase activity and AA concentration, which is associated with the increased photosynthetic activity of mid-leaf tissues and reflected in increasing TBA_{ap0} and $TBA_{ap1.5}$. The intensity of AOS increases in the transition from low-resistant to disease-resistant variety, resulting in a predominance of cytochrome oxidase activity in the transition from the variety "Donetsk Golden" to "Globe" and even an increase in the value compared to tissues of the apex, indicating a decrease free radical peroxide destruction of membrane biopolymers.

Analysis of cross-varietal comparison of the values of PAS tissue indicators of onion-turnip scales revealed an inverse dependence of the level of superoxide generation on the level of variety resistance to diseases with a significant increase in the share of microsomal products. The concentration of TBA_{ap0} and $TBA_{ap1.5}$ also increased during the transition from high-resistant to low-resistant varieties, but the analysis of cytochrome oxidase activity revealed a 6.05-fold predominance of the value of the Globus variety established for onions over Donetsk Golden ($p<0.05$). , and the advantage over the values of the tissues of the onion leaf in 3.02 times ($p <0,05$). It was found that the concentration of AA, the activity of SOD and catalase significantly increase according to the resistance of onion varieties to disease, and the activity of GSH-peroxidase and the concentration of GSH – decreases. The obtained

results allow us to conclude the strengthening of the role of the antioxidant part of PAS in ensuring the resistance of the tissues of onion scales to diseases.

Attention is drawn to the experimentally detected increase in the generation of $\bullet O_2^-$ in the tissues of the onion arrow with an increase in the resistance of the variety to disease while reducing the level of TBA_{ap0} and $TBA_{ap1,5}$. The inter-varietal difference in catalase, SOD, AA, and GSH activity is characterized by an increase in their numerical values during the transition to a highly disease-resistant variety, and cytochrome oxidase activity is generally highest among photosynthetic organs and decreases with decreasing variety resistance. A possible explanation for this distribution is the formation of other ROSs in addition to O_2 and the predominance of the AA link in ensuring tissue resistance to disease.

Intervarietal analysis of the value of the indicators of PAS of root tissues is similar to the tissues of onion scales, which is probably explained by the affiliation of these organs to non-photosynthetic vegetative. Thus, in the transition from high- to low-resistant onion varieties, a significant increase in superoxide generation, an increase in the concentration of TBA_{ap0} and $TBA_{ap1.5}$, a decrease in the activity of SOD and catalase, the concentration of AA. Instead, there is a slight increase in GSH peroxidase activity and GSH concentration. The degree of free radical peroxide destruction decreases with increasing resistance of the variety, as evidenced by the recorded increase in cytochrome oxidase activity during the transition to a highly resistant variety.

Cross-varietal comparison of the values of PAS of onion flower tissues shows that the level of background and stimulated generation $\bullet O_2^-$ decreases in accordance with the decrease in the stability of the variety. A similar series of decreases in the value of the indicator was found in relation to TBA_{ap0} and $TBA_{ap1,5}$. It is established that flower tissues have the highest value of all studied enzymatic and non-enzymatic antioxidants and are characterized by a significant increase in their activity during the transition from low-resistant variety "Donetsk Golden" to high-resistant variety "Globus". It was recorded that the tissues of the flower of the Globus variety also have the lowest level of FRPO of biopolymers of membranes, as evidenced by a significant increase in cytochrome oxidase activity during the transition from high- to low-disease-resistant varieties. Therefore, with increasing resistance of onion varieties to disease, there is an increase in both parts of the PAS in the tissues of its flower.

The inter-varietal analysis of the value of the indicators of the state of PAS of onion seeds, which is at rest, shows that the level of generation $\bullet O_2^-$ decreases with decreasing index of resistance of the variety. A similar pattern was found for the concentration of TBA_{ap0}. The concentration of low molecular weight antioxidants in onion seeds increases with increasing resistance of plant varieties to disease, which is also characteristic of most of the studied enzyme AO. In general, it was found that the level of FRPO biopolymers remains the lowest in the stable variety "Globus" and increases during the transition to "Donetsk Golden".

According to the experimentally obtained results, the initiation of the germination process stimulates an increase in the activity of enzymatic antioxidants, the values of which increase with increasing resistance of plant varieties to disease. Therefore, it can be concluded that for dormant onion seed tissues, the prooxidant PAS is predominant, which may play a role in controlling cell division (Janků et al., 2019; Tsebrzhinskiy, 1992), activating the germination process enhances the activity of both links of PAS, the values of which change according to changes in the resistance of onion varieties to disease.

The results of the analysis suggest that: first, the most significant indicators of PAS, which are associated with plant resistance to disease, in all parts of onions, are the concentration of $\bullet O_2^-$ and AA, catalase activity, SOD and cytochrome oxidase; secondly, when conducting biochemical studies that reflect the dependence of the resistance of the variety to diseases with the state of PAS of onions, it is advisable to use the tissues of the flower, leaf, and seed, activated before germination.

Conclusions

As a result of the conducted scientific research, the connection of the state of the prooxidant-antioxidant system with the level of resistance of the variety to diseases and the distribution of the components of the prooxidant-antioxidant system in different plant organs was established. This allowed us to draw the following conclusions:

1. The resistance of the variety to diseases depends on the following indicators of the prooxidant-antioxidant system of plants: level of generation $\bullet O_2^-$, the content of TBA-active products, ascorbic acid, glutathione, superoxide dismutase activity, glutathione peroxidase, cytochrome oxidase.

2. In the tissues of photosynthetic vegetative organs of onions, there is a strengthening of both parts of the prooxidant-antioxidant system; in tissues that are not capable of photoproduction, there is an advantage of the antioxidant link in accordance with the increased resistance of the variety to disease.

3. The greatest activity of both parts of the prooxidant-antioxidant system is characteristic of onion flower cells, which is associated with their receptor, protective, and regulatory value. Onion seed tissues, which are at rest, have the advantage of a prooxidant link and increase the concentration of low molecular weight antioxidants. Initiation of germination processes enhances the activity of both parts of the prooxidant-antioxidant system, as evidenced by an increase in the basic concentration $\bullet O_2^-$ by 26.98% ($p < 0.05$), an increase in the stimulated concentration with NADP●H – by 6.55% ($p < 0.05$), stimulated by yeast – by 175.39% ($p<0.001$), stimulated by NaF – by 362.34% ($p < 0.001$); ascorbic acid – by 4.5% ($p < 0.05$), catalase activity – by 30.31% ($p <0.05$), superoxide dismutase – by 76.82% ($p < 0.001$), cytochrome oxidase – by 58, 69% ($p <0.001$).

4. A characteristic feature of the state of PAS of onion varieties "Globe" was a close dependence between the concentrations of $\bullet O_2^-$ with GSH ($r = + 0.65$) and with the activity of catalase ($r > + 0.77$) in seed tissues, the connection with AA ($r > + 0.63$) and SOD ($r = + 0.75$) in onion-turnip tissues, as well as with GSH-peroxidase in leaf apex tissues ($r = + 0.93$) and leaf middle ($r = + 0.67$) onions. Variety "Rainbow" is characterized by a close dependence of the concentration of $\bullet O_2^-$ with AA ($r > + 0.65$) and catalase ($r < – 0.63$) in the tissues of the apex of the leaf; catalase correlates with GSH-peroxidase ($r = + 0.86$) in the tissues of the middle of the leaf; in flower tissues, TBA_{ap} and SOD are closely related ($r = + 0.67$), $\bullet O_2^-$ and GSH-peroxidase ($r = 0.86$); in root tissues – $\bullet O_2^-$ directly correlates with AA, catalase, SOD and GSH ($r > + 0.63$), and in seed tissues – SOD with GSH and TBA_{ap} ($r > + 0.63$). For the tissues of the onion flower variety "Donetsk Golden" revealed a directly proportional dependence of the concentration of TBA_{ap} with the activity of catalase and cytochrome oxidase ($r > + 0.63$); in seeds, the associated feedback is GSH-peroxidase and TBA_{ap} ($r < – 0.63$); at the roots – directly associated catalase with TBA_{ap} ($r = + 0.71$); revealed an inverse relationship of TBA_{ap} with GSH and GSH-peroxidase ($r < – 0.63$) in the tissues of the scales and leaves of onions, as well as a direct connection with catalase ($r > + 0.63$) in the tissues of the arrow, which is likely, are variety-specific traits.

References

Apel K., Hirt H. (2004) Reactive oxygen species: metabolism, oxidative stress, and signal transduction. Plant Biol. Vol. 55. P. 373 – 399. https://doi.org/10.1146/annurev.arplant.55.031903.141701

Aver'yanov A.A. (1991) Aktivnyye formy kisloroda i immunitet rasteniy [Active forms of oxygen and plant immunity] Uspekhi sovrem. biologii. 111, 5, 722–737. (in Russian).

Baiano A., del Nobile M.A. (2015) Antioxidant compounds from vegetable matrices: Biosynthesis, occurrence, and extraction systems. Crit. Rev. Food Sci. Nutr.;56:2053–2068. doi: 10.1080/10408398.2013.812059.

Dmytriyev O.P., Kravchuk Z.M. (2005) Aktyvni formy kysnyu ta imunitet roslyn [Active forms of oxygen and immunity of plants]. Tsytolohyya y henetyka, 39 (4), 64–75. (in Ukrainian).

D'yakov Y.T., Ozeretskovskaya O.L., Dzhavakhiya V.G. (2002) Obshchaya i molekulyarnaya fitopatologiya. Mir, Moskva. (in Russian).

Foyer CH, Noctor G. (2005). Oxidant and antioxidant signaling in plants: A re-evaluation of the concept of oxidative stress in a physiological context.Plant Cell Environ. 28:1056–107134. https://doi.org/10.1111/j.1365-3040.2005.01327.x

Gill, S. S., Tuteja, N. (2010). Reactive oxygen species and antioxidant machinery in abiotic stress tolerance in crop plants. *Plant Physiol. Biochem.* 48, 909–930. doi: 10.1016/j.plaphy.2010.08.016

Halliwell B. Reactive species and antioxidants. Redox biology is fundamental theme of aerobic life. Plant Physiol. 2006;141:312–322. doi: 10.1104/pp.106.077073.

Hasanuzzaman M., Nahar K., Anee T.I., Fujita M. (2017) Glutathione in plants: Biosynthesis and physiological role in environmental stress tolerance. PMBP. 23:249–268. doi: 10.1007/s12298-017-0422-2.

Hasanuzzaman M. M. H. M., Borhannuddin B. T. I. A, Khursheda P., Kamrun N., Jubayer A. M., Masayuki F. (2019) Regulation of Ascorbate-Glutathione Pathway in Mitigating Oxidative Damage in Plants under Abiotic Stress. Antioxidants (Basel) Sep; 8(9): 384. doi: 10.3390/antiox8090384.

Janků M, Luhová L, Petřivalský M (2019). On the Origin and Fate of Reactive Oxygen Species in Plant Cell Compartments. Antioxidants (Basel). 8(4): 105. doi: 10.3390/antiox8040105

Kasote D. M., Katyare S.S., Hegde M.V., Bae H. (2015) Significance of Antioxidant Potential of Plants and its Relevance to Therapeutic Applications. *Int J Biol Sci*; 11(8):982-991. doi:10.7150/ijbs.12096.

Kohen R, Nyska A. (2002) Oxidation of biological systems: oxidative stress phenomena, antioxidants, redox reactions, and methods for their quantification. Toxicol Pathol. 30:620–50. DOI:10.1080/01926230290166724

Kolupaev Y. E. (2007) Aktyvnye formy kysloroda v rastenyyakh pry deystvyy stressorov: obrazovanye y vozmozhnye funktsyy [Active forms of oxygen in plants under the action of stressors: formation and possible functions] Visnyk Kharkivs'koho natsional'noho ahrarnoho universytetu. Seriya: Biolohiya. 3, 6-26. (in Russian).

Kostyuk V.A. (2004) Bioradikaly i bioantioksidanty [Bioradicals and bioantioxidants]. BGU, Mn. (in Russian).

Maksimov I.V. (2006) Pro/antioksidantnaya sistema i ustoychivost' rasteniy k patogenam [Pro/antioxidant system and plant resistance to pathogens]. Uspekhi sovrem. biologii. 126, 3, 250–261. (in Russian).

Marrocco I, Altieri F, Peluso I. (2017). Measurement and Clinical Significance of Biomarkers of Oxidative Stress in Humans. Oxid Med Cell Longev. 2017: 6501046. doi: 10.1155/2017/6501046

Merzlyak M. N. (1999). Aktivirovannyj kislorod i zhiznedejatel'nost' rastenij [Activated oxygen species in plants] Sorosovskij obrazovatel'nyj zhurnal, 9, 20 – 26. (in Russian)

Pacheco J. H. L., M. A. Carballo, and M. E. Gonsebatt, (2018). "Antioxidants against environmental factor-induced oxidative stress," in Nutritional Antioxidant Therapies: Treatments and Perspectives, K. H. Al-Gubory, Ed., vol. 8, pp. 189–215, Springer, Cham, Switzerland. https://doi.org/10.1007/978-3-319-67625-8

Polesskaja O.G. (2007) Rastitel'naja kletka i aktivnye formy kisloroda: uchebnoe posobie [Plant cell and reactive oxygen species]. KDU, Moskva. (in Russian).

Shao H.B., Chu L.Y., Shao M.A., Jaleel C.A., Mi H.M. (2008) Higher plant antioxidants and redox signaling under environmental stresses. C R Biol. 331:433–41. https://doi.org/10.1016/j.crvi.2008.03.011

Smirnoff N. (2005) Antioxidants and reactive oxygen species in plants. Blackwell Publishing, NY.

Smirnoff N., Arnaud D. (2019) Hydrogen peroxide metabolism and functions in plants. New Phytol.;221:1197–1214. doi: 10.1111/nph.15488.

Song W., Derito C.M., Liu M.K., He X., Dong M., Liu R.H. (2010) Cellular antioxidant activity of common vegetables. J. Agric. Food Chem. 58:6621–6629. doi: 10.1021/jf9035832.

Tarchevskiy I.A. (2002). Signal'nyye sistemy kletok rasteniy [Signal systems of plant cells] Nauka. Moskva, 294. (in Russian).

Tsebrzhinskiy O.I. (2002) Differentsirovannoye spektrofotometricheskoye opredeleniye produktsii superoksida v tkanyakh NST-testom [Differentiated spectrophotometric

determination of superoxide production in tissues by the HCT test]. Aktual'ní problemi suchasnoĭ meditsini. 1 (2), 96–97. (in Russian).

Tsebrzhinskiy O.I. (1992) Nekotoryye aspekty antioksidantnogo statusa [Some aspects of antioxidant status] Fiziologiya i patologiya perekisnogo okisleniya lipidov, gemostaza iimmunogeneza. Poltava. 120–155. (in Russian).

Xu, D.-P.; Li, Y.; Meng, X.; Zhou, T.; Zhou, Y.; Zheng, J.; Zhang, J.-J.; Li, H.-B. (2017) Natural Antioxidants in Foods and Medicinal Plants: Extraction, Assessment and Resources. *Int. J. Mol. Sci. 18*, 96. https://doi.org/10.3390/ijms18010096

Ye Y, Li J, Yuan Z (2013). "Effect of antioxidant vitamin supplementation on cardiovascular outcomes: a meta-analysis of randomized controlled trials". PLOS ONE. 8 (2): e56803. *doi:10.1371/journal.pone.0056803*

Distribución geográfica y análisis de la dieta del Mochuelo de Hoyo *Athene cunicularia*, en el estado Falcón, Venezuela

Vanessa G. Salas A.*
Francisco J. Contreras M.**
Ángela Martino ***
Juan C. Fernández Ordoñez****
Eucleris García*****

RESUMEN

Objetivo: Conocer la distribución geográfica y estimar la composición de la dieta del Mochuelo de hoyo *Athene cunicularia* en el estado Falcón, Venezuela. **Metodología:** investigación descriptiva. Para determinar la dieta fueron monitoreadas 19 madrigueras en las que se colectaron 62 egagrópilas de 27 individuos, en distintos periodos, enero – abril y agosto – noviembre del 2018, agosto – octubre del 2019 y enero – marzo del 2020. Para obtener información sobre su distribución, se marcaron puntos de coordenadas de todas las zonas de ocurrencia o de ubicación confirmada y posteriormente se realizó un modelo de distribución potencial con el Software Maxent 3.2.1 para predecir su distribución en áreas no observadas **Resultados:** Se identificaron 632 ítems presa, *Athene cunicularia* posee un consumo marcado de invertebrados (75%) con preferencias de especies del orden *Coleoptera* y otro (56%) de vertebrados. Se confirmaron 11 sitios de establecimiento y el análisis de distribución potencial, define que esta especie podría localizarse en gran parte del estado Falcón, en el eje Central, la Península de Paraguaná, el Occidente y pequeñas áreas en el Oriente, **Conclusión:** La dieta de *Athene cunicularia* en el estado Falcón, se compara con la común ecología trófica de esta especie, sin embargo, posee con una marcada variabilidad en el consumo, adaptada a la disponibilidad presente en los ecosistemas semidesérticos y desérticos, donde puede existir mayor disponibilidad de presas.

PALABRAS CLAVE: Dieta; distribución; egagrópilas.

*Centro de Investigaciones en Ecología y Zonas Áridas (CIEZA) de la Universidad Nacional Experimental Francisco de Miranda (UNEFM) Falcón, Venezuela. orcid.org/0000-0002-1874-461X. E-mail: VANESSAGSALAS@GMAIL.COM

**Programa Licenciatura en Ciencias. Ambientales, Universidad Nacional Experimental Francisco de Miranda (UNEFM) Falcón, Venezuela.

***Unidad de Ecología Animal del Centro de Investigaciones en Ecología y Zonas Áridas (CIEZA) de la Universidad Nacional Experimental Francisco de Miranda (UNEFM) Falcón, Venezuela.

**** Fundación Científica Ara Macao, Instituto Nacional de Parques (INPARQUES), estado Cojedes-Venezuela.

***** Instituto Nacional de Parques (INPARQUES), estado Falcón-Venezuela.

Recibido: 09/04/2020 Aceptado: 11/06/2020

Geographical distribution and diet analysis of the Mochuelo de Hoyo *Athene cunicularia*, in the State of Falcón, Venezuela

ABSTRACT

Objetive: To know the geographical distribution or to estimate the composition of the diet of the Little screech in the state Falcón, Venezuela. **Methodology:** descriptive research. To determine the diet, 19 burrows were monitored in which 62 pellets were collected from 27 indivviduals, in different prtiods, january – april and august – november 2018, august - october 2019 and january – march 2020. To obtain information on their distribution, coordinate points of all the zones of occurrence or confirmed location were marked and later a distribution model was performed with the Maxent 3.2.1 sofware to predict its distribution in unobserved areas. **Results:** 632 prey ítems were identified *Athene cunicularia* has a marked consumption of invertebrates of vertebrates. 11 establishment sites were confirmed and the analysis of potential distribution defines that this species could be located in much of the falcón state. In de central axis, the Paraguaná Peninsula, the west and small áreas of the east. **Conclusión:** The diet of *Athene cunicularia* in the falcon state is compared to the common trophic ecology of this species, however, it has a marked variability present in semi-desert and desert ecosystems, where there may be greater evailability of prey.

KEYWORDS: Diet; Distribution; pellets.

Introducción

El Mochuelo de hoyo, es un ave rapaz conocida por su nombre científico como *Athene cunicularia*, es un pequeño búho de la familia *Strigidae*, de hábitos parcialmente diurno-crepusculares y de nidificación subterráneas, realizando hoyos o madrigueras sobre el suelo, aunque en oportunidades aprovechan madrigueras de otras especies o cualquier infraestructura que cumpla con las condiciones (Marks *et al*., 1999). Así mismo, se le considera como un indicador de la calidad del hábitat, debido a su ecología trófica diversa, es una especie monógama que se reproduce entre noviembre y abril (Hilty, 2003), de tamaño pequeño entre unos 18 a 26 cm y puede pesar entre 120 y 250 gramos, de grandes ojos amarillos, postura erguida y patas largas, es de color marrón con manchas blanquecinas, en el pecho con barras marrones (Ascanio *et al*., 2017).

Athene cunicularia habita en áreas abiertas de escaza vegetación, posee amplia distribución en América, habita en el oeste de Canadá, el oeste de los Estados Unidos, México, América

Central y América del Sur, existiendo más de 18 subespecies en el mundo (Haug *et al*., 1993). En Venezuela se encuentran establecidas tres subespecies, *A. c apurensis* ubicado al OESTE, *A. c brachyptera* en el NORTE e isla de margarita (Restall *et al*., 2006) y *A. c minor* al NORTE del país (Ascanio *et al*., 2017).

La lista roja de la Unión Internacional para la Conservación de la Naturaleza (IUCN, 2009) considerada a *Athene cunicularia* en Venezuela bajo la categoría de preocupación menor, Sin embargo, esta especie se encuentra en peligro de extinción en Canadá y está amenazada en México, también, se encuentra incluida en el apéndice II de la Convención Sobre el Comercio Internacional de Especies Amenazadas de Fauna y Flora Silvestre (CITES), donde se encuentran especies que no están amenazadas de extinción pero que podrían llegar a estarlo.

Por otro lado, como todo búho de la familia Strigidae, por no poseer buche para triturar sus alimentos, regurgita las partes no digeribles de su presa a través de una capsula compuesta por pelos, élitros, plumas y huesos, llamados también egagrópilas. Estas capsulas brindan información confiable sobre su rol como controlador biológico, permiten determinar la presencia y abundancia relativa de sus presas (Rodríguez, 2015), es por ello que, a nivel mundial, es una especie estudiada en gran medida por su estructura alimentaria o dieta, tales como, los estudios realizados por, Andrade *et al*., 2010, Bastián *et al*., 2008, Bellocq, (1988), Martínez *et al*., (2018), entre otros, en Venezuela existen escasos o nulos estudios relacionados a la dieta. Limonggi, (2014) estudio su dieta en un área limitada del estado Guárico y Vásquez *et al*., (2017) en el estado sucre.

En el estado Falcón, es una especie aún menos estudiada, Colveé, (1996) también estudió su ecología alimentaria en la Península de Paraguaná, investigación de hace más de 20 años, en zonas donde la perturbación sobre el ecosistema ha aumentado. Por otra parte, Ascanio *et al*., (2017), Hilty, (2003) y Restall *et al*., (2006) presentan la distribución de la avifauna venezolana, donde se pone en duda la presencia de esta especie en otras áreas de Falcón, hecho por el cual se hace necesario brindar información actualizada sobre su distribución en el estado Falcón.

En este sentido, Los objetivos fueron conocer las características sobre la dieta de una población de *Athene cunicularia* representada por 11 parejas y 5 individuos solitarios presentes

entre la Península de Paraguaná, la ciudad de Santa Ana de Coro y La Vela de Coro, así como, describir la amplitud de su distribución confirmada y posible en el estado Falcón.

1. Materiales y Métodos

El área de estudio comprendió la costa de Carirubana de la Península de Paraguaná, la ciudad de Santa Ana de Coro y la zona de agricultura y rural de la Vela de Coro (Figura 1). Estas zonas se caracterizan por ecosistemas xerófitos con una temperatura promedio anual que se ubica entre 21,8°C y 24,6°C con una mínima de 18,1°C y una máxima de 27,8°C. La precipitación media anual registrada varía desde los 540 mm a 1600 mm, determinada está directamente por la altitud (Decreto 1.040, 2018).

Los menores promedios de precipitación anual ocurren en la de Serranía de San Luis, la evaporación media anual oscila entre 936 mm y 2170 mm, evaporándose más de lo que puede llover, estas condiciones determinan como característica general del área la existencia de déficit hídricos al menos 8 meses al año, particularmente en el período de enero - mayo. Los meses más húmedos corresponden a los picos de precipitación en los meses de junio-julio y noviembre-diciembre (Decreto 1.040, 2018).

Dieta: Se llevaron a cabo de 1 a 3 salidas de campo por cada mes, para un total de 19 salidas a los sectores Butare y las Malvinas de la Vela de Coro, Kilometro siete y el Conejal de la Ciudad de Santa Ana de Coro y las Costas de Carirubana. El análisis de las egagrópilas permitió documentar la dieta del Mochuelo de hoyo durante dos periodos, sequia: (enero – abril) de los años 2018 y 2020, así como, del periodo de lluvia: (agosto, octubre – agosto, noviembre) de los años 2018 y 2019. Por otro lado, se obtuvo información en dos escenarios diferentes (agroecosistemas y áreas rurales parcialmente habitadas) (Torres *et al.*, 1994).

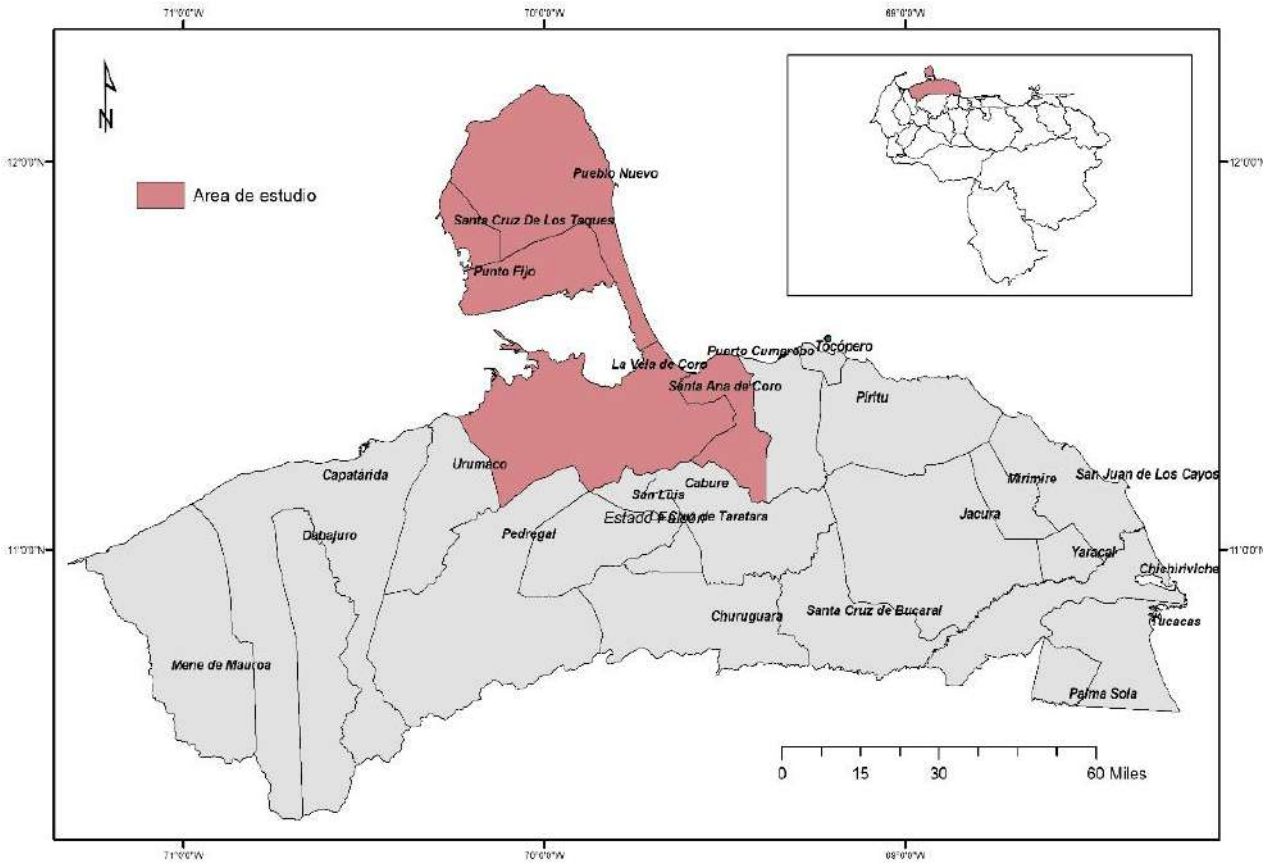

Figura 1. Área de estudio y zonas de colecta de egagrópilas.

Fueron colectadas de forma manual un total de 62 muestras de egagrópilas, que se encontraban dentro y a los alrededores de las madrigueras de *Athene cunicularia* en 19 madrigueras pertenecientes a 11 parejas y 5 individuos solitarios para un total de 27 Mochuelos de Hoyo. Estas una vez colectadas, fueron depositadas en bolsas plásticas ziploc e identificadas con fecha y sector de la madriguera. Posteriormente fueron trasladadas al laboratorio y con ayuda de pinzas y en algún caso de forma manual, fueron disgregadas en seco sobre una placa de Petri (Vásquez *et al.*, 2018). En una lupa estereoscópica y en casos con un microscopio, se llevó a cabo un procedimiento que consistió en separar el volumen de los individuos vertebrados e invertebrados extraídos de cada egagrópila (Torres, 2010).

Para algunas identificaciones taxonómicas de los ítems presa encontrados, se utilizaron fragmentos cráneo-mandibulares como, cráneos enteros o maxilas y mandíbulas para roedores, huesos porosos en aves, pieles y mandíbulas para reptiles y anfibios todo esto en el caso de los vertebrados, para invertebrados se consideraron restos de exoesqueleto de muestras quitinosas

útiles como, élitros para escarabajos; tarsos y mandíbulas para ortópteros, para escorpiones las pinzas y aguijones, entre otros (Vásquez *et al*., 2018). Posteriormente fueron utilizadas guías fotográficas de colecciones de referencias, tales como, González – Sponga (1996), Rexford, (1994), Raymond, (1992) y Mijares y Arends (2000). Sin embargo, no fue posible identificar algunos ítems.

Para estimar la base alimenticia de *Athene cunicularia*, se transformaron los valores a porcentaje en la separación del volumen entre vertebrados e invertebrados (Duffy y Jackson, 1986), para la identificación de las presas se agrupó en familias, posteriormente se calculó la frecuencia relativa. (Torres *et al*., 1994).

Distribución: Se obtuvieron registros visuales y el marcaje de coordenadas geográficas (UTM) a través de un geoposicionador (GPS) Garmin Etrex 10, en zonas donde se confirmaba la presencia de la especie, así mismo, se visitaron áreas que por medio de la comunicación personal se informó sobre su localización y se procedió a su confirmación en campo. La localización de los individuos y las madrigueras se dio por el hábito de *Athene cunicularia* de vocalizar cuando un intruso se acerca demasiado a su madriguera. En este sentido, se llevaron a cabo de 1 a 3 salidas de campo a cada sector, para un total de 19 salidas.

Los puntos de registro se mapearon en un Sistema de Información Geográfica (SIG) ArcView 3.3 (Esri, 1996) para obtener una cartografía de áreas de distribución confirmada. Posteriormente, se desarrolló un modelo de distribución geográfica potencial de *A. cunicularia* en el estado Falcón a través de un análisis realizado por el programa Maxent 3.2.1, donde se determina los puntos de ocurrencia o de ubicación confirmada de la especie y poder predecir su distribución en áreas no observadas, esto, a partir de una serie de variables bioclimáticas disponibles en la base de datos WorldClim (descrita en detalle en, www.worldclim.org) con una resolución de 1 Km y generar los modelos de distribución, que brindan información de 19 variables de temperatura, isotermalidad y precipitación, en este sentido, se logró ubicar zonas cuyas características se asemejan a las áreas de establecimiento confirmadas de *Athene Cunicularia*. Del resultado obtenido, se simplificó la información a un mapa temático de distribución geográfica potencial, empleando (SIG), a través del software ArcView 3.3 (Esri, 1996), (Jasso y Chapa 2008).

Cabe destacar que Maxent 3.2.1 es un programa que aplica el principio de máxima entropía, es decir, que todos los valores tienen la misma probabilidad de ocurrir (Phillips *et al.*, 2006). El algoritmo busca la distribución más cercana a la homogeneidad, pero restringiéndose según la información biológica disponible y las condiciones ambientales del área de estudio y así calcula la distribución geográfica más probable para una especie a partir de información incompleta. (Jasso y Chapa 2008).

2. Resultados

Durante el periodo enero – abril del 2018, se colectaron 9 egagrópilas, por su parte, de agosto - noviembre del mismo año se colectaron 17 egagrópilas, para un total de 26. Durante el periodo agosto – octubre del año 2019, se colectaron un total de 29 egagrópilas y, por último, de enero a marzo del 2020 un total de 11 egagrópilas, todas ellas en zonas caracterizadas como agroecosistemas y áreas rurales parcialmente habitadas (Tabla 1).

Áreas	**Periodos Evaluados**			
	Sequia		**Lluvia**	
	Enero – abril 2018	**Enero marzo 2020**	**Agosto - noviembre 2018**	**Agosto-Octubre 2019**
Butare (La Vela de Coro) (Agroecosistema)		11 egagrópilas		
Las Malvinas (La Vela de Coro) (Zona rural parcialmente habitada)				17 egagrópilas
Kilometro Siete (Ciudad de Coro) (Zona rural parcialmente habitada)	9 egagrópilas			
El Conejal (Ciudad de Coro) (Agroecosistema)			13 egagrópilas	
Costas de Carirubana (Península de Paraguaná) (Zona rural parcialmente habitada)				12 egagrópilas

Tabla 1. Cantidad de egagrópilas colectadas según el periodo y área evaluada.

Fueron identificados 623 items presa, los cuales evidenciaron que los recursos alimenticios de *Athene cunicularia* en ambos periodos de sequía y lluvia, se basan en un alto

consumo de invertebrados con un promedio de (75%), (Grafico 1), destacando la clase insecta, siendo representada por el orden coleóptero cuyas especies de mayor biomasa fueron de la familia Scarabaeidae (69%), seguido de la familia Arachidae (12.3%) y Diplocentridae (9.9%) (Tabla 2).

Ítem presa		
	N°	%
Coleoptera	-	-
Scarabidae	321	69.3
Arachidae	57	12.3
Scorpiones	-	-
Diplocentridae	-	-
Diplocentrus flavus	46	9.9
Sphingidae	39	8.4
Total Invertebrados	**463**	**99.9**
Amphibia		
Bufonidae	12	7.1
Rhinela marina		
Squamata	-	34.3
Gekonidae	58	
Cnemidophurus lemnicastus	-	
Gonatodes vittatus	-	
Teiidae	42	24.8
Ameiva sp.		
Rodentia	-	
Muridae	-	
Mus musculus	46	27.2
Aves	11	6.7
Total Vertebrados	**169**	100
Total presas	**623**	
N° Egagrópilas	**62**	

Tabla 2. Frecuencia relativa de las presas consumidas por *Athene cunicularia* en el estado Falcón, Venezuela.

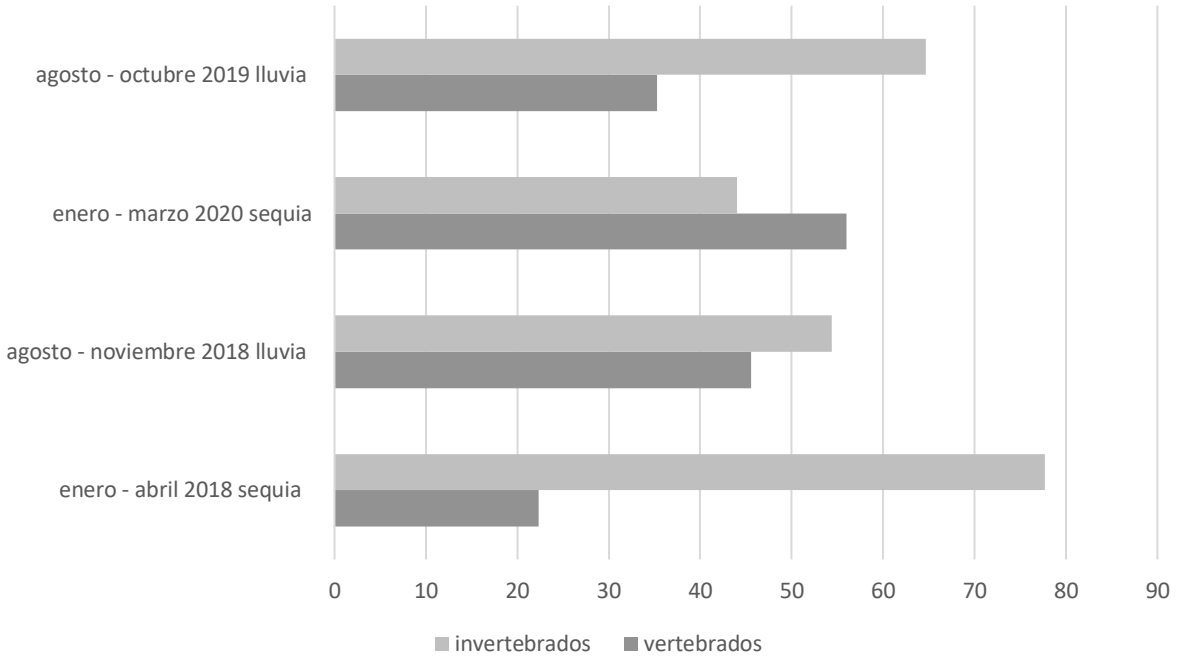

Grafico 1. Se evidencia el alto consumo de invertebrados en la mayoría de los periodos evaluados (75% Invertebrados), a diferencia de un periodo de sequía, donde el mayor consumo fue de vertebrados, posiblemente a las características de la zona evaluada (agroecosistema).

Sin embargo, existió un explosivo consumo de vertebrados (56%) en uno de los periodos de sequía evaluados, en el caso específico, la preferencia se dirigió al consumo de especies de la familia Gekonidae (*Cnemidophurus lemnicastus, Gonatodes vittatus*) en un (61%), Teiidae (*Ameiva* sp) en un (30%) y Muridae (*Mus musculus*) con un (48%), esto puede deberse a la zona de recolección de las egagrópilas, caracterizada por agroecosistemas de siembra de hortalizas y verduras, con madrigueras ubicadas al borde de lagunas activas, donde estas especies de vertebrados son comunes y abundantes, es importante señalar que en otro agroecosistema con menos actividad productiva y en un periodo de lluvia, la alimentación se basó en el consumo de invertebrados. (Grafico 2).

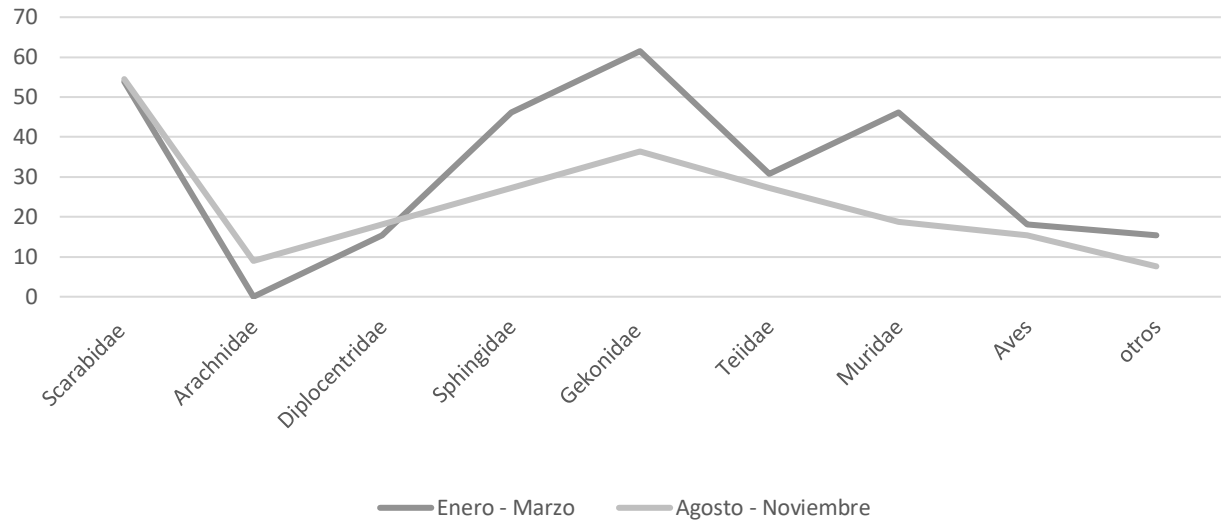

Grafico 2. Relación de consumo de vertebrados e invertebrados en dos zonas caracterizadas como agroecosistemas y en periodos diferentes (lluvia y sequia), nótese que en un agroecosistema con poca actividad productiva y en periodo de lluvia existe un bajo consumo de las especies encontradas (periodo agosto – noviembre), a diferencia de un agroecosistema en periodo de sequía, pero con alta actividad productiva (periodo enero – marzo) que permitió que la dieta se concentrara en el consumo de estas especies.

Por otro lado, se visitaron 17 sectores de La Vela de Coro, Santa Ana de Coro, la Península de Paraguaná y la Costa oriental: (Butare, las Malvinas, Los Olivos, Las Calderas, Kilometro siete, las Eugenias, el Conejal, Tenerías, Sector Cararapa y Dunas activas del Parque Nacional Médanos de Coro, el Isiro, las Costas de Carirubana, Tacuato, Adicora, La Bocaina y Punta Macolla), de todas las zonas recorridas solo se pudo confirmar la presencia de la especie en el 68.7% de las áreas, destacando que la especie había sido confirmada con evidencias fotográficas en dos sectores a mediados de los años 2010 y 2011 (Tabla 3).

Zonas recorridas	Confirmada	No Confirmada	Evidencia fotográfica de su avistamiento años anteriores	Coordenadas
Butare	X			N -69.654 – O- 11.431
las Malvinas	X			N -69.652 – O- 11.434
Los Olivos	X			N- -69.677 – O-11.448
Las Calderas	X			N- -69.666 – O -11.451
Kilometro siete	X			N- -69.716 – O- 11.429
Las Eugenias		X		-
El Conejal	X			N -69.754 –O – 11.428
Tenerías	X			N- 69.737 – O – 11.418
Sector Cararapa	X			N- -69.729 – O -11.623
Dunas activas del Parque Nacional Médanos de Coro		X	X	-
El Isiro		X		-
Las Costas de Carirubana	X			N -70.217 – O- 11.708
Tacuato		X	X	-
Adicora		X		-
La Bocaina	X			N -69.806 – O- 11.848
Punta Macolla	X			N -70.212 – O- 12.086
Tucacas	X			N -68.374 – O- 10.752

Tabla 3. Zonas Confirmadas/No confirmadas durante el chequeo en campo.

Una vez planteado el modelo de distribución geográfica potencial se puede decir que la ubicación de *Athene cunicularia* está influenciada y adaptada a dos variables climatológicas, por la temperatura media del mes más seco y la precipitación del mes más húmedo, En este sentido, las posibles zonas de localización de mayor posibilidad de ocurrencia se delimitan en gran parte de la Península de Paraguaná, en la zona xerófita costera occidental y central, así como en pequeños tramos de la costa oriental del estado Falcón (Imagen 1), zonas donde se requiere ampliar su distribución, así mismo, se ha determinado que estas áreas, son en gran parte, zonas afectadas

por la ganadería, la agricultura y la presión urbana, donde existe una alta probabilidad de establecimiento si se suman las caracterizas de selección del hábitat como; espacios abiertos de escaza vegetación.

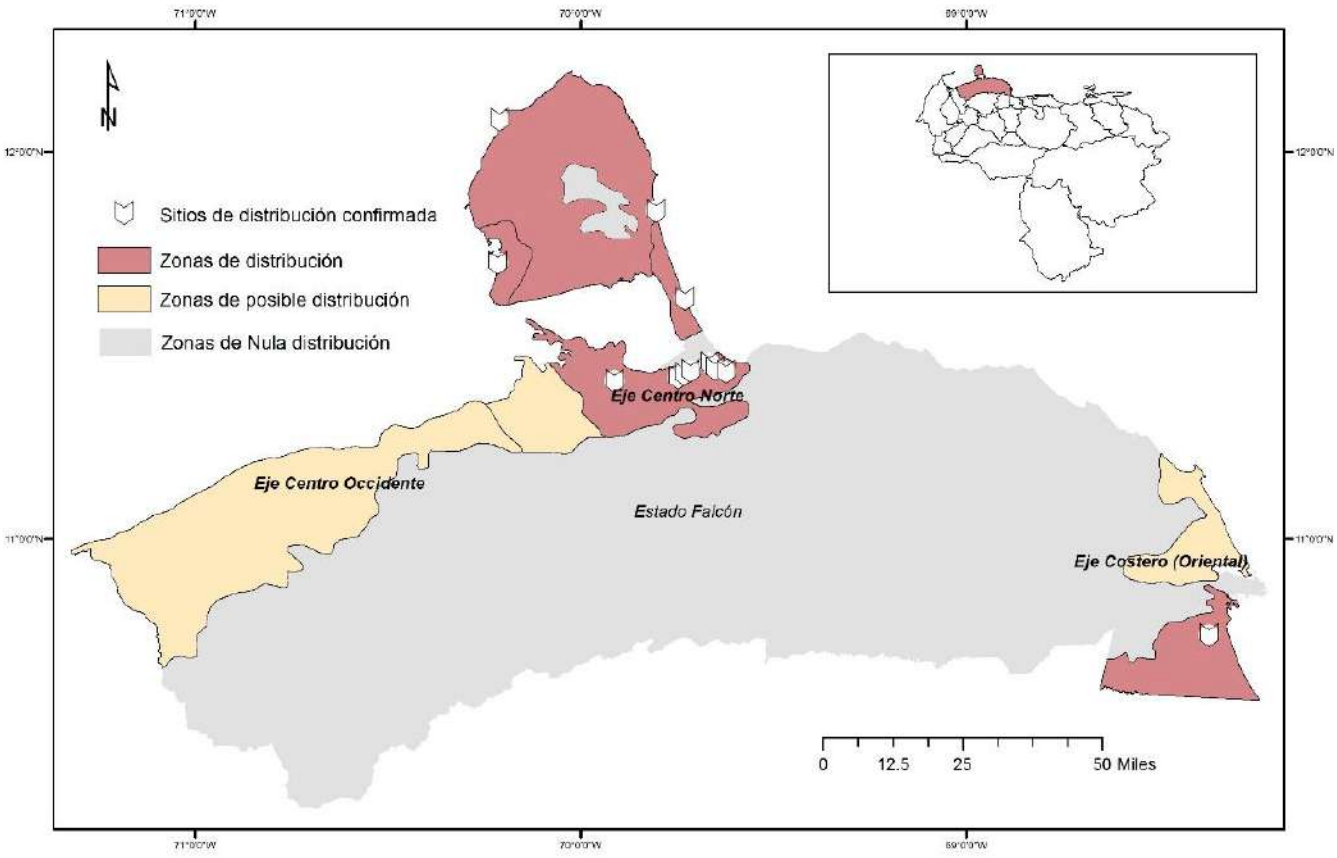

Figura 2. Distribución potencial del *Athene cunicularia* en el estado Falcón, Venezuela.

3. Discusión

Los resultados obtenidos en este trabajo coinciden en parte con la común dieta descrita de *Athene cunicularia*, Vásquez *et al*., (2018), Limongi, (2014), Schlatter *et al*., 1980, Torres-Contreras *et al*., 1994; Zunino y Jofre, (1999), Nabtea *et al*., (2008), y Rodríguez, (2015), coinciden que su dieta está basada principalmente al consumo de invertebrados tanto en periodo de lluvia como el de sequía, elevando su consumo de vertebrados en periodos lluviosos, sin embargo, este estudio afirma su conducta oportunista, ya que, el Mochuelo de hoyo a pesar de las variaciones climatológicas de las zonas áridas puede variar su dieta de acuerdo a la área que habita.

Se evidenció que en dos agroecosistemas con condiciones productivas diferentes y en periodos climatológicos diferentes, la dieta cambia drásticamente, esta diferencia puede deberse al grado de sequedad, humedad y disponibilidad de alimento presente en cada zona, lo que reafirma también su rol como controlador biológico de las especies abundantes. Según Zunino y Jofré (1999) a medida que el Mochuelo de hoyo se interna hacia zonas más desérticas se produce un aumento en la dieta con fauna asociada a las zonas áridas, como son las lagartijas, ratones, escorpiones y pequeños insectos.

Así mismo, nuestro resultado se relaciona con el análisis realizado por Pairo *et al*, (2017) y Baladrón *et al.* (2016), en la selección de los bordes de los cultivos como lugar para localizar el nido donde se proporcionan mejores oportunidades de caza y el aumento en la disponibilidad de presas, asociado a la presencia de la siembra, agua, y áreas despejadas para la caza.

Por otro lado, aunque se desconoce a cerca de las estimaciones poblacionales de *Athene cunicularia*, se podría decir que el área de distribución del Mochuelo de hoyo se encuentra altamente intervenido, lo que puede inducir al desplazamiento de sus poblaciones, en todas las zonas donde se ubica el Mochuelo de hoyo, se identificaron diferentes amenazas sobre su hábitat, por ejemplo, sobre las dunas de los Médanos de Coro constantemente existe una intervención por buggys y motos cuatro ruedas a pesar de que existe una medida precautelaría dictaminada por la fiscalía ambiental que prohíbe su circulación, a esta acción puede deberse su desaparición sobre estas áreas. Al Norte del Parque Nacional Médanos de Coro, en las adyacencias de la localidad de Tacuato, existe un aumento de la actividad agrícola específicamente del cultivo de melón (*Cucumis melo*) y aunque es una actividad productiva, este tipo de sembradíos requieren un el alto uso de pesticidas que podría afectar la base de la alimentación de *Athene cunicularia* y que mermen sus poblaciones. Hecho que podría elevar su categoría de amenaza y por tanto inducir a un episodio más de pérdida en el equilibrio de un ecosistema de un ave considerada como controlador biológico de plagas como lo son roedores e insectos.

El Mochuelo de hoyo podría distribuirse en las zonas planteadas en el modelo de distribución potencial por lo que se necesitarán estudios de campo más detallados para dilucidar sobre su distribución.

Conclusiones y recomendaciones

El Mochuelo de hoyo es un depredador oportunista que realiza cierta selección de su alimento de acuerdo a la abundancia de presas en su entorno, siendo aún más oportunistas en ecosistemas de zonas áridas, donde las condiciones climatológicas las define la altitud y siendo una especie que se ubica en las zonas bajas, busca adaptarse y cumplir con su rol especialista de controlar plagas, un controlador de especies consideradas plagas para las actividades agrícolas.

Es necesario ampliar el conocimiento común a la comunidad para la conservación del Mochuelo de hoyo, a través de la educación ambiental. Así como, establecer constantes jornadas de vigilancia y control para el mantener a perpetuidad del estado natural, el hábitat del Mochuelo de hoyo.

Agradecimientos

A la Fundación Idea Wild, al Centro de Investigaciones en Ecología y Zonas Áridas (CIEZA) de la Universidad Nacional Experimental Francisco de Miranda (UNEFM), Fundación Científica Ara Macao y en especial a todo el equipo Guardaparques del Parque Nacional Médanos de Coro área administrada por el Instituto Nacional de Parques (INPARQUES).

Referencias

Ascanio D., Rodríguez G. y Restall R. (2017). Birds of Venezuela. Helm Field Guides. 592pp..

Andrade, A.; Nabte, M.J.; Kun, M.E. (2010). Diet of the Burrowing Owl (Athene cunicularia) and its seasonal variation in Patagonian steppes: implications for biodiversity assessments in the Somuncurá Plateau Protected Area, Argentina. Studies on Neotropical Fauna and Environment 45(2): 101-110.

Baladrón, A. V., J. P. Isacch, M. Cavalli, and M. S. Bó. (2016). Habitat selection by Burrowing Owls (Athene cunicularia) in the Pampas of Argentina: a multiple-scale assessment. Acta Ornithologica 51(2):137-150. DOI: 10.3161/ 00016454AO2016.51.2.001.

Bastian, A.M.S., E.D. Fraga, A. Mäder, S.A. Garcia, and M. Sander (2008). Análise de egagrópilas de coruja-buraqueira, Athene cunicularia (Molina, 1782) no câmpus da unisinos, São Leopoldo - RS (Strigiformes: Strigidae). Biodiversidade Pampeana, Pucrs, Uruguaiana 6(2): 70-73.

Bellocq, M.I. (1988). Dieta de Athene cunicularia (Aves, Strigidae) y sus variaciones estacionales en ecosistemas agrarios de la Pampa, Argentina. Physis Sección C 46 (110): 17-22.

Colveé, S. (1996). Ecología alimentaria del mochuelo de hoyo (Athene cunicularia) en la Península de Paraguaná. Tesis de Maestría. Universidad Simón Bolívar. Caracas, Venezuela

Decreto 1.040 (2018). Plan de Ordenación del Territorio del estado Falcón (POTEF). Documento Técnico. Secretaria de Ambiente y Ordenación del Territorio de la Gobernación del estado Falcón.

Duffy, D. C. & S. Jackson (1986). Diet studies of seabirds: A review of methods. Colonial Waterbirds 1: 1-17.

Environmental Systems Research Institute (ESRI) (1996). ArcView GIS, the geographic information system (GIS) for everyone. New York Street.

González – Sponga M. (1996). Guía para identificar escorpiones en Venezuela. Cuadernos Lagoven. 203pp

Hilty, S. (2003). Birds of Venezuela. 2da Edición. Princeton University Press. Princeton, New Jersey.

Haug, E., Millsap B., and Martell M. (1993). Burrowing Owl (Speotyto cunicularia). In A. Poole and F. Gill (eds.). The birds of North America. The Academy of Natural Sciences, Philadelphia, Pennsylvania and the American Ornithologists' Union, Washington DC, USA.

IUCN (2009). Red List of Threatened Species. Disponible en www.iucnredlist.org Consultado el día: 19/11/2012.

Jasso, M., Chapa, L. (2008). Distribución potencial de las aves del altiplano potosino. Tesis de Maestría en ciencias ambientales. Instituto Potosino de Investigación Científica y Tecnología A.C. México 127pp

Limongi T. (2014). Caracterización de la dieta y comportamiento alimentario de *Athene cunicularia* (Mochuelo de Hoyo) en el Hato Masaguaral. Edo. Guárico, Venezuela. Trabajo Especial de Grado. Universidad de Carabobo. 93pp.

Martínez, J. A., Martínez, J. E., Mañosa, S., Zu-berogoitia, I. & Calvo, F. (2006). How to manage human–induced mortality in the Eagle Owl Bubo bubo. Bird Conservation International, 16: 265–278

Marks J.S, Cannings R.J y Mikkola, H. (1999). Family Strigidae (typical owls). Pp. 76–242 en: del Hoyo J, Elliott A y Sargatal J (eds) Handbook of the birds of the world. Volume 5. Barn owls to hummingbirds. Lynx Edicions, Barcelona.

Martínez, M., Echevarrial A., Ortiz Pablo., y Fanjul M. (2018) Dieta de la Lechucita Vizcachera (Athene Cunicularia) en un Humedal de Altura de la Provincia de Tucumán, Noroeste de Argentina Ornitolofia neotropical (2018) 29:359-365.

Medina C., Zelada W., Pollack L., Huamán E., y Gómez A. (2013). Dieta de la lechuza de los arenales, *Athene cunicularia*, en Trujillo y en el Cerro Campana, La Libertad (Perú). REBIOL 2013; 33(2): 99-106, Julio – Diciembre. Revista Científica de la Facultad de Ciencias Biológicas. Universidad Nacional de Trujillo. Trujillo. Perú.

Mijares A., y Arends A. (2000). Herpetofauna of Estado Falcón, Northwestern Venezuela: A Checklist with Geographical and Ecological Data. Smithsonian Herpetological Information Service no. 12. 30pp.

Nabtea M., Pardiñas U., y Sabaa S. (2008). The diet of the Burrowing Owl, Athene cunicularia, in the arid lands of northeastern Patagonia, Argentina. Journal of Arid Environments 72 1526–1530.

Pairo, P., Leveau L., y Bellocq I. (2017). Selección del hábitat de nidificación de la lechuza vizcachera (Athene cunicularia) en agroecosistemas de la Pampa Ondulada. Ecología Austral 27:375-384 Asociación Argentina

Phillips, S. J., Anderson, R. P., & Schapire, R. E. (2006). Maximun Entropy Modeling of species geographic distributions. Ecological Modelling, 190, 231-259de Ecología.

Rodríguez Reyes Enzo (2015). Abundancia relativa y dieta del búho terrestre *Athene cunicularia punensis* (Chapman, 1914) en las zonas circundantes de la comuna Atahualpa, Provincia de Santa Elena, Ecuador. Universidad de Guayaquil Facultad de Ciencias Naturales, escuela de biología, tesis para la obtención del título de biólogo.

Restall R., Rodner C. y Lentino M. (2006). Birds of Northern South America An Identification Guide. Volumen 2. 656pp

Raymond, T. (1992). Mariposas de Venezuela. Ediciones CORPOVEN. 275pp

Rexford, L. (1994), Mamíferos silvestres de Venezuela. Armitano Editores C.A. 344pp.

Sainz-Borgo, C. (2016). Registro de dos eventos de mobbing en zonas urbanas de la ciudad de Caracas (Venezuela), *Revista de la Universidad del Zulia*, 7 (18), 69-73.

Schlatter, R., Yánez, P., Núñez H., y Jaksic (1980). The Diet of Burrowing Owl in Central Chile and its relation to prey size. Auk. 97 (3): 616-619.

Torres, María J. (2010). Dieta y conducta de predación de Athene cunicularia sobre Pelecanoides garnotii en isla Choros, norte de Chile. Tesis. Univeridad Catolica del Norte. Coquimbo, Chile. 53 pp. [Spanish with English Abstract]

Torres-Contreras H, Aranguiz E., y Jaksic F. (1994). Dieta y selectividad de presas de *Speotyto cunicularia* en una localidad semi-árida del norte de Chile a lo largo de siete años (1987-1993). Revista Chilena de Historia Natural 67: 329 -340, 1994

Vásquez-Avila1 B., Nivelo-Villavicencio C., Picón P., Armijos M., Vásquez C. y Astudillo P. (2018) La Lechuza Campanaria Tyto alba (Strigiformes:Tytonidae) como regulador de plagas en un ecosistema urbano alto andino en el sur del Ecuador. Revistas Avances en ciencias e ingeniería 10(16), 42 – 51.

Zunino S., y Jofre C. (1999). Dieta de Athene cunicularia en la isla Chorros, Reserva Nacional Pingüino de Humboldt, IV Región. Boletín chileno de ornitología 6: 2-7. Unión de Ornitólogos de Chile.

Factors influencing the development of ecotourism in tourist towns in Kermanshah Province, Iran

Heshmat Moradi*
Alireza Poursaeed **
Marjan Vahedi***
Mohammad Bagher Arayesh ****

ABSTRACT

This study was carried out to explain the development of ecotourism in the tourist villages of the Kermanshah province, using a quantitative-qualitative method. Qualitative data analysis was performed using the maxqda12 software. The statistical sample in the qualitative section was snowball and 20 experts. In the quantitative section, the stratified random sampling method with the Morgan ratio was used. The research tool was an interview with a questionnaire prepared by an investigator derived from the qualitative phase of the research and the background. Data analysis with SPSS24 and PLS2 software indicated that the study model was adequate. On the other hand, it was discovered that all the dimensions of the conceptual research model were extracted from the qualitative and literary studies of the research literature to measure the factors and had a good function in the measurement of these concepts. The multivariate determination coefficient for the main structural equation was 85.5%, indicating that the independent variables of the study included economic, social, and cultural factors, participation, attractions, management, policy formulation, and infrastructure factors. Economic, social and cultural factors, attractions, ecotourism, participatory management and policy-making infrastructures have priorities, second to seventh, respectively. The first priority focuses on anticipating changes in the development of ecotourism

KEY WORDS: Ecotourism development; Ecotourism; Tourism; Kermanshah.

* PhD Student, Department of Agricultural Extension and Education, Ilam branch, Islamic Azad University, Ilam, Iran.

** Associate Professor /, Department of Agricultural Extension and Education, Ilam branch, Islamic Azad University, Ilam, Iran. ***Corresponding author* /E-mail: a_poursaeed@yahoo.com

*** Assistant Professor / Department of Agricultural Extension and Education, Ilam branch, Islamic Azad University, Ilam, Iran.

**** Assistant Professor / Department of Agricultural Extension and Education, Ilam branch, Islamic Azad University, Ilam, Iran.

Recibido: 10/04/2020 Aceptado: 18/06/2020

Factores que influyen en el desarrollo del ecoturismo en pueblos turísticos de la Provincia de Kermanshah, Irán

RESUMEN

Este estudio se realizó para explicar el desarrollo del ecoturismo en las aldeas turísticas de la provincia de Kermanshah, utilizando un método cuantitativo-cualitativo. El análisis de datos cualitativos se realizó utilizando el software maxqda12. La muestra estadística en la sección cualitativa fue bola de nieve y 20 expertos. En la sección cuantitativa, se empleó el método de muestreo aleatorio estratificado con proporción de Morgan. La herramienta de investigación fue una entrevista con cuestionario elaborado por un investigador derivado de la fase cualitativa de la investigación y los antecedentes. El análisis de datos con el software SPSS24 y PLS2 indicó que el modelo en estudio era adecuado. Por otro lado, se descubrió que todas las dimensiones del modelo conceptual de la investigación se extrajeron de los estudios cualitativos y literarios de la literatura de investigación para medir los factores y tuvieron una buena función en la medición de estos conceptos. El coeficiente de determinación multivariante para la ecuación estructural principal fue del 85,5%, lo que indica que las variables independientes del estudio incluyeron factores económicos, sociales y culturales, participación, atracciones, gestión, formulación de políticas y factores de infraestructura. Los factores económicos, sociales y culturales, las atracciones, el ecoturismo, las infraestructuras participativas de gestión y de formulación de políticas tienen las prioridades, segunda a séptima, respectivamente. La primera prioridad se centra en anticiparse a los cambios en el desarrollo del ecoturismo

PALABRAS CLAVE: Desarrollo del ecoturismo; Ecoturismo; Turismo; Kermanshah.

Introduction

Tourism as one of the largest and most prosperous industries in the world has received increasing attention from governments, and in many countries tourism policies have been regarded as the design and formulation of large-scale national programs and policies and as an effective tool for following the development process (Faraji et al, 2017). One of the models that some countries have been focusing on for the development of sustainable tourism in the last two decades has been the discussion of the identity and indigenous structures in tourism that have shaped the phenomenon of ecotourism (Husseini, 2014). Ecotourism is a responsible environmental travel and visit of the early natural areas to understand its benefits and related

cultural features (Ehsani, 2016). Ecotourism is a sustainable strategy to monetize and conserve natural resources (Davoodi, 2015). Therefore, ecotourism should be considered not as a program but as a major and macro strategy. Many countries with the potential to develop ecotourism have devised and implemented ecotourism development and investment plans to create the infrastructure needed to attract ecotourism visitors. In fact, ecotourism is a sustainable strategy for earning money while maintaining natural resources (Davoodi, 2015; Abbas et al., 2019).

Due to the potential of Iran in tourism attractions and unique climate diversity in the world, this industry occupies a valuable place in the world and is in the 64th place among 150 member countries of the World Tourism Organization (Manochehri, 2015).Also in 2017 it is ranked 93 out of 136 tourism countries in the world, which has the potential to achieve better rankings. The worst ranking among the components of the Travel and Tourism Competitiveness Index in 2017 was related to environmental sustainability, followed by the prioritization of travel and tourism and tourism services infrastructure (Tehran Chamber of Commerce, Industries, Mines and Agriculture, 2018).

The economy of Kermanshah province is mainly agricultural and is the agricultural center of Iran. But the weakening of agricultural potentials, mainly dry farmland and the intensification of successive droughts have led to rural migration (BigMohamadi and Hatemi, 2010). It has also caused extreme unemployment in the province, with the province having the highest unemployment rate with 26.6% and since this province is one of the most important and richest provinces of the country in the field of tourism and is among the top 5 provinces for the number of tourists, the total number of tourists in different seasons is 1003940 people (Iran Statistical Center, 2015),And about half of the tourists visit the target villages of tourism(Vermaghan, CharmalehOlia, Fash, Hajij, Shamshir, Khanghah, Piran, SarabHarasam, SorkhehDeizeh, Harir, Shalan, Kandouleh, Galin, Nojiyeran (Nojobaran)).But in terms of ecotourism development indicators, there is a huge difference between different regions of the province. This and other issues such as: creating employment, increasing income, reducing immigration it has led to the development of tourism in villages that have the potential to develop ecotourism.

In addition, Kermanshah province has high potential in the field of ecotourism industry depending on the conditions of the country, including: pristine nature, jungle highlands and

mountains, rivers, mineral waters, forests, ancient history, sights, old markets, Diverse architectural styles, diverse climates and, most importantly, a variety of different cultures, thus necessitating the use of these resources in order to develop ecotourism and the province's development with proper management and planning. Some villages in the province have been providing tourism services in recent years, but the benefits of this type of tourism in the development as well as the development of ecotourism development strategies have not been considered by agricultural and rural development planners and policy makers, and have not considered ecotourism as a means of direction. Resolving the problems of rural people with unused environmental protection, not even enough research has been done, so it is necessary to plan for the development of ecotourism as a result of rural development and development with regard to the characteristics and capabilities of the villages. Since these villages have been registered with the Cultural Heritage Organization and are part of our cultural heritage, they need to be given a great deal of attention so that by planning properly they can improve their ecotourism and help reduce problems. And this research seeks to answer the question of what factors are effective in the development of ecotourism in tourism target villages of Kermanshah province?

1. Theoretical Foundations

Ecotourism is nature-based tourism and involves understanding the natural environment that contributes to ecological sustainability. In other words, ecotourism is a type of natural and sustainable tourism that is made possible by indigenous stakeholders and utilizing the natural potentials of tourism (Mersangar, 2006). And ecotourism is a tourism that considers itself responsible for the totality of plant and animal species, land, and ecosystems of an area alongside local communities with all their cultural needs and characteristics (Gigović et al, 2016). Tourism has a history dating back to human activities. And in ancient times the different classes of societies traveling on different ends had in effect some kind of tourism activity. Famous explorers, adventurers, and tourists such as Marcopolo, Magellan, Vasco da Gama, and Christopher Columbus have somehow embarked on tourism trips to a society shaped by Hegel's interpretation of modernism (MacCannel, 1976). In the 19th century, the expansion of railways

provided access to rural areas for many, and the development of the tourism industry expanded eco-tourism, and in the twentieth century not only did the demand for ecotourism grow rapidly, but its scope also varied. A brief look at the tourism situation in Iran and Turkey, which has perhaps undergone a growing trend in the last 30 years or so, has even overtaken Iran in some cases, according to the World Tourism and Tourism Council (WTTC). Turkey's 2015 share of direct participation in the travel and tourism sector in GDP reached $ 32 billion in 2015 and is projected to reach $ 48 billion in 2026 if the index reaches 2015 in Iran. It reached $ 7 billion and is projected to reach $ 14 billion by 2026 (Heidari, 2009). It should be noted, however, that the nascent industrial ecotourism industry has been introduced into the scientific and academic literature of our country since the early 1980s and has not yet received sufficient attention at the planning and executive levels of the country (Razvani & Bayat, 2013). And in Kermanshah province, there is also a new category that requires the active participation of people, policymakers, planners and researchers.

1.1. Research Background

The role of ecotourism development in the local economy is widely known, but what is remotely plausible is the people's role in the development of this industry also consider ecotourism (Daniel, 2013). Garcia (2017) unpleasant driving situation can create a high level of dissatisfaction and affect the subsequent behavior of tourists towards the destination. From the perspective of Blancas et. al, (2015). The most important indicators of ecotourism development include: the number of crimes registered by the police at the destination per 1000 persons, the cost of government to restore order and public safety, the ratio of tourists to the population, the percentage of employment created in the tourism sector, the ratio To other jobs.

Sepahvand et al. (2018) examined the views of three groups of people, officials, and tourists on the formulation of specific laws and regulations, optimal use of attractions and, in a study entitled, Strategic Planning for the Development of Rural Ecotourism (Case Study: Village of Bisheh Station). Preventing demolition, and creating tourism fairs to showcase different types of cultural geography such as crafts, art, local cover, food, music, customs and local rural celebrations can lead to the development of ecotourism in the village of Bisheh Station. Khosravi

(2007) in his thesis entitled Strategic Analysis of Ecotourism Development in Galiksh City Using SWOT model, concluded that diversification of services, accommodation, recreation and health services in order to satisfy tourists and subsequently increase tourists in order to create tourism. New activities for residents of the study area, training crisis management to local forces to increase safety and formulate special laws and regulations to optimally and efficiently use the region's natural attractions and prevent damage to forest lands, farms and water, soil and air pollution the development of eco-tourism is effective.

The results of Salici (2018) research on local partnerships and ecotourism development (case study of JannatRoodbar village) conducted through field and citation method showed that financial support for rural infrastructures; construction of council office and village assistance; Good hygiene, support for agriculture and animal husbandry, assistance to repair the roof of old and traditional buildings, continue the implementation of the conductor plan and pavement of rural areas in the development of suitable ecotourism. In a study on the impact of ecotourism on the development of rural tourism, Baghani (2017) considers the development of educational programs, development and support of ecotourism as effective in the development of rural tourism and ecotourism.

Shatarian et al. (2017) in article titled Prioritization of Factors Influencing the Development of Rural Nature in the Village of BarzakKashan by Combining ANP and DEMATEL Techniques, Organizing the development of the area's nature tourism, organizing tours of the area and developing intermediaries (advertising and information offices, etc.) and improving the way tourists are treated, are effective in promoting ecotourism. Omidi Najafabadi et al., 2016), education, holding conferences, festivals and exhibitions, creating information websites, and distributing booklets and brochures consider ecotourism effective. Karami (2017) Lack of publicity about tourism and ecotourism attractions in the region, low number of regional resorts and amenities and lack of proper monitoring system, poor transportation, lack of proper planning and facilities, lack of access to the development of ecotourism is effective. Birendra and Suman (2018) Residents' participation in the ecotourism development program, visitor satisfaction, local support for ecotourism development, periodic evaluation of policy makers and tourism planners involved with the project on the importance of ecotourism can be helpful in

ecotourism development. The success indicators of the Ecotourism Development Project include environmental protection, economic prosperity, promotion of local arts and culture, local participation and a fair share of resources. Funda (2018) concluded in a study entitled Ecotourism of the World and Turkey on Socio-Cultural and Economic Dimensions, that in areas where there is potential for ecotourism, planning for the development of ecotourism should be undertaken. The hotel or dormitory should be built, the awareness of the people of the area should be increased and the economic priorities should be given to the local people. Erkara et al., (2017) believes that the level of social welfare and the level of community preparedness to participate in environmental protection are effective on the development of ecotourism.

1.2. Conceptual model and research hypotheses

An examination of the background studies and causal conditions affecting the central issue (development of ecotourism) in field interviews reveals the various factors influencing ecotourism development such as economic, social and administrative factors, governance, infrastructure, and infrastructure. They have a direct and indirect impact on the development of ecotourism. In reviewing the research background, some of these factors have been used to design the conceptual model of ecotourism development, and based on the conceptual model presented in Figure 1, the following seven basic hypotheses are discussed (Tab 1):

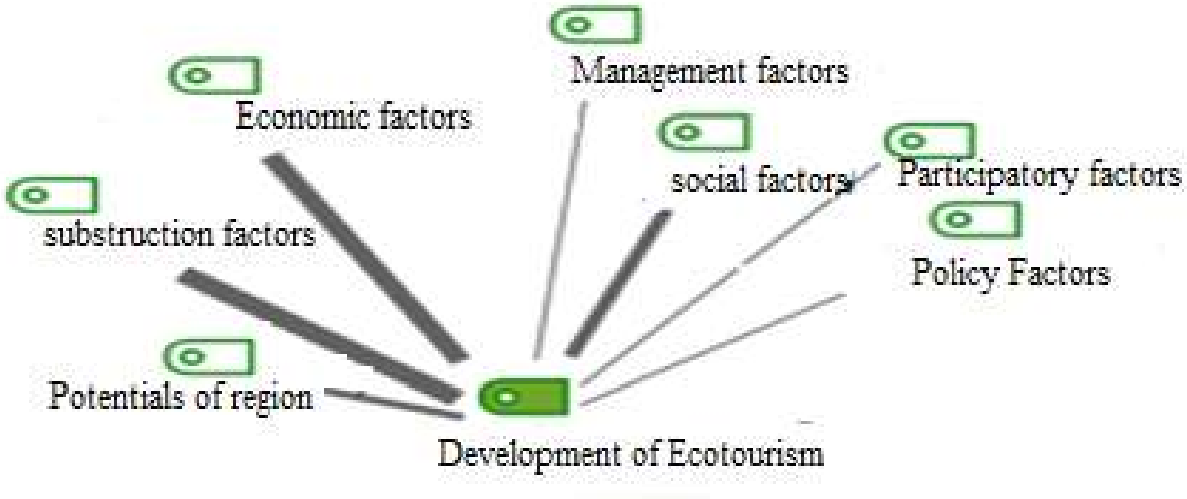

Figure 1.

Tab 1: Conceptual research model with maxqda12 software

Research hypothesis	Assumption test
1.Policy factors are effective in the development of ecotourism	H0:β=0H1: β≠0
2. Social and cultural factors contribute to the development of ecotourism.	H0:β=0H1: β≠0
3. Participatory factors are effective in the development of ecotourism.	H0:β=0H1: β≠0
4. Economic factors contribute to the development of ecotourism	H0:β=0H1: β≠0
5. Gravity factors and potentials of the region are effective in the development of ecotourism	H0:β=0H1: β≠0
6. Management factors influence ecotourism development.	H0:β=0H1: β≠0
7. Infrastructure factors, ecotourism services and facilities are effective in developing ecotourism	H0:β=0H1: β≠0

2. Research Methods

The research method used in this study can be investigated from different aspects. From a research perspective or paradigm, this research is considered a mixed (quantitative - qualitative) type. In terms of purpose, the present study is an applied one; it is a descriptive-analytical one. And in terms of time, it is retrospective. The statistical population of this study consists of two groups.

The first group, which are experts and experts in the field of tourism, whose views have been used to extract factors that influence the ecotourism development of tourism target villages in Kermanshah province.

The second group is the head of the households of the beneficiary villages (2678 family) and ecologists and tourists, which according to statistics of Kermanshah province Cultural Heritage Office in 2017 was about 530 thousand. The sample size in the qualitative section was purposive

sampling of snowball, which included 20 experts and professors, cultural heritage tourism experts, city tourism managers from whom information was collected through open interviews.

The sampling method in the quantitative section was stratified random sampling with proportional allocation using Morgan table. Only 203 questionnaires from tourists and 236 questionnaires from heads of households in the target tourism villages were returned or analyzed. In this study, three main methods of interviewing experts, documentary and field studies were used to collect data. Face-to-face interviews with open-ended and semi-structured questions were used for the qualitative research method and a small part of the closed-ended questionnaire was used for data collection. To determine the validity of the questionnaire, a panel of experts was used. To check the validity of the questionnaire, 30 villagers and tourists (out of the study area) were selected by a completely random method and the research questionnaire (108 questions) was completed by them.

The variables were then refined using Cronbach's alphamethod. After collecting and sorting quantitative data, descriptive and analytical statistical methods were used for data analysis. All calculations were performed using SPSS24 and pls2 software.

2.1. Qualitative Research Findings

1-Open coding

Open coding includes key interviews, concepts, and the main catagory described in Tab 2.

2-Axial coding

This coding is shown in Figure 2

3. Selective coding

According to the results and the final model of the research findings indicate causal conditions affect the central issue and lead to local community participation in conservation, management and decision making, participation in ecotourism sector investment, empowerment (people, investors and other organizations). Gaining economic benefits for

stakeholders, preserving local cultures and making optimal use of cultural heritage and ultimately indigenous people and ecotourism development, and promoting ecotourism with factors such as stakeholder participation and ecotourism education And intervention factors such as financial management of ecotourism (financing of ecotourism costs) And investing in ecotourism), policymaking (social security, formulation of ecotourism laws and the application of new technologies in ecotourism), a sense of belonging and good management of ecotourism (ecotourism privatization, ecotourism security and good management) combined and leading to strategies Management (energy management, benefits management and waste management), advertising marketing such as setting up information centers, creating traditional exhibitions, festivals and rituals, and ultimately educational and promotional strategies such as ecotourism education, environmental protection and cultural heritage, and How to deal with tourists and promote ecotourism are coming back.

Finally, applying these strategies can have both positive and negative consequences, including: positive economic outcomes such as reduced unemployment, a new local product market, the development of handicrafts, improved service quality, the creation of new infrastructure and increased levels. The prosperity and quality of life of local people will have negative consequences, such as a shift in interest income, economic imbalances, and the shifting of the workforce from agriculture to tourism. It also has positive environmental consequences such as reduced environmental degradation, gasification to the villages, protection of cultural heritage and biodiversity benefits, and negative consequences such as increased traffic and noise and increased pollution of climate and soil. Applying these strategies to the development of ecotourism may have positive social and cultural consequences such as cultural exchanges and social interactions, development of educational programs and the preservation of cultural heritage, and negative consequences such as imitating local people from tourist culture, transmitting disease from human to animal, Diminishing the principles, beliefs and values and forcing the locals to it The cup is a traditional activity (Figure 2).

Table 2: Open Coding

Category	concepts	Interview Key
Excellent conditions	Ecotourism infrastructure and facilities	Ecotourism resorts need to be developed.
		Building a hotel can be helpful in developing ecotourism and sustaining tourists.
		Parking and a place for setting up tents, barracks and water, etc. have been created in some villages.
		Asphalting and improving the roads of the villages, more tourists come to these villages.
		Creating toilets, green spaces and children's play equipment
	Policy factors	Development of special laws and regulations for environmental protection
		Establishment of environmental protection base in villages
		Economic priorities must be given to the local people.
		Government financial support for local workshops and handicrafts
	Attractions and potentials of the region	Offering traditional food in tents and restaurants
		Using natural building materials in the village
		Performing music, holding local ceremonies and celebrations
		Existence of beautiful natural cultural landscapes and attractions
		Introduction and sale of medicinal plants in the region
		Beautifying the paths leading to the village
	Management factors	Giving economic priorities to the local people
		Surveys of policymakers and planners involved in the ecotourism project
		Surveys of tourists and locals
		Rural waste disposal management
		Training local people and tourists on environmental issues
	Social factors and cultural	Tourist satisfaction with hosting, facilities and services provided
		Create a seasonal exhibition of local products
		Pleasant and unpleasant experience from previous trips of tourists
		Distribution of brochures and pamphlets at the entrances of villages
		Installation of signs prohibiting fires and cutting down trees and observing hygiene
		Providing rural life experience for tourists

		Production and broadcast of TV programs about the attractions of the village
	Participatory factors	The participation of villagers in providing accommodation services to tourists
		Sharing indigenous peoples in the use of pastures
		Involve local people in the management, planning and decision-making of the village
		Local people's participation in environmental protection
	Economic factors	Local investors invest in environmental housing
		Export development of some local products
		Suitable marketing for selling local products
		Improving the quality of handicrafts
		Indigenous people's activity in selling livestock and agricultural products
		Spending tourism revenue in the village
		Divide local people's income from ecotourism
		Invest in herbs and traditional medicine
		Foreign investment in the village
		Development of small and medium handicraft production companies
		Pay low-interest financial and credit facilities to start small businesses
Axial category	Ecotourism development	Local community participation in environmental protection
		The participation of the local community in the management and decision-making of the village
		Gain economic benefits
		Empowering people, investors and other organizations
		Local community participation in tourism investment
		Preserving local cultures
		Increase of jobs
		Optimal use of cultural heritage
Background conditions	Water management	Optimal use of water
	Education	Environmental protection training in schools
		Development of public awareness through excellent tourism training centers
		Training border guards and law enforcement to protect the environment.
		Increase public awareness of environmental protection through charismatic individuals
	Participation	All-round participation of the people, the government and the private sector in preserving cultural and historical monuments
		Creating tourism infrastructure in the village with the participation of the people and the government

	The cooperation of ecotourism stakeholders	Cooperation of the Radio and Television in promoting and implementing ecotourism training programs
		Cooperation of organizations, villagers and rural councils in environmental protection
Interfering factors	Sense of belonging	Prevent the change of pasture user and ecotourism attractions
		Application of old architectural facades in the construction of new houses
	Policy	The role of the police in protecting the environment
		The role of local people in environmental protection
		The role of the Cultural Heritage Organization in identifying and introducing attractions
		Licensed by the Cultural Heritage to create ecotourism facilities
		Laws and guidelines on cultural heritage in the field of environmental protection
		Transfer of new and low-consumption technologies to the village
	Good eco-tourism management	Reinforce buildings against earthquakes
		Expansion of roads and fencing in road construction sites
	Security in ecotourism	Recreational boat insurance
		Handicraft insurance
		Assign residence supervision to the private sector
		Housing supervision by the private sector
		Assignment of exploitation of attractions to the private sector
		Residence permits, restaurants and hotels to the private sector
	Management of government institutions	The role of government in protecting natural resources
		Responsibility of the Cultural Heritage Organization in introducing cultural and natural heritage
		The role of government in providing ecotourism infrastructure
	Ecotourism Financial Management	Establishing a fund to help restore and restore courtyards and historical sites
		Apply financial incentives for optimal energy and water consumption
		Use municipal revenues to develop ecotourism services and facilities
Ecotourism development	Educational and promotional	Use of crimes committed by border smugglers to restore historic buildings and religious shrines
		Training to protect the environment and how to deal with each other

		Construction of small cultural and historical museums
		Promoting the tradition of using religious places and sites
	Marketing	Guide the student camps of the Path of Light to these areas
		Create small and medium workshops and local production factories
		Starting small businesses in the field of ecotourism
		Seasonal exhibition of local products in the villages
		Festivals and traditional and religious rites
		Village council and village administration, and information offices
		Editing and broadcasting TV programs
		Media advertising about tourism and village attractions
	Managing people in Ecotourism	TV shows, promotional CDs, brochures and ...
		Observance of construction standards in energy consumption
		Fuel consumption management
		Energy saving by people
		Use of livestock waste as fertilizer in agricultural lands
Impacts of ecotourism development	Social and cultural impacts	Collect solid waste and recycle it
		Transmission of diseases from humans to animals and local people
		Increasing the desire of villagers to use luxury and decorative goods
		Educational programs for the development and support of ecotourism
		Destruction of the principles and values of the beliefs and customs of the local people
		Cultural exchanges and social interactions between locals and tourists
		Protecting the cultural and historical heritage of the villages
		Use of animal waste for fertilizer
		Forcing people to do dance activities and ..
		Ignoring the rules to earn as much as possible from available resources
		Increase accommodation facilities such as hotels, restaurants, tents and campsites
		Increase the level of well-being and quality of life
		Demand for economic infrastructure has increased
		New markets for local products and handicrafts
		Development of works of art and handicrafts
		Transfer of work from agriculture to ecotourism
		Economic imbalance of regions
		Ecotourism in the busy season has reduced unemployment
	Economic impacts	Increased air, soil and water pollution and noise pollution
		Rapid development of ecotourism amenities
		Avoid the extinction of rare animal and plant species
		Reduce environmental degradation
		Gas supply to tourist target villages
		Sensitivity of local people to different types of environment

Figure 2: The model presented by the selective coding of factors affecting ecotourism development

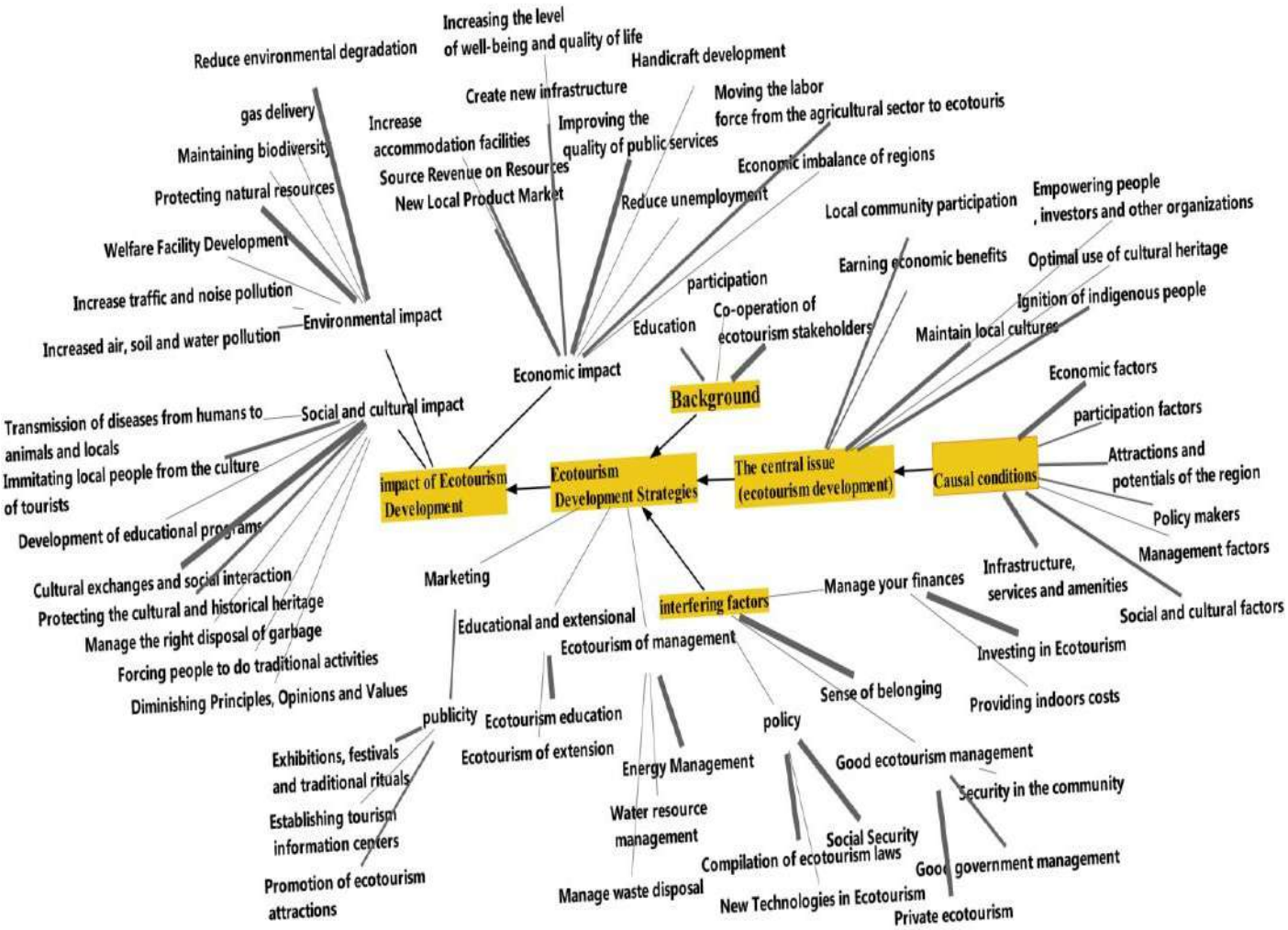

4. Qualitative Research Findings

The demographic characteristics of tourists and heads of households in the target villages are based on Table 3.

Table 3: Frequency Distribution of Sample Members by Individual Tourism Characteristics and Head of Families.

Sex (tourists)	Variable	Abundance	Abundance Percent
	Man	184	90.6
	Female	19	9.4
	Total	203	100
Married (tourists)	Single	170	83.7
	Married	33	16.3
	Total	203	100
Education (tourists)	illiterate	2	1
	Diploma and Diploma	99	48.8
	Associate Degree	22	10.8
	Bachelor	53	26.1
	Masters degree and higher	27	13.3
	Total	203	100
Age (tourists)	15-23 years	14	6.9
	24-32 years	24	11.8
	33-41 years old	58	28.6
	42-50 years	73	36
	50 years and more	34	16.7
	Total	203	100
Occupation (tourists)	Governmental	104	51.2
	Free	73	36
	Unemployed	26	12.8
	Total	203	100
Age of Head of Households	29-23 years	15	6.4
	36-30 years	37	15.7
	43-37 years	53	22.9
	50-44 years	71	30.1
	More than 50	59	25
	Total	236	100
Head of household	Man	217	91.9
	Female	19	8.1
	Total	236	100
The head of households	Governmental	63	18.8
	Free	112	33.7

	Agriculture and Animal Husbandry	114	33.8
	Unemployed	47	14
	Total	336	100
Education of the head of households	illiterate	8	3.4
	Diploma and Diploma	140	59.3
	Associate Degree	13	5.5
	Bachelor	63	26.7
	Masters and higher	12	5.1
	Total	336	100

The results showed that 83.7% of the surveyed tourists are married and 16.3% are single. 81.8% of household heads were married and 8.2% were single. The survey findings showed that most of the tourists (51.2%) have freelance jobs, 36% government jobs and 12.8% unemployed. The highest percentage of heads of households surveyed (33.8%) were agricultural and livestock, 33.4% freelance, 18.8% government and 14% unemployed. Findings related to factors affecting ecotourism development are as follows. 80.6% of the tourists were male and 8.4% were female. Also, 81.8 percent of the household heads were male and 8.1 percent were female. Therefore, it can be concluded that most of the subjects in both groups are men. The mean age of tourists was 41.2 years and standard deviation was 10.7 years, with the youngest being 23 years and the highest being 73 years. The mean age of the head of households was 44 years, with the youngest being 23 years and the highest age being 76 years. In both groups, the most common age group was less than 45 years. Findings from the respondents' education indicate that a small percentage of illiterate tourists (1) and 48.8% of tourists have a high school diploma and below, 10.8% have a high school diploma and 26.1% have a bachelor's degree and 13.3% of tourists have a high school diploma. Postgraduate Education and Higher Education the majority of the sample studied is postgraduate and higher. Also, 3.4% were head of illiterate households, 58.3% had a bachelor's degree and below, 5.5% had a bachelor's degree, 26.7% had a bachelor's degree, and 5.1% had a bachelor's degree or higher. The education of the majority of members is a sample of diplomas and diplomas.

5. Investigating Factors Affecting Tourism Development from Respondents' Viewpoints

Findings show that in terms of infrastructure, the views of both groups, the increase of eco-tourism resorts, the construction of hotels, the creation of new educational and health and service infrastructure, the establishment of parking spaces for tents, ports and water, etc. The establishment of local tourism guides at the entrance to the village has been given top rankings for ecotourism development.

Table 4: Investigating the Factors Affecting Tourism Development from Respondents' Viewpoints

Tourists				Households				Variables
Rating	CV	Average Ratings	Deviation Criterion	Rating	CV	Average Ratings	Standard deviation	
1.Infrastructure, services and ecotourism facilities								
3	0.3	3.4	1.04	3	0.33	3.45	1.15	Deployment of local tourism guides at the village entrance
6	0.34	3.26	1.1	4	0.35	3.52	1.22	Creating a bathroom; green space and children's playgrounds
5	0.33	3.6	1.19	1	0.3	3.73	1.13	Increase in eco-tourism
2	0.29	3.49	1	2	0.32	3.24	1.03	Provides parking and parking space for tents, benches and water.
4	0.31	3.46	1.06	5	0.36	3.27	1.17	Distribution of leaflets and booklets at the entrance of the villages to the tourists
6	0.34	3.35	1.15	1	0.3	3.5	1.05	Construction of the hotel
1	0.25	3.71	0.94	2	0.32	3.48	1.1	Creating new educational, health and service infrastructure
2. Policy								
5	0.4	3.09	1.25	3	0.39	3.08	1.2	Reduce the formalities for investment

2	0.37	3.11	1.14	5	0.42	2.78	1.18	Increased road safety
3	0.38	2.86	1.08	2	0.37	2.96	1.1	Establishment of an environmental checkpoint in the villages
3	0.38	3	1.14	4	0.41	2.77	1.15	Neighboring security
1	0.34	2.99	1.01	1	0.33	3.01	1	Develop special laws and regulations to protect the environment
3. Potentials and Attractions of the Area								
5	0.33	3.27	1.08	3	0.31	3.45	1.08	The presence of beautiful natural cultural landscapes and attractions
4	0.32	3.46	1.12	7	0.37	3.33	1.23	Resources and potentials of the village
6	0.35	3.24	1.15	6	0.36	3.32	1.2	Various and favorable climate of the villages
1	0.27	3.48	0.92	4	0.32	3.16	1	Using natural building materials in the village
5	0.33	3.4	1.11	2	0.29	3.39	0.99	Protecting historical monuments and religious sites
3	0.29	3.4	0.98	3	0.31	3.2	0.98	Beautifying the roads leading to the village
2	0.28	3.51	0.97	1	0.28	3.35	0.95	Music performances, local celebrations and celebrations
4. Management								
3	0.3	3.51	1.06	4	0.33	3.41	1.12	Managers' experience and education
2	0.28	3.64	1.04	5	0.35	3.46	1.21	Survey of tourists
1	0.27	3.32	0.91	3	0.32	3.47	1.11	Survey of policy makers and planners involved with ecology
3	0.3	3.2	0.96	1	0.3	3.4	1.03	Proper disposal of village waste
4	0.32	3.23	1.03	2	0.31	3.35	1.04	Pay attention to the views of indigenous people in village planning and decision making
5. Social and cultural								
2	0.36	3.17	1.14	1	0.35	3.24	1.12	Tourist satisfaction with the facilities and services provided
1	0.34	3.31	1.12	2	0.36	3.11	1.13	Providing tourists with the opportunity to experience rural life

5	0.51	2.63	1.34	7	0.43	2.88	1.24	Preserving the creations and works of the past
3	0.41	3	1.23	3	0.37	3.11	1.16	Enjoyable and unpleasant experience of previous tourists' journey
3	0.41	3.24	1.32	4	0.39	3.06	1.21	The humility and courtesy of the locals
6. Participatory								
1	0.31	3.61	1.11	3	0.35	3.55	1.25	Indigenous peoples share rangelands
3	0.41	2.74	1.12	4	0.37	2.86	1.07	People's participation in management, planning and village decision making
2	0.38	3.2	1.22	2	0.34	3.32	1.13	Establishment of tourism cooperatives
4	0.42	3.07	1.28	1	0.31	3.37	1.06	Rural participation in providing accommodation services to tourists
7. Economic								
3	0.22	3.52	0.78	3	0.27	3.63	0.97	Paying low interest finance and credit facilities to start small businesses
3	0.22	3.53	0.76	2	0.26	3.65	0.97	Spending the proceeds of tourism on the village
1	0.19	4	0.77	1	0.24	3.96	0.93	Development of small and medium-sized handicraft companies
2	0.21	4.1	0.88	4	0.28	3.91	1.1	Improve the quality of handicrafts
8. Ecological Development Indicators								
2	0.23	3.27	0.76	3	0.23	3.24	0.74	Local community participation in village management and decision making
3	0.3	3.73	1.12	4	0.27	3.75	1.01	Optimal use of cultural heritage
1	0.22	3.41	0.76	1	0.2	3.42	0.68	Preserving local cultures
1	0.22	3.3	0.74	2	0.22	3.37	0.74	Local community participation in tourism investment
2	0.23	3.39	0.77	3	0.23	3.36	0.77	Earn economic benefits

In terms of policy making, the formulation of specific laws and regulations to protect the environment has been ranked first by the policy maker, ranking second and third, respectively, from the perspective of household heads, the use of local environmentalists, and the reduction of administrative formalities for investment, respectively. Which has the greatest impact on ecotourism development. But from the perspective of tourists from neighboring countries' security, increased road safety and the deployment of rural environments have been ranked second and third in tourism development. In the area of potentials and attractions in the area, music performances, local celebrations and celebrations are top priority, preservation of historical monuments and religious sites and beautification of roads leading to the village rank second and there are beautiful natural and cultural landscapes and attractions.

The third priority was the one that had the greatest impact on eco-tourism development. From the tourists' point of view, the use of natural building materials in the village, music performances, local celebrations and beautification of the roads leading to the village were among the most important factors affecting eco-tourism development which made the first to third priority in eco-tourism development have dedicated themselves. In terms of management, proper waste management, consideration of indigenous peoples' views in village planning and decision-making, and surveys of policy makers and planners involved with the eco-project were the first to third priorities, respectively, which had the greatest impact on ecosystem development. From the perspective of tourists, surveys of policy makers and planners involved with ecotourism project, first and second priority managers' experience and education and survey of tourists and proper management of rural waste management were the most important factors affecting eco-tourism development.

Both groups shared a common view of the main variables in the social and cultural factor that included, a pleasant and unpleasant experience of previous tourists' journeys, satisfaction of tourists with the facilities and services offered, and the provision of a rural life experience for tourists and the attitude and attitude of locals. As a participatory factor, the villagers' participation in providing accommodation services to tourists, establishing tourism cooperatives and indigenous peoples' use of rangelands is, from a tourist's perspective, including: indigenous peoples' use of rangelands, tourism cooperatives and local people's

participation in management are the planning and decisions of the village. In the economic realm, the development of small and medium-sized enterprises is the production of handicrafts, the spending of tourism revenue on the countryside, and the payment of low-interest financial and credit facilities to start small businesses. Likewise, the three main variables of the economic perspective, from the tourists' perspective, are: Priority development of small and medium-sized handicrafts companies, Improvement of the quality of handicrafts and spending of tourism income in the village and payment of low interest financial and credit facilities to start up. They are small businesses. And in terms of ecotourism development index, preservation of local cultures, participation of local community in investment in tourism sector and economic gain, respectively, they had first to third priority of indicators of ecotourism development and from tourist's point of view, preservation of local cultures, participation The local community has been a top priority in investing in tourism and preserving local cultures is a top priority and optimal use of cultural heritage is a top priority among the indicators of eco-tourism development.

6. Fitting the model and testing the research hypotheses

In this study, the fitting of the model derived from the effect of causal conditions on the axial category in the qualitative section will be investigated. Since in the measurement models a set of observable variables reflects a unique hidden variable that must have the homogeneity and unidimensionality of that model. For this purpose, there are some indicators at the software level to check the reliability of a measurement model. At this point, the weight of the indices related to the hidden external variables is measured. One of these indices is representative or single reliability (reliability of each of the observable variables) (Mohsenin and Esfandyani, 2017). The other two indices used for validity are composite reliability index (CR) and mean variance extracted index (AVE). In order to evaluate the individual reliability of each observed variable, the operating load of each index (observed variable) on the relevant hidden variable should be considered (Henseler and Sarstedt, 2015), if the standard operating load is at least 0.7, Reliability index is required and some others have stated minimum required load factor of 0.5 (Hulland, 1999). Given acceptable values of the fit indices and factor loadings of items for each variable

that for most questions exceeds 0.5. However, a feature called GOF is used to measure model fit obtained by PLS software. But Henseler and Sarstedt (2015) found the index presented by Goodness of Fit Test to evaluate the inefficiency of the inefficient model. In this respect, the most valid characteristic used to evaluate the model fit is the SRMR, which experts believe should be below .08. The standardized value of SRMR in this study was .023. This indicates that the model fits well. Therefore, it can be stated that the research measurement model is at a desirable level and the components sufficiently explain the variance of the conceptual model variables of the research and there is no need for software modification (Table 5).

Table 5: Modified model fit indices for respondents' data

AVE	CR	Cronbach's alpha	Factor Loading	Items	factors
50.7	91.8	90.1	75.4	Local people invest in building ecotourism residences	Economic factors
			75	Export promotion of some local products	
			56.2	Proper marketing to sell local products	
			70.4	Improve the quality of handicrafts	
			78.2	Native people's activities in selling livestock and crops	
			74.8	Spending the proceeds of tourism on the village	
			61.6	Contributing local people to the ecological income	
			69.8	Invest in Medicinal Plants and Traditional Medicine	
			76.6	Development of small and medium-sized handicraft companies	
			68.3	Foreign investment in the village	
			73.9	Paying low interest finance and credit facilities to start small businesses	
52	86.6	81.7	74.1	Introducing and selling herbs	Potentials and Attractions of
			71.9	Music performances, local celebrations and celebrations	
			69	Traditional catering in tents and restaurants	

			74.7	Using natural building materials in the village	
			74.4	There are beautiful natural and cultural landscapes and attractions	
			68.2	Beautifying the roads leading to the village	
57.6	79.6	63.3	86.7	Survey of policymakers, tourists and locals about village planning	Management
			83.4	Proper disposal of village waste	
			53.1	Pay attention to the views of indigenous people in village planning and decision making	
58.1	84.7	76.3	73.6	Rural participation in providing accommodation services to tourists	partnership
			70.1	Indigenous peoples share rangelands	
			78.1	Involvement of local people in management, planning and village decisions	
			82.8	Involvement of local people in environmental protection	
50.7	91.8	90.1	68.9	Educate locals and tourists on environmental issues	Social and cultural
			70.8	Tourist Satisfaction with Hosting, Facilities and Services Provided	
			82	Creating a seasonal exhibition of local produce	
			71.2	Enjoyable and unpleasant experience of the previous tourist trip	
			53.2	Distribution of leaflets and booklets at the entrance of the villages	
			74.6	Installation of a ban on lighting fires and cutting down trees and maintaining hygiene	
			74.2	Providing tourists with the opportunity to experience rural life	
			53.8	Produce and broadcast television programs about village attractions	
58.4	84.8	76.2	75.9	Develop special laws and regulations to protect the environment	policy
			83.3	Giving local people economic priorities	
			67.6	Establishment of an environmental checkpoint in the villages	

			78.1	Government funding for local workshops and crafts	
56.5	86.6	80.8	79.8	Construction of the hotel	Infrastructure
			76.6	Creating a bathroom; green space and children's playgrounds	
			70.6	Asphalt and road improvement of villages	
			71.8	Provides parking and parking space for tents, benches and water.	
			76.8	Increasing ecotourism resorts	
64.4	87.8	81.5	82.6	Local community participation in environmental protection	Development of Ecotourism
			80.6	Earn economic benefits	
			79.4	Preserving local cultures	
			78.4	Indigenous people ignite	

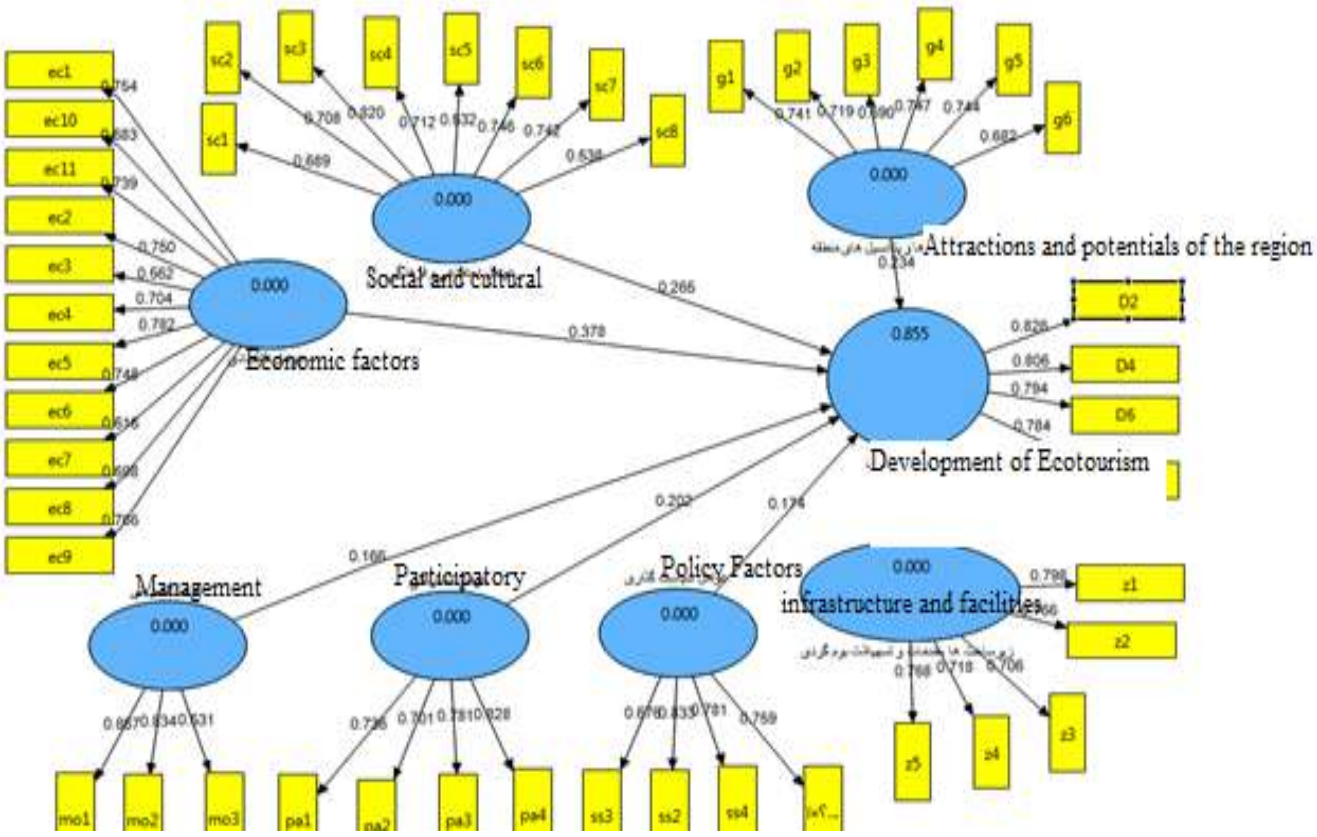

Figure 3: Pls 2 software output and T values

According to the results of the t-test, all path coefficients were significant at 99% confidence level and played a significant role in measuring their structures. According to the standard coefficient it can be said that the region's attractions and potentials (0.223), infrastructure, ecotourism services and facilities (0.077), policy factors (0.174), participatory factors (0.220), Economic factors (0.378), managerial factors (0.166) and social and cultural factors (0.256) influence the development of ecotourism. According to the results of the t-test, all path coefficients were significant at 99% confidence level and played a significant role in the measurement of their structures (Figure 3). Table 5 summarizes the results of the research hypotheses according to the respondents. Since the value of T for all hypotheses is greater than 2.58, all hypotheses are confirmed. Also, considering the path coefficient positive for each of the seven hypotheses, we can say that these seven variables are positive and direct to influence ecotourism development. In order to analyze the value of the path coefficient, it can be stated that, for example, if one percent of economic factors increase, the development of ecotourism for respondents (tourists and head of households of tourism target villages) would increase 38 percent of ecotourism development.

Conclusion

This study was conducted to explain the development of ecotourism in tourism target villages of Kermanshah province. In the current study, ecotourism development is considered as a central issue. The key areas of ecotourism development in this research include the sub-categories of local community participation in conservation, management and decision-making in the ecotourism sector, empowerment of stakeholders (people, investors and other organizations), economic benefit for stakeholders It is intended to benefit, preserve local cultures, and make optimal use of the cultural heritage, and ultimately the indigenous people. These categories, as observed by Shatrian et al. (2018), Karami (2017), and Blancas et al. (2015), are also cited in a statement by the World Ecumenical Association in 2000.The causal conditions are considered to be factors contributing to the development of ecotourism, including economic factors, advertising and information, infrastructure, ecotourism services and facilities, resources, attractions, education, policy, social factors, and so on. It is the cultural, managerial, and

supportive factors that make the economic factor 66 the most abundant among the other factors. And the most important variables affecting the development of ecotourism are interviewees, media outlets, rural attractions, private sector investment, welfare and health facilities, and public participation in environmental protection.

These factors have been mentioned in Omidi Najafabadi et al., (2015) and Blancas et al. (2015). The underlying conditions in this study include the participation and cooperation of tourism stakeholders and ecotourism education. This finding is similar to the (Lane, 2018) and (Hea, 2018) which state that all stakeholders should be involved in tourism development. Quantitative findings showed that most of the subjects in both groups (tourists and heads of households concerned) were men and in both groups the highest frequency was in the age group of less than 45 years. Respondents indicated that a small percentage of the tourists were illiterate (1) and the majority of the educated members of the sample were diplomas and diplomas. The highest percentage of tourists (51.2%) had freelance jobs and the highest percentage of surveyed households (33.8%) had agricultural and animal husbandry jobs.

Findings from factors affecting ecotourism development show that from both groups' viewpoints, increasing the number of ecotourism residences, formulating specific laws and regulations to protect the environment, enforcing music, organizing local celebrations, proper waste management Villages, the pleasant and unpleasant experience of the previous tourist journey, the participation of the villagers in providing accommodation services to the tourists, the development of small and medium-sized handicrafts companies have been top notch. In the inferential section, the findings of the study indicated that 7 main factors including infrastructure, policy factors, attractions and potentials of the region, managerial factors, social and cultural factors, economic factors, participatory factors accounted for 63.5% of the total variance explained. The results indicated that economic factors had a significant effect on ecotourism development. The results have already been confirmed by Khosravi (2007), Baghani (2017), Erkara et.al. (2017) and Birendra & Suman (2018). Management factors also influence ecotourism development. The results confirm the findings of Hajinejad and Yari (2013) and Birendra & Suman (2018).

The results showed that social and cultural factors influence the development of ecotourism. These results are consistent with the research by Garcia (2017) and Shatarian et al (2017). The policy factor also influences the development of ecotourism. The results confirm the research of Funda (2018), Erkara et.al. (2017) and Baghani (2017). In this study, it was found that the factor related to infrastructure, services and facilities of ecotourism had a significant effect on the development of ecotourism, the results of which are consistent with the research of Ghaderi (2004) and Salehi et al. (2016). Also, the region's attractions and potentials have a significant impact on ecotourism development. The participatory factor has a significant impact on the development of ecotourism, which is consistent with the findings of Khosravi (2007) and Daniel (2013). Also, the results of the path coefficients in the model confirm that economic priority factor and socio-cultural factors, factors of regional attractions and potentials, participatory factors, policy factors, managerial and infrastructure factors, services and Ecotourism facilities have the second to seventh priorities, respectively.

Given the quantitative findings of research that is above the average of the averages of effective factors in ecotourism development and the inferential findings of positive, direct and significant effects of these factors in ecotourism development, it is suggested to reconstruct and repair important historical monuments. And archeology, organizing, equipping and preparing mirages and spas, creating and completing hotels and guesthouses for higher tourist satisfaction, a shared vision of the goals and missions of tourism management programs, forming a committee of experts and stakeholders. Tourism as a consultative committee for tourism development Developing road communication networks, providing a peaceful, clean place for tourist use, and protecting the ancient artifacts and landscapes of Kermanshah province.

In future research, reliable results can be obtained by removing the identified dimensions for each variable with low factor loadings. Future researchers can use other software to analyze qualitative data and evaluate concept model fit. One of the innovations of the present study was that for the first time explaining the development of ecotourism with the help of coding has been done. The application of quantitative-qualitative method is one of the newer methods which was less used in the field of ecotourism. While the variables and concepts extracted from the interviews are broad concepts. Another innovation of the present study is the distribution of

questionnaires obtained from interviews with experts and testing of conceptual model extracted by pls2.Despite efforts to fully implement this research, and to provide a framework that contributes to the broadening of the literature on ecotourism development, several limitations remain to be addressed in future research. Including: limited access and inability to interview all experts in this area, ignoring foreign tourists and limited research to the target villages of Kermanshah tourism.

References

Abbas, M.; Shabbir, M. S.; Qayum Mir, N.; Bibi, A.; Siddiqi, A. F. (2019). Ecological Consequences of Climate Change on Pioneer Business, *Revista de la Universidad del Zulia*, 10 (28), 250-259.

Baghani, M. (2017). Impact of Ecotourism on Rural Tourism Development: A Case Study of Saffronia Tourism Area of Sabzevar. M.Sc., Semnan University, Faculty of Tourism, 16: 825–830.

Big Mohammadi, H. and Hatami, M. (2010). Geographical Analysis of Migration Process in East Azarbaijan Province (2006-2006), Geographical Survey of Environmental Statistics, 6: 594–607.

Birendra K.C. R. & Suman, S. N. (2018). Residents' perspectives of a newly developed ecotourism project: an assessment of effectiveness through the lens of an importance–performance analysis, *Journal of Tourism Research*, 23(6), pp 560-572.

Blancas, F. Lozanooyola, M. Gonalez, M. (2015). A European Sustainable Tourism Labels proposal using a composite indicator, Environmental Impact Assessment, Review 54, pp 38-54.

Daniel, J. (2013). Economics Impacts of Tourism,the flasher Press London ,Washington, D.C,6(15), 421-431.

Davoodi, A.S. (2015). An Analysis of the Challenges of Ecotourism Development in Payam Valley, Marand County, Thesis for Master Degree, University of Tabriz, Faculty of Geography and Planning, 27: 84–93.

Ehsani, A. (2016). A Road to Sustainable Tourism, [in Persian], Tehran:Mahkameh Publications.

Erkara, A., Roza, B. & Nurlan, T. (2017). Model of sustainable development of tourism industry in Kazakhstan (regional perspective), VIEŠOJI POLITIKA IR ADMINISTRAVIMAS PUBLIC POLICY AND ADMINISTRATION 2017, 16 (2), pp: 179–197.

Faraji, A. Nematpour, M. And Ashry, A. (2017). Systematic Analysis of the Positive and Negative Impacts of Iranian Tourism Development on the Future Research Approach, Quarterly Journal of Social Tourism Studies, Volume 5, Number 9, pages 151-190.

Funda. Ü. (2018). DünyadaveTürkiye'deEkoturizm, Sosyal-KültürelveEkonomikKatkıları. UlusalÇevreBilimleriAraştırmaDergisi, 1(2), pp: 69-72.

Garcia, M. (2017), "Towards a new approach of destination loyalty drivers: satisfaction, visit intensity and tourist motivations", Current Issues in Tourism, 20(3), pp. 238-260.

Ghaderi, A. (2004). The Role of Rural Tourism in Rural Development, PhD Thesis in Geography and Rural Planning, Tarbiat Modares University, Tehran.

Gigović, L., Pamučar, D., Lukić, D. &Marković, S., (2016). GIS-Fuzzy DEMATEL MCDA Model for the Evaluation of the Sites for Ecotourism Development: A Case Study of Dunavskiključ" Region, Serbia, Land Use Policy, 44: 127 –132.

Hajinejad, A. and Yari, m. (2013). Strategic Ecotourism Planning Using the Combined Model TOPSIS- and SWOT (Case Study of Koohdasht Boulevard Forest Park), Journal of Geography and Development, Volume 11, Number 32, Pages 181-177.

Hea, P. (2018). Evolutionary Analysis of Sustainable Tourism, Annals of Tourism Research, 69 (2018) 76–89.

Heidari A. (2009). Measuring and Explaining the Competitive Advantage of Advanced Technology Enterprises Based on a Model Designed with a Causal Map Approach, Doctoral Thesis, University of Tehran, School of Management.

Henseler, R. & Sarstedt, M. (2015). A new criterion for assessing discriminant validity in variance-based structural equation modeling. Journal of the Academy of Marketing Science, 43(1), 115-135. https://doi.org/10.1007/s11747-014-0403-8

Hulland, J. (1999). Use of partial least squares (PLS) in strategic management research: a review of four recent studies, Strategic Management Journal, Volume20, Issue2,pp: 195-204

Husseini, G. (2014). Wildlife Tourism New Solution for Tourism Development in Qomishlu Region, MA Thesis. Islamic Azad University of Najaf Abad Branch., 263 pages.

Iran Statistics Center (2015). Statistical Yearbook.

Karami, F. (2017). Evaluation of Ecotourism Development Strategies in Arasbaran Region. M.Sc. in Tourism Planning, University of Tabriz, Faculty of Geography and Planning, Department of Geography, 128 pages.

Khosravi, A. (2007). Strategic Analysis of Ecotourism Development in Galiksh City Using SWOT Model. M.Sc., Institute of Higher Education and Development, Faculty of Rural Development and Development, 85 pages.

Lane, B. (2018). Will Sustainable Tourism Research Be Sustainable in the Future? An Opinion Piece, Tourism Management Perspectives, 25 (2018), 161–164.

MacCannel, D. (1976). The Tourist: A New Theory of the Leisure Class. New York: The Macmilan Press LTD: 17, p: 178.

Manochehri, M. (2015). Evaluation of nature hiking ability of dining area using satellite imagery and GIS, MSc thesis, Faculty of Natural Resources, Mazandaran University. 4: 31-37.

Mersangar, M.S. (2006). Ecotourism Strategy Based on Sustainable Development, Journal of Forests and Rangelands, 169; 313–321.

Mohsenin, Sh. and Esfandiani, M. R. (2017). Structural equations based on the partial least squares approach with the help of Smart-PLS software (educational and practical). Tehran, Mehraban Book Publishing Institute, Second Edition, p: 70

Omidi Najafabadi, M. Haghbin, A. Farajullah Hosseini, J. (1395). Investigating the factors affecting the development of eco-tourism; Case study: Little Lavasan, Quarterly Journal of Agricultural Extension and Education Research, Year 9, No. 3, pp. 11-22.

Razvani, M. and Bayat (2013). Analysis of Rural Tourism Position in Large Development Plans of the Country (with Emphasis on Five-Year National Development Plans), 8: 4428–4433.

Salehi, S. (2016). ―Bvmgrdy development in the village of Janat Rudbar with an emphasis on the participation of local communities‖. Administration of Cultural Heritage, Handicrafts and Tourism Organization of Mazandaran[In Persian].

Salici, A. (2018). Application of ecotourism opportunities spectrum method in ecotourism resources: a cas study of samandag costal areas in southern turkey. *Applied Ecology and Environmental Research* , 16(3), pp.2701-2715 .

Sepahvand, R. Jafari, M.P. and Amin, A. (2018). Strategic Planning for Rural Ecotourism Development (Case Study: Village of Bisheh Station), Human Geography Research, 207: 604–611.

Shatarian, M. Kiani Salami, P., Gholami, P. And, Lately, Z. (2017). Prioritizing the Factors Influencing the Nature Development of Rural Areas of Borzak-Kashan by Combining ANP and DEMATEL Techniques, Journal of Geographical Applied Research, 331: 361–375.

Shatrian, M. KianiSalmi, P. and Zormand, P. (2018). Causal Identification and Explanation of Factors Affecting Entrepreneurial Opportunities in Desert Areas Using Ecotourism Approach (Case Study: Maranjab Desert, Iranian Journal of Geography Association, 141: 291–299.

Tehran Chamber of Commerce, Industries, Mines and Agriculture. (2018). Iran's position in the Travel and Tourism Competitiveness Index 2017, Vice President of Economic Studies, available at http://otaghiranonline.ir/ Accessed 25 October 2018.

Comparative floral and pollen morphology of some invasive and native impatiens species

Yulia Konstantinovna Vinogradova *
Alla Georgievna Kuklina **
Ekaterina Vasilyevna Tkacheva ***
Andrey Sergeevich Ryabchenko ****
Maksim Igorevich Khomutovskiy *****
Olga Vladimirovna Shelepova ******

ABSTRACT

To evaluate the hypothesis of competitive superiority of invasive species, we compared the invasive *Impatiens parviflora* DC. and *I. Glandulifera* royle, the naturalized *I. Nevskii* pobed. and the native *I. Noli-tangere* L. in the flowers' morphometric characters at different phases of anthesis. The characters in which alien species have a competitive superiority over closely related *I. Noli-tangere* are revealed. Morphological variability was studied by morphometric observations of the following characters: bud: length and diameter; spurred sepal: length and width; spur: length and diameter; lateral sepal: length and width; largest petal: length and death; large lobe of lateral petal: length and width; small lobe of lateral petal: length and width; anther: length; stamen's filament: length; calyptra: length and width; ovary: length and diameter; length of a style, length of a stigma. There is a tendency for alien Impatiens species of the earlier development of androecium and gynoecium: caliptra is formed at the stage of uncolored bud, the pistil is differentiated in ovary, short style and stigma is formed at the stage of colored bud. No other flowers' morphometric characters, representing competitive advantage of the invasive *I. Glandulifera* and *I. Parviflora* over the native *I. Noli-tangere* and naturalized *I. Nevskii* were identified.

KEYWORDS: *Impatiens*, alien species, invasion, floral biology.

* Doctor of biological Sciences, Chief researcher_Flora Department, Tsitsin Main Moscow Botanical Garden of the Russian Academy of Sciences (Moscow, Russia) ORCID: 0000-0003-3353-1230.
** Candidate of biological Sciences, Senior researcher_Flora Department, Tsitsin Main Moscow Botanical Garden of the Russian Academy of Sciences, (Moscow, Russia) ORCID: 0000-0002-9783-7776.
*** Candidate of biological Sciences, Senior researcher Library for Natural Sciences of the Russian Academy of Sciences (11/11 Znamenka street, 119991, (Moscow, Russia) ORCID: 0000-0001-5893-8243.
**** Candidate of biological Sciences, Senior researcher Laboratory of physilogy and immunity of plants, Tsitsin Main Moscow Botanical Garden of the Russian Academy of Sciences (Moscow, Russia) ORCID: 0000-0001-5200-1273.
***** Candidate of biological Sciences, Senior researcher Laboratory of Landscape Architecture, Tsytsin Main Moscow Botanical Garden of the Russian Academy of Sciences (Moscow, Russia)//Candidate of biological Sciences, Leading researcher Department of Geobotany, Biology Faculty of Lomonosov Moscow State University (Moscow, Russia). ORCID: 0000-0003-1121-6512.
****** Candidate of biological Sciences, Senior researcher Laboratory of physilogy and immunity of plants, Tsitsin Main Moscow Botanical Garden of the Russian Academy of Sciences (Moscow, Russia) ORCID: 0000-0003-2011-6054.

Recibido: 04/05/2020 Aceptado: 01/07/2020

Comparación de morfología floral y polen de algunas especies de Impatiens invasoras y nativas

RESUMEN

Para evaluar la hipótesis de la superioridad competitiva de las especies invasoras, comparamos la invasiva Impatiens parviflora DC. e I. Glandulifera royle, la I. Nevskii pobed naturalizada y el nativo I. Noli-tangere L. en los caracteres morfométricos de las flores en diferentes fases de la antesis. Se revelan los caracteres en los que las especies exóticas tienen una superioridad competitiva sobre I. Noli-tangere estrechamente relacionada. La variabilidad morfológica se estudió mediante observaciones morfométricas de los siguientes caracteres: brote: longitud y diámetro; sépalo estimulado: largo y ancho; espuela: longitud y diámetro; sépalo lateral: largo y ancho; pétalo más grande: longitud y muerte; lóbulo grande de pétalo lateral: largo y ancho; lóbulo pequeño de pétalo lateral: largo y ancho; antera: longitud; filamento del estambre: longitud; caliptra: largo y ancho; ovario: longitud y diámetro; longitud de un estilo, longitud de un estigma. Hay una tendencia para las especies exóticas de Impatiens del desarrollo anterior de androceo y gineceo: el caliptra se forma en la etapa de yema incolora, el pistilo se diferencia en ovario, el estilo corto y el estigma se forma en la etapa de yema coloreada. No se identificaron los caracteres morfométricos de otras flores, que representan una ventaja competitiva de la I. Glandulifera e I. Parviflora invasoras sobre la I. Noli-tangere nativa y la I. Nevskii naturalizada.

PALABRAS CLAVE: Impatiens, especies exóticas, invasión, biología floral.

Introduction

Potentially invasive species can be identified before they start to spread by comparing their traits with those of successful invaders. A powerful tool for delimiting the traits associated with invasiveness are analyses of a number of species of the same genus. Since the influence of traits on invasion success may differ with respect to the stage of the plant's life cycle, comparative studies should address the whole life cycle (Cuda et al., 2016).

This study is a continuation of a series of works on the micromorphological study of flower organs in invasive taxa belonging to *Lupinus* L. (Vinogradova et al., 2012), *Robinia* L. (Vinogradova et al., 2013) and *Caragana* Fabr. (Kuklina et al., 2015; Vinogradova, 2016). It was found that the signs by which invasions can be predicted, apparently, are not common to all taxa. Even among worst invasive species, there is not any plant with all the characteristics of the "ideal weed" (Vinogradova et al., 2010). In this article, we compared flower biology of alien *Impatiens* species with the native *Impatiens noli-tangere* L.

Impatiens noli-tangere, - native in Europe from Scandinavia to the Apennines and temperate Asia to the Pacific (Pobedimova, 1949). Pollinated by bees.

I. glandulifera Royle (= *I. roylei* Walp.) is an Asian ornamental plant introduced to Europe in the XIXth century from the Himalayas, becoming established as an escape from cultivation in Europe and North America (Clements et al., 2008; DAISIE, 2019; Maslo and Šaric, 2019). The species is included in the Black Book of the Flora of Central Russia (Vinogradova et al., 2010) and the Black Book of the Flora of Siberia (Ebel et al., 2016). As a result of the expansion of *I. glandulifera*, the native populations of *I. noli-tangere* are declining (Daumann, 1967). *I. glandulifera* outcompetes native plant communities for pollinators (Bartomeus et al., 2010).

I. parviflora DC., is one of the most widespread invasive plant species in Central Europe (DAISIE, 2019; Maslo and Šaric, 2019). This species disturbs the natural vegetation composition in many European forests where it is frequently mixed with the native *I. noli-tangere*. Extinctions have sometimes been reported for *I. noli-tangere*, and knowledge is lacking about the possible contribution of *I. parviflora* to this phenomenon (Godefroid and Koedam, 2010). Nevertheless, both mechanisms and consequences of its invasion are still poorly understood (Reczynska et al., 2015; Jarcuska et al., 2016; Florianova and Munzbergova, 2017; Skálová et al., 2019).

I. nevskii Pobed., naturally grows in Central Asia (Pobedimova, 1949). Currently, the taxonomic status of *I. nevskii* is not defined: "not establish this name either as an accepted name or as a synonym with original publication details: Fl. URSS 14: 746 1949 (The Plant List). Our early research showed that *I. parviflora* and *I. nevskii* have overlapping natural distribution ranges, a similar ecology, similar phenology, morphology of flowers and seeds both in nature and in the garden experiment, which causes doubt of the species autonomy of *I. nevskii* (Maitulina, 1988; Vinogradova et al., 2010).

Flowers of all studied species are hermaphrodite, strongly zygomorphic, combined in racemes. Sepals 3, petaloid; the lowest (the posterior sepal is at the bottom of the flower because of the twisting of the pedicel) large and spurred; the 2 lateral small. Petals 5, the upper one is large, the 4 lower usually united in pairs on each side of the flower. Stamens 5, filaments broad, short, connate above; anthers connate round the ovary forming a deciduous calyptra. Ovary with a short style, and a single stigma or 5 stigmas (Gleason and Cronquist, 1993; Clapham et al., 1962).

The purpose of this study is an attempt to identify the characteristics contributing to the wide resettlement of alien *I. parviflora* and *I. glandulifera*. The objective of this study is a comparative analysis of the micromorphology of the flower during different stages of development in taxa of the genus *Impatiens*: native *I. noli-tangere*, invasive *I. parviflora*, invasive *I. glandulifera* and alien *I. nevskii* showing low capability of naturalization.

1. Materials and methods

We studied four species of *Impatiens* spontaneously growing in the Main Botanical Garden Russian Academy of Sciences (Moscow, Russia). Some samples were collected in other localities (Table).

Table. Localities of studied *Impatiens* samples

Taxon	Locality	Latitude	Longitude
I. noli-tangere	Russia, Moscow, Ostankino, protected oak forest in the Main Botanical Garden named after N.V. Tsitsin Russian Academy of Sciences	55°49′N	37°35′E
I. glandulifera	Russia, Moscow, Zelenograd district, bank of the Skhodnya river	55°98′N	37°19′E
I. glandulifera	Russia, Moscow, Ochakovo, General Dorokhov street, bank of the Setun- river	55°69′N	37°47′E
I. parviflora	Russia, Moscow, Ostankino, protected oak forest in the Main Botanical Garden named after N.V. Tsitsin Russian Academy of Sciences	55°49′N	37°35′E
I. parviflora	Russia, Moscow, Mytishchi, the national reserve «Losinyy Ostrov»	55°89′N	37°76′E
I. nevskii	Russia, Moscow, Main Botanical Garden named after N.V. Tsitsin Russian Academy of Sciences	55°98′N	37°19′E

For the analysis, the flowers were collected from 5-10 individuals per the species at the following stages of development: (I) the phase of beginning of budding (buds are green), (II) the phase of budding (buds are colored, (III) the phase of beginning of flowering, (IV) the phase of full flowering, (V) – ending of flowering and beginning of fruiting. The morphological and biometric traits of different organs of the flower were determined using a Keyence VHX 1000 digital microscope. The sampling was 10 fresh

flowers at each of the first two phases of development and 30–40 flowers at the subsequent phases. The morphological variability was defined by morphometric investigations of the following characteristics: bud length (BL), bud diameter (BD), spurred sepal, length (SSL), spurred sepal, width (SSW), length of the spur (SL), diameter of the spur (SD), lateral sepal, length (LSL), lateral sepal, width (LSW), largest petal, length (LPL), largest petal, width (LPW), large lobe of lateral petal, length (LLPL), large lobe of lateral petal, width (LLPW), small lobe of lateral petal, length (SLPL), small lobe of lateral petal, width (SLPW), anther, length (AL), stamen's filament, length (FL), calyptra, length (CL), calyptra, width (CW), ovary, length (OL), ovary, diameter (OD), length of style (STL), length of stigma (OSL). The size of the freshly collected pollen without water on a glass slide was calculated; the pollen fertility was determined by staining the pollen grains with acetocarmine under slight heating. The total number of pollen grains for each species to determine their size is 30-50. The average volume of the pollen was determined according to the formula for ellipsoid: $4/3\pi(l/2)(d/2)^2$. The scanning electron microscope LEO 1430 VP (Zeiss, Oberkochen, Germany) was used for examining the pollen and its exine surface of different taxa of *Impatiens*. Specimens were observed in a high vacuum, at magnification from x400 (overview) to x5000, accelerating voltage of 20 kV, and operating distance of 9 mm. Air-dried specimens were mounted directly on copper plates, underwent cathode sputtering with gold in argon, and then were viewed in a high vacuum. Special fixation of the material was not applied because of specimens' air-drying, which resulted in maximal preservation of the biological objects' native structure. Basic statistical analyses were performed using Microsoft Excel and PAST 2.17. Data was analysed with ANOVA test and differences between means compared through the Tukey-Kramer test ($\alpha = 0.05$). The statistical significance of differences of morphometric traits was tested by the Student's *t*_test.

2. Results

Impatiens noli-tangere (Fig.1)

Phase I (Beginning of budding): The inflorescences started to form in early June. The buds are green, 3.3×1.9 mm in lenght, the corolla is completely hidden in the calyx. Lateral sepal is 3–4 mm long and 0.3–0.5 mm wide. Spurred sepal is 3-3.5 mm long and 0.8

mm depth, but the spur isn't visible yet. The largest uncoloured petal is 2.9-3.2 mm long and 1.3–1.5 mm wide.

Phase II (Budding): The buds are greenish-yellow, 5.2×3.1 mm. Lateral sepal is 3.8–5.2 mm long and 2.8–3.6 mm wide. Spurred sepal is 4-5.1 mm long and 2.8-5 mm depth with a spur 4-4.5 mm long and 0.4 mm diameter. The corolla projects over the calyx. The largest petal is 3.7×2.9 mm. Each of the five stamens have filament ~0.4 mm long and white free anther 2.5-3.1 mm long. The undifferentiated ovary length is 1.8 mm.

Phase III (Beginning of flowering): The open buds are yellow, 8.1×4.5 mm. Yellow lateral sepal is 3.9 mm long and 4.0 mm wide. Spurred sepal is 7 mm long and 5.3 mm depth with a curved spur 8.2 mm long and 0.8 mm diameter. The largest petal is 7.0×4.8 mm, bright yellow with small brown spots.

The large lobe of lateral petal is 8.5×4.4 mm, and the small one is 4.1×2.0 mm. Staminal filament is 0.9 mm, the length of anthers is 1.8-2.9 mm. The pistil (3.1 mm long) is slightly differentiated into the ovary (2.5×0.7 mm) and stigma (0.3 mm long). The style isn't visible.

Phase IV (Full flowering): The size of the lateral sepal increases (6.5-6.9×3.9-4.0 mm). Spurred sepal is 7.2 mm long and 9.5 mm depth with a curved spur 10.7 mm long and 3.2 mm diameter. The largest petal is 7.6×10.9 mm. The large lobe of lateral petal is 15.3×13.6 mm, and the small one is 6.9-7.6×3.3-3.5 mm. The anthers connate round the ovary forming a calyptra 3.6×1,5 mm. They release pollen and decrease in size. The pistil total length reaches 3.2–4.6 mm (the stigma is 0.3 mm and the ovary is 2.5–3.8 mm long and 0.8–0.9 mm in diameter). The style isn't visible.

Ending of flowering and beginning of fruiting (Phase V): The corolla turns brown and falls off. The staminal filaments drive off at the base, and the calyptra falls off completely together with them. The fruit is formed only in two or three flowers per raceme and contains 2-3 seeds.

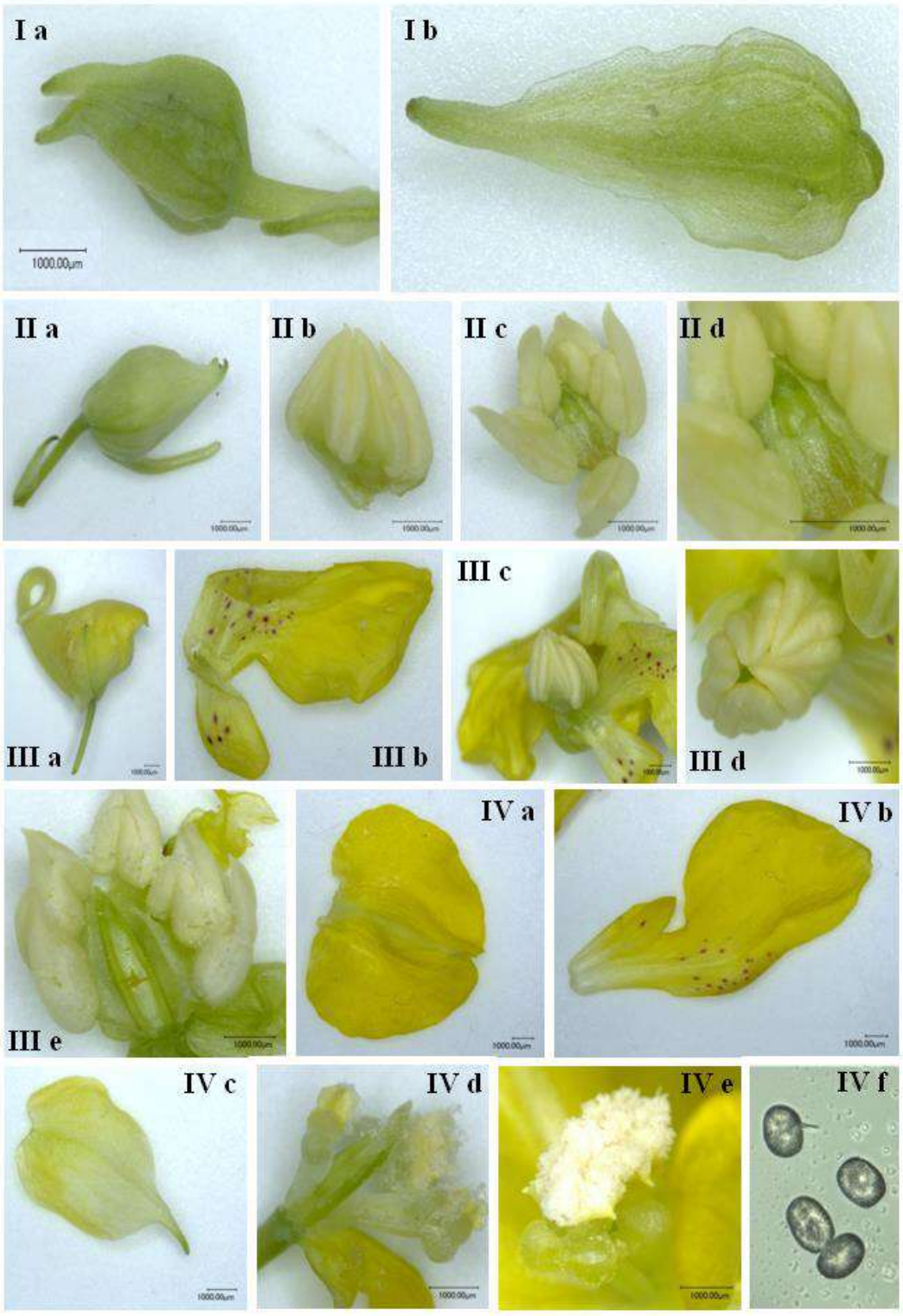

Figure 1. *Impatiens noli-tangere*

I – Beginning of budding: a –bud; b – large petal; II – Budding: a – bud; b – androecium; c – stamens and ovary; f – ovary; III – Beginning of flowering: a –bud; b – lateral petal; c – androecium and corolla; d – androecium; e – ovary; IV – Full flowering: a – large petal; b – lateral petal; c – lateral sepal; d – ovary and corolla; f – pollen.

Impatiens glandulifera (Fig.2)

In contrast to *I. noli-tangere*, *I. glandulifera* begins to bloom a half month earlier and continues to bloom almost to frost. The raceme has an average up to ~100 flowers during the growing season. Flowers are purplish, pink, and rarely white.

Phase I (Beginning of budding): The buds are green 4.7–5.8×4.0–5.2 mm, the corolla is completely hidden in the calyx. Lateral sepal is 6.5–7.6 mm long and 3.9–4.8 mm wide. Spurred sepal is 7.2–9.1 mm long and 2.6–5.6 mm depth, with a spur 1.8–2.6 mm long and 0.5–0.8 mm diameter. The largest uncolored petal is 5.7–6.1 mm long and 5.6–6.1 mm wide. The large lobe of lateral petal is 6.6–7.4×2.8–3.2 mm, and the small one is 3.1–4.1×2.6–3.6 mm. Stamens have filament 1.5–1.9 mm long and white free anther 4.0–4.6 mm long. The pistil is differentiated in ovary (1.4–1.6 mm length) and stigma (0.5 mm length).

Phase II (Budding): The buds are colored, 9.6–9.7×5.5–8.6 mm. Lateral sepals are 7.4–10.3 mm long and 3.7–5.5 mm wide. Spurred sepal is 11.3–13.2 mm long and 4.4–7.5 mm depth with a spur 3.8–6.5 mm long and 0.9–1.2 mm diameter. The corolla projects over the calyx. The largest petal is 7.3–10.1×9.6–9.7 mm. The large lobe of lateral petal is 7.9–12.1×4.7–6.9 mm, and the small one is 4.2–6.1×6.0–9.4 mm. The stamens have filament 2.2–3.9 mm long and white free anther 4.4–5.8 mm long. The pistil is differentiated in ovary 2.4–3.6×1.4 mm, style 0.1–0.7×0.3 mm and stigma 0.5–0.7×0.1–0.3 mm.

Phase III (Beginning of flowering): The open buds are pink or purple. Lateral sepal is 9.4 mm long and 4.2 mm wide. Spurred sepal is 13.0–14.0 mm long and 7.3 mm depth with a spur 5.4–6.6 mm long and 1.2 mm diameter. Staminal filament is 3.7–4.9 mm, the length of anthers is 4.8–5.2 mm. The anthers connate round the ovary forming a calyptra.

Phase IV (Full flowering): The size of the lateral sepal increases 7.1–9.4×4.1–5.3. Spurred sepal is ~17 mm long and 19 mm depth with a short erect spur 5–6 mm long and 1–2 mm diameter. The largest petal is 12–14×19–22 mm. The large lobe of lateral petal is 28.3–39.6×13.7 mm, and the small one is 11.0–11.7×8.9–10.0 mm. The anthers connate round the ovary forming a calyptra 4.7×4.2 mm. They release pollen and decrease in size. The pistil total length reaches 4.5–5.1 mm (the stigma is 0.6–1.0 mm, the style is 0.4 mm, and the ovary is 3.5–3.8 mm long and 1.6 mm in diameter.

Ending of flowering and beginning of fruiting (Phase V): As well as *Impatiens noli-tangere*, the corolla turns brown and falls off. The staminal filaments drive off at the base, and the calyptra falls off completely together with them. Almost every flower forms a fruit.

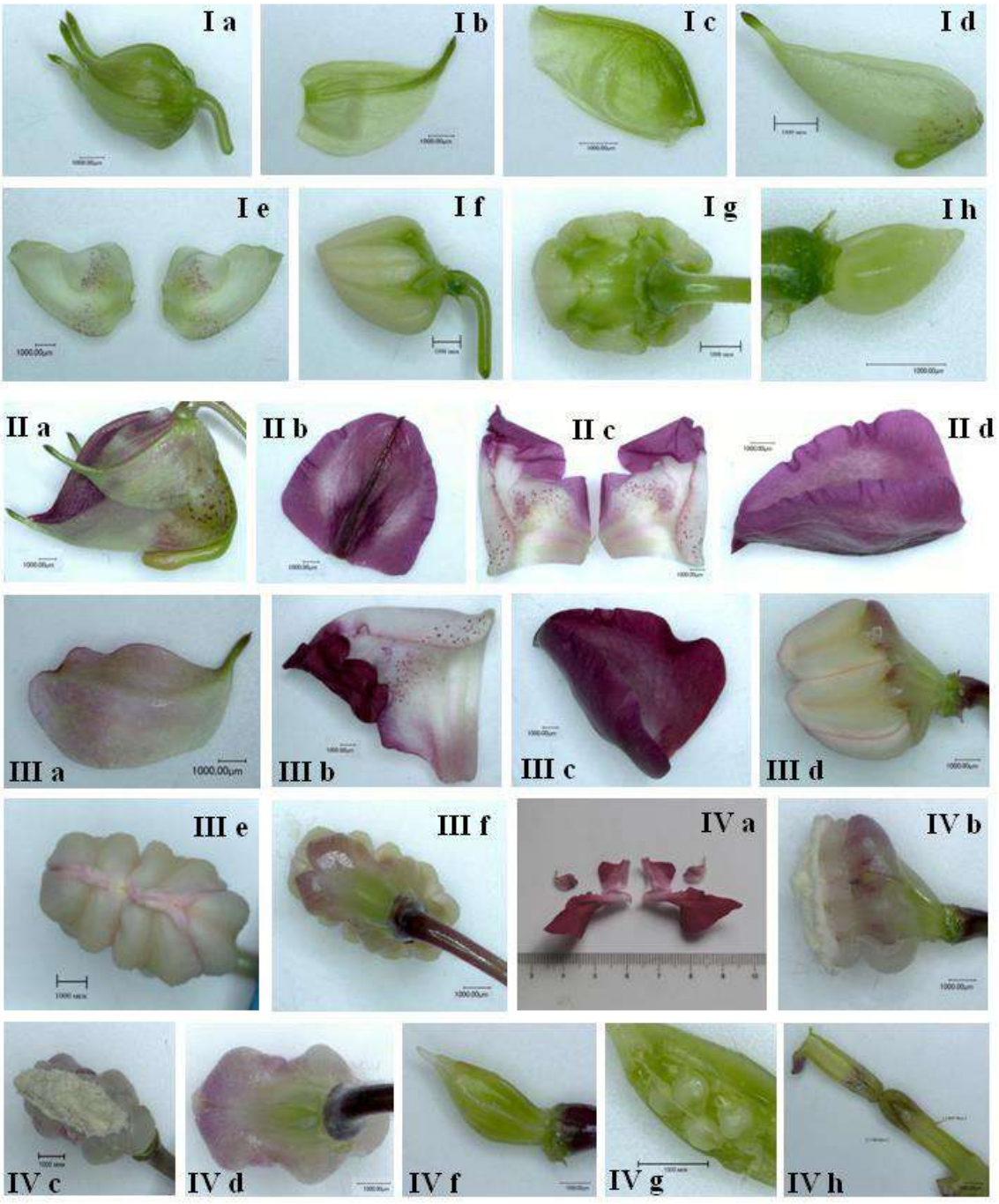

Figure 2. *Impatiens glandulifera*

I – Beginning of budding: a – bud; b – lateral sepal; c – large petal; d – spurred sepal; e – two lateral petals; f – androecium; g – stamen's filament; h – ovary; II – Budding: a – bud; b – large petal; c – two lateral petals; d – largest petal; III – Beginning of flowering: a – lateral sepal; b – lateral petal; c – largest petal; d – androecium; e – calyptra, top view; f – calyptra and stamen's filament, bottom view; IV – Full flowering: a – two lateral petals; b – calyptra, side view; c – calyptra, top view; d – calyptra and stamen's filament, bottom view; e – ovary; f – ovules.

Impatiens parviflora (Fig.3)

In contrast to *I. noli-tangere*, *I. parviflora* begins to bloom a half month earlier and continues to bloom almost to frost (similar with *I. glandulifera*). The raceme has an average up to 50 flowers during growing season.

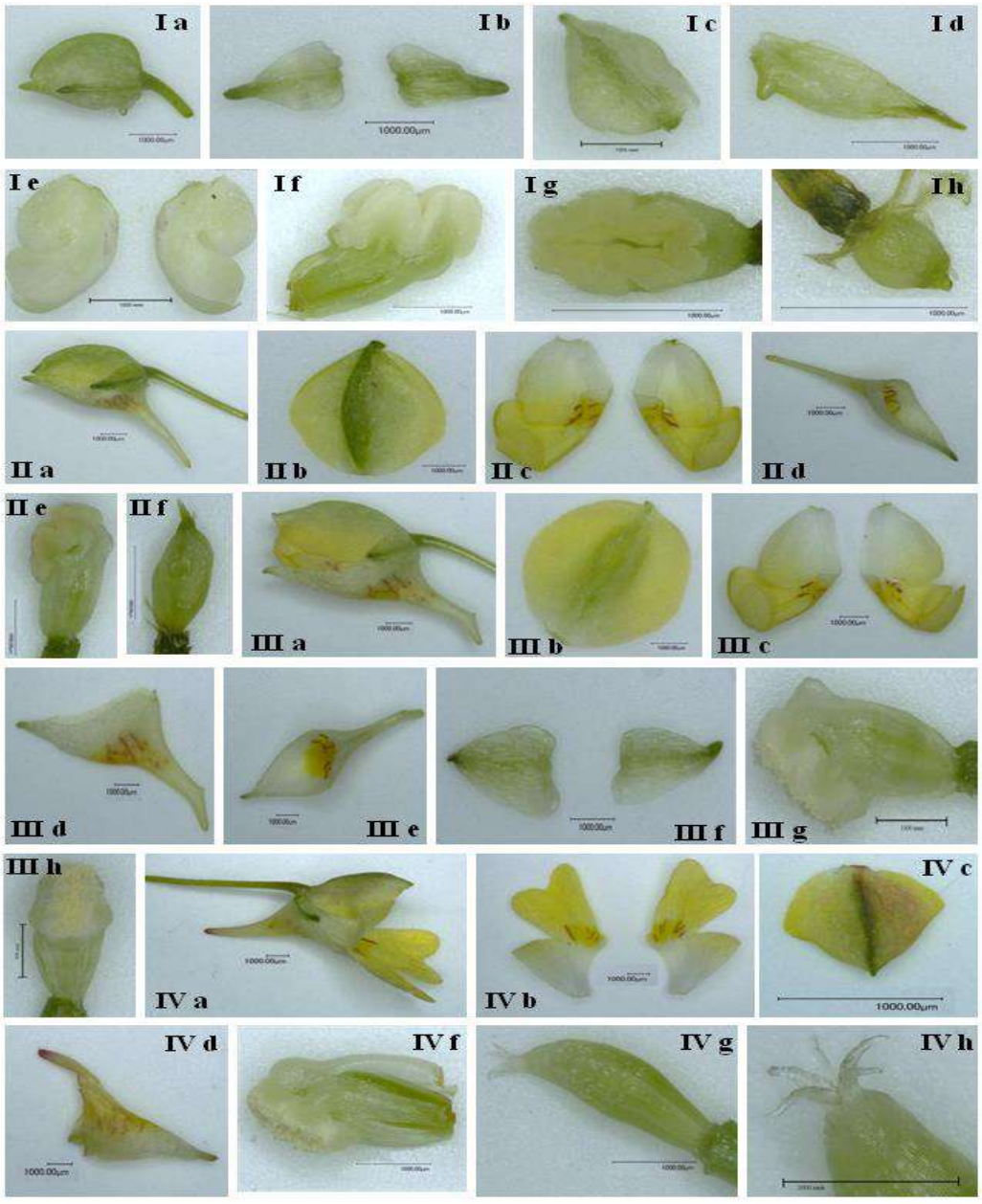

Figure 3. *Impatiens parviflora*

I – Beginning of budding: a – bud; b – lateral sepal; c – large petal; d – spurred sepal; e – two lateral petals; f – androecium; g – calyptra, side view; h – ovary; II – Budding: a –bud; b – large petal; c – two lateral petals; d – spurred sepal; e – androecium; f – ovary; III – Beginning of flowering: a – bud; b – large petal; c – two lateral petals; d – spurred sepal, side view; e – spurred sepal, top view; f – lateral sepal; g – androecium; h – ovary; IV – Full flowering: a – flower, side view; b – two lateral petals; c – large petal; d – spurred sepal, side view; f – androecium, side view; g – ovary; h – five stigmas.

Phase I (Beginning of budding): The buds are green, smaller than both above mention species, 2.6-3.1×2.0-2.1 mm. Lateral sepal is 1.7–1.9 mm long and 1.0–1.2 mm wide. Spurred sepal is 2.8-3.3 mm long and 0.7-0.8 mm depth, with a spur 0.1-1.0 mm long and 0.1-0.3 mm diameter. The largest uncolored petal is 2.6-3.9 mm long and 2.0-3.7 mm wide. The large lobe of lateral petal is 2.2-3.2×1.0-1.1 mm, and the small one is 1.1-1.6×1.0-1.3 mm. Stamens have filament 1.0-1.3 mm long. White anthers 4.0-4.6 mm long connate round the ovary forming a calyptra 1.0-1.3×0.8-1.0 mm. The pistil is differentiated in the ovary (0.6-0.8 mm length), the style (0.1 mm length) and stigma (0.1-0.2 mm length).

Phase II (Budding): The buds became colored, 3.6-5.7×2.7-3.7 mm. Lateral sepals are ~2.7 mm long and 1.2–1.6 mm wide. Spurred sepal is 3.9-5.8 mm long and 0.9-2.1 mm depth with a spur 0.9-4.9 mm long and 0.3-0.9 mm diameter. The corolla projects over the calyx. The largest petal is 2.9-3.9×3.0-3.8 mm. The large lobe of lateral petal is 3.3-5.2×1.6-2.5 mm, and the small one is 1.6-2.7×1.9-2.5 mm. The stamens have filament 1.6-2.4 mm long. White anthers 0.7-1.0 mm long form a calyptra 1.5×1.1 mm. The pistil is differentiated in ovary 1.3-1.9 mm length, style 0.1 mm length and stigma 0.3 mm length.

Phase III (Beginning of flowering): The open buds are pale-yellow. Lateral sepal doesn't increase as compare with phase II. Spurred sepal is 6 mm long and 2-3 mm depth. The largest petal is 5.0×4.6 mm. Staminal filament is 2.4-2.5 mm, calyptra is 1.7×1.1 mm.

Phase IV (Full flowering): Spurred sepal is 5.7-6.2 mm long and 4.2-5.6 mm depth. The largest petal is 5.3×5.2 mm. The large lobe of lateral petal is 9.0-11.0×3.5-3.9 mm, and the small one is 4.4×2.8-4.6 mm. Staminal filament is 2.4-2.5 mm, calyptra is 1.7×1.1 mm. The pistil is differentiated in ovary 2.0 mm length, style 0.3 mm length and stigma 0.3 mm length.

Ending of flowering and beginning of fruiting (Phase V): Almost every flower forms a fruit.

Impatiens nevskii (Fig.4)

I. nevskii differs from *I. parviflora* only in the lilac (vs. yellow) color of the corollae. No differences in all other studied parameters were noted. Multivariate analysis and pairwise Hotelling's tests of morphological variability of quantitative traits of I. nevskii and I. parviflora showed the fail of statistically significant differences (Wilks' lambda 0.9; P <

0.0001) between the species. This gave us reason to "close" this species and consider it to be the lilac-flowered form of *I. parviflora* (Maitulina, 1988).

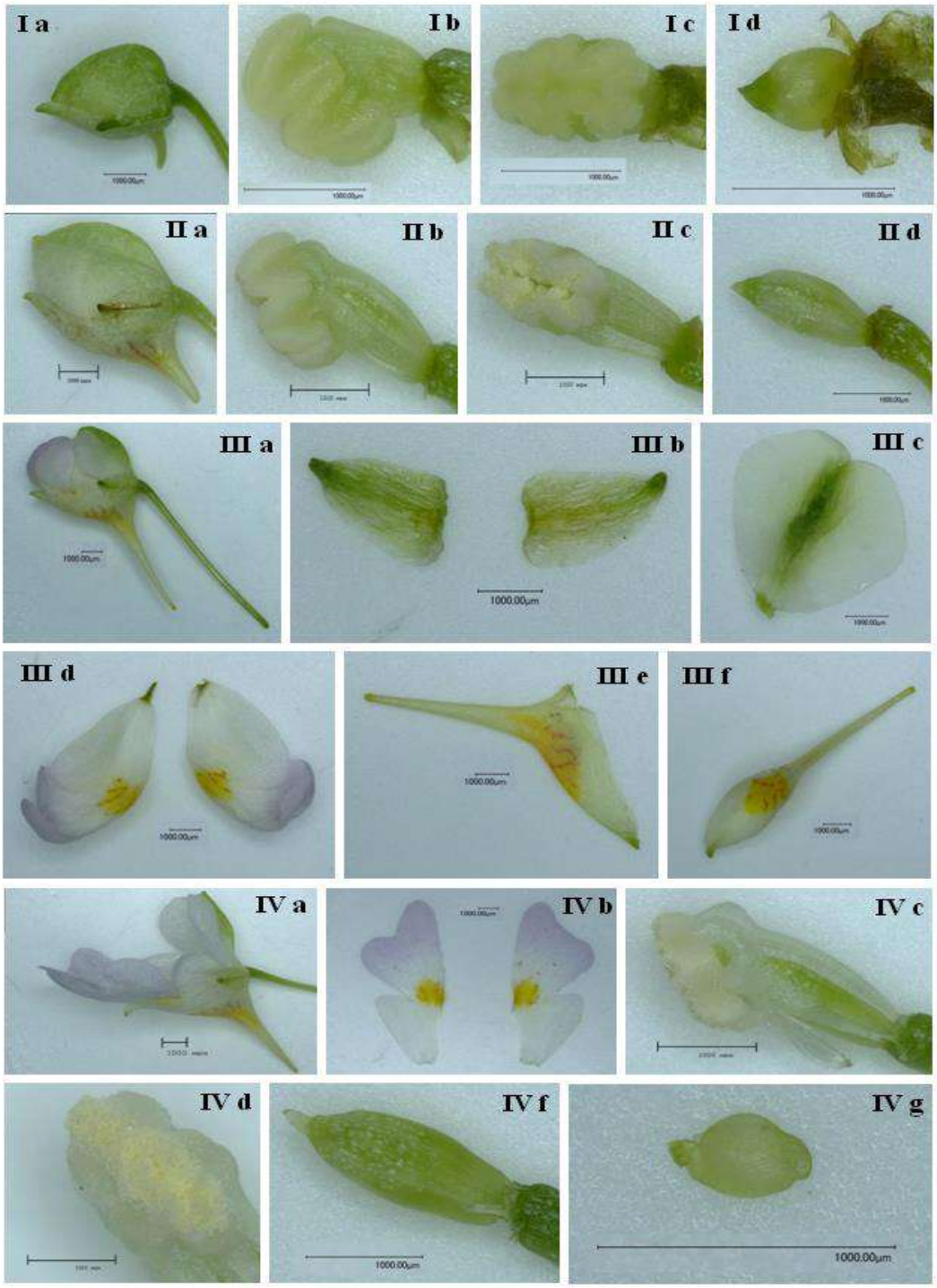

Figure 4. *Impatiens nevskii*

I – Beginning of budding: a – bud; b – androecium, top view; c – calyptra, top view; d – ovary; II – Budding: a – bud; b – androecium, top view; c – calyptra, top view; d – ovary; III – Beginning of flowering: a – bud; b – two lateral sepals; c – large petal; d – two lateral petals; e – spurred sepal, side view; f – spurred sepal, top view; IV – Full flowering: a – flower, side view; b – two lateral petals; c – androecium, side view; d – calyptra, top view; f – ovary; g – ovules.

The discriminant analysis between the four species made it possible to completely separate them. The plot (Fig. 5) shows that the *I. noli-tangere* and *I. glandulifera* data clouds diverge greatly. And only samples *I. nevskii* and *I. parviflora* tend to cluster close to each other.

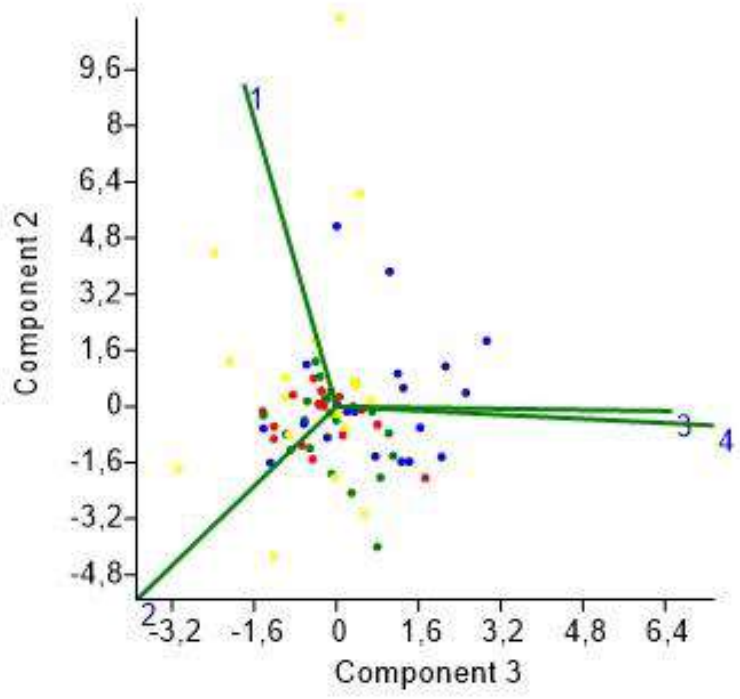

Figure 5. Morphometric parameters of flower in *Impatiens* species at different phases of development

1 - *I. noli-tangere*, 2 - *I. glandulifera*, 3 - *I. parviflora*, 4 - *I. nevskii*.

We studied the variability of sizes and shapes of the pollen in the four taxa (Figs. 6 and 7).

All studied taxa have medium-sized colpate pollen (Vinogradova and Kuklina, 2016; The Plant List). In native *I. noli-tangere*, the pollen grains are small: the mean length of polar axis (l) is 24.91±0.29 μm, and their mean equatorial diameter (d) is 17.71±0.26 μm; shape index (the ratio of length to diameter) is 1.4. The pollen fertility is quite low, 39%.

In invasive *I. glandulifera*, the pollen sizes are small, too: the mean length of polar axis (l) is 27.16±0.21 μm, and their mean equatorial diameter (d) is 16.36±0.18 μm; shape index is 1.7. The pollen fertility is high, up to 98%.

In invasive *I. parviflora*, the pollen is finer: the mean length of polar axis (l) is 32.39±0.25 µm, and their mean equatorial diameter (d) is 22.00±0.27 µm; shape index is 1.5. The pollen fertility is high, up to 98%.

In naturalized *I. nevskii*, the pollen is the largest: the mean length of polar axis (l) is 34.94±0.29 µm, and their mean equatorial diameter (d) is 20.49±0.21 µm; shape index is 1.7. The pollen fertility is high, up to 95%.

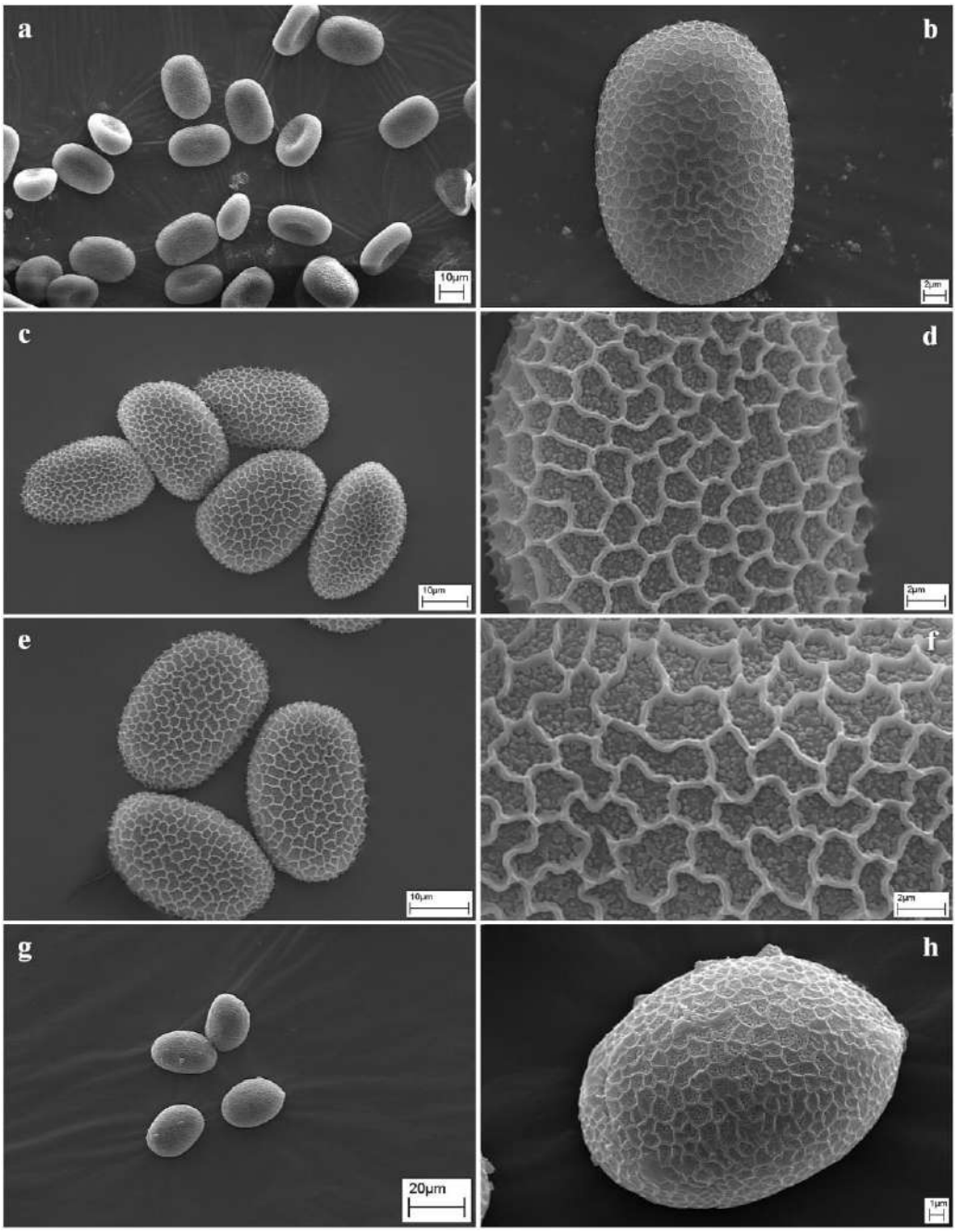

Figure 6. Pollen and its exine surface of different taxa of *Impatiens*

a, b – *I. glandulifera;* c, d – *I. parviflora;* e, f – *I. nevskii;* g, h – *I. noli-tangere.*

Thus, the size of the pollen grain decreases in the order *I. parviflora* → *I. nevskii* → *I. noli-tangere* → *I. glandulifera*. The largest pollen grains are observed for *I. parviflora* and *I. nevskii*. In *I. parviflora*, the volume fluctuates from 4987 to 11433 (mean 8291±235 μm^3). In *I. nevskii*, the volume fluctuates from 5645 to 9517 (mean 7710±175 μm^3). These two species aren't statistically different each from other on this parameter. The pollen grains of *I. glandulifera* are twice smaller: the volume fluctuates from 2013 to 6166 (mean 3873±104 μm^3). Native *I. noli-tangere* isn't different from invasive *I. glandulifera* on the average volume of pollen: it fluctuates from 2020 to 5719 (mean 4131±142 μm^3).

Four species differ also in a shape of pollen. Pollen grains are elongate (l/d› 1.5) for *I. glandulifera* and *I. nevskii*. Pollen grains of *I. parviflora* are oval (l/d = 1.5), and pollen grains of *I. noli-tangere* are rounded (l/d ‹1.5).

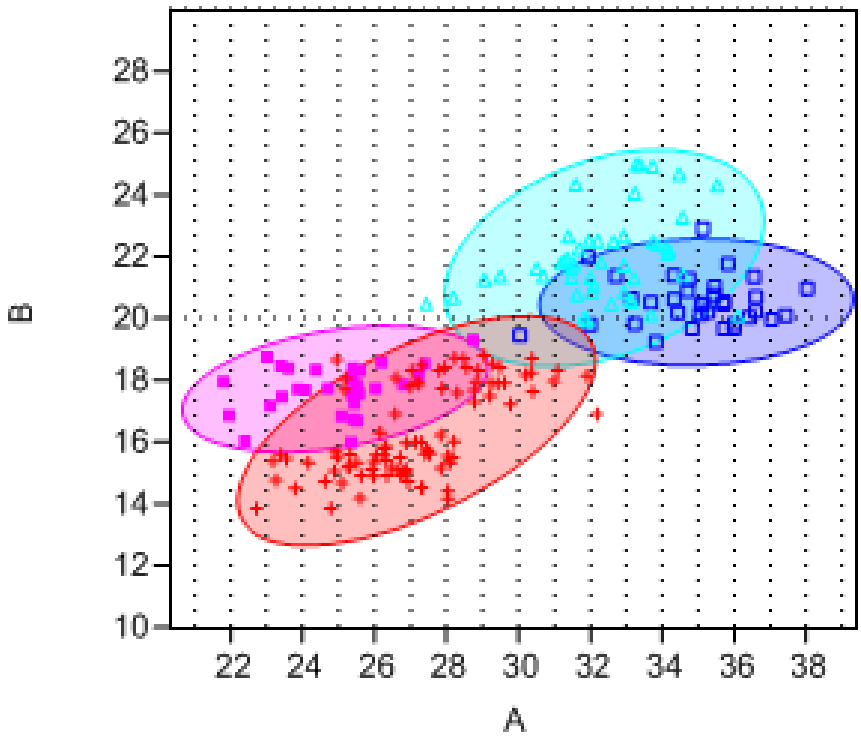

Figure 7. Morphometric parameters of pollen in different taxa of *Impatiens*

I. nevskii (dark blue), *I. parviflora* (light blue), *I. noli-tangere* (violet), *I. glandulifera* (red).

In alien *I. glandulifera* and *I. parviflora*, almost every flower forms a fruit; in *I. nevskii*, fruiting is less abundant, while in native *I. noli-tangere*, the fruits are formed only in two or three flowers per raceme (Fig. 8). Earlier we determined, that floral biology differed among species, and *I. glandulifera* is a cross-pollination species, while *I. parviflora* is a self-pollination one (Maitulina, 1988; Vinogradova, 2008). Other botanists obtained the same results. So, *I. glandulifera* and *I. noli-tangere* presented large quantities of sucrose-dominant nectar, contrary to *I. parviflora* (Vervoort et al., 2011).

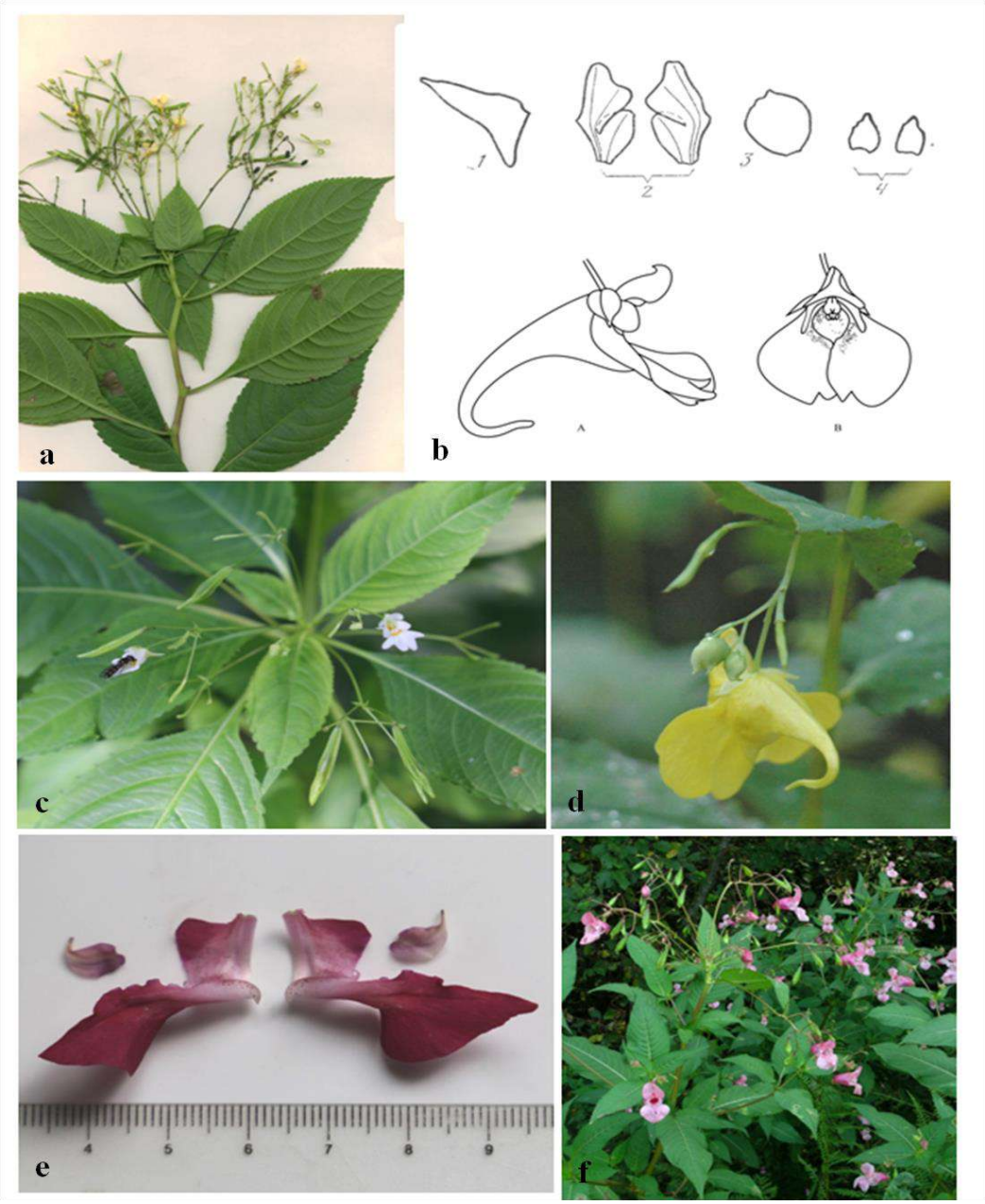

Figure 8. Morphology of inflorescences in different taxa of Impatiens

a - herbarium specimen of *I. parviflora*; *b* - scheme of flower's structures of *Impatiens* spp.; c – *I. nevskii*; *d* – *I. noli-tangere*; *e* - two lateral petals of *I. glandulifera*; *f* – *I. glandulifera*.

In Ireland, *Bombus pascuorum* is a highly effective pollinator of *I. glandulifera* due to its high visitation frequency, the morphological fit with flowers and individuals removing large pollen quantities (Nienhuis and Stout, 2009). *I. parviflora* had high autonomous selfing ability (81.4% fruit set) linked to complete self-compatibility, whereas *I. glandulifera*, showed lower autonomous selfing (9.3% fruit set), with high self-compatibility (Vervoort et al., 2011).

It is known that the reproductive traits and the breeding system could indicate some trends that might favour population spread and invasion (Jacquemart et al., 2015; Florianova and Munzbergova, 2018). However, the flower development of the four *Impatiens* species proceeds quite similarly. With aging of the flower, the corolla sizes increase, the pistil is differentiated, and the sepals and corolla became colored. At all the stages of the flower development, the pistil is shorter than the stamens. At all the stages of development, *I. parviflora* and *I. nevskii* have the smallest sizes of the flower organs.

The study of the features of the flower development in the four taxa of the genus *Impatiens* allowed distinguishing in them five phases of development, which differ not only in terms of quantitative but also in terms of qualitative criteria. The phase I finishes when the corolla acquires a form peculiar to the species and becomes longer than the calyx. At the same time, sepals and petals become colored. The phase II finishes, when the corolla disperses from the calyx. The phase III finishes when anthers burst and release pollen. The phase IV finishes when the brownish corolla shanks off, and virtually all the pollen pours out from the anthers.

The factors responsible for invasion success of *I. glandulifera* and *I. parviflora* are poorly known, though they may be related to frost tolerance and its popularity as an ornamental plant (Najberek et al., 2017). There is information, that light availability in dense forest canopy could influence on abundance the local population of *I. parviflora* (Barabasz-Krasny et al., 2018). Influences natural enemies and arbuscular mycorrhizal fungi have on plant performance, should take into consideration, too (Tanner et al., 2014). According to our observations, the native *I. noli-tangere* is more susceptible by diseases than *I. parviflora*. Polymorphism in the structure of DNA in plants from natural populations of *I. noli-tangere* is lower (7.3%) than in invasive populations of *I. glandulifera* (45.6%) and *I. parviflora* (49.7%) (Kupcinskiene et al., 2015).

There is a tendency for alien *Impatiens* species to earlier development of androecium and gynaeceum: caliptra is formed at the stage of uncolored bud, the pistil is differentiated in ovary, short style and stigma at the stage of colored bud. Not any other flower morphometric traits which would offer more competitiveness of invasive *I. glandulifera* and *I. parviflora* as compared to the native *I. noli-tangere* and naturalized *I. nevskii* were identified.

Conclusions

There aren't any taxonomic traits for differentiate *I. parviflora* from *I. nevskii* in the morphology of the floral sphere, excepting the color of sepals and petals.

The invasive *I. glandulifera* has competitive advantage over other studied species in terms of large sizes of organs of the floral sphere. The invasive *I. parviflora* has no competitive advantage over *I. nevskii* and *I. noli-tangere* in the floral sphere. On the contrary, it is inferior to native *I. noli-tangere* and it is similar with slightly naturalized *I. nevskii*. The invasive *I. parviflora* has the largest pollen grains, but in the same time invasive *I. glandulifera* has the smallest pollen grains. Thus, the hypothesis concerning the competitive advantage in the secondary distribution range of "the more powerful" plants is not supported by our results in full.

Compared to the native *I. noli-tangere*, flowers of alien *Impatiens* species, develop faster. For example, the calyptra is observed in the earliest phase of development, into uncolored buds; the pistil is differentiated in ovary, short style and stigma at the stage of colored bud.

Acknowledgements

The work was carried out in accordance to Institutional research project № 19-119080590035-9 and to Russian Foundation for Basic Research (RFBR) № 19-54-26010\19.

References

Barabasz-Krasny, B., Mozdzen, K., Soltys-Lelek, A., Stachurska-Swakon, A. (2018). Biological Traits of *Impatiens parviflora* DC. under Different Habitat Conditions. Notulae Botanicae Horti Agrobotanici Cluj-Napoca, 46 (1), 277-285. doi: 10.15835/nbha46110970.

Bartomeus, I., Vila, M., Steffan-Dewenter, I. (2010). Combined effects of *Impatiens glandulifera* invasion and landscape structure on native plant pollination. Journal of Ecology, 98 (2), 440-450. doi: 10.1111/j.1365-2745.2009.01629.x.

Clapham, A.R., Tutin, T.G., Warburg, E.F. (1962). Flora of the British Isles. Cambridge: Univ. Press.

Clements, D.R., Feenstra, K.R., Jones, K., Staniforth, R. (2008). The biology of invasive alien plants in Canada. 9. *Impatiens glandulifera* Royle. Canadian Journal of Plant Science, 88 (2), 403-417. doi: 10.4141/CJPS06040.

Cuda, J., Skalova, H., Janovsky, Z., Pysek, P. (2016). Juvenile biological traits of Impatiens species are more strongly associated with naturalization in temperate climate than their adult traits. Perspectives in Plant Ecology Evolution and Systematics, 20, 1-10. doi: 10.1016/j.ppees.2016.02.007.

DAISIE: Delivering Alien Invasive Species Inventories for Europe. Available at: http://www.europe-aliens.org (Accessed January 2019).

Daumann, E. (1967). Zur Bestaubungs – und Verbrietungsokologie dreier Impatiens – Arten. Preslia, 39 (1), 43-58.

Ebel', A.L., Kupriyanov, A.N., Strel'nikova, T.O. et al. (2016). Chernaya kniga Sibiri [Black book of Siberia]. SO RAN: Novosibirsk. (In Russian)

Florianova, A., Munzbergova, Z. (2017). Invasive *Impatiens parviflora* has negative impact on native vegetation in oak-hornbeam forests. Flora, 226, 10-16. doi: 10.1016/j.flora.2016.11.006.

Florianova, A., Munzbergova, Z. (2018). Drivers of natural spread of invasive Impatiens parviflora differ between life-cycle stages. Biological Invasions, 20, 2121-2140. doi: 10.1007/s10530-018-1691-6.

Gleason, H.A., Cronquist, A. (1993). Manual of Vascular Plants of Northeastern United States and Adjacent Canada. New York.

Godefroid. S., Koedam. N. (2010). Comparative ecology and coexistence of introduced and native congeneric forest herbs: *Impatiens parviflora* and *I. noli-tangere*. Plant Ecology and Evolution, 143 (2), 119-127. doi: 10.5091/plecevo.2010.397.

Jacquemart, A.L., Somme, L., Coli, C., Quinet, M. (2015). Floral biology and breeding system of *Impatiens balfourii* (Balsaminaceae): An exotic species in extension in temperate areas. Flora, 214, 70-75. doi: 10.1016/j.flora.2015.06.001.

Jarcuska, B., Slezak, M., Hrivnak, R., Senko, D. (2016). Invasibility of alien *Impatiens parviflora* in temperate forest understories. Flora, 224, 14-23. doi: 10.1016/j.flora.2016.06.005.

Kuklina, A.G., Vinogradova, Yu.K., Tkacheva, E.V. (2015). About Flowering Biology of Alien Species. 3. *Caragana arborescens* Lam. and *C. laeta* Kom. Russian Journal of Biological Invasions, 6 (4), 238-251. doi: 10.1134/S2075111715040037.

Kupcinskiene, E., Zybartaite, L., Paulauskas, A. (2015). Comparison of genetic diversity of three Impatiens species from Central Europe and Baltic region. Zemdibyste-Agriculture, 102 (1), 87-94. doi: 10.13080/z-a.2015.102.011.

Maitulina, Yu.K. (1988). K biologii i sistematike sredneaziatskikh vidov roda Nedotroga [On the biology and systematics of Central Asian species of the genus Nedotroga]. Byulleten' Glavnogo Botanicheskogo sada, 150, 59-64. (In Russian)

Maslo, S., Šaric, Š. (2019) Small Balsam, *Impatiens parviflora* DC. (Balsaminaceae): A new alien species to the flora of Bosnia and Herzegovina. Phytologia Balcanica, 25 (1), 31-35.

Najberek, K., Nentwig, W., Olejniczak, P., Krol, W., Bas, G., Solarz, W. (2017). Factors limiting and promoting invasion of alien *Impatiens balfourii* in Alpine foothills. Flora, 234, 224-232. doi: 10.1016/j.flora.2017.08.002.

Nienhuis, C.M., Stout, J.C. (2009). Effectiveness of native bumblebees as pollinators of the alien invasive plant *Impatiens glandulifera* (Balsaminaceae) in Ireland. Journal of Pollination Ecology, 1 (1), 1-11.

Pobedimova, Ye. G. (1949). *Impatiens* L. in a book Flora SSSR 14. Moscow-Leningrad: AN SSSR, 746-747. (In Russian)

Reczynska, K., Swierkosz, K., Dajdok, Z. (2015). The spread of *Impatiens parviflora* DC. in Central European oak forests - another stage of invasion? Acta Societatis Botanicorum Poloniae, 84 (4), 401-411. doi:10.5586/asbp.2015.039.

Skálová, H., Moravcová, L., Čuda, J., Pyšek, P. (2019). Seed-bank dynamics of native and invasive Impatiens species during a five-year field experiment under various environmental conditions. Neobiota, 50, 75-95. doi:10.3897/neobiota.50.34827.

Tanner, R.A., Jin, L., Shaw, R., Murphy, S.T., Gange, A.C. (2014). An ecological comparison of *Impatiens glandulifera* Royle in the native and introduced range. Plant Ecology, 215 (8), 833-843. doi: 10.1007/s11258-014-0335-x.

The Plant List. Available at: http://www.theplantlist.org/ (Accessed January 2019).

Vervoort, A., Cawoy, V., Jacquemart, A-L. (2011). Comparative Reproductive Biology in Co-Occurring Invasive and Native Impatiens Species. International Journal of Plant Sciences, 172 (3), 366-377. doi:10.1086/658152.

Vinogradova, Yu.K. (2016). Bio-Morphological Characters of Alien Legume Species, Influencing Their Invasion in Natural Plant Communities. American Journal of Plant Science, 7, 2390-2398. doi: 10.4236/ajps.2016.716209.

Vinogradova, Yu. K. (2008). Mikroevolyutsiya nedotrogi zhelezkonosnoy (*Impatiens glandulifera* Royle) v protsesse formirovaniya vtorichnogo areala [Microevolution of nedotroga ferruginosa (*Impatiens glandulifera* Royle) in the process of secondary area formation]. Byulleten' Glavnogo Botanicheskogo sada, 194, 3-18. (In Russian)

Vinogradova, Y., Kuklina, A. (2016). Flowering calendar and morphometric features of pollen for some invasive species in the Middle Russia. Hortus botanicus, 11, 2-13. doi: 10.15393/j4.art.2016.3342.

Vinogradova, Yu. K., Mayorov, S.R., Khorun, L.V. (2010). Chernaya kniga flory Sredney Rossii: chuzherodnyye vidy rasteniy v ekosistemakh Sredney Rossii [Black book of the flora of Central Russia: alien plant species in the ecosystems of Central Russia]. Moscow: GEOS. (In Russian)

Vinogradova, Yu. K., Tkacheva, E.V., Brindza, J., Mayorov, S.R., Ostrowsky, R. (2013). On flowering patterns of alien species: 2. *Robinia pseudoacacia*, *R.× ambigua*, and *R. neomexicana*. Russian Journal of Biological Invasions, 4 (2), 74-86. doi:10.1134/S2075111713020094.

Vinogradova, Yu. K., Tkacheva, E.V., Mayorov, S.R. (2012). About Flowering Biology of Alien Species: 1. *Lupinus polyphyllus* Lindl. Russian Journal of Biological Invasions, 3 (3), 163-171. doi: 10.1134/S2075111712030083.

Global successful experiences of the health tourism brand and presentation of a native model

Amin Afsharifar *

ABSTRACT

The current study aims to benchmark the global successful experiences of health tourism branding and presenting its native pattern. This study is analytical-descriptive in nature and practical approach in terms of the target sought. The questionnaire was designed to measure the effective variables on health tourism branding. A researcher-made questionnaire, whose dimensions and indicators were based on the literature and research background, was used to measure the dependent variable of the research. Acer brand value questionnaire was used for assessing the dependent variable of the research. The statistical population of this research is the professors of the medical sciences universities and tourism and marketing management group and the directors and assistants of the Cultural Heritage, Handicrafts and Tourism Organization of Fars and Bushehr provinces that regarding the lack of access to all members of the research community, sampling was done by available sampling. Finally, 87 valid questionnaires were obtained. After examining the research model using the path analysis method, the findings showed that all paths between the research variables were confirmed at 95% confidence level and were significant. This means that policy making, infrastructure, marketing, communication and information, medicine and health have a positive and significant impact on health tourism branding. However, the findings indicated that the highest path coefficient for the relationship between the infrastructure and branding of health tourism is 0.365.

KEYWORDS: benchmarking; successful experience; branding; health tourism; pattern.

* School of Business and Law, Edith Cowan University, Joondalup, Australia, WA.

Recibido: 02/03/2020 Aceptado: 06/05/2020

Experiencias globales exitosas de la marca de turismo de salud y presentación de un modelo nativo

RESUMEN

El presente estudio tiene como objetivo comparar las experiencias globales exitosas de la marca de turismo de salud y presentar su patrón nativo. Este estudio es de naturaleza analítica-descriptiva y enfoque práctico en términos del objetivo buscado. El cuestionario fue diseñado para medir las variables efectivas en la marca de turismo de salud. Se utilizó un cuestionario realizado por un investigador, cuyas dimensiones e indicadores se basaron en la literatura y los antecedentes de la investigación, para medir la variable dependiente de la investigación. El cuestionario de valor de marca Acer se utilizó para evaluar la variable dependiente de la investigación. La población estadística de esta investigación son los profesores de las universidades de ciencias médicas y el grupo de gestión de turismo y marketing y los directores y asistentes de la Organización del Patrimonio Cultural, Artesanía y Turismo de las provincias de Fars y Bushehr que, en relación con la falta de acceso a todos los miembros de la comunidad de investigación, el muestreo se realizó mediante muestreo disponible. Finalmente, se obtuvieron 87 cuestionarios válidos. Después de examinar el modelo de investigación utilizando el método de análisis de ruta, los resultados mostraron que todas las rutas entre las variables de investigación se confirmaron con un nivel de confianza del 95% y fueron significativas. Esto significa que la formulación de políticas, la infraestructura, el marketing, la comunicación y la información, la medicina y la salud tienen un impacto positivo y significativo en la marca del turismo de salud. Sin embargo, los resultados indicaron que el coeficiente de ruta más alto para la relación entre la infraestructura y la marca del turismo de salud es 0.365.

PALABRAS CLAVE: evaluación comparativa; experiencia exitosa; marca; turismo de salud; patrón

Introduction

Tourism is one of the most dynamic and the fastest growing industries in the world. The United Nations recognized the industry as one of the main means of economic development, employment and a source of higher income. In developed countries, tourism generates income diversification and reduces incoherence in the economy, while in developing countries; the industry has an opportunity to export in a faster method than traditional methods (Vetitnev et al, 2016). On the other hand, one of the most important sectors of tourism, which has become one of the largest and most profitable parts of the world's economy, is the health tourism category.

In fact, this industry has affected the flow of capital, income and balance and investment, which, has driven the movement and transfer the capital and help the growth of countries that have recognized the importance of this industry more than any other economic and industrial activity in the world. It has been estimated that every health traveler is three times as likely as a regular tourist (Reisman, 2010). Health travelers can travel from their permanent place of residence to a destination, in order to obtain their physical and mental health and wellbeing. In this context, the globalization of healthcare means patients crossing borders with treatment being the main objective. Today healthcare is regarded as a global phenomenon.

The establishment of multinational hospitals, the competitiveness of global healthcare prices, the internationalization of standards, and the convergence of the level of specialized technologies, are all signs of global health development. Also, people traveling to other countries for health-related issues, are mainly affected by the changes made in consumer values, increasing neurological stress and workload, Population aging, high costs of treatment and healthcare in developed countries, new attitudes toward mental and psychological activities, lack of effective insurance, secrecy (anonymity), lack of facilities in the country of origin, possibility of cure and treatment with the benefit of holidays (Kazemi, 2008).

In spite of the importance of health tourism in creating a sustainable income, very few studies have been carried out in the field of health tourism and its branding in Iran. This is despite the fact that, when compared with the countries of the region, Iran has huge health and medical related capabilities, such as skilled manpower and medical equipment and facilities. For that. We should also consider the national objective of Iran in maintaining a brand image as the main hub of health tourism in the region, based on the goals of developing its 20-year landscape at 1404 horizon. Therefore, this research seeks to resolve the research gap in this area through the use of successful global experiences in order to provide a suitable pattern and model for that matter.

1. Theoretical fundamentals and research background

1.1. The Concept of Health Tourism

Health tourism is one of the most important branches of the tourism industry, with high economic and social turnover, in which people travel to health and medical care destinations to be provided with unique medical services and facilities. As this has had civic organizations in more qualified and talented countries focus their attention on this sector of the tourism industry and involve durable and efficient domestic policies act to their favor. The term "health tourism" was introduced by Goodrich in 1987, and then began to spread to universities in the United States and England.

The definitions circling this concept somewhat vary. Resiman (2010) quoted by the global organization tourism defines health as a type of tourism whose purpose is to retrieve, promote, and reach the physical and mental health of the person for more than 24 hours and less than one year. Dursun & Cemal (2010) state that health tourism is a kind of travel that is also responsible for health and medical care in addition to entertainment, leisure and comfort. Connell et al (2006) point out that health tourism is a journey organized from the person's living environment to another place to maintain, improve and regain physical and mental health of the individual. Tourism experts categorize health according to the type and function of the tourist's desired service into three categories: Health tourism that is tourist's travel to areas with attractions and natural services (such as spa springs) for refreshment and not for treatment. Therapeutic tourism, however, is to travel to consume natural resources (such as spa springs), rather for treatment or for restoration, and of course under the supervision of a physician. In the context of medical tourism, which is another type of health tourism, a traveler (patient) travels to medical centers for the use of special medical services, such as all sorts of surgeries and therapies (Garrod, 2003).

1.2.Study of successful health tourism experiences

Today, many developing countries regard health tourism as a gold mine and are keenly looking for the growth and development of this industry in their country, (Awadzi & Panda 2006). For example, the quality of health services in Singapore is highly appreciated. Safety, trustworthy services, with advanced research and international credibility in the field of medicine, has made it a leading Asian center in health tourism developments. India, on the other hand, is one of the most popular destinations for cardiac surgery and hip bone graft surgery for the international medical tourists. In other areas of

national health and wellbeing, India is also recognized as a global leader in services provided for this section of tourists. The main reasons for this country's success include skilled hospital staffing, new technologies, health care quality, diverse medical packages offered, lack of waiting time, public fluency in English, and broad access to information through the Internet. In this country, the government has also shared its role through the Ministry of Health and Welfare of the Family and the Ministry of Tourism and has a headquarters and strategic role in infrastructure preparation and human resource development (Saravana and Krishna, 2015).

Malaysia is another successful country in attracting medical tourists. One of the reasons for Malaysia's success in attracting medical tourists is the low payroll, the skill of the workforce, the connection with English language, access to alternative therapies, the attractive natural environment, and the health and technology facilities (Sri and Bakar,2011). Also, medical tourism is a growing part of Thailand's industry. The cost of treatment in Thai hospitals is very low in comparison with the United States, while care and nursing are offered at a high level. On the other hand, Mexico has become one of the most popular destinations for American health tourists in recent years. This country, due to its vicinity and the relatively low medical costs relative to the United States, has been regarded as a noticed destination to Americans and Canadians. Gastric surgery, eye examinations and checking are the basic medical services provided for tourists. According to studies, medical expenses in Mexico are between 13% and 31% lower than in the United States (Ricafort, 2011).

2. Research background

Han and Sean Hyun (2015) concluded that there was a significant relationship between perceived qualities, satisfaction and trust in staff and medical clinics, and affected the intention to return to the clinic and destination country in medical tourism. Meanwhile, satisfaction and trust are important mediators. In a research, the most important factors affecting the development of the health tourism industry are, respectively, the development of public infrastructure, human resources development, information and marketing system development, and product development strategy (Noori et al, 2011). Ricafort (2011) has selected 20 factors influencing the topic from the tourists'

point of view and ultimately prioritizes the influential factors. The results of the research show that among these factors, "professional doctors" has the highest score. Haribabu et al (2010) conducted their research focusing on competitive challenges in medical tourism in Singapore. The results show that Singapore has a high level of competitive ability and has been able to attract many tourists in the health tourism business. A study in Hong Kong that identified the factors influencing the development of health tourism was that the laws, regulations, government support, costs and medical needs of the local community were among the most important factors affecting the development of health tourism (Heung et al, 2010). Another study has suggested that factors such as demographic changes in advanced countries, along with increased problems with their health care system, such as the long waiting line of patients, high cost of health services and the lack of an effective insurance system, have led the flow of patients from these countries out of National borders for receiving high quality and low cost health services (Beth, 2010).

3. Introduction of Indices and Conceptual Model of the Research

After examining the same research, the dimensions and indicators that affect health tourism branding are presented in the following table:

Table 1: Dimensions and Indicators Effective on Branding Health Tourism Excerpts from the Background of the Research

Authors	Component (Indicator)	Factor (dimension)	Row
Ma (2008), Ranjan Debata et al (2013)	Supporting the private sector to invest in health tourism	Policy making	1
Kumar (2009)	Developing up-to-date standards and regulations in the field of health tourism		2
Ma (2008), Ranjan Debata et al (2013)	Design and development of policies related to health tourism		3
Ranjan Debata et al (2013), Connell (2006)	Establishing coordination and cooperation between all organizations and establishment related to health and tourism		4
Nagarajan(2004)	Long-term planning to attract health tourists		5
Heung et al (2010), Ranjan Debata et al (2013), Mohamad et al (2012)	Creation and development of health-related infrastructure	Infrastructure	1

Mohamad et al (2012)	Development of modern medical and therapeutic technologies		2
Vetitnev et al (2016),Altin et al (2011), Mohamad et al (2012)	Create and develop cheap resorts for patient entourage		3
Nagarajan (2004)	Designing and developing a coherent marketing strategy in the field of health tourism	Marketing	1
Kumar (2009)	Use of up-to-date and efficient promotional techniques in the field of health tourism		2
Kumar (2009)	Design and development of distribution and sale channels for international health and medical services		3
Ranjan Debata et al (2013), Kumar (2009)	Study and study of health tourism market		4
Chen et (2012), Kumar (2009)	Needs assessment of potential customers in the field of health tourism		5
Ma (2008)	International cooperation in health care	Communication and information	1
Mohamad et al (2012)	Creating a system for registration, control and documentation of health tourists		2
Connell (2006), Carrera & Bridges (2006)	The existence of an appropriate and efficient notification system for the identification of medical and therapeutic capabilities		3
Kumar (2009)	Proper use of cyberspace capacity		4
Connell (2006)	Establishing an inter-channel for the exchange of information and communication among all the organizations and organizations active in the field of health tourism		5
Ranjan Debata et al (2013), Carrera & Bridges (2006)	Cost of treatment	Medical and therapeutic	1
Ma (2008), Ranjan Debata et al (2013)	Medical coverage of the destination country		2
Ma (2008),Altin et al (2011)	Availability of suitable medical facilities		3
Carrera & Bridges (2006)	There are specialist doctors with international certificates		4
Altin et al (2011), Carrera & Bridges (2006)	Applying fluent foreign language skills in the field of treatment		5
Ranjan Debata et al (2013), Altin et al (2011)	Quality of health care offered at health centers		6
Carrera & Bridges (2006)	Getting important healthcare quality approvals by health centers		7

After identifying the dimensions for each of these indicators, the conceptual model of the research is as follows. In the model, the five dimensions of policy, infrastructure, marketing, communication and information, and medical and therapeutic services are regarded as the independent variables and branding health tourism is the dependent variable, which is measured using the Acer Model (1996). It includes five dimensions of brand loyalty, brand perceived quality, brand association, brand awareness, and willingness to accept brand extension.

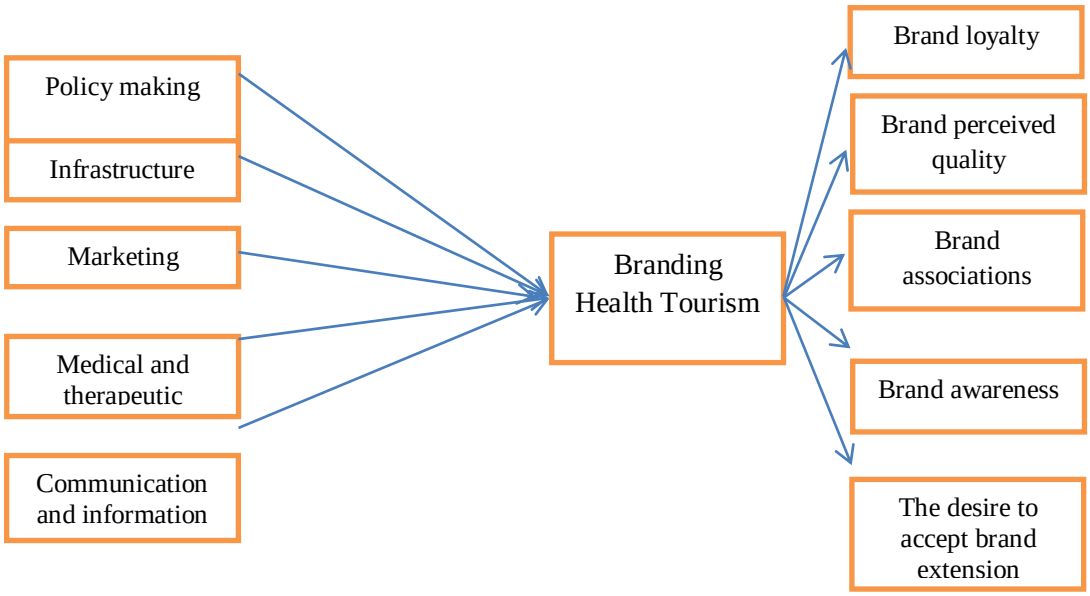

Figure1. Conceptual model of research

4. Research Methodology

This study is analytical-descriptive in terms of nature and practical in terms of target. Questionnaires were also used as the tool to collect data. In order to measure the variables affecting health tourism branding, a researcher made questionnaire whose dimensions and indicators are based on literature and research background (Table 1), and used to measure the dependent variable of the research is the Acer Brand Value Questionnaire, which is typically a 32-question and 5-dimensional questionnaire. Also, the two questionnaires have a Likert spectrum of 5 options (strongly agree to completely opposed).

On the other hand, for evaluating the validity of the researcher-made questionnaire, the factor analysis method was based on the opinions of the experts and the Cronbach's

alpha coefficient was used to assess the reliability of the questionnaire statements. Also, SPSS software version 19 was used for data analysis and PLS software was used for modeling structural equations and studying relationships of variables in the research model. The results related to validity (using factor analysis method) and reliability (using Cronbach's alpha method) are presented in the following two tables which indicate validity (due to the increase of each factor load of the components from the value of 0.5 in each dimension it is specified) and the stability (due to the larger coefficient of alpha of all of the structures of 0.7).

The statistical community of this research are the professors of medical sciences universities and tourism and marketing management group, and finally the directors and assistants of the Cultural Heritage, Handicrafts and Tourism Organization of Fars and Bushehr provinces. Due to the lack of access to all members of the research community, sampling was done by available sampling. Finally, 87 valid questionnaires were obtained.

Table 2: Results of Validity Study Using Factor Analysis

Load factor	Component (Indicator)	Factor (dimension)	Row
0.775	Supporting the private sector to invest in health tourism	Policy making	1
0.712	Developing up-to-date standards and regulations in the field of health tourism		2
0.743	Design and development of policies related to health tourism		3
0.645	Establishing coordination and cooperation between all organizations and establishment related to health and tourism		4
0.785	Long-term planning to attract health tourists		5
0.726	Creation and development of health-related infrastructure	Infrastructure	1
0.823	Development of modern medical and therapeutic technologies		2
0.792	Create and develop cheap resorts for patient entourage		3
0.675	Designing and developing a coherent marketing strategy in the field of health tourism	Marketing	1
0.785	Use of up-to-date and efficient promotional techniques in the field of health tourism		2
0.686	Design and development of distribution and sale channels for international health and medical services		3
0.788	Study of health tourism market		4
0.629	Needs assessment of potential customers in the field of health tourism		5
0.805	International cooperation in health care	Communication and	1
0.687	Creating a system for registration, control and documentation of health tourists		2

0.567	The existence of an appropriate and efficient notification system for the identification of medical and therapeutic capabilities	information	3
0.655	Proper use of cyberspace capacity		4
0.715	Creating a cross-channel for the exchange of information and communications between all devices and organs		5
0.823	Cost of treatment	Medical and therapeutic	1
0.733	Medical coverage of the destination country		2
0.749	Availability of suitable medical facilities		3
0.685	Existence of specialist doctors with international certificates		4
0.845	Applying fluent foreign language skills in the field of treatment		5
0.769	Quality of health care offered at health centers		6
0.625	Getting important healthcare quality approvals by health centers		7

Table3: Reliability test using Cronbach's alpha coefficient

Dimensions of the questionnaire	Number of questions	Reliability test using Cronbach's alpha coefficient	Result
Policy making	5	0.82	Confirmed
Infrastructure	3	0.86	confirmed
Marketing	5	0.79	confirmed
Communication and information	5	0.81	confirmed
Medical and therapeutic	7	0.8	confirmed
Whole questionnaire	25	0.77	confirmed

5. Research findings

5.1. Normality test

|The Kolmogorov-Smirnov test was used to investigate the normality of the distribution of research data related to the questions. Two questionnaires (researcher-made questionnaire and Acer brand value questionnaire) were used. The results are listed in the table below.

Table 4: Results of Kolmogorov-Smirnov test

parameters		Questionnaire questions Researcher made	Brand equity questionnaire questions
(Number of respondents)		87	87
(Normal parameters)	(Average)	3.587	3.187
	(Standard deviation)	0.5240	.6007

(The biggest differences)	(Absolute value)	.087	.090
	(Positive)	.087	.090
	(Negative)	-.047	-.044
Z (Kolmogorov-Smirnov statistics)		1.313	1.256
(The significance level)		0.102	.085

The results of the above table indicate that the data related to the research questionnaires follow the significance level of 0.05 of the normal distribution due to larger ones.

5.2. Testing the status of existing research variables

After determining the distribution of the research data, to evaluate the status of the research variables, a one-way T test (with regards to the normal distribution of data) was used with a cut-off point of 3, as described in the following table.

Table5: Unilateral T test for variables in the research model (independent and dependent)

Test Value = 3					
Variables	**Number**	**Average**	**The t statistics**	Degrees of freedom	The significance level
Policy making	87	4.1026	7.413	86	.000
Infrastructure	87	3.8579	7.523	86	.000
marketing	87	3.7135	7.868	86	.000
Communication and information	87	3.4194	6.149	86	.000
Medical and therapeutic	87	3.7613	4.318	86	.000
Branding Health Tourism	87	3.3341	8.172	86	.000

The results of the above table show that all six variables that make up the research model are significant at 95% confidence level, while the highest average is related to the policy variables and the infrastructure.

5.3. Testing the research model

In this research, based on the conceptual model of the research, five assumptions were considered. To investigate these assumptions, the structural equation model was used with the help of PLS software. The results of the test of path coefficients t are described below. It should also be noted that, based on a rule of thumb, values higher than 0.2 in the

above sample indicate a significant relationship, but in order to achieve a more accurate result, bootstrapping test in the form of t-test coefficients was conducted.

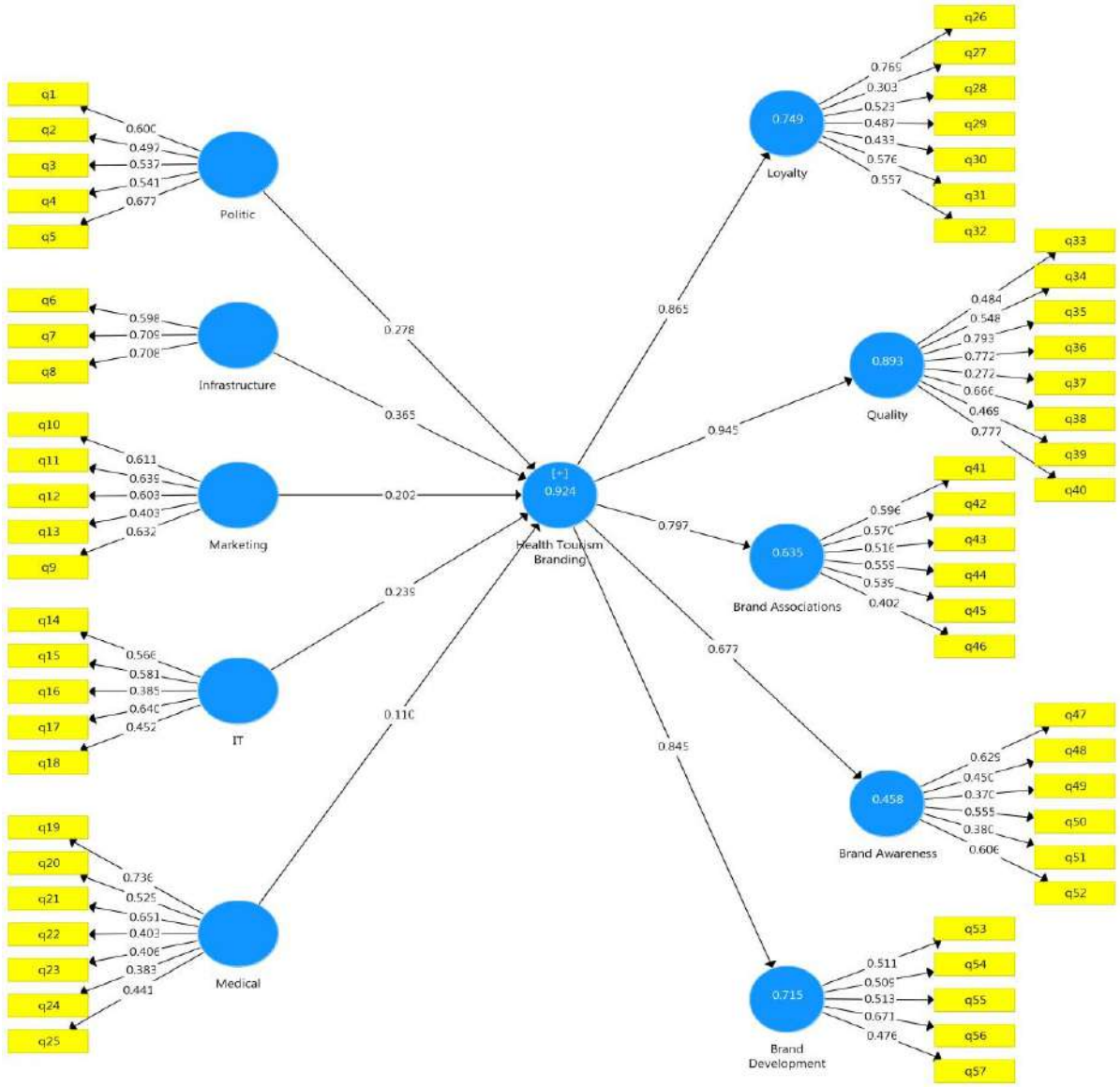

Figure 2: Chart path coefficients

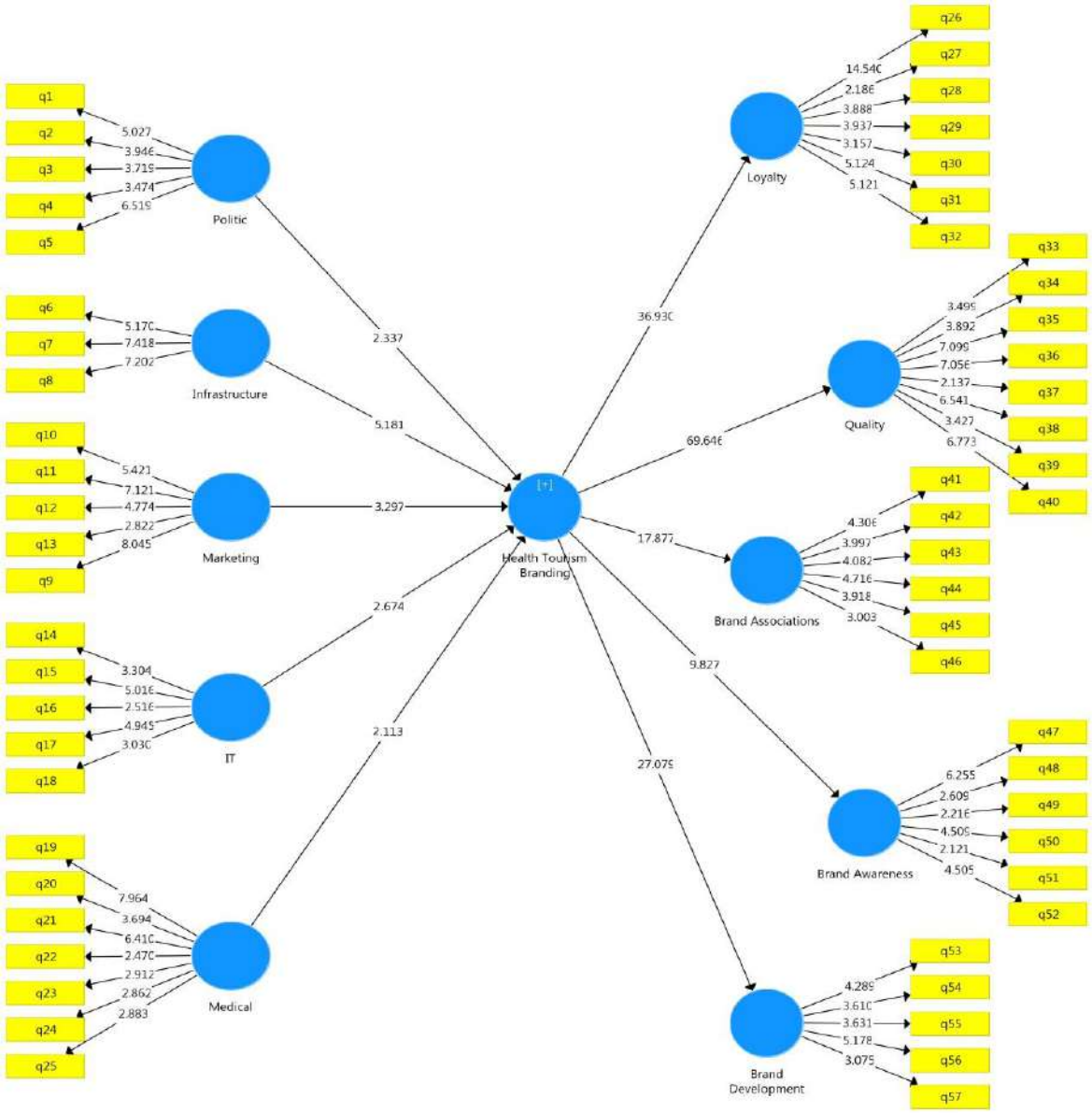

Figure3: Chart of coefficients t

Based on the results of the above table, it should be noted that, according to the values of the t statistic that is greater than 1.96 (at 95% confidence level), all the paths between the variables are approved and also with regards to the significant values (amounts smaller than 0.05) all values are obtained and therefore, it can be stated that all five main paths of the research model (from independent to dependent variables) are approved at 95% confidence level. Also, the highest path coefficient is related to the relationship between infrastructure and branding of health tourism with a value of 365%. According to the above results, it should be mentioned that the direct effect of 5 independent variables of the research model on the dependent variable of the model, i.e.

branding of health tourism, is 0.278, 0.336, 0.220, 0.239 and 0.110, which is an indication of the ability of this model in improving the health tourism branding variance.

Table 6: Path Test Results

Scientific path		statictics t	Standard path coefficient) β(	Significance level	Test result
from	to				
Policy making	Branding Health Tourism	2.337	0.278	0.0012	confirmed
Infrastructure	Branding Health Tourism	5.181	0.365	0.0012	confirmed
Marketing	Branding Health Tourism	3.297	0.202	0.0012	confirmed
Communication and information	Branding Health Tourism	2.674	0.239	0.0012	confirmed
Medical and therapeutic	Branding Health Tourism	2.113	0.110	0.0012	confirmed

On the other hand, regarding the fit test and the quality of the structural model of the research model, we can cite the following two indicators:

1. The root mean of the standard squared residuals (SRMR)

According to Heung et al. (2010), in relation to this fitting scale, values of less than 0.8 represent good fit, which according to the calculated data, the SRMR value for the standard state (real data) is 124/0 and for the estimated mode (Bootstrap sample data) is 0.99, which is much less than 0.8.

2. The root mean of the remaining covariance squares (RSM)

This scale follows the logic fitting to the SRMR, but refers to covariance. The benchmark introduced by Lohmler (1989) has set the threshold value of 0.20 for the proposal. That is, a value less than 12/0 represents a good fit of the model and higher levels of proportionality. The value obtained in this study is 0.11 which indicates the acceptable fit of the model.

Conclusion

This research was conducted with the aim of benchmarking the successful global health tourism branding and providing its native model based on a quantitative research strategy. After examining the research model using the path analysis method, the findings showed that all the paths between the research variables were confirmed at 95% confidence level and therefore, all the assumptions of the research were confirmed. This means that the variables of policy, infrastructure, marketing, communication and information, medicine and health have a positive and significant impact on health tourism branding. However, the findings indicated that the highest path coefficient for the relationship between the infrastructure and branding of health tourism is 365%. Therefore, the focus on this factor and its components should be prioritized among other responsible factors in relation to other factors. On the other hand, the study of the effect of the variables of the research model indicates that this model has a good effect on health tourism branding variance. The findings are based on the research of Han and Sin Hyun (2015), Ricaford (2011), HariBabu et al. (2010), Beth (2010), Garrod (2003), each determining the factors affecting the branding of health tourism which are compatible and consistent. In discussing the above findings, it can be said that the discussion on health tourism is multifaceted (Chertakova et al., 2019) and in order for a successful and appropriate model to be presented in this area, it is necessary to have different segments active in the fields of treatment, marketing, politics, communication and national sovereignty. According to the findings of this research, two factors of infrastructure and policy making were considered more important and of high priority, which require special attention. Hopefully, the model presented in this study would be a platform for all those who pursue an activity in this prominent sector of the tourism industry.

Refrences

Awadzi, W., & Panda, D. (2006). Medical Tourism: Globalization and the marketing of medical services. Consortium Journal of Hospitality & Tourism, 11(1).

Beth, K. (2010). Traveling for medical care in a global world. Medical Anthropology, 29(4): 344-362.

Chertakova, E. M.; Yarovova, T. V.; Opanova, Z.; Lavrova, G. N.; Kachalova, L. P. (2019). A conceptual model of creative activity and personal self-development, *Revista de la Universidad del Zulia*, 10 (28), 331-344.

Connell, J. (2006), Medical tourism: sea, sun, sand and surgery, Tourism Management. 2006; 6(27): 1093-1100.

Dursun, A., & Cemal, Y. (2010). General directorate of health services, medical research tourism. Retrieved from http://saglik.gov.tr/SaglikTurizmi/dosya/1-74211/h/yurtdisi-arastirmasimedical-tourism-overseas-researchd-.pdf

Garrod, B. (2003). Local participation in the planning and management of ecotourism: A revised model approach. Journal of Ecotourism, 2(1), 33-53.

Han, H., & Hyun, S. S. (2015). Customer retention in the medical tourism industry: Impact of quality, satisfaction, trust, and price reasonableness. Tourism Management, 46, 20-29.

Haribabu H., Naga Lakshmi C., Mohan A. V. (2010). Interaction between Universities and Technology Clusters in Emerging Economies - Case Study of Cyberjaya, Malaysia - A Greenfield development and Cyberabad, India - A Brownfield Development, In VIII Triple Helix International Conference on University, Industry and Government Linkages, Books of abstracts 2010

Heung, V. C., Kucukusta, D., & Song, H. (2010). A conceptual model of medical tourism: Implications for future research. Journal of Travel & Tourism Marketing, 27(3), 236-251.

Kazemi, Z. (2008). "Study of Effective Factors for Attracting Medical Tourist in Iran". Masetr Thesis, Lulea: Lulea University of Technology.

Noori, G. H., Taghizadeh, Z., & Shirani, Z. (2011). Iran's role in the Muslim world with an emphasis on nature tourism health care (Functions, Challenges and Solutions). In the first International Conference on Tourism and Sustainable Development Management, Islamic Azad University, MARVDASHT.

Reisman, D. A. (2010). Health tourism: Social welfare through international trade. Edward Elgar Publishing.

Ricafort, K.M.F. (2011). A Study of Influencing Factors That Lead Medical Tourists to Choose Thailand Hospitals as Medical Tourism Destination (Master Dissertation), Webster University, Cha-am, Thailand.

Saravana, K.G. and Krishna, R.R. (2015). Status, growth and impact of medical tourism in India, International Journal of Pharmaceutical Sciences Review and Research, 34(1): 284-291

Sri, T.D. and Bakar, A.S. (2011). Medical Tourism – Malaysia, International Medical University (IMU), Kuala Lumpur, Malaysia.

Vetitnev, A., Kopyirin, A., & Kiseleva, A. (2016). System dynamics modeling and forecasting health tourism demand: the case of Russian resorts. Current Issues in Tourism, 19(7), 618-623.

The share of health care spending in the structure of GDP as a criterion for the healthcare system effectiveness

Danil Alekseevich Zyukin *
Anna Yurievna Bystritskaya **
Artem Alekseevich Golovin ***
Olga Vladimirovna Vlasova ****

ABSTRACT

Effective work of the healthcare system is becoming increasingly important in modern conditions, which actualizes the task of finding tools to increase the effectiveness of its functioning; this should ultimately lead to a decrease in morbidity and an increase in life expectancy. One of the main criteria for social development in modern conditions is the share of health care spending as a percentage of GDP; since this reflects the degree of attention and concern of the state about the health and life of citizens. The research hypothesis states that the share of health care costs does not affect the quality of the health care system, which is expressed in the average life expectancy of the population. To confirm the hypothesis, an analysis was made of the degree of influence of the share of expenditures on health care development on GDP on average life expectancy in the context of countries using a simple pair correlation and correlation between ranks; A cluster analysis of the countries was also carried out on the basis of their grouping according to the level of health spending as a percentage of GDP. It has been established that there is no connection between the share of health expenditures from GDP in countries and average life expectancy in them, which confirms the failure to use this indicator as a criterion for assessing the development of the health system. A cluster analysis of the countries under consideration showed that the effectiveness of the health care system is a complex category, depending not only on the level of state funding, but also on a number of other aspects.

KEYWORDS: healthcare, WHO, ranking of countries, share of healthcare expenditures, life expectancy, healthcare system efficiency.

*Candidate of Economic Sciences, Senior Researcher Kursk State Agricultural Academy named after I.I. Ivanov Russia, ORCID: https://orcid.org/0000-0001-8118-2907

** Candidate of Economic Sciences, Associate Professor, Head of the Department of Economics and Accounting Kursk State University. Russia.

*** Candidate of Economic Sciences, Associate Professor of the Department of Customs and the World Economy Southwestern State University. Russia ORCID: https://orcid.org/0000-0001-6688-3561

**** Candidate of Economic Sciences, Associate Professor of the Department of Economics and Management Kursk State Medical University, Russia.

Recibido: 03/04/2020 Aceptado: 01/06/2020

La participación del gasto en salud en la estructura del PIB como criterio para la efectividad del sistema de salud

RESUMEN

El trabajo efectivo del sistema de salud se está volviendo cada vez más importante en las condiciones modernas, lo que actualiza la tarea de encontrar herramientas para aumentar la efectividad de su funcionamiento; esto debería conducir a una disminución de la morbilidad y un aumento de la esperanza de vida. Uno de los criterios principales para el desarrollo social en las condiciones modernas es la proporción del gasto en atención de salud como porcentaje del PIB; ya que esto refleja el grado de atención y preocupación del Estado sobre la salud y la vida de los ciudadanos. La hipótesis de la investigación establece que la parte de los costos de atención médica no afecta la calidad del sistema de atención médica, que se expresa en la expectativa de vida promedio de la población. Para confirmar la hipótesis, se realizó un análisis del grado de influencia de la participación del gasto en el desarrollo de la atención de salud en el PIB sobre la esperanza de vida promedio en el contexto de los países que utilizan una correlación simple de pares y una correlación entre los rangos. También se realizó un análisis de conglomerados de los países sobre la base de su agrupación de acuerdo con el nivel de gasto en salud como porcentaje del PIB. Se ha establecido que no existe una conexión entre la participación del gasto en salud del PIB en los países y la esperanza de vida promedio en ellos, lo que confirma la falta de uso de este indicador como criterio para evaluar el desarrollo del sistema de salud. Un análisis de conglomerados de los países considerados mostró que la efectividad del sistema de atención de salud es una categoría compleja, que depende no solo del nivel de financiación estatal, sino también de otros aspectos.

PALABRAS CLAVE: asistencia sanitaria, OMS, clasificación de países, porcentaje de gastos en asistencia sanitaria, esperanza de vida, eficiencia del sistema sanitario

Introduction

The most important goal of state health policy at the present stage is to improve the demographic situation, the state of public health, and to ensure the availability and quality of medical care for citizens. Effective work of the health system is becoming increasingly important: the emergence of a new coronavirus infection in 2019 and its transformation into a world pandemic in 2020 showed that the health care system in most countries was not perfect and was not ready for such threats, which already led to the deaths of tens of thousands of people (Podgalo et al., 2019). In this regard, the task of searching for tools to increase the effectiveness of its functioning is being updated, which ultimately should lead to a decrease in the incidence and increase in average life expectancy (Tagaeva and Kazantseva, 2016).

The most important characteristic of human potential and state of health can be considered an indicator of life expectancy. Life expectancy is considered as one of the basic indicators of socio-economic well-being of the population (Tuaeva and Sugarova, 2013; Polezharova et al., 2020). Tracking the dynamics of average life expectancy in the country and comparing the results by region and district helps identify problem areas in which the demographic problem is most acute. This makes it possible to respond in the framework of regional and national social policies (Vlasova, 2017).

Bloomberg experts consider the life expectancy of the average citizen as the main indicator (60% of weight) when assessing the level of effectiveness of healthcare systems (Russia Became the Last in Health Care Efficiency Rating, 2016). Other indicators are government spending on health as a share of GDP per capita and the cost of per capita medical services. The first of these indicators is a reflection of the degree of attention and concern of the state to the health and life of citizens (Panova, 2015). Therefore, the prevailing share of health care expenditures in the structure of GDP in comparison with developed countries criticizes the liberal part of Russian society, which considers the level of the indicator not sufficient to ensure the provision of quality medical care accessible to all citizens of the country. Sergeeva NM, comparing this indicator of Russia with the countries of Europe, notes that its level is stably inferior to all but Ukraine in recent years (Sergeeva, 2018). There are undoubtedly differences in the health systems that have developed in the world; this figure will be naturally higher in countries with a larger private sector (Perkhov and Lutsko, 2019).

The share of government spending is considered the main criterion for the development of healthcare; the health system cannot exist solely on the basis of budgetary funds (Zyukin et al., 2019). The experience of the most developed European countries confirms this; there is a high life expectancy of the population, but a significant part of medical expenses is transferred to insurance medical organizations or carried out at the expense of the patient (Travnev, 2017). There is also a fair opinion that the achievement of healthcare efficiency while ensuring a high life expectancy is the result of the effective work of all elements of the system: from the necessary level of financing to the rational use of available resources, as well as increasing the motivation of medical personnel to work and conscientious performance of their duties (Kuznetsov, 2019; Muñoz, 2019).

1. Theoretical basis

The effectiveness of the functioning of health systems is most often determined on the basis of the average life expectancy of the population, since it is believed that the more efficient the health system is, the higher the life expectancy of the population in a certain territory (Kadyrov et al., 2019). However, effectiveness is affected by a system of many factors of different nature of action. The relative importance of healthcare as an economic sphere is manifested through the indicator of the share of healthcare expenditures in the structure of GDP. Our position is based on the fact that this indicator among the countries is not an objective criterion for the work of the health care system, and therefore it is also not able to influence life expectancy. The share of health care expenditures in the GDP structure is not indicative of Russia as a large country in terms of population and especially in geographical size, which still retains elements of Soviet state medicine. At the same time, other, especially the general improvement in the economic situation in the country, which has slowed down significantly in recent years, have become the priority reasons for ensuring an increase in the life expectancy of the population of Russia. Therefore, the research hypothesis says that the share of health care spending does not affect the quality of the health care system, which is expressed in the average life expectancy of the population.

2. Methodology

The work used data published by the Center for Humanitarian Technologies, reflecting the rating among 183 countries in terms of health care spending (The rating of the countries of the world in terms of health spending, 2006–2020) and average life expectancy of the population (Rumyantseva, 2018). To confirm the hypothesis, an analysis was made of the degree of influence of the share of health care spending in the GDP structure on average life expectancy in the context of countries using a simple pair correlation and correlation between ranks based on the construction of data scattering diagrams. A cluster analysis was also carried out, on the basis of which a grouping was made among countries by the level of health spending as a percentage of GDP. The number of groups was determined based on the Sturgess formula. A confirmation of the hypothesis that there is no connection between the share of health care spending in the structure of GDP and life expectancy is the insignificance of the pair correlation coefficient, the inadequacy of the approximation model for their

relationship and the absence of a logical connection in the groups obtained depending on the level of the regressor factor.

3. Results

An assessment of the impact of the share of health care expenditures on average life expectancy in the context of 183 countries on the basis of constructing a dispersion diagram showed that there is no stable correlation between these indicators. This is confirmed by the results obtained, since the direction and compression of the cluster points relative to the regression line emphasizes the absence of a significant correlation between the studied data series (Figure 1).

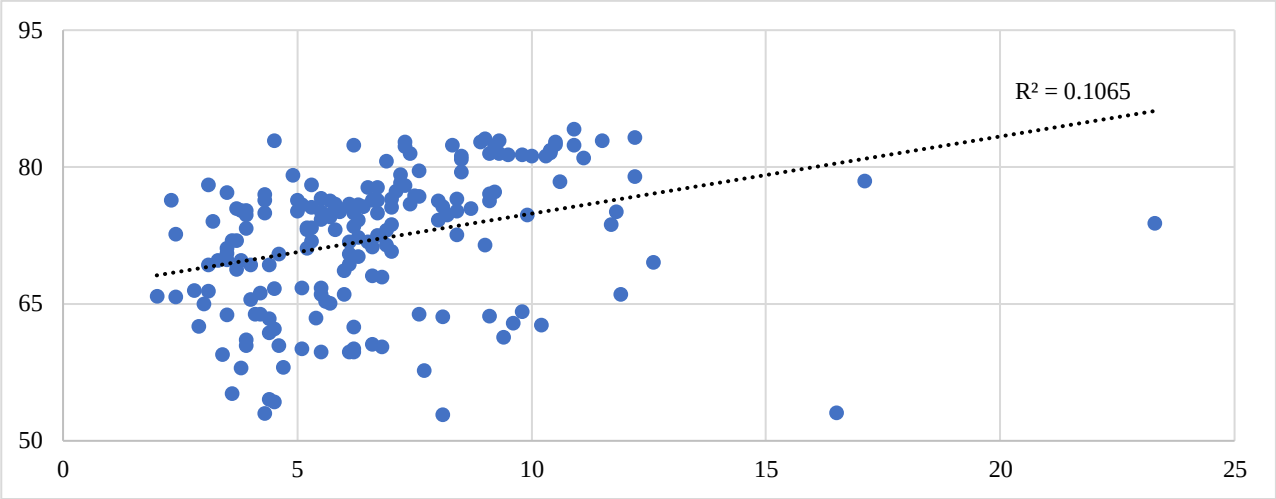

Figure 1. Assessment of the relationship between the average life expectancy and the level of health expenditure on GDP in the context of 183 countries in 2018

An analysis of the correlation of the ranks of the studied indicators also confirmed the absence of a relationship between life expectancy and the level of health care spending in different countries; This is evidenced by the scattering diagram obtained, on which the cluster points relative to the regression line are randomly located and have a large spread (Figure 2).

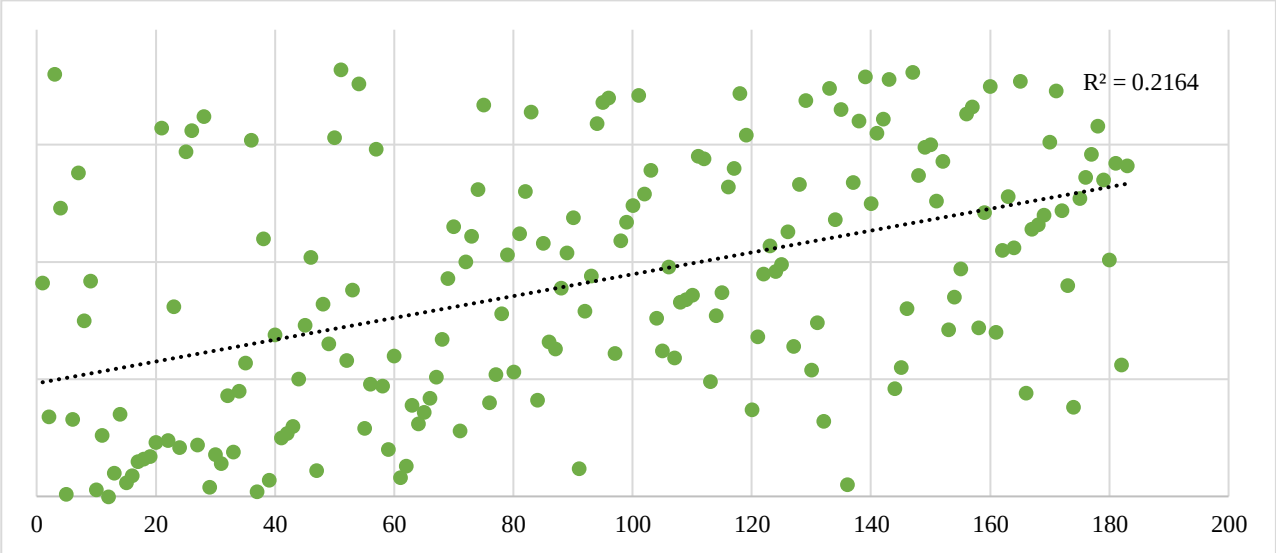

Figure 2. Assessment of the relationship between the ranks in the context of 183 countries by average life expectancy and the level of health care expenditures from GDP in 2018

All countries were divided into 8 groups during cluster analysis based on the Sturgess formula. During the clustering process, 3 countries were excluded from the sample - Sierra Leone, the USA and the Marshall Islands, in which the level of health expenditures was significantly separated from other countries and amounted to 16.5%, 17.1% and 23.3%, time, as in other countries, the variation of the studied indicator ranges from 2-12.6%.

As a result, the first group with the lowest level of expenditures (2-3.3%) included 12 countries, most of which belong to East Asia and Africa and have a low level of socio-economic development (the exception is Qatar). The average group level of health spending is 3%, and the average life expectancy in these countries is 69 years. The second group, where the level of health spending varies from 3.3-4.7%, includes 39 countries from different continents of the world and having different levels of socio-economic development. At the same time, the average level of health care spending in the group is 4.0%, and the average life expectancy is 67 years, which is lower than in the first group. As a result of clustering, 31 countries, including Russia, were included in the third group of countries with a level of health spending in the range of 4.7-6.0%; the average level of health expenditures from GDP in which was 5%, and the average life expectancy was 72 years.

The fourth group is the largest and includes 41 states of the world, where the share of health care spending varies between 6-7.3% of GDP, and the average group spending level was 7% with an average life expectancy of 81 years, which is the highest value among all

clusters. The fifth group included 20 countries with different levels of socio-economic development with a share of health expenditures of 7.3-8.6% of GDP and an average life expectancy of 74 years. The sixth group of countries included 19 countries, including many countries in Europe, where the level of health spending is 8.6-10% of GDP. At the same time, the average group expenditure level is 9%, and the average life expectancy is only 76 years. 11 countries were included in the seventh group of countries with a fairly high level of health care spending, where health care spending varies between 10–11.3%, and their average life expectancy is 80 years (Table 1).

Table 1. Cluster analysis of 183 countries by level of health spending in 2018

Group number	The number of countries and the interval of the group by the share of health spending in GDP	Country	The average value of health spending, in% of GDP	Life expectancy, years
1	2,0 - 3,3% (12 countries)	Papua New Guinea, Brunei, Bangladesh, Laos, Pakistan, Angola, Eritrea, Qatar, Indonesia, Gabon, Venezuela	3,0	69
2	3,3 - 4,7% (39 countries)	Equatorial Guinea, UAE, Kazakhstan, Bhutan, Fiji, Djibouti, Saint Vincent and the Grenadines, Nigeria, Thailand, Vanuatu, India, Malaysia, Mongolia, Mali, Sri Lanka, Kuwait, Seychelles, Benin, DRC, Timor-Leste, Ethiopia, Tanzania, Guyana, Mauritania, Oman, Turkey, Antigua and Barbuda, CAR, Philippines, Ghana, Gambia, Cote d'Ivoire, Singapore, Kenya, Zambia, Chad, Congo, Egypt, Cameroon	4,0	67
3	4,7 - 6,0% (31 countries)	Bahrain, China, Romania, Peru, Myanmar, Mozambique, Grenada, Cape Verde, Solomon Islands, Dominic, Saint Lucia, Tonga, Russia, Haiti, Mexico, Samoa, Jordan, Senegal, Botswana, Guinea, Yemen, Vietnam , Mauritius, Saudi Arabia, Saint Kitts and Nevis, Sudan, Morocco, Guatemala, Colombia, Sao Tome and Principe, Madagascar	5,0	72
4	6,0 - 7,3% (41 countries)	Jamaica, Suriname, Belize, Cambodia, Guinea-Bissau, Luxembourg, Latvia,	7,0	81

		Dominican Republic, Uganda, Burundi, Niger, Macedonia, Belarus, Uzbekistan, Nepal, Bahamas, Poland, Trinidad and Tobago, Algeria, Kyrgyzstan, Turkmenistan, Togo , Estonia, Albania, Lithuania, Ukraine, Rwanda, Burkina Faso, Cyprus, Azerbaijan, Bolivia, Tunisia, Barbados, El Salvador, Tajikistan, Slovakia, Czech Republic, Croatia, South Korea, Israel, Panama		
5	7,3 - 8,6% (20 countries)	Ireland, Hungary, Argentina, Costa Rica, Montenegro, Comoros, Swaziland, Lebanon, Paraguay, Iran, South Africa, Lesotho, Bulgaria, Iceland, Ecuador, Honduras, Georgia, Greece, Slovenia, Chile	8,0	74
6	8,6 - 10,0% (19 countries)	Nicaragua, Italy, Spain, Moldova, Portugal, Uruguay, Serbia, Namibia, New Zealand, Bosnia and Herzegovina, Australia, Malta, Zimbabwe, Finland, Liberia, United Kingdom, Malawi, Armenia, Belgium	9,0	76
7	10,0 - 11,3% (11 countries)	Afghanistan, Denmark, Austria, Andorra, Netherlands, Canada, Norway, Maldives, Japan, Sweden, Germany	11,0	80
8	11,3 - 12,6% (10 countries)	France, Palau, Brazil, Kiribati, Switzerland, Cuba, Micronesia Sierra Leone, USA, Marshall Islands	12,0	76

Source: made by the author based on data from the Center for Humanitarian Technologies (The rating of the countries of the world in terms of health spending, 2006-2020; Rating of countries in terms of life expectancy, 2016-2020).

The eighth group of countries with the highest expenditures on healthcare development included 10 entities, among which 7 have healthcare expenditures ranging from 11.3-12.6%, as well as 3 countries with extremely high healthcare expenditures (Sierra Leone, USA and Marshall Islands). Moreover, the average level of health spending among 7 countries is 12%, and the average life expectancy is only 76 years. Despite the fact that health care spending in Sierra Leone is about 16.5%, the average life expectancy in this African republic is only 53 years, which confirms the hypothesis that the share of health care spending is not a determining factor in the quality of the system health care and, accordingly, does not significantly affect the life expectancy of the population. In the United States, despite 17.1%

of healthcare costs, life expectancy is 78.5 years, although, for example, this indicator in Japan with a spending level of 10.9% is 84.2 years. The highest level of health spending is observed in the Marshall Islands (23.2%), but the average life expectancy is only 73.9 years.

4. Discussions

The uneven development of health systems in different countries is revealed by ratings on indicators such as life expectancy, the number of healthy people in society, and the effectiveness of medical care (Rumyantseva, 2018). However, the ratings of countries on the effectiveness of the health system in practice are still not always indicative. For example, according to a Bloomberg rating in 2016 (Lu Wei and Del Giudice), Italy took the first place, which was most affected by the consequences of the spread of COVID-19.

Many scientists agree that life expectancy is an important indicator of the effectiveness of the health system. At the same time, the share of health care expenditures in the context of assessing the quality of work of this system reflects only the attention of a particular state to its healthcare system as an important component of the social sphere (Poklonova et al., 2015).

Despite the fact that the World Health Organization annually publishes ratings of countries according to the level of health care spending, this indicator is not an objective criterion for international comparisons, since all countries have different levels of GDP, area, size and socio-demographic characteristics of the population (Travnev, 2017). The indicator of per capita health expenditures is more objective from the point of view of assessing the health system, since it is calculated in countries in a single currency (most often in US dollars), and the determination of its size per inhabitant makes it possible to take into account the differentiation of countries by area and population (Diaghileva, 2014).

So, Obrizan M. and Wehby G.L. revealed the heterogeneity of the results in their study of the impact of health care spending in countries on life expectancy in 2006-2011 using quantile regression. Their results suggest that increasing health care costs in countries with low life expectancy can have an important impact on life expectancy and significantly reduce global inequality in life expectancy and development by reducing the distribution of life expectancy in the world (Obrizan and Wehby, 2018).

At the present stage of development, the degree of state participation in the policy of financing the health system has begun to change, but there is some convergence in policies adopted in different countries to improve financial incentives and encourage the effective use of medical services. The key factor for success in the competition of hospitals is changes in the efficiency of hospitals, and not the attitude to public or private ownership, which also strongly determines the share of health care expenditures in the structure of GDP as practice shows (Stabile and Thomson, 2014).

The main problem of ensuring the growth of life expectancy of the population of Russia is the use of outdated treatment technologies (for example, surgical intervention instead of more effective therapy), the lack of a focus on healthcare for the recovery of patients, the underdevelopment of preventive medicine, violation of citizens' rights (tacit focus on saving) in the manner of providing free medical care (access to diagnostic equipment, prescribing procedures, issuing free medicines) (Rumyantseva, 2018). The present value of future medical expenses is an important determining factor in decisions made over time, such as financing long-term medical care, investment in fixed assets (Ewing et al., 2003). In most Russian regions, this approach to building a business in the healthcare system is still not relevant, so the real cost of medical services is difficult to assess, which determines less involvement of business entities in this sphere in the country's GDP. Scenario planning tools are poorly used, which are necessary for the system to assess the dynamics of the impact of new technologies, such as big data & cloud & in healthcare industry (Akhlaghinia et al., 2019).

Conclusion

The research confirms the hypothesis that the share of government spending on GDP does not affect the average life expectancy of the population as one of the most important criteria for the effectiveness of the health system. Based on the result of the correlation analysis carried out in the context of 183 countries, it was found that there is no connection between the share of health expenditures from GDP in countries and average life expectancy, which confirms the failure to use this indicator as a criterion for assessing the development of the health system. A cluster analysis of the countries under consideration showed that the highest life expectancy (81 years) is observed in those countries where the average level of health spending is about 7%. Life expectancy is not high in countries where health spending

is the highest share of GDP. This allows us to conclude that the effectiveness of the health care system is a complex category, depending not only on the level of state funding, but also on a number of other aspects. Since ensuring the high efficiency of national health systems is one of the priority tasks in modern conditions in modern conditions, the search for mechanisms to achieve it is an important area. Currently, WHO does not have a unified methodology for the objective assessment of the effectiveness of countries' health systems, which complicates the task of identifying and systematizing existing social problems in order to develop measures to solve them.

References

Akhlaghinia, N., Rajabzadeh, A., Yazdian, A., Moghbel, A. (2019). Scenario planning for emergent technology (big data & cloud) in healthcare industry. Amazonia Investiga, 7 (15), 299-305.

Diaghileva, N.V. (2014). The effectiveness of public spending on health services. Bulletin of the Orenburg State Agrarian University, 6 (50), 205-208.

Ewing, B.T., Piette, M.J., Payne, Ja.E. (2003). Forecasting medical net discount rates. Journal of Risk & Insurance, 70 (1), 85.

Kadyrov, F.N., Obukhova, O.V., Brutova, A.S. (2019). Health care financing in 2019: new priorities and channels for the movement of funds. Health Care Manager, 1, 70-78.

Kuznetsov, V.V. (2019). Modern aspects of the study of the effectiveness of healthcare to improve the quality of life of the population. Quality and life, 1 (21), 84-89.

Lu Wei, Del Giudice V. Italy's Struggling Economy Has World's Healthiest People. Available at: https://www.bloomberg.com/news/articles/2017-03-20/italy-s-struggling-economy-has-world-s-healthiest-people.

Muñoz, O. (2019). Cultura, gestión pública, gerencia y sistema de relacionamiento, *Revista Latinoamericana de Difusión Científica*, 1 (1), 68-83.

Obrizan, M., Wehby, G.L. (2018). Health expenditures and global inequalities in longevity. World Development, 28-36.

Panova, L.V. (2015). Health care financing as a contextual health factor. Petersburg Sociology Today, 6, 384-407.

Perkhov, V.I., Lutsko, V.V. (2019). Macroeconomic spending on healthcare in Russia and abroad. Modern problems of healthcare and medical statistics, 2, 334-345.

Podgalo, D.D., Sokolova, M.G., Atroshchenko, A.M. (2019). Health problems in the Russian Federation and ways to solve them. Economics and production organization efficiency, 30, 74-80.

Poklonova, E.V., Starodub, V.A., Zagora, I.P. (2015). The costs of social policy: status and trends. Economics and Entrepreneurship, 11-2 (64), 112-117.

Polezharova, L. V.; Goncharenko, M. A.; Gryechishkin, A. V. (2020). International tax models towards multinational companies from the perspective of national welfare, *Revista de la Universidad del Zulia*, 11 (29), 337-366.

Rating of countries in terms of life expectancy (2006–2020). The Humanitarian Encyclopedia: Research. Center for Humanitarian Technologies. Available at: https://gtmarket.ru/ratings/life-expectancy-index/life-expectancy-index-info.

Rumyantseva, E.E. (2018). Monitoring national health systems. World economy and international relations, 62 (2), 92-99.

Russia Became the Last in Health Care Efficiency Rating (2016). RBC. Available at: http://www.rbc.ru/society/29/09/2016/57ecd9499a79476f928bb8f.

Sergeeva, N.M. (2018). Comparative assessment of health care costs in Russia and European countries. Azimuth of scientific research: economics and management, 7 (3, 24), 256-259.

Stabile, M., Thomson, S. (2014). The changing role of government in financing health care: an international perspective. Journal of Economic Literature, 52 (2), 480-518.

Tagaeva, T.O., Kazantseva, L.K. (2016). Modern problems of public health and healthcare in Russia. Transactions of Novosibirsk State University of Architecture and Civil Engineering (Sibstrin), 19 (3, 63), 191-201.

The rating of the countries of the world in terms of health spending (2006–2020). The Humanitarian Encyclopedia: Research. Center for Humanitarian Technologies. Available at: https://gtmarket.ru/ratings/expenditure-on-health/info.

Travnev, L.N. (2017). Social expenditures of the state and the search for new instruments for financing social policy. Economics: yesterday, today, tomorrow, 7 (2A), 5-17.

Tuaeva, L.A., Sugarova, I.V. (2013). The effectiveness of spending on the health system. Terra Economicus, 11 (3-3), 94-97.

Vlasova, O.V. (2017). The study of life expectancy in the Central Federal District. Karelian Scientific Journal, 6 (4, 21), 335-337.

Zyukin, D.A., Belyaev, S.A., Vlasova, O.V., Nadzhafova, M.N., Reprintseva, E.V., Sergeeva, N.M. (2019). On the trends in the expansion of the market of paid medicine in the federal districts of the Russian Federation. Vestnik NGIIE, 3 (94), 62-73.

Drug delivery via super-paramagnetic $(N2)n[SiO2(OH)2]8$ Core-Shell catalyst

Somayeh Khosravi*
Majid Monajjemi**

ABSTRACT

The MNPs @ $[SiO_2(OH)_2]_8$ catalyzers were stablished via ab-initio and quantum mechanics & Molecular mechanic (QM/MM) simulation. The studies focus on how to improve the dispersion of composite particle for achieving high magnetic performances. The results revealed that the Fe3O4 @$[SiO_2\ (OH)_2]_8(N_2)_8$ as a cabalist exhibited better thermodynamic stability and dispersion than the magnetite nanoparticles. Furthermore, the particle size and magnetic properties of the $[SiO_2\ (OH)_2]_8(N_2)_8$ composite nanoparticles can be controlled by changing the functional groups. The electrical properties such as NMR Shielding, electron densities, energy densities, potential energy densities, ELF, LOL, of electron density, eta index, ECP, ESR and hyperfine interactions for Fe_3O_4@ $[SiO_2(OH)_2]_8(N_2)_8$ have been calculated. As the catalyst could be easily recovered by magnetic separation and recycled for a few times without significant loss of its catalytic activity, we have calculated to obtain the stronger non bonded interaction in the Fe_3O_4@ $[SiO_2(OH)_2]_8(N_2)_8$ system. This system can be used for antibiotics drug delivery instead of injection. The chemical shielding and several factors as the same electronegativity, magnetic anisotropy of π-systems will be changed due to the number of electrons The chemical shielding is a vector orientation function for all of the shielding parameters that can change in several places inside the shielding region .

KEYWORD: super-paramagnetic Nano particle, QM/MM simulation, Fe3O4, $[SiO_2\ (OH)_2]8$, non-bonded interactions

*Department of Chemistry, Science and Research Branch, Islamic Azad University, Tehran, Iran

**Department of Chemical Engineering, Central Tehran Branch, Islamic Azad University, Tehran, Iran. E-mail: Maj.monajjemi@iauctb.ac.ir

Recibido: 29/04/2020 Aceptado: 17/06/2020

Suministro de fármacos a través de paramagnéticos (N2) n [SiO2 (OH) 2] 8 Catalizador Core-Shell

RESUMEN

Los catalizadores MNPs @ [SiO2 (OH) 2] 8 se establecieron mediante simulación ab-initio y mecánica cuántica y mecánica molecular (QM / MM). Los estudios se centran en cómo mejorar la dispersión de partículas compuestas para lograr altos rendimientos magnéticos. Los resultados revelaron que el Fe3O4 @ [SiO2 (OH) 2] 8 (N2) 8 como cabalista exhibió una mejor estabilidad y dispersión termodinámica que las nanopartículas de magnetita. Además, el tamaño de partícula y las propiedades magnéticas de las nanopartículas compuestas [SiO2 (OH) 2] 8 (N2) 8 se pueden controlar cambiando los grupos funcionales. Las propiedades eléctricas tales como NMR Shielding, densidades de electrones, densidades de energía, densidades de energía potencial, ELF, LOL, de densidad de electrones, índice eta, ECP, ESR e interacciones hiperfinas para Fe3O4 @ [SiO2 (OH) 2] 8 (N2) 8 han sido calculados. Como el catalizador podría recuperarse fácilmente mediante separación magnética y reciclarse varias veces sin una pérdida significativa de su actividad catalítica, hemos calculado obtener la interacción no unida más fuerte en el sistema Fe3O4 @ [SiO2 (OH) 2] 8 (N2) 8. Este sistema se puede usar para la administración de antibióticos en lugar de la inyección. El blindaje químico y varios factores como la misma electronegatividad, la anisotropía magnética de los sistemas π se cambiarán debido a la cantidad de electrones. El blindaje químico es una función de orientación vectorial para todos los parámetros de blindaje que pueden cambiar en varios lugares dentro de la región de blindaje.

PALABRAS CLAVE: nanopartículas superparamágicas, simulación QM / MM, Fe3O4, [SiO2 (OH) 2] 8, interacciones no unidas

Introduction

Since the magnetism in Fe_3O_4 was discovered, the material revolutionized the area of science with its wonderful properties. The materials have been at the core of the tremendous application such as electric motor, electromagnet, transformer, video/audiotape, and biomedical technologies etc. Fe_3O_4 is an electronic conductor with conductivities extremely higher than Fe_2O_3, and this is ascribed to electron exchange between the Fe^{III} and Fe^{II} centers. It is ferromagnetic with a curie temperature of 855 K and the ferromagnetism properties of Fe_3O_4 arises because the electron spin of both iron ions in the octahedral structures is coupled and the

spin of the Fe^{3+} in the tetrahedral structure is coupled but anti-parallel to the previous one. This magnetic particle also falls under the categories of such functional materials owing to its several wonderful properties such as high Curie temperature (~850 K), and low electronic resistivity at lab temperatures. Fe_3O_4 is an important catalyst in the Haber process in the water gas shift reaction (Farhami, 2017). The latter uses a high temperature shift catalyst (HTS) of iron oxide stabilized by chromium oxide. This iron-chrome catalyst is reduced at reactor start up to generate Fe_3O_4 from α-Fe_2O_3 & Cr_2O_3 to CrO_3. These kind magnetite particles are the earliest discovered magnet that crystallizes in the inverse cubic spinel structures. Each cubic spinel cell contains eight interpenetrating oxygen and the tetrahedral sites, occupied by one-third of the iron atoms, form a diamond structures. The remaining Fe atoms are located at the octahedral sites with the nearest-neighbor atoms lined up as strings along six different {110} directions. In other words Fe_3O_4 consists of a cubic close packed array of oxide ions where all of the Fe^{2+} ions occupy half of the octahedral sites and the Fe^{3+} are split evenly across the remaining octahedral sites and the tetrahedral sites. In this work we have investigated the catalysis's properties of Fe3O4 nanoparticles @[SiO2 (OH)2]8 to compare with $[SiO_2(OH)_2]_8(N_2)_8$ in the area of silicon effects of chemical synthesizes while the nano-Fe_3O_4@SiO2 supported ionic liquid Fe3O4@SiO2-IL can be successfully applied for perform the reaction of organic molecules (Bourgeois, 2000).

1. Computational details

Part of the systems including Fe3O4@ $[SiO2 (OH)_2]_8$, Fe3O4@ $[SiO_2(OH)_2]_8(N2)_8$ (Fig.1) and Fe_3O_4@SiO2-IL nanoparticles have been modeled with QM/MM method and the calculations are carried out with the DFT methods. In this investigation, differences in force field are illustrated by comparing the calculated energies with AMBER and OPLS force fields. Furthermore, Hyper-Chem professional release 7.01 programs applied for the additional calculations. For non-covalent interactions between core and shell, the B3LYP method is unable to describe van der Waals by medium-range interactions. Therefore, the ONIOM methods including 3 levels of 1-high calculation (H), 2-medium calculation (M), and 3-low calculation (L) have been performed in our study for calculating those non-bonded interactions (Frackowiak, 2002).

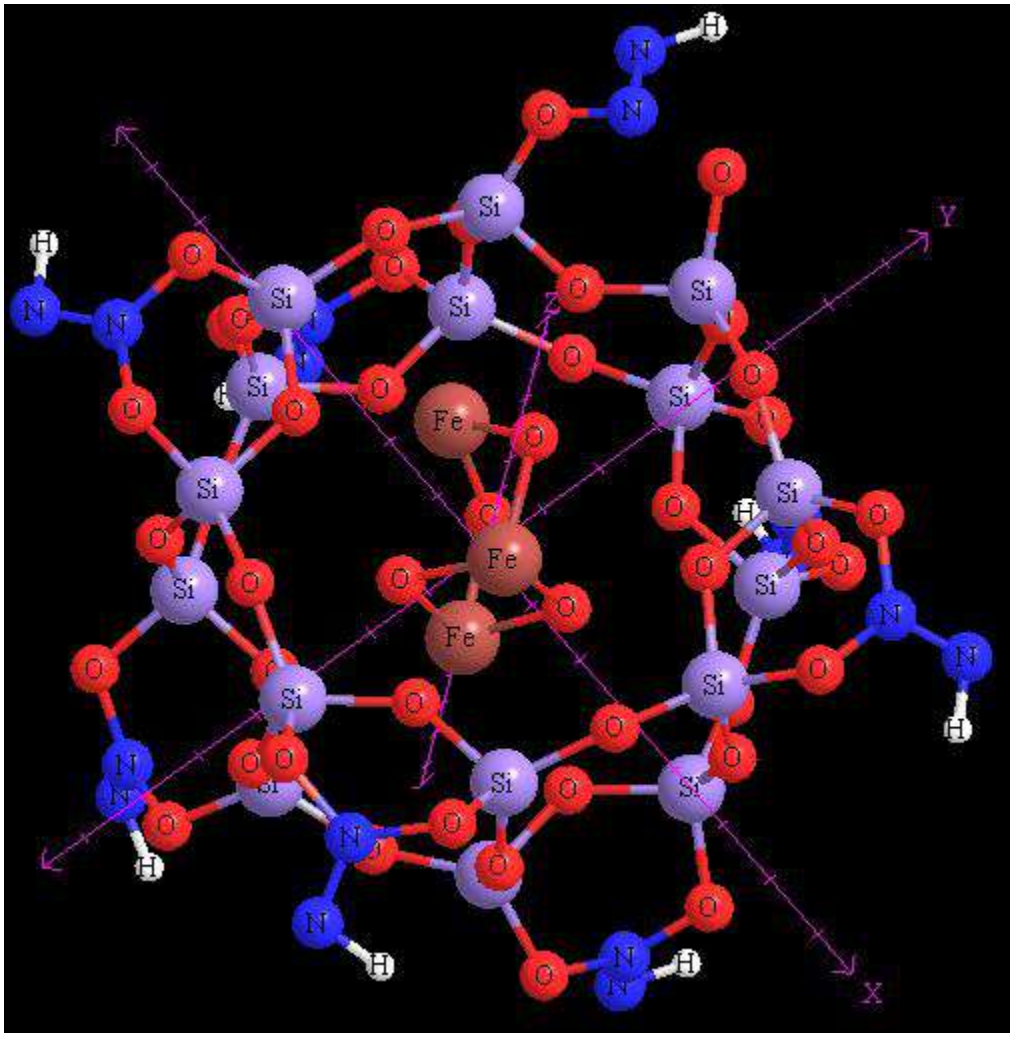

Fig.1.Non bonded interaction between Various Optimized $SiO2(OH)2]8(N2)n\ (n = 0 - 8)$ of core-shell nanoparticles.

The ab-initio and DFT methods are used for the model system of the ONIOM layers and the semi empirical methods of pm6 (including pseudo=lanl2) and Pm3MM are used for the medium and low layers, respectively **(**Monajjemi, 2009**)**. B3LYP and the most other popular and widely used functional are insufficient to illustrate the exchange and correlation energy for distant non-bonded medium-range systems correctly. Moreover, some recent studies have shown that inaccuracy for the medium-range exchange energies leads to large systematic errors in the prediction of molecular properties. Geometry optimizations and electronic structure calculations have been carried out using the m06 (DFT) functional. This approach is based on an iterative solution of the Kohn-Sham equation of the density functional theory in a plane-wave

set with the projector-augmented wave pseudo-potentials. The Perdew-Burke-Ernzerhof (PBE) exchange-correlation (XC) functional of the generalized gradient approximation (GGA) is also used. The optimizations of the lattice constants and the atomic coordinates are made by the minimization of the total energy (Monajjemi, 2011).

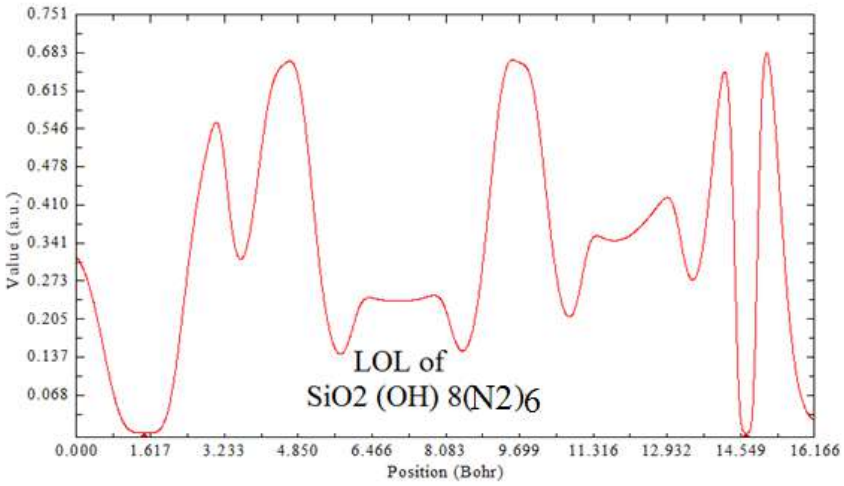

Fig.2: LOL for system of SiO2 (OH) 8(CO)x { X=6}

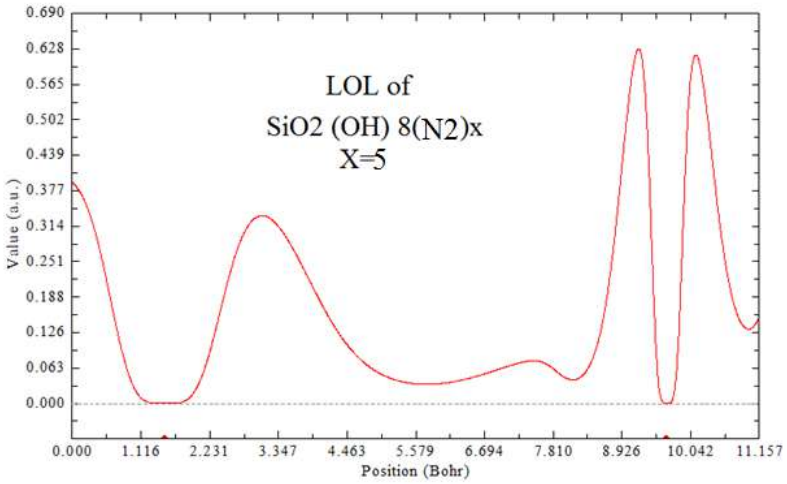

Fig.3: LOL for two systems of SiO2 (OH) 8(N2) x {X=5 }

The charge transfer and electrostatic potential-derived charge were also calculated using the Merz-Kollman-Singh Chelp or chelpG the charge calculation methods based on molecular electrostatic potential (MESP) fitting are not well-suited for treating larger systems whereas some of the innermost atoms are located far away from the points at which the MESP is computed. In such a condition, variations of the innermost atomic charges will not head towards

a significant change of the MESP outside of the molecule, meaning that the accurate values for the innermost atomic charges are not well-determined by MESP outside the molecule (Madani, 2017). The representative atomic charges for molecules should be computed as average values over several molecular conformations.

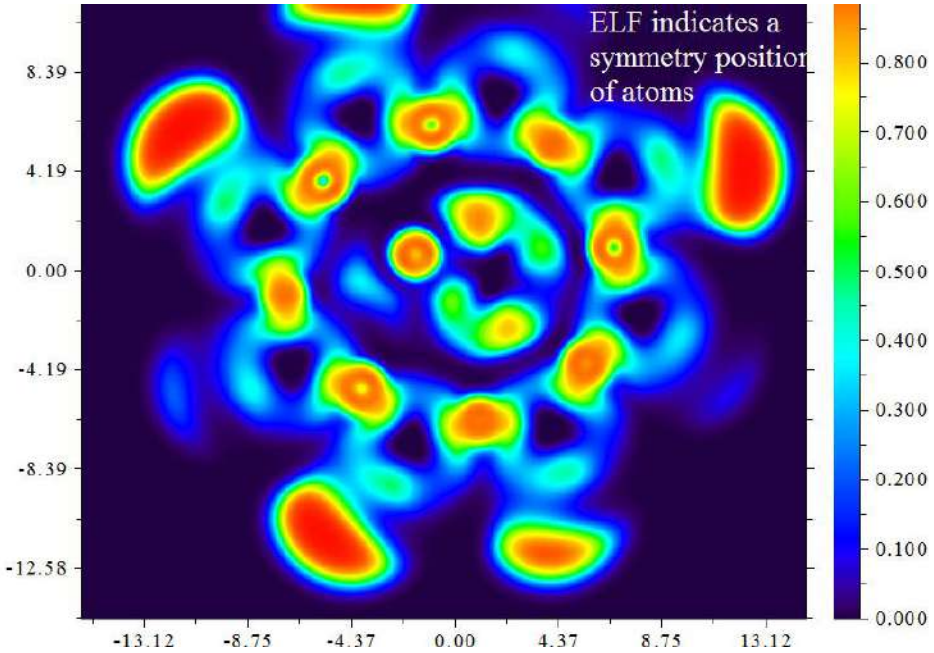

Fig.4. Color-field map of ELF for complexes [SiO2 (OH)2]8 (N2)4 indicates a symmetry position of systems

A detailed overview of the effects of the basis set and the Hamiltonian on the charge distribution can be found in references. The charge density profiles in this study has been extracted from first-principles calculation through an averaging process as described in reference. The interaction energy for capacitor was calculated in all items according to the equation as follows:

$$\Delta E_S(eV) = \{E_C - (\sum_{i=1}^{n}(Fe3O4 - [\mathrm{SiO2(OH)2]8(N2)n\ (n = 0 - 8)} + \sum_{i=6}^{14}(Fe3O4 - \mathrm{SiO2(OH)2]8(N2)n\ (n = 0 - 8)\}\ (1)$$

Where the "ΔE_S" is the no bonded and stability energies of systems. The electron density (Both of Gradient norm & Laplacian), value of orbital wave-function, electron spin density, electrostatic potential from nuclear atomic charges, electron localization function (ELF), localized orbital locator (LOL defined by Becke & Tsirelson), total electrostatic potential

(ESP), as well as the exchange-correlation density, correlation hole and correlation factor, and the average local ionization energy using the Multifunctional Wave-function analyzer have also been calculated in this study. The contour line map was also drawn using the Multiwfn software (Lu, T., Chen, F., 2012). The solid lines indicate positive regions, while the dash lines indicate negative regions. The contour line corresponding to VdW surface (electron density=0.001 a.u., which is defined by R. F. W Bader) is plotted in this study. This is specifically useful to analyze distribution of electrostatic potential on VdW surface. Such a contour line has also been plotted in gradient line and vector field map by the same option. The relief map was used to present the height value at every point. Shaded surface map and shaded surface map with projection are used in our representation of height value at each situation (Frackowiak, 2002).

2. Theoretical background

2.1. The electron density

The electron density has been defined as $\rho(r) = \eta_i \left|\varphi_i(r)\right|^2 = \sum_i \eta_i \left|\sum_l C_{l,i}\,\chi_i(r)\right|^2$(2). [119-121] Where η_i is occupation number of orbital (*i*), φ is orbital wave function, χ is basis function and *C* is coefficient matrix, the element of i_{th} row j_{th} column corresponds to the expansion coefficient of orbital *j* respect to basis function *i*. Atomic unit for electron density can be explicitly written as e/Bohr^3. $\nabla\rho(r) = [(\frac{\partial\rho(r)}{\partial(x)})^2+(\frac{\partial\rho(r)}{\partial(y)})^2+(\frac{\partial\rho(r)}{\partial(z)})^2]^{\frac{1}{2}}$ (3) $\nabla^2\rho(r) = \frac{\partial^2\rho(r)}{\partial x^2} + \frac{\partial^2\rho(r)}{\partial y^2} + \frac{\partial^2\rho(r)}{\partial z^2}$(4)[18-20].

The positive and negative value of this function correspond to electron density is locally depleted and locally concentrated respectively. The relationships between $\nabla^2\rho$ and valence shell electron pair repulsion (VSEPR) model, chemical bond type, electron localization and chemical reactivity have been built by Bader.

2.2. Kinetic energy density K(r)

The kinetic energy density is not uniquely defined, since the expected value of kinetic energy operator $\langle \varphi \left| -\left(\frac{1}{2}\right)\nabla^2 \right| \varphi \rangle$ can be recovered by integrating kinetic energy density from

alternative definitions. One of commonly used definition is: $k(r) = -\frac{1}{2}\sum_i \eta_i \varphi_i^*(r)\nabla^2\varphi_i(r)$ **(5)**[119-121] Relative to *K*(r), the local kinetic energy definition given below guarantee positivizes everywhere; hence the physical meaning is clearer and is more commonly used. The Lagrangian kinetic energy density, "G(r)" is also known as positive definite kinetic energy density.

$G(r) = \frac{1}{2}\sum_i \eta_i \ |\nabla(\varphi_i|^{\ 2} = \frac{1}{2}\sum_i \eta_i\{[(\frac{\partial\varphi_i(r)}{\partial(x)})^2 + (\frac{\partial\varphi_i(r)}{\partial(y)})^2 + (\frac{\partial\varphi_i(r)}{\partial(z)})^2]\}$ **(6)**. *K*(r) and *G*(r) are directly related by Laplacian of electron density $\frac{1}{4}\nabla^2\rho(r) = G(r) - K(r)$ **(7)**.

2.3. Electron localization function (ELF)

Becke and Edgecombe noted that spherically averaged like spin conditional pair probability has direct correlation with the Fermi hole and then suggested electron localization function (ELF) [123]. ELF(r) $= \frac{1}{1+[D(r)/D_{0(r)}]^2}$ **(8)** where D(r) $= \frac{1}{2}\sum_i \eta_i \ |\nabla\varphi_i|^{\ 2} - \frac{1}{8}[\frac{|\ |\nabla\rho_\alpha|^{\ 2}}{\rho_\alpha(r)} + \frac{|\ |\nabla\rho_\beta|^{\ 2}}{\beta(r)}]$ **(9)** and $D_{0(r)} = \frac{3}{10}(6\pi^2)^{\frac{2}{3}}[\rho_\alpha(r)^{\frac{5}{3}} + \rho_\beta(r)^{\frac{5}{3}}]$ **(10)** for close-shell system, since $\rho_\alpha(r) = \rho_\beta(r) = \frac{1}{2}\rho$, *D* and *D*0 terms can be simplified as D(r) $= \frac{1}{2}\sum_i \eta_i \ |\nabla\varphi_i|^{\ 2} - \frac{1}{8}[\frac{|\nabla\rho|^{\ 2}}{\rho(r)}]$ **(11)**, $D_{0(r)} = \frac{3}{10}(3\pi^2)^{\frac{2}{3}}\rho(r)^{\frac{5}{3}}$ **(12)**.

Savin *et al*. have reinterpreted ELF in the view of kinetic energy, which makes ELF also meaningful for Kohn-Sham DFT wave-function or even post-HF wave-function. They indicated that *D*(r) reveals the excess kinetic energy density caused by Pauli repulsion, while *D*0(r) can be considered as Thomas-Fermi kinetic energy density. Localized orbital locator (LOL) is another function for locating high localization regions likewise ELF, defined by Schmider and Becke in the paper[25]. $LOL(r) = \frac{\tau(r)}{1+\tau(r)}$ **(13)**, where $(r) = \frac{D_0(r)}{\frac{1}{2}\sum_i \eta_i \ |\nabla\varphi_i|^{\ 2}}$ **(14)**, $D_0(r)$ for spin-polarized system and close-shell system are defined in the same way as in ELF. Local information entropy is a quantification of information, this theory was proposed by Shannon in his study of information transmission in noise channel, and nowadays its application has been largely widened to other areas, including theoretical chemistry. Parr *et al.* discussed the relationship

between information entropy and atom partition as well as molecular similarity. This simulation and modeling of systems have been done based on our previous work.

3. Result and discussion

Modified magnetic materials are nowadays well-known and have been investigated intensively due to their potential applications in many areas, such as biology, medicine and the environment. These applications include enzyme and protein separations, RNA and DNA purifications (Deng, 2010).

The term "Ab Initio" is given to computations which are derived directly from theoretical principles, with no inclusion of experimental information. The most common type of ab initio calculation is called a Hartree-Fock calculation, in which the primary approximation is called the central field approximation. A method, which avoids making the HF mistakes in the first place, is known as Quantum Monte Carlo (QMC). Also, in contrast to the MD method which is entirely deterministic, the MC simulation method is based on the use of probabilistic concepts. In this method, a system composed of *N* interacting atoms is given a group of initial coordinates.

The evolution of this initial configuration is then generated by these successive random displacements of the atoms. There are some flavors of QMC vibrational, diffusion, and Green's functions. These methods work with a clearly correlated wave function and evaluate integrals numerically using a Monte Carlo integration. These calculations can be very time consuming, but they are apparently the most accurate methods known today. Ab initio calculations give very good qualitative results and can give increasingly accurate quantitative results as the molecules in question become smaller, generally. There are three steps in carrying out any quantum mechanical calculation in Hyper-Chem 8.0 program package. First, set up a molecule with an appropriate starting geometry. Second, choose a calculation method and its associated choices. Third, choose the type of calculation with the relevant options. The Monte Carlo simulations always detect the so-called "important phase space" regions which are of low energy. Because of defects of the force field, this lowest energy basin usually does not correspond to the native state in most cases, so the rank of native structure in those decoys produced by the force field itself is poor. In this study, difference in force field is illustrated by comparing the energy

calculated by using force fields, MM+, Amber, and OPLS. Also, we investigated polar solvent and the temperature effects (between 260K and 400K) on the stability of SWBNNT bonded to CFA (or CGA) in various solvents. The quantum mechanics (QM) calculations were carried out with the Hyper-Chem 8.0 program. This study mainly focuses on the magnetic properties of Fe3O4 in a non-bonded system with $SiO2(OH)2]8(N2)n\ (n = 0 - 8)$shell surfaces. The non-bonded interaction is shown in figs1- 8. As it is indicated in tables 1-10, the electrical properties can be obtained from changes in the non-bonded interactions. Electron densities, energy densities, Potential energy densities, ELF, LOL, Ellipticity of electron density, eta index and ECP for $SiO2(OH)2]8(N2)n\ (n = 0 - 8)$ were calculated of each simulation (Tables 1-10).

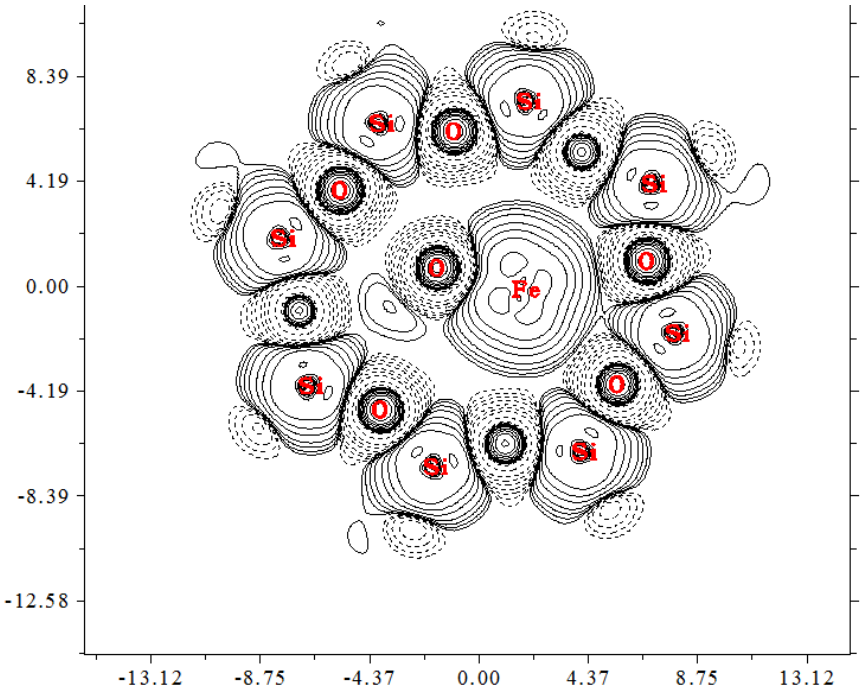

Fig.5: Density of Hamiltonian kinetic energy for [SiO2 (OH)2]8

According to the equation 13, 14 the largest electron localization is located on Fe3O4 where the electron motion is more likely to be confined within that region. If electrons are completely localized in the Fe3O4, they can be distinguished from the ones outside. As shown in tables 1-10 the large ELF is close to the Fe3O4 atoms. The regions with large electron localization need to have large magnitudes of Fermi-hole integration which would lead the Fe3O4 towards superparamagnetic. The fermi hole is a six-dimension function and as a result,

it is difficult to be studied visually. Based on equations 12, 13 and 14, Becke and Edgecombe noted that the Fermi hole is a spherical average of the spin which is in good agreement with our results in tables and Figs.

Table1: All Electron Densities of non-bonded interactions for $SiO2[(OH)2]8$complexes

Atom(number)	Density of all electron(10^{-3})	Density of alpha (10^{-3})	Density of Beta (10^{-3})	Spin Density
Fe(1)	0.29	0.16	0.16	0.0
Fe(2)	0.21	0.12	0.12	0.0
Fe(3)	0.33	0.15	0.14	0.01
O(1)	0.13	0.05	0.04	-0.01
O(2)	0.25	0.15	0.15	0.0
O(3)	0.33	0.17	0.15	0.02
O(4)	0.21	0.14	0.13	-0.02

Table.2: Gap energies for various [SiO2 (OH)]8(N2)n (n=0-8)

[SiO2(OH)2]8 (N2)n	HOMO (e.V)	LUMO (e.V)	Gapenergy (e.V)
n=0	-3.234562	-0.234515	3.000047
n=1	-3.956745	-0.298765	3.65798
n=2	-3.879656	-0.287659	3.591997
n=3	-3.873456	-0.234987	3.636489
n=4	-3.768545	-0.277531	3.491014
n=5	-3.150873	-0.254573	2.896300
n=6	-3.457843	-0.298342	3.159501
n=7	-3.376543	-0.232485	3.144058
n=8	-3.768456	-0.309566	3.458890

ELF indicates that it is actually a relative localization and must be accounted within the range of [0, 1]. A large ELF value corresponds to largely localized electrons which indicate that a covalent bond, a lone pair or inner shells of the atom is involved. According to equation 16, LOL can be interpreted similar to ELF in terms of kinetic energy, though; LOL can also be interpreted in terms of localized orbitals. Small (large) LOL value usually appears in boundary (inner) region of localized orbitals due to the large (small) gradient of orbital wave-function in this area. The value range of LOL is identical to ELF, namely [0, 1]. LOL has a similar expression as ELF.

Table3: Energies of non-bonded interactions for Fe3O4@ [SiO2 (OH)2]8 (N2)4

[SiO2(OH)2]8 (N2)4	Lagrangian kinetic [G(r)]energy(10^{-3})	Hamiltonian kinetic [K(r)]energy(10^{-2})
Fe(1)	0.35	0.46
Fe(2)	0.36	0.37
Fe(3)	0.34	0.41
O(1)	0.13	-0.13
O(2)	0.16	-0.17
O(3)	0.22	-0.24
O(4)	0.24	-0.25

Table4: Laplacian, ELF, LOL and Local information entropy of non-bonded interactions of Fe3O4@ [SiO2 (OH)2]8 (N2)4

Atom(number)	Laplacian of electron density(10^{-1})	Electron localization function (ELF) (10^{-3})	Localized orbital locator (LOL) (10^{-1})	Local information entropy (10^{-4})
Fe(1)	-0.21	0.44	0.13	0.56
Fe(2)	-0.31	0.41	0.34	0.19
Fe(3)	-0.35	0.16	0.23	0.25
O(1)	0.13	0.51	0.23	0.22
O(2)	0.41	0.16	0.55	0.35
O(3)	0.36	0.42	0.21	0.40
O(4)	0.15	0.21	0.43	0.20

As it is indicated in tables, LOL is low and constant for those $SiO2(OH)2]8(N2)n(n = 0 - 8)$ compounds. The results of ELF and LOL indicate that the Fe3O4 starts to act as a super magnetic in any situation inside of shell.

Table5: Average local ionization energy, RDG and ESP of non-bonded interactions for Fe3O4@ [SiO2 (OH)2]8 (N2)3

Atom(number)	Reduced density gradient(RDG) (10^{+1})	Average local ionization energy	ESP from nuclear charge (10^{4})	ESP from electron charge (10^{2})
Fe(1)	0.42	0.43	0.13	-0.17
Fe(2)	0.35	0.56	0.15	-0.50
Fe(3)	0.41	0.31	0.11	-0.45
O(1)	0.23	0.60	0.17	-0.14
O(2)	0.24	0.21	0.16	-0.43
O(3)	0.35	0.35	0.13	-0.33
O(4)	0.23	0.16	0.12	-0.31

Table6: Lambada2, Wave function value, Ellipticity of electron density and Eta index of non-bonded interactions for Average local ionization energy, RDG and ESP of non-bonded interactions for Fe3O4@ [SiO2 (OH)2]8 (N2)2

Atom(number)	Lambada2 (10^{-3})	Wave function value $10^{-4})$	Ellipticity of electron density	Eta index
Fe(1)	-0.25	0.84	0.42	-4.3
Fe(2)	-0.24	0.73	0.45	-1.3
Fe(3)	-0.22	0.60	0.43	0.80
O(1)	0.18	0.51	-0.14	0.75
O(2)	0.25	0.53	-0.26	0.52
O(3)	0.23	0.42	-0.17	0.43
O(4)	0.23	-0.37	-0.24	0.31

As it is shown in Fig1-10, there are fluctuations within a decreasing amount for electron density, energy density, ELF and LOL, while there is no fluctuation for ESP which is actually periodic.

Currently, a number of drugs are used in the treatment of the cancer, but most of them were produced controlled effect on the cancer cells. The usual applications of hetero-cycles are as vast as it is diverse and is not extensively encompassed in the scope of that study. The most drugs belong to a class of hetero-genius structures. Heterocyclic structures played an important behavior in the metabolism of all cells; maximum number of them is 6 (or sometimes 5) membered hetero-cycles including one to three hetero-atoms. Recently, imidazole fragment has been attracting much concentration because of its role as attractive scaffold for biochemical

active hetero-cyclic drugs. Generally, chemical-physics and biochemical properties like acceptor and donor capabilities, hydrogen bond, π-π interactions, van der Waals, coordination bond with a metal and in total hydrophobic force has caused much interest in anticancer studies for such compounds. These properties are important of understanding for its reactivity enable derivative for binding with various nucleic acids, enzymes and biological structures. A large number of the important heterocyclic compounds are used in the medical activities such as histidine and proline which are amino acids. It is notable pyridoxine, folic acid, thiamine, riboflavin, biotin, B_{12} and E families of the vitamins are included of heterocyclic structures. For investigation of antifungal activity compounds, Singh et al have synthesized 1,3, 4oxadiazolo-(3,2a)-s-triazin-7-thione and Abdle,et-al have synthesized some novel 1, 3, 4oxadiazole derivatives. Fungi are hetero-tropic micro-organisms that are distinguished. Dhar has synthesized 1,3,4-oxadiazolo-[3,2-a]-1,3,4-dithiazines and found anti-fungal. In compound Ar=2- ClC6H4, Ar'=2-ClC6H4OCH2.Methyl 5- (l-hydroxy-2-propenyl)-3-thiophenecarboxylate was stirred at room temperature with 10 equivalents of freshly prepared manganese dioxide to give methyl 5-(2-propenoyl)-3- thiophene carboxylatein 60% yield. The proton nmr spectrum exhibit explicitly a doublets for two hydrogens due to the de-shielding effect of the carbonyl. Infra-red spectroscopy helps to confirm the structure of two carbonyls around 1650 cm^{-1} for the allylic ketone and 1700 cm^{-1} for the ester Figs1-3. Since a carcinogen is applied into a body, cancerous cell will not immediately result. This is due to the "latency effect" where certain of time elapses before there is growth of the tumor. The initial application of a carcinogen will result in the formation of the irreversible initiated cells. Time may then elapse before a second agent, known as the promoter, will act reversibly on the initiated cell giving a premalignant lesion. Changes in the premalignant lesion, such as increased growth rate, increased invasiveness and metastases, result from the 3rd stage of the process known as progression. Those changes are usually associated with the changing in the number and arrangement of genes which encode for various proteins.

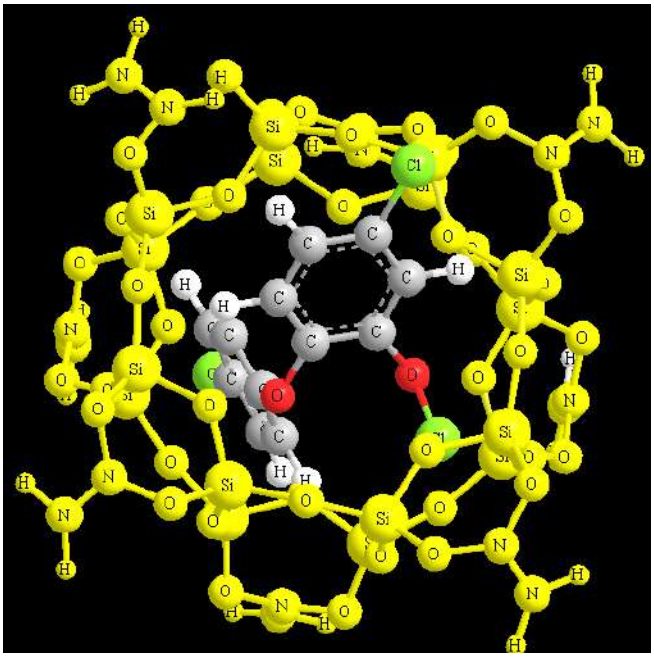

Fig.6: Tricloson antibiotic delivery via [SiO2 (OH)2]8

The chemical shielding and several factors as the same electronegativity, magnetic anisotropy of π-systems will be changed due to the number of electrons The chemical shielding is a vector orientation function for all of the shielding parameters that can change in several places inside the shielding region (Figs 6-11).

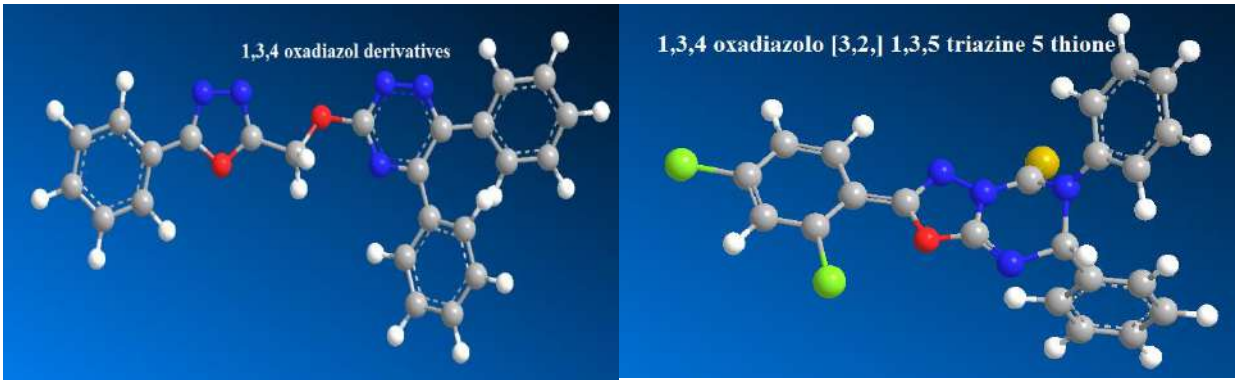

Fig.7. optimization of 1,3,4 oxadiazol derivatives and 1,3,4 oxadiazolo [3,2,] 1,3,5 triazine 5 thione

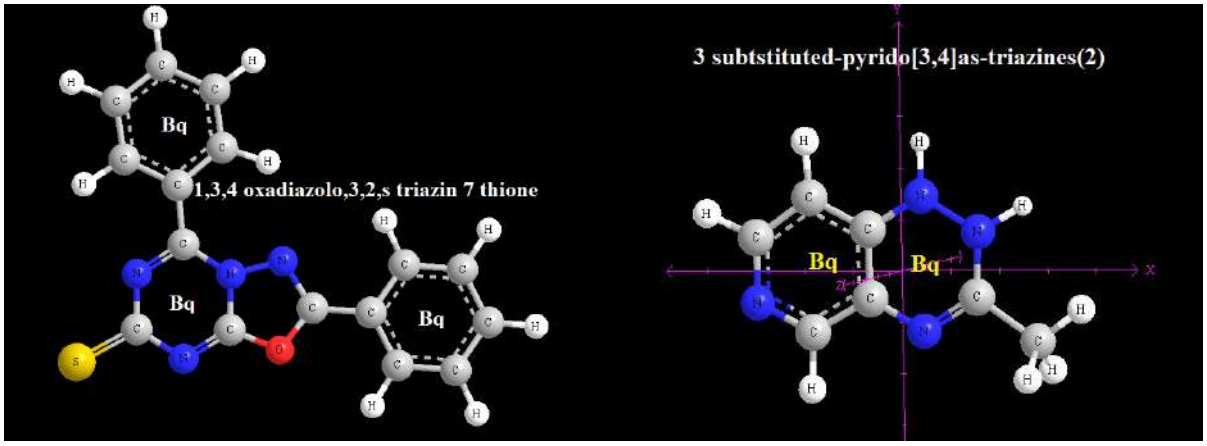

Fig.8. optimization of 1,3,4 oxadiazolo,3,2,s triazin 7 thione and 3 subtstituted-pyrido[3,4]as-triazines(2).

Optimization& NMR constants with orientations of the principal components& Haeberlen-Mehring, or Herzfeld-Berger [parameter] for several heterocyclic compounds in random situations has been calculated through DFT methods tables1, 2. In small distance around the center, the asymmetric-parameter (η), and the skew (**κ**), exhibited. gaussian distribution based on their fluctuation behavior[15], which is relate on its distance of molecular ring. In contrast, of that parameters, the isotropy $\sigma_{iso}(r)$ Has not a fluctuating behavior and increase in around the center of the rings with a linear relationship. The slopes of that line is changed for various distances of heterocyclic compounds. The isotropy in all NMR calculations are positive which indicates negative values for aromaticity.

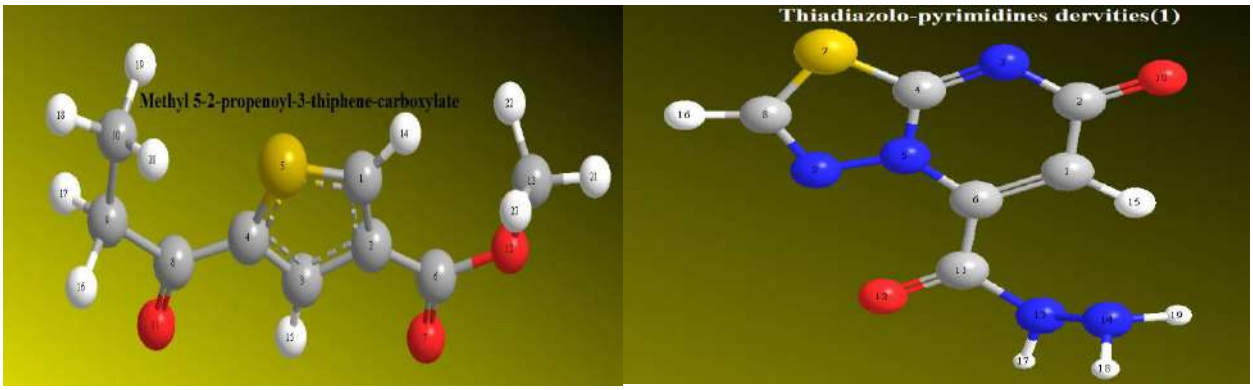

Fig.9. optimization of Methyl 5-2-propenoyl-3-thiphene-carboxylate and Thiadiazolo-pyrimidines derivatives (1)

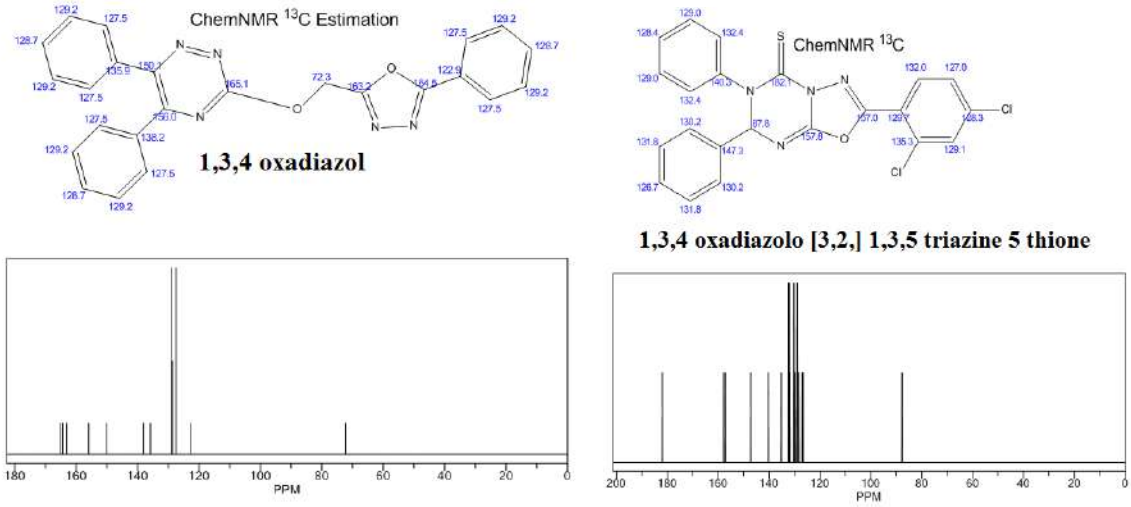

Fig.10. NMR estimation of some oxadiazol compounds

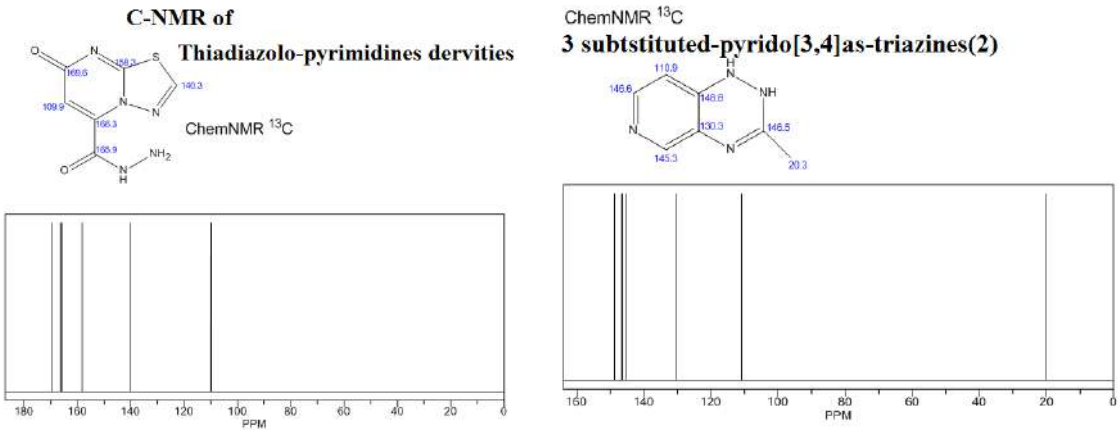

Fig.11. NMR estimation of some Thiadiazol compounds

Conclusion

Once a compound that fulfills all of these requirements has been identified, it will begin the process of drug development prior to clinical trials. Modern drug discovery involves the identification of screening hits, medicinal chemistry and optimization of those hits to increase some properties. One or more of these steps may involve computer-aided drug design and drug-delivery via silica compounds such as $(N2)n[SiO2(OH)2]8$ Core-Shell catalyst. A fascinating result of the theoretical analysis of antibiotics- S-NICS methods were the stable model for drug delivery. The observed behavior must reflect intrinsic properties of the mechanism of its structure and provides useful constraints for the development of mechanistic models.

References

Bourgeois, L., Bando, Y., Han, W.Q., Sato, T. (2000). Structure of boron nitride nanoscale cones: Ordered stacking of 240° and 300° disclinations *Phys. Rev*. B, (61), 7686.

Deng, Y.; Cai, Y.; Sun, Z.; Liu, J.; Liu, C.; Wei, J.; Li, W.; Liu, C.; Wang, Y.; Zhao, D.; (2010). Multifunctional Mesoporous Composite Microspheres with Well-Designed Nanostructure : A Highly Integrated Catalyst System, J. AM. CHEM. SOC., *132*, 8466–8473.

Farhami, N., Monajjemi, M., Zare, K. (2017). Non Bonded Interactions in cylindrical capacitor of (m, n) @ (m', n') @ (m",n") Three Walled Nano Carbon Nanotubes. *Oriental Journal of Chemistry* (*33*), 3024- 3030, http://dx.doi.org/10.13005 /ojc/ 330640

Frackowiak, E., Béguin, F. (2002). Electrochemical storage of energy in carbon nanotubes. *Carbon*, *(40)*, 1775-1787, https://doi.org/10.1016/S0008-223(02)00045-3

Iijima Sumio (1991). Synthesis of Carbon Nanotubes. *Nature*, (354), 56-58.

Lee, V.S., Nimmanpipug, P.,Mollaamin, F., Kungwan, N., Thanasanvorakun, S., Monajjemi, M.(2009). Investigation of single wall carbon nanotubes electrical properties and mode analysis: Dielectric effects. *Russian journal of physical chemistry A* (*83*), 2288-2296, https://doi.org/10.1134/S0036024409130184.

Lu, T., Chen, F. (2012). Multiwfn: A Multifunctional Wavefunction Analyzer. *J. Comp. Chem*., *33*, 580-592, https://doi.org/10.1002/jcc.22885.

Madani, M.S., Monajjemi, M., Aghaei, H. (2017), The Double Wall Boron Nitride Nanotube: Nano-Cylindrical Capacitor, *Oriental Journal of Chemistry*, (*33*), 1213-1222 , http://dx.doi.org/10.13005/ojc/330320.

Monajjemi, M., Chegini, H., Mollaamin, F., Farahani, P. (2011). Theoretical Studies of Solvent Effect on Normal Mode Analysis and Thermodynamic Properties of Zigzag (5,0) carbon nanotube. *Fullerens Nanotubes carbon and nanostructures* (*19*), 469-482, https://doi.org/10.1080/1536383X.2010.494783.

Sociomedical factors affecting the birth rate in the Russian Federation

Alla Ivanovna Ovod *
Irina Gennadievna Komissinskaya **
Kirill Vladimirovich Khorlyakov ***

ABSTRACT

The article considers the number of women giving birth in Russia in the context of the existing demographic problems caused by the depopulation of the country. The study evaluates the social, economic and medical factors influencing the dynamics of the number of women giving birth in the Russian Federation based on correlation and regression analysis, and also provides a short-term forecast for their further change. The implementation of the increase in the number of women giving birth in Russia is one of the current important sociodemographic tasks for the State; This will improve the demographic situation and will lay the foundations for the formation of a sufficient human resource, which will later form the country's high human capital. According to the results of forecasting the dynamics of the number of women in the work in the short term, it was determined that the downward trend in the number of women in the work will continue, since the negative impact of medical factors will remain unchanged. changes, while economic and social factors will not change.

KEYWORDS: Russian Federation; social policy; demographic situation; reproduction of the population; birth rate; number of women in work, sociomedical factors.

*Doctor of pharmaceutical Sciences, Professor of the Department of Management and Economics of Pharmacy, Kursk State Medical University of the Ministry of Health of the Russian Federation, https://orcid.org/0000-0001-9380-1138.

** Doctor of pharmaceutical Sciences, Professor, Head of the Department of Pharmacy, Kursk State Medical University of the Ministry of Health of the Russian Federation.

*** Post-graduate student of the Department of Management and Economics of Pharmacy, Kursk State Medical University of the Ministry of Health of the Russian Federation.

Recibido: 29/04/2020 Aceptado: 25/06/2020

Factores sociomédicos que afectan la tasa de nacimiento en la Federación Rusa

RESUMEN

El artículo considera el número de mujeres parturientas en Rusia en el contexto de los problemas demográficos existentes causados por la despoblación del país. El estudio evalúa los factores sociales, económicos y médicos que influyen en la dinámica del número de mujeres parturientas en la Federación Rusa en base a análisis de correlación y regresión, y también ofrece un pronóstico a corto plazo para su cambio adicional. La implementación del aumento en el número de mujeres parturientas en Rusia es una de las tareas sociodemográficas actuales importantes para el Estado; esto mejorará la situación demográfica y sentará las bases para la formación de un recurso humano suficiente, que posteriormente formará el alto capital humano del país. De acuerdo con los resultados de pronosticar la dinámica del número de mujeres en el trabajo a corto plazo, se determinó que continuará la tendencia a la baja en el número de mujeres en el trabajo, ya que el impacto negativo de los factores médicos se mantendrá sin cambios, mientras que los factores económicos y sociales no cambiarán.

PALABRAS CLAVE: Federación Rusa; política social; situación demográfica; reproducción de la población; tasa de natalidad; número de mujeres en trabajo, factores sociomédicos.

Introduction

Today, the demographic situation in Russia is complicated: there is a natural population decline, which has been outlined since the 90s of the 20th century (Maltseva, 2017). Despite the fact that there was a positive dynamics and population growth by 2013, a change in the political situation in 2014 led to another economic crisis that negatively affected the socio-demographic situation (Potapova, 2015). In this regard, today, as before, the problem of increasing fertility is an urgent social problem that requires drastic measures (Ignatenkov, 2017). The overall indicator characterizing the demographic situation is the birth rate of the population, but the number of women in labor as the main reproducing resource of the country's population is also important (Zyuzina, 2016). In this regard, the study of the number of women in labor in the country and the factors influencing their dynamics is an important area of socio-economic analysis.

1. Theoretical basis

Increasing the number of women in labor in Russia is one of the significant current socio-demographic tasks for the state, the implementation of which will improve the demographic situation and lay the foundation for the formation of a sufficient human resource; this will subsequently allow the formation of a high human capital of the country (Dedkov, 2018). To achieve this goal, it is necessary to identify factors and problem areas that impede the increase in the birth rate in Russia, which can conditionally be divided into social, economic and medical (Zyukin et al., 2016). Therefore, it is important to consider indicators of the development of the country's social and medical infrastructure, as well as basic economic indicators, as factors in the formation of the current demographic situation (Andreev and Andreeva, 2016; Sharma et al., 2019).

2. Methodology

The number of women in labor in Russia as an indicator of the demographic situation should be considered in conjunction with a number of socio-economic indicators characterizing the current situation in the country. During the study, 18 socio-economic indicators were selected and grouped in 3 main areas: social, economic and medical factors (Ovod et al., 2020). The choice of socio-economic indicators as factors affecting the number of women in labor in the Russian Federation was carried out on the basis of logical analysis.

The study period is 2006-2018; 2006 was chosen as the base year, since it precedes the implementation of the large-scale national project “Health”, from which the modernization of the industry began. Cost indicators are shown at a comparable price level in 2018 based on consumer price indices for research purposes.

In the course of the study, a hypothesis was put forward that, as each of the selected indicators has a direct impact on the effective sign, the formed groups of indicators as a whole have a certain effect on the number of women in labor. To confirm the hypothesis, a pair correlation analysis was carried out and the results were interpreted based on the Chaddock scale. Assessment of the overall influence of groups of factors was carried out on the basis of standardization of indicators for their comparability. As a result, a regression model of a standardized type was constructed, based on the values of the beta coefficients of which the nature and degree of influence of the groups of factors on the number of women in labor in the Russian Federation was determined. Based on the obtained model, a forecast was made

of the dynamics of the number of women in labor in Russia for the short term and 4 possible scenarios were generated.

The reliability and complexity of the study is determined using the materials of the statistical digest "Russia in Figures" (Russia in numbers, 2019). The use of statistical methods and correlation and regression analysis as the main tools forms an objective quantitative assessment of the impact of socio-economic indicators on the number of women in labor in Russia.

3. Results

During the study, a system of factors was formed that influenced the number of women in labor in Russia. The proposed system includes economic, social and medical factors (Figure 1).

A correlation analysis of selected factors with an effective sign showed that the closest direct relationship (0.89) is the number of women in labor in the Russian Federation with average per capita incomes. Because the factor of income and the availability of appropriate financial opportunities for its maintenance is crucial when deciding on the birth of a child. This is due to the fact that when a woman decides, she loses her previous level of earnings, and in most cases the amount of the allowance paid is small. Therefore, a qualitative increase in the level of per capita income in the country is one of the aspects to improve the demographic situation.

Also, among social factors, a close correlation between the number of women in labor in the Russian Federation is observed with the value of paid services per capita. This fact is interconnected with factor S1 and is due to the fact that the growth in per capita income of the population allows people to receive medical services on a paid basis, including pediatric ones. The desire to receive medical care in private medical centers is due to a lack of confidence in the budgetary health care system. Therefore, the presence of an appropriate level of per capita income initially determines the possibility of increased consumption of paid medical services and affects the number of women in labor in the Russian Federation. Among social factors, there is an inverse close relationship (-0.77) of the number of women in labor with a share of the population with incomes below the subsistence level, which also lends itself to the logic of socio-economic analysis and indicates the dominant position of the income factor when deciding on the birth of children.

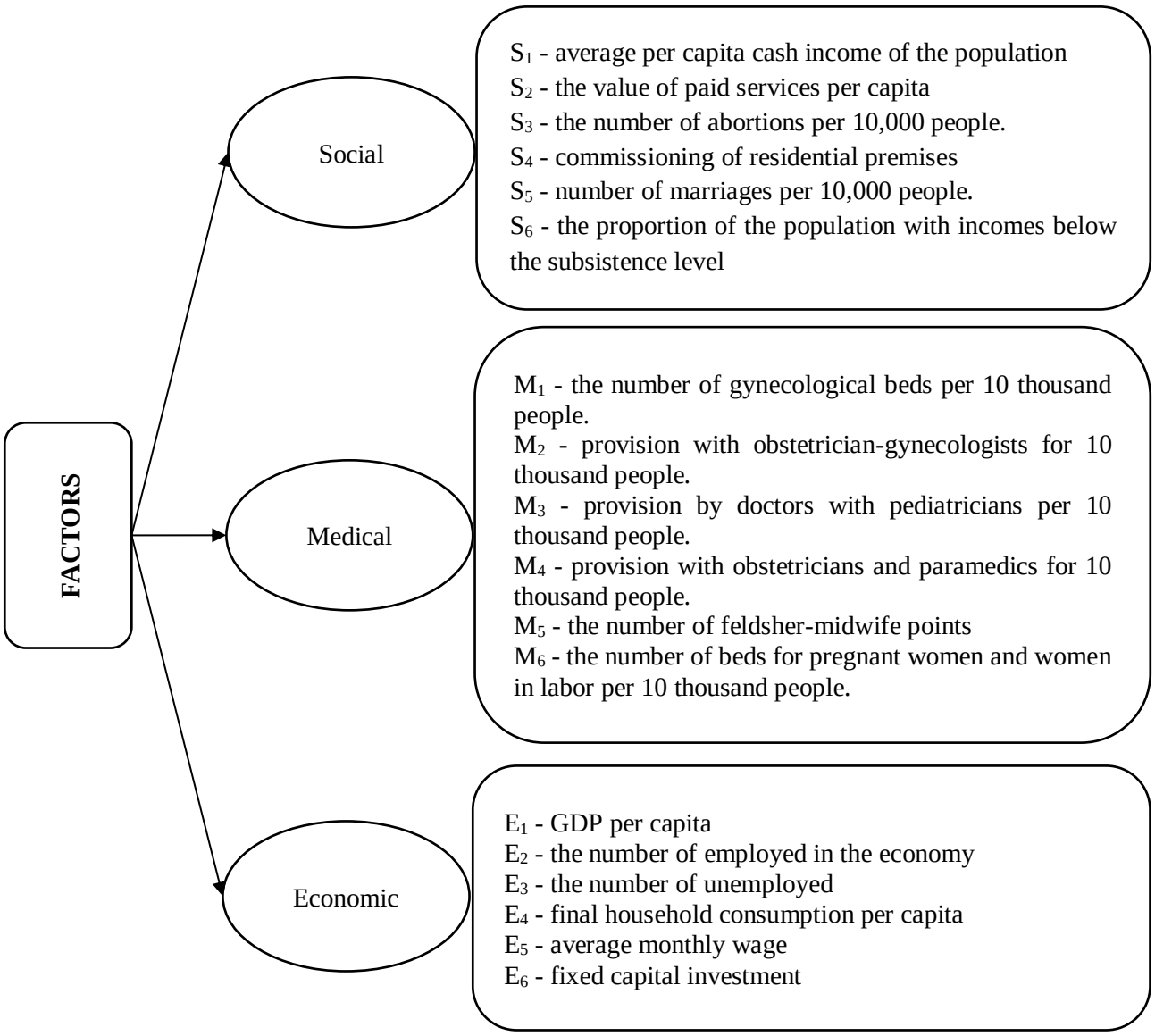

Figure 1. System of factors affecting the number of women in labor in Russia

Compiled by the authors

In addition, an inverse moderate correlation was found (-0.58) in the number of women in labor with the number of abortions per 10 thousand, which indicates that a decrease in the number of abortions contributes to an increase in the number of completed pregnancies, resulting in an increase in the number of women in labor. However, a decrease in the frequency of abortion occurs under the influence of a number of socio-economic factors. The remaining social factors, namely the commissioning of living space and the number of marriages per 10 thousand people, do not have a significant impact on the increase or decrease in the number of women in labor in the country. This is due to the fact that today the housing market in the Russian Federation is quite large; and the fact of introducing

additional areas has practically no effect on childbirth. This is also due to the fact that housing in new buildings is expensive and often inaccessible to certain segments of the population, especially large families, and therefore the purchase of secondary housing is more affordable. As the study showed, the factor of family and marriage also does not significantly affect the number of women in labour in the Russian Federation, which is due to a decrease in the importance of the institution of the family in modern society and also due to the fact that, according to statistics, about a third of women give birth outside the marriage and without a partner, becoming mothers alone (Figure 2).

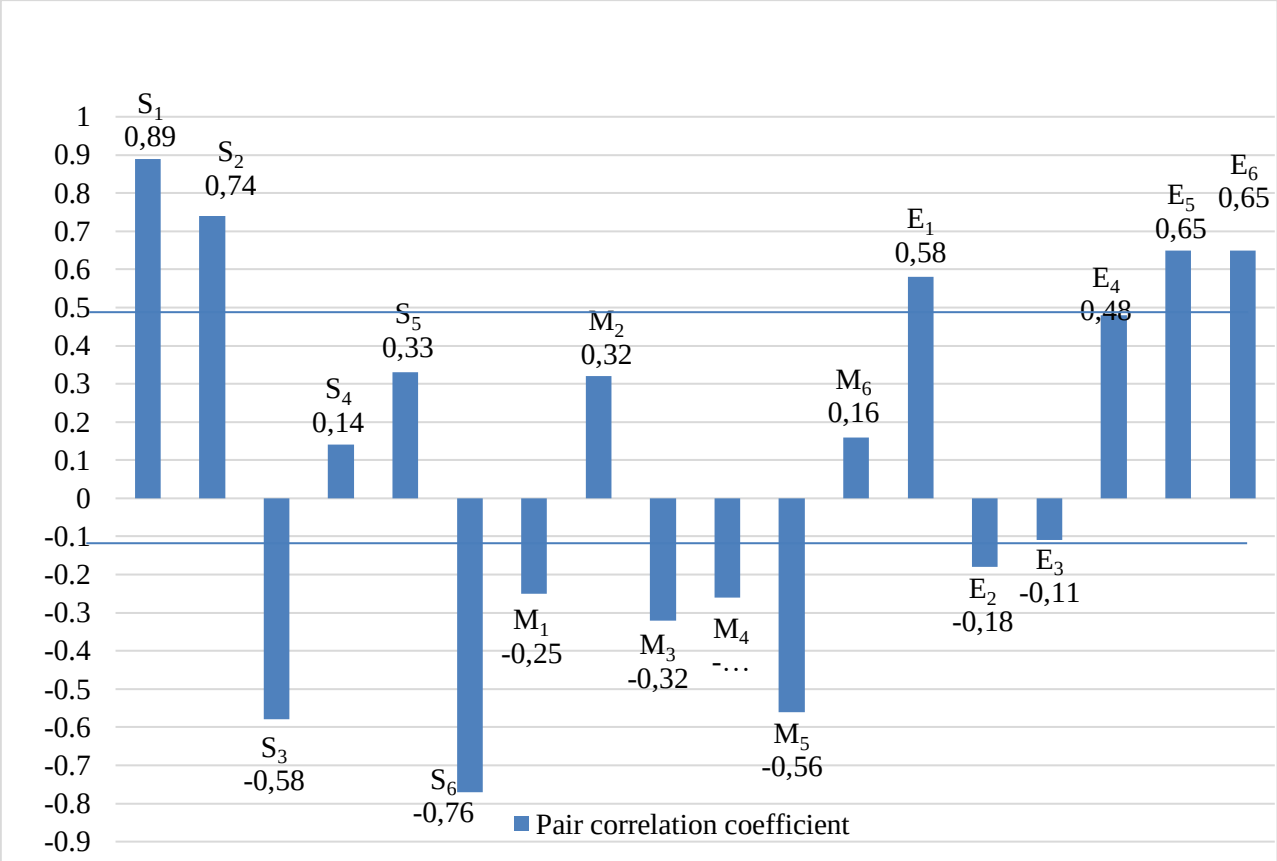

Figure 2. The values of the coefficients of pairwise correlation of the number of women in labor with factors

Calculated by the author based on data from the statistical digest "Russia in numbers" (Russia in numbers, 2019)

A correlation analysis of the influence of medical factors on the number of women in labor in Russia showed the absence of a close and stable relationship between the effective sign and the selected factors. Moderate feedback (-0.56) was identified only with the number

of feldsher-midwife points. The direct nature of the relationship was determined with such a factor as the availability of doctors per 10 thousand people; this is natural, since the need for doctors in the healthcare system is determined on the basis of the population. The increase in the number of women in labor and, accordingly, the number of children born determines the increasing need for doctors. However, the tightness of communication is weak (0.32), which indicates that this factor does not significantly affect the number of women in labor in Russia. Similar trends were identified for the factor of the number of beds for pregnant women and women in labor per 10 thousand people, the relationship of the effective sign with which is very weak (0.16). A weak and inverse correlation in nature was revealed with such factors as the number of gynecological beds, the provision of doctors with pediatricians, obstetricians and paramedics per 10 thousand people; this is explained by modernization processes in healthcare, which results in a reduction in capacity in the industry, recognized as ineffective. At the same time, it must be understood that a further reduction in available capacities can lead to a shortage, as a result of which the availability and quality of medical care will decrease.

Also important for assessing factors affecting the number of women in labor in Russia is the economic component, which in turn determines the development of social and medical factors. The significant influence of economic factors is confirmed by the results of a correlation analysis, which shows that the number of women in labor in Russia has a direct and moderate relationship with the size of GDP per capita, average monthly wages and investments in fixed assets. In turn, the number of people employed in the economy and the number of unemployed has practically no effect on the number of workers in labor in Russia, which is associated with the development of self-employment as a separate phenomenon on the labor market, as a result of which people are between the employed and the unemployed without entering these groups. Consequently, the level of remuneration and the volume of investment in fixed assets among the largest impacts of economic factors on the number of women in labor in the country.

According to the results of the study, the model $y=1{,}5238*F_1+0{,}2981*F_2+1{,}1237*F_3$ was obtained, the adequacy of which is confirmed by the F-criterion, and the degree of description of the effective attribute is 69.9%. As a result, it was found that social and economic factors contribute to an increase in the number of women in labor in the Russian Federation, with social factors increasing by 127.6% and economic factors by 26.7%. In turn,

medical factors have a negative effect on the effective sign, contributing to its reduction by 28.1%, which is due to problems of the domestic health care system. Consequently, the change in the number of women in labor in Russia is most affected by socio-economic factors, the most significant of which are the average per capita income and poverty level in the country.

In accordance with the existing trends, a negative change in the number of women in labor in Russia should be expected in the short term, which will reach 1,448 thousand people by 2021 according to the forecast. It is predicted that the following emerging trends will continue in the short term: stagnation in changes in economic and social factors, increased negative impact of the medical component in accordance with the obtained linear regression model. The operability of the forecasting model can be verified when statistics for 2019 are generated.

At the same time, under the influence of various social, economic, and political factors, it is possible to develop one of the proposed scenarios for changing the number of women in labor in Russia, which were compiled using the standard error tool. Moreover, it is assumed that the deviation of the simulated value in both directions does not exceed two standard errors of the regression equation, which determine the probability at the level of 95%.

In accordance with the optimistic scenario, the number of women in labor in Russia will reach 1,686 thousand people in 2019 and will decrease by 3.9% and amount to 1,448 thousand people by 2021. It is assumed that such a development of events is possible with a change in the current situation and the emergence of a positive influence of social, economic and medical factors determining the number of women in labor in Russia.

We believe that the number of women in labour will increase to 1600 thousand people with a moderately optimistic scenario by 2019; but the reduction in the number of women in labor in the country to 1534 thousand people, which is 4.1%, will happen by 2021 under the influence of socio-economic problems. Such a scenario is possible if social and economic factors have a positive impact on the number of women in labour in Russia, stimulating an improvement in the demographic situation, including due to the growth of population incomes and the emergence of additional social guarantees, and the factors of the medical component will retain the current negative impact, contributing to their reduction (table 1).

Table 1. Scenarios of changes in the number of women in labour in the Russian Federation in 2019-2021

Scenario	Projected number of women in labour, thousand people			Change in 2021 to 2019
	2019	2020	2021	
Simulated value	1513	1507	1448	-4,3
Optimistic	1686	1679	1620	-3,9
Moderately optimistic	1600	1593	1534	-4,1
Conservative	1427	1420	1361	-4,6
Negative	1340	1334	1275	-4,9

Compiled by the authors

According to the conservative development scenario, the number of women in labor in the country will reach 1,427 thousand people by 2019, and will decrease by 4.6% and amount to 1,361 thousand people by 2021. We believe that such a development is possible if the factors of the social component have a positive impact on the increase in the number of women in labor in the country, which is possible due to an increase in the amount of social benefits and other guarantees. At the same time, it is predicted that factors of the economic component will have a negative effect on the number of women in labor, including due to a decrease in real incomes of the population, depreciation of the ruble and other economic problems. Global changes in the work of the health system are also not expected, as a result of which medical factors will retain their negative impact.

The negative scenario implies a reduction in the number of women in labor by almost 5% over 3 years, as a result of which this indicator will amount to 1275 thousand people by 2021 compared to 1340 thousand people in 2019. Such a development of events, in our opinion, is possible in the case of a negative development vector of the influence of all social, economic and medical factors, which is possible in case of further deterioration of the economic situation in the country and the emergence of another economic crisis.

4. Discussions

The reproduction of the Russian population is significantly influenced by the socioeconomic problems that have developed in the country and require solutions (Fedorov, 2014). So, one of the key factors preventing active natural population growth is economic growth, due to the relatively low standard of living of the population and average per capita income. Studies of European values and macro-level indicators of economic growth and income inequality for 46 countries observed from 1981 to 2012 show that economic growth improves the subjective well-being of families and increases their social trust in the state in the long run (Mikucka et al., 2017). The recession of the Russian economy while maintaining high inflation rates leads to a decrease in real incomes of the population, which reduces the financial ability of families to have a baby (Akhmeduev, 2020).

The economic reforms carried out in recent years of the country also negatively affect fertility and the desire to give birth. For example, an increase in retirement may deprive young families of the physical assistance for caring for young children that they receive from grandmothers who will be forced to work until they are 60 years old (Zyukin et al., 2018).

Together with the economic factor, it is worth highlighting the lack of appropriate housing conditions and means for their significant improvement (Kostenko and Ryabova, 2018). The Maternity Capital program began to play a significant role, through which many families were able to improve their living conditions, which became an incentive for having a baby. Despite the positive impact of this program on existing demographic problems, it has not been possible to achieve a steady increase in the birth rate, and the number of women in labor in recent years has tended to decrease (Markov and Alekseeva, 2019).

In addition, the imperfection of social policy is recognized as one of the negative aspects: the social guarantees existing today are only nominal and there is no significant social support for the population (Zyukin et al., 2018). Economic instability, the lack of proper support from the state in conjunction with insecurity in their own forces leads to the fact that the population does not decide on the birth of a child (Chernyavskaya, 2014). Therefore, one of the significant directions for improving the demographic situation should be to increase social guarantees, which will become real support for Russian families (Ovod et al., 2020). One of the principal directions of increasing the number of women in labour is the expansion of their social and economic preferences (Baird, 2004). Russia is a

multinational country, therefore there are problems of social inequality in relation to pregnant women and mothers with young children in various socio-cultural clusters. This problem is relevant and is more substantively considered in the scientific literature of European studies, where the observance of social rights of citizens at a very high level (Binelli et al., 2015).

Preservation of current trends is predicted to lead to aggravation of demographic problems: the number of women in labor will continue to decline, the natural population decline will increase (Tikhomirova and Tikhomirov, 2018). In addition to internal socio-economic problems, foreign policy contradictions that have escalated in recent years have a significant negative impact on the situation, which helps to divert not only the attention of the country's government from internal problems, but also leads to an outflow of financial resources to foreign policy issues to the detriment of the social sphere (Temiryaev, 2019).

Separately, it is worth highlighting the existing problems in the healthcare industry, caused not only by a shortage of necessary resources, but also by the low availability of services provided, including in terms of obstetric care (Bakai, 2017). The modernization and optimization carried out in the industry, as practice has shown, only aggravated the situation as a result of a reduction in capacities, which in the future can lead to a limitation of the increase in the number of women in labor, since the healthcare system will not be able to serve a large number of patients at one time (Alpeeva et al., 2017). In addition, the quality of the services provided, which is not high today, continues to decline, which is unacceptable for obstetric care, since not only the health of the mother and child, but also their life may depend on it (Tikhomirov and Tikhomirova, 2019).

Conclusion

The study showed that the number of women in labour in Russia is most affected by the income factor, which is confirmed by the presence of a direct and close relationship with the size of average per capita incomes and feedback with the poverty level. The identified trend indicates that the level of financial well-being is crucial when deciding on the birth of a child. At the same time, the continuing trend of population depopulation is due to economic instability and a decrease in real incomes of the population. Therefore, it can be noted that

the internal socio-economic situation does not contribute to increasing the birth rate in the country.

An assessment of the group-wide results revealed that the largest positive contribution to the increase in the number of women in labor in Russia was made by social factors (127.6%). The economic component also positively affects the increase in the number of women in labor in the country, and the medical component contributes to their reduction, which, in our opinion, is associated with domestic health problems due to the low quality and accessibility of the services provided. In addition, insufficiently effective work of healthcare in conjunction with environmental problems leads to a decrease in the physical ability of the population to bear children, especially at a more mature age.

Based on the results of forecasting the dynamics of the number of women in labor in the short term, it was determined that the downward trend in the number of women in labor will continue, since the negative impact of medical factors will remain unchanged, and economic and social factors will not change.

References

Akhmeduev, A. (2020). Globalization and population precariation: challenges and tendencies of the new world order. *Amazonia Investiga*, 9 (25), 242-250.

Alpeeva, T.A., Ermakova, K.L., Shtokolova, K.V. (2017). On the effectiveness of using the hospital bed and medical personnel in the region's healthcare system. *Regional Bulletin*, 1 (6), 21-23.

Andreev, B.A., Andreeva, A.D. (2016). The study of the dependence of changes in the birth rate on the factors of social well-being in Russia. *The First Step in Science*, 12 (24), 17-23.

Baird, M. (2004) Orientations to paid maternity leave: understanding the Australian debate. *The Journal of Industrial Relations*, 46 (3), 259-274.

Bakai, E.O. (2017). The economic and statistical analysis of healthcare in modern Russia. *Economics and Entrepreneurship*, 1 (78), 861-867.

Binelli, C., Loveless, M., Whitefield, S. (2015). What is social inequality and why does it matter? Evidence from Central and Eastern Europe, *World Development*, 70, 239-248.

Chernyavskaya, E.Yu. (2014). Problems of reproduction of human resources in modern Russia. Business. Education. Law, 3 (28), 186-191.

Dedkov, E.N. (2018). The demographic policy of Russia: the relationship of economic development and population reproduction. *Russian Political Science*, 3 (8), 120-127.

Fedorov, G. (2014). The concept of geo-demographic situation and geo-demographic typology of the subjects of the Russian Federation. *Bulletin of Geography*. Socio-economic Series, 25 (25), 101-114.

Ignatenkov, G.K. (2017). Modern demographic problems of the Russian Federation and ways to solve them. *New Science: Strategies and Development Vectors*, 3 (4), 66-69.

Kostenko, R.V., Ryabova, A.D. (2018). Demographic problems in the Russian Federation and ways to solve them. *Bulletin of Modern Research*, 12.2 (27), 290-292.

Maltseva, T.N. (2017). Actual problems of demographic policy in the Russian Federation. *Forum of Young Scientists*, 6 (10), 1150-1155.

Markov, S.N., Alekseeva, A.V. (2019). Maternal capital as an instrument of financial support for the Russian family. *Financial Economics*, 9, 483-488.

Mikucka, M., Dubrow, J.K., Sarracino, F. (2017). When does economic growth improve life satisfaction? Multilevel analysis of the roles of social trust and income inequality in 46 countries, 1981–2012. *World Development*, 93, 447-459.

Ovod, A.I., Khorlyakov, K.V., Komissinskaya, I.G. (2020). The influence of socio-economic factors on the number of women in labour in the Russian Federation. Azimuth of Scientific *Research: Economics and Management*, 1 (30), 168-172.

Potapova, O.N. (2015). Socio-demographic problems and the foundations of the national economy of Russia. Political Internet electronic scientific journal of the Kuban State Agrarian University, 109, 171-182.

Russia in numbers (2019). Short Stats /Rosstat-M., 2019, 549 p.

Sharma, S. K.; Shukla, J. B.; Singh, J.; Singh, S. (2019). Effects of density dependent migration on the spread of infectious diseases: A Mathematical Model, *Revista de la Universidad del Zulia*, 10 (27), 184-201.

Temiryaev, G.A. (2019). The impact of sanctions on the Russian economy. *Forum of Young Scientists*, 1-3 (29), 583-587.

Tikhomirova, T.M., Tikhomirov, N.P. (2018). Problems of substantiation of measures to exit Russia from the demographic crisis. *Plekhanovsky Scientific Bulletin*, 2 (14), 142-148.

Tikhomirov, N.P., Tikhomirova, T.M. (2019). Assessment and management of the reproduction potential of the Russian population. *Federalism*, 3 (95), 51-71.

Zyukin, D.A., Bystritskaya, A.Yu., Dendak, G.M. (2018). Raising the retirement age as a way of avoiding the insolvency of the financial model of the state. *Azimuth of Scientific Research: Economics and Management*, 3 (24), 104-108.

Zyukin, D.A., Reprintseva, E.V., Sergeeva, N.M., Perkova, E.Yu., Galkina, N.G. (2016). The study of the relationship of socio-economic factors in the development of the region's health system. *International Journal of Applied and Basic Research*, 1-2, 218-221.

Zyuzina, Yu.O. (2016). Demographic and family policy in the Russian Federation: current status, problems and prospects. *Scientific journal Discourse*, 1 (1), 203-207.

Biopsicosociología del orgasmo en el varón y en la hembra: fundamentos y diferencias

Andrés Reyes *
Mariana Añolis **
Édixon Ochoa ***
María Matera ****

RESUMEN

La respuesta sexual se encuentra mediada por factores anatomo-hormono-neuro-vasculoendoteliales. Ha sido explicada a través de varios modelos como el tetrafásico (Masters y Johnson, 1966), el trifásico (Kaplan, 1979), y el pentafásico (Bancroft, 1983), entre otros. El orgasmo se ubica como una de estas fases en estos modelos. Éste se define como un conjunto de sensaciones corporales sumamente placenteras y de excitación intensa, que libera tensiones y que produce satisfacción. Existen pocas diferencias entre el orgasmo del varón y de la hembra; desde un punto de vista funcional, el orgasmo del varón está estrechamente relacionado con la eyaculación, mientras que en la hembra no existe una conexión tan obvia y directa. En este estudio se recopilaron las semejanzas y diferencias presentes en el orgasmo del varón y de la hembra, referidas a los fundamentos anatómicos, fisiológicos, neuroendocrinos, neurológicos, psicológicos, socioculturales y espirituales.

PALABRAS CLAVE: respuesta sexual; orgasmo; varón; hembra; diferencias.

* Comunidad Estudiantil para la Difusión e Investigación de la Anatomía Humana (CEDIAH). Escuela de Medicina. Facultad de Medicina. Universidad del Zulia (LUZ). Maracaibo, Venezuela. E-MAIL: aerc2302@gmail.com ORCID: https://orcid.org/0000-0002-4181-1649

** Comunidad Estudiantil para la Difusión e Investigación de la Anatomía Humana (CEDIAH). Escuela de Medicina. Facultad de Medicina. Universidad del Zulia (LUZ). Maracaibo, Venezuela. ORCID: https://orcid.org/0000-0001-7841-3153

*** Profesor. Unidad curricular electiva Sexología Médica. Cátedra de Psicología Médica. Departamento de Ciencias de la Conducta. Unidad curricular Orientación II. Centro de Orientación "Dra. Consuelo Faría" (COFAMED). Escuela de Medicina. Facultad de Medicina. Universidad del Zulia (LUZ). Maracaibo, Venezuela.

**** Comunidad Estudiantil para la Difusión e Investigación de la Anatomía Humana (CEDIAH). Escuela de Medicina. Facultad de Medicina. Universidad del Zulia (LUZ)// Servicio de Cirugía General. Hospital Universitario de Maracaibo, Venezuela.

Recibido: 29/04/2020 Aceptado: 19/06/2020

Biopsychosociology of orgasm in male and female: fundamentals and differences

ABSTRACT

The sexual response is mediated by anatomo-hormonal-neuro-vasculoendothelial factors. This has been explained through several models, like the four-phase (Masters y Johnson, 1966), the three-phase (Kaplan, 1979), the penta-phase (Bancroft, 1983), among others. Orgasm is located as one of these phases in these models. This is defined as a set of extremely pleasant bodily sensations and intense arousal that releases tensions and produces satisfaction. There are few differences between male and female orgasm, from a functional point of view, male orgasm is closely related to ejaculation while in female there is no such obvious and direct connection. This study compiled the similarities and differences that occur in the male and female orgasm regarding the anatomical, physiological, neuroendocrine, neurological, psychological, sociocultural and spiritual fundamentals.

KEYWORDS: sexual response; orgasm; male; female; differences.

Introducción

La respuesta sexual humana es toda actividad caracterizada por la presencia de activación cortical y/o medular en el sistema nervioso; correlacionada con un fenómeno de tumescencia, contractilidad muscular lisa y/o estriada y un fenómeno de detumescencia (tanto a escala genital como extragenital), efecto de una estimulación sexual; y mediada por factores anatomo-hormono-neuro-vasculo-endoteliales (FLASSES, AMSM y AISM, 2014).

Dicha estimulación sexual implica la activación de reacciones neurológicas, vasculares, musculares y hormonales (Kaplan, 1974; Portillo, 2017), lo cual se ha explicado a través de distintos modelos, tales como: El tetrafásico (Masters y Johnson, 1966) (fig. 1), el trifásico (Kaplan, 1979), el pentafásico (Bancroft, 1983), el tridimensional (Schnarch, 1991), el continuo de (Whipple y Mc Greer, 1997) y el ciclo de la erótica (Lacalle, 2009) (fig. 2). En todos estos modelos se menciona al orgasmo como una de sus fases (FLASSES, AMSM y AISM, 2014).

El vocablo **orgasmo** proviene del griego *orgasmós* (ὀργασμός), que significa 'hinchazón, plenitud, deseo de lujuria'; éste a su vez deriva de *orgé* (ὀργέ), 'ardor, impetu' y del verbo *orgáoo* (ὀργάοο), 'arder en deseos' (Duvauchelle, 1995). Es una experiencia difícil de describir, a pesar de haber sido experimentado por la mayoría de las personas, quienes lo definen como la sensación más intensa de placer sexual (Kaplan, 1974; Portillo, 2017; Levin, 2011; Komisaruk et al, 2004). Puede conceptuarse como "Una descarga expulsiva de tensión neuromuscular en la respuesta sexual humana" o "Un breve episodio de relajación física relacionado a vasocongestión y miotonía, incrementado por el desarrollo de la estimulación de la respuesta sexual". Sin embargo, una definición más completa expone que el orgasmo es un conjunto de sensaciones corporales sumamente placenteras y de excitación intensa que libera tensiones y produce inmensa satisfacción (Komisaruk et al, 2004).

Tanto la hembra como el varón experimentan cambios en la circulación, la respiración y la musculatura pélvica durante el orgasmo (Levin, 2007). La actividad cerebral del mismo es similar tanto en la hembra como en el varón y puede inducir cambios mentales profundos porque, a su vez, se presentan emociones como intenso placer, relajación de la tensión, sensación de inevitabilidad y pérdida del control conductual consciente (Georgiadis et al, 2006).

Las diferencias descritas entre el varón y la hembra son muy pocas (Levin, 2011). Desde un punto de vista funcional, el orgasmo del varón está estrechamente relacionado con la eyaculación, mientras que en la hembra no existe una conexión tan obvia y directa, debido a que el fluido orgásmico es inconstante (Georgiadis et al, 2006). Por ello, la presente investigación tiene como objetivo determinar los fundamentos anatómicos, fisiológicos, neuroendocrinos, neurológicos y psicológicos del orgasmo, estableciendo diferencias entre el orgasmo del varón y de la hembra.

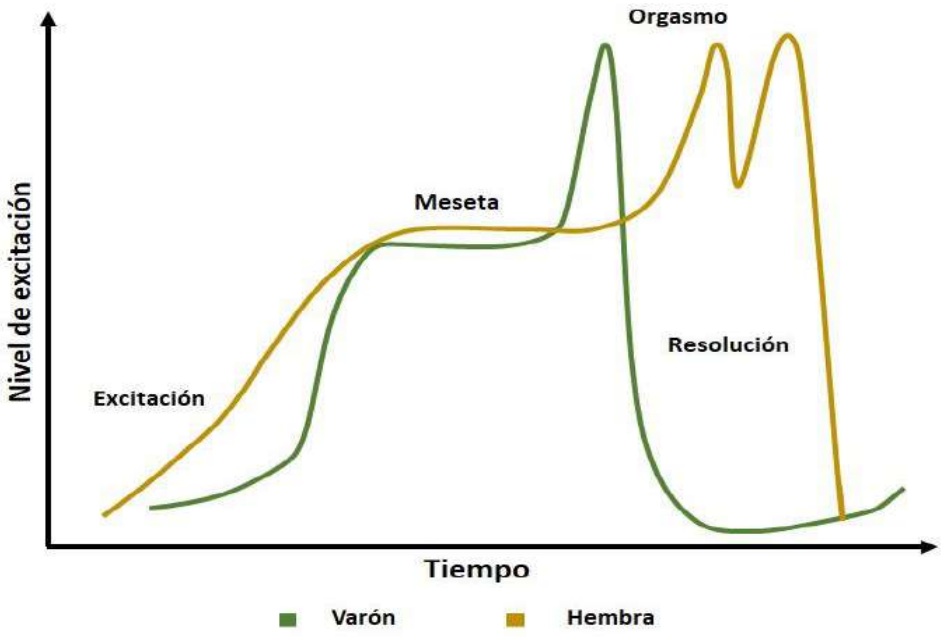

Figura 1. Modelo tetrafásico de respuesta sexual humana (Masters y Johnson, 1966)

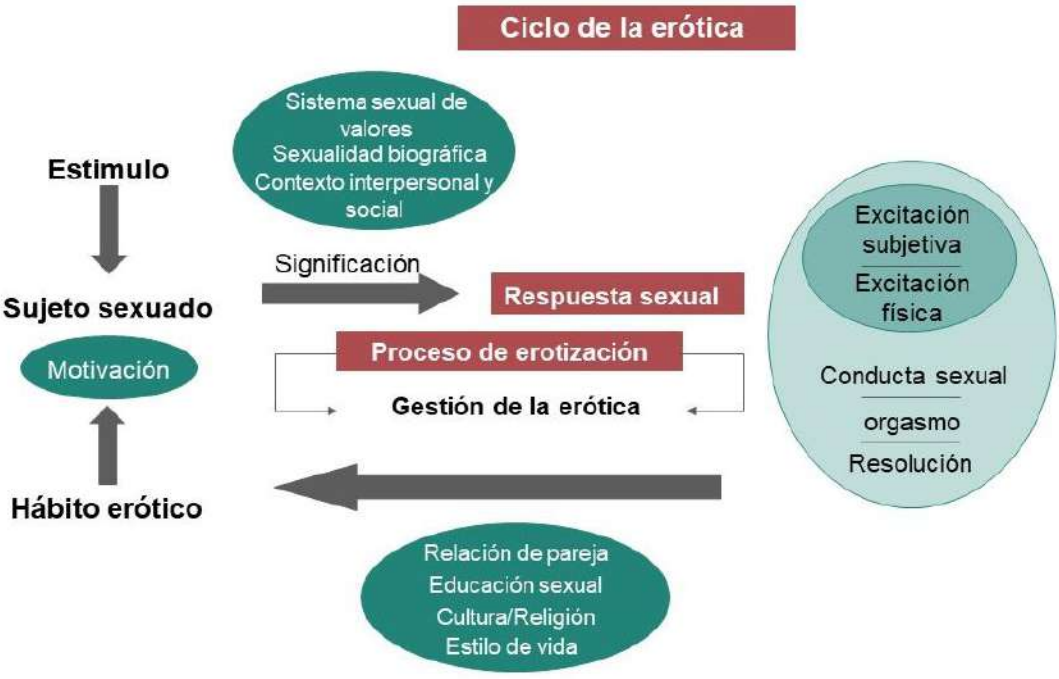

Figura 2. Ciclo de la erótica (Lacalle et al, 2009).

1. Fundamentos anatómicos

En la hembra, los genitales externos corresponden al monte de Venus, los labios mayores, los labios menores, el clítoris y el vestíbulo vaginal. El monte de Venus es un triángulo invertido de tejido adiposo, encima de la sínfisis púbica y se relaciona con dos pliegues gruesos, denominados labios mayores. Cada labio tiene dos caras, una externa que está pigmentada y cubierta de vello púbico y la cara interna que es lisa y compuesta de glándulas sebáceas (Emhardt et al, 2016; Graziottin y Gambini, 2015). Entre ellos se ubican dos pliegues pequeños denominados labios menores, que rodean el vestíbulo de la vagina y se dividen en dos porciones: una superior que va a formar el prepucio del glande del clítoris y una inferior que forma el frenillo del clítoris, son ricos en tejido eréctil, vascular y una gran cantidad de terminaciones nerviosas (Emhardt et al, 2016; Graziottin y Gambini, 2015).

El clítoris es una estructura eréctil formada por un cuerpo cavernoso y glándulas que cubren al prepucio, los cuerpos cavernosos convergen y siguen las ramas públicas formando la crura que representa su porción oculta que se encuentra cubierta por el isquiocavernoso. El vestíbulo vaginal se encuentra en la entrada de la vagina y cumple una función sexual y protectora. Éste se convierte en un lugar de alta congestión durante la fisiología sexual, contribuyendo a la congestión genital y formación de la plataforma orgásmica (Emhardt et al, 2016).

Los genitales internos están conformados por las trompas de Falopio, que son dos estructuras tubulares que se relacionan con los ovarios, los cuales son dos órganos ovalados situados en ambas fosas iliacas. La vagina, es una estructura fibromuscular, tubular con una extensión de 6 – 12 cm desde la vulva al cérvix. Se encuentra rodeada de musculatura pélvica estriada, formando dos capas paralelas: la más superficial se compone de tres músculos ubicados en dos triángulos, el isquiocavernoso, el bulbo esponjoso y el transverso (Emhardt et al, 2016). El útero es un órgano muscular que se sitúa en la pelvis entre la vejiga y el recto (Emhardt et al, 2016; Graziottin y Gambini, 2015).

En el varón, los órganos genitales externos corresponden al pene, que se encuentra situado por debajo de la sínfisis púbica y por arriba del escroto. Posee la capacidad de la erección, que lo hace apto para sus funciones copuladoras (Latarjet y Ruiz, 2005). Su longitud promedio en el adulto es de 9,16 cm en estado flácido, mientras que en la erección alcanza un promedio de 13,12

cm (Veale et al, 2015). Asimismo, consta de una extremidad proximal o raíz del pene, una cara dorsal y la uretra; en su extremo distal se sitúa el glande, que se encuentra rodeado por el prepucio, y está constituido por formaciones eréctiles: los cuerpos cavernosos y el cuerpo esponjoso. El escroto es un saco cutáneo contentivo de los testículos (Latarjet y Ruiz, 2005).

Los genitales internos del varón son los testículos, órganos glandulares y ovoides. El epidídimo, que comprende la vía colectora y secretora, está conformado por una cabeza, un cuerpo y una cola. Las vías espermáticas están constituidas por los conductos deferentes, que inician su trayecto desde la cola del epidídimo, se dirigen al conducto inguinal y luego descienden hacia la vejiga urinaria, terminando en la unión con el conducto excretor de la vesícula seminal. Las vesículas seminales son un par de glándulas bilaterales, anexas a los conductos deferentes, situadas detrás de la vejiga y delante del recto y, unidas con el conducto deferente, forman el conducto eyaculador, que se dirige en sentido inferior, medial y posterior a un trayecto de 15 a 20 cm, hasta desembocar en la pared posterior de la uretra prostática (Latarjet y Ruiz, 2005).

Por otra parte, la uretra masculina pertenece tanto al sistema urinario como al aparato genital, mide 16 cm aproximadamente y se origina en el cuello vesical, traspasa la próstata y el diafragma urogenital para luego hacerse perineal y, rodeada por las formaciones eréctiles, atraviesa el pene hasta desembocar en el orificio externo de la uretra. Por ello, se divide en uretra prostática, membranosa, bulbar y esponjosa (Latarjet y Ruiz, 2005). La próstata es un órgano musculo glandular, que interviene en la función sexual y es atravesada por los conductos eyaculadores (Levin, 2018). Las glándulas bulbouretrales son dos, están ubicadas a ambos lados del músculo esfínter externo de la uretra y desembocan en la uretra esponjosa (Latarjet y Ruiz, 2005).

2. Fundamentos fisiológicos

Aunque el orgasmo posee un componente subjetivo muy marcado, existen ciertos patrones comunes entre el varón y la hembra (Komisaruk et al, 2004). En ambos se producen contracciones de los músculos pélvicos, pulsátiles, altamente intensas y placenteras al inicio del orgasmo. En el componente cardiovascular, al inicio del orgasmo, el varón y la hembra

experimentan las cifras más elevadas de presión arterial, frecuencia cardíaca y frecuencia respiratoria registrables durante todo el ejercicio de la función sexual. Además, durante el orgasmo la mayoría de los hombres y mujeres emiten vocalizaciones involuntarias (Levin, 2011).

En la hembra, el orgasmo suele estar asociado con la estimulación de los genitales y áreas extragenitales, tales como los pezones y las mamas. El inicio del orgasmo ocurre con sensaciones pulsátiles de intenso placer, perceptibles con las contracciones del útero, los músculos pélvicos, la vagina y el ano (Levin, 2011). También ocurre el engrosamiento del tercio posterior de la vagina, formándose la plataforma orgásmica. Ésta se halla constituida por los músculos perineales, encargados de las contracciones orgásmicas y la emisión uretral (Puppo, 2013).

Las contracciones rítmicas y estereotipadas de la plataforma orgásmica ocurren en los músculos bulbocavernosos, pubococcígeo, isquiocavernoso, transverso del periné, elevador del ano y esfínter externo del ano, además del útero (Puppo, 2013). Los bulbos vestibulares ocasionan la contracción de la vagina, observable cada 0,8 segundos debido a la contracción rítmica del músculo bulbocavernoso (Levin, 2011). El fenómeno de la "eyaculación en la hembra" se refiere a la expulsión, a través de la uretra, de un fluido diferente a la orina que es producido por glándulas intrauretrales (Jannini et al, 2012). Desde un punto de vista fisiológico, el término "emisión uretral" es el más adecuado (Puppo y Puppo, 2016).

La hembra es multiorgásmica por naturaleza, por lo que no es refractaria al orgasmo desde el punto de vista físico. Si su respuesta sexual no se encuentra inhibida y su aparato genital aún se mantiene en la fase de meseta, puede volver a ser eróticamente estimulada y, segundos después del primer orgasmo, alcanzar otro u otros hasta extenuarse físicamente, pudiendo rechazar toda estimulación (Arango, 2008). El orgasmo de la hembra no se asocia completamente con la presencia de la emisión uretral (Puppo, 2013; Puppo y Puppo, 2016). Sin embargo, algunas pueden presentar orgasmos con emisión uretral, tras la cual sigue un período refractario posteyaculatorio, no pudiendo experimentar un orgasmo inmediatamente posterior a ello (Levin, 2011).

Durante las fases precedentes al orgasmo, en el momento en que éste ocurre y ulterior al mismo, se registra un aumento de la temperatura en los genitales externos. A lo largo de la fase de excitación, los labios mayores y menores de la hembra son las áreas más cálidas. Sin embargo,

tan pronto como se desencadena la fase orgásmica, el clítoris se torna la estructura genital externa que proporciona el mayor aumento de calidez (Woodard y Diamond, 2010).

En el varón, los principales componentes del orgasmo son la erección y la eyaculación (Graziottin y Gambini, 2015). Es importante destacar que eyaculación y orgasmo no son sinónimos, pero la eyaculación es un componente importante del orgasmo del varón. Durante el orgasmo, los espermatozoides fluyen del epidídimo hasta los conductos deferentes propulsados por contracciones musculares, adquiriendo un componente que funciona como vehículo a partir de la vesícula seminal. Los conductos deferentes se contraen casi sincrónicamente con la vesícula seminal, drenando hacia la uretra prostática, simultáneamente acompañada con la emisión de la vesícula seminal. Durante esta fase, los fluidos prostáticos drenan en la uretra prostática mediante contracciones regulares y recurrentes, palpables a través del recto (Alwaal et al, 2015).

La segunda fase corresponde a la expulsión, debida a un reflejo parasimpático en el que participan la vejiga, la uretra y los músculos perineales, para propulsar el semen durante la eyaculación. Durante el orgasmo, los músculos bulbocavernosos se contraen rítmicamente con una acción de bombeo para la expulsión del semen (Puppo y Puppo, 2016). Tras la eyaculación, se presenta un período donde el varón no puede repetir inmediatamente la erección o la eyaculación, denominado "Periodo Refractario Posteyaculatorio", cuya duración promedio es de 20 minutos y su finalidad es desconocida (Alwaal et al, 2015; Sayin y Shenck, 2019). Se han descrito hombres multiorgásmicos, considerando como aquellos varones capaces de experimentar más de un orgasmo en un lapso < 20 minutos (Wibowo et al, 2016).

3. Fundamentos neuroendocrinos

Existen una serie de neurotransmisores y hormonas que actúan en un conjunto de procesos bioquímicos estrechamente relacionados con el orgasmo y su desarrollo. Éstas son las siguientes:

Dopamina: Se relaciona con el sistema límbico, representa el neurotransmisor del placer en ambos sexos, modula la motivación, el placer, la sensación de éxtasis, la duración de la experiencia sexual en los humanos, su comportamiento sexual y la libido, facilita la eyaculación

en el varón y prolonga la duración del orgasmo de la hembra (Sayin y Shenck, 2019). Sus efectos ocurren de manera predominante en el núcleo accumbens (Arango, 2008).

Serotonina: Antagonista de la dopamina en ambos sexos. Actúa en el hipotálamo lateral en el tracto mesocorticolímbico dopaminérgico, disminuye la libido, reduce el placer sexual, bloquea el orgasmo y su intensidad en la hembra y retarda la eyaculación del varón (Sayin y Shenck, 2019).

Norepinefrina: Mediador del sistema nervioso autónomo, durante la respuesta sexual aumenta la libido, la capacidad de alcanzar el orgasmo y la sensación de placer durante el orgasmo (Krüger et al, 1998). Facilita la función sexual en ambos sexos y puede inducir la eyaculación rápida en el varón (Sayin y Shenck, 2019).

Testosterona: Mayormente sintetizada por las células de Leydig en el varón y por las glándulas suprarrenales en la hembra, aumenta la libido en ambos sexos. Es la responsable de la producción de espermatozoides. Las concentraciones séricas de testosterona libre determinan la duración de la actividad sexual del varón. Si aquellas aumentan, el período refractario se acorta, se prolonga la erección y aumenta el volumen de emisión seminal, (Sayin y Shenck, 2019). Además, aumenta la frecuencia orgásmica en ambos sexos y la incitación al coito (Exton et al, 2001).

Prolactina: Denominada la hormona de la saciedad sexual, es secretada posterior al orgasmo en ambos sexos, siendo responsable de la sensación de vértigo y de ebriedad junto a las endorfinas. (Sayin y Shenck, 2019). Posterior al orgasmo, se registran concentraciones pronunciadas de la misma en plasma, lo cual sugiere que actúa como mecanismo de retroalimentación negativa en el sistema nervioso central para controlar la excitación postorgásmica (Exton et al, 2001). Cuando aumenta, se reducen las concentraciones de testosterona, induciendo el período refractario. Es capaz de disminuir la libido y la atracción sexual en los hombres (Sayin y Shenck, 2019).

Oxitocina: Producida en las neuronas supraópticas del núcleo paraventricular del hipotálamo, cumple un papel fundamental tanto en el orgasmo como en la conducta sexual de ambos sexos. Es la responsable de las contracciones uterinas y vaginales en el orgasmo de la hembra, mientras que en el varón influye en la erección y la eyaculación. Regula, además, el

estado de ánimo y las emociones, promoviendo las sensaciones de amor pasional, apego, empatía y tranquilidad posteriores al orgasmo (Sayin y Shenck, 2019).

4. Fundamentos neurológicos

La experiencia orgásmica implica un fenómeno de integración neuronal en las áreas corticales de asociación y existe una variabilidad en la calidad de esta experiencia (Arango, 2008). La actividad cerebral al momento del orgasmo suele ser muy similar, tanto en la hembra como en el varón. En ambos se activan regiones como el hipotálamo lateral, los núcleos accumbens, la región ventral del tegmento, la región ventral del núcleo pálido, la ínsula, la corteza de la cíngula, la corteza prefrontal, la corteza orbitofrontal y el septum (Sayin y Shenck, 2019). Sin embargo, existen algunas excepciones en la amígdala, el lóbulo temporal, la porción inferior del tallo encefálico, así como en la duración del período refractario postorgásmico (Jannini et al, 2012).

La activación del tegmento ventral se proyecta al núcleo accumbens, se activa la sustancia gris periacueductal y el núcleo dorsal de rafe. La cíngula anterior y la ínsula se activan en el orgasmo al igual que a la estimulación al dolor. La amígdala proporciona el componente emocional al orgasmo y, además, conjuntamente con el hipotálamo posterior activa al sistema nervioso autónomo, que induce el aumento de la frecuencia cardíaca y del flujo sanguíneo, característicos del orgasmo. Sin embargo, el hipocampo es el responsable del papel de la fantasía en el orgasmo, mientras que el núcleo paraventral del hipotálamo es indispensable para la liberación de oxitocina y la eyaculación (Jannini et al, 2018).

El cerebelo también se activa, tanto en el orgasmo de la hembra como del varón, incrementando la tensión muscular, Por otra parte, la corteza de la cíngula se activa fuertemente en el orgasmo y presenta dos funciones importantes: una simulación para activar el sistema nervioso autónomo y, además, generar los sentimientos intensos del orgasmo (Jannini et al, 2018).

En la hembra se ha observado un descenso en la actividad de la neocorteza, asimismo se exhibe un incremento de la actividad en las regiones subcorticales del cerebro (Georgiadis et al, 2006). De igual manera, se evidencia una activación más profunda de la ínsula izquierda (Levin, 2011; Sayin y Shenck, 2019; Georgiadis et al, 2009). Por otra parte, ocurre el decrecimiento de la

actividad en la corteza orbitofrontal, lo cual representaría la desinhibición conductual, como también del córtex temporal inferior, que está asociado con el incremento de la excitación sexual (Jannini et al, 2018; Georgiadis et al, 2016). Debido a la activación exagerada de la cíngula anterior, las manifestaciones autonómicas del orgasmo en la hembra se presentan con doble magnitud, debido a una intensa activación de la vía simpática (Jannini et al, 2018).

En el varón se ha observado una activación más extensa de la sustancia gris periacueductal (Levin, 2011; Georgiadis et al, 2009), que tiene un papel prominente en el control del comportamiento reproductivo. Además, se asocia con la activación mayormente intensa del claustro izquierdo y la porción ventral occipitotemporal de la corteza (Georgiadis et al, 2009). También se ha descrito una activación primaria en las zonas de transición del mesodiencéfalo, mientras se describe un descenso en la amígdala durante la eyaculación. Se ha descrito actividad neocortical en pocas áreas, las cuales son exclusivas del hemisferio derecho (Levin, 2011; Wise et al, 2017).

5. Fundamentos psicológicos

En cuanto a la experiencia mental, tratar de definir el orgasmo con palabras resulta difícil en varones y hembras, debido especialmente a la pérdida de la concentración voluntaria. La experiencia psicológica en ambos es bastante similar, cuando no idéntica (Levin, 2011). Al estudiar cualquier faceta humana, es necesario establecer una relación entre el cuerpo y la persona, precisando así la influencia psicológica en la obtención del orgasmo (Sira, 2011).

En la hembra, se encuentra influenciada por la orientación psicosocial y la receptividad para la obtención del orgasmo (Sira, 2011). La apreciación del cuerpo se relaciona con la calidad percibida de la excitación, orgasmo y satisfacción de la función sexual (Satinsky et al (2012). Una vez iniciado, puede ser interrumpido por el ambiente (Levin, 2011). Las hembras pueden presentar disminución de la ansiedad, felicidad, euforia, relajación, sensación subjetiva de corriente eléctrica y tensión muscular, así como la alteración del estado de conciencia (Sayin, 2017). Es frecuente que la mujer finja el orgasmo por considerar que, cuanto mayor sea la intensidad de la respuesta sexual, mayor será el placer subjetivo obtenido por el varón. Un

estudio realizado en 487 mujeres estableció la existencia de tres estadios en la progresión subjetiva de la mujer hacia el orgasmo (Sira, 2011).

En el primer estadio, el orgasmo se inicia con una sensación de "suspensión o detenimiento", que dura sólo un instante, siguiéndole un empuje aislado de inmensa actividad sexual, orientada hacia el clítoris e irradiada hacia la pelvis. Hay mujeres que registran diferentes intensidades de respuesta, desde niveles suaves hasta el choque. La sensación de vivencia clitorídea – pélvica ha sido explicada por muchas mujeres como una sensación de expulsión. Con frecuencia se refiere la sensación de abrirse para recibir algo. El segundo estadio se describe como una sensación de "ola de calor", que invade el área pélvica y se extiende a todo el cuerpo. Con respecto al tercer estadio, se manifiesta una contracción involuntaria en vagina o en el perineo bajo, definida como "latido pélvico" (Sira, 2011).

En el varón, se refiere una sensación de placer y plenitud posterior al orgasmo durante la eyaculación, que suele ser mayor en comparación con la hembra y, una vez iniciado en fase de "sensación de inevitabilidad eyaculatoria", no puede ser interrumpido (Levin, 2011). Cuanto mayor sea el volumen seminal expelido, mayor será la sensación subjetiva de placer. En él se describen dos estadios (Sira, 2011).

El primer estadio consiste en una sensación de inevitabilidad eyaculatoria, descrita como la sensación de "sentir que viene la eyaculación" y un segundo estadio que posee dos fases: primero, las contracciones del esfínter de la uretra estimulan la sensación contráctil, variando en intensidad y apreciación subjetiva. Experimentan un grado de tal anestesia que las porciones finales del eyaculado se expelen casi sin presión. Durante la segunda fase, donde el semen es expelido bajo presión a través de la uretra, se tiene una apreciación específica del volumen seminal. Dicha apreciación subjetiva se puede ejemplificar con la diferencia de intensidad del orgasmo en la eyaculación luego de un período de abstinencia: cuanto sea mayor el volumen eyaculado mayor será la sensación subjetiva de placer (Sira, 2011).

6. Fundamentos Socioculturales

La calidad de la relación de pareja se encuentra altamente ligada a la frecuencia con la que se obtiene el orgasmo y la calidad de la respuesta sexual (Mah y Bink, 2005). Se describe la

presencia de factores ambientales, culturales y sociales influyentes en la experiencia del orgasmo (Masters y Johnson, 1978). Sin embargo, para ellos, la inadaptación sexual en el varón y la influencia cultural en la actividad sexual de aquél no se relacionan con su obtención del orgasmo, a contrapelo de la obtención del orgasmo de la hembra (Llanes et al, 2013).

Se ha sugerido que los factores psicosociales son determinantes en la interpretación subjetiva del orgasmo experimentado en la hembra, además de la satisfacción y el placer. Se ha evidenciado que, tanto el placer como la satisfacción orgásmica de la hembra, se vinculan con las relaciones intrapersonales e interpersonales, así como también con los factores del contexto o lugar donde se ejerza la función sexual. La experiencia de placer y satisfacción orgásmica en el varón recibe una pequeña consideración, pero alguna evidencia sugiere que sus experiencias subjetivas se relacionan con influencias psicosociales. Algunas de estas experiencias enfatizan la importancia de la calidad de los orgasmos en la relación del varón (Guasch, 1993).

En muchas hembras que nunca han experimentado orgasmos parece estar implicada una educación religiosa severa y negativa respecto del sexo. Además, la hembra es calificada como "femenina", es decir, dulce, amorosa, delicada, sentimental, dependiente de lo afecto y lo económico, pero se le reprime sexual y eróticamente, por lo que su respuesta sexual puede verse afectada, especialmente en la obtención del orgasmo (Masters et al, 1987). Se dice que "la mujer tiene que buscar un orgasmo", más allá de buscar una necesidad individual, pero estas situaciones pueden generar malestar o bienestar dentro de la salud sexual por lo que puede afectar la fase del orgasmo (Arango, 2008).

La salud sexual es un fundamento de la salud en general, por tanto, demanda un espacio dentro del derecho a la salud integral. No obstante, es violentada, lo cual atenta contra los individuos debido a los estereotipos estéticos y conductuales (femenino/masculino) que impone la sociedad. Una mujer que responde a estos cánones está constreñida por los papeles conductuales que debe seguir: desgenitalizar su cuerpo, no apropiarse de su placer, desconocer sus genitales y su funcionamiento. Hereda mitos y prejuicios, además de un sentimiento de culpa sobre ellos, por tanto, sobre la respuesta sexual, así como su actitud y conquista ante el erotismo y el orgasmo (Arango, 2008).

La hembra suele fingir el orgasmo para generar placer al varón, para terminar el encuentro sexual, sentirse sexualmente normales, evitar reacciones negativas y reforzar las habilidades sexuales del varón. Por el contrario, es más común que los hombres simulen el orgasmo por su propio beneficio para producir incentivo para una nueva erección (DeLamater et al, 2015).

7. Fundamentos espirituales

La espiritualidad y la sexualidad son determinantes en la identidad, creencias y comportamientos del ser humano. A pesar de que suelen verse como dos entidades totalmente opuestas en la existencia, se han desarrollado investigaciones las cuales han revelado relaciones entre ellas (Costa et al, 2016). Tanto el deseo sexual como su ejecución poseen una relación inherente con el ámbito espiritual. El orgasmo juega un papel fundamental en la sexualidad humana, siendo una experiencia en la que se trasciende al mismo ser (Ellens, 2009).

Ahora bien, el autoejercicio de la función sexual (masturbación) y el coito casual acostumbran a ser ejercicios sexuales gratificantes y placenteros a la vez, pero suelen estar acompañados de una impresión de sentirse vacío e incompleto. En consecuencia, el orgasmo es una experiencia que consiste en entregarnos completamente hacia el otro individuo. Consumar el orgasmo con una persona con la que se comparta una arraigada sensación emocional, conlleva una especie de paz suprema (Ellens, 2009).

Es común que exista el deseo de encontrar una conexión sexual sustentada en creencias y comportamientos (Armstrong, 2019). Cuando un individuo asume la importancia de la espiritualidad en la sexualidad, ya sea en la suya propia o en una relación, se compromete a alcanzar un grado mayor de satisfacción (Kusner et al, 2014). Una vez llegado al punto máximo de conexión de la sexualidad con la espiritualidad, el cuerpo actúa como un intermediario entre el placer emocional y el espiritual, experimentando así, nuevos niveles de placer orgásmico (MacKnee, 2002).

En algunas culturas del mundo oriental, se ha logrado conseguir el orgasmo a través de la meditación espiritual, es decir, si ocurre la interconexión entre la energía sexual y la energía espiritual. Tal conexión no discrimina expresiones fenotípicas, edad, cultura, religión o

nacionalidad, debido a que la energía espiritual proviene del espíritu y en éste no existen diferencias entre unos y otros (Henderson, 2015).

En el caso de las hembras, mientras mayor sea su disposición a abrirse a su espiritualidad, alcanzarán frecuentemente el orgasmo durante el ejercicio de la función sexual (Costa et al, 2016). Suele suceder que el varón propague la idea de una vinculación directa del ejercicio de la función sexual con altos niveles de energía espiritual, ante la finalidad de concretar encuentros sexuales con algunas hembras (Henderson, 2015; Ochoa y Pitter, 2018).

Consideraciones finales

Existen ciertas diferencias entre el orgasmo del varón y la hembra. Entre éstas destacan que el orgasmo de la hembra carece de función reproductiva, puede constantemente ser repetitivo, usualmente no presenta período refractario, no se relaciona directamente con la emisión uretral y, una vez iniciado, puede ser interrumpido o inhibido por factores psicológicos, socioculturales y ambientales. Asimismo, la espiritualidad representa un papel sustancial en la obtención del orgasmo en la hembra.

Por su parte, el orgasmo del varón mayormente no es repetitivo debido a la presencia de un período refractario constante, ejerce una función vinculada directamente con la reproducción y está estrechamente relacionado con la eyaculación. Al contrario de la hembra, no se halla muy influenciado por el entorno social, el contexto sexual o los prejuicios culturales; y su magnitud de la espiritualidad se haya menguada en la consecución del mismo.

Finalmente, se recomienda la realización de nuevas investigaciones que propicien la exploración de las singularidades orgásmicas del varón y la hembra, en aras de una mayor comprensión de dichos fenómenos, así como también para el desarrollo de competencias más efectivas, tanto en el tratamiento de las alteraciones en la fase orgásmica de la respuesta sexual, como en el fomento de experiencias sexuales sanas, libres, conscientes, responsables y sin problematizaciones, todo ello enmarcado en la promoción de la salud sexual.

Referencias

Alwaal A., Breyer B., Lue T. (2015). Normal male sexual function: Emphasis on orgasm and ejaculation. Fertil Steril. 104:1051-1060.

Arango, I. (2008) Sexualidad Humana. Editorial Manual Moderno.

Armstrong, J. (2019). God Likes Sex: Conversations Integrating Spirituality and Sexuality. DMin. 2 (1)

Bancroft J. (1983) Human sexuality and its problems. Churchill Livingstone, New York.

Costa R., Oliveira T., Pestana J., Costa D. (2016). Self-transcendence is related to higher female sexual desire. Personality and Individual Differences, 96, 191–197.

De Lamater J., Plante R. (2015). Handbook of the Sociology of Sexualities. Editorial Springer. p-p 138.

Duvauchelle C. (1995). Etimología del lenguaje en las Ciencias de la Salud. Maracaibo - Venezuela. Ediciones Astro Data S.A.

Ellens J. H. (2009). The Spirituality of Sex: Psychology, religion and spirituality. Editorial Greenwood Publishing Group p.p 54-56.

Emhardt E., Siegel J., Hoffman L. (2016). Anatomic variation and orgasm: Could variations in anatomy explain differences in orgasmic success? Clin Anat. 29 (05), 665-672.

Exton, M., Kruger, T., Bursch, N., Haake, P., Knapp, W., Schedlowski, M., Hartmann, U. (2001). Endocrine response to masturbation-induced orgasm in healthy men following a 3-week sexual abstinence. World Journal of Urology. 19, 377-382.

FLASSES, AMSM, AISM (2014). MSD III. Manual de diagnóstico de sexología. 3ª Edición. Caracas - Venezuela. Editorial CIPV.

Guasch O. (1993). Para una sociología de la sexualidad. Rev española de investigaciones sociológicas. 64, 105-122.

Georgiadis J., Kortekaas R., Kuipers R., Nieuwenburg A., Pruim J., Reinders A., Holstege G. (2006). Regional cerebral blood flow changes associated with clitorally induced orgasm in healthy women. Eur J Neurosci 24: 3305-3316.

Georgiadis, J., Reinders, A., Paans, A., Renken, R., Kortekaas, R. (2009). Men versus women on sexual brain function: prominent differences during tactile genital stimulation, but not during orgasm. Human Brain Mapping. 30, 3089-3101.

Georgiadis J., Kortekaas R., Kuipers R., Nieuwenburg A. et al. (2016). Regional cerebral blood flow changes associated with clitorally induced orgasm in healthy women. The European journal of neuroscience. 24, 3305-3316.

Graziottin A., Gambini D. (2015). Anatomy and physiology of genital organs – women. In: Neurology of Sexual and Bladder Disorders. Milan.130, 39-60.

Henderson R. (2015). Emotion and Healing in the Energy Body: A Handbook of Subtle Energies in Massage and Yoga. Editorial Simon and Schuster.

Jannini EA., Rubio A., Whipple B., Buisson O., Komisaruk BR., Brody S. (2012). Female orgasm(s): One, two, several. J Sex Med. 9, 956-965.

Jannini E.A., Wise N., Frangos E., Komisaruk BR. (2018). Peripheral and Central Neural Bases of Orgasm. In Texbook of Sexual Function and Dysfunction: Diagnosis and Treatment, First Edition. 13, 179-195.

Kaplan H. (1974). New Sex Therapy: Active treatment of sexual dysfunction. Editorial Routledge, pp. 5-12.

Kaplan, H. (1979). Disorders of sexual desire and other new concepts and techniques in sex therapy (Vol. 2). Simon y Schuster.

Komisaruk B., Whipple B., Crawford A., Grimes S., Liu W-C, Kalnin A, et al. (2004). Brain activation during vaginocervical self-stimulation and orgasm in women with complete spinal cord injury; fMRI evidence of mediation by the vagus nerves. Brain Res. 1024, 77-88.

Krüger T., Exton M., Pawlak C., von zur Muhlen A., Hartmann U., Schedlowski M. (1998). Neuroendocrine and cardiovascular response to sexual arousal and orgasm in men. Psychoneuroendocrinology 23:401-11.

Kusner G.K., Mahoney A., Mahoney K.I., DeMaris A. (2014). Sanctification of marriage and spiritual intimacy predicting observed marital interactions across the transition to parenthood. J. Fam. Psychol, 28(5).

La Calle P., Herraíz, M.A., Coronado P., Moltalvo J. (2009). Flujo Genital Femenino: estudio y consideraciones clínicas. [Tesis Doctoral] Madrid. Facultad de Medicina. Departamento de Ginecología y Obstetricia. Hospital Clínico Universitario San Carlos.

Latarjet M., Ruiz A. (2005). Anatomía Humana. Editorial Panamericana. p.p. 1567-1598.

Levin R.J. (2011). Physiology of orgasm. Cancer and sexual health. 35-49.

Levin R.J. (2018). Prostate induced orgasms: a concise review illustrated with a highly relevant case study. Clin Anat. 31, 81-5.

Levin R.J. (2007). The human sexual response - similarities and differences in the anatomy and function of the male and female genitalia. In: Janssen E, editor. The psychophysiology of sex. Bloomington: Indiana University Press. 39-56.

Llanes L., Acosta G., Castelo L. (2013). Eyaculación y placer sexual en el varón: una relación compleja y multideteminada. Rev Sexología y Sociedad. 19 (1): 44-63.

MacKnee C. (2002). Profound Sexual and Spiritual Encounters among Practising Christians: A Phenomenological Analysis. Journal of Psychology & Theology 30(3): 234-245.

Mah K., Binik Y.M. (2005). Are orgasms in the mind or the body? Psychosocial versus physiological correlates of orgasmic pleasure and satisfaction. Journal of Sex &Marital Therapy 31, 187-200.

Masters, W., Johnson, V. (1966). Human sexual response. Little, Brown.

Masters, W., Johnson V. (1978) La Respuesta sexual humana. Editorial Inter-Médica.

Masters, W., Johnson, V., Kolodny, R. (1987). La Sexualidad Humana. Grijalbo

Ochoa, E.; Pitter, W. (2018). Menstruación, abstinencia sexual y ejercicio de la función sexual según la ley judía: una perspectiva sexológica, *Revista de la Universidad del Zulia*, 9 (24), 54-71.

Portillo S., Pérez T., Royuela A. (2017). Disfunción sexual femenina: estudio de prevalencia en mujeres premenopáusicas. Prog Obstet Ginecol. 60(4), 320-327.

Puppo V. (2013). Anatomy and physiology of the clitoris, vestibular bulbs, and labia minora with the review of the female orgasm and the prevention of female sexual dysfunction. Clin Anat. 26, 134-52.

Puppo V., Puppo G. (2016). Comprehensive review of the anatomy and physiology of male ejaculation: Premature ejaculation is not a disease. Clin Anat. 29(1), 111-9.

Satinsky S., Reece M., Dennis B., Sanders S., Bardzell S. (2012). An Assessment of body appreciation and its relationship to sexual function in women. Body image 9, 137-144.

Sayin HÜ. (2017). Female Orgasmic Consciousness: New Horizons (Review). SexuS Journal. 2(4), 117-145.

Sayin HÜ., Shenck CH. (2019). Neuroanatomy and neurochemistry of sexual desire, pleasure, love and orgasm. SexuS Journal Winter. 4,11.

Schnarch, D. (1991). Constructing the sexual crucible: An integration of sexual and marital therapy. WW Norton & Company.

Sira M. (2011). Entre sábanas, consejos practicos para mejorar tu vida sexual y de pareja. Editorial Norma p.p. 49-53.

Veale D., Miles S., Bramley S., Muir G., Hodsoll J. (2015). Am I normal? A systematic review and construction of nomograms for flacid and erect penis length and circumference in up to 15 521. BJU Int; 115, 97886.

Whipple, B., Brash-McGreer, K. (1997). Management of female sexual dysfunction. Sexual function in people with disability and chronic illness. A health professional's guide, 509-534.

Wibowo E., Wassersug R. (2016). Multiple orgasms in men—what we know so far. Sex Med Rev. 4, 136-48.

Wise N., Frangos E., Komisaruk B. (2017). Brain activity Unique to Orgasm in Women: An fMRI Analysis. J Sexual Med. 14(11), 1380-1391.

Woodard T., Diamond M., (2010). Physiologic Measures of Sexual Function in Women: A Review. National Institutes of Health. 92 (1), 19-34.

Estrategias motivacionales para mejorar las relaciones interpersonales en los docentes de la Escuela Profesional de Tecnología Médica de la Universidad de Chiclayo

Yris Adriana Mendoza Deza *
Dora Victoria Vásquez Gastelumendi *
Carlos Alberto Ríos Campos **
Freddy Manuel Camacho Delgado ***
Karina Silvana Gutiérrez Valverde ****

RESUMEN

Se realizó la investigación con el objetivo de diseñar estrategias motivacionales para mejorar las relaciones interpersonales en los docentes de la Escuela Profesional de Tecnología Médica, Facultad de Ciencias de la Salud – Universidad de Chiclayo. Para ello se aplicaron encuestas, observación, entrevistas estructuradas y en profundidad y testimonios sobre el nivel de relaciones interpersonales. Luego, se procedió a examinar el problema en relación con las teorías de Kurt Lewin, Douglas Mcgregor y Daniel Goleman que sirvieron de fundamento a nuestra propuesta de estrategias motivacionales. Se concluyó que la mayoría de docentes presentan malas relaciones interpersonales, lo que se manifiesta en mala comunicación, ausencia de socialización, falta de identidad institucional, falta de identidad con los conceptos de respeto, autonomía y libertad, entre otros. Las estrategias motivacionales son esenciales, ya que nos permiten trabajar con todos los docentes de manera dinámica e interactiva afinando e incrementando el nivel de las relaciones interpersonales.

PALABRAS CLAVE: Estrategias organizacionales; clima laboral; comunicación; desmotivación.

* Licenciado en Tecnología Médica, Hospital Luis Heysen Incháustegui, Perú. E-mail: yris_adri2@hotmail.com
** Docente Investigador, Universidad Politécnica Amazónica, Perú. E-mail: crios@upa.edu.pe
*** Docente Principal, Universidad Nacional Intercultural Fabiola Salazar Leguía de Bagua. E-mail: fcamacho@ unibagua.edu.pe
**** Docente universitaria. Universidad Nacional de Frontera, Perú. E-mail: kgutierrez@unfs.edu.pe

Recibido: 13/03/2020 Aceptado: 25/05/2020

Motivational strategies to improve interpersonal relationships in teachers of the Professional School of Medical Technology at the University of Chiclayo

ABSTRACT

The research was carried out with the aim of designing motivational strategies to improve interpersonal relationships among teachers at the Professional School of Medical Technology, Faculty of Health Sciences - University of Chiclayo. For this, surveys, observation, structured and in-depth interviews and testimonies on the level of interpersonal relationships were applied. Then, we proceeded to examine the problem in relation to the theories of Kurt Lewin, Douglas Mcgregor and Daniel Goleman that served as the foundation for our proposal of motivational strategies. It was concluded that the majority of teachers present bad interpersonal relationships, which is manifested in poor communication, absence of socialization, lack of institutional identity, lack of identity with the concepts of respect, autonomy and freedom, among others. Motivational strategies are essential, since they allow us to work with all teachers in a dynamic and interactive way, refining and increasing the level of interpersonal relationships.

KEYWORDS: Organizational strategies; working environment; communication; demotivation.

Introducción

Toda realidad problemática tiene dos aspectos, uno objetivo y el otro subjetivo, el mismo que da cuenta de la realidad interior de la persona y que sirve de energía a la voluntad de la persona, la que se revela en nuestro comportamiento cotidiano.

Desde el enfoque de una educación centrada en el desarrollo de las fortalezas y talentos, los desafíos que aparecen como prioritarios refieren al cambio de mentalidad de los educadores desde un modelo de déficit a uno de capacidades (Muñoz, Conejeros, Contreras & Valenzuela, 2016).

La Universidad, como institución creadora y transmisora de ciencia, técnica y cultura, tiene la responsabilidad, no sólo de preparar para el ejercicio de las actividades profesionales al alumno, sino que tiene un compromiso de excelencia para la docencia, la investigación y la transferencia (Garrote, Garrote & Jiménez, 2016).

La evidencia presentada apunta a la importancia de continuar educando a los líderes institucionales sobre los beneficios de utilizar estrategias que promuevan y apoyen las necesidades psicológicas de autonomía, competencia y vínculo de sus empleados (Muñoz & Ramírez, 2014; Vásquez, 2019).

El término motivación deriva del verbo latino moveré, cuyo significado es mover, por lo tanto, motivación es la necesidad de activar la conducta dirigiéndola hacia la meta propuesta (Alemán, Navarro de Armas, Suárez, Izquierdo & Encinas, 2018).

La competencia comunicativa interpersonal es fundamental para el desarrollo de las organizaciones, su estudio se realiza a través de cinco subcompetencias: empatía, autocontrol emocional, retroalimentación, centrado en el problema, escucha activa, las cuales se desarrollan a través de un entrenamiento socio-psicológico (Hernández, Herrera & Mena, 2019).

Una comunicación interpersonal incorrecta tiene repercusiones negativas tanto para el paciente como para los profesionales (Lapeña-Moñux, Cibanal-Juan, Pedraz-Marcos, & Macía-Soler, 2014).

Las habilidades sociales y de comunicación interpersonal involucran las interacciones entre las personas y entre sí mismos, entre las personas y grupos; lo que se busca, entonces, es que la persona maneje correctamente estos aspectos, conductual, personal y situacionalmente (Flores, Garcia, Calsina & Yapuchura, 2016).

Un conflicto es un proceso dinámico y complejo que se alimenta de emociones. Por lo tanto, para entender los procesos de gestión de conflicto, es necesario estudiar la influencia de las variables emocionales que rodean las disputas (Montes, Rodríguez & Serrano, 2014).

Cabe señalar que es de gran importancia avanzar en el estudio del perdón en las relaciones interpersonales, ya que puede ayudarnos a mantener relaciones sanas y un adecuado funcionamiento psicológico (Beltrán-Morillas, Valor-Segura & Expósito, 2015).

El trabajo contiene elementos de estrategia motivacional que comprometen a docentes universitarios, por ende, se da cuenta del aspecto subjetivo del campo de observación.

Metodológicamente el problema de investigación, tiene que ver con el objeto de estudio, relaciones interpersonales docentes en la Escuela Profesional de Tecnología Médica de la Facultad de Ciencias de la Salud – Universidad de Chiclayo.

Posible solución del problema, ¿de qué manera influirán las estrategias motivacionales al mejoramiento de las relaciones interpersonales en los docentes de la Escuela Profesional de Tecnología Médica de la Facultad de Ciencias de la Salud – Universidad de Chiclayo?

El objetivo general, diseñar estrategias motivacionales para mejorar las relaciones interpersonales en los docentes de la Escuela Profesional de Tecnología Médica de la Facultad de Ciencias de la Salud – Universidad de Chiclayo. Los objetivos específicos, diagnosticar las relaciones interpersonales de los docentes: comunicación, trabajo en equipo, liderazgo y conflicto, investigar el modo cómo se relaciona la base teórica con la propuesta, elaborar la propuesta en función a las razones de la investigación.

El campo de acción, estrategias motivacionales para mejorar las relaciones interpersonales en los docentes de la Escuela Profesional de Tecnología Médica de la Facultad de Ciencias de la Salud – Universidad de Chiclayo.

La hipótesis, si se diseñan estrategias motivacionales sustentadas en las teorías de Kurt Lewin, de Douglas McGregor y de Daniel Goleman, entonces mejorarán las relaciones interpersonales en los docentes de la Escuela Profesional de Tecnología Médica de la Facultad de Ciencias de la Salud – Universidad de Chiclayo.

Se realizó el análisis del problema de estudio. Comprende la situación geográfica del Perú, de la Provincia de Chiclayo y una breve descripción de la Universidad de Chiclayo. Tendencias de las relaciones interpersonales docentes universitarias; relaciones interpersonales docentes en la Universidad de Chiclayo y la razón metodológica.

La Universidad de Chiclayo (UDCH) está ubicada en la Ciudad Universitaria Km. 3.5 Carretera a Pimentel. Chiclayo, Perú (Universidad de Chiclayo, 2013).

Se abordó el marco teórico, el cual está comprendido por el conjunto de trabajos de investigación que anteceden al estudio y por la síntesis de las principales teorías que sustentan la propuesta. Luego el marco conceptual.

Se realizó el análisis e interpretación de los datos. También la propuesta en relación a las teorías mencionadas; los elementos constitutivos de la propuesta: Realidad problemática, objetivos, fundamentación, estructura, cronograma, presupuesto y financiamiento. La estructura de la propuesta como eje dinamizador está conformada por tres talleres con sus respectivas temáticas. Se presentaron las conclusiones, recomendaciones, bibliografía y anexos.

1. Metodología

La importancia de la metodología es que proporciona un sentido de visión, de a dónde quiere ir el analista con la investigación. Las técnicas y procedimientos (el método), por otra parte, proporcionan los medios para llevar esta visión a la realidad (Strauss & Corbin, 2002).

El trabajo está diseñado en dos fases: En la primera se consideró el diagnóstico situacional y poblacional que nos permitió seleccionar las técnicas de investigación. En la segunda fase se operacionalizaron las variables, haciendo hincapié en la variable independiente que guarda relación con la elaboración de la propuesta. La investigación adoptó el siguiente diseño:

Fuente: Elaboración propia.

2. Resultados

2.1. Resultados de guía de observación

INDICADOR	SIEMPRE	AVECES	CASI NUNCA	NUNCA	TOTAL
COMUNICACIÓN:					
- Dispone de suficiente información en relación con el trabajo, eventos a realizarse y otros.	0	2	15	3	20
- Recibe información de su superior y sus colegas.	0	1	2	17	20
- Existe interacción con directivos y colegas.	0	0	2	18	20
TRABAJO EN EQUIPO:					
- En la Escuela nos comunicamos permanentemente.	0	1	1	18	20
- En mi trabajo todos nos llevamos bien.	0	0	4	16	20
- Tengo confianza con mis compañeros de trabajo.	0	0	5	15	20
PERCEPCIÓN DE LA ORGANIZACIÓN:					
- La imagen negativa que se tiene en la sociedad de la Institución.	17	3	0	0	20
- La Institución tiene conflictos internos.	18	2	0	0	20

- Se siente orgulloso de trabajar en esta institución.	0	1	1	18	20
SATISFACCIÓN GENERAL:					
- Satisfecho en el trabajo.	0	1	1	18	20
- Satisfecho con la relación con el jefe.	0	1	2	17	20
- Satisfecho con la relación que tengo con mis compañeros.	0	2	2	16	20

Fuente: Guía de observación aplicada a los docentes de la Escuela Profesional de Tecnología Médica de la Universidad de Chiclayo.

2.1.1. Interpretación

Comunicación, con respecto a este indicador se puede observar que no existe interacción con directivos y colegas (18), así mismo nunca reciben información de su superior y sus colegas (17), tampoco disponen de suficiente información en relación con el trabajo, eventos a realizarse y otros (15). Trabajo en equipo, los gestores nunca se comunican permanentemente (18), tampoco se llevan bien (16), mucho menos se denota confianza entre los compañeros de trabajo (15).

Percepción de la organización, se determinó que la Institución tiene conflictos internos (18), además se tiene una imagen negativa de la Institución (17) y que los gestores no sienten orgullo de trabajar en su Institución (18). Satisfacción general, en este indicador podemos decir que los gestores observados no se sienten satisfechos con la relación con su jefe (17), tampoco se sienten satisfechas en el trabajo (18), ni con la relación que se tienen con los compañeros (16).

2.2. Resultados de la encuesta

Análisis: Del 100% de docentes encuestados, el 65% afirma que las relaciones interpersonales son malas y 10% muy malas respectivamente. Por otro lado, el 15% afirma que muy buenas y 10% buenas relaciones interpersonales. Se concluye que poco menos de las tres

cuartas partes de la muestra, es decir, el 75% de los docentes tienen inadecuadas relaciones interpersonales.

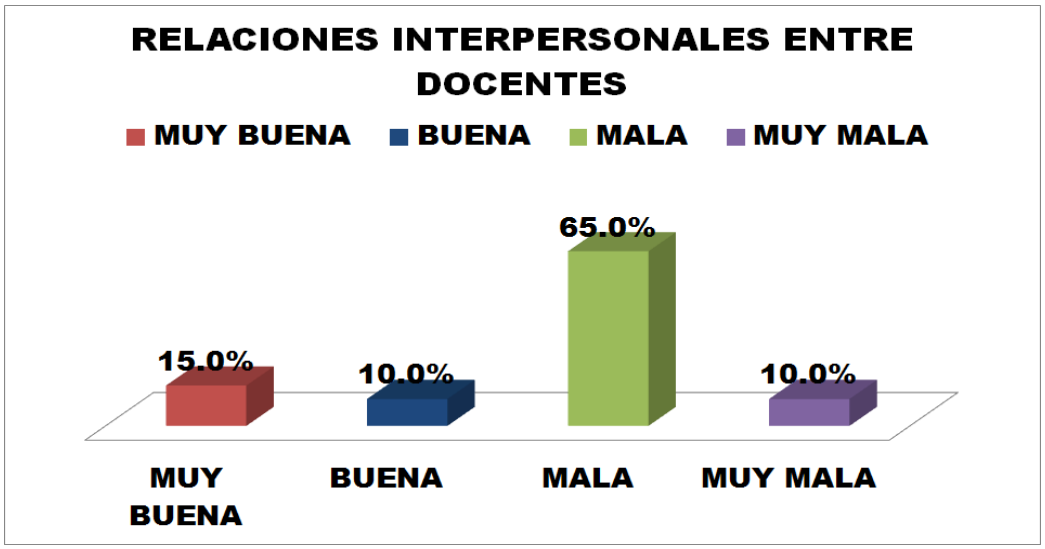

Figura Nº 01: Relaciones Interpersonales entre Docentes

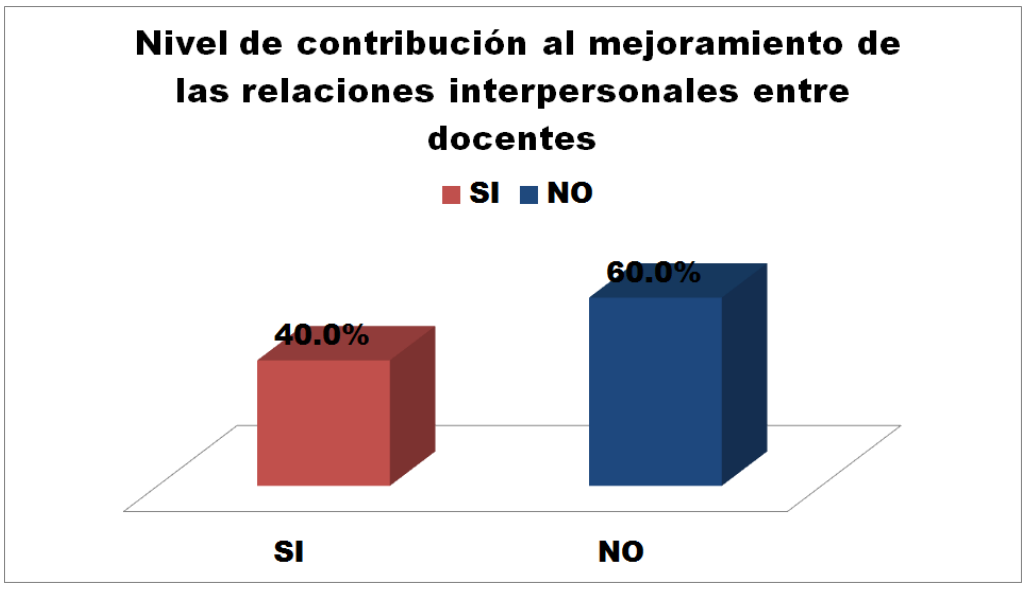

Figura Nº 02: Nivel de contribución al mejoramiento de las relaciones interpersonales entre docentes.

Análisis: 60% de docentes sostienen que no hay voluntad por mejorar las relaciones interpersonales, mientras que el 40% expresa lo contrario. Se deduce que poco más del 50%

de la muestra, es decir 60% no tienen predisposición por mejorar las relaciones interpersonales.

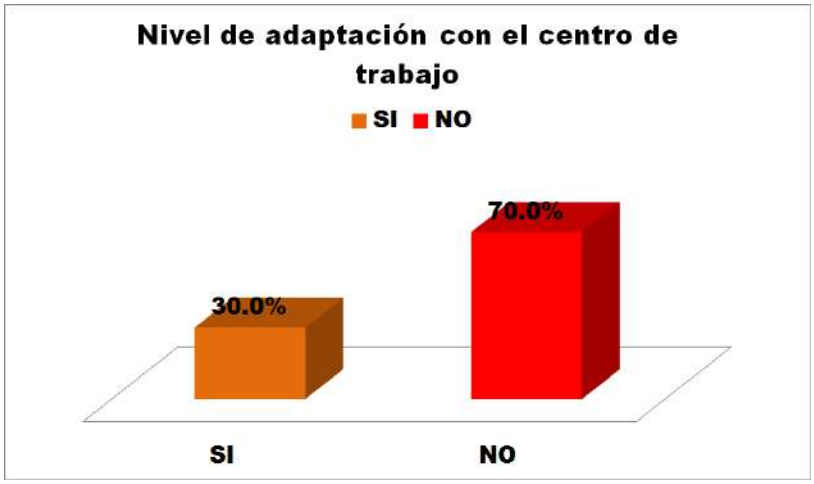

Figura Nº 03: Nivel de Adaptación con el Centro de Trabajo

Análisis: Del 100% de docentes encuestados, el 70% indican que no se adaptan al clima institucional de su centro de trabajo, mientras que el 30% responde lo contrario. Vemos que estamos frente a una realidad donde poco menos de las tres cuartas partes de la muestra, es decir, el 70% de los docentes no se han incorporado al ambiente de su centro de trabajo.

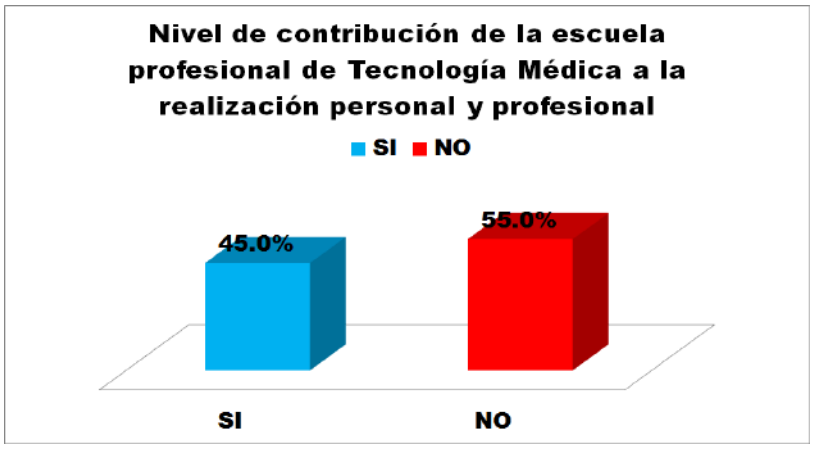

Figura Nº 04: Nivel de contribución de la Escuela Profesional de Tecnología Médica a la Realización Personal y Profesional.

Análisis: 55% afirman que la Escuela Profesional de Tecnología Médica no contribuye a su realización personal ni profesional. En conclusión, poco más del 50% de los docentes nos hace ver que su Escuela Profesional no contribuye a su formación personal ni profesional, debido a que el 75% de ellos existe inadecuadas relaciones interpersonales.

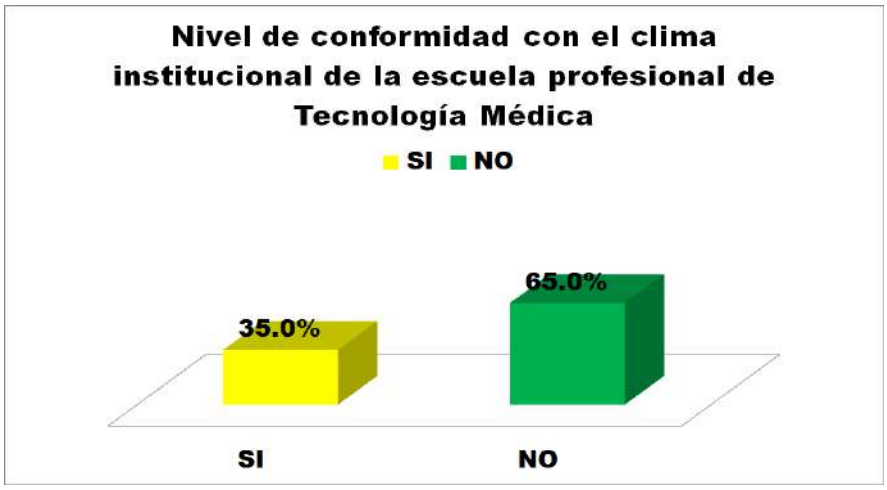

Figura Nº 05: Nivel de Conformidad con el Clima Institucional de la Escuela Profesional de Tecnología Médica.

Análisis: Del 100% de docentes encuestados, el 65% no están de acuerdo con el clima institucional de la Escuela Profesional de Tecnología Médica, sin embargo, el 35% está conforme. Vemos que la mayoría de docentes, no están de acuerdo con el clima institucional de su centro de trabajo, debido a las malas relaciones interpersonales y a la inadaptación en su centro de trabajo.

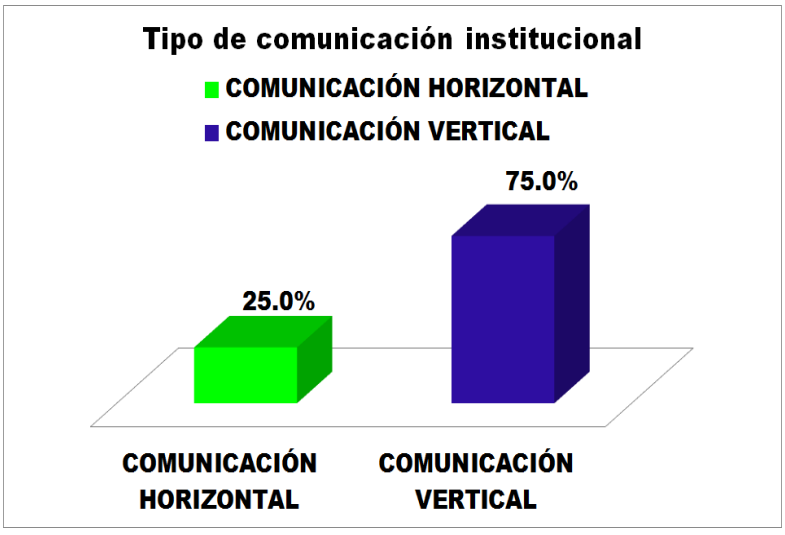

Figura Nº 06: Tipo de comunicación institucional.

Análisis: 75% afirman que predomina un tipo de comunicación vertical y solo el 25% indica lo contrario. En síntesis, la mayoría de docentes reconocen que la comunicación es

arbitraria, debido a las malas relaciones interpersonales entre docentes, mostrando inconformidad en su centro de trabajo.

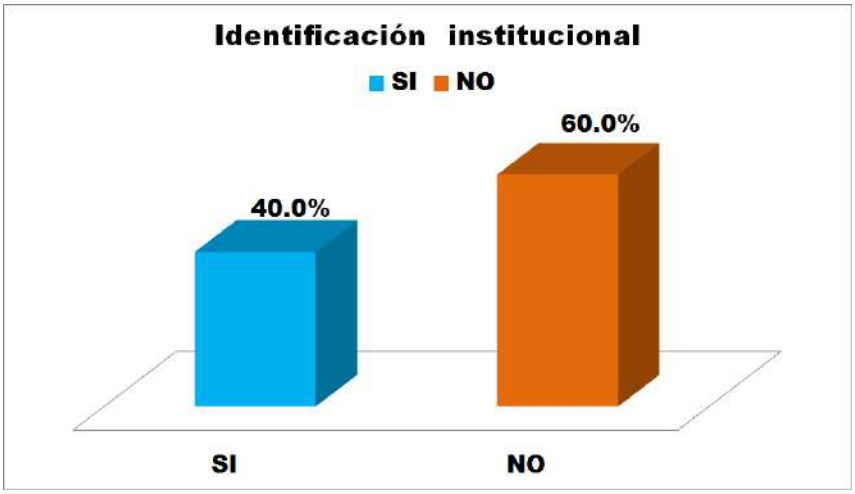

Figura Nº 07: Nivel de identificación institucional

Análisis: Del 100% de docentes encuestados, el 60% expresan no sentirse identificados con la Escuela Profesional de Tecnología. Vemos que la mayoría de docentes no se siente identificado con su centro de trabajo, debido a la comunicación verticalista.

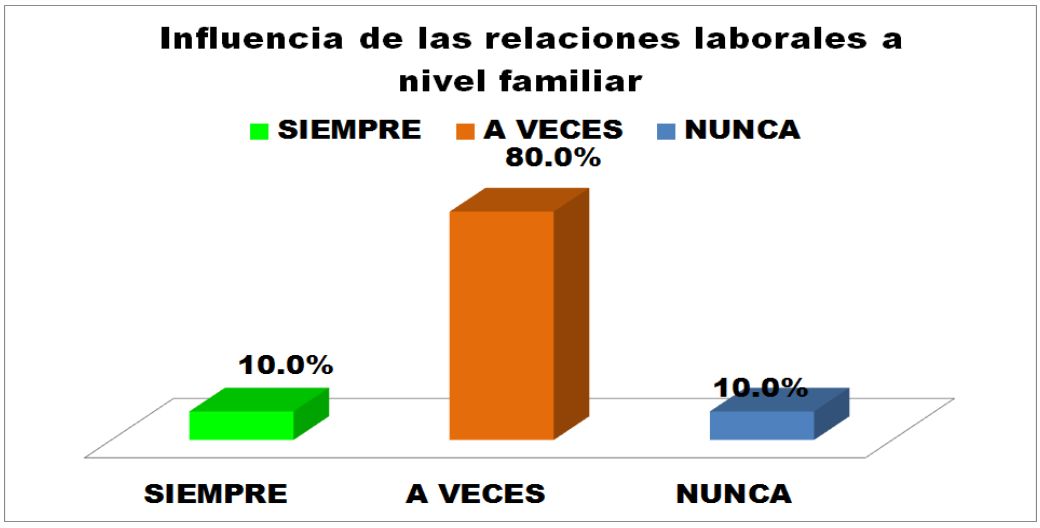

Figura Nº 08: Influencia de las Relaciones laborales a nivel familiar.

Análisis: 80% de docentes reconocen que a veces las relaciones laborales influyen en sus relaciones familiares; el 10% afirma que siempre influyen y solo el 10% contestaron que no influyen. Se concluye que las tres cuartas partes de la muestra, es decir, el 80% afirman que a veces las relaciones laborales influyen el seno familiar, en consecuencia, al existir malas

relaciones interpersonales entre docentes, una comunicación verticalista de orden superior a inferior, entre otras perjudican no solo su ámbito laboral, sino también en su hogar.

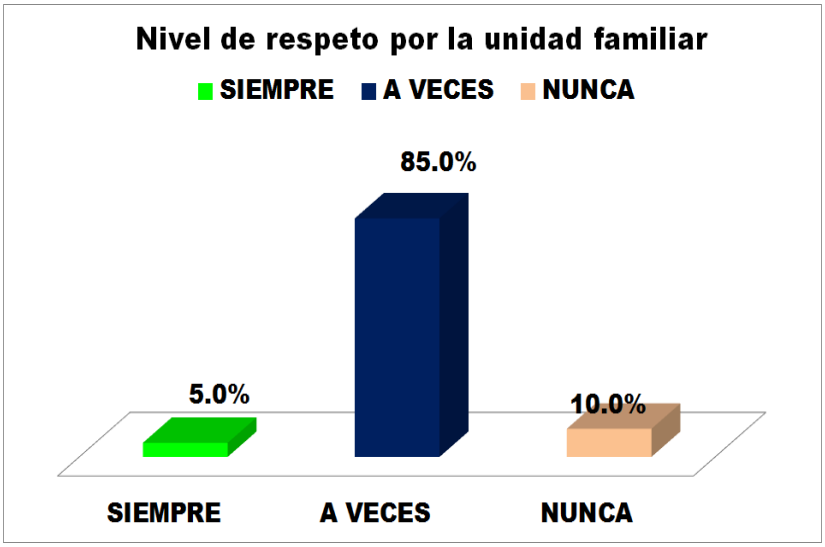

Figura Nº 09: Nivel de respeto por la unidad familiar.

Análisis: Del 100% de docentes encuestados, el 85% reconocen que a veces existe respeto por la unidad familiar; el 5% indican si hay respeto familiar y el 10% afirma que no lo hay. La mayoría de docentes concluyen que a veces existe respeto por la unidad familiar.

Figura Nº 10: Nivel de Identificación con los conceptos de autonomía, respeto y libertad.

Análisis: 80% no se identifican con los conceptos de autonomía, respeto y libertad. La mayoría de docentes no se identifican con los conceptos aludidos; ya que no se identifica con

su institución universitaria donde labora y mucho menos con la Escuela Profesional de Tecnología Médica.

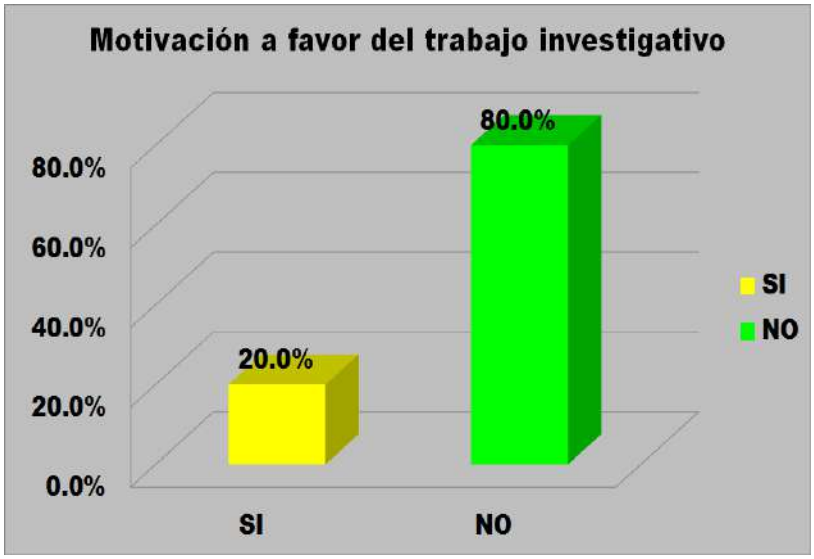

Figura Nº 11: Nivel de motivación a favor del trabajo investigativo.

Análisis: Del 100% de docentes encuestados, el 80% reconocen que no existe motivación a favor de la investigación. Se deduce que la mayoría de docentes reconocen que no existe motivación investigativa.

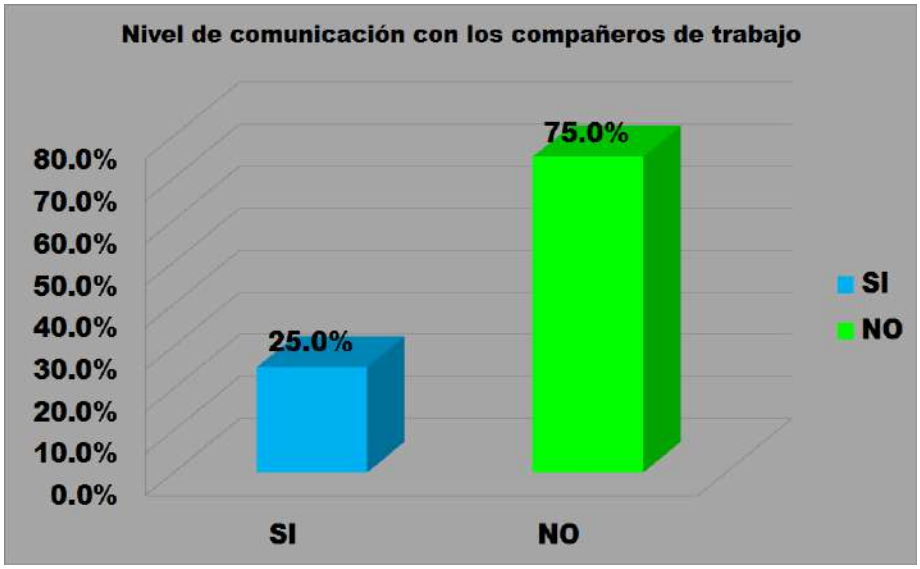

Figura Nº 12: Nivel de comunicación con los compañeros de trabajo.

Análisis: 75% reconocen no tener comunicación permanente con sus colegas, mientras que el 25% expresa que si lo hay. Vemos que la mayoría de docentes afirma no tener

comunicación permanente entre ellos; esto debido a las malas relaciones interpersonales, a la comunicación verticalista. Por tanto, no se adaptan a su centro de trabajo.

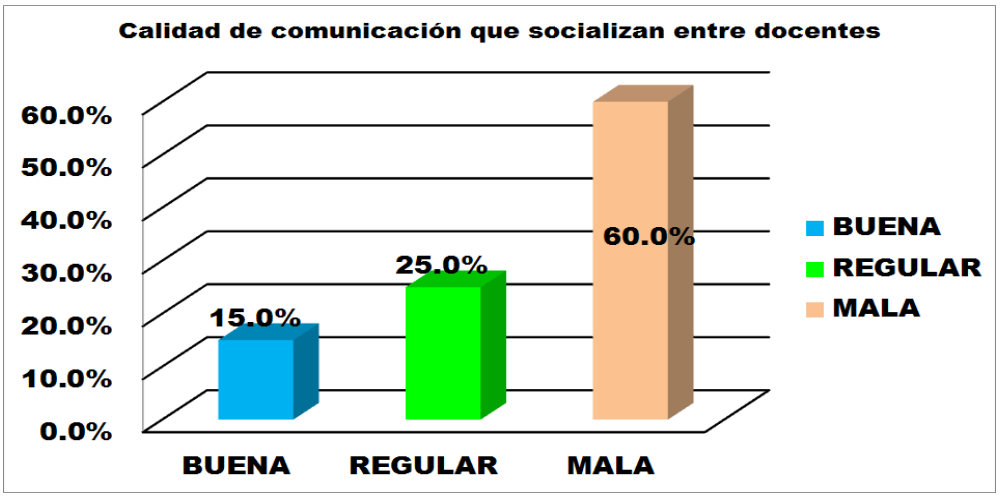

Figura Nº 13: Calidad de comunicación que socializan entre docentes.

Análisis: Del 100% de docentes encuestados, el 60% sostiene que la comunicación entre ellos es mala y 25% regular; mientras que solo el 15% afirma que es buena. Vemos que la mayoría de los docentes reconocen que las relaciones no son agradables, ya que no existe una adecuada comunicación.

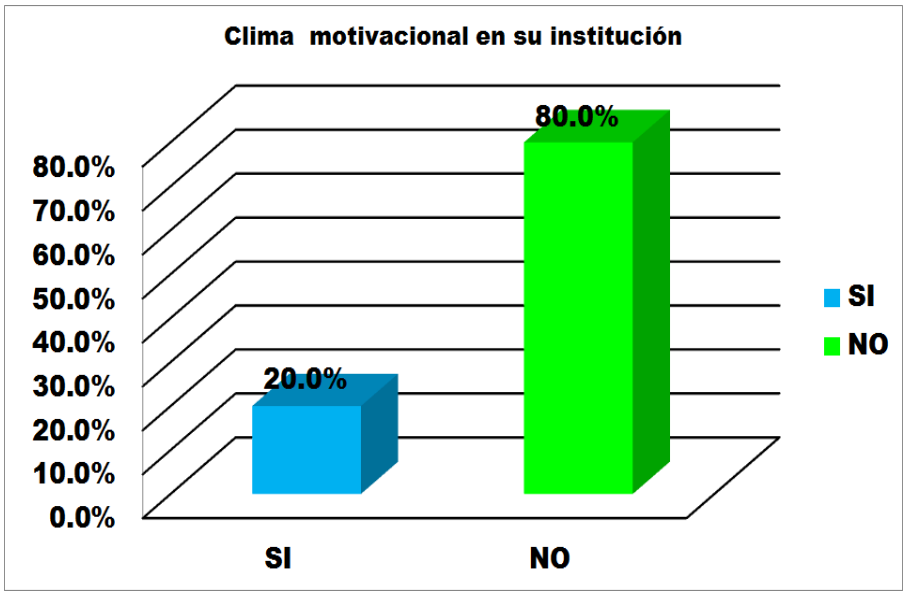

Figura Nº 14: Existencia de un clima motivacional en su institución.

Análisis: 80% reconocen que no existe un clima motivacional en su Institución mientras que el 20% indica que si lo hay. La mayoría de docentes afirman que no existe clima motivacional en su centro de trabajo, debido a que no existe una buena comunicación entre colegas y por ende no hay motivación para desarrollar su trabajo investigativo.

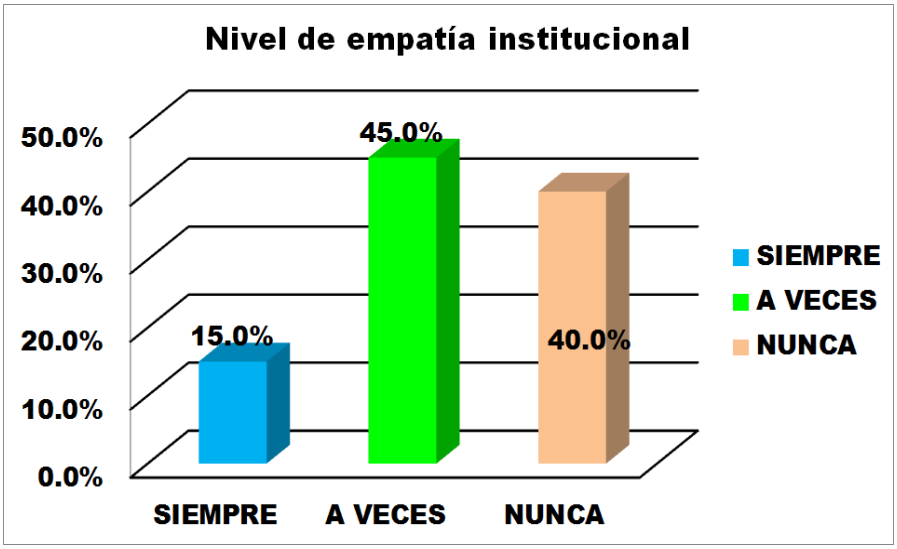

Figura Nº 15: Nivel de empatía institucional.

Análisis: Del 100% de docentes encuestados, el 45% afirman que a veces existe empatía institucional; el 40% no lo hay, mientras que el 15% expresa lo contrario. Se concluye que la mayoría de docentes reconocen que no existe comprensión institucional, debido a las malas relaciones interpersonales entre colegas y a la desmotivación institucional.

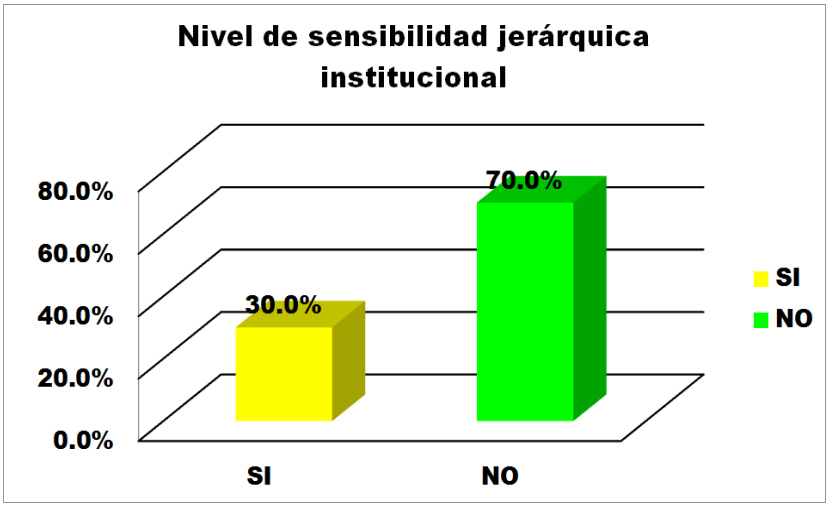

Figura Nº 16: Nivel de sensibilidad jerárquica institucional.

Análisis: 70% reconocen que sus autoridades no son sensibles a sus requerimientos y sólo 30% reconoce que son sensibles. Esto permite afirmar, que, al existir una comunicación verticalista de las autoridades, no les interesa el ánimo de los docentes.

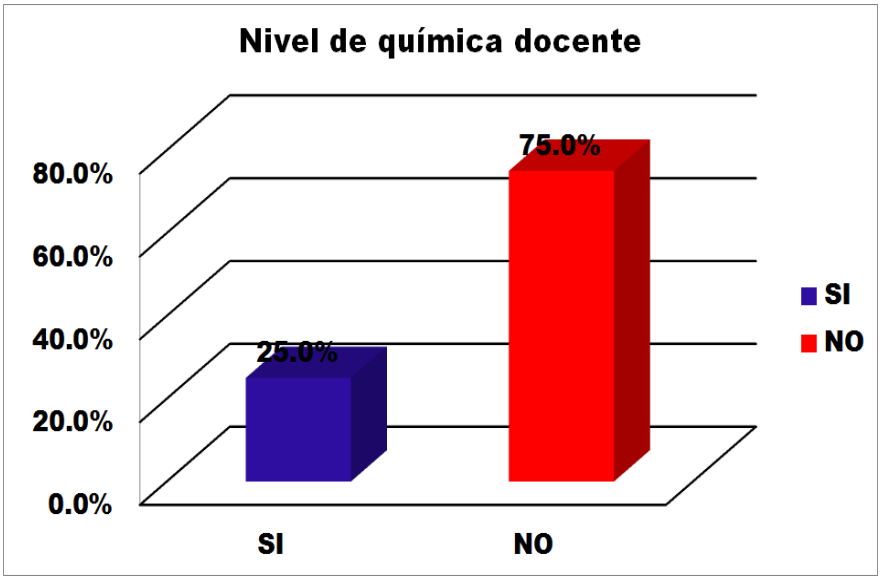

Figura Nº 17: Nivel de química docente.

Análisis: Del 100% de docentes encuestados, el 75% afirman que no existe química docente, esto es, no se entienden ni se atienen entre ellos, mientras que el 25% expresa lo contrario. Vemos que la mayoría de docentes reconocen que no existe sinceramiento ni transparencia entre ellos.

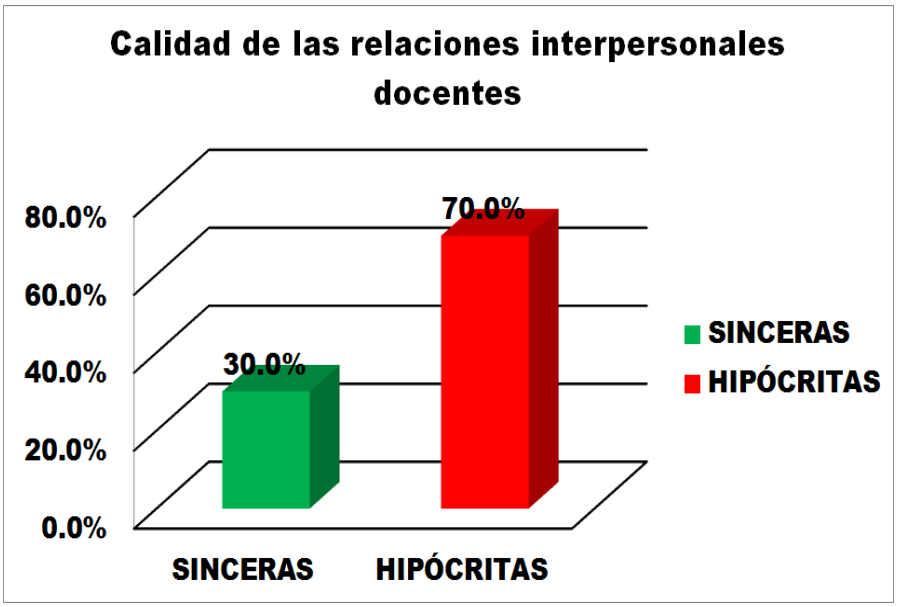

Figura Nº 18: Calidad de las Relaciones Interpersonales Docentes.

Análisis: 70% reconocen que las relaciones interpersonales son hipócritas y solo el 30% indica que son sinceras. Observamos que la mayoría de docentes reconocen que las relaciones interpersonales son fingidas, esto permite aseverar que no existe sinceramiento ni transparencia entre ellos.

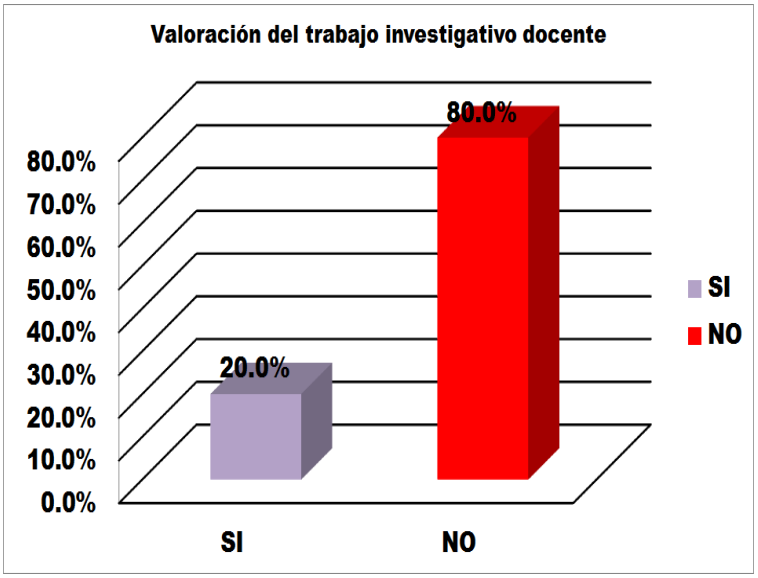

Figura Nº 19: Valoración del trabajo investigativo docente.

Análisis: Del 100% de docentes encuestados, el 80% afirman que no se valora el trabajo investigativo docente, mientras el 20% expresa que sí. La mayoría de docentes reconocen que no se le da la prestancia del caso al trabajo investigativo docente.

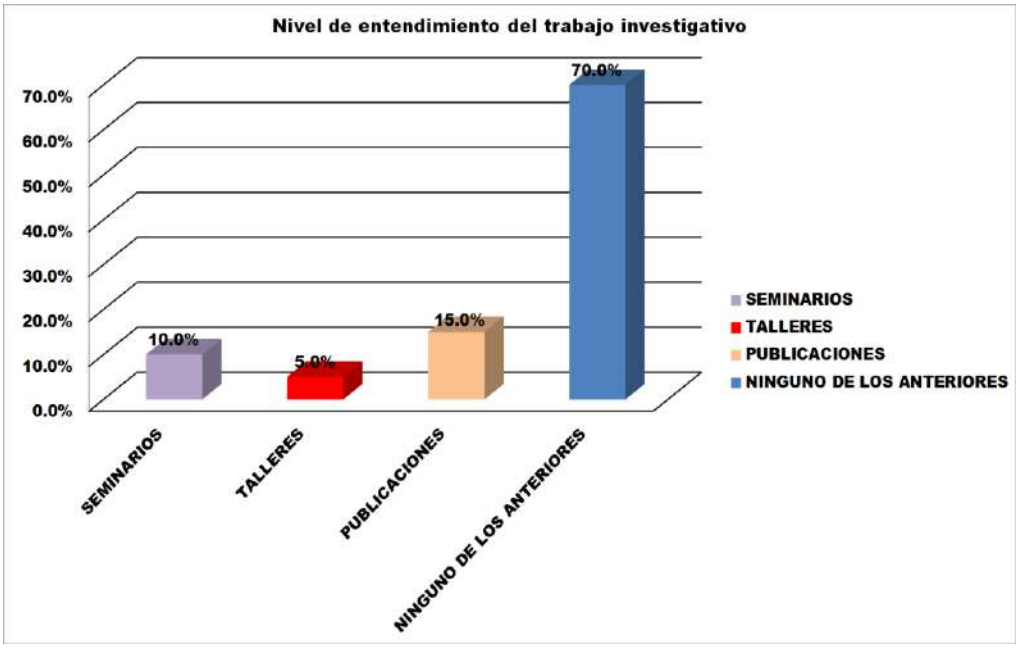

Figura Nº 20: Nivel de Entendimiento del Trabajo Investigativo.

Análisis: 70% no entienden el significado del trabajo investigativo docente; el 15% expresa que el trabajo investigativo implica publicaciones; el 10% seminarios y el 5% talleres. En su mayoría los docentes no comprenden que se entiende por trabajo investigativo docente.

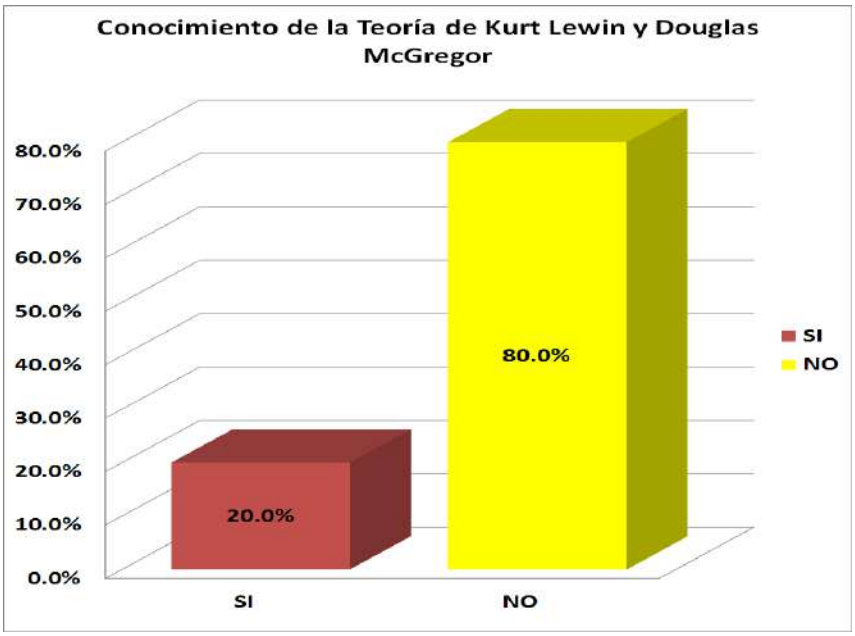

Figura Nº 21: Conocimiento de la Teoría de Kurt Lewin y Douglas McGregor.

Análisis: Del 100% de docentes encuestados, el 80% no tienen conocimiento de la Teoría de Kurt Lewin y Douglas McGregor, solo el 20% si conocen la teoría. La mayoría de docentes desconocen las Teoría deKurt Lewin y Douglas McGregor.

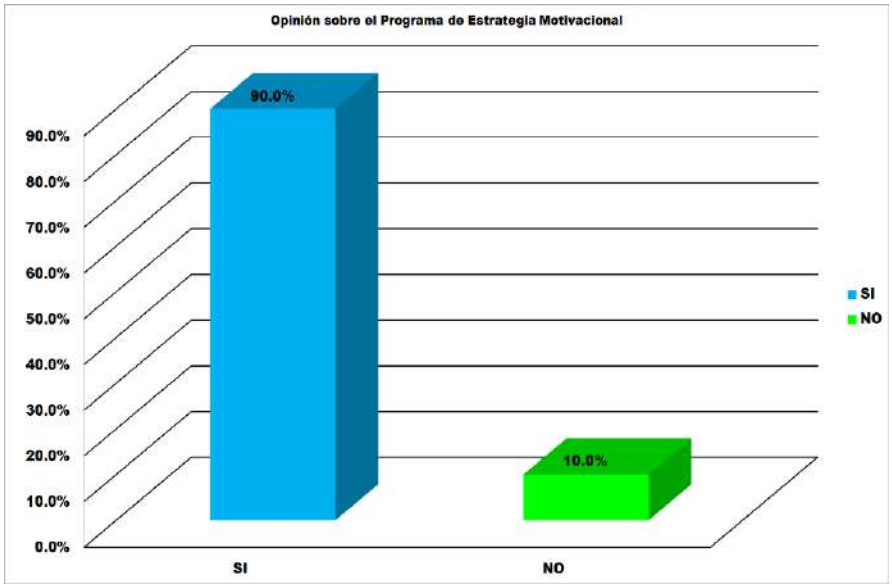

Figura Nº 22: Opinión Sobre el Programa de Estrategia Motivacional.

Análisis: 10% sostienen que un Programa de Estrategia Motivacional no mejorará las relaciones interpersonales docentes, mientras que un 90% respondió que sí. Casi todos los docentes reconocen que un Programa de Estrategia Motivacional mejorará las relaciones interpersonales docentes.

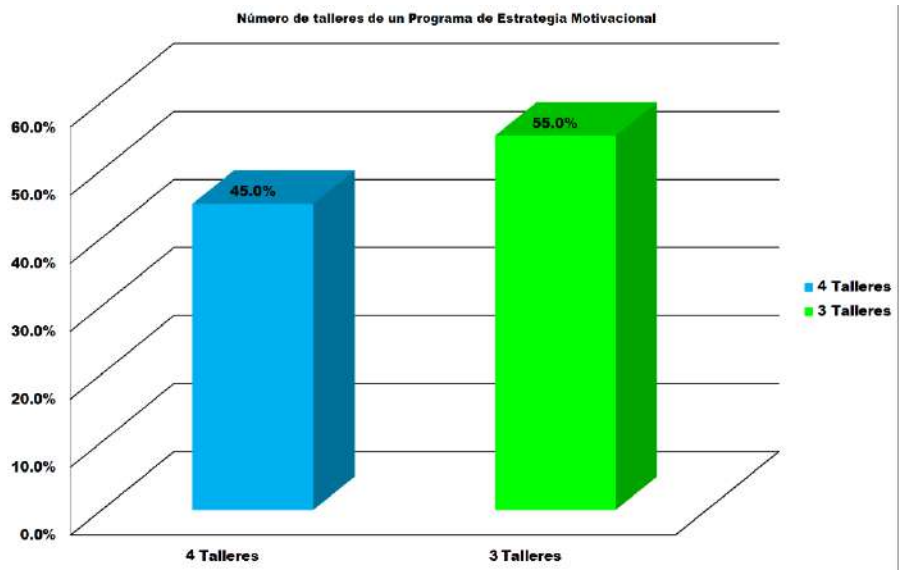

Figura Nº 23: Número de Talleres de un Programa de Estrategia Motivacional

Análisis: Del 100% de docentes encuestados, el 55% son de la opinión que un Programa de Estrategia Motivacional deberá concretizarse a través de 3 talleres; mientras que el 45% opina que debe estar estructurado por 4 talleres. Observamos que la mayoría de docentes son de la opinión que el programa en su estructura deberá tener 3 talleres.

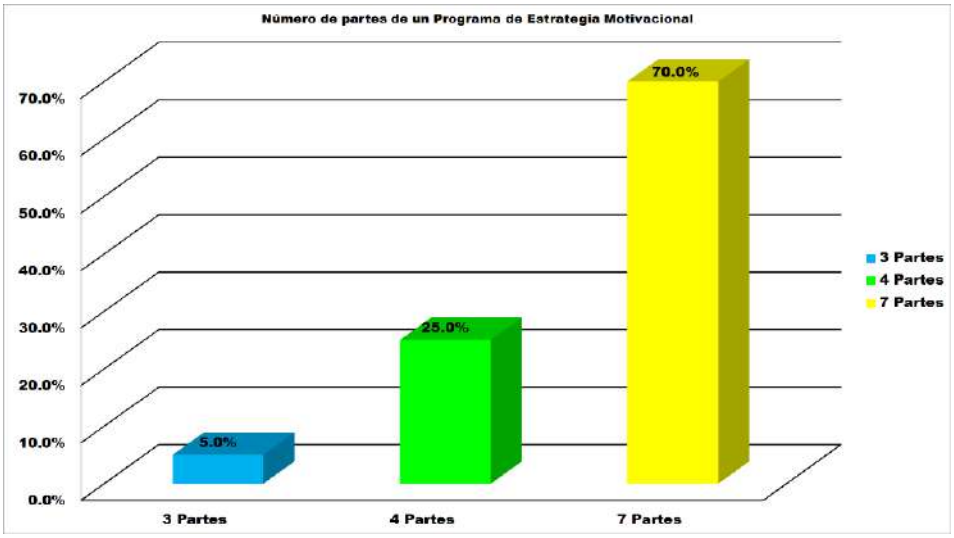

Figura Nº 24: Número de Partes de un Programa de Estrategia Motivacional.

Análisis: 70% de docentes creen que el Programa de Estrategia Motivacional debe tener 7 partes, mientras 25% de docentes afirman que el Programa sólo debe tener 4 partes y sólo un 5% indica que el programa debe contener 3 partes. En su mayoría los docentes son de la opinión que el programa debe tener 7 partes.

3. Discusión

La Universidad de Chiclayo, fue creada mediante Ley Nº 24086, el 11 de Enero de 1985, dando inicio a sus labores académicas con las Carreras Profesionales de Arquitectura y Urbanismo y la Facultad de Ciencias de la Salud, con la Escuela Profesional de Obstetricia.

Posteriormente, se modifica el Art. 02 de la Ley de Creación mediante Ley Nº 2478 el 22 de Diciembre de 1987, ampliando las Carreras Profesionales de Ciencias de la Salud, con las Escuelas Profesionales de Tecnología Médica con la especialidad de Radiología, Terapia Física y Rehabilitación y Laboratorio Clínico; Facultad de Educación con las Escuelas Profesionales de Educación Inicial y Educación Especial.

En el año 1992 la Universidad de Chiclayo adquiere su plena autonomía eligiendo a sus máximas autoridades. En el año 1993 se aprueban las Carreras Profesionales de Derecho, Ingeniería Informática y de Sistemas, Psicología, Administración de Empresas, Contabilidad, Economía; del mismo modo se amplía la Facultad de Educación con Educación Primaria y Secundaria. A la fecha la Universidad de Chiclayo cuenta con 9 facultades y 16 escuelas profesionales, habiéndose creado la Facultad de Medicina Humana y la Escuela Profesional de Enfermería. Al presente año se cuenta con la apertura de las Escuelas de Ingeniería Civil y Marketing.

En la actualidad tiene una infraestructura moderna distribuida en el campo universitario ubicado en el Km. 4.5 de la carretera al Balneario de Pimentel y el edificio de la Urb. Miraflores donde funciona la Facultad de Derecho. Asimismo, las funciones administrativas se realizan en el local de Miraflores Mz H Lote 9 y la Escuela de Post Grado en Juan Manuel Iturregui 133.

La Misión de la Universidad de Chiclayo es la de formar profesionales de excelencia en las diferentes ramas del saber y la práctica: Conocimiento claro del entorno local, regional, nacional e internacional. Capacidad permanente para generar ciencias e investigación, tecnología y trabajo productivo. Compromiso con los procesos del cambio social, vigencia

del estado de derecho, democracia participativa, verdad y justicia y demás principios de la convivencia ciudadana. Frente a ello, la Universidad de Chiclayo tiene como visión alcanzar el liderazgo a nivel local y nacional.

4. Propuesta Teórica: "Estrategias motivacionales para mejorar las relaciones interpersonales"

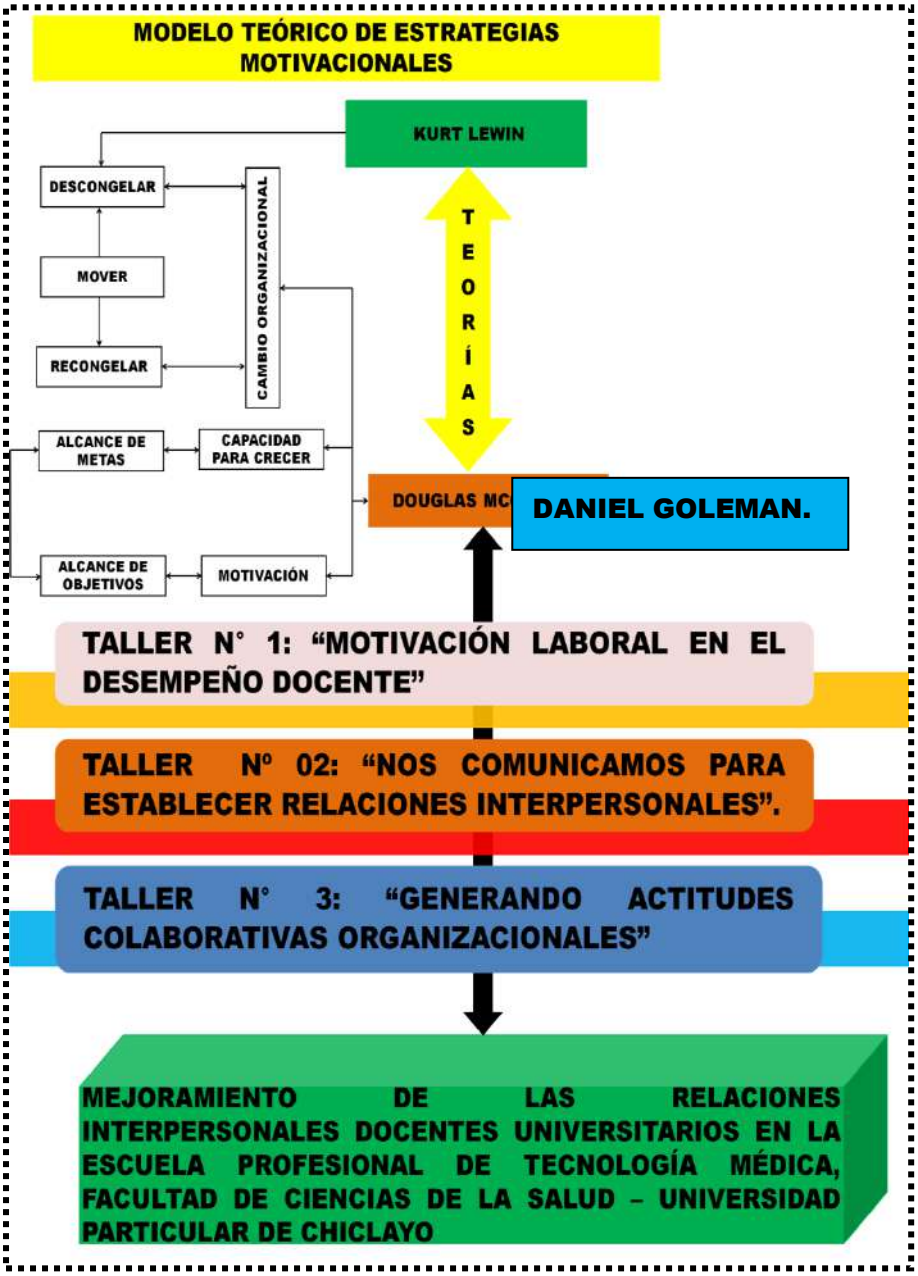

Las estrategias motivacionales como técnicas que persiguen lograr objetivos para mejorar la calidad educativa no han sido desarrolladas ni aplicadas en nuestra institución universitaria. No hay hasta ahora actividades que hagan uso de exposiciones individuales y

colectivas orientadas a las relaciones interpersonales, o análisis de resultados relacionados ha dicho tema.

Esta realidad ha motivado nuestro interés para proponer estrategias motivacionales tomando en cuenta la motivación, información y orientación para realizar aprendizajes de socialización y convivencia en los docentes. Para tal efecto se ha tenido en cuenta el trabajo individual y colectivo que deberán desarrollarse en los próximos talleres a través de los cuales se concretizan las estrategias motivacionales.

El objetivo general de la propuesta fue, mejorar las relaciones interpersonales en los docentes de la Escuela Profesional de Tecnología Médica, Facultad de Ciencias de la Salud – Universidad de Chiclayo, mediante estrategias motivacionales con la finalidad de potenciar su capacidad de socialización y convivencia.

Los objetivos específicos fueron, conocer la esencia de las relaciones interpersonales y descubrir las capacidades individuales para establecerlas, incrementar y reforzar cualidades de socialización y convivencia, y otras habilidades y conceptos aplicables al desarrollo de relaciones interpersonales y proponer la aplicación de conocimientos y habilidades relativas a las relaciones interpersonales para lograr un equipo sólido.

Conclusiones

La mayoría de docentes presentan malas relaciones interpersonales, se manifiesta en la mala comunicación, ausencia de socialización, falta de identidad institucional, falta de identidad con los conceptos de respeto, autonomía y libertad, entre otros.

La base teórica sirvió de fundamento a la propuesta.

Las estrategias motivacionales son esenciales, ya que nos permiten trabajar con todos los docentes de manera dinámica e interactiva afinando e incrementando el nivel de las relaciones interpersonales.

Referencias

Alemán, B., Navarro de Armas, O., Suárez, R., Izquierdo, Y. & Encinas, T. (2018). La motivación en el contexto del proceso enseñanza-aprendizaje en carreras de las Ciencias Médicas. *Revista Médica Electrónica*, *40*(4), 1257-1270. Recuperado de http://scielo.sld.cu/scielo.php?script=sci_arttext&pid=S1684182420180004000032&lng=es&tlng=es.

Beltrán-Morillas, A., Valor-Segura, I., & Expósito, F. (2015). El perdón ante transgresiones en las relaciones interpersonales. Psychosocial Intervention, 24(2), 71-78. https://dx.doi.org/10.1016/j.psi.2015.05.001

Flores, E., Garcia, M., Calsina, W., & Yapuchura, A. (2016). Las habilidades sociales y la comunicación interpersonal de los estudiantes de la Universidad Nacional del Altiplano - Puno. *Comuni@cción*, 7(2), 05-14. Recuperado de http://www.scielo.org.pe/scielo.php?script=sci_arttext&pid=S2219-71682016000200001&lng=es&tlng=es.

Garrote, D., Garrote, C., & Jiménez, S. (2016). Factores Influyentes en Motivación y Estrategias de Aprendizaje en los Alumnos de Grado. REICE. Revista Iberoamericana sobre Calidad, Eficacia y Cambio en Educación, 14(2),31-44. Recuperado de https://www.redalyc.org/articulo.oa?id=551/55144743002

Hernández, V., Herrera, K. & Mena, M. (2019). Entrenamiento socio-psicológico para mejorar la competencia comunicativa interpersonal: estudio de un caso. Comuni@cción, 10(1), 5-20. https://dx.doi.org/https://doi.org/10.33595/2226-1478.10.1.326

Lapeña-Moñux, Y., Cibanal-Juan, L., Pedraz-Marcos, A., & Macía-Soler, M. (2014). Las relaciones interpersonales de los enfermeros en asistencia hospitalaria y el uso de habilidades comunicativas. Texto & Contexto - Enfermagem, 23(3), 555-562. https://dx.doi.org/10.1590/0104-07072014002010013

Montes, C., Rodríguez, D. & Serrano, G. (2014). Estrategias de manejo de conflicto en clave emocional. Anales de Psicología, 30(1), 238-246. https://dx.doi.org/10.6018/analesps.30.1.135171

Muñoz, C., Conejeros, M., Contreras, C., & Valenzuela, J. (2016). La relación educador-educando: Algunas perspectivas actuales. Estudios pedagógicos (Valdivia), 42(especial), 75-89. https://dx.doi.org/10.4067/S0718-07052016000300007

Muñoz, A. & Ramírez, M. (2014). La motivación de los empleados: más allá de la "zanahoria y el garrote". Recuperado de http://www.scielo.org.co/pdf/adter/n24/n24a8.pdf

Muñoz, O. (2019). Cultura, gestión pública, gerencia y sistema de relacionamiento, *Revista Latinoamericana de Difusión Científica*, 1 (1), 68-83

Strauss, A., & Corbin, J. (2002). Bases de la investigación cualitativa. Chile: Universidad de Antioquía.

Vásquez Gastelumendi, D. V.; Ríos Campos, C. A.; Santamaría Baldera, N.; Gutiérrez Valverde, K. S.; Camacho Delgado, F. M.; Aguirre Zaquinaula, I. R.; Estela Urbina, R. O. (2019). Estrategias organizacionales para fortalecer el clima laboral en la Escuela Profesional de Tecnología Médica - Facultad de Ciencias de la Salud de la Universidad de Chiclayo, *Revista de la Universidad del Zulia*, 10 (28), 112-136.

Universidad de Chiclayo. (2013). Región Lambayeque. Recuperado de http://www.altillo.com/universidades/peru/Universidad_de_Chiclayo_UDCH.asp

Realidad virtual en la reducción del dolor y la ansiedad en niños sometidos a venopunción

Sonia Tejada-Muñoz *
Iris Tomasita Tafur- Santillán **
Rosa Jeuna Diaz-Manchay ***
Lisseth Dolores Rodriguez-Cruz ****
Manuel Emilio Milla-Pino *****
Sonia Celedonia Huyhua-Gutierrez ******
Manuel Jesús Sánchez-Chero *******

RESUMEN

El objetivo del estudio fue verificar el efecto de la realidad virtual en la reducción de la ansiedad y el dolor en niños de 6 a 10 años sometidos a venopunción en el Departamento de Pediatría del Hospital Regional Virgen de Fátima en Chachapoyas- Perú, 2019. Estudio analítico, prospectivo, cuasi-experimental; la muestra fue de 50 niños distribuidos en un grupo control (25) y un grupo intervenido (25) sometidos a la aplicación de realidad virtual. Los resultados muestran que los videojuegos reducen significativamente el dolor (X2 = 43; p = 0.0000) y la ansiedad (X2 = 38.33; p; = 0.0000) en los niños sometidos a venopunción. Está comprobado que la realidad virtual reduce significativamente la ansiedad y el dolor en los niños sometidos a venopunción, y es una herramienta tecnológica de distracción, económica y fácil de usar para el profesional de la enfermería que puede ser implementada en hospitales de países con alto índice de pobreza.

PALABRAS CLAVE: Realidad virtual; procedimientos invasivos; dolor; ansiedad; hospitalización pediátrica; Enfermería.

* Profesor Asociado. Facultad de Ciencias de la Salud Universidad Nacional Toribio Rodríguez de Mendoza de Amazonas - Perú. https://orcid.org/0000-0002-1181-8540. E-mail: sonia.tejada@untrm.edu.pe
** Enfermera especialista en pediatría. Departamento de Pediatría del Hospital Regional Virgen de Fátima, Chachapoyas, Amazonas - Perú. https://orcid.org/0000-0002-3725-5280. Email: iristafursantillan622@hotmail.com
*** Coordinadora de Asuntos Académicos de la Escuela de Enfermería de la Universidad Católica Santo Toribio de Mogrovejo, Chiclayo, Perú. https://orcid.org/0000-0002-2333-7963. Email: rdiaz@usat.edu.pe
**** Docente de la Escuela de Enfermería de la Universidad Católica Santo Toribio de Mogrovejo de Chiclayo, Perú. https://orcid.org/0000-0003-1742-9498. Email: lrodriguez@usat.edu.pe
***** Docente Investigador. Universidad de Jaén, Perú. https://orcid.org/0000-0003-3931-9804. Email: manuel.milla@unj.edu.pe
****** Docente Asociado. Facultad de Ciencias de la Salud Universidad Nacional Toribio Rodríguez de Mendoza de Amazonas, Perú. https://orcid.org/0000-0003-4823-2778. Email: sonia.huyhua@untrm.edu.pe
******* Docente Investigador. Universidad Nacional de Frontera., Perú. https://orcid.org/0000-0003-1646-3037. E-mail: msanchezch@unf.edu.pe

Recibido: 13/05/2020 Aceptado: 26/06/2020

Virtual reality in reducing pain and anxiety in children undergoing venipuncture

ABSTRACT

The objective of the study was to verify the effect of virtual reality in reducing anxiety and pain in children aged 6 to 10 undergoing venipuncture in the Pediatric Department of the Regional Hospital Virgen de Fátima in Chachapoyas - Peru, 2019. Study analytical, prospective, quasi-experimental; the sample was 50 children distributed in a control group (25) and intervened group (25) submitted to the virtual reality application. The results show that video games significantly reduce pain (X2 = 43; p = 0.0000) and anxiety (X2 = 38.33; p; = 0.0000) in children undergoing venipuncture. It is proven that virtual reality significantly reduces anxiety and pain in children undergoing venipuncture, and is a distraction technology tool, economical and easy to use for the nursing professional that can be implemented in hospitals in countries that have high poverty index.

KEYWORDS: Virtual reality; invasive procedures; pain; anxiety; pediatric hospitalization; Nursing.

Introducción

Durante la hospitalización en el área de pediatría, es común realizar procedimientos invasivos con fines terapéuticos o diagnósticos (Toledo et al., 2019), los cuales a menudo provocan dolor y ansiedad (Eijlers et al., 2019), siendo para los niños la venopunción uno de los procedimientos clínicos más dolorosos y aterradores (Atzori et al., 2018), lo que implica inicialmente distraerlos como medida para calmar su dolor (Zamora et al., 2014). Existen medidas no farmacológicas para reducir el dolor en los niños durante la venopunción, de acuerdo a su edad, así en neonatos y lactantes prevalece el uso de sacarosa oral, en la primera infancia se utiliza medidas afectivas y de distracción, mientras en la edad escolar predominan las técnicas de distracción, (Cocera-Martínez, 2016). Al respecto, Plaza y Gómez (2015) en su estudio concluyen que la distracción audiovisual es efectiva para disminuir la intensidad de dolor durante la administración de la vacuna Triple Vírica.

Una de las funciones autónomas de las enfermeras pediátricas, es reducir el dolor que ocasionan los procedimientos invasivos como la venopunción, sin embargo, a pesar que existen estudios que demuestran la eficacia de algunas medidas estratégicas no farmacológicas, su aplicación es escasa (Cocera-Martínez, 2016). La venopunción es un procedimiento que causa dolor y ansiedad a los niños, y una forma de reducir estas molestias

es usar la realidad virtual (RV) (Toledo et al., 2019). Distraer la atención del dolor con la ayuda de la RV, particularmente en niños, puede ayudar a las enfermeras a trabajar de manera más efectiva (Piskorz y Czub, 2018). Al respecto, la RV es una intervención moderna que puede usarse para proporcionar entretenimiento durante los procedimientos clínicos especialmente para los niños (Eijlers et al., 2019; Kenney & Milling, 2016; Chan et al., 2018).

En ese sentido, existen algunos estudios en países desarrollados, donde han comprobado que la RV ayuda significativamente a disminuir del dolor en procedimientos que utilizan agujas, como la venopunción en la hospitalización de pediatría (Chan et al., 2019; Aracil, 2016), en tratamiento oncológico de pediatría (Atzori et al., 2018), en el servicio de urgencias pediátricas (Valbuena et al., 2018), en extracción de sangre (Piskorz y Czub, 2018), también para aliviar la ansiedad preoperatoria y mejorar la inducción de anestesia en niños sometidos a cirugía electiva (Ryu et al., 2017). Con la RV se logró disminuir el dolor en los niños durante los cambios de apósitos en heridas crónicas (Hua et al., 2015). Asimismo, hay estudios con RV que demuestran la disminución de la ansiedad en los niños hospitalizado y en sus familiares (Toledo et al., 2019).

Sin embargo, la investigación en RV en hospitales de países subdesarrollados como es Perú, aún no se han reportado referentes relacionados directamente al uso de esta tecnología, por lo que se torna un estudio en beneficio de los pacientes pediátricos y de sus familiares acompañantes, por otro lado, sirva para motivar a las enfermeras a su aplicación en la práctica clínica.

Este estudio tuvo como objetivo: Comprobar el efecto de la realidad virtual en la reducción de la ansiedad y el dolor en niños de 6 a 10 años hospitalizados en el servicio de Pediatría del Hospital Regional Virgen de Fátima en Chachapoyas - Perú, 2019.

1. Materiales y métodos

Se efectuó un estudio analítico, prospectivo, cuasiexperimental (Hernández, 2018). La muestra fue de 50 niños de 6 a 10 años hospitalizados por cualquier diagnóstico médico y que tiene indicado el procedimiento de venopunción; quienes cumplieron con los criterios de inclusión: lúcidos, orientados en tiempo, espacio y persona cuyas madres autorizaron su participación en el estudio; fueron asignados a uno de los 2 grupos de la investigación

mediante tabla de aleatorización: Grupo control (Grupo 1= 25) vs Grupo intervenido sometido a realidad virtual (Grupo 2= 25).

Para el uso de la realidad virtual se empleó el modelo VR Shinecon Virtual Reality 3D Glasses VR Headset Casque Realidad Virtual with Gamepad for pone Android 4.3 – 6 inh Smartphone + Game contoller (con ajuste de la distancia interpupilar) asociado a un dispositivo telefónico y a unos auriculares para una mayor inmersión en el mundo virtual. La técnica de distracción utilizada fue la proyección de cortos dibujos animados. Las Variables recogidas: edad, sexo, diagnóstico, escalas de dolor y ansiedad, estas últimas fueron valorados por personal sanitario y el niño.

La escala de las caras de Wong y Baker (WBFS, 2019), ha sido validada por Hicks et al (2001), consta de seis caras con distintas expresiones desde una cara feliz hasta una muy triste, organizadas de "la más alegre" a "la más triste" a fin de que correspondieran a un niño o niña escolar, con "nada de dolor" hasta "mucho dolor". También se asignó un número del 0 al 10 a cada cara en orden ascendente y distribuidos de la manera siguiente: 0 – No dolor, 2 dolor leve, 4 – 6 dolor moderado, 8 – dolor intenso, 10 – Máximo dolor imaginable. Esta numeración se utilizó únicamente para recoger los datos.

Asimismo, se usó la escala de Gronniger Discale (valorada de 0 a 5), escala observacional diseñada por Humphrey et al. (1992), para medir la ansiedad durante un procedimiento médico de corta duración. Maneja el distrés o ansiedad del niño en cinco niveles (1-5) de menor a mayor grado de ansiedad; tiene en cuenta dos variables principales que son el llanto y la tensión muscular que están consideradas en todos los instrumentos revisados como las conductas que con mayor frecuencia se presentan, además de ser relativamente fácil definirlas en forma operacional, se clasifica en cinco grados: 1- calmado, 2- Tímido/nervioso, 3- Ansiedad moderada pero todavía bajo control, 4- tensión y llanto continuo, 5- pánico.

Los niños hospitalizados en el servicio de pediatría de este hospital demostraron sentimientos reducidos de dolor (medido por caras) durante todo el procedimiento de la venopunción cuando se utiliza el dispositivo de distracción de realidad virtual. Las puntuaciones de ansiedad informados por el personal de enfermería durante el procedimiento fueron reducidas altamente significativas para el grupo experimental que para el grupo control.

El estudio fue aprobado por el Vicerrectorado de Investigación de la Universidad Nacional Toribio Rodríguez de Mendoza de Amazonas, previo visto bueno del Comité de ética. Todos los pacientes o representantes legales (madres) fueron informados y firmaron el consentimiento informado necesario para su inclusión en el mismo.

Se realizó el análisis estadístico con el programa SPSS Statistics v21. Se usó la prueba de rangos con signo de Wilcoxon en virtud de la escala ordinal en que se midieron las variables respuestas y que las muestras antes y después intra grupos son relacionadas o pareadas, asimismo se usó la Prueba de Mann Whithey en virtud de la escala ordinal en que se midieron las variables respuestas y que las muestras intergrupos son independientes.

2. Resultados

Tabla 01. Ansiedad y dolor en niños sometidos a venopunción antes y después de la sesión de realidad virtual en el grupo control y experimental, Chachapoyas - 2019

COMPARACIÓN	PRUEBA DE RANGOS CON SIGNO DE WILCOXON		OBSERVACIÓN
	Aprox normal	P-valor	
AA1 vs. AD1	0.730 ns	0.4652	IGUAL
DA1 vs. DD1	1.214 ns	0.2249	IGUAL
AA2 vs. AD2	4.359 **	0.0000	DIFERENTES
DA2 vs. DD2	4.359 **	0.0000	DIFERENTES

ns : No significativo (p › 0.05)
(*) : Significativo (p ‹ 0.01)
(**) : Altamente significativo (p ‹ 0.05)
AA1 : Ansiedad antes Grupo 1
AD1 : Ansiedad después Grupo 1
DA1 : Dolor antes Grupo 1
DD1 : Dolor después Grupo 1
AA2 : Ansiedad antes Grupo 2
AD2 : Ansiedad después Grupo 2
DA2 : Dolor antes Grupo 2
DD2 : Dolor después Grupo 2

Tabla 02. Ansiedad y dolor después de la sesión de realidad virtual en el grupo experimental, Chachapoyas – 2019.

VARIABLE	PRUEBA DE LA MEDIANA		OBSERVACIÓN
	CHI-CUADRADO	P-valor	
ANSIEDAD	38.33 **	0.0000	Grupo 2
DOLOR	43.00 **	0.0000	Grupo 2

ns : No significativo ($p > 0.05$)
(*) : Significativo ($p < 0.01$)
(**) : Altamente significativo ($p < 0.05$)

3. Discusión

Está demostrado que, la venopunción es el procedimiento médico más frecuente en los servicios de hospitalización, sobre todo, esto genera mucha ansiedad, miedo y dolor en los niños, pudiendo continuar ese miedo hasta la edad adulta debido a dichas experiencias, (Cuervo & Alonso, 2016), ante ello, es importante utilizar medidas no farmacológicos para distraer a los niños, así en los últimos años se está innovando con la realidad virtual, esta tecnología informática sumerge al individuo en un entorno interactivo, multisensorial tridimensional (Kenney & Milling, 2016), simulado por computadora al que se accede a través de un dispositivo montado en la cabeza, lo que excluye la visión del mundo real; de este modo la distracción con la realidad virtual sería una intervención no farmacológica útil en los procedimientos donde se utilicen agujas, sobre todo en pacientes pediátricos (Chan et al., 2019; Sil et al. 2014), indicaron mejoras significativas en el umbral y tolerancia del dolor en niños al usar videojuegos y un casco de realidad virtual.

En esta investigación al comparar las muestras relacionadas o pareadas intra grupos se ha encontrado evidencias que nos impulsan a afirmar que en el grupo 1 (control) existe un comportamiento similar en cuanto a las variables ansiedad y dolor para las mediciones antes y después, mientras que en el grupo 2 (Realidad virtual) el comportamiento es diferente entre los valores antes y después para cada una de las respuestas estudiadas (Tabla 01). Asimismo la comparación inter grupos, objeto de estudio, presenta evidencias que conducen a pensar que el grupo 2 tienen mayores valores tanto de la variable ansiedad como de la variable dolor

ya que el estadístico de prueba resultó altamente significativo, rechazándose así la hipótesis nula que expresa un comportamiento similar entre los grupos y aceptándose la hipótesis alternativa que señala la existencia de un comportamiento distinto entre los grupos con respecto a las dos variables respuestas estudiadas. Así se ha podido demostrar que al aplicar los lentes de realidad virtual a los niños hospitalizados sometidos a venopunción se logró la reducción altamente significativa del dolor y la ansiedad (p = 0.0000) (Tabla 02). Los hallazgos del presente estudio son similares al estudio de Valbuena et al. (2018), quienes aplicaron en el grupo de intervención RV durante la venopunción a los pacientes pediátricos, mientras que en el grupo control se emplearon los métodos de distracción habituales, posteriormente evaluaron las escalas de dolor (escala Wong- Baker y numérica, WBFS, 2019) y de ansiedad (Gronninger discale, Humphrey et al. 1992), ellos concluyeron que la RV es una instrumento efectivo para disminuir los niveles de dolor y ansiedad, aunque sus resultados no fueron estadísticamente significativos porque fue muy poco el tamaño muestral (el grupo intervención (n=9) y el grupo control (n=8)).

También, se ha encontrado coincidencias con la investigación de Piskorz & Czub (2018), en una clínica de nefrología pediátrica (N=38; edad media 11 años, rango 7-17); al grupo experimental se les aplicó distracción con RV y manifestaron una intensidad de dolor significativamente menor que los controles (media = 15,16 ± 20,51 frente a 37,05 ± 30,66; t= 2,59, df = 36, p <0,02, d = 0,863); se obtuvieron resultados similares para el nivel de estrés (11.16 ± 18.58 vs 41.89 ± 40.89; t = 2.98, df = 36, p <.01, d = 0.993); no hubo correlaciones con la edad. Mientras, Atzori et al. (2018), hicieron un estudio con 15 pacientes (edad media 10.92, SD = 2.64) que padecen enfermedades oncológicas y recibieron una venopunción con "No RV" y una venopunción con "Sí RV" en dos días separados (orden de tratamiento aleatorizado); durante la RV, los pacientes informaron reducciones significativas en el "Tiempo dedicado a pensar en el dolor", reportaron diversión y una "fuerte sensación de estar dentro del mundo generado por computadora".

Asimismo, en el estudio de Chan et al (2019), la intervención de RV que utilizaron fue segura y efectiva para los niños de 4 a 11 años sometidos a venopunción, disminuyendo el dolor, la ansiedad, la angustia y la necesidad de restricción en dos entornos hospitalarios. Igualmente, Eijlers et al. (2019), finiquitan que la investigación de realidad virtual en pediatría se ha centrado principalmente en la distracción durante los procedimientos clínicos y se

encontró que era significativamente más efectiva para reducir el dolor (14 estudios) y la ansiedad (7 estudios).

Atzori et al (2018), concluyen que la RV puede considerarse una técnica de distracción efectiva para el manejo del dolor en niños y adolescentes durante la punción venosa; además, promueve la diversión provocando emociones positivas, más que las técnicas tradicionales de distracción; y ayuda a enfrentar este procedimiento de una manera no estresante. De este modo, la RV puede ser un instrumento eficaz para menguar el dolor y el estrés pediátricos debido a la punción venosa, puede ser aplicada fácilmente por las enfermeras en su práctica clínica (Piskorz & Czub, 2018). Además, algunos estudios que han utilizado la RV como distracción para disminuir el dolor y la ansiedad en los niños sometidos a venopunción, aseguran que esta intervención no reporta efectos secundarios o reacciones adversas (Toledo et al., 2019; Atzori et al., 2018).

Por otro lado, Toledo et al. (2019), en su estudio reportaron elevada satisfacción de los pacientes pediátricos y sus familiares en relación al uso de la RV, confirmaron que disminuye el dolor y la ansiedad, facilitando la ejecución de pruebas o exámenes diagnósticos. Cabe mencionar, que la RV también puede ayudar a reducir el uso de opioides en los pacientes con dolor crónico, Gupta et al. (2018).

Chan et al (2018) sugieren usar RV para quemaduras, fisioterapia; incluso en el futuro, la rehabilitación con realidad virtual podría ser fácil de realizar en casa con mínima supervisión clínica (Matsangidou et al., 2017). Por lo mencionado, se necesitan más investigaciones que establezcan la eficacia de los costos y los entornos clínicos óptimos para el uso de la RV (Chan et al., 2018). De esta manera se infiere, que la realidad virtual es una tecnología que puede ser utilizada para diferentes contextos tanto hospitalarios como comunitarios, así como para disminuir el dolor y ansiedad en pacientes con diferentes patologías, medios de diagnóstico y tratamientos, que necesitan distracción o relajación enfocando su mente en las imágenes que se visualizan a través de la realidad virtual, esto además de mejorar la satisfacción del paciente y de su familiar acompañante, mejora la imagen institucional.

Es labor de los enfermeros y enfermeras, hacer del proceso de la hospitalización pediátrica un entorno armónico que genere una experiencia positiva, reduzca el dolor, la ansiedad, el miedo a las agujas y minimice traumas durante la enfermedad y hospitalización

del niño; por lo que es un imperativo moral incorporar técnicas de distracción como la realidad virtual, pues favorecen significativamente la producción de endorfinas minimizando el dolor y la ansiedad en los niños sometidos a venopunción.

Conclusiones

En este estudio se evidenció que el efecto de la realidad virtual es altamente significativo en la reducción de la ansiedad (p = 0.0000) y el dolor (p = 0.0000) en niños de 6 a 10 años que fueron sometidos a venopunción; por ello constituyen una herramienta tecnología de distracción para el profesional de enfermería además es una intervención alternativa económica y de fácil uso para ser implementada en los hospitales de la región y el país. Pero se recomienda realizar más estudios que reproduzcan los resultados de esta investigación, que permita concretar estudios controlados aleatorios.

Limitaciones del estudio: Hubo dos padres que no firmaron el consentimiento informado, y dos niños que no se dejaron colocar los lentes de realidad virtual.

Referencias

Aracil NG. (2016). Efectividad de medidas no farmacológicas para la disminución del dolor y la ansiedad durante la venopunción en población pediátrica. Recuperado de https://dialnet.unirioja.es/servlet/tesis?codigo=61178.

Atzori B, Hoffman HG, Vagnoli L, et al. (2018). Virtual Reality Analgesia During Venipuncture in Pediatric Patients With Onco-Hematological Diseases. Front Psychol. doi:10.3389/fpsyg.2018.02508

Chan E, Foster S, Sambell R, Leong P. (2018). Clinical efficacy of virtual reality for acute procedural pain management: A systematic review and meta-analysis. PLOS ONE. 13(7):e0200987. doi:10.1371/journal.pone.0200987

Chan E, Hovenden, Michael, Ramage, Emma, et al. (2019). Virtual Reality for Pediatric Needle Procedural Pain: Two Randomized Clinical Trials. J Pediatr. 209:160-167.e4. doi:10.1016/j.jpeds.2019.02.034

Cocera-Martínez L. (2016). Efectividad de las medidas analgésicas empleadas para el alivio del dolor durante la punción venosa en niños. Recuperado de http://tauja.ujaen.es/jspui/handle/10953.1/3719.

Cuervo CC, Alonso PS. (2016). Uso de métodos frente al dolor durante la venopunción en niños. NURE Investig Rev Científica Enferm. (83):14.

Eijlers R, Utens EMWJ, Staals LM, et al. (2019). Systematic Review and Meta-analysis of Virtual Reality in Pediatrics: Effects on Pain and Anxiety. Anesth Analg. 129(5):1344-1353. doi:10.1213/ANE.0000000000004165

Gupta A, Scott K, Dukewich M. (2018). Innovative Technology Using Virtual Reality in the Treatment of Pain: Does It Reduce Pain via Distraction, or Is There More to It? Pain Med. 19(1):151-159. doi:10.1093/pm/pnx109

Hernández S, Mendoza C. (2018). Metodología de la investigación: Las rutas cuantitativa, cualitativa y mixta. 1ra ed. México: McGraw-Hill Interamericana.

Hicks, Carrie L, Baeyer Carl L, Spafford Pamela A, Korlaar, Inez V, Goodenough, Belinda. (2001). The Faces Pain Scale – Revised: toward a common metric in pediatric pain measurement. Pain. 93(2):173-183. doi:10.1016/S0304-3959(01)00314-1

Hua, Yun, Qiu, Rong, Yao, Wen-yan, Zhang, Qin, Chen, Xiao-li. (2015). The Effect of Virtual Reality Distraction on Pain Relief During Dressing Changes in Children with Chronic Wounds on Lower Limbs. Pain Manag Nurs. 16(5):685-691. doi:10.1016/j.pmn.2015.03.001

Humphrey GB, Boon CMJ, Heuvell GFEC van L van Den, Wiel HBM van De. (1992). The Occurrence of High Levels of Acute Behavioral Distress in Children and Adolescents Undergoing Routine Venipunctures. Pediatrics. 90(1):87-91.

Kenney, M. P., & Milling, L. S. (2016). The effectiveness of virtual reality distraction for reducing pain: A meta-analysis. *Psychology of Consciousness: Theory, Research, and Practice, 3*(3), 199–210. https://doi.org/10.1037/cns0000084

Matsangidou M., Ang C.S., Sakel M. (2017). Clinical utility of virtual reality in pain management: a comprehensive research review. Br J Neurosci Nurs.13(3):133-143. doi:10.12968/bjnn.2017.13.3.133

Piskorz J., Czub M. (2018). Effectiveness of a virtual reality intervention to minimize pediatric stress and pain intensity during venipuncture. J Spec Pediatr Nurs. 23(1):e12201. doi:10.1111/jspn.12201

Plaza Sánchez L., Gómez Galán R. (2015). Efectividad en la aplicación de un método de distracción audiovisual en niños durante la vacunación. Rev Cuba Enferm. 31(3):0-0.

Ryu J-H, Park S-J, Park J-W, et al. (2017). Randomized clinical trial of immersive virtual reality tour of the operating theatre in children before anaesthesia. BJS Br J Surg. 104(12):1628-1633. doi:10.1002/bjs.10684

Sil S., Dahlquist LM, Thompson C, et al. (2014). The effects of coping style on virtual reality enhanced videogame distraction in children undergoing cold pressor pain. J Behav Med.37(1):156-165. doi:10.1007/s10865-012-9479-0

Toledo, B., Pérez, J.A., Morente,L, et al. (2019). Disminuyendo el dolor en los procedimientos invasivos durante la hospitalización pediátrica: ¿ficción, realidad o realidad virtual? An Pediatría. 91(2):80-87. doi:10.1016/j.anpedi.2018.10.019

Valbuena S.M, Fernández IF, Robla MV, Vega IBV, Ruiz TG, Fernández JAF. (2018). Eficacia de una intervención enfermera con realidad virtual en urgencias pediátricas: un ensayo clínico aleatorizado. Tiempos Enferm Salud Nurs Health Times. (5):32-37.

Wong-Baker Faces Pain Rating Scale. (2019). Wong-Baker FACES Foundation. Recuperado de https://wongbakerfaces.org/.

Zamora LMR, Lara M, Martha R. (2014). Distractor para «calmar» el dolor por la venopunción en los niños. Rev Mex Pediatría. 81(6):209-213.

Normas para la presentación de trabajos

1. Principios de la Revista

La REVISTA DE LA UNIVERSIDAD DEL ZULIA es un órgano científico de difusión de trabajos parciales o definitivos de investigadores y/o equipos de investigación nacionales y extranjeros. Su naturaleza es multidisciplinaria e interdisciplinaria, por ello su temática se divide en tres grandes ejes: a. *ciencias sociales y arte*; b. *ciencias del agro, ingeniería y tecnología*; c. *ciencias exactas, naturales y de la salud*. Su publicación es cuatrimestral. Cada número, de los tres del año, se corresponde con uno de los tres ejes temáticos. La *Revista de la Universidad del Zulia*, por su carácter histórico y patrimonial, está adscrita a la CÁTEDRA LIBRE HISTORIA DE LA UNIVERSIDAD DEL ZULIA.

2. Métodos de Envío y de Evaluación de los Trabajos

Los autores interesados en publicar su trabajo en la *Revista de la Universidad del Zulia* deberán remitir tres copias del mismo sin identificación en sobre cerrado a la siguiente dirección: Avenida Guajira, Fundadesarrollo, planta baja de la Sede Rectoral de La Universidad del Zulia. Este sobre debe estar acompañado de otro, el cual contendrá el original del trabajo con la identificación del autor o autores, indicando: nombre, apellido, institución que representa (universidad, instituto, centro de investigación, fundación), correo electrónico. Así mismo en este sobre se presentará una comunicación escrita firmada por todos los autores y dirigida al Director de la Revista. En esta comunicación se manifestará el interés de los autores de proponer su trabajo para la publicación en la *Revista de la Universidad del Zulia*, previa evaluación del Comité de Arbitraje. Se agregará también a este sobre una síntesis curricular de cada autor con una extensión no mayor de diez (10) líneas. Los artículos pueden agregarse a la plataforma OJS de la revista. También se podrá presentar el trabajo dirigiéndolo al siguiente correo electrónico: revistadeluz@gmail.com. El currículo de los autores se enviará en archivo adjunto, distinto al que contendrá el trabajo. Los artículos propuestos para esta revista deben ser inéditos y no deben haber sido propuestos simultáneamente a otras publicaciones. Todos los trabajos serán evaluados por parte de un Comité de Árbitros-Especialistas de reconocido prestigio, seleccionado por el Comité Editorial de la Revista. La evaluación de los Árbitros se realizará mediante el procedimiento conocido como par de ciegos: los árbitros y los autores no conocerán sus identidades respectivas. Los criterios de Evaluación son los siguientes: a. Criterios formales o de presentación: 1) originalidad, pertinencia y adecuada extensión del título; 2) claridad y coherencia del discurso; 3) adecuada elaboración del resumen; 4) organización interna del texto; 5) todos los demás criterios establecidos en la presente normativa. b. Criterios de contenido: 1) dominio de conocimiento evidenciado; 2) rigurosidad científica; 3) fundamentación teórica y metodológica; 4) actualidad y relevancia de las fuentes consultadas; 5) aportes al conocimiento

existente. Al recibirse la respuesta del Comité de Árbitros designado se informará a los autores por correo electrónico la decisión correspondiente; en caso de ser aceptado el trabajo deberá remitirse por correo electrónico la versión digital del mismo.

3. Presentación de los trabajos

Los trabajos deben presentar un resumen de 150 palabras como máximo y hasta cinco palabras claves; tanto el resumen como las palabras claves estarán en español e inglés. Igualmente el título y el subtítulo del trabajo serán presentados también en español e inglés. La extensión máxima del trabajo será de veinte (20) páginas, y diez (10) como extensión mínima (salvo excepciones plenamente justificadas). Todos los trabajos serán presentados en hoja tipo carta, impresos por una sola cara, con numeración continua y con márgenes de tres (3) centímetros a cada lado. El texto se presentará a espacio y medio, en fuente Times New Roman, tamaño 12.

4. Cuerpo del artículo

Se dividirá en Introducción, Desarrollo y Conclusiones (o Consideraciones Finales, según sea el caso). La introducción incluirá el propósito u objetivo general perseguido. El Desarrollo se organizará en secciones y subsecciones debidamente identificadas con subtítulos numerados completamente en arábigos de acuerdo al sistema decimal, respondiendo a una sucesión continua y utilizando un punto para separar los niveles de división. La Introducción y Conclusión están exceptuadas de esta numeración. Las fechas y horas se expresarán numéricamente. En caso de existir ilustraciones (gráficos, mapas, fotos) debe hacerse referencia a los mismos en el texto. Estas ilustraciones serán contadas dentro de la extensión máxima del artículo. Las notas explicativas o aclaratorias deben reducirse al mínimo necesario y colocarse al pie de páginas debidamente señalizadas. Los materiales complementarios se recogerán en anexos, los cuales se identificarán con una letra y un título y se colocarán después de la bibliografía. Los anexos serán contados también dentro de la extensión máxima del artículo.

5. Citado

El citado se realizará en el texto utilizando la modalidad autor-fecha, establecido en el *Reglamento para la presentación de trabajos en la Universidad del Zulia*, indicando, en caso de ser cita textual, apellido(s) del autor, seguido de coma, año de publicación de la obra, seguido de dos puntos y el (los) número(s) de la(s) página(s), por ejemplo: de acuerdo a Rincón (1998: 45) o (Rincón, 1998: 45); si no es cita textual sino una paráfrasis no se indicará el número de página, ejemplo: de acuerdo a Rincón (1998) o (Rincón, 1998). Si hay varias obras del mismo autor publicadas en el mismo año, se ordenarán literalmente en orden alfabético; por ejemplo, (Rincón, 2008a: 12), (Rincón, 2008b: 24). Si son dos autores, se colocarán solamente el primer apellido de cada uno, por ejemplo: Según Morales y Fleires (2008: 90) o (Morales y Fleires, 2008: 90), siguiendo el mismo criterio explicado anteriormente para las citas textuales y las paráfrasis. En caso de ser tres autores o más se colocará el apellido del autor principal

seguido de "et al", ejemplo: (Rincón *et al.*, 2008: 45). Deben evitarse, en lo posible, citas de trabajos no publicados o en imprenta, también referencias a comunicaciones y documentos privados de difusión limitada, a no ser que sea estrictamente necesario. En caso de fuentes documentales, electrónicas u otras que por su naturaleza resulten inviables o complejas para la adopción del citado autor-fecha, sugerido en estas normas, puede recurrirse u optarse por el citado al pie de página.

6. Referencias bibliográficas

Las referencias (bibliográficas, hemerográficas, orales y/o documentales) se presentarán al final del texto, según lo establecido en el *Reglamento para la presentación de trabajos en la Universidad del Zulia*. El orden de las referencias es alfabético por apellido. Las diferentes obras de un mismo autor se organizarán cronológicamente, en orden ascendente, y si son dos obras o más de un mismo autor y año, se mantendrá el estricto orden alfabético por título.

Fecha de evaluación_____

Instrumento de Evaluación del Árbitro

I.- Criterios formales o de presentación

CRITERIOS DE EVALUACIÓN	EXCELENTE	MUY BUENO	BUENO	REGULAR	DEFICIENTE OBSERVACIONES
Originalidad, pertinencia y adecuada					
Extensión del título					
Claridad y coherencia del discurso					
Adecuada elaboración del resumen					
Contiene abstract y palabras claves					
Objetivo, metodología y resultados.					
Organización interna del texto					

II. - Criterios de contenido

CRITERIOS DE EVALUACIÓN	EXCELENTE	MUY BUENO	BUENO	REGULAR	DEFICIENTE OBSERVACIONES
Dominio de conocimiento evidenciado					
Rigurosidad científica					
Fundamentación teórica y metodológica					
Actualidad y relevancia de las fuentes consultadas					
Aportes al conocimiento existente					

III. – Sugerencia de publicación

De acuerdo a la información obtenida usted recomendaría (favor marcar con una X):

Publicar sin modificaciones: _____ Publicar con ligeras modificaciones_____
Publicar con modificaciones sustanciales_____ No publicar_____

Fundamentación de la decisión:

REVISTA DE LA UNIVERSIDAD DEL ZULIA

FUNDADA EN 1947

PATRIMONIO DE LA

UNIVERSIDAD DEL ZULIA

FUNDADA EN 1891

MARACAIBO-VENEZUELA

Julio de 2020

REVISTA DE LA UNIVERSIDAD DEL ZULIA
CIENCIAS EXACTAS, NATURALES Y DE LA SALUD///
AÑO 11 N° 30, Mayo-Agosto 2020
ISSN 0041-8811

Contenido